

R-483

ADVANCED PROPFAN ENGINE TECHNOLOGY (APET) AND SINGLE-ROTATION GEARBOX/ PITCH CHANGE MECHANISM

By
D.F. Sargisson

General Electric Company

FINAL REPORT

*IN-07
DATE OVERRIDE*

97828

Prepared for



National Aeronautics and
Space Administration

Lewis Research Center
Cleveland, Ohio
44135

Contract NAS3-23044

(NASA-CR-168113) ADVANCED PROPFAN ENGINE
TECHNOLOGY (APET) AND SINGLE-ROTATION
GEARBOX/PITCH CHANGE MECHANISM (General
Electric Co.) 483 p Avail: MIS HC
A21/MF AC1

N87-28553

Unclas
0097828

CSCL 21E G3/07

1. Report No. NASA CR-168113		2. Government Accession No.		3. Recipient's Catalog No.	
4. Title and Subtitle ADVANCED PROPFAN ENGINE TECHNOLOGY (APET) AND SINGLE-ROTATION GEARBOX/PITCH CHANGE MECHANISM				5. Report Date June 1985	
				6. Performing Organization Code	
7. Author(s) D. F. Sargisson (General Electric Company)				8. Performing Organization Report No. R83AEB592	
				10. Work Unit No.	
9. Performing Organization Name and Address General Electric, Aircraft Engine Business Group, Advanced Engineering Technology Dept., Cincinnati, Ohio, 45215				11. Contract or Grant No. NAS3-23044	
				13. Type of Report and Period Covered Contractor Report	
12. Sponsoring Agency Name and Address National Aeronautics and Space Administration Lewis Research Center, 21000 Brookpark Road, Cleveland, Ohio 44135				14. Sponsoring Agency Code	
15. Supplementary Notes Project Manager, Gerald A. Kraft, Advanced Turboprop Project Office, NASA Lewis Research Center, Cleveland, Ohio 44135					
16. Abstract <p>This study compares the projected performance, in the 1990's time period, of equivalent technology level high bypass ratio turbofan powered aircraft (at the 150 passenger size) versus advanced turboprop propulsion systems. Fuel burn analyses, economic analyses, and pollution (noise, emissions) estimates, have been made. Three different cruise Mach numbers were investigated for both the turbofan and turboprop propulsion systems. Aerodynamic design and performance estimates have been made for nacelles, inlets, and exhaust systems. Air to oil heat exchangers have been investigated for (oil cooling) advanced gearboxes at the 12,500 SHP level. The results and conclusions of this study are positive in that high speed turboprop aircraft will exhibit superior fuel burn characteristics and lower Direct Operating Costs when compared with equivalent technology turbofan aircraft. In addition to the conceptual design of the propfan gearbox made during early tasks in this study, an additional Task (Task VII) extended the conceptual design data to the status of a Preliminary Design. Also a new Task (Task VIII) made a conceptual design of an advanced electro-mechanical propfan pitch change mechanism controlled by an all-digital fiberoptic data link. These additional tasks have materially assisted in defining areas of a modern turboprop which would benefit greatly from the application of advanced concepts and technology.</p>					
17. Key Words (Suggested by Author(s)) Propfan, Gearbox, Turboprop, Turboprop Engine, Pitch Change, Fiberoptic Data Link, Turboprop Propulsion System			18. Distribution Statement [REDACTED] until July 1987		
19. Security Classif. (of this report) unclassified		20. Security Classif. (of this page) unclassified		21. No. of pages	22. Price*

TABLE OF CONTENTS

<u>Section</u>	<u>Page</u>
FOREWORD	iv
1.0 SUMMARY RESULTS AND CONCLUSIONS	3
2.0 INTRODUCTION	9
3.0 PROGRAM OVERVIEW	15
4.0 TOPICAL DISCUSSION OF THE STUDY (TASKS I THROUGH VI, AND TASKS VII, VIII AND IX)	75
5.0 CONCLUSIONS	437
APPENDIX I - HEAT EXCHANGERS	449
APPENDIX II - ACOUSTICS	467
APPENDIX III - ENGINE WEIGHT AND DIMENSION CALCULATION MODEL	485

PRECEDING PAGE BLANK NOT FILMED

FOREWORD

This document presents the results of a contract study (NAS3-23044) conducted for the National Aeronautics and Space Administration (NASA) by the General Electric Company, Aircraft Engine Business Group. The program was administered by the Advanced Technology Programs Department with K. Schuning serving as Program Manager. The Technical Manager assigned for the Study was D.F. Sargisson.

The study was directed by NASA-Lewis Research Center and G.A. Kraft was the NASA Study Program Manager.

A large range of technical subjects were addressed during the study period and a number of widely differing technical disciplines were involved. The following is a list of the principal General Electric personnel who have made major contributions to this study.

For Tasks I through VI

Engine Design

Aero/Mechanical	J. Ciokajlo/G. Smith
Cost and Weight	G. Smith

Engine Cycle and Performance Analyses

Cycle Definitions and	J.E. Johnson/R. Steinmetz
Performance Decks	J. Morrow

Gearbox Design

Theory	R.J. Willis (AEBG, Lynn)
Mechanical Design	C. Broman/C. Toraason
Cost and Weight	C. Toraason/A. Ludwig
Heat Exchangers	R. Petsch
Lubrication	D. Hester

Propeller Performance

	R.G. Giffin
--	-------------

Nacelle and Inlet Aerodynamics

Inlet	D. Paul
Exhaust and Nacelle Design	A. Kuchar
Configuration Analyses	R. Petsch

Aircraft Synthesis and Performance Analyses

Requirements	W. Joy
Aircraft Synthesis	W. Joy
Trade-offs/Performance	R. Hines

Installation Technology W. Joy/R. Petsch

Acoustic Technology S. Lavin/P. Ho

Engine Emissions J. Taylor

It is also appropriate that General Electric acknowledges the advice and counsel of three principal aircraft companies, who have supported this study, particularly in the area of airplane performance methodology, weight estimating procedures, acoustic trade-off data for fuselage noise attenuation, nacelle placement and other installation criteria. These companies are:

Lockheed	California and Georgia
Douglas	Long Beach
Boeing	Seattle

A number of Hamilton-Standard personnel have also contributed data for this study and their efforts are likewise acknowledged.

For Tasks VII through IX

Electric Machinery	E. Richter/T. Miller, General Electric Corporate R&D Center
Fiberoptic Technology	G. Carlson, GE, CR&D Center
Traction Drives	G. White/R. Anderson, TRI Inc.
Propeller Mechanisms	C.M. Toraason, GE P. Barnes, Hamilton-Standard M. Mayo, Hamilton-Standard

SECTION 1.0

SUMMARY RESULTS AND CONCLUSIONS

1.0 SUMMARY RESULTS AND CONCLUSIONS

The Advanced Propfan and Engine Technology Definition Study (hereafter referred to as APET, or the APET Study) forms a part of the technology base required to substantiate the performance benefits that have been predicted for airplane propulsion systems which include the estimated full-scale Hamilton Standard propfan performance characteristics. Several previous industry studies conducted for NASA support the position that the development of the propfan would provide a significant contribution to the continuing commercial airplane technology dominance, by the United States, of the International Market. However, the studies already reported have not covered specific airplane engine and gearbox design characteristics (and related installation layout) that are required to produce, together with the propfan, the best performance consistent with acceptable noise characteristics. Therefore, the APET Study, sponsored by NASA Lewis, is an essential element in the realization of the full potential performance benefits that can occur from an optimum propfan propulsion system.

This study contract initially covered the six tasks that are listed below:

APET Program Tasks

- Task I - Selection of Evaluation Procedures and Assumptions
- Task II - Engine Configuration and Cycle Evaluation
- Task III - Propulsion System Integration
- Task IV - Engine/Aircraft Evaluation
- Task V - Advanced Prop-Fan Engine Technology (APET) Plan
- Task VI - Reporting Requirements

Task I provided the rationale for the conduct of the study. Task II evaluated a candidate set of turbofan and turboshaft engines correctly sized for the missions defined in Task I, and selected one turbofan engine and two turboshaft engines that were then carried into the later study tasks; Task III provided installation factors for the selected engines and produced Preliminary Design Layouts of engines, gearboxes, nacelles and sub-systems integrated with

PRECEDING PAGE BLANK NOT FILMED

the aircraft wing; Task IV evaluated the airplane performance, operating costs and acoustic signatures while carrying out the specified missions, Task V produced a set of recommendations and plans for the technology development of key components identified in this study; Task VI covered the necessary reporting, which includes this document.

A range of cruise speeds between Mach 0.70 and 0.80 was examined for the selected missions and six point-design airplanes were synthesized and "flown" on the computer to obtain a matrix of performance results. Some off-design missions were also run to determine quantitatively the value of the technology assumptions on both fuel burn and cost. Acoustic and emission signatures were also estimated and compared against existing rules and those that may be in force in the next decade.

The results and conclusions from this study are positive. High cruise speed turboprop powered airplanes will, when examined with consistent propulsion technology relative to turbofan engines, exhibit superior fuel burn and operating cost indices while meeting all the requisite regulations for acoustic and emission signatures. Many aspects of the study and its results have direct Military relevance. These aspects can now be explored with some confidence, using the propulsion systems designed for APET.

As a result of the above 6 tasks, NASA decided to enlarge the APET study by the addition of 3 more tasks. These were:

Task VII - The Preliminary Design of a gearbox to be selected from the candidates already identified.

Task VIII - The Conceptual Design of an advanced electromechanical pitch change mechanism which integrates with the propfan and the gearbox of Task VII.

Task IX - Reporting Requirements.

The primary objective of Task VII was to identify the technologies which require support for an advanced gearbox to drive the propfan. The time period for application was selected as the early 1990's and NASA required that the "advanced" gearbox to be directly compared with a gearbox using state-of-the-art technologies in gears, bearings, housings, lubrication and lubricant choices, system integration methods, costs and weights. This task also required that the "advanced" gearbox to be compatibly designed with regard to the Pitch Change Mechanism being conceptually designed in Task VIII.

Both offset and concentric gearboxes were preliminarily designed. The offset gearbox is not reported here because its design was undertaken by the Westland Helicopter Company in England at no cost to the contract. The concentric gearbox is a reprobable item and has been included.

It is noteworthy that the offset design made by Westland to General Electric ground rules was a significant advance over any contemporary offset gearbox in terms of low parts count and thus greatly enhanced reliability. The advance was made possible by substituting "conformal" gear technology for current "involute" gear technology. The technology data base available to Westland on "conformal" gears is unique to the western world and has been developed over a period of some 15 years. Conformal gear sets in a helicopter transmission have both military and commercial application and over 300 Westland "Lynx" helicopters are in world-wide service.

The concentric gearbox which was preliminarily designed also included advancements of significance. Higher temperature gearsets and lubrication were used in conjunction with a modulated flow oil system. Also, the main system components such as the oil tank and oil-to-air heat exchanger were integrated into the gearbox housing design, saving weight and increasing reliability in the process. The housing itself was proposed as a fabricated titanium structure which comprises local castings welded to sheet-metal structures using advanced manufacturing techniques.

Task VIII had as its primary objective the design of a radically different PCM for the propfan. Earlier work by General Electric had defined the propfan PCM to be an essential technology item requiring intense effort. The history

of hydromechanical systems in propeller PCM's may seem to be adequate for current applications but the propfan raises many questions as to the desirability of proceeding down a hydromechanical path. The Centrifugal Twisting Moment (CTM) of the scimitar shaped propfan blade combined with its relatively high rotational speed gives rise to actuator forces that are an order of magnitude greater than conventional, unswept, blades. Also, the control of the total propulsion system is based on the use of a Full Authority Digital Electronic Control (FADEC) and there are some obvious merits in having electronic signaling interface directly with electronic components rather than using electrohydraulic servo valves.

General Electric used the resources of the Corporate Research and Development Center to assist in the definition of advanced electromechanical components and the conceptual design of an all fiberoptic signal and control system that crosses the stationary-to-rotating boundary (gearbox to propfan) via an uniquely designed optical slipring with low optical loss. It should be emphasized that the system concepts being reported herein are radially different from any previous propeller control system, and they are attempting to ensure that the propfan, when fully developed, will be supported by a PCM with improved reliability and integrity (system safety) compared with current propellers.

SECTION 2.0
INTRODUCTION

TABLES

<u>Table</u>		<u>Page</u>
2-1.	Twin-Engined Turboprop Airplanes.	10

2.0 INTRODUCTION

An important element of NASA's Aircraft Energy Efficiency Program (ACEE) is the Advanced Turboprop Project (ATP). This project is being directed and administered by the NASA Lewis Research Center.

In parallel to the ATP, NASA Lewis has contracted for the Advanced Propfan Engine Technology definition studies (hereafter called APET) with three principal US propulsion companies.

The objectives of the APET definition study were to:

- Identify candidate engine and drive systems which, when coupled with an advanced propfan, will improve the energy efficiency of future U.S. commercial aircraft so that substantial fuel savings can be realized and permit U.S. built commercial aircraft and engines to retain their dominant place in the world aircraft market.
- Assist NASA in formulating a plan for a follow-on hardware effort that will provide the key technology required for U.S. engine manufacturers to develop the candidate engines and drive systems which are critical to the viability of a propfan propulsion system.

As part of the ATP a new concept of propeller rotor is being progressively evaluated through both theoretical and empirical efforts. This rotor, now being developed by Hamilton-Standard under contract to NASA, is generally referred to as a "Propfan". Typically, in a single row actuator disk it will employ eight or ten blades. Each of the blades incorporates advanced technology geometry for improving aerodynamic (thrust and efficiency) performance at high cruise Mach numbers (in the order of $M = 0.70$ to 0.80) and additional geometric refinements to reduce rotor noise generation. The propfan also uses advanced technology in its structure to reduce weight significantly compared with an all-metal, old technology, propeller blade. Previous studies have indicated that a propfan propulsion system, flying at an equivalent cruise Mach number to the current turbofan powered airplanes, can reduce fuel consumption by more than fifteen percent when compared with a turbofan propulsion system using equivalent core engine (gas-generator) technology. These studies are listed in References 1 through 22.

The scope of the first 6 Tasks of the APET studies required consistent comparisons between airplanes, designed for equivalent commercial operations, employing turbofan and turboprop propulsion systems. These comparisons are projected into the technology levels realizable during the early part of the next decade.

The definition of the turbofan airplane, using an existing data base is considered straightforward. The definition of the turboprop is much less well based and is discussed below.

It has been over twenty years since industry designed or developed commercial turboprop aircraft and engines for use by the major trunk airlines. The cruise speed of these aircraft was in the Mach 0.5 to 0.6 range, with Mach number-never-exceed (M_{NE}) values of around 0.65. The Mach restrictions, in general, were not related to the propulsion systems themselves, but were limiting factors for the aircraft aerodynamic (wing) and structural design. Also, again in general terms, these designs called for a balance between takeoff performance and related criteria such as field length, second-segment climb with one engine inoperative (OEI) and the cruise altitude power available. The majority of the larger airplanes were 4-engined, whereas the APET studies were directed towards short-to-medium haul twin engined aircraft.

Large, twin turboprop aircraft which have been produced for the commercial or military market are listed in Table 2-1. In the Western World, the "Transall" with a takeoff gross weight (TOGW) of over 112,000 pounds is the heavy weight leader with engines of over 6,000 shaft horsepower (SHP) each.

Table 2-1. Twin-Engined Turboprop Airplanes.

Model	Design Role	TOGW-LB	SHP Required	Comments
(GE) APET	150-Pax/1000 n.mi	130,000	2 x 10,000 2 x 14,000	M = 0.7 cruise M = 0.8
Consortium Transall	Military Transport	112,435	2 x 6,100	M = 0.5 to 0.6
Breguet Atlantique	ASW	98,105	2 x 6,100	M = 0.5 to 0.6
Lockheed L-400	100 PAX	84,000	2 x 4,662	Lockheed proposed twin of basic Hercules
Aeritalia G.222	Military Transport	58,400	2 x 3,400	M = 0.5
Convair 580	48 PAX	57,000	2 x 3,025	M = 0.4 to 0.45
Antonov AN-26	Military Transport	53,000	2 x 2,820	Also commercial versions
Fokker F27	40-50 PAX	45,000	2 x 2,230	M = 0.4 to 0.45

Aircraft maximum range/payload design point has a definite impact on airplane size and weight, and installed propulsion thrust requirements. General Electric has recently completed an economic survey of 70 major airlines worldwide, with particular emphasis on the route structures and equipment being used for stage lengths equal to and below 1000 miles. As a result, the APET baseline airplane was defined for a 1000 nautical miles maximum payload/range point for this study.

The significance of the material being reported lies mainly in the consistency of the direct comparisons between turbofan and turboprop commercial aircraft designed with identical ground rules. Also noteworthy are the contributions offered by modern gearbox and PCM technology, nacelle concepts and their aerodynamic characteristics, cycle considerations for advanced turboshaft engines, propfan selection criteria, acoustic and emission estimates.

The scope of Tasks VII and VIII in this study demanded more detailed engineering judgement. Task VII refined a gearbox from the earlier Tasks to the level of a Preliminary Design where design loads, gear and bearing details, housing design criteria and installation integration were all taken by design layouts to the stage where accurate weights and costs could be generated. Also equally important were the exercises involving maintainability and reliability and the impacts thereon of various options in modularity. Task VIII is much more radical and introduces the possibility that the propfan PCM could well be an autonomous electromechanical system under the control of a frequency modulated digital signal having its origin in the propulsion FADEC and its terminal in an electronic control module rotating, with the propfan, at the forward end of the propfan structural hub.

Finally, it is believed that the recommendations and the technology development plans that are being proposed will provide NASA with a well constructed roadmap for high horsepower, high cruise speed, turboprop propulsion systems.

SECTION 3.0
PROGRAM OVERVIEW

<u>Section</u>		<u>Page</u>
3.1	Study Procedures and Assumptions	15
3.2	The APET Airplanes	21
3.3	Reference Turbofan Engine	37
3.4	APET Turboshaft Engines	41
3.5	Performance Comparisons	51
3.6	Gearboxes	55
3.7	Nacelles and Nacelle Technology	61
3.8	Mission Analyses and Results	69

PRECEDING PAGE BLANK NOT FILMED

SECTION 3.1
STUDY PROCEDURES AND ASSUMPTIONS

<u>Section</u>		<u>Page</u>
3.1.1	Fuel Price Forecast	15
3.1.2	Direct Operating Cost Method	15
3.1.3	Environmental Constraints	15

TABLES

<u>Table</u>		<u>Page</u>
3.1-1	APET DOC Assumptions.	16

3.0 PROGRAM OVERVIEW

3.1 STUDY PROCEDURES AND ASSUMPTIONS

The APET contract called for the submission of a document that, subject to the NASA Program Manager's approval, defined all the ground rules and methods that were to be used throughout the technical efforts that are reported here. This document covered the following major topics.

3.1.1 Fuel Price Forecast

As is discussed later in Section 4.1.3, fuel prices forecast for the mid-1990's time period are based on projections from a number of sources that included Government Agencies, Oil Industry Analysts, and economic forecasts that are generated internally by the General Electric Company. NASA/GE agreed that the fuel price to be used in the economics assessments would be fixed at \$1.50 per gallon, plus or minus 50¢.

3.1.2 Direct Operating Cost (DOC) Method

Three DOC methods were analyzed. They were (1) NASA method contained in Reference 30, (2) the Eurac Method contained in Reference 31 - Common DOC Method for Short/Medium Range Aircraft, and (3) the ATA Method updated by Boeing in their presentation Reference 32. All three methods gave very similar results and with NASA's agreement, General Electric selected Method Number 3. Table 3.1-1 shows the assumptions made for the DOC calculations reported in this study.

3.1.3 Environmental Constraints

Both emission and acoustic regulations now in force and those expected by the mid-1990 time period, were required items in the study. Emissions are regulated by the "Current Standards - Newly Certified Large Engines" published in the Federal Register dated July 17, 1973. Hydrocarbon (HC), nitrous oxides (NOX), carbon monoxide (CO) and smoke number are specified for both turbofan and turboshaft engines. Further specifications cover Time-in-Mode at Percent Rated Power for the purposes of regulating the time (in minutes) that are to be used for analytical predictions. These current regulations are likely to

Table 3.1-1. APET DOC Assumptions.

Methods Used	Basically ATA Method as modified by Boeing (1979) with minor changes
Cost Basis Aircraft	- All Costs in 1981 Dollars - "Rubberized," Scalable in Size
Economic Conditions	1981 (Except for Fuel - See below)
Spares - Airframe - Engine - Nacelle	6% of Airframe Price 30% of Engine Price 6% of Nacelle Price
Depreciation	15 Years to 10% Residual Value (on Total Investment)
Annual Utilization	Boeing 1979 Method, with minor changes
Block Distance	300 N Mi
Insurance	0.5% per Year (on Fly-Away Price)
Fuel Price	\$1.50 ± \$.50 per US Gallon (Valid from 1992 and Afterwards)
Maintenance - Engine - Airframe	GE Preliminary Design In-house Method Boeing 1979 Method with Labor Rate \$14.19/Manhour
Crew Costs	Boeing 1979 Method (Updated to 1981 Dollars)

be updated by a Notice of Proposed Rule Making (NPRM) dated March 24, 1978 which revise the gaseous standards, including Smoke Number, and converts the regulations into S.I. units.

For the acoustic regulations, it was proposed that the current FAR 36 (Stage 3) rules which apply to turbofan airplanes should be expanded to include turbopropfan-powered airplanes. For the mid-1990's changes in the current regulations could occur as a result of efforts being undertaken by Working Groups C and D of the ICAO and by the SAE Committee A-21. However, no judgment was made that the Stage 3 rules should be amended to more stringent levels for the farfield noise takeoff and approach specifications. It was noted that no regulations are in existence for cabin interior noise, and that passenger acceptance levels are the subject of individual airlines negotiations with the aircraft manufacturers as part of the airplane specification they are offered. In order to make the necessary trade of airframe weight deltas due to the acoustic treatment required to attenuate propfan nearfield noise, it was decided that an interior level in the 82-84 dBA band would be used.

SECTION 3.2

THE APET AIRPLANES

<u>Section</u>		<u>Page</u>
3.2.1	Configuration and Size Selection	21

FIGURES

<u>Figure</u>		<u>Page</u>
3.2-1.	APET Flight Profile (With Reserves).	23
3.2-2.	APET Leg Definition.	24
3.2-3.	APET Study Airplane/Engine Sizing Guidelines.	25
3.2-4.	70 Airline-Worldwide Survey of Route Structure.	26
3.2-5.	70 Airline-Worldwide Survey of Route Structure.	26
3.2-6.	70 Airline-Worldwide Survey of Route Structure.	26
3.2-7.	70 Airline-Worldwide Survey of Route Structure.	26
3.2-8.	Short Range Aircraft-Stage Length Utilization.	27
3.2-9.	APET Baseline Turbofan Aircraft Configuration-150 PAX - Mach Cruise 0.8 Design.	29
3.2-10.	APET Baseline Propfan Airplane Configuration -150 PAX - Mach Cruise 0.8 Design.	30
3.2-11.	APET Baseline Propfan Airplane Configuration - 150 PAX - Mach Cruise 0.7 Design.	31
3.2-12.	APET Wing Planform Families.	32
3.2-13.	APET Aircraft-Propfans - Mach 0.8 Design.	32
3.2-14.	APET Aircraft Fuel Efficiency.	31

TABLES

<u>Table</u>		<u>Page</u>
3.2-1.	APET Aircraft Abbreviated Specification.	22
3.2-2.	APET Aircraft Sizing Results.	33
3.2-3.	Aircraft Component Weight Estimation.	34

3.2 THE APET AIRPLANES

Six APET airplanes were designed for this study; three were turbofan engine powered and three were turbopropfan engine powered. Each of the propulsion types was exercised on three point design airplanes which had cruise design values of Mach 0.70, Mach 0.75, and Mach 0.80. All the airplanes had the same constraints, i.e., they were all designed to achieve the maximum payload range point of 150 passengers at 1000 nautical miles while observing identical rules for field length, altitude cruise capability, engine inoperative cruise altitude, maximum approach speed, wing aspect ratio, alternate field length, and reserve fuel allowance. The abbreviated specification for these airplanes is shown in Table 3.2-1. The flight profile selected is shown in Figure 3.2-1, and the mission leg details are defined in Figure 3.2-2.

3.2.1 Configuration and Size Selection

As discussed above, there are two varieties of APET airplanes:

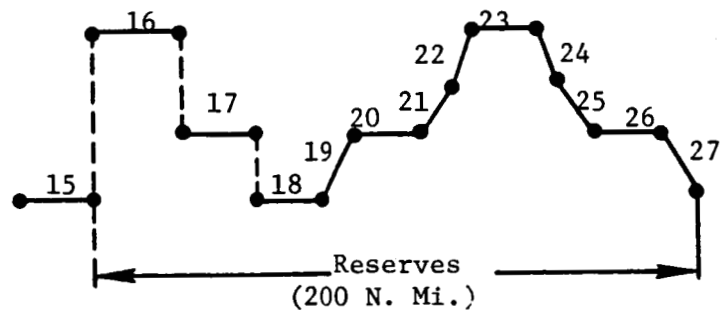
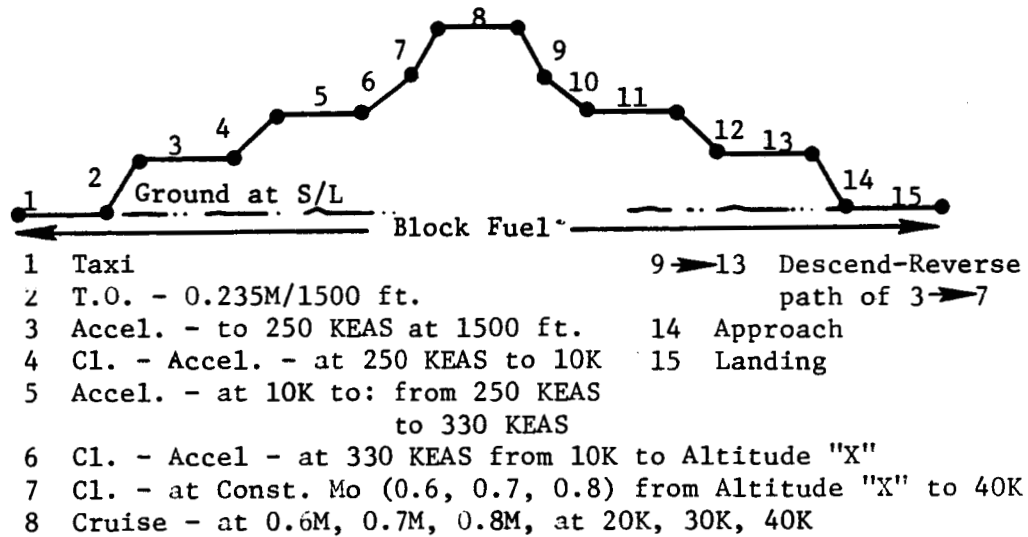
1. A turbofan powered airplane with 7.5 bypass ratio engines installed in Long Duct Mixed Flow (LDMF) nacelles.
2. A turboprop-powered airplane powered by Hamilton Standard 10-bladed propfans driven by high pressure ratio turboshaft engines.

Each variety was exercised over three cruise Mach numbers, namely $M = 0.70, 0.75, \text{ and } 0.80$.

From a number of sources, including a General Electric survey of worldwide operations by 70 domestic and foreign airlines, it is apparent that a 150 passenger airplane design with range limited to 1000 nautical miles with full payload (150 PAX plus 5000 lb cargo) would have a large potential market. This size also challenges the technology of engines, propfans and gearboxes as the shaft powers required are more than twice the levels demonstrated by production propulsion systems of western origin. A summary of the factors that were considered in the selection of the size and performance characteristics of the APET airplane/propulsion systems is shown in Figure 3.2-3, while Figures 3.2-4 through -7 are included to show the results of the 70 airline survey referred to earlier. Figure 3.2-8 illustrates the very high proportion of domestic flights that are scheduled for 1000 statute miles (or less).

Table 3.2-1. APET Aircraft Abbreviated Specification.

Aircraft Technology/Timing	-	Service Introduction after 1990
Maximum Number of Passengers	-	150
Passenger Arrangement	-	All Tourist Class, Six-Abreast, 32" Pitch
Design Range Capability (Full Payload including 5000 lb Cargo)	-	1000 N Mi
Average Stage Length	-	300 N Mi
Field Length (Sea Level)	-	6000 Ft (Sea Level) at Max TOGW
Alternate Field Length	-	Denver (Hot Day); Weight for Trip to S. Fran. (100% LF)
Engine-Out Ceiling	-	15,000 Ft
Design Cruise Mach Number	-	Varies: 0.7 to 0.8
Required Cruise Altitude Capability	-	35,000 Ft-Design Range Mission.
Maximum Approach Speed (Knots)	-	135 Kts. (At MLW = 0.975 x Max. TOGW)
Number of Engines	-	2
Engine Location	-	On Wing
Propulsion Types	-	Turbofan and Turboprop (Propfan)
Cruise Speed/Altitude	-	Will Vary with Design Mach and Stage Length
Takeoff Gross Weight (TOGW)	-	Variable
Wing Design	-	Sweep and Thickness Varies with Design Mach
Wing Aspect Ratio	-	11 (For all Values of Design Mach No.)
Measures of Merit	-	Maximum TOGW
	-	Fuel Burn at 300 N Mi Stage Length
	-	DOC at 300 N Mi Stage Length



- 16 Loiter - 45 Min. at Cr Conditions (as for 8)
- 17 Loiter - 30 Min. at 0.35M/15K
- 18 → 22 Cl. Same Conds. As 2 → 7
- 23 Cr. - 0.55M at 25K

24 → 27 Descend, Same path as 9 → 13

KEAS = Equivalent Airspeed in Knots

Figure 3.2-1. APET Flight Profile (With Reserves).

Leg	Definition
1	Taxi-out, 9 minutes at ground idle thrust (6% of FN _{GLS} Max for E ³)
2	Takeoff - to 0.235 Mach/1500 feet; 1.25 minutes at FN _{GL} Max (0.2 Mach)
3	Accel - at 1500 feet to 250 KEAS
4	Climb-Accel - at 250 KEAS to 10,000 feet
5	Accel - at 10,000 feet to climb speed (250 to 330 KEAS)
6	Climb-Accel - at climb speed (250 to 330 KEAS) to "X" altitude
7	Climb - at constant Mach (Mach = 0.6 to 0.8; Alt - "X" to 40,000 feet
8	Cruise - Mach = 0.6 to 0.8; Alt = 25,000 to 40,000 feet
9	Descend - Const. Mach to "X" altitude
10	Descend-Decel - at 280 KEAS to 10,000 feet
11	Decel - at 10,000 feet 250 KEAS
12	Descend-Decel - at 250 KEAS to 1500 feet
13	Decel - at 1500 feet to 0.235 Mach/1500 feet
14	Approach/Landing - 2 minutes at FN _{GL} Max (0.2 Mach) to get fuel burn; 6 minutes block time
15	Taxi-in - 5 minutes at ground idle
1-15	Gives block fuel and time
16	Loiter - 45 minutes at cruise conditions
17	Loiter - 30 minutes at 0.35 Mach/15,000 feet
18-22	Climb-Accel - Same as main mission (250 KEAS first climb part, 280 KEAS second climb part)
23	Cruise - 0.55 Mach/25,000 feet
24-27	Descend-Decel - 280 KEAS and 250 KEAS first and second parts of descent, respectively
16-27	Gives reserves - 200 N. Mi. Total Dist.

Figure 3.2-2. APET Mission Leg Definition.

ASM = Available Seat Miles

PAX = Number of Passengers

- Engine should be at a size that allows credible up or down scaling. (8000 - 16000 SHP range).
- Aircraft range capability to be consistent with expected future aircraft usage in 1990's.
- Should challenge current technology for improvements in:
 - Shaft engines
 - Gearboxes
 - Propellers
 - Airframe weight
- Aircraft size to be tailored for short/short-medium haul: Best ASM/Gallon and DOC is the goal.
- Aircraft design range will be limited so as not to penalize economics by "overdesign".
- 150 and 100 PAX sizes have been considered. Selected 150 PAX size appears to meet all the objectives above.

Figure 3.2-3. APET Study Airplane/Engine Sizing Guidelines.

THE TOTAL ASM PIE DIVISION
70 AIRLINE SURVEY WORLDWIDE

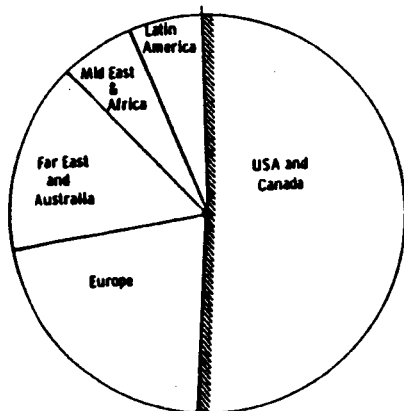


Figure 3.2-4

- 898.6 Billion (Total Pie)
- 4600+ Pax Aircraft
- 194 Freight Aircraft (not incl. Combi's)

THE ASM PIE DIVISION
WORLDWIDE

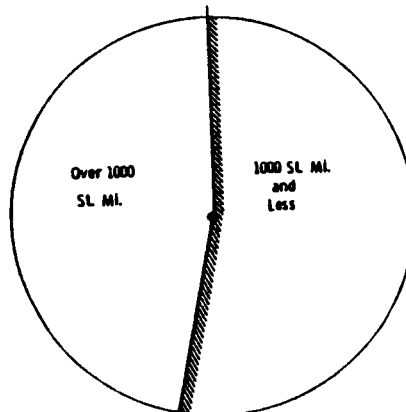


Figure 3.2-5

70 Airline Survey
Total ASM 898620.8 Million
"Short" ASM 478926.0 Million

THE SHORThAUL < 1000 ST MI OR LESS
PIE DIVISION, WORLDWIDE

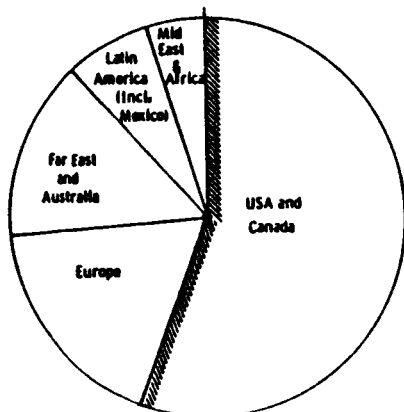


Figure 3.2-6

- 478.9 Billion Pie

SHORThAUL
WORLDWIDE ASM DIVISION
70 AIRLINE SURVEY
Turboprops DC-9-80
Short jets B720

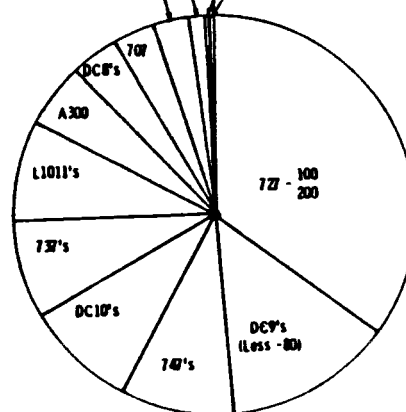


Figure 3.2-7

- Trunk & Regional Carriers
 - Flights - To or Less Than 1000 ST Mi
- Annual ASM 478.9 Billion

Figure 3.2-4 thru 7. 70 Airline - Worldwide Survey of Route Structure.

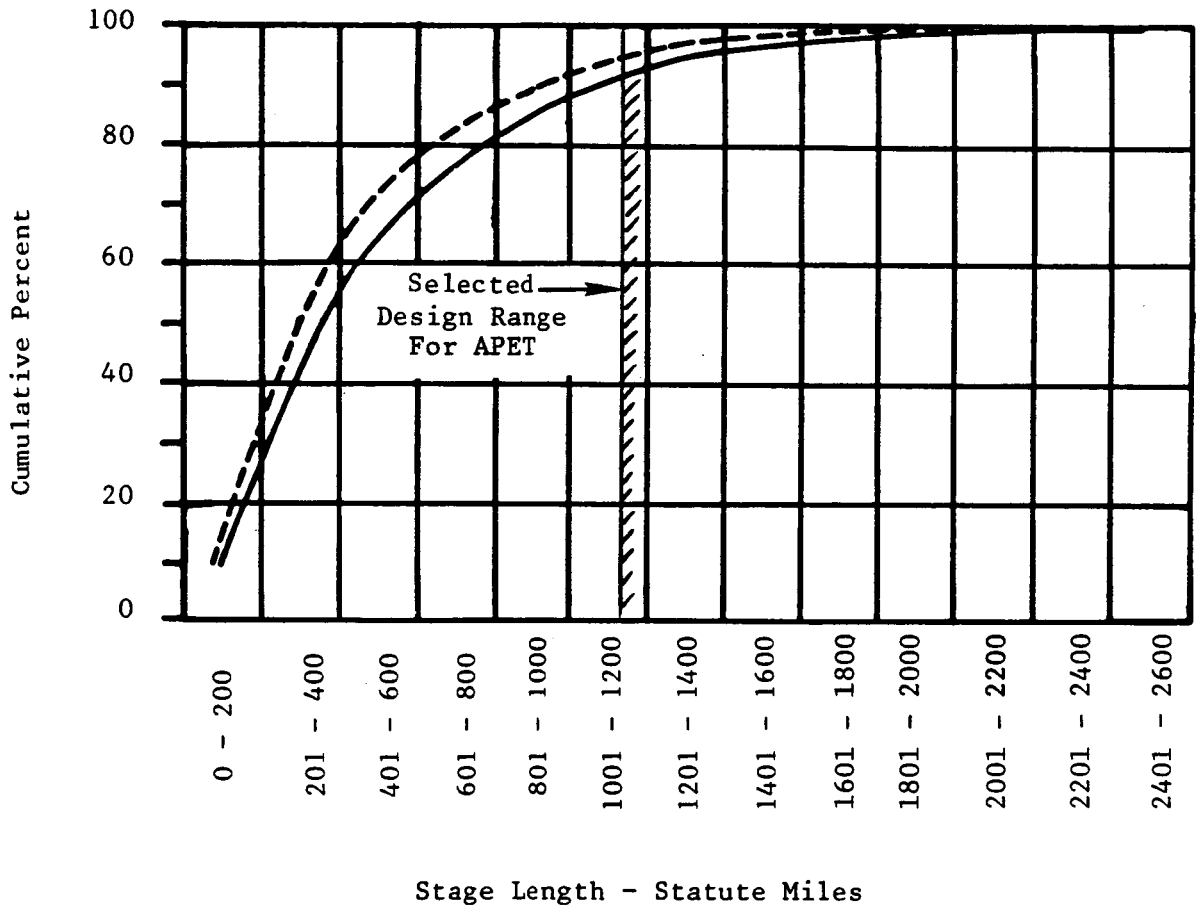
SHORT RANGE AIRCRAFT - STAGE LENGTH UTILIZATION

North American Operations

BAC-111/DC9/737/727

----- 1978 O. A. G. *

———— 1980 O. A. G.



* OAG = Official Airline Guide

Figure 3.2-8. Short Range Aircraft - Stage Length Utilization.

Together, these figures given clear substantiation to the importance of the short-haul market, both internationally and domestically, and support the selection of a 1000 N. Mi. maximum range/payload requirement as being reasonable. Also, it can be noted from Figure 3.2-8, the fifty percentile value of flights crosses the 300-400 statute mile stage length curve and serves to support the selection of a median value of 300 N. Mi. as representing a reasonable value which to use for the figures of merit in ensuing economic evaluations.

The airplanes designed for this study are shown in Figures 3.2-9, 3.2-10, and 3.2-11 while Figure 3.2-12 illustrates the family of wings that were evaluated. An aspect ratio (AR) of 11 was chosen for all of the airplanes as it is predicted that the use of advanced metallic alloys and composite materials could well achieve this level of AR by the mid-1990's. In fact, this value might well be judged to be conservative - especially for cruise Mach numbers near 0.70. The range/payload curve for one of the study airplanes - in this case the $M = 0.80$ turboprop-powered airplane - is shown here as Figure 3.2-13. This figure has some noteworthy points. The figure of Merit range/payload point was selected at 65% load factor (LF) at 300 nautical miles range. The seventy airline survey already alluded to showed that this selection of stage length could account for some 50% of the likely usage pattern for the projected APET airplane. Also seen on the figure is that although the airplane is design limited to 1000 nautical miles (with full payload) it becomes very flexible with anything less than 100% LF. This effect, shown by the flatness of the curve between the identified points (3) and (5) on the figure is due to the fuel efficiency of the airplane/propulsion system combination.

As will be discussed in more detail in Section 4.2, wing and thrust sizing for APET airplanes was undertaken using well known parameters. In this section, which is devoted to an overview of the study results, Table 3.2-2 is included to summarize the wing and thrust sizing values that were used for the flight analyses. The results, in terms of the often used measure of flight efficiency - Available Seat Miles per Gallon (ASM/GAL) - are shown on Figure 3.2-14. Here, all six APET airplanes are portrayed versus the current designs of airplanes employing high bypass-ratio turbofan engines. It may be seen that the APET Mach 0.75 turboprop has about twice the fuel efficiency of any existing airplane at a range of 500 nautical miles.

SPECIFICATIONS

MAX TOGW - 111,970 LBS
 MAX LANDING WGT - 106,170 LBS
 ZERO FUEL WGT - 100,770 LBS
 OP. WGT EMPTY - 94,300 LBS
 MAX FUEL CAPACITY - 4140 US GAL
 WING AREA - 928 FT² AR - 11.0

TAIL AREA:
 VERTICAL - 131 FT²
 HORIZONTAL - 134 FT²

PASSENGER ACCOMMODATIONS:
 160 - ALL TOURIST - 32 IN PITCH
 DESIGN MACH NUMBER - 0.8 /
 ENGINES - 2 - 17,410 LBS F₄ (SLLB)

ORIGINAL FACED
 OF POOR QUALITY

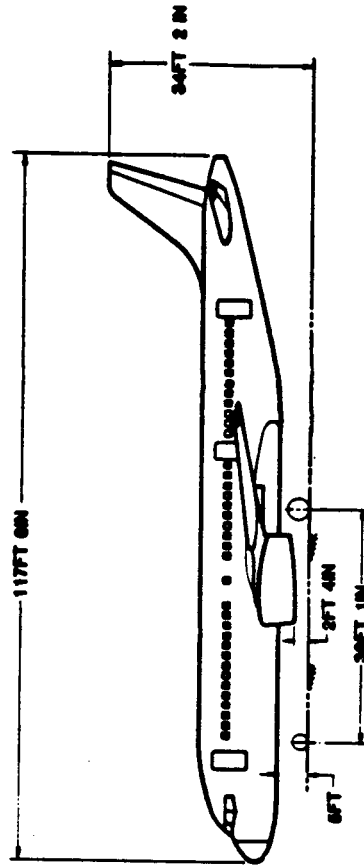
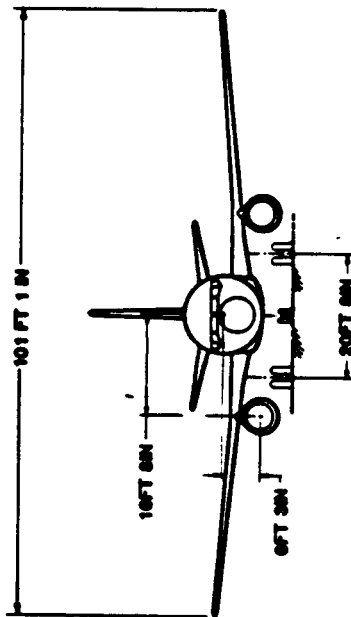
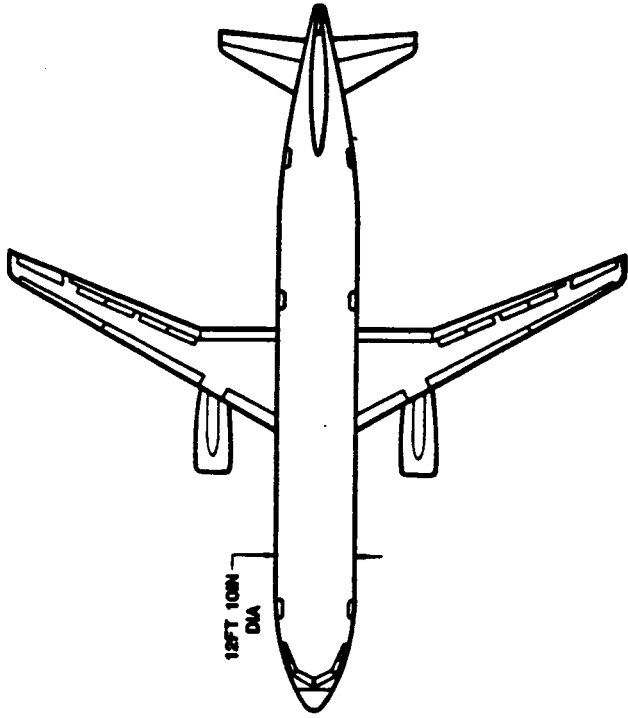
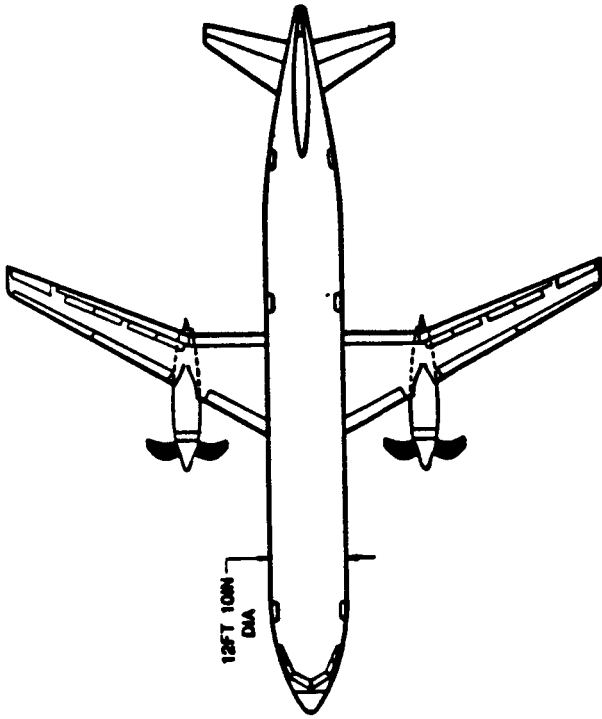


Figure 3.2-9. APET Baseline Turbofan Aircraft Configuration - 150 Pax Mach Cr. 0.80 Design.

ORIGINAL PAGE IS
OF POOR QUALITY



SPECIFICATIONS	
MAX TOGW	- 110,000 LBS
MAX LANDING WGT	- 100,210 LBS
ZERO FUEL WGT	90,000 LBS
OP. WGT EMPTY	64,400 LBS
MAX FUEL CAPACITY	3820 US GAL
WING AREA	- 878 FT ² AR - 11.0
TAIL AREAS :	
VERTICAL	- 182 FT ²
HORIZONTAL	- 123 FT ²
PASSENGER ACCOMMODATIONS :	
180 - ALL TOURIST	- 32 IN PITCH
DESIGN MACH NUMBER	- 0.8
ENGINES	- 2 - 11,300 SHP EA (S.L.S.)
PROPELLERS	13 FT 0.5 IN DIA EA

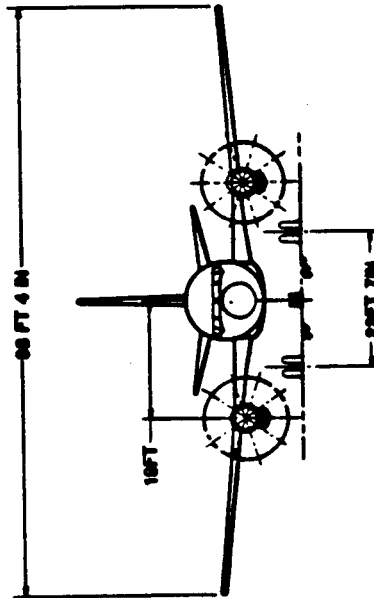
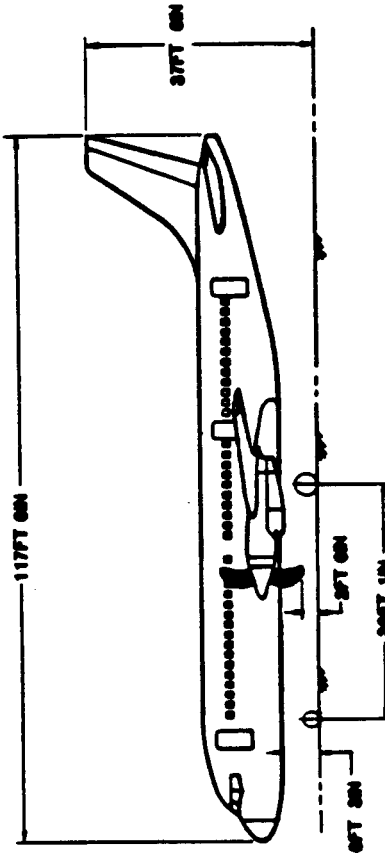
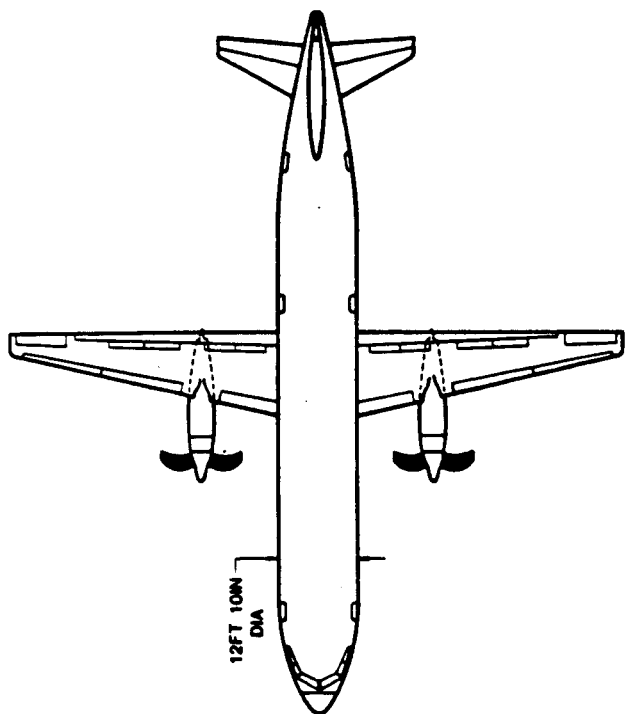


Figure 3.2-10. AEPT Baseline Propfan Airplane Configuration - 150 Pax Mach Cr. 0.80 Design.

ORIGINAL PAGES
OF POOR QUALITY



SPECIFICATIONS	
MAX TOGW	- 107,310 LBS
MAX LANDING WGT	- 104,630 LBS
ZERO FUEL WGT	94,680 LBS
OP. WGT EMPTY	63,100 LBS
MAX FUEL CAPACITY	3630 US GAL
WING AREA	- 632 FT ²
AR	- 11.0
TAIL AREAS :	
VERTICAL	- 164 FT ²
HORIZONTAL	- 134 FT ²
PASSENGER ACCOMMODATIONS :	
180	- ALL TOURIST - 32 IN PITCH
DESIGN MACH NUMBER - 0.7	
ENGINES - 2 - 10,720 SHP EA (S.L.S.)	
PROPELLERS 12 FT 2 IN DIA EA	

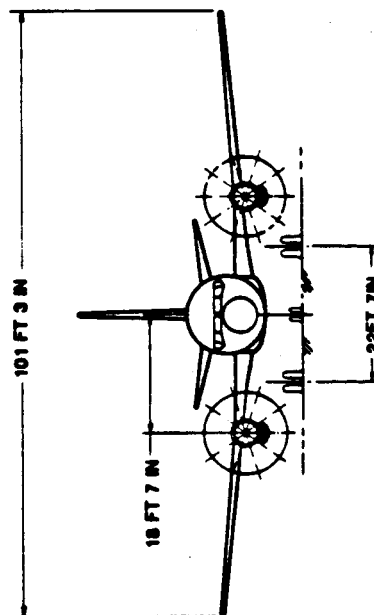
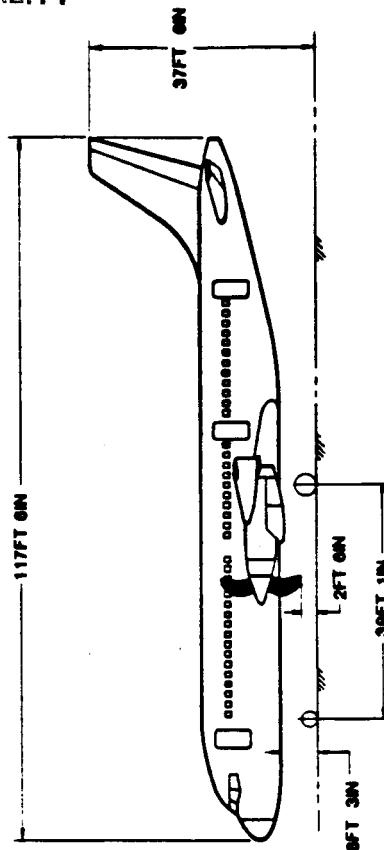


Figure 3.2-11. AEPT Baseline Propfan Airplane Configuration - 150
Pax Mach Cr. 0.70 Design.

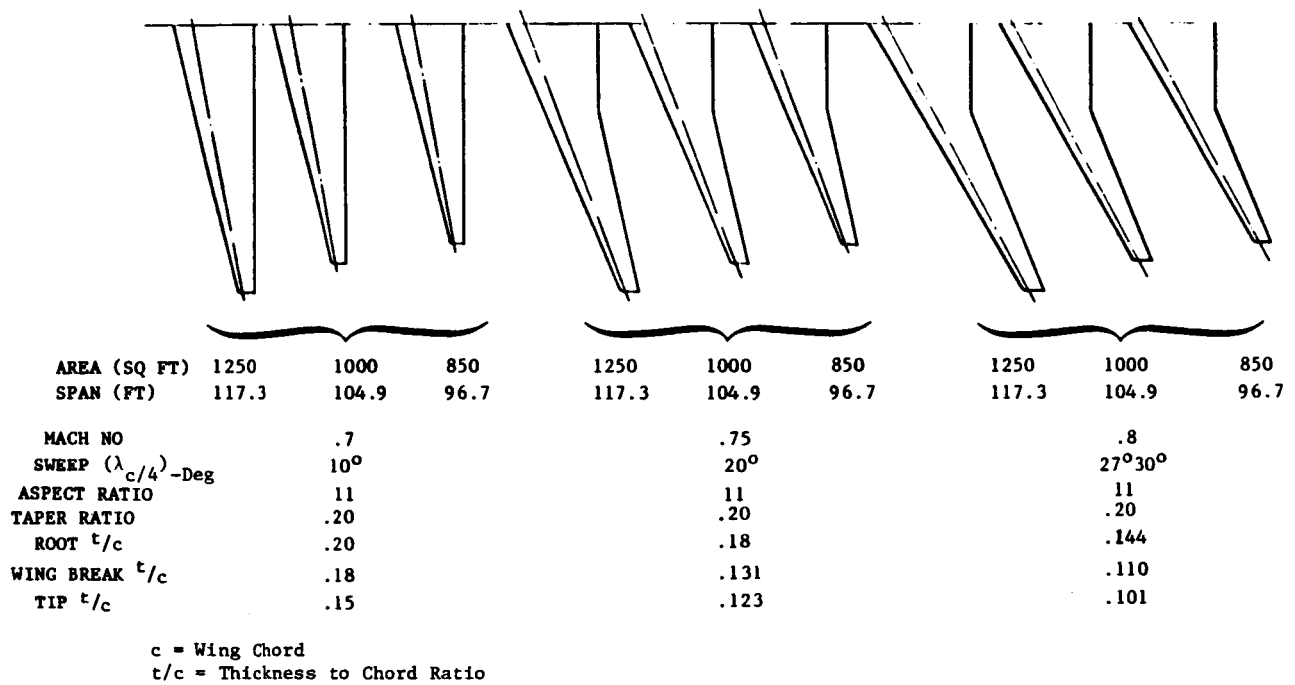


Figure 3.2-12. APET Wing Planform Families.

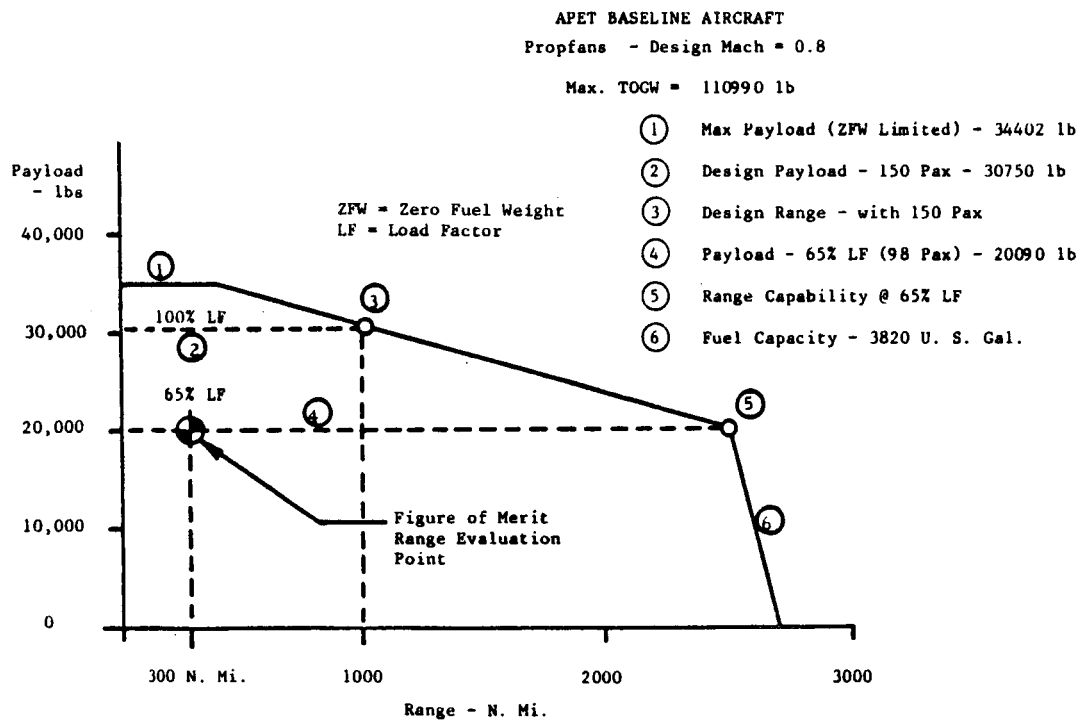


Figure 3.2-13. APET Baseline Aircraft Propfans - Design Mach = 0.8.

ORIGINAL PAGE IS
OF POOR QUALITY

Table 3.2-2. APET Aircraft Sizing Results.

Powerplant Type	Propfan			Turbofan		
	0.7	0.75	0.8	0.7	0.75	0.8
Design Mach No.	0.7	0.75	0.8	0.7	0.75	0.8
Selected (W_0/S_W)	115.2	120.5	126.2	115.2	120.5	120.6
Selected $\Sigma F_n/W_0$ @ .02M/SL	0.261	0.264	0.268	0.235	0.240	0.249
Wing Sized By:	Buffet	Buffet	Fuel Cap.	Buffet	Buffet	Fuel Cap.
Engine Sized By:	Denver TO					
Resulting TOGW	107309	108845	110986	108036	109305	111970

W_0 = Takeoff Gross Weight
 S_W = Wing Area
 F_n = Net Thrust

APET AIRCRAFT FUEL EFFICIENCY

1000 NMI Design Range

65% Load Factor

TP = Turboprop
TF = Turbofan

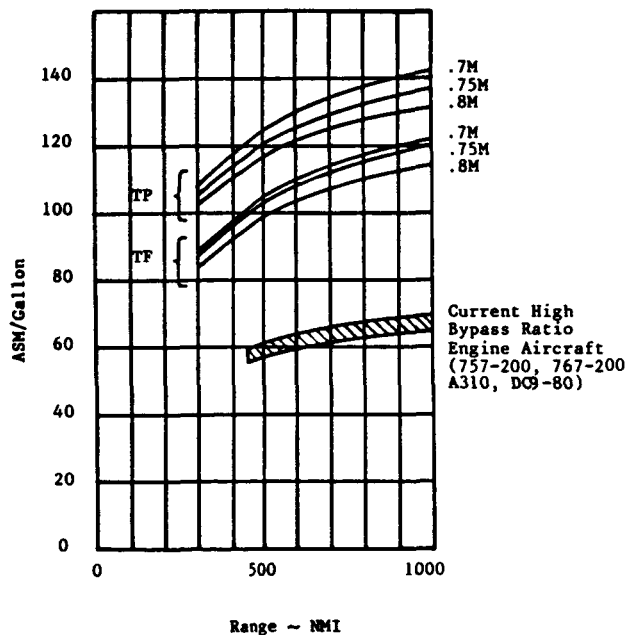


Figure 3.2-14. APET Aircraft Fuel Efficiency 1000 NMI Design Range 65% Load Factor.

Estimates for airplane weights used a projection of a 1972 weight scenario for the airframe (including avionics but less the propulsion system). This scenario is from a data base contained in the Reference 33 modified by General Electric, where necessary, to fit the APET airplane definition. From this data base the "1990's weight" is estimated by applying weight reduction factors to the principal weight components of the airplane structure and systems. These factors are shown on Table 3.2-3.

Table 3.2-3. Aircraft Component Weight Estimation.

Component/System	Reference Weight ⁽¹⁾	Weight Reduction Factors, (Est.) ⁽²⁾
Wing - Bending Structure Wing - Shear and Other Str. Tail Fuselage Landing Gear Fuel System Flight Controls - Hydraulics Electrical Pneumatics and Air Cond. Anti-Icing Instruments Avionics Furnishings OWE Items	Base ↓	0.9 0.8 0.85 0.90 0.9 1.0 0.8(3) 1.0(3) 0.8(3) 1.2(3) 1.0 0.75 0.9 1.00
<p>(1) "1972 Technology"</p> <ul style="list-style-type: none"> - Represents Technology of 727/737/DC9, etc. - Data base from S.A.I./Douglas Report (Ref 33) (NASA CR-151970) - S.A.I./Douglas Formulas - Modified by G.E. <p>(2) "1995 Technology"</p> <ul style="list-style-type: none"> - Represents APET Technology - Estimated using S.A.I./Douglas data base with Weight Reduction Factors - 2% Weight Contingency added - Austere passenger furnishings and accommodations (because aircraft is used on short stage lengths). <p>(3) All Electric Airplane</p>		

SECTION 3.3

REFERENCE TURBOFAN ENGINE

<u>Section</u>		<u>Page</u>
3.3.1	Definition	37
3.3.2	Cycle Selection	37
3.3.3	Engine Weight and Dimensions	37

FIGURES

<u>Figure</u>		<u>Page</u>
3.3-1.	APET Baseline Turbofan Engine Changes From FPS Standard E ³ .	38

3.3 REFERENCE TURBOFAN ENGINE

3.3.1 Definition

A scaled down version of the E³ Flight Propulsion System (FPS) was designed for this study. Similar to the full-scale engine, the scaled version employs a single-stage fan and a single stage booster with continuous bleed. Due to an increase in bypass ratio of the scaled-down engine (from ≈ 6.8 for the FPS to ≈ 7.5 for the APET turbofan) the number of LP turbine stages was increased from five to six. The HP compressor, a 10-stage unit, is retained as is a 2-stage HP turbine. The combustor has been redesigned from a double dome configuration to a single dome, low smoke, low emissions configuration. The engine is installed in a Long Duct Mixed Flow (LDMF) nacelle where a common fan and core nozzle is used in conjunction with a high efficiency convoluted mixer. The engine and nacelle cross section is shown on Figure 3.3-1, which also identifies the differences included relative to the full-scale E³ propulsion system.

3.3.2 Cycle Selection

To achieve a 4000 pound thrust level at maximum climb thrust level and Mach = 0.80 flight speed at 35 thousand feet on a standard day plus 18° F, a sea level static thrust engine of approximately 17,600 pounds results from the engine defined above. A fan corrected airflow of about 730 pounds per second and a corrected core flow near 57 pounds per second are required to make the thrust at a cycle set-up temperature level of 2258° F at the maximum climb altitude point. A contingency maximum climb temperature of 2490° F is required in this engine for Denver hot-day performance.

3.3.3 Engine Weight and Dimensions

A basic engine weight of 3,013 pounds was estimated for the APET turbofan uninstalled. Installed with a mixer, reverser, inlet and other installation items it weighed 4,453 pounds. A further allowance of 445 pounds should be added for the wing pylon to obtain a fully installed weight of 4,898 pounds.

The fan selected had a diameter of 59.6 inches and the engine length from the fan rotor leading edge to the aft flange of the engine rear frame was calculated to be 90 inches.

ORIGINAL PAGE IS
OF POOR QUALITY.

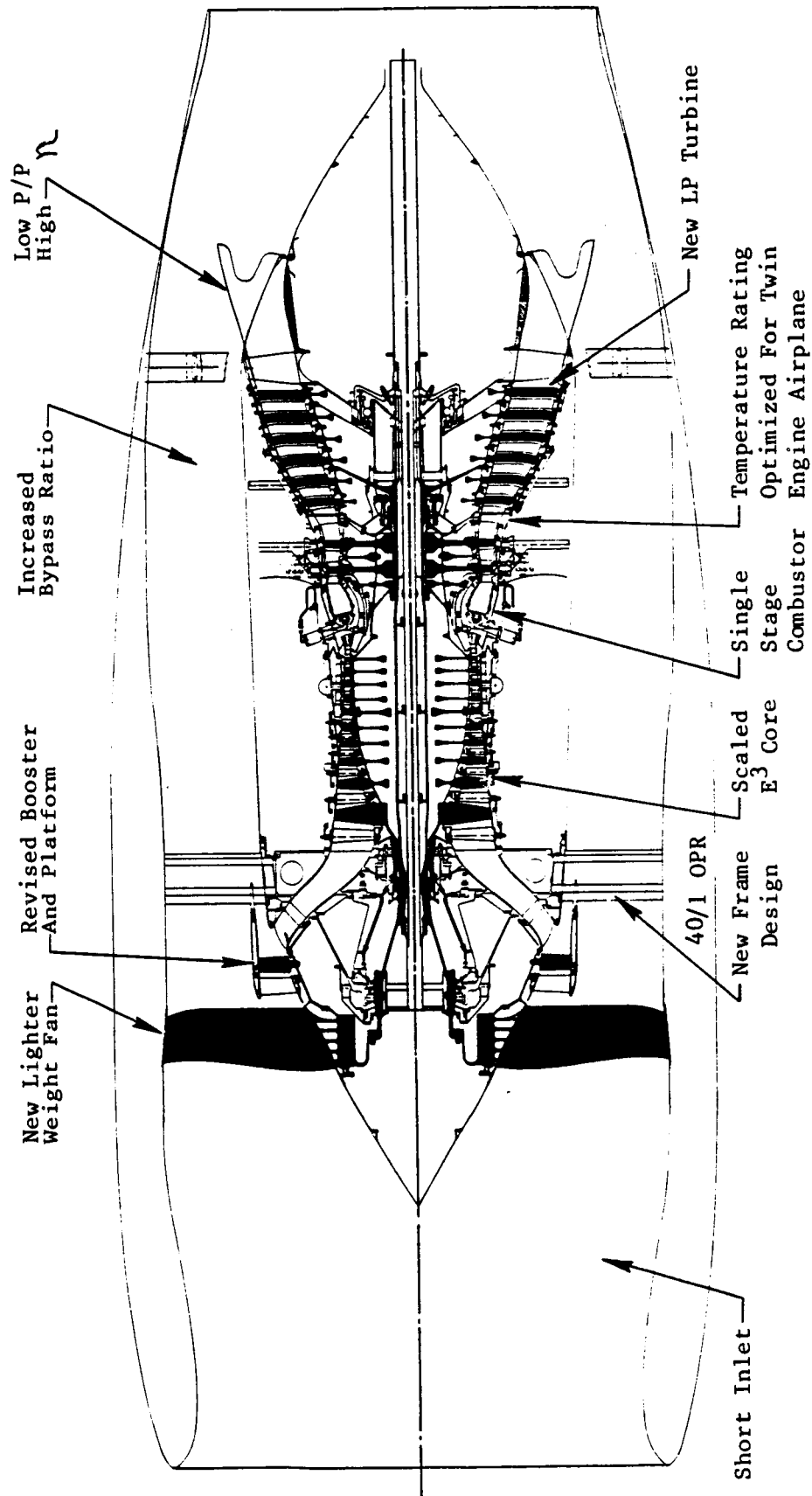


Figure 3.3-1. APET Baseline Turbofan Engine Changes from FPS Standard E₃.

SECTION 3.4

APET TURBOSHAFT ENGINES

<u>Section</u>		<u>Page</u>
3.4.1	Candidate Engines	41
3.4.2	Cycle Assumptions	41
3.4.3	Propfan Variables	41

FIGURES

<u>Figure</u>		<u>Page</u>
3.4-1.	APET Turboprop Gas Generator - Axial Flow Compressor.	42
3.4-2.	APET Turboprop Gas Generator - Axi-Centrifugal Compressor.	43
3.4-3.	Turboprop Configuration Studies.	46
3.4-4.	APET Installed Climb Path Comparison (Thrust in lbs).	48
3.4-5.	APET Installed Climb Path Comparison (Thrust lbs vs. SHP).	48

TABLES

<u>Table</u>		<u>Page</u>
3.4-1.	Candidate Turboshift Engines.	42
3.4-2.	APET Turboprop Configuration Studies - Cycle Assumption Comparisons.	44
3.4-3.	APET Turboprop Configuration Studies - Component Aerodynamic Comparisons.	45

3.4 APET TURBOSHAFT ENGINES

3.4.1 Candidate Engines

Six candidate engines were defined for this study. They are shown in tabular form on Table 3.4-1. From these candidates NASA/GE selected engines defined as 2(b) and 3(b) for more detailed design and analysis.

Engines 2(b) and 3(b) have very similar performance and weight. They are depicted on Figures 3.4-1 and 3.4-2, respectively.

Both engines are 2-shaft gas generators which at the baseline size deliver 13,000 shaft horsepower to the propfan reduction gearbox. As can be noted from the figures, very similar cycle characteristics are shown despite the fact that engine 2(b) is an all-axial design while engine 3(b) employs an axi-centrifugal compressor system. Either engine could use a 3 or a 4 stage power turbine depending on the level of technology addressed in a development program.

3.4.2 Cycle Assumptions

Tables 3.4-2 and 3.4-3 are included to show the cycle comparisons and the component aerodynamic comparisons of the two selected study engines. The effects of variation in cycle pressure ratio and turbine gas temperature on the size of the APET turboshaft engine is given in Figure 3.4-3. Booster, core corrected flow sizes are portrayed as booster pressure ratio is varied; this implies an overall engine pressure ratio change as a direct function of boost pressure. Effects on HPT size, maximum take-off compressor delivery temperature (T3) as well as gearbox shaft horsepower and SFC effects are all depicted in this figure. Studies of similar cycle effects of parameter variation led to the final selection of the 1.75 boost pressure ratio and the Overall Pressure Ratio (OPR) just above 40 to one.

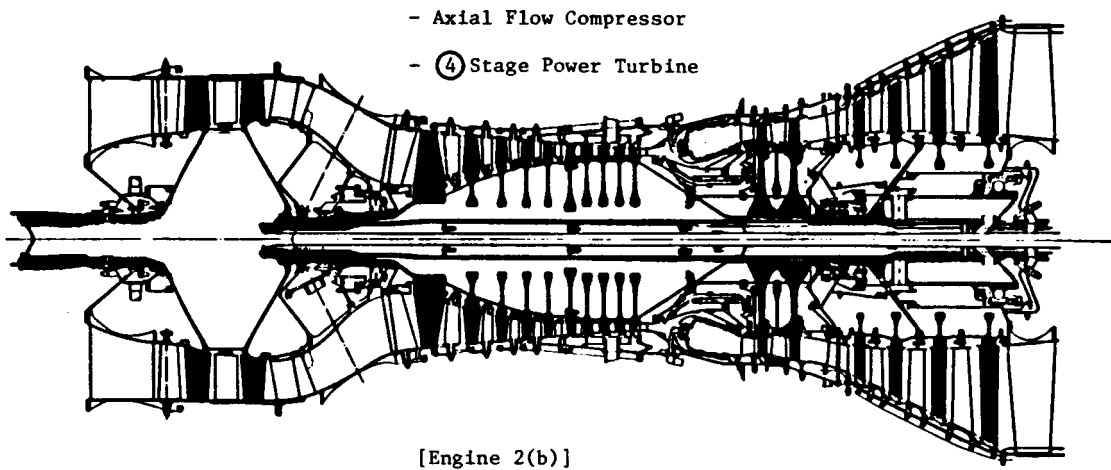
3.4.3 Propfan Variables

The selection of engine cycle parameters required prior examination of propfan variables, for the uninstalled and installed propulsion systems.

Table 3.4-1. Candidate Turboshaft Engines.

Case #	Engine Description	Low Pressure Compressor Stages	High Pressure Compressor Stages	HP Turbine Stages	LP Turbine Stages	Overall Pressure Ratio
1	Unboosted 2-Shaft	-0-	10 Axial	2	3	23:1
2(a)	Boosted 2-Shaft	1, high r/R	10 Axial	2	3	38:1
2(b)	Boosted 2-Shaft	2, low r/R	10 Axial	2	3 or 4	38:1
3(a)	Boosted 2-Shaft	1, high r/R	5 Axial 1 Centrifugal	2	3	38:1
3(b)	Boosted 2-Shaft	2, low r/R	5 Axial 1 Centrifugal	2	3 or 4	38:1
*4	Boosted	2, low r/R	10 Axial	*	*	38:1

*This engine used a single stage HP turbine, a single stage intermediate turbine, and a 3-stage LP turbine acting to drive the third shaft as a free turbine.

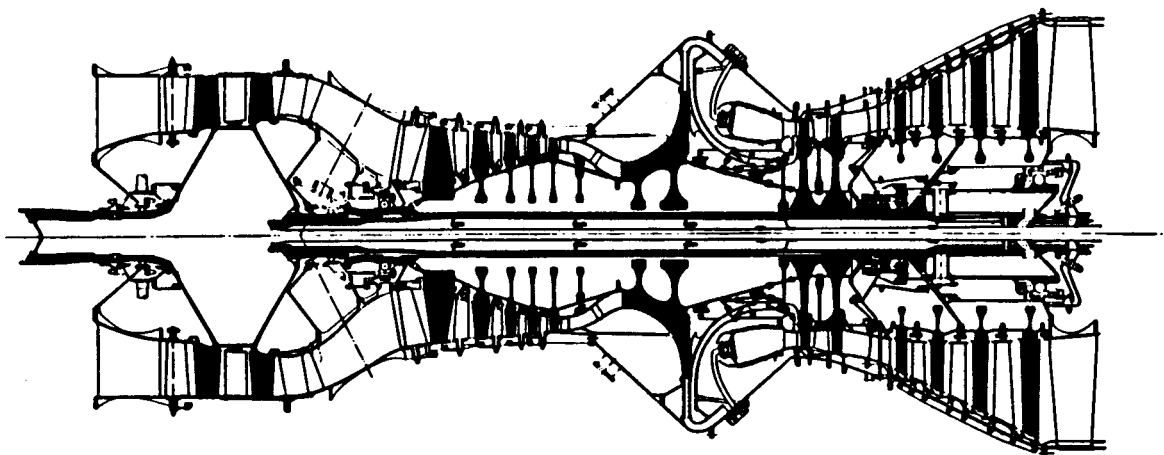


[Engine 2(b)]

<u>BOOSTER</u>	<u>CORE</u>	<u>POWER TURBINE</u>
$V_{Tip}/\sqrt{\theta} = 9.24$	Scaled E^3	$P/P = 7.6$
$r/r = .67$	$V_{Tip}/\sqrt{\theta} = 1498$	$\psi_{PAvg} = .95$
$PR = 1.75$	$PR = 23$	

Figure 3.4-1. APET Turboprop Gas Generator.

ORIGINAL PARTS
OF POOR QUALITY



<u>Booster</u>		<u>Core (PR_{OA} = 23)</u>	<u>Power Turbine</u>
$V_{Tip}/\sqrt{\theta} = 924$	Axial	- $V_{Tip}/\sqrt{\theta} = 1498$	P/P = 7.6
r/r = .67		PR = 7.12	$\psi_{P Avg} = .95$
PR = 1.75	Centrifugal	- $V_{Tip}/\sqrt{\theta} = 1407$	
		PR = 3.23	

[Engine 3(b)]

Figure 3.4-2. APET Turboprop Gas Generator Axi-Centrifugal Compressor Four-Stage Power Turbine.

Table 3.4-2. APET Turboprop Configuration Studies.

Cycle Assumption Comparisons

	All Axial	Axi Centrifugal
• <u>At M0.80/35000° + 18°</u>		
Thrust	4000	4000
PR Overall	40.2	40.2
T41 - ° F	2390	2390
$W\sqrt{\theta}/\delta$ LP	69.9	70.3
PR _{LP}	1.75	1.75
η_{LP} Poly/Adia	0.888/0.881	0.888/0.881
ΔP Gooseneck	1.5%	1.5%
$W\sqrt{\theta}/\delta$ Core	44.2	44.5
PR Core	23.0	23.0
η_C Poly/Adia	0.898/0.848	0.897/0.846
ΔP Combustor	4.95%	6.0%
$\eta_{Combustor}$	0.995	0.995
No. HPT Stages	2	2
$W\sqrt{T}/P$ HPT	6.53	6.65
η_t (Cycle)	0.914	0.915
$\Delta h/T$ LPT	0.101	0.100
P/P LPT	7.6	7.4
η_{LPT}	0.920	0.920
P8/P0	1.50	1.50
Total Cooling Air	17.0	17.0
Total Chargeable	9.3	9.3
η_{Prop}	0.809	0.809
SFC	Base	+0.5%
Propeller HP @ 0.8/35K + 18°	6450	6445
Propeller HP @ 0.2/SL + 27°	12500	12500

Table 3.4-3. APET Turboprop Configuration Studies.

Component Aerodynamic Comparisons

	All Axial	Axi Centrifugal
A) <u>Booster/LP Spool</u>		
No. Stages	2	2
$W/\sqrt{\theta}/\delta$	69.9	70.3
W_A/A_A	39.0	39.0
V Tip $\sqrt{\theta}$	924	924
r/r	0.67	0.67
PR	1.75	1.75
B) <u>Compressor</u>		
No. Stages	10	5+1
$W/\sqrt{\theta}/\delta$	44.2	44.5/8.43
W_A/A_A	38.0	38.0/32.3
V Tip/ $\sqrt{\theta}$ Axial	1498	1498
V Tip/ $\sqrt{\theta}$ Impeller	---	1407
PR	23.0	7.12 x 3.23 = 23
Last Blade Height	0.51"	0.42"
C) <u>HP Turbine</u>		
No. Stages	2	2
$W/\sqrt{T}/P$	6.53	6.65
$\Delta h/T$	0.086	0.086
P/P	5.14	5.16
ψ Pitch (Avg.)	0.66	0.66
1st Stage Blade Height	1.12	1.13"
D) <u>LP Turbine</u>		
No. Stages	4	4
$\Delta h/T$	0.100	0.100
P/P	7.6	7.6
ψ Pitch (Avg.)	0.95	0.95
AN^2	$42.5 * 10^9$	$42.5 * 10^9$
Altitude Thrust = 4000 #		

Cycle PR, T41 Impact on Performance Component Sizes, T3 Levels

- 4000# M_{XCL} Thrust Sized Engines
- T41 = 2350°F M_{XL} , 2450°F @ T-O
= 2450°F M_{XL} , 2550°F @ T-O

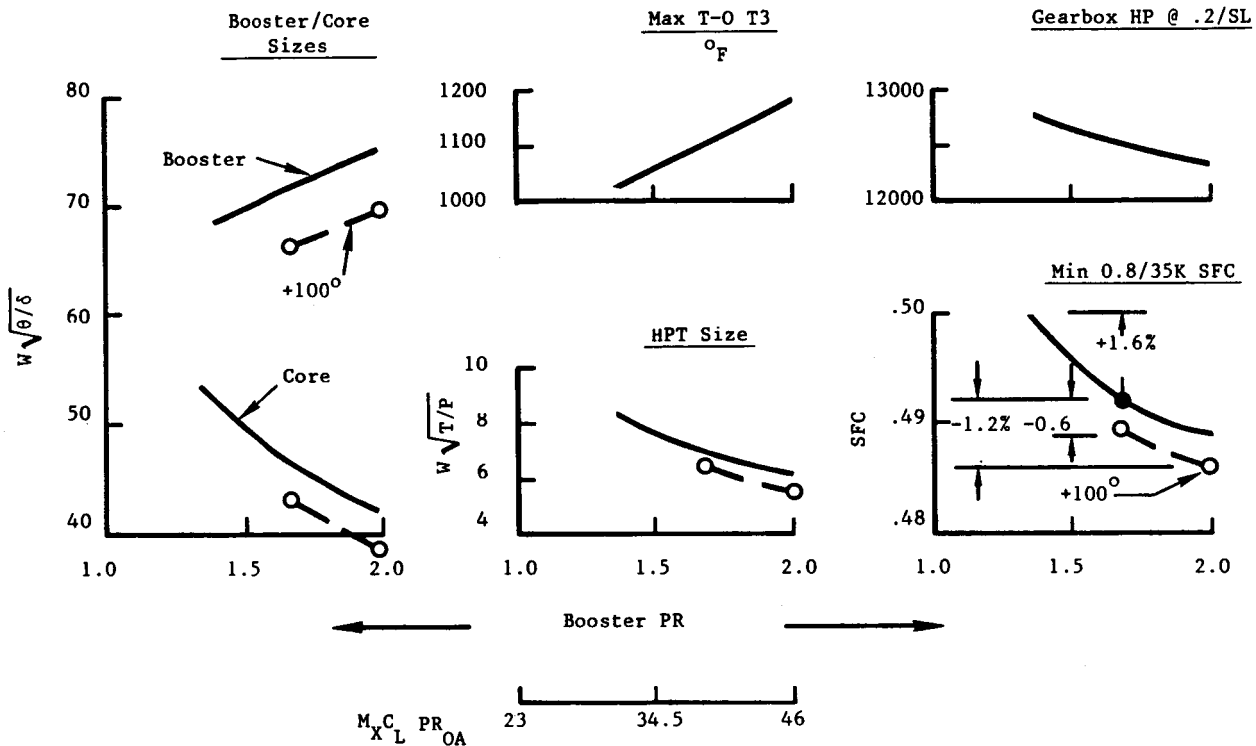


Figure 3.4-3. Turboprop Configuration Studies.

Propfan variables of tip speed and disc loading (SHP/D^2) for Mach numbers between 0.70 and 0.80 at altitude were examined. Propfan variables effects on take-off and climb-out performance were also established. The relative climb performance of the competing turbofan and turbopropfan powered airplanes are shown as Figures 3.4-4 and -5. The conclusion that can be drawn is that the superior climbout performance (in terms of fuel burned) of the propfan powered airplane is a potent factor in selecting propfan parameters for the short/medium ranges of particular interest in the APET airplane analyses. A high propfan tip speed is beneficial in both takeoff and cruise modes of flight. A moderate disc loading in the range of 20 to 30 SHP/D^2 is beneficial for cruise performance if diameter and weight effects on the airplane are neglected. Also, the lower the disc loading, the higher is the value of torque ratio across the reduction gearbox drive train. (For the same tip speed, a larger diameter propfan with lower power loading, inevitably requires an increase in driving torque).

An examination of propfan diameter effects on airplane geometry also shows disadvantages for the lower loaded propfans:

- Landing gear length (weight) is increased
- Nacelle lateral placement on the wing requires a further outboard location, giving rise to greater asymmetric thrust moments
- A larger tail volume coefficient is required
- Propfan, gearbox, and installation weights are increased.

A discussion on the evaluation of selection criteria for the propfan disc loading and tip speed will be found later in this report in Section 4.4.

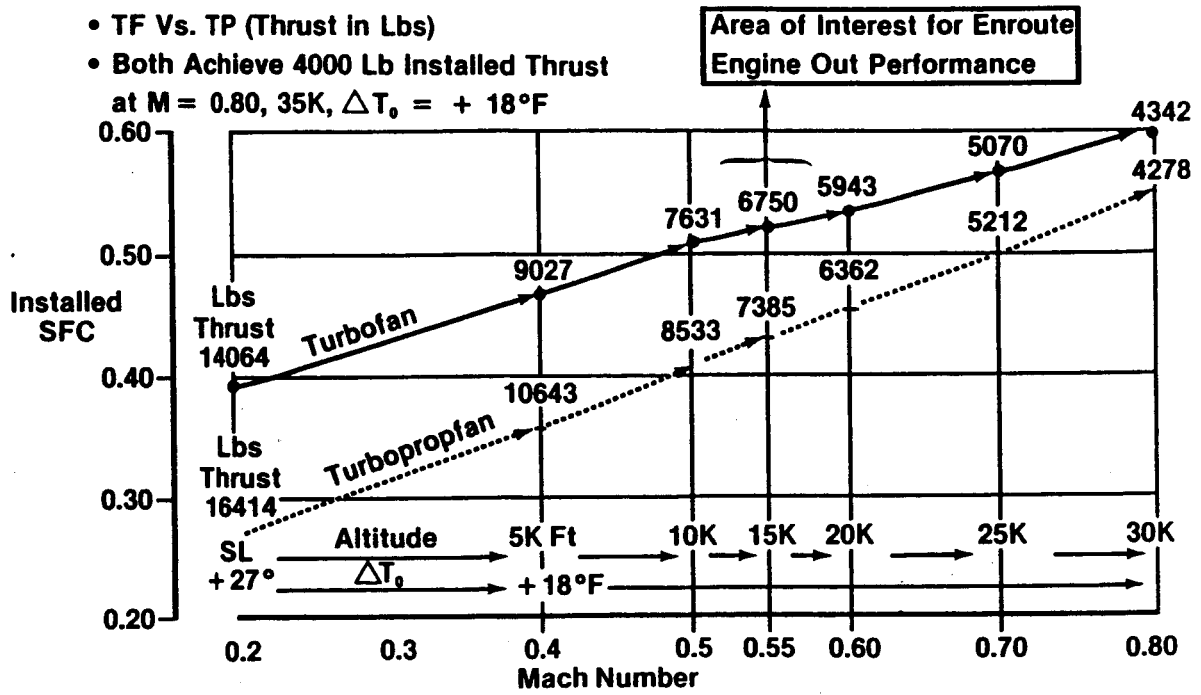


Figure 3.4-4. APET Installed Climb Path Comparison.

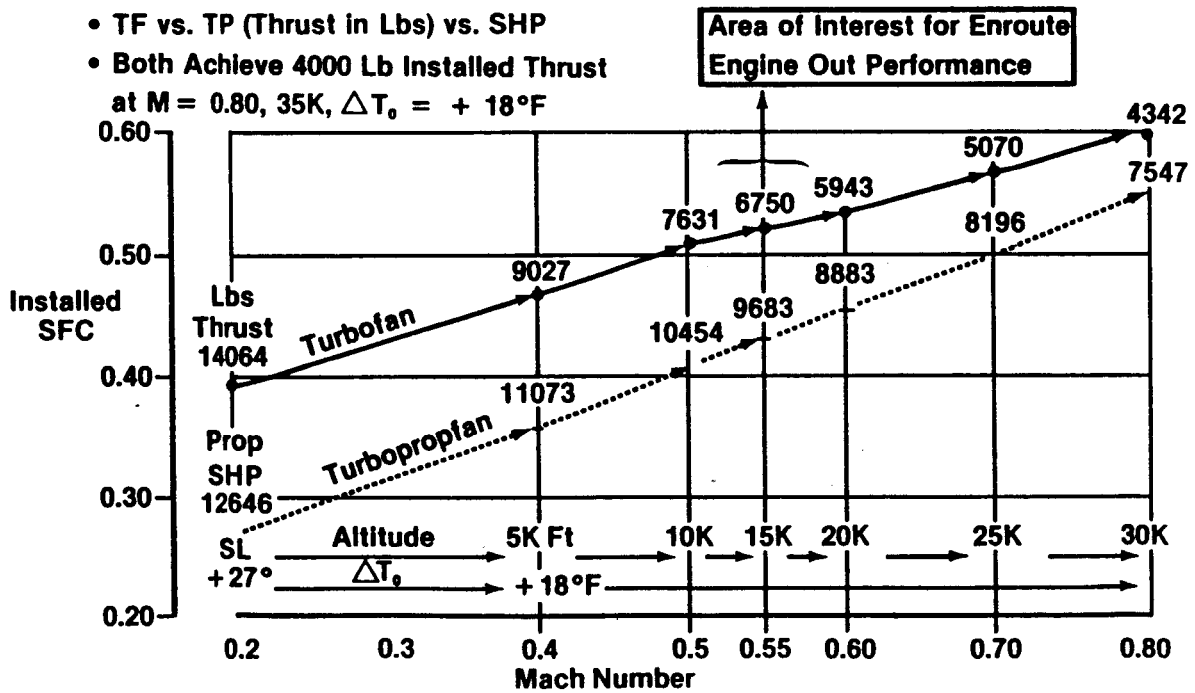


Figure 3.4-5. APET Installed Climb Path Comparison.

SECTION 3.5
PERFORMANCE COMPARISONS

FIGURES

<u>Figure</u>		<u>Page</u>
3.5-1.	APET Turbofan and Turboprop Installation Loss Bookkeeping.	52

TABLES

<u>Table</u>		
3.5-1.	APET Uninstalled Comparisons.	51

3.5 PERFORMANCE COMPARISONS

Performance comparisons between the uninstalled, and installed, turbofan and turboprop engine installations addressed the principal factors that contribute additional drag of selected configurations, and for the turboprop detailed assessments were made for the nacelle shape, engine inlet and exhaust systems, heat exchanger design parameters for the gearbox air-to-oil cooler installations, wetted areas and additive drag due to propfan supersonic effects. By NASA direction, interference effects between the nacelles and wings were not included for either form of propulsion systems, because high-speed turboprop wind tunnel programs at Ames Research Center are still in progress, and final data is not yet available. Likewise, the beneficial effect of swirl recovery by the wing was not included at this time, for the same reason.

Uninstalled performance comparisons were based on an estimate that the APET MCR = 0.80 airplane would require approximately 4000 lb of net thrust at the end of climb on a hot day, whether powered by turbofan or turboprop engines. The cycle assumptions used in Tables 3.4-2 and -3 were expanded to estimates of the take-off and climb performance that could be expected from both the turbofan and turboprop engines. Table 3.5-1 shows these comparisons in terms of percent of net thrust available and establishes the potential superiority of the propfan system all the way from Sea Level Takeoff to the selected start of cruise altitude point.

For the installed systems, a bookkeeping system was established and built into the performance computer decks. This system is illustrated by Figure 3.5-1 which shows the factors, and their magnitudes, for a typical high speed cruise point.

Table 3.5-1. APET Uninstalled Comparisons.

			Ref. TF	Base TP
●	MO.80/35K + 18°	- FN	4000	4000
		- SFC	Base	-10.6%
●	MO.2/SL + 27°	- FN	Base	+18.1%
		- SFC	Base	-31.0%
●	MO.2/5330 + 52°	- FN	Base	+13.2%
		- SFC	Base	-31.7%
●	MO.6/20000 ft + 18°	- FN	Base	+ 8.0%
		- SFC	Base	-16.4%
*Denver, Hot Day Takeoff.				

M = 0.80, 35K, Max CR.

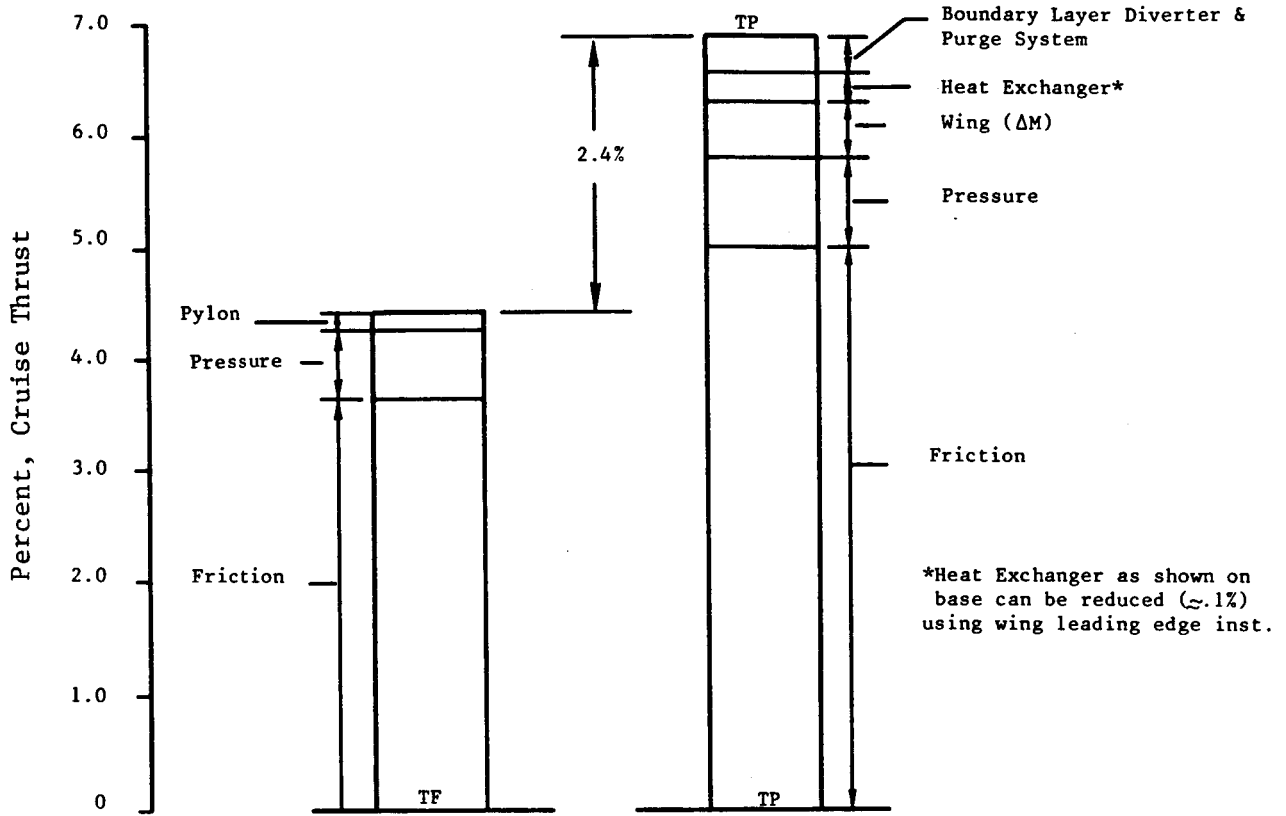


Figure 3.5-1. APET Turbofan & Turboprop Installation Loss Bookkeeping.

SECTION 3.6

GEARBOXES

<u>Section</u>		<u>Page</u>
3.6-1.	Gearbox Selection	55
3.6-2.	Gearbox Materials	57
3.6-3.	Condition Monitoring	57
3.6-4.	Lubrication	57

FIGURES

<u>Figure</u>		<u>Page</u>
3.6-1.	APET Gearbox Study - Effect of Scaling and Propeller Technology.	56

3.6 GEARBOXES

The attributes considered to be most desirable (not necessarily in the order of importance for ranking purposes) are as follows:

1. High efficiency of torque transfer
2. Low weight for the transmitted torque
3. Initial Price. (Here simplicity is a great virtue)
4. Reliability (The same comment as for 3 above).

Building from an established data base, a number of candidate gearboxes, both in-line and offset configurations, were preliminary designed and screened.

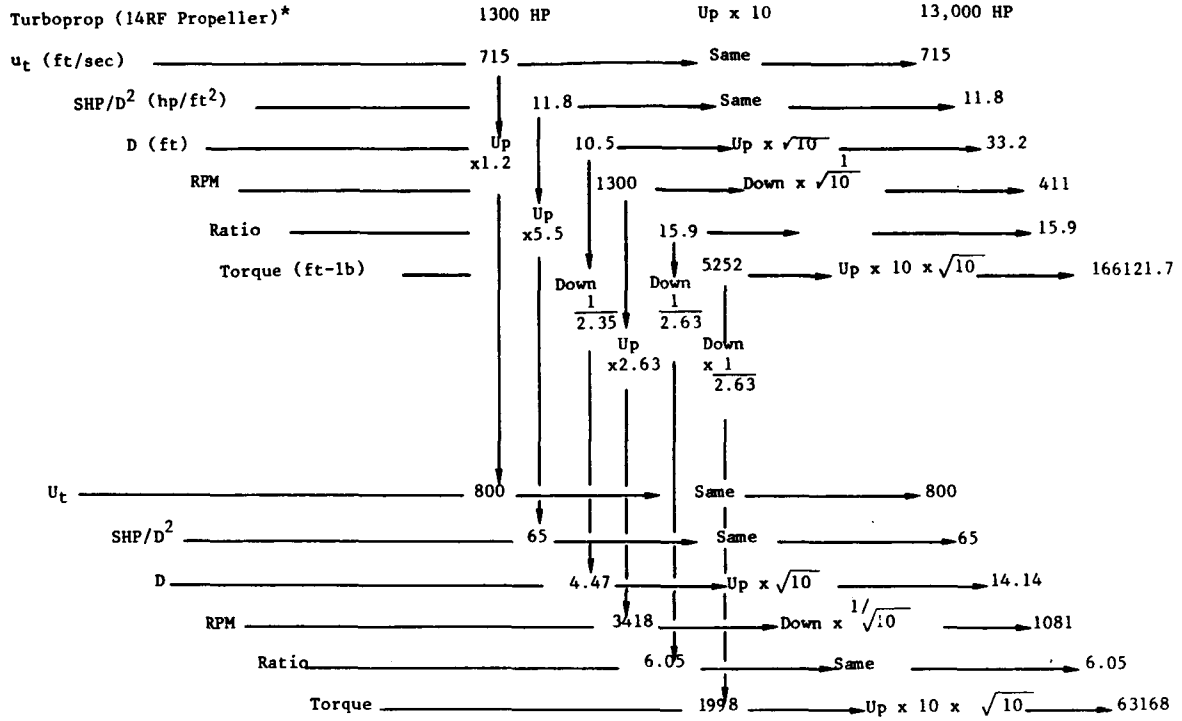
It is appropriate at this point to emphasize the contribution that is made to gearbox size and weight reduction, by the use of the propfan. If the thrust of a conventional propeller were scaled up by a factor of ten, the gearbox torque would of necessity be scaled up by a factor of ten times the square root of ten. The high tip speed and power density (SHP/D²) of the propfan allows a reduction in torque by a factor of 1/2.63, and thus the propfan dedicated gearbox greatly benefits from a lower stage ratio and a reduced torque. This is illustrated in Figure 3.6-1 where all the factor differences between a conventional propeller's effects on gearbox sizing are shown comparatively with the requirements for a propfan gearbox.

3.6.1 Gearbox Selection

From the slate of candidate gearboxes, both an offset and an in-line gearbox were selected for further requirements including weight and cost estimating. All of the gearboxes that have been considered, including the two that were selected for further efforts, are fully described in Section 4.6 of this report.

The offset gearbox was estimated to weigh 1068 lbs and the in-line gearbox was estimated to weigh 94 lbs more. Both these estimates are likely to be reduced with further efforts that are scheduled in the APET follow-on tasks that have been contracted by NASA, and which will be reported late in 1984.

Effect of Scaling & Propeller Technology



* The 14RF Propeller is a Hamilton Standard Designation for a Modern Commuter Aircraft Propeller

Figure 3.6-1. APET Gearbox Study.

3.6.2 Gearbox Materials

For this study, main drive gear materials of Vasco X2 Mod or equivalent have been selected. Bearings are of M50 alloy and titanium alloys have been used, where possible for main shafts. Auxiliary gears to drive the lubrication system, the power offtake for aircraft accessories and the like are selected from AISI 9310 material. The main housings have been estimated, at this time, in cast aluminium metal. Magnesium alloys and/or titanium fabricated housings will be considered in the further refinements of the current designs.

3.6.3 Condition Monitoring

Effective vital function, as well as diagnostic, instrumentation will be needed in the future turboprop gearboxes. Information processors can fault isolate to a line replaceable unit (LRU). The follow-on APET studies will include a substantial effort to select and define critical sensors, sensor technologies, processing and memory units, and an interactive system which is capable of being interrogated and monitored by the Full Authority Digital Engine Control (FADEC).

3.6.4 Lubrication

Current US turboprops use shared oil systems with the engine gas generator. The selection of the oil for this system has historically been made in favor of the synthetic oils that perform best in the hot bearing environment of the turbine stages of the engine. For APET, higher viscosity oils with boundary additives have been evaluated using the TELSCE Computer Program (Reference 42). This, with other analytical techniques, has suggested that a good balance of physical properties, cost and near-term availability may be afforded by the use of an Emgard EP 75W-90 (Frigid-Go) formula. This type of lubricant, in a non-shared oil system i.e. one dedicated to the propeller gearbox alone, has good potential to improve both load-carrying capabilities of the gears, and increase the scoring life factors. Coupled with superior filtration systems, modular gearbox construction, suitable functional instrumentation etc. the future for high torque gearboxes reliability will be greatly improved relative to existing gearboxes.

SECTION 3.7

NACELLES AND NACELLE TECHNOLOGY

<u>Section</u>		<u>Page</u>
3.7.1.	Geometric Selection	61
3.7.2.	Inlet Studies	61
3.7.3.	Exhaust Nozzles	64
3.7.4.	Nacelle Designs	64
3.7.5.	Engine and Gearbox Dynamic Suspension	64

FIGURES

<u>Figure</u>		<u>Page</u>
3.7-1.	Model Configuration Used in a Wind Tunnel Program.	62
3.7-2.	APET Study Nacelles.	63

PRECEDING PAGE BLANK NOT FILMED

3.7 NACELLES, AND NACELLE TECHNOLOGY

An historical survey was made of a number of previous installations of turboprop engines. Installations of the later T-56 models and those of the Roll-Royce "Tyne" engine are of particular interest because they represent the highest horsepower installations made by airframe manufacturers in the Western World. The survey showed a number of limiting factors if airplane speeds are projected into the Mach 0.70 to 0.80 range. Nacelle design technology for APET type performance is a key technical issue.

3.7.1 Geometric Selection

Apart from the NASA sponsored RECAT studies carried out in the middle nineteen-seventies, there have been only a limited number of reports that assist in the process of selecting the nacelle geometric location. NASA Ames wind tunnel program for high speed nacelle research on a swept-wing is of particular importance, and the results from the NASA tests have been used to justify the nacelle types and locations reported in this study. Fore and aft location for an on-the-wing nacelle is by no means an established science with well understood ground rules. Likewise, the spanwise location is equally uncertain with regard to secondary effects such as cabin noise (and sound attenuation weight penalties), asymmetric thrust and drag, ground clearance criteria and the like.

Figure 3.7-1 illustrates one of the models that have been used in the NASA high-speed wind-tunnel program while Figure 3.7-2 shows the entire family of nacelles and locations that have been considered during this APET study.

At this time there appears to be no front running favorite arrangement for location or for nacelle type. Further efforts will be required before a well-based decision of geometry could be made.

3.7.2 Inlet Studies

Both single and dual offset inlet designs have been analyzed. The first was used with an offset gearbox propulsion system arrangement while the second was used with an in-line configuration.

ORIGINAL PAGES
OF POOR QUALITY

**MODEL CROSS SECTIONS
(2.50"/1.00" APPROX)**

MODEL STA (in)	R (in)	H (in)
0.5	3.000	0.00
1.0	3.000	0.000
1.5	3.000	0.000
2.0	3.000	0.000
2.5	3.000	0.000
3.0	3.000	0.000
3.5	3.000	0.000
4.0	3.000	0.000
4.5	3.000	0.000
5.0	3.000	0.000
5.5	3.000	0.000
6.0	3.000	0.000
6.5	3.000	0.000
7.0	3.000	0.000
7.5	3.000	0.000
8.0	3.000	0.000
8.5	3.000	0.000
9.0	3.000	0.000
9.5	3.000	0.000
10.0	3.000	0.000
10.5	3.000	0.000
11.0	3.000	0.000
11.5	3.000	0.000
12.0	3.000	0.000
12.5	3.000	0.000
13.0	3.000	0.000
13.5	3.000	0.000
14.0	3.000	0.000
14.5	3.000	0.000
15.0	3.000	0.000
15.5	3.000	0.000
16.0	3.000	0.000
16.5	3.000	0.000
17.0	3.000	0.000
17.5	3.000	0.000
18.0	3.000	0.000
18.5	3.000	0.000
19.0	3.000	0.000
19.5	3.000	0.000
20.0	3.000	0.000
20.5	3.000	0.000
21.0	3.000	0.000
21.5	3.000	0.000
22.0	3.000	0.000
22.5	3.000	0.000
23.0	3.000	0.000
23.5	3.000	0.000
24.0	3.000	0.000
24.5	3.000	0.000
25.0	3.000	0.000
25.5	3.000	0.000
26.0	3.000	0.000
26.5	3.000	0.000
27.0	3.000	0.000
27.5	3.000	0.000
28.0	3.000	0.000
28.5	3.000	0.000
29.0	3.000	0.000
29.5	3.000	0.000
30.0	3.000	0.000
30.5	3.000	0.000
31.0	3.000	0.000
31.5	3.000	0.000
32.0	3.000	0.000
32.5	3.000	0.000
33.0	3.000	0.000
33.5	3.000	0.000
34.0	3.000	0.000
34.5	3.000	0.000
35.0	3.000	0.000
35.5	3.000	0.000
36.0	3.000	0.000
36.5	3.000	0.000
37.0	3.000	0.000
37.5	3.000	0.000
38.0	3.000	0.000
38.5	3.000	0.000
39.0	3.000	0.000
39.5	3.000	0.000
40.0	3.000	0.000
40.5	3.000	0.000
41.0	3.000	0.000
41.5	3.000	0.000
42.0	3.000	0.000
42.5	3.000	0.000
43.0	3.000	0.000
43.5	3.000	0.000
44.0	3.000	0.000
44.5	3.000	0.000
45.0	3.000	0.000
45.5	3.000	0.000
46.0	3.000	0.000
46.5	3.000	0.000
47.0	3.000	0.000
47.5	3.000	0.000
48.0	3.000	0.000
48.5	3.000	0.000
49.0	3.000	0.000
49.5	3.000	0.000
50.0	3.000	0.000

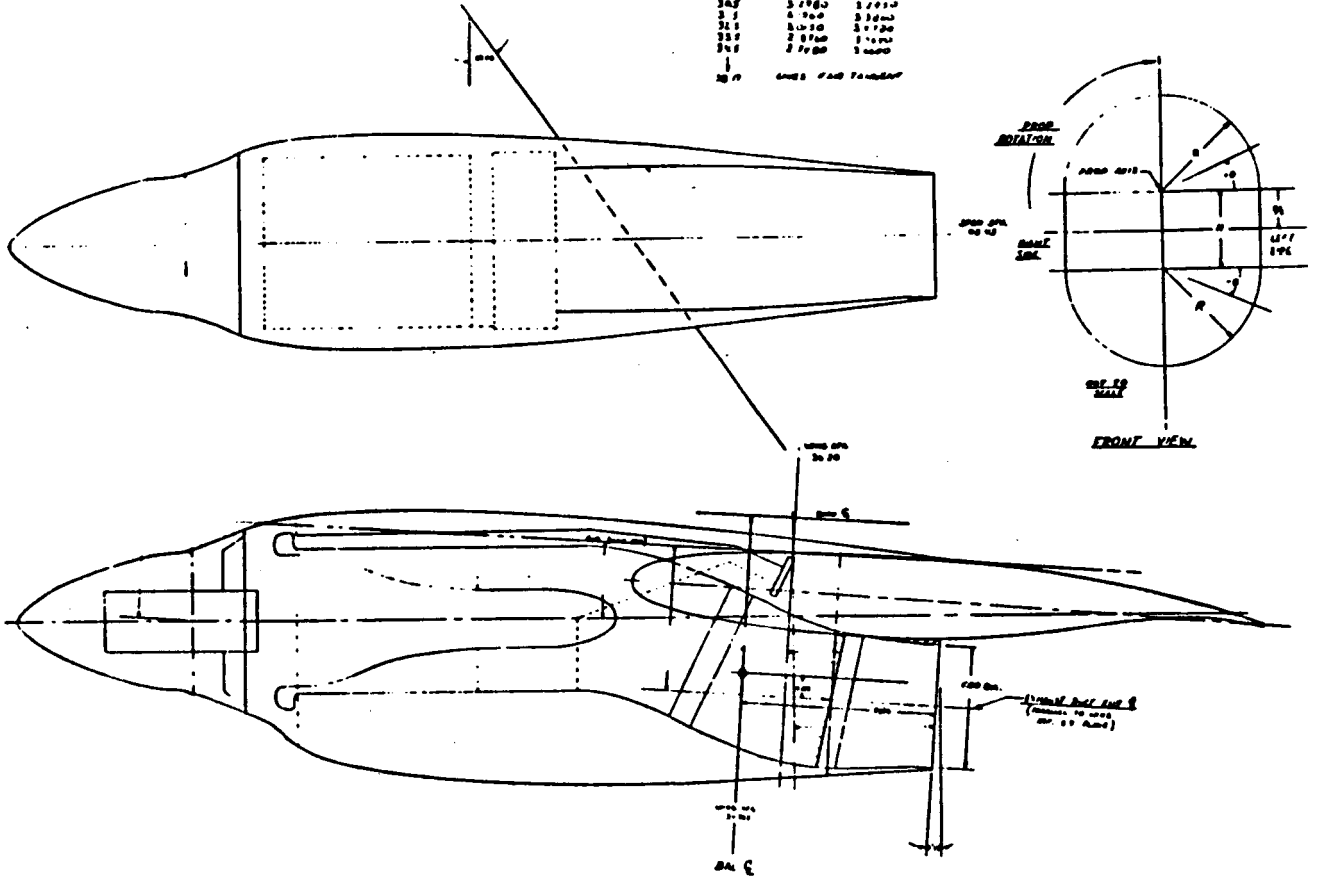


Figure 3.7-1. Model Configuration Used in a Wind Tunnel Program.

ORIGINAL PARTS
OF POOR QUALITY

- ALL PROPFANS ARE 13.2 FT DIA
- ALL PROP TO GROUND CLEARANCES ARE 2.5 FT
- ALL WING CHORDS ARE 10 FT
- PROP DIA = 1.0 FOR SKETCHES 1
DISTANCE TO 1/4 CHORD = THRU 4 RATIO=1.30
FOR 5 & 1.28 FOR 6
- 1/4 CHORD DISTANCE TO GROUND
SKETCH 1=10.12 FT
SKETCH 2 8.93 FT
SKETCH 3 11.02 FT
SKETCH 4 8.74 FT
SKETCH 5 8.29 FT
SKETCH 6 10.12 FT

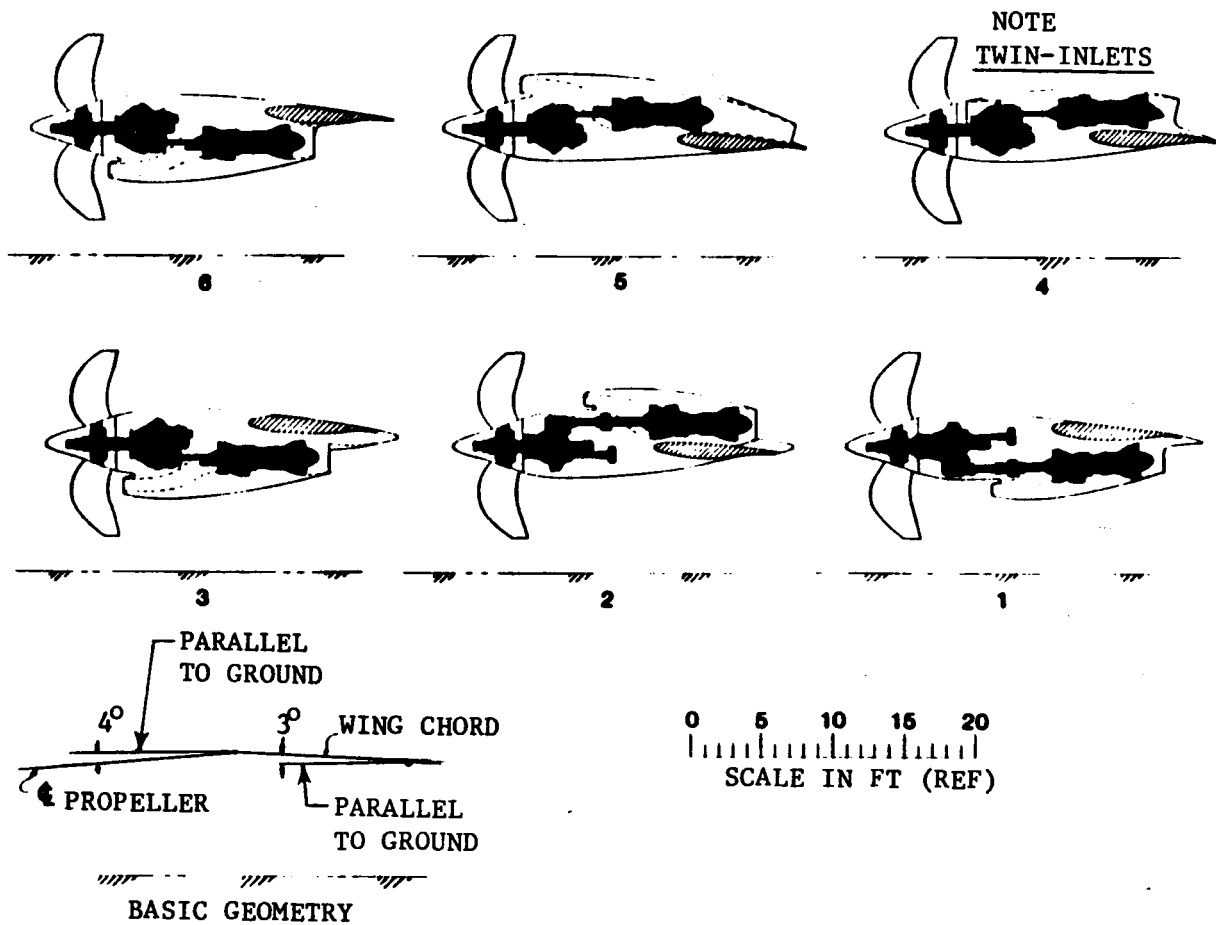


Figure 3.7-2. APET Study Nacelles.

The estimated performances of these inlets were very close to each other and other factors than aero performance and recovery would have to be used before a selection could be justified. Both these inlet designs are reported in detail in Section 4.7 of this report.

3.7.3 Exhaust Nozzles

These were analyzed on both an uninstalled and an installed basis, with considerations of boattail angle and flow suppression being taken into effect. The low pressure ratio turboprop exhaust system finally selected was based on a 10° boattail angle and a fully submersed nozzle plug.

Although adequate analytical data is available for the level of effort required by this study, more detailed analyses and model tests would be required in any definitive propulsion system design.

3.7.4 Nacelle Designs

These consisted essentially of taking the engines and gearboxes previously selected, coupling them with the preferred inlet and exhaust systems and combining them with faired contours to enclose the overall selected propulsion system. Considerations of the wing effect on nacelle contouring and the close-out geometry dictated by an under-the-wing installation are illustrated and described in Section 4.7 of this report. Nacelle drags estimates were made using conventional techniques for both friction and pressure drags including the super velocity effects in the propfan wake.

3.7.5 Engine and Gearbox Dynamic Suspension

All turboprops must be analyzed through dynamic ranges for the purposes of reducing propulsion system induced vibration (isolation techniques) as well as the safety aspects for whirl-flutter stability. The engine systems and nacelle designs included in this report are all believed to be capable of lightweight suspension dynamics in a design program that includes the full aerodynamic characteristics of the propfan and the nacelle and wing elasticity values.

It is expected that the APET follow-on contract tasks will include some dynamic considerations, and efforts will be made to identify some technical approaches to suspension dynamics that have the potential of major improvements relative to conventional elastomeric supports.

SECTION 3.8
MISSION ANALYSES AND RESULTS

FIGURES

<u>Figure</u>		<u>Page</u>
3.8-1.	APET Aircraft Fuel Efficiency.	70
3.8-2.	APET Economic Results - Baseline Cases.	71
3.8-3.	APET Result - Fuel Burn vs. Technology vs. MXCR vs. Range, 65% Load Factor.	71

TABLES

3.8-1.	APET Study Results - Description of APET Baseline Aircraft.	70
3.8-2.	APET Aircraft Noise Levels.	72

PRECEDING PAGE BLANK NOT FILMED

3.8 MISSION ANALYSES AND RESULTS

All six APET airplanes (three turbofan powered and three turboprop powered) were optimized in terms of gross weight, wing loading, thrust-to-weight ratio for the design mission - 150 passengers at a 1000 N. Mi range. Also each design was optimized for its propulsion type and for its selected flight Mach number.

Three measures of merit were considered; fuel burn, available seat miles per gallon (ASM/GAL) and direct operating cost (DOC).

Off-design characteristics in terms of assumed airplane weight and range were also considered, as was a reduction of the selected aspect ratio of 11 down to 9.

A summary of the point design airplanes flying with a 65% load factor (LF) is presented on Table 3.8-1, while Figure 3.8-1 shows the ASM/GAL values versus range for the same LF. The design point cases for the DOC of both the turbofan and turboprop aircraft are depicted on Figure 3.8-2, where also are shown the effects of an off-design case - the Mach 0.80 designs being constrained to fly at a cruise Mach of 0.70 and an altitude comparison between operating at 30 and 35 thousand feet.

Figure 3.8-3 describes the levels, or steps, of technology that are estimated to take an airplane using 1972 weight technology and having a design range of 2000 N. Mi all the way to the final selected values of the APET airplanes.

Also as part of the mission results, estimates were made of the acoustic signature of three of the APET airplanes. These were:

1. The Mach 0.80 Turbofan
2. The Mach 0.80 Turboprop
3. The Mach 0.70 Turboprop

Using NASA and SAE data for the propfan noise and an established base from other sources for the engine component noise and airframe noise, the takeoff, cutback, sideline and approach noise levels were estimated. A summary of these results is shown in Table 3.8-2.

Table 3.8-1. APET Study Results - Description of APET Baseline Aircraft.

Propulsion Type	Turboprop			Turbofan		
	0.70	0.75	0.80	0.70	0.75	0.80
Design Mach No.	0.70	0.75	0.80	0.70	0.75	0.80
Design Range (100% LF) - NMI	1000	1000	1000	1000	1000	1000
TOGW - lbs	107309	108845	110986	108036	109305	111970
Wing Area - ft ²	932	903	879	938	907	929
F _n SLS - lbs	---	---	---	15853	16381	17410
SHP - hp	10720	10998	11390	---	---	---
Prop. Dia. - ft	12.15	12.335	12.55	---	---	---
Fuel Capacity - US Gal	3630	3715	3820	3950	4020	4140
O.W.E - lbs	63120	64082	65488	61692	62483	64388
Fuel Burn - 1000 nmi (65% LF)	7063	7313	7618	8204	8397	8746
Fuel Burn - 300 nmi (65% LF)	2799	2855	2922	3412	3458	3578
ASM/Gal - 1000 nmi (65% LF)	142.3	137.4	131.9	122.5	119.7	114.9
ASM/Gal - 300 nmi (65% LF)	107.7	105.6	103.2	88.4	87.2	84.3

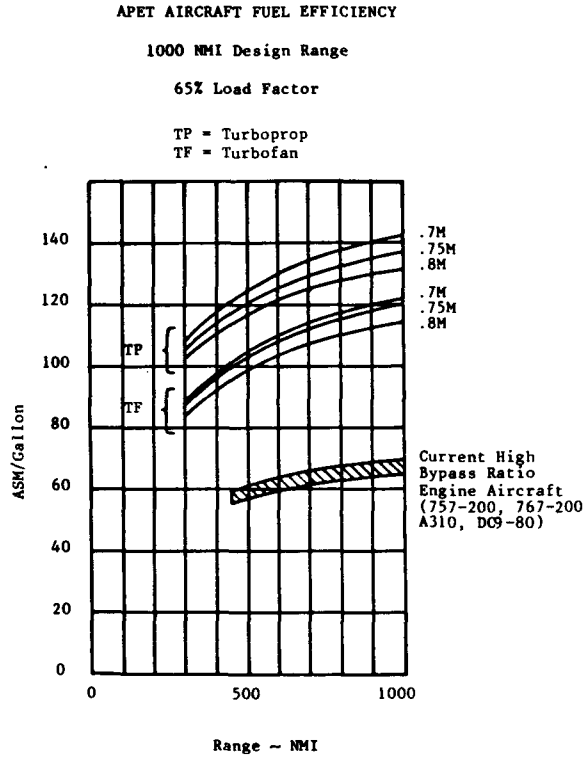


Figure 3.8-1. APET Aircraft Fuel Efficiency 1000 NMI Design Range 65% Load Factor.

ORIGINAL FIGURE
OF POOR QUALITY

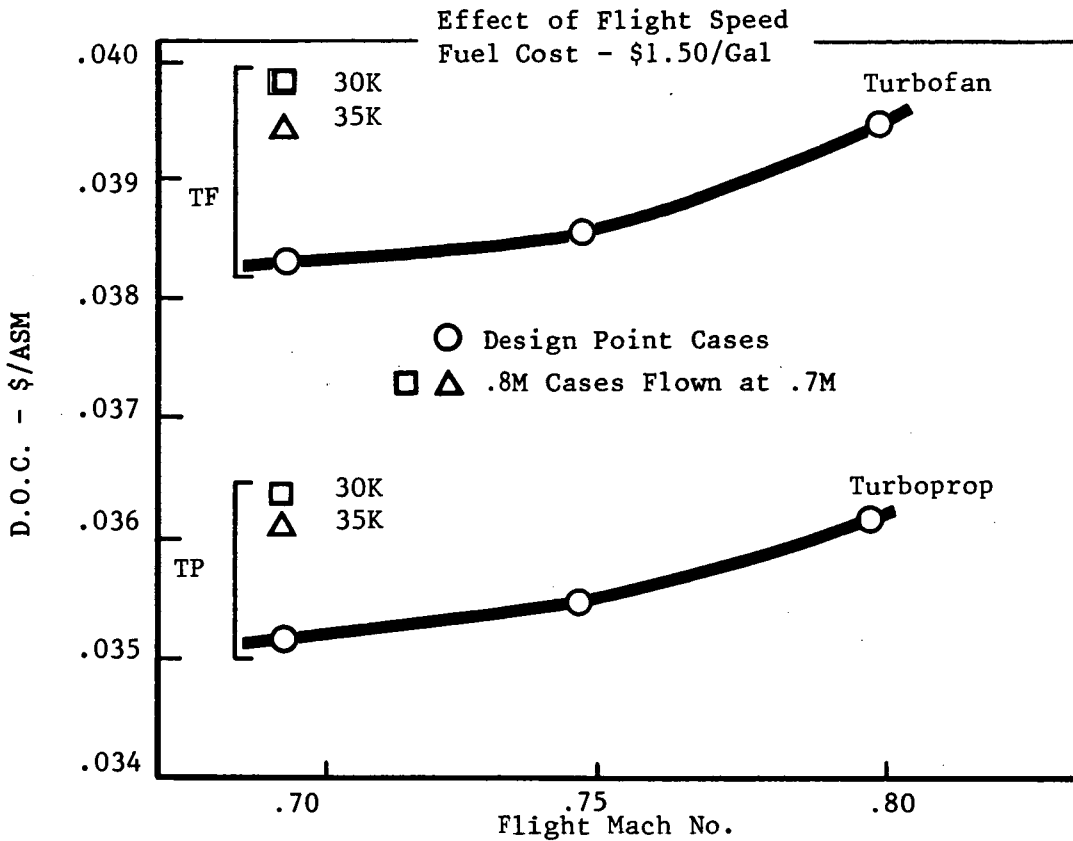


Figure 3.8-2. APET Economic Results - Baseline Cases.

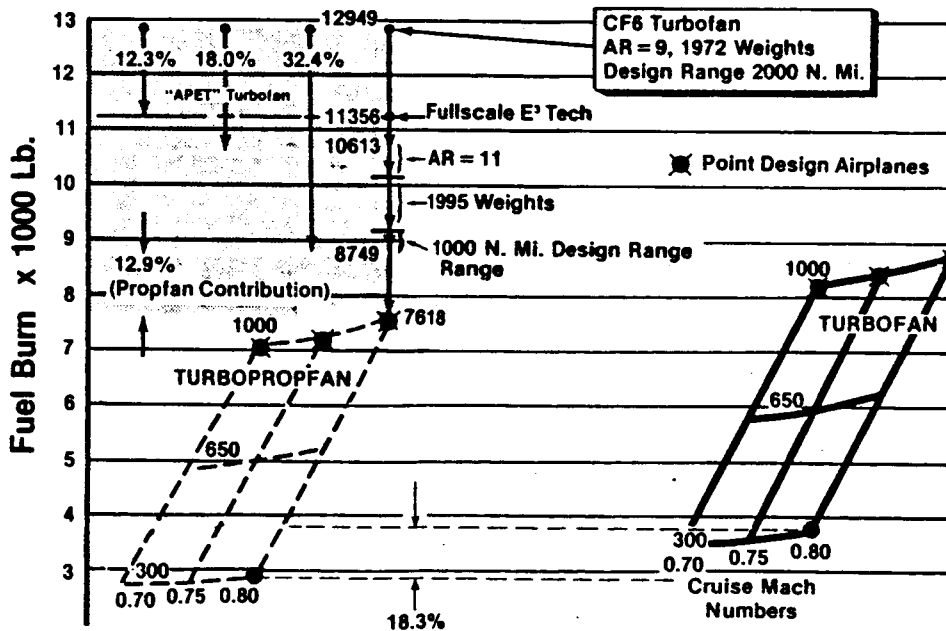


Figure 3.8-3. Fuel Burn Versus Technology Versus MCR Versus Range, 65% Load Factor.

Table 3.8-2. APET Aircraft Noise Levels.

Condition	0.8 Mach Turbofan TOGW = 111,970 lbs			0.8 Mach Turboprop TOGW = 110,986 lbs			0.7 Mach Turboprop TOGW = 107,309		
	FAR 36 (EPNdB)	Estimated Level (EPNdB)	Margin (EPNdB)	FAR 36 (EPNdB)	Estimated Level (EPNdB)	Margin (EPNdB)	FAR 36 (EPNdB)	Estimated Level (EPNdB)	Margin (EPNdB)
Takeoff	89.3	85.8	3.5	89.3	90.5	-1.2	89.1	90.2	-1.1
Cut Back	89.3	85.3	4.0	89.3	88.9	0.4	89.1	88.7	0.4
Sideline	95.4	91.3	4.1	95.4	95.4	1.9	95.2	93.2	2.0
Approach	99.3	94.9	4.4	99.2	97.2	2.0	99.1	96.7	2.4

In addition to far field noise estimates, values were calculated for the sound pressure level at the fuselage wall. A cabin wall transmission loss was then applied which determined an "A" weighted interior SPL. The methodology used and the results obtained are discussed in Appendix II. Interior noise levels are estimated to lie within the desired value of 82-84 EPNdB.

It can be noted from the farfield values presented in Table 3.8-2 that the APET airplanes will all meet the current (Stage 3) noise regulations, using cutback at takeoff.

SECTION 4.0

TOPICAL DISCUSSION OF THE STUDY

<u>Section</u>		<u>Page</u>
	<u>Tasks I through VI</u>	
4.1	Ground Rules	75
4.2	The APET Airplanes	87
4.3	Reference Turbofan Engine	113
4.4	APET Turboshift Engines	123
4.5	Impact of Design Features on Engine Deterioration Modes	157
4.6	Gearboxes, Lubrication and Heat Exchangers	163
4.7	Nacelles and Nacelle Technology	221
4.8	Mission Analysis	283
4.9	Acoustics	301
4.10	Emissions	307
4.11	Military Relevance	313
4.12	Recommendations	319
	<u>Tasks VII and VIII</u>	
4.13	Preliminary Design of an Advanced Single Rotation Gearbox	339
4.14	Conceptual Design of an Advanced Pitch Change Mechanism	377
4.15	Recommendations for Pitch Change Mechanism	421

SECTION 4.1
GROUND RULES

<u>Section</u>		<u>Page</u>
4.1.1	Study Procedures and Assumptions Document	75
4.1.2	Historical Survey	75
4.1.3	Operating Costs	76
4.1.4	Acoustics	79
4.1.5	Emissions	81

FIGURES

<u>Figure</u>		<u>Page</u>
4.1-1.	Conventional Turboprop History.	78
4.1-2.	APET Fuel Price Forecast.	80
4.1-3.	Estimating Airframe Unit Prices.	80
4.1-4.	EPA Smoke Emission Standards - Turbojet/Turbofan Engines.	83
4.1-5.	EPA Smoke Emission Standards - Turboprop Engines.	83

TABLES

<u>Table</u>		<u>Page</u>
4.1-1.	Historical Summary of Turboprops.	77
4.1-2.	Current Standards - Newly Certified Large Engines.	82
4.1-3.	Current EPA Prescribed Cycles for Emissions Calculations.	82
4.1-4.	NPRM Standards - Newly Certified Large Engines.	84

4.0 TOPICAL DISCUSSION OF THE STUDY

4.1 GROUND RULES

4.1.1 Study Procedures and Assumptions Document (Reference 23)

The APET study technical analyses were preceded by the creation of an interim report with the above title. This report was submitted to NASA in April 1982, for approval by the Project Manager, which approval was duly obtained. The document outlined the methodology that would be used to analyze many of the technical parameters that were to be addressed and reported on throughout the study period.

General Electric discussed the methods being proposed with three principal Aircraft Design Companies to further ensure that a rational base set of assumptions would be followed by equally rational analytical efforts. Many of the suggestions made by these companies were followed where possible, although for some issues such as "Fuel Price Forecasting" General Electric elected to use in-house data and forecast values, while for others such as "propfan source noise," General Electric relied on data provided by Hamilton Standard.

The following sections summarize the "Study Procedures and Assumptions Document" and for the interested reader the results of the analyses are contained within Sections 4.2 through 12, and in the three Appendices.

4.1.2 Historical Survey

In Section 2 (Introduction) of this report, Table 2-1 has summarized some of the larger twin-engined turboprop airplanes that have seen significant numbers built and a large total of operating hours accrued in either military or commercial service. Using conventional, current, technology levels for the airplane and engines it was postulated that the APET turboprop airplanes might weigh in the neighborhood of 130,000 pounds (TOGW) and require engines each of 10,000 SHP for MCr equal 0.70 and 14,000 SHP for MCr equal 0.80. For the benefits in weight that were predicted due to advanced technology airplanes and engines, it was to be expected that these values might be reduced somewhat

through the study activities. The values being quoted here are for the 150 passenger size with a maximum payload/range point designed for 1000 nautical miles.

In order not to delay the design activity start point, General Electric decided to design a "baseline" system at the 12,500 SHP level and determine what are the valid scaling factors for the engines and transmission systems that result from changes (up or down) from the baseline level.

The airplane size (150 passenger), the design maximum payload range point (1000 nautical miles), the initial cruise altitude of 35,000 feet, the runway length of 6,000 feet, plus other factors affecting engine thrust and airplane wing sizing were all catalogued in an abbreviated airplane specification that was submitted to NASA. This specification, which has already been shown as Table 3.2-1 in the Program Overview will not be duplicated here. However, for those interested, a more detailed summary of historical data on 2 and 4-engined turboprops is shown on Table 4.1-1, while Figure 4.1-1 is included to show where the APET baseline was expected to lie at 130,000 pounds TOGW and 2 x 12,500 SHP propulsion systems. It is clear that the APET family of turbo-prop designs, because of their high cruise Mach number, are in a class that is substantially different from previous experience.

4.1.3 Operating Costs

Three methods of estimating Direct Operating Cost (DOC) were exercised during the APET studies. They were:

1. Eurac method (Reference 31)
2. Boeing modification of the ATA method (Reference 32)
3. NASA TM 80196 dated January 1980, "Computer Programs for Estimating Civil Aircraft Economics." (Reference 30)

All three programs outputs were compared when using identical inputs and the resultant values were judged to be very similar. Because of general acceptance by the U.S. Airline Industry, the Boeing modified ATA method, updated to 1981 economic parameters, was selected for this study.

Fuel price forecasting for the 1990 time period relied on data from a number of sources including Government Agencies, Oil Industry projections, and

Table 4.1-1. Historical Summary Turboprop.

Aircraft Type	No. Engines and Engine Type	Total Installed, shp	No. PAX	TOGW lbs X1000	Maximum Payload Distance, N. Mi.	Maximum Distance Full Fuel, N. Mi.
CL44D4	4 Tyne 12	22920	160	210	2900	4850
Britannia 320	4 Proteus 765	17800	139	185	3620	4530
Vanguard 951	4 Tyne 506	19940	115	135	1800	2620
Electra L188	4 Allison 501	15000	99	116	1400	2690
Viscount 800	4 Dart 525	6960	71	64.5	1120	1670
Convair 600	2 Dart 542	6050	56	57	390	695
NAMC YS-11	2 Dart 542	6120	60	51.8	770	1725
HS 748 2B	2 Dart 536	4560	60	46.5	1367	1867
HP Herald 700	2 Dart 532	4260	60	45	625	1675
HS 748 Series 2	2 Dart 531	4210	58	44.5	1000	1780
Fokker F-200	2 Dart 532	4460	48	43.5	1610	1610
Russian Commercial Variant of "Bear" Bomber						
TU 114	4 Kusnetsov	48000	220	414	?	9000

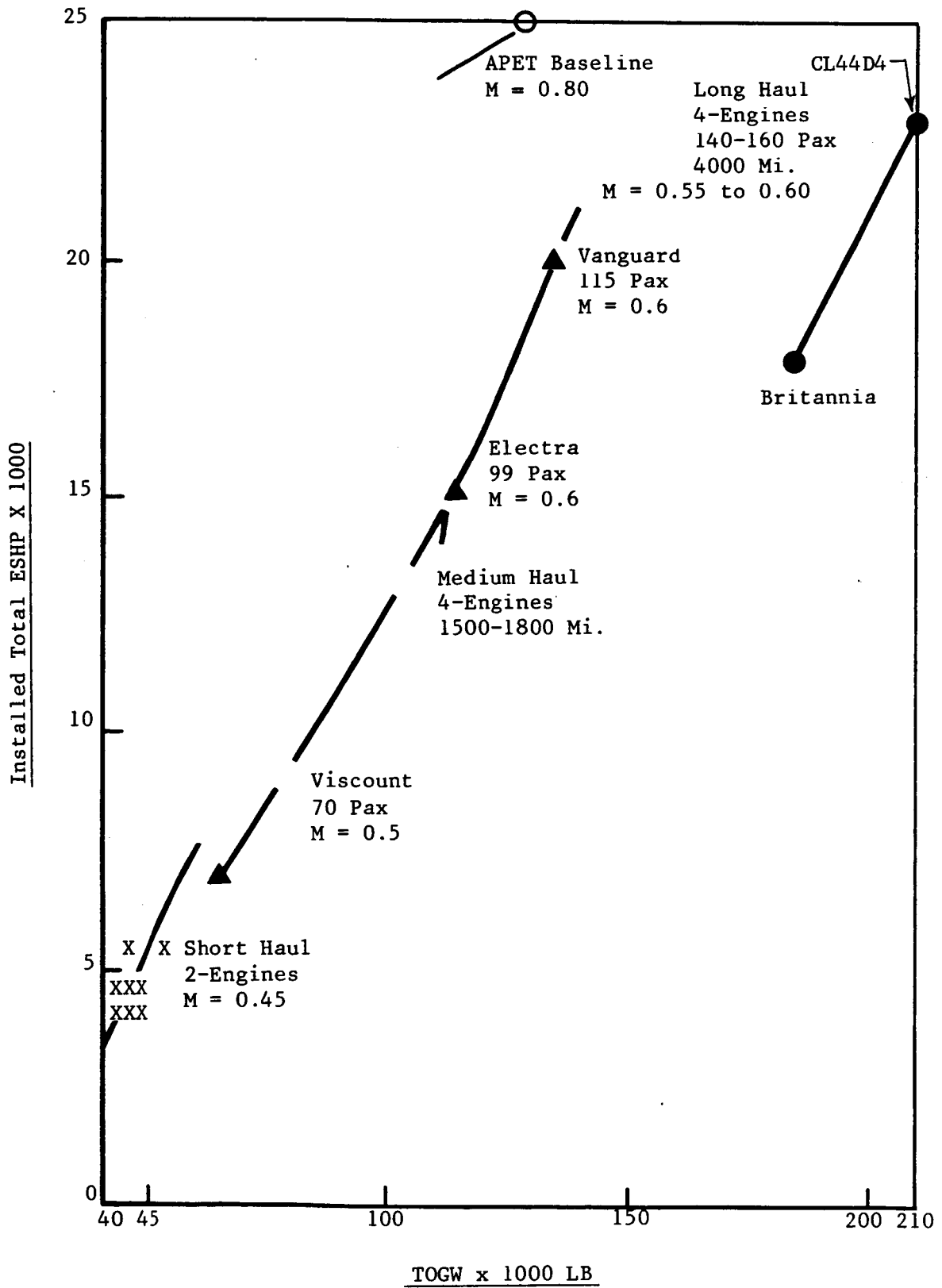


Figure 4.1-1. Conventional Turboprop History.

economic forecasts long used by the General Electric Company. Figure 4.1-2 shows the scatter or variability that results from these data sources. Following discussions with the NASA program office it was decided that a base price of a \$1.50 per gallon ± 0.50 would be used in the ensuing analyses.

Unit aircraft flyaway prices were proposed by dividing the aircraft into two categories:

1. Airframe (including Avionics)
2. Propulsion

Estimating relationships were devised to permit airframe price variation as a function of size and for this the data contained in the following reports was used:

- Douglas Aircraft Company, Inc. report. (Reference 33)
- Society of Allied Weight Engineers Paper. (Reference 25)

These data are summarized in Figure 4.1-3.

General Electric proposed to use in-house data for engines, gearboxes, and nacelles and Hamilton Standard data for the propfan and controls. In-house data and methods were also to be applied to those costs associated with maintenance actions and spare parts pricing, with the exception of the propfan where Hamilton-Standard data was used.

4.1.4 Acoustics

General Electric considered two types of acoustic environmental constraints: (1) those that are based on regulations in force at the time of the study (1982), and (2) those that are anticipated by 1995.

For (1) above, FAR 36/Stage 3) is applicable while for (2), guidance was sought from the activities of the International Civil Aviation Organization (ICAO) under working group C, and also some of the activities reported by the Society of Automotive Engineers (SAE) Committee A-21. These regulations that are either in force or are anticipated, apply to the noise levels exterior to the airplane. For interior noise acceptability levels it was proposed that informal discussions were held with appropriate Government and Industry personnel. These discussions determined that there are no mandatory requirements

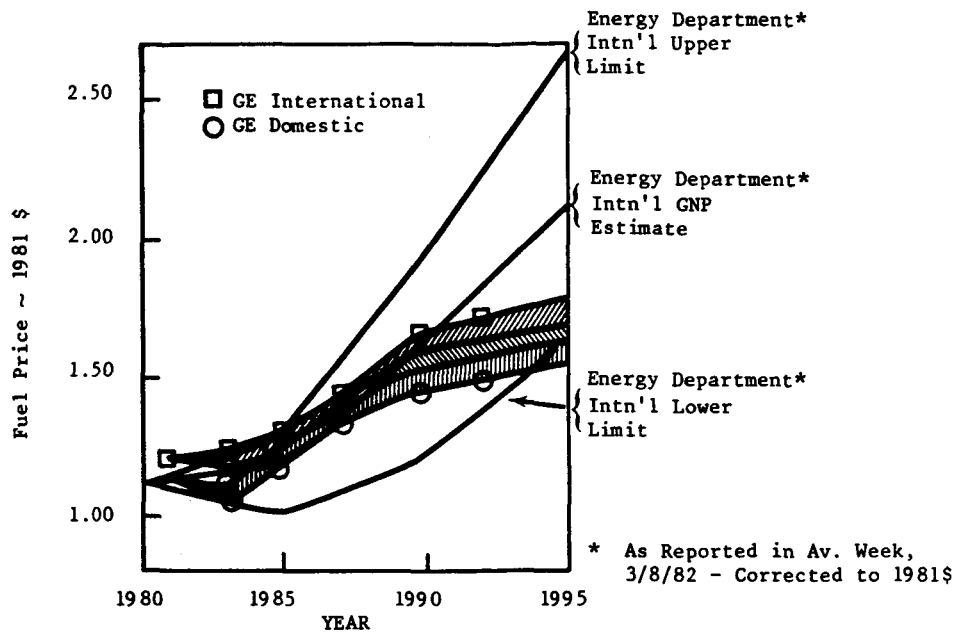


Figure 4.1-2. APET Fuel Price Forecast.

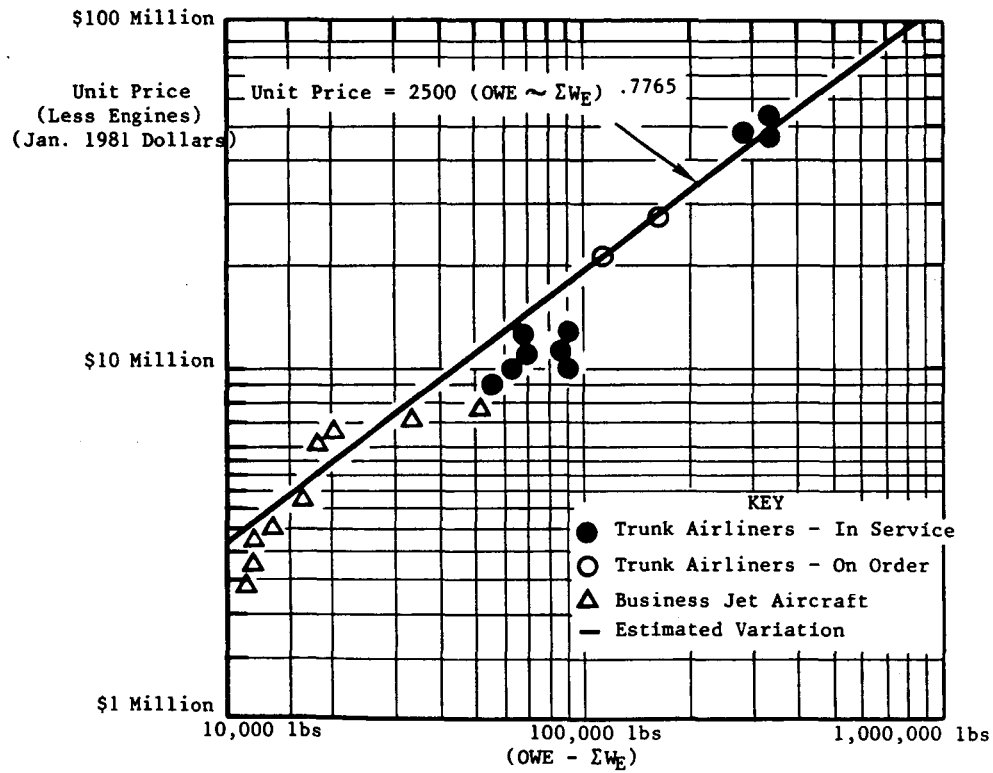


Figure 4.1-3. Estimating Airframe Unit Prices.

that covers interior noise levels and that the major commercial aircraft design companies actually negotiate the levels that are guaranteed to the customer via the airplane model specification that is being proposed prior to a sale. Because of this lack of a mandatory requirement it was thought that interior noise levels of 82-84 dBA would appear to satisfy the study objective.

4.1.5 Emissions

The current standards for newly certified large engines have been issued by the U.S. Environmental Protection Agency (EPA) and cover permissible levels of HC, CO, NO_x, and smoke number for engines above 8,000 pounds thrust as published in the Federal Register dated July 17, 1973. The EPA also has developed prescribed cycles for emissions calculations which allocate fixed time levels for the taxi-idle, takeoff, climbout, and approach parts of the flight regime. On March 24, 1978, some proposed revisions to the earlier publication were contained as a Notice of Proposed Rule Making (NPRM) where SI units were introduced for the new standards. Table 4.1-2 provides the current standards for newly Certificated large engines and Figures 4.1-4 and -5 illustrate the smoke emission standards to be met by turbojet/turbofan engines and turboprop engines respectively. Table 4.1-3 summarizes the regulations of time-in-mode at percent rated power while Table 4.1-4 summarizes the revisions proposed for particulate emissions and Smoke Number in International Standard Units.

Table 4.1-2. Current Standards - Newly Certified Large Engines.

(Federal Register - July 17, 1973)

	Large Turbojet/ Turbofan Engines (>8000 lb Thrust)	All Turboprop Engines
HC	0.4*	4.9 ⁺
CO	3.0*	26.8 ⁺
NO _x	3.0*	12.9 ⁺
Smoke No.	(Fig. 4.1-4)	(Fig. 4.1-5)
*Lbs/1000 lb-Thrust Hrs/Cycle		
⁺ Lbs/1000 HP-Hrs/Cycle		

Table 4.1-3. Current EPA Prescribed Cycles for Emissions Calculations.

Time-in-Mode at Percent Rated Power

Mode	Turbojet/Turbofan Engines		Turboprop Engines	
	Time, minutes	Power, percent	Time, minutes	Power, percent
Taxi-Idle	26	*	26	*
Takeoff	0.7	100	0.5	100
Climbout	2.2	85	2.5	90
Approach	4.0	30	4.5	30

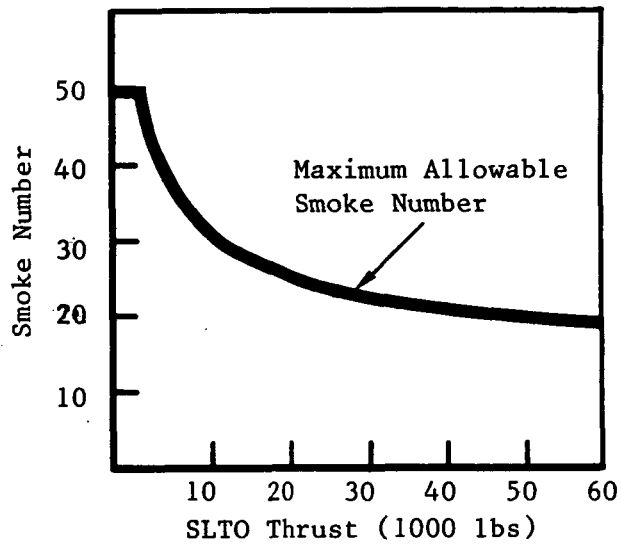


Figure 4.1-4. EPA Smoke Emission Standards-Turbojet/Turbofan Engines.

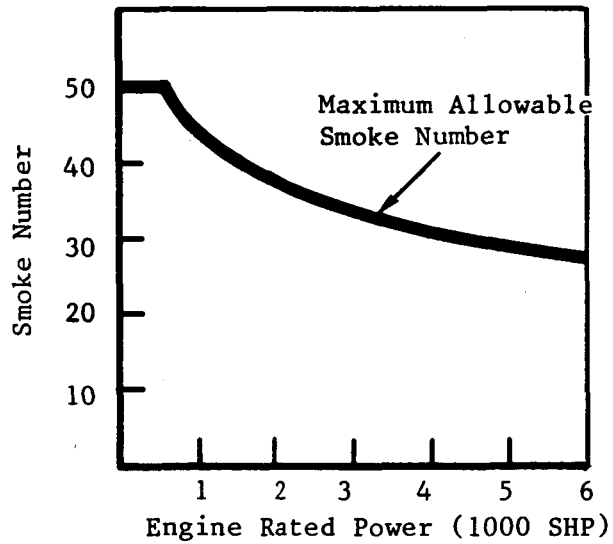


Figure 4.1-5. EPA Smoke Emission Standards-Turboprop Engines.

Table 4.1-4. NPRM Standards - Newly Certificated Large Engines.

(Federal Register - March 24, 1978)

	Large Turbojet/ Turbofan Engines (>27 kN Thrust)	Large Turboprop Engines (>2000 kW Power)
HC	3.3*	0.045**
CO	25.0*	0.34**
NOx	33.0*	0.45**
Smoke No.	79* (kN Thrust)-0.265	277* (kW Power)-0.280
<p>*Grams per Cycle/kN Thrust</p> <p>**Grams per Cycle kW Power</p>		

SECTION 4.2

THE APET AIRPLANES

<u>Section</u>		<u>Page</u>
4.2.1	Configuration and Size Selection	87
4.2.2	Aerodynamic Assumptions and Criteria	93
4.2.3	Performance Objectives	97
4.2.4	Performance Computer Programs	104
4.2.5	Weight Estimating Procedures	106

FIGURES

<u>Figure</u>		<u>Page</u>
4.2-1.	APET Nominal Aircraft Configuration - 150 PAX - Mach Cruise 0.8 Design.	89
4.2-2.	APET Baseline Propfan Airplane Configuration - 150 PAX - Mach Cruise 0.8 Design.	90
4.2-3.	APET Wing Planform Families.	91
4.2-4.	APET Baseline Propfan Airplane Configuration - 150 PAX - Mach Cruise 0.7 Design.	92
4.2-5.	Tail Sizing Criteria.	94
4.2-6.	APET Aircraft Low-Speed L/D Characteristics.	96
4.2-7.	APET Assumed Buffet Limits Cruise Flight - 1G.	96
4.2-8.	APET Baseline Aircraft - Propfan - Mach 0.8 Design.	99
4.2-9.	APET Wing Sizing Criteria.	102
4.2-10.	APET Engine Sizing Criteria.	102
4.2-11.	APET Aircraft Design - Typical Engine and Wing Sizing Study.	103

SECTION 4.2

FIGURES (Concluded)

<u>Figure</u>		<u>Page</u>
4.2-12.	APET Design-Sizing Study.	103
4.2-13.	APET Study - Work Flow.	105

TABLES

<u>Table</u>		<u>Page</u>
4.2-1.	APET Aircraft Study Guidelines.	97
4.2-2.	APET OWE Items - 150 PAX.	98
4.2-3.	Technology Study - Effects of Varying Technology Assumptions.	100
4.2-4.	APET Aircraft Technology - Effect on Comparison of Turboprop vs. Turbofan.	100
4.2-5.	APET Drag Characteristics.	101
4.2-6.	APET Aircraft Sizing Results.	104
4.2-7.	Aircraft Component Weight Estimation.	107
4.2-8.	APET - Typical Weight Buildup.	109

4.2 THE APET AIRPLANE

4.2.1 Configuration and Size Selection

The APET airplane is an advanced technology commercial 150 passenger size design which could be introduced into service circa 1995. There are two basic series, each of which has three variants. These two series are:

1. A turbofan powered airplane with 7.5 bypass ratio engines installed in Long Duct Mixed Flow (LDMF) nacelles
2. An advanced turboprop powered airplane with Hamilton-Standard 10 bladed propfans driven by high-pressure ratio turboshaft engines.

The three variants are the results of the variation of the design cruise Mach number which was set at $M=0.70$, 0.75 and 0.80 . All the designs are of conventional low wing layout with engines installed on the wing. All the airplanes are twin engined.

Overall design goal is to keep the aircraft weight to a minimum, which is consistent with the fuel-efficient performance goals that are the object of this study. Consequently, as indicated in the Introduction (Section 2) the design stage length for maximum payload is set at 1000 n. miles. The selection of the APET design stage length has also been discussed in Section 3.2, where a number of factors have been enumerated and displayed to show the reasons chosen for the size and missions of the APET airplanes.

Aircraft designs were created using a data base largely composed of NASA contractor reports. Early in the design process, some different preliminary design groups were briefed on assumptions being used. Many of the comments and suggestions received during these briefing sessions were utilized to improve the design process and to produce a more credible design. The resulting series of designs is felt to be representative of a design capable of initial operation in the 1990's.

The fuselage contains a passenger cabin having a single aisle layout with all-tourist, six-abreast seating. Seat pitch of 32 inches has been selected for consistency with the operational short haul role. Galley, lavatory and other specialized passenger amenities are held to a minimum of bulk

size and weight - also consistent with short-haul operation. Underfloor cargo space is restricted to an allowance for passenger luggage plus space for up to 5000 pounds of cargo. A two-crew cockpit is assumed and standard provisions for flight attendants are included. These design objectives result in a fuselage which is circular in cross-section with a diameter of 154 inches and overall length of 117 feet 6 inches. Figures 4.2-1 and 4.2-2 are included to show the airplane 3-views for the turbofan and turbopropfan powered airplanes respectively. The figures are restricted to the competitive airplanes suitable for MCR of 0.80 in both cases.

A "family" of wings has been created to match the cruise Mach number selection and these are shown in Figure 4.2-3. It may be noted that all wings have the identical aspect ratio of eleven. The wing family has a fixed planform for each Mach number and the area was selected after computer synthesis of the optimum wing loading. Wing planform is selected to provide space for landing gear when retracted. Spanwise variations of thickness-to-chord ratio were chosen to be a compromise among several pertinent considerations including:

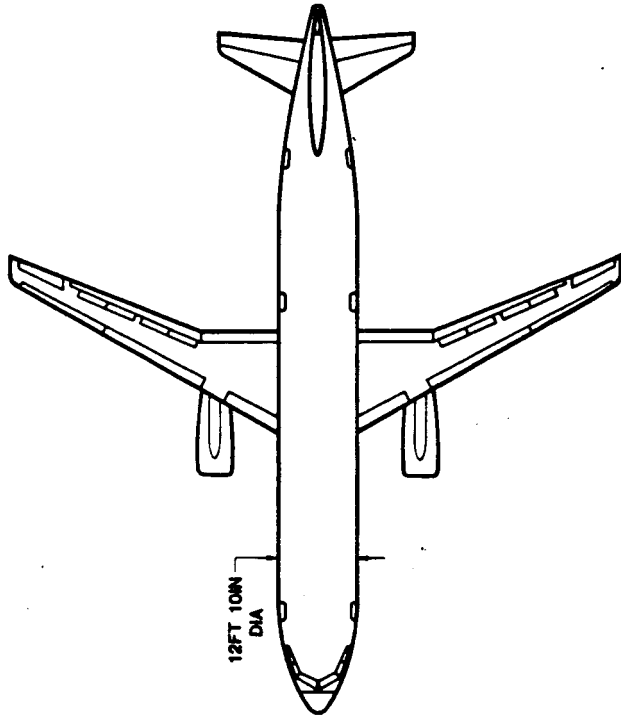
- Structural weight
- Drag in cruise mode
- Fuel volume
- Landing gear storage

All wings achieve performance levels associated with supercritical aerodynamics. All aircraft fuel is carried in integral tanks within the wing structural box, including that portion of wing in the fuselage carry-through region.

Figure 4.2-4 presents a 3-view of the propfan-powered aircraft designed for 0.7 Mach number.

Tail design is conventional. Horizontal tail size is based on a tail volume coefficient consistent with the type of flap system used, and is also based on the use of a relaxed criteria for stability and control employing a neutral type static margin. Vertical tail sizing is based primarily on the effects of yawing moments caused by engine out - asymmetric thrust conditions. Dual-hinged rudder systems are not used, although they may make an effective trade

ORIGINAL PAGE IS
OF POOR QUALITY



SPECIFICATIONS	
MAX TOGW -	111,970 LBS
MAX LANDING WGT -	109,170 LBS
ZERO FUEL WGT -	100,770 LBS
OP. WGT EMPTY -	84,390 LBS
MAX FUEL CAPACITY -	4140 US GAL
WING AREA -	929 FT ² AR - 11.0
TAIL AREAS :	
VERTICAL -	131 FT ²
HORIZONTAL -	134 FT ²
PASSENGER ACCOMMODATIONS :	
180 - ALL TOURIST -	32 IN PITCH
DESIGN MACH NUMBER -	0.8
ENGINES -	2 - 17,410 LBS F. (S.L.S.)

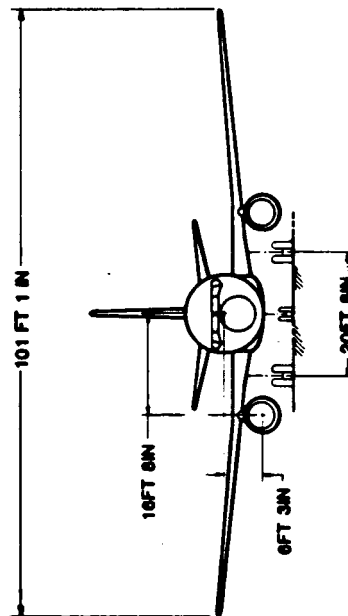
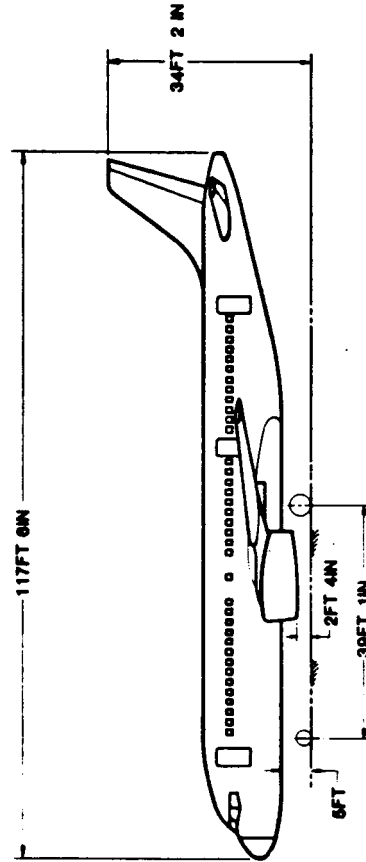
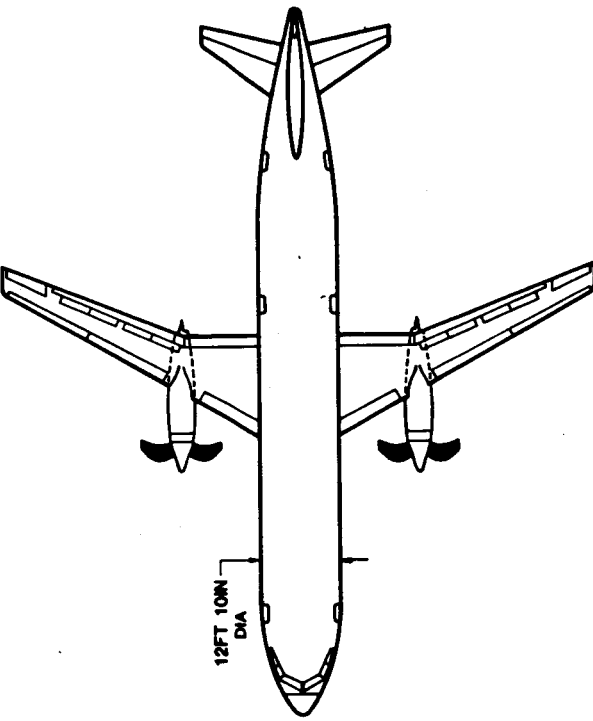


Figure 4.2-1. APET Nominal Aircraft Configuration-150 Pax
Mach Cr. 0.80 Design.



SPECIFICATIONS	
MAX TOGW	- 110,990 LBS
MAX LANDING WGT	- 108,210 LBS
ZERO FUEL WGT	99,890 LBS
OP. WGT EMPTY	65,490 LBS
MAX FUEL CAPACITY	3820 US GAL
WING AREA	- 879 FT ²
AR	- 11.0
TAIL AREAS :	
VERTICAL	- 152 FT ²
HORIZONTAL	- 123 FT ²
PASSENGER ACCOMMODATIONS :	
150	- ALL TOURIST - 32 IN PITCH
DESIGN MACH NUMBER	- 0.8
ENGINES	- 2 - 11,390 SHP EA (S.L.S.)
PROPELLERS	12 FT 6.5 IN DIA EA

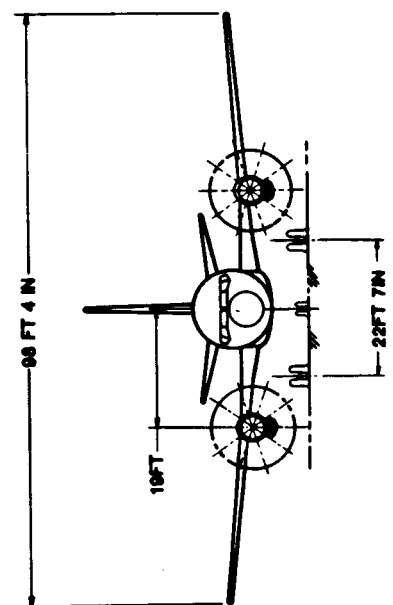
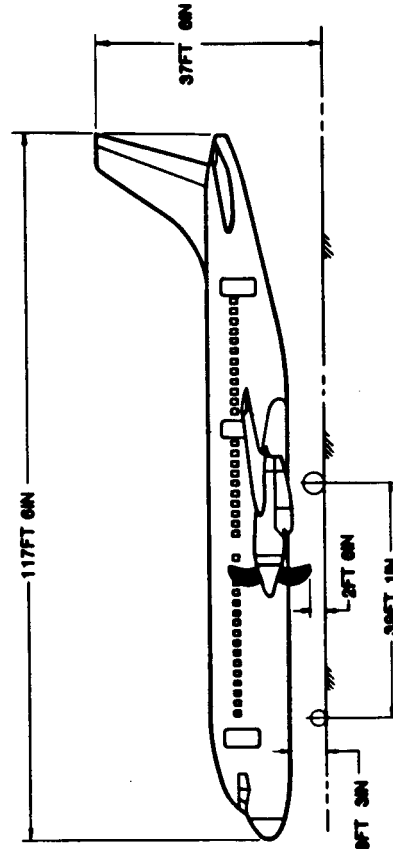


Figure 4.2-2. APET Baseline Propfan Airplane Configuration-150 Pax
Mach Cr. 0.80 Design.

APET WING PLANFORM FAMILIES

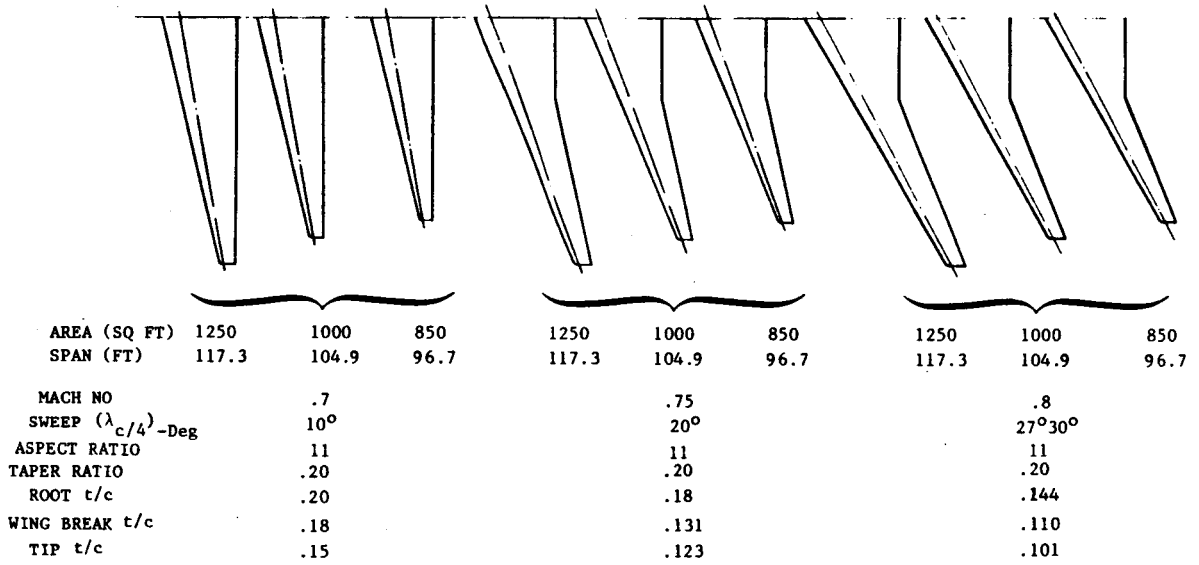
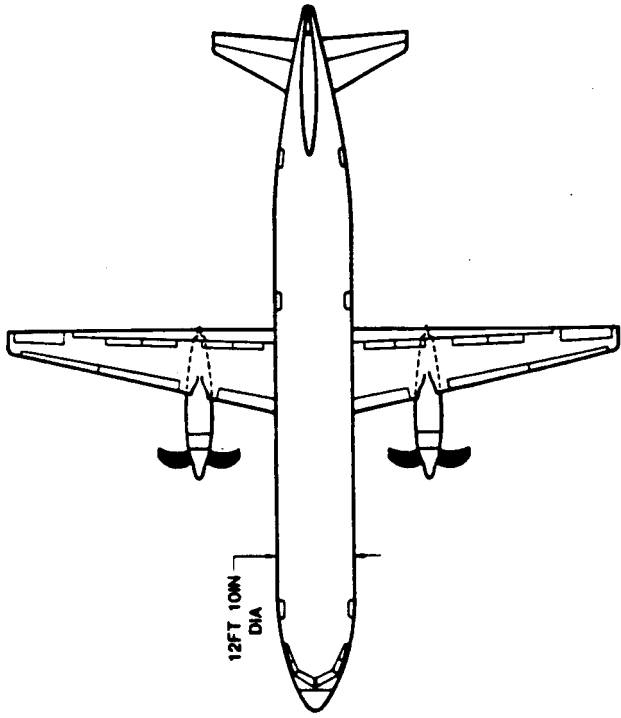


Figure 4.2-3. APET Wing Planform Families.

APET Baseline Propfan Airplane Configuration-150 Pax Mach Cr. 0.70 Design.



SPECIFICATIONS	
MAX TOGW	- 107,310 LBS
MAX LANDING WGT	- 104,630 LBS
ZERO FUEL WGT	96,590 LBS
OP. WGT EMPTY	63,100 LBS
MAX FUEL CAPACITY	3630 US GAL
WING AREA	- 932 FT ² AR - 11.0
TAIL AREAS :	
VERTICAL	- 164 FT ²
HORIZONTAL	- 134 FT ²
PASSENGER ACCOMMODATIONS :	
150	- ALL TOURIST - 32 IN PITCH
DESIGN MACH NUMBER	- 0.7
ENGINES	- 2 - 10,720 SHP EA (S.L.S.)
PROPELLERS	12 FT 2 IN DIA EA

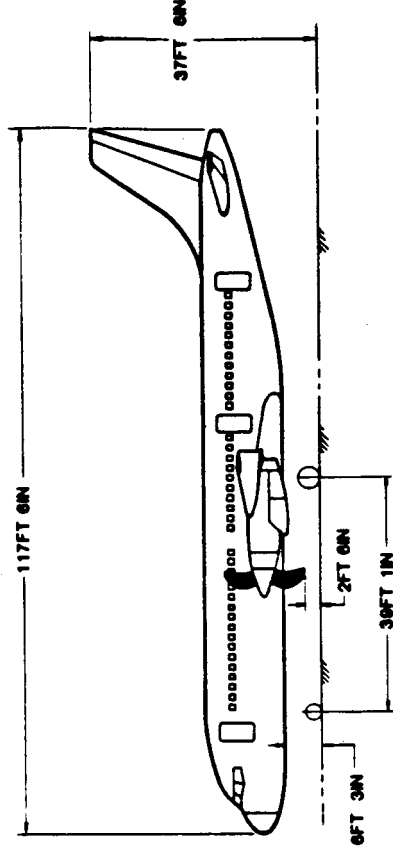
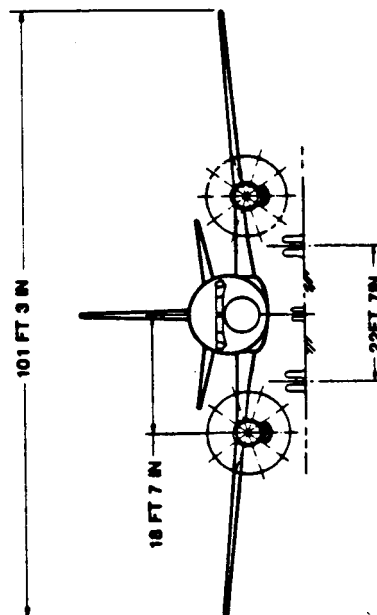


Figure 4.2-4. APET Baseline Propfan Airplane Configuration-150 Pax Mach Cr. 0.70 Design.

study especially for the propfan propulsion system. Figure 4.2-5 gives a schematic representation of the relationships that have been used in sizing the tail surface areas.

The selected landing gear is of conventional design in that the nose gear retracts forward into the bottom fuselage and the main gear retracts sideways into an area aft of the wing box in wing and the fuselage, below the passenger floor. Standard size criteria applies to wheels, tires and brakes and an anti-skid system would be standard as also would be the use of carbon-carbon brakes heat sink material. Landing gear length is computed differently for the turbofan powered airplane compared to the turbopropfan powered airplane and gear weights are adjusted accordingly.

Obviously there are substantial differences in the selection of nacelle designs for the two competing propulsion systems and these are discussed in detail in Section 4.7 of this report. It suffices to say here that the parameters used to locate the turbofan nacelle are conventional and that the turbopropfan nacelles location use a compromise between:

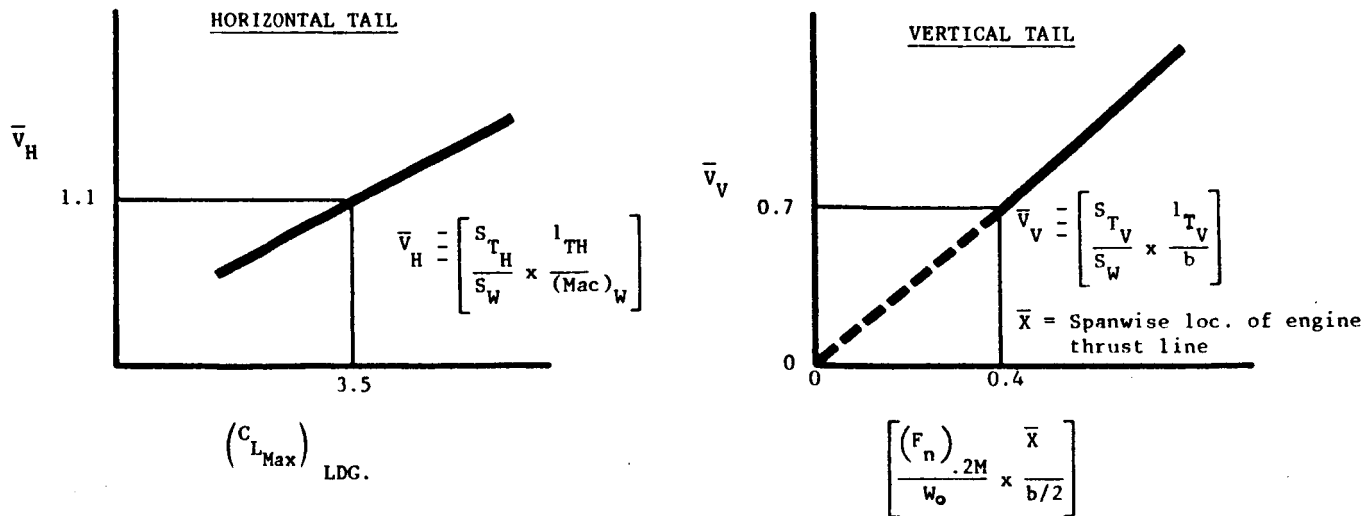
- cabin noise (and associated additional acoustic treatment weight)
- Engine-out asymmetric thrust
- Propfan tip to wing clearance for low $1 \times P$ excitation factors.

(The $1 \times P$ excitation factor is a product of uneven distribution of flow through the propfan actuator disk. It is exhibited as a cyclic force applied to the propfan drive shaft giving rise to cyclic bending moments.)

Estimated nacelle drag characteristics included in the airplane performance analysis are also discussed in Section 4.7.

4.2.2 Aerodynamic Assumptions and Criteria

The APET airplane aerodynamic assumptions and criteria are conventional with the possible exception of the supercritical airfoil selected for a wing with an AR of eleven. Drag levels are based on skin-friction and form drag values that are exhibited by current transport aircraft designs. A time sharing computer program has been used to calculate the drag of the various components (i.e., wing, fuselage, tail, etc.). Nacelle drag is included in the calculation although in the bookkeeping system used in this study, nacelle drag was debited to thrust produced in the engine performance computer programs.



S_{T_H} = Horizontal tail area, ft²

l_{T_H} = Distance of 1/4 chord of horizontal tail from aircraft center of gravity, ft

S_W = Wing area, ft²

Mac_W = Wing Mean Aerodynamic Chord, ft

$(C_{L_{Max}})_{LDG}$ = Lift Coefficient with flaps at landing position

S_{T_V} = Vertical Tail Area, ft²

l_{T_V} = Vertical Tail Length, ft

b = Wing span, ft.

$(F_n)_{.2M}$ = Thrust of one engine at takeoff power at 0.2 Mach flight speed, pounds

\bar{X} = Distance of the thrust line from the aircraft fuselage centerline, ft

W_0 = Takeoff gross weight, pounds

Figure 4.2-5. Tail Sizing Criteria.

Although the selected aspect ratio of eleven is high in comparison to current aircraft with swept wings, it was considered to be a realistic value for an advanced, post 1990, airplane design. Unusual features such as natural laminar flow wings, "winglets", or cranked wings have not been used; and the objective is clearly to improve takeoff, climb and cruise specific fuel consumption values within a comparatively simple framework of advanced technology.

The high lift systems use flap configurations that are based on recent NASA Airframe Contractor studies and typically exhibit maximum C_L levels of 2.5 and 3.5 for the takeoff and landing configurations, respectively. Low speed drag estimates for second-segment climb calculations have been based on a relationship curve of $L/D/\sqrt{AR}$ vs C_L/\sqrt{AR} presented by Torenbeek in his book, "Synthesis of Subsonic Airplane Design," (published in Delft in 1976) as updated by recent NASA data. A presentation of these parameters is included as Figure 4.2-6 which provides the data for the variation in the expected APET airplane climbout drag characteristics as the wing flap angle selection is also varied. The values for aircraft low-speed drag obtained from the figure represent second-segment climb conditions with symmetric powerplant operation. For purposes of engine sizing, in second-segment engine-out configuration, additional drag was estimated for windmilling engines or feathered propeller and for the deflected flight controls necessary to maintain selected heading.

Overall, it is believed that the aerodynamic assumptions and criteria are representative for the quoted time period and may well be improved on as more advanced concepts and technologies find their way into future production commercial airplanes. In any event, this study shows that for equivalent airframe technology assumptions for both the turbofan powered airplane and the turboprop fan powered airplane the difference in aircraft performance is virtually a constant at identical ranges. Thus, the absolute values used in the aerodynamic assumptions are of lesser significance than the necessity for ensuring comparable technology levels for the two competing propulsion systems.

Buffet limits for cruise operations are based on a compilation of flight data on 15 subsonic transport and military cargo aircraft. Curves used in analysis are presented in Figure 4.2-7. The normal 0.3g margin is assumed for cruise operating conditions.

Symmetric Flight - Flap Setting Varies-Turbofan Aircraft

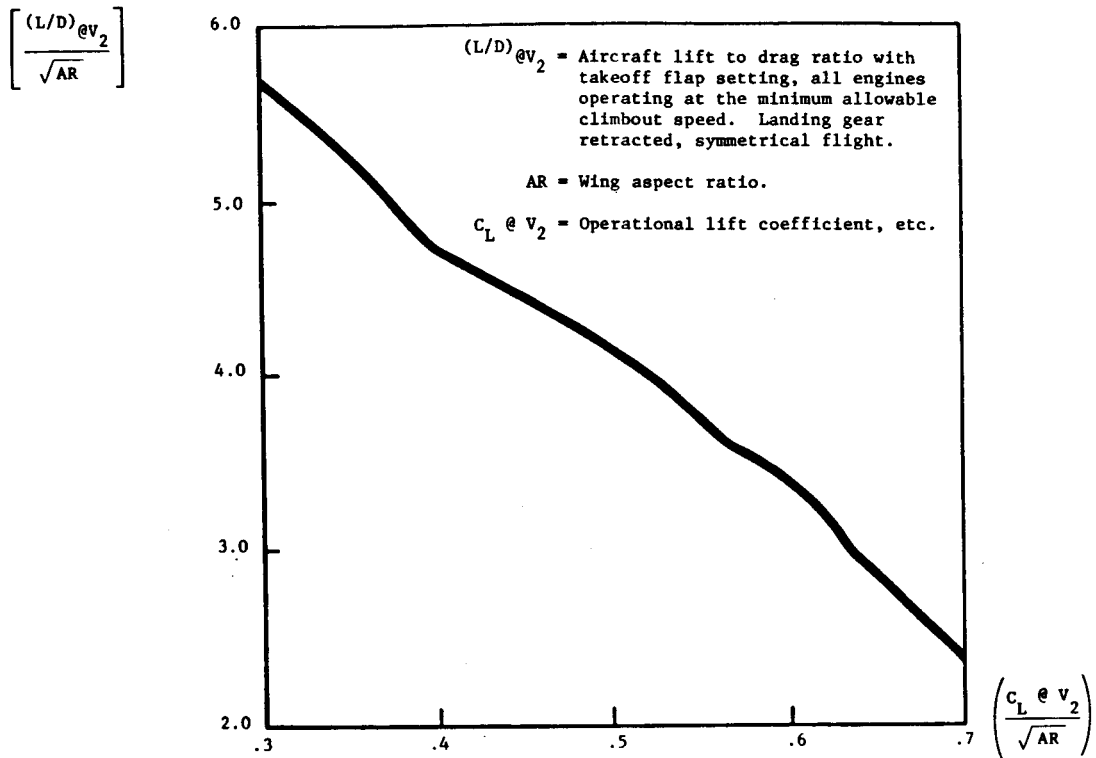


Figure 4.2-6. APET Aircraft Low-Speed L/D Characteristics.

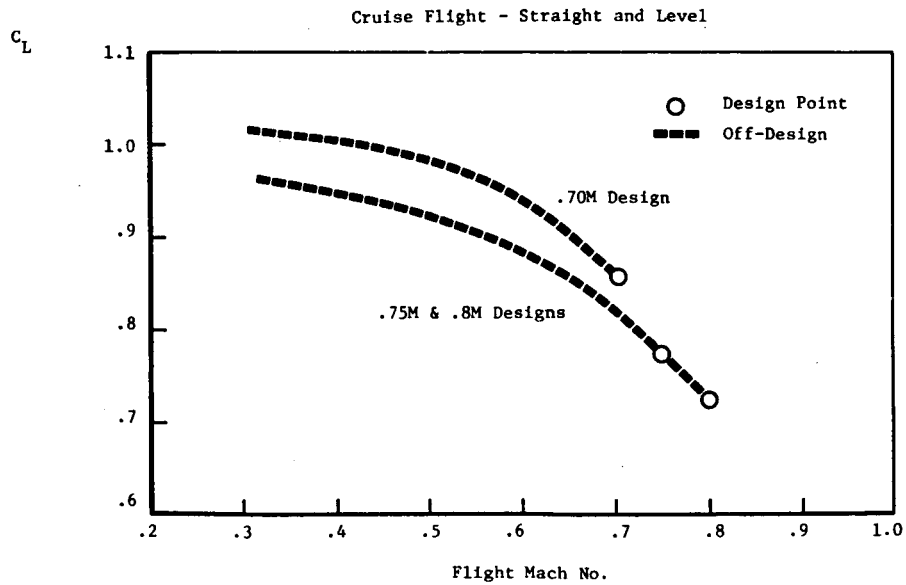


Figure 4.2-7. APET Assumed Buffet Limits.

4.2.3 Performance Objectives

The general ground rules discussed in Section 4.1 are combined with definitive aircraft specifications and listed in Table 4.2-1. The basic philosophy was to define an advanced technology aircraft operating under flight and economic conditions as are known today (i.e., runway lengths, certification requirements, speed limits and stage lengths). A specific requirement was the full-payload design stage length and this was chosen to be 1,000 N. miles. The APET aircraft was designed to this basic stage length.

Table 4.2-1. APET Aircraft Study Guidelines.

Aircraft Technology/Timing	- Service Introduction after 1990
Maximum Number of Passengers	- 150
Passenger Arrangement	- All Tourist Class, Six-Abreast, 32" Pitch
Design Range Capability (Full Payload)	- 1000 N Mi
Average Stage Length	- 300 N Mi
Field Length (Sea Level)	- 6000 Ft (Sea Level) at Maximum TOGW
Alternate Field Length	- Denver (Hot Day); Weight for Trip to San Francisco (100% LF)
Engine-Out Ceiling	- 15,000 Ft
Design Cruise Mach Number	- Varies: 0.7 to 0.8
Required Cruise Altitude Capability	- 35,000 Ft - Design Range Mission
Maximum Approach Speed	- 135 Kts. (At MLW = 0.975 x Maximum TOGW)
Number of Engines	- 2
Engine Location	- On Wing
Propulsion Types	- Turbofan and Turboprop (Propfan)
Cruise Speed/Altitude	- Will Vary with Design Mach and Stage Length
Takeoff Gross Weight	- Variable (Fall-Out)
Wing Design	- Sweep and Thickness Varies with Design Mach
Wing Aspect Ratio	- 11 (For All Values of Design Mach No.)
Measures of Merit	- Maximum TOGW - Fuel Burn at 300 N Mi Stage Length - DOC at 300 N Mi Stage Length

The "basic" stage length choice is significant. A very long stage length (relative to PAX and Cargo) provides flexibility in extending the aircraft to high revenue through flights. However the built-in weight penalties for this capability reduce revenue on the more popular (high load factor) short range flights. A study of current and past North American Air traffic indicates that the most economically viable aircraft would have a "basic" range of 1000 N. miles with high usage in the 300 N. mile stage length range. Using the maximum load "basic" range of 1000 N. miles as an aircraft design criteria sets the fuel capacity and weight of the aircraft. The off-design performance resulting from fuel efficiency enhances the flexibility of the aircraft. As shown in Figure 4.2-8, a 1000 N.M. A/C can have a profitable operation in the 300-1000 N. mile range at full capacity with a "return to base" or supplemental route capability of approximately 2500 N. miles with a 65 percent payload.

Assuming the "Basic" 300-1000 mile duty cycle passenger amenities and services can be scaled down appropriately (as opposed to a 4 hr. trans-continental flight). The basic OEW Items assumed for this purpose are shown in Table 4.2-2.

Table 4.2-2. APET OEW Items - 150 PAX.
(Pounds)

Flight Crew (2)	340
Cabin Crew (4)	520
Crew Baggage	130
Briefcases	50
Food, Beverages	1100
Food Service Equipment	
Potable Water	150
Toilet Chemicals	40
Misc. Cabin Equipment	300
Wash Water	
Emergency Equipment	300
Unusable Fuel	250
Engine Oil	170
Bins for Baggage	<u>750</u>
	4100

APET BASELINE AIRCRAFT
 Propfans - Design Mach = 0.8

Max. TOGW = 110990 lb

- ① Max Payload (ZFW Limited) - 34402 lb
- ② Design Payload - 150 Pax - 30750 lb
- ③ Design Range - with 150 Pax
- ④ Payload - 65% LF (98 Pax) - 20090 lb
- ⑤ Range Capability @ 65% LF
- ⑥ Fuel Capacity - 3820 U. S. Gal.

ZFW = Zero Fuel Weight

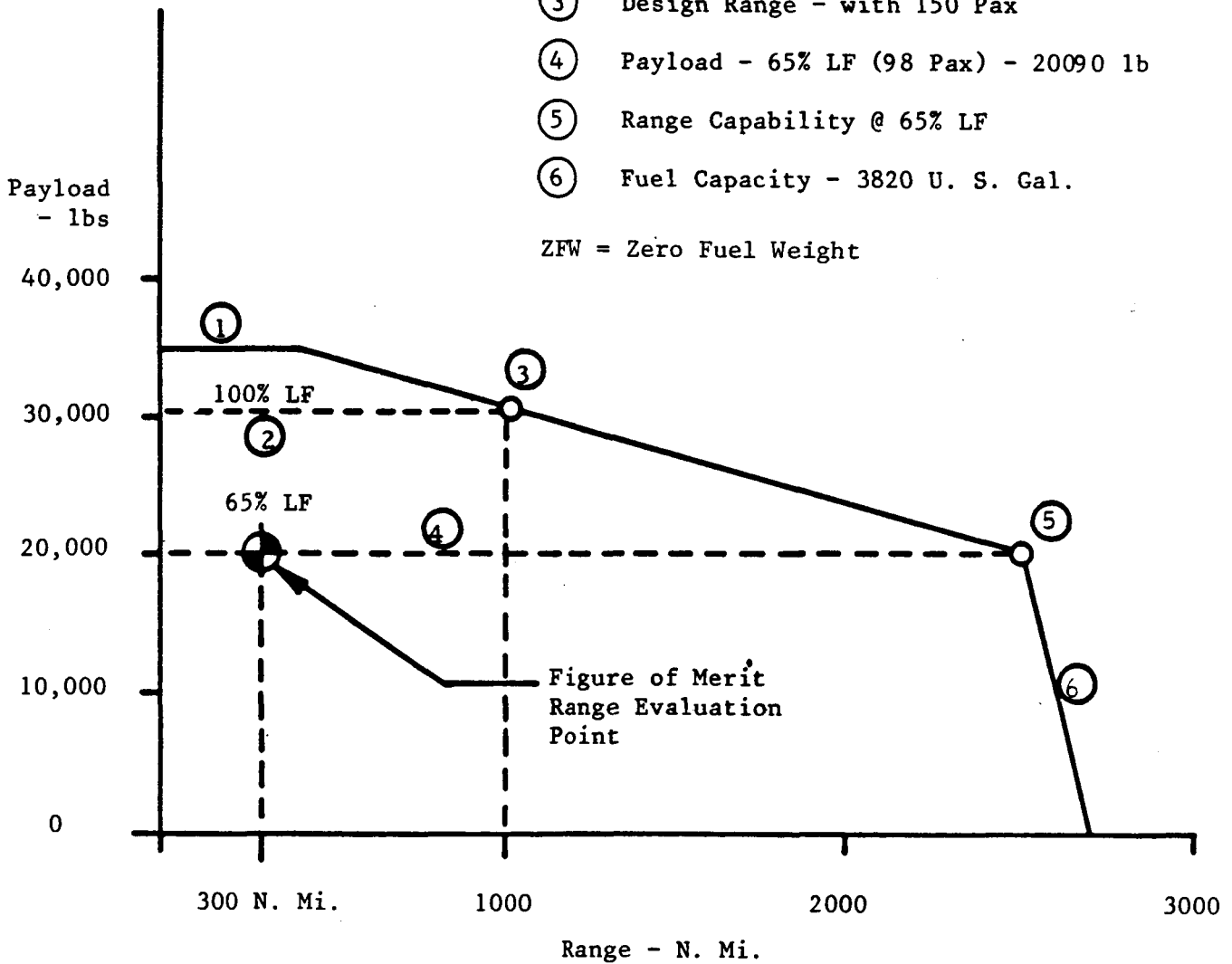


Figure 4.2-8. APET Baseline Aircraft Propfans - Design Mach = 0.8.

A perspective of assumed 1995 APET technology relative to established technology is in order. Table 4.2-3 enumerates the magnitude and chronology of technology relative to the selected APET airplane parameters.

Table 4.2-3. Technology Study Effects of Varying Technology Assumptions.

Code	Engine Technology	Airframe Aero	Airframe Weight	Design Range	TOGW	Percent Reduction In TOGW	Fuel Burn 1000 NMI (65% LF)	Percent Reduction in Fuel Burn	Fuel Burn 300 NMI (65% LF)	Percent Reduction in Fuel Burn
1	CF6	AR = 9	1972	2000	155606*	>7.7	12949*	>18.0	5335*	>18.2
2	"APET"	AR = 9	1972	2000	143583	>1.8	10613	> 3.7	4361	> 2.6
3	"APET"	AR = 11	1972	2000	140860	>9.6	10131	> 7.1	4222	> 7.6
4	"APET"	AR = 11	1995	2000	125823	>8.9	9212	> 3.6	3818	> 4.5
5	"APET"	AR = 11	1995	1000	112000		8749		3579	

*Baseline Values for Percentage Calculations

An obvious question asked in evaluating "advanced" technology is "what is real?" Absolute level of future entities is difficult to assess. However, relative changes on a common base is a realistic place to start. Table 4.2-4 compares turboprop versus turbofan technology gains on a current (old) technology basis and an advanced technology basis (new). The simple statement of this table is that neither the turbofan or the turboprop have been awarded an advantage, relative to each other, in advanced technology that they do not have in current technology (based on the parameter of Fuel Burn).

Table 4.2-4, APET Aircraft Technology.

• Effect on Comparison of Turboprop Versus Turbofan

Technology Level Used	TOGW Ratio*	Fuel Burn Ratio* (R = 300)
"1972" Weights AR = 9 Design Range = 2000 NMI	"Old" 0.987	0.815
"1995" Weights AR = 11 Design Range = 1000 NMI	"New" 0.992	0.817

*Ratios are based on $\frac{\text{Turboprop}}{\text{Turbofan}}$

Table 4.2-5 summarizes the calculated aerodynamic characteristics of a 0.8 M APET aircraft. These are general and offered as an order of magnitude type representation. They are based on evaluation of flight test data for other real aircraft.

Table 4.2-5. APET Drag Characteristics.

Typical Cases - Propulsion System Not Installed									
Design Mach No.	0.8	→							
Wing Sweep - degrees	27.5°	→							
Average Wing (t/c)	0.1225	→							
Wing Aspect Ratio	11	→							
Wing Area	900	900	900	1000	1000	1000	1130	1130	1130
Flight Mach No.	0-0.70	0.75	0.80	0-0.70	0.75	0.80	0-0.70	0.75	0.80
C _{D₀}	0.01914	0.01914	0.0201	0.01819	0.01819	0.0191	0.01724	0.01724	0.0181
k	0.0432	0.0445	0.0551	0.0432	0.0445	0.0551	0.0432	0.0445	0.0551
C _{L₀}	0.1	→							

$$C_D = C_{D_0} + k (C_L - C_{L_0})^2$$

C_{D₀} = Airplane drag coefficient at C_L = C_{L₀}.

C_{L₀} = Airplane lift coefficient for defining the drag polar offset.

k = The induced drag factor.

After the payload and economic considerations have been resolved the actual procedure of sizing aircraft wing and engine must occur. The mathematical methods have been with us for years, the criteria and procedures vary, within limits, relative to regulations and manufacturer. Figures 4.2-9 and 4.2-10 state the criteria used for wing and propulsion system sizing. These items are a result of Government regulations and a consensus of aircraft manufacturers' statement of requirements.

The procedure, once the criteria are defined, is mathematically complex but fully understood. Thrust-to-weight versus wing-loading relative to the design criteria are calculated (Figure 4.2-11), this addresses safety concerns. T/W versus wing-loading and fuel burn and TOGW versus wing-loading and thrust-to-weight address economic concerns, (Figure 4.2-12). Fuel burn and weight are directly convertible to dollars. The summary of sizes, points are shown in Table 4.2-6.

Factors Affecting Choice of Wing Size (Wing Loading)

- Takeoff Field Length
- Second-Segment Climb Gradient
- Enroute Engine-Out Climb Gradient
- Landing Field Length
- Limiting Value of Approach Speed
- Buffet Limits (Cruise)
- Wing Fuel Volume
- Wing Weight

Figure 4.2-9. APET Wing Sizing Criteria.

Thrust will be Sized for:

- Takeoff Field Length - 6000 Feet - Sea Level (ISA + 27° F).*
- Denver Field Length (OAT = 92° F).*
- Enroute Engine-Out Ceiling - 15,000 Feet (ISA + 18° F).
- End of Climb Thrust Required (ISA + 18° F) - Thrust Margin for 300 fpm Rate of Climb.

*Also must meet second-segment climb gradient requirements.

Note - Engine-Out Sizing Conditions Include:

Aircraft Symmetric Drag - Low Speed (With High Lift Devices)
- High Speed (Clean)

Windmilling Drag (Or Feathered Drag)

Rudder/Aileron Drag.

Figure 4.2-10. APET Engine Sizing Criteria.

ORIGINAL PAGE IS
OF POOR QUALITY

EF
n. 2M SL
Max. 10GW

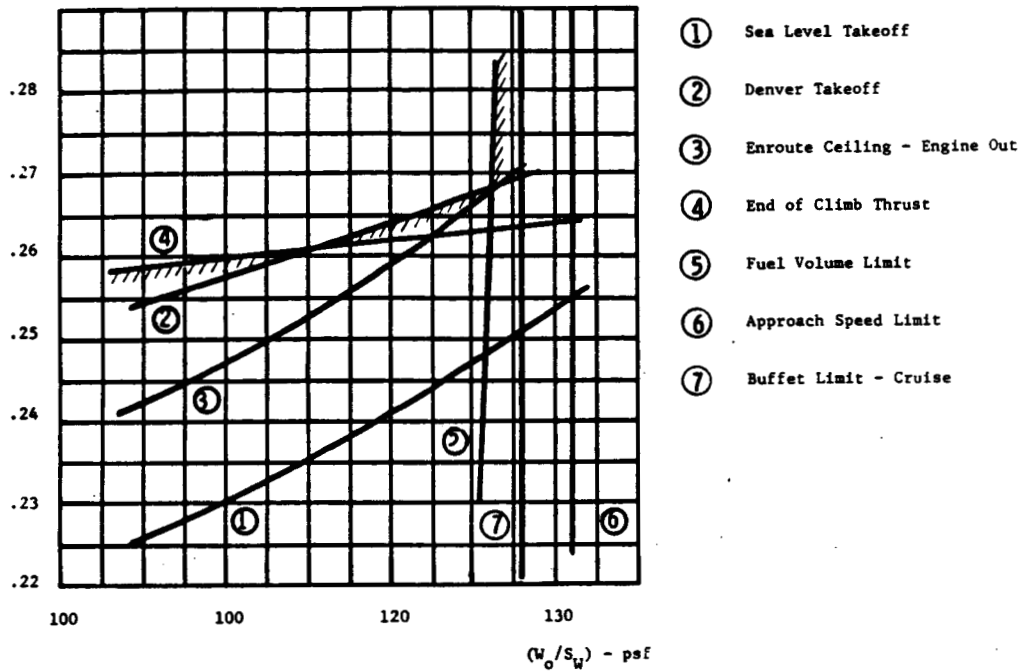


Figure 4.2-11. APET Aircraft Design Typical Engine and Wing Sizing Study Design Mach Number = 0.8 Propfan Propulsion.

Propfan - Design Mach = 0.8

$$\frac{\text{SHP}}{D^2} = 37.5$$

SHP = Shaft horsepower
D = Propfan diameter, feet

— Locus of combinations which meet all sizing limits (Wing and Engine)

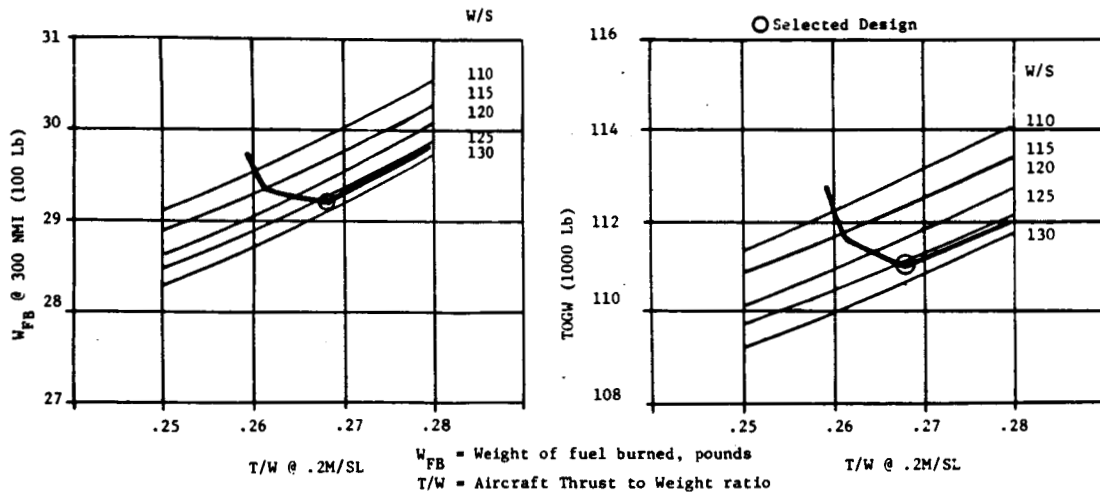


Figure 4.2-12. APET Design - Sizing Study.

Table 4.2-6. APET Aircraft Sizing Results.

Design Mission - 1000 NMI

Powerplant Type	Propfan			Turbofan		
	0.7	0.75	0.8	0.7	0.75	0.8
Design Mach No.	0.7	0.75	0.8	0.7	0.75	0.8
Selected (W_0/S_W)	115.2	120.5	126.2	115.2	120.5	120.6
Selected $F_n, W_0 @ 0.2M/SL$	0.261	0.264	0.268	0.235	0.240	0.249
Wing Sized By:	Buffet	Buffet	Fuel Capacity	Buffet	Buffet	Fuel Capacity
Engine Sized By:	Denver TO	Denver TO	Denver TO	Denver TO	Denver TO	Denver TO
Resulting TOGW	107309	108845	110986	108036	109305	111970

4.2.4 Performance Computer Programs

The analysis described in the preceding sections was performed using the G.E. mission analysis computer program. This program is capable of calculating mission performance of either turbojet, turbofan or turboprop transport airplanes for the following modes of operation:

- Takeoff (fuel allowance only)
- Constant altitude acceleration
- Constant Mach number climb
- Constant altitude and Mach number cruise
- Constant Mach number climb to optimum Breguet cruise altitude
- Constant altitude and Mach number cruise after discontinuous change in altitude and Mach number
- Breguet cruise
- Constant altitude deceleration

- Decelerated descent along $q = f(XM^2)$ path
- Constant Mach number descent
- Maneuver mode (used for reserves)

The nondimensional aircraft drag characteristics (drag polar) and weight are inputted to the program. A matrix of engine performance data (net thrust as a function of altitude and Mach number) is run on the cycle deck and placed in a file. This file is read by the mission program.

The mission program "flies" a "rubber" airplane. That is, aircraft weight, engine weight and engine thrust are adjusted (scaled) to match the mission requirements. The output of the mission program (aircraft weight, fuel burn) reflect the complex interaction of engine thrust - SFC characteristics and aircraft design.

The computer program is also capable of determining the effects of small changes and, hence, can be used to obtain sensitivity factors.

As a result of recent in-house commercial aircraft studies, a systematic computerized approach for executing the mission analysis portion of this study has been devised. Figure 4.2-13 describes the general work flow and identifies the various inputs and considerations that were included in the study. The work flow is rather straightforward and generally does not involve iterative loops.

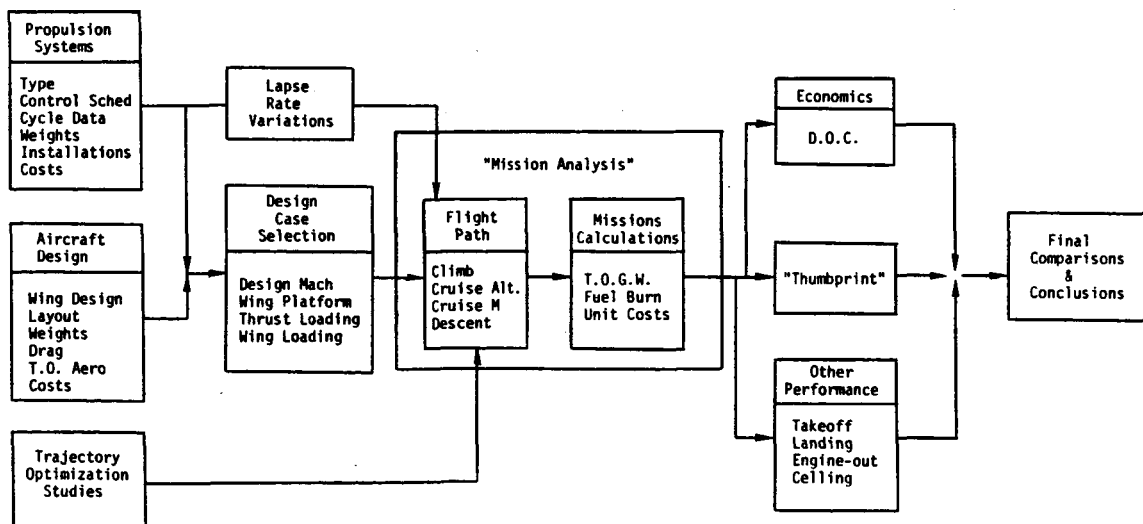


Figure 4.2-13. Study Work Flow.

C-2

4.2.5 Weight Estimating Procedures

Aircraft main assembly, component, system and subsystem weights have been estimated using formulae that have, for current technology level commercial aircraft, provided reliable answers in previous studies. The methodology of determining the projected (lower) weights for a post-1990 state-of-the-art airplane is a two-step process. First, current aircraft weights have been estimated for the size class of the APET airplane by using a base from published data of existing aircraft types as contained in Reference 33. Where necessary, the formulae in this report have been modified to reflect additional available data on the commercial airplanes and have also been supplemented by other formulae to cover subsystems not contained in the published report (e.g., passenger furnishings and OWE items). This resultant group of formulae serves to predict what might be called "1972" weight technology.

The second step concerns the weight reduction factors that could be assumed to reflect the weight changes to be expected as advanced technology is projected into airplane designs of the 1995 time period. This technology will typically include such items as:

- Supercritical wing technology
- Advanced aluminum alloys
- Composite materials in non-primary structures
- Advanced manufacturing processes
- Advanced avionics and on-board computers
- Advanced system, component and subsystem designs.

The weight reduction factors selected for this study are shown in Table 4.2-7, and were based on surveys of published data and were modified after discussions with the principal airframe design companies. The factors shown are believed to provide some reasonable but challenging goals for the airplanes of the 1995 time period.

Furnishings and equipment weights have been held to a minimum by using passenger accommodations with comfort levels between those currently used by commuter aircraft and those now used by trunk airlines and also be reducing and/or omitting certain equipment now required for long-haul operations (but

Table 4.2-7. Aircraft Component Weight Estimation.

Component/System	Reference Weight ⁽¹⁾	Weight Reduction ⁽²⁾ Factors, (Est.)
Wing - Bending Structure Wing - Shear and Other Str. Tail Fuselage Landing Gear Fuel System Flight Controls - Hydraulics Electrical Pneumatics and Air Cond. Anti-Icing Instruments Avionics Furnishings OWE Items	Base 	0.9 0.8 0.85 0.90 0.9 1.0 0.8 ⁽³⁾ 1.0 ⁽³⁾ 0.8 ⁽³⁾ 1.2 ⁽³⁾ 1.0 0.75 0.9 1.00
<p>(1) "1972 Technology"</p> <ul style="list-style-type: none"> - Represents Technology of 727/737/DC9, etc. - Data base from S.A.I./Douglas Report (NASA CR-151970) (Ref 33) - S.A.I./Douglas Formulas - Modified by G.E. <p>(2) "1995 Technology"</p> <ul style="list-style-type: none"> - Represents APET Technology - Estimated using S.A.I./Douglas data base with Weight Reduction Factors - 2% Weight Contingency added - Austere passenger furnishings and accommodations (because aircraft is used on short stage lengths). <p>(3) All Electric Airplane</p>		

not needed for short-haul operation). A crew of 6 persons has been assumed - two in the cockpit crew and four in the cabin. Cabin furnishings weights have been based on use of two lavatories and two galleys. Cabin furnishing estimates have been extracted from a data base which includes only short-haul aircraft (F28, 737, 727, etc.). Cabin furnishings include a basic amount of acoustic treatment material suitable for a turbofan aircraft.

By concentrating on the "short-haul" aspects there can be some reduction and in some cases omissions of weight items that would normally be included at 100 percent factors. Overall the Operational Weight Empty (OWE) is estimated to be in the 84 to 85 percent band compared with today's equivalent airplane rated

at 100 percent. These values apply directly to the turbofan powered airplane and other factors must be introduced to account for the differences required for turboprop power.

Three of the weight items which are different when the propfan is used are:

Landing Gear	(Generally longer and heavier)
Vertical Tail	(Generally larger area and heavier)
Acoustic Treatment	(More, due to different noise characteristics)

Propfan weights which include the blades, hub, pitch change mechanism, controls and anti-icing features have been directly taken from Hamilton-Standard parametric weight data packages. Gearbox and engine weights have been generated two ways. One is a parametric method using in-house computer programs while the other involves producing a layout drawing and converting this via computer vision terminals into weight data. Nacelle and systems weights also used a combination of parametric and direct calculations.

Engine weights are calculated by a computer program that is directly linked to the design program. Weights are modified in the computer system whenever detail engine designs, or new engine hardware is developed and physically weighed. These programs have stood the test of time and have been used in numerous commercial and military engine studies.

For the mission analyses programs, it was necessary to estimate the weight breakdown of each of the six baseline airplanes - three turbofans and three turboprop fans at design cruise Mach numbers of 0.70, 0.75 and 0.80. One of these weight breakdowns is given as a typical example in Table 4.2-8 for the Mach cruise 0.80 turbofan powered airplane. Weight data for the other five aircraft are given in Figure 3.8-1 (already shown). Elsewhere in this report, (See Section 4.8 of this report) the full range of the variation in Takeoff Gross Weights (TOGW) is given in tabular form for the six point design airplanes.

Table 4.2-8. APET - Typical Weight Buildup.

- Turbofans - 0.8M Design Load
- "1995" Weight Technology

	<u>Pounds</u>
Wing	9987
Tail	1247
Fuselage	14850
Landing Gear	4468
Propulsion (Installed)	9372
Fuel System	639
Flight Controls	1417
Electrical	2540
Air Conditioning, APU	2375
Anti-Icing	265
Furnishings and Eq. (TF)	9653
Added Cabin Acoustics	0
Instruments	553
Avionics	1793
Loading and Handling	0
Miscellaneous	<u>133</u>
Calculated Empty Weight	(59292)
Contingency (2% of Airframe Wt)	<u>996</u>
Empty Weight	(60288)
OWE Items	<u>4100</u>
OWE	64388
Passengers (150)	30750
Cargo	0
Fuel (Design Range)	<u>16832</u>
TOGW	111970

SECTION 4.3
REFERENCE TURBOFAN ENGINE

<u>Section</u>		<u>Page</u>
4.3.1	Definition	113

FIGURES

<u>Figure</u>		<u>Page</u>
4.3-1.	APET Baseline Turbofan Engine Changes From FPS Standard E ³ .	114
4.3-2.	Reference APET Turbofan Description.	115
4.3-3.	APET Baseline Turbofan - Weight and Dimensions.	116
4.3-4.	Final APET Turbofan - Engine Sizes.	117

PRECEDING PAGE BLANK NOT FILMED

4.3 REFERENCE TURBOFAN ENGINE

4.3.1 Definition

A baseline APET turbofan engine has been designed with technology assumptions believed valid for service introduction in the year 1995.

As previously discussed, the APET turbofan is based on a scaled-down version of the E³ Flight Propulsion System (FPS) engine, in an equivalently scaled-down nacelle. Figure 4.3-1 shows the general layout of the design and includes notation that highlights the major differences from the full-scale FPS system. Figure 4.3-2 is included to show the similarities, and the differences where they exist, between the full and sub-scale systems.

The E³ turbofan (full scale) engine compression system employs a single stage fan, single stage booster with continuous bypass bleed (driven by a 5-stage LP turbine) pressurizing a 10-stage axial compressor driven by a 2-stage HP turbine. A low smoke, low emissions burner design supplies the hot gas used for driving both sets of turbines and for mixing with the bypassed fan airflow. A high efficiency, low delta pressure, advanced technology mixer exhausts the total engine flow via a common propelling nozzle.

Initial airplane and propulsion sizing studies showed that the required characteristic thrust size dictated a cycle match point at the end of climb, at maximum climb power. This match point yields, for Mach 0.80 flight speed, 35,000 ft. altitude on a Standard Day + 18° F, a thrust level of 4000 pounds.

The demonstrated core performance of the full-scale E³ engine has been selected as a target value for the significantly smaller core size of the APET Turbofan. (APET is approximately 47 percent of the full-scale E³.) This target is difficult to achieve when scaling a highly efficient set of components down to a smaller flow size; and in order to make the goal, certain component efficiency values need to be improved to offset the reduction in efficiency that results from tip clearance losses and Reynolds number effects. The component assumptions that are made between E³ and APET are also shown in Figure 4.3-2 where it may be noted that the number of LP turbine stages has been

PRECEDING PAGE BLANK NOT FILMED

- Cycle Parameters at M0.80/35000' + 18° M_xC₁
 - PR Fan Tip = 1.55
 - PR Fan Hub = 1.75
 - PR Core = 23.0
 - PR Overall = 40.2
 - BPR = 7.1
 - Turbine Temp. = 2258?2490° F (M_xC₁/Denver)

- Configuration - Mixed Flow
 - 1 Stage Fan
 - 1 Stage Booster with Continuous Bleed
 - 10 Stage Core
 - 2 Stage HPT
 - 6 Stage LPT

- Component Assumptions Relative to GE E³ FPS Cycle
 - Fan η = +1.2%
 - Core η = No Change
 - HPT = +0.2%
 - LPT = +0.8%
 - ΔCooling Air = -2.35 Pts

In Full
E³ Size

- Component Sizes
 - For 4000 lb M_xC₁ Thrust 10.8/35K + 18°
 - Fan $W\sqrt{\theta/\delta}$ = 728
 - BPR = 7.1 SLS FN = 17600 lb
 - Core $W\sqrt{\theta/\delta}$ = 56.6

Figure 4.3-2. Reference APET Turbofan Description.

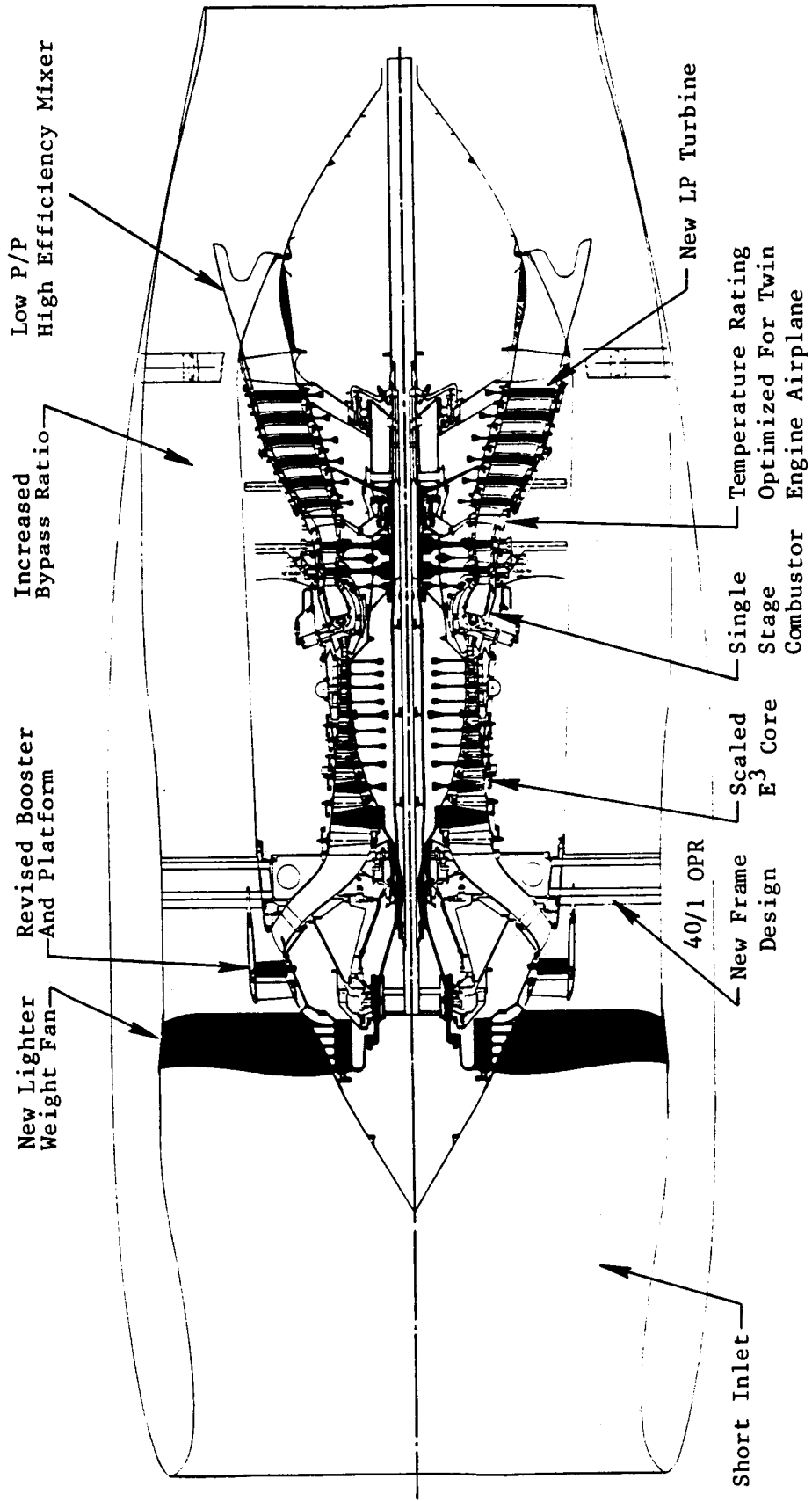


Figure 4.3-1. APET Baseline Turbofan Engine Changes from FPS Standard E³

increased from the five (used on the full-scale E³) to six on this scaled version.

For this thrust size, using the scaled E³ components, a preliminary design was made for an engine with a fan diameter of 59.6 inches and a flow of 731 pounds/second. These and other data including a weight breakdown are shown in Figure 4.3-3.

The nominal turbofan powered airplane for MCR = 0.80 is as shown in Figure 3.1-1. Installation factors for an isolated turbofan engine are well known and need not be amplified in this study report; however, it is important to note that some on-the-wing effects have been excluded by NASA direction. This exclusion will also apply to some of the factors for the turboprop, as is amplified later in this report.

Fan Dia.	=	59.6 inches	Basic Engine Weight	=	3103 lb
*Length	=	90.0 inches	Mixer and Reverser	=	615 lb
			Installation	=	735 lb
			Pylon	=	<u>445</u>
					4898 lb

*Length is defined as Fan Rotor leading edge to aft flange of engine rear frame.

Figure 4.3-3. APET Baseline Turbofan - Weight and Dimensions.

For the case of the turbofan installation, there is no universally acceptable criteria for estimating the incremental drag from isolated to a fully installed propulsion nacelle, especially for the long duct mixed flow configuration being used as this study's baseline. For the case of the turboprop installation, it appears appropriate that these incremental effects be added at some later point in time. The ongoing NASA-Ames wind tunnel program is showing dramatic drag improvements with wing leading edge extensions, wing-to-nacelle fillets and contoured nacelles (non-axisymmetric). Certainly it seems that the

turboprop increment can be held to a value that is similar to the turbofan with the process of refinements that are being actively explored by NASA and their Industry Contractors.

The turbofan installation loss bookkeeping system identified a 3.6% thrust loss due to the nacelle friction drag with a further 0.7% loss for the pressure drag. The inlet and exhaust losses are bookkept in the engine cycle format as they are also for the turboprop installation.

The final APET turbofan engine sizes for the three different cruise Mach numbers considered are summarized on Figure 4.3-4 where fan and core engine corrected airflow as well as fan diameter and installed thrust are shown for each cruise Mach number studied.

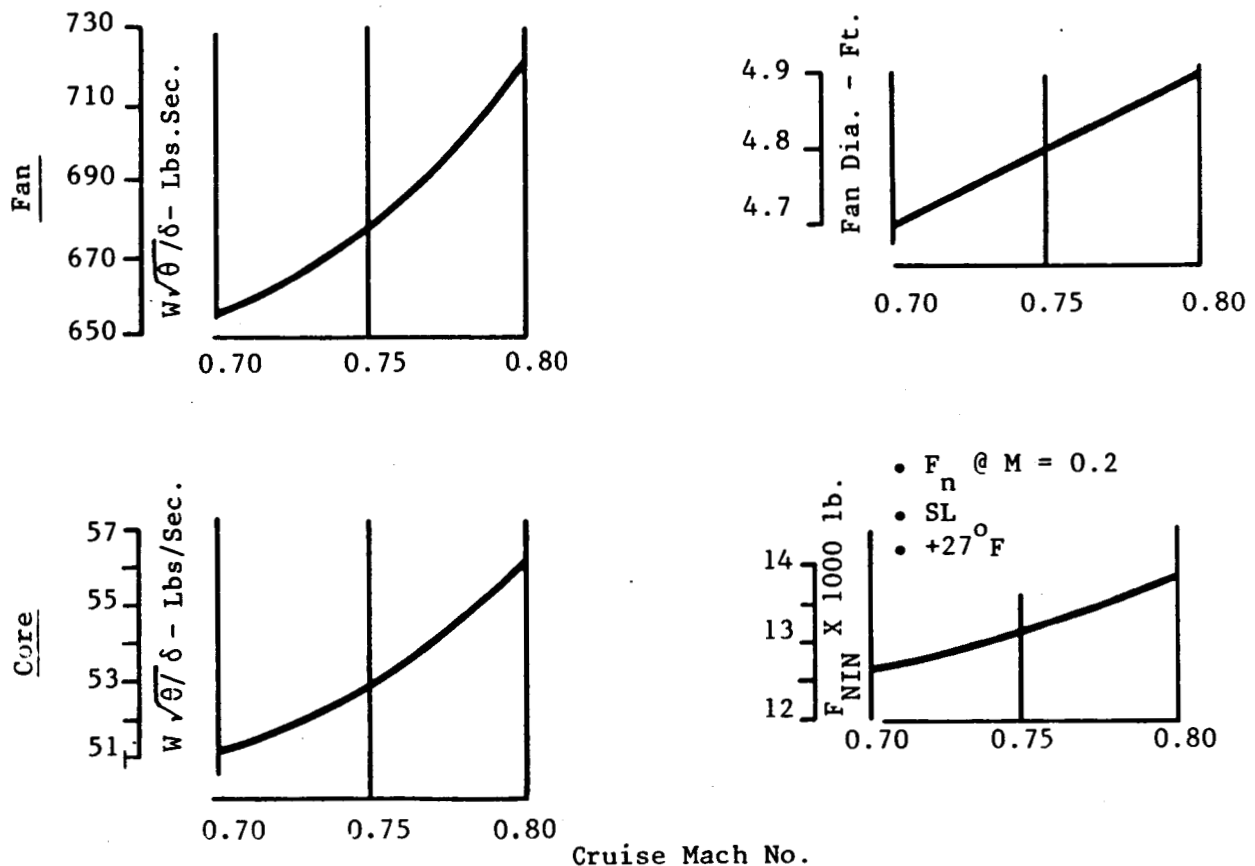


Figure 4.3-4. Final APET Turbofan Engine Sizes.

SECTION 4.4

APET TURBOSHAFT ENGINES

<u>Section</u>		<u>Page</u>
4.4.1	Candidate Engines and Descriptions	123
4.4.2	Selected Study Engines and Cycles	131
4.4.3	Engine Weight and Cost	142
4.4.4	Cycle Selection Summary	142
4.4.5	Other Cycle Parameters	145
4.4.6	Propeller Selection	149

FIGURES

<u>Figure</u>		<u>Page</u>
4.4-1.	APET Engine Number 1 - Unboosted Turboprop - (All Axial Compression System) - 2 Shaft Engine.	125
4.4-2.	APET Engine Number 2A - Boosted Turboprop - (All Axial Compression System) - 2 Shaft Engine.	126
4.4-3.	APET Engine Number 2B - Boosted Turboprop - (All Axial Compression System) - 2 Shaft Engine.	127
4.4-4.	APET Engine Number 3A - Boosted Turboprop - (Axi-Centrifugal Compression System) - 2 Shaft Engine.	128
4.4-5.	APET Engine Number 3B - Boosted Turboprop - (Axi-Centrifugal Compression System) - 2 Shaft Engine.	129
4.4-6.	APET Engine Number 4 - Boosted Turboprop - (All Axial Compression System) - 3 Shaft Engine.	130
4.4-7.	APET Turboprop Gas Generator - Axial Flow Compressor - Four Stage Power Turbine.	133

PRECEDING PAGE BLANK NOT FILMED

119

PAGE 118 INTENTIONALLY BLANK

SECTION 4.4 (Continued)

FIGURES (Continued)

<u>Figure</u>		<u>Page</u>
4.4-8.	APET Turboprop Gas Generator - Axi-centrifual Compressor - Four Stage Power Turbine.	133
4.4-9.	APET Turboprop Gas Generator - Axial Flow Compressor - Three Stage Power Turbine.	134
4.4-10.	APET 2B "Baseline" Engine (12,500 SHP).	136
4.4-11.	APET 3B "Baseline" Engine (12,500 SHP).	137
4.4-12.	Cycle Pressure Ratio and T41 Impact on Performance Component Sizes at T3 Levels.	140
4.4-13.	Final APET Turboshaft Engine Sizes.	141
4.4-14.	APET Baseline (Axi-Axi) Engine and Gearbox.	143
4.4-15.	APET Alternate (Axi-Axi) Engine with Split Gearbox.	143
4.4-16.	APET Engine (Axi-Axi) with Concentric Gearbox.	144
4.4-17.	Baseline APET Boosted Turboprop Description.	145
4.4-18.	Propfan Propeller Performance - 10 Blade Configuration.	147
4.4-19.	APET Uninstalled Performance Comparisons.	147
4.4-20.	APET Propeller Tip Speed Study.	148
4.4-21.	The Propeller System.	150
4.4-22.	Ten-Blade, 1986 Propfan Projections- Drag Coefficient Versus Mach Number.	152
4.4-23.	Single Rotation 10-Blade Propfan - Max. Pitch Change Flow Versus Diameter.	152
4.4-24.	Drag and Propeller Speed Versus Windmilling SHP at Pitchlock (Mach 0.2, Sea Level).	153
4.4-25.	Drag and Propeller Speed Versus Windmilling SHP at Pitchlock (Mach 0.74, 35,000 ft.).	153

SECTION 4.4 (Concluded)

FIGURES (Concluded)

<u>Figure</u>		<u>Page</u>
4.4-26.	Windmilling Drag and Percent Tip Speed Versus Design SHP/D ² and Tip Speed (Mach 0.2, Sea Level).	154
4.4-27.	Windmilling Drag and Percent Tip Speed Versus Design SHP/D ² and Tip Speed (Mach 0.2, Sea Level).	154

TABLES

<u>Table</u>		<u>Page</u>
4.4-1.	Candidate Turboshaft Engines.	124
4.4-2.	APET Turboprop Configuration Studies - Cycle Assumption Comparisons.	138
4.4-3.	APET Turboprop Configuration Studies - Component Aerodynamic Comparisons.	139
4.4-4.	APET Uninstalled Comparisons.	149

4.4 APET TURBOSHAFT ENGINES

4.4.1 Candidate Engines and Descriptions

Six candidate turboshaft engines were defined and a preliminary design was completed for each. The design process used calculates the flowpath from given input cycle parameters and determines casing configuration; number of stages required; blade to vane axial spacing; numbers of blades and vanes required; burner configuration; frame and bearing and shafting layouts. All the engines have been designed to produce 12,500 SHP at SL static conditions. The computer programs provide data in a form that allows rapid design definition by drawings and automated calculation of both weight and costs. These computer programs are continually being refined by comparison to experimental and production engine hardware and have been extensively used in other commercial and military studies. Table 4.4-1 lists the principal characteristics of the six candidates examined while Figures 4.4-1 through -6 show these engines driving a baseline propfan reduction gearbox and propfan. All the engines are enclosed within a nacelle contour that includes a single, offset, inlet duct as the source of air supply.

The original engine definitions matched the full-size E³ engine in cycle pressure ratio; and all were sized to produce 4000 lb. of thrust (with the selected propfan) at Maximum Climb Power, 35,000 ft. altitude, Mach 0.80 flight speed, and a free air ambient temperature of Standard Day + 18° F. Because of lapse rate differences and a range of temperature ratings studied, there were significant differences in shaft horsepower transmitted through the propeller gearbox to the propfan. In order not to delay the process of preliminary design for the gearbox and the nacelle/engine installation, it was decided to fix a baseline value of 12,500 SHP at the propfan drive face. In terms of SHP at the engine output shaft (booster front frame station), this equates to approximately 13,000 SHP engine delivery power level. Note that approximately 300 gearbox horsepower is reserved for driving airframe accessories while a further loss occurs due to inefficiency in the drive system itself. Thus, when using the computer deck and the scaling laws for APET engines, it is essential to note that the SHP produced by the deck is at the engine shaft before it powers the propfan gearbox.

Table 4.4-1. Candidate Turboshaft Engines.

Case No.	Engine Description	Low Pressure Compressor Stages	High Pressure Compressor Stages	HP Turbine Stages	LP Turbine Stages	Overall Pressure Ratio
1	Unboosted 2 Shaft	-0-	10 Axial	2	3	23:1
2(a)	Boosted 2-Shaft	1, high r/R	10 Axial	2	3	38:1
2(b)	Boosted 2-Shaft	2, low r/R	10 Axial	2	3 or 4	38:1
3(a)	Boosted 2-Shaft	1, high r/R	5 Axial 1 Centrifugal	2	3	38:1
3(b)	Boosted 2-Shaft	2, low r/R	5 Axial 1 Centrifugal	2	3 or 4	38:1
4	Boosted 3-Shaft	2, low r/R	10 Axial	*	*	38:1

*This engine used a single stage HP turbine, a single stage intermediate turbine, and a 3-stage LP turbine acting to drive the third shaft as a free turbine.

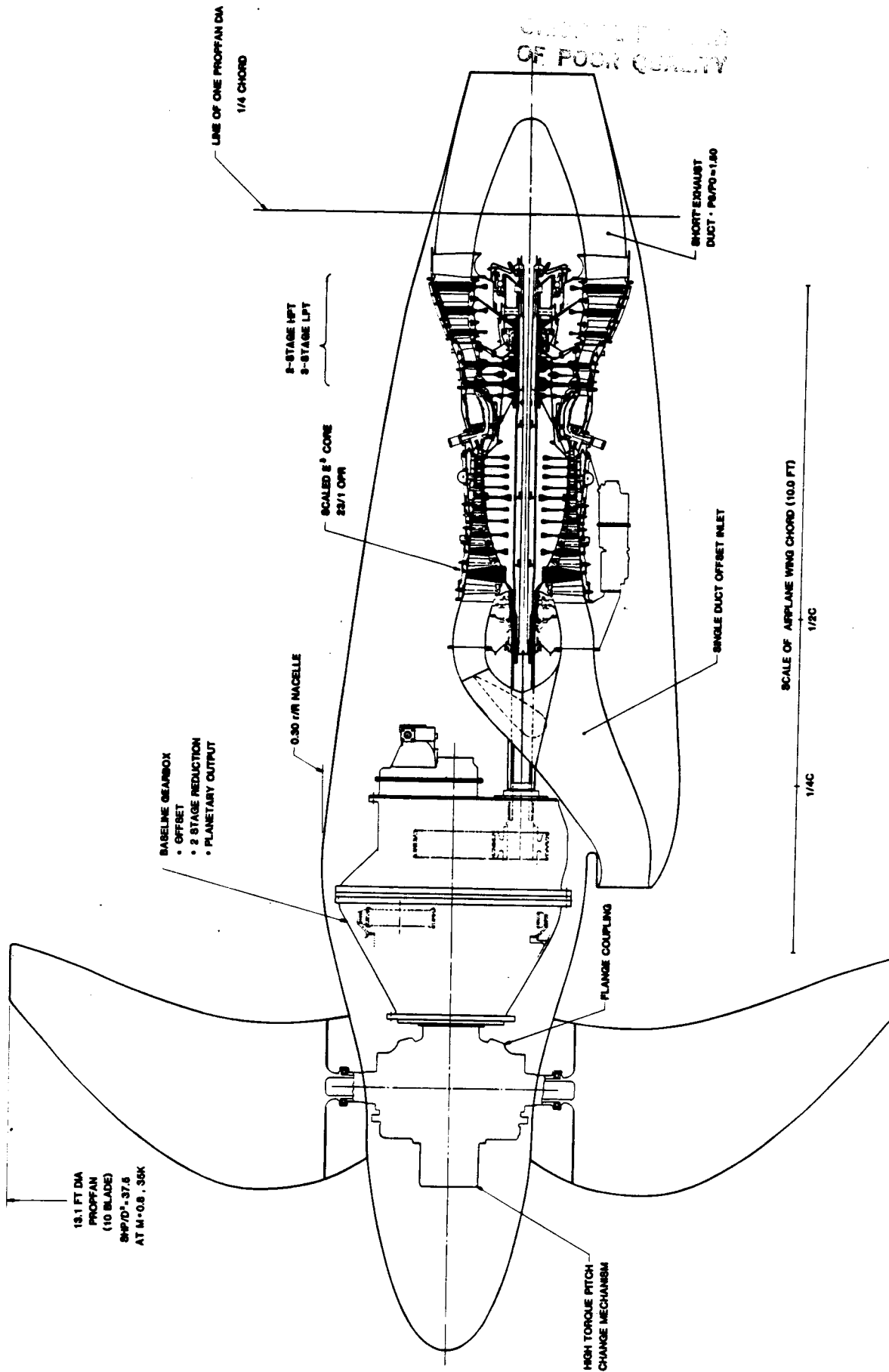


Figure 4.4-1. APET Engine No 1-Unboosted Turboprop
 (All Axial Compression System)
 2 Shaft Engine.

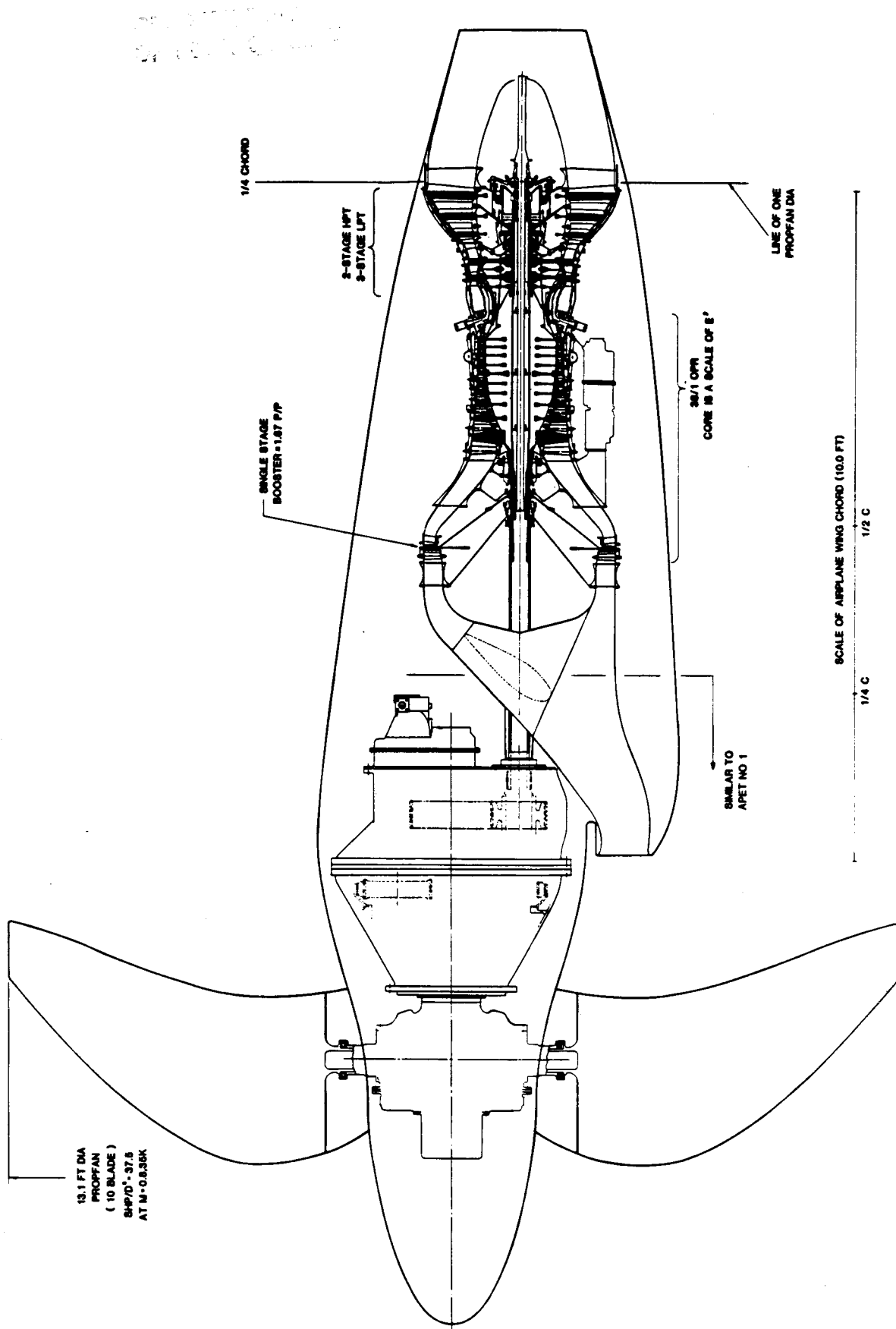


Figure 4.4-2. APET Engine No 2A-Boosted Turboprop
 (All-Axial Compression System)
 2 Shaft Engine.

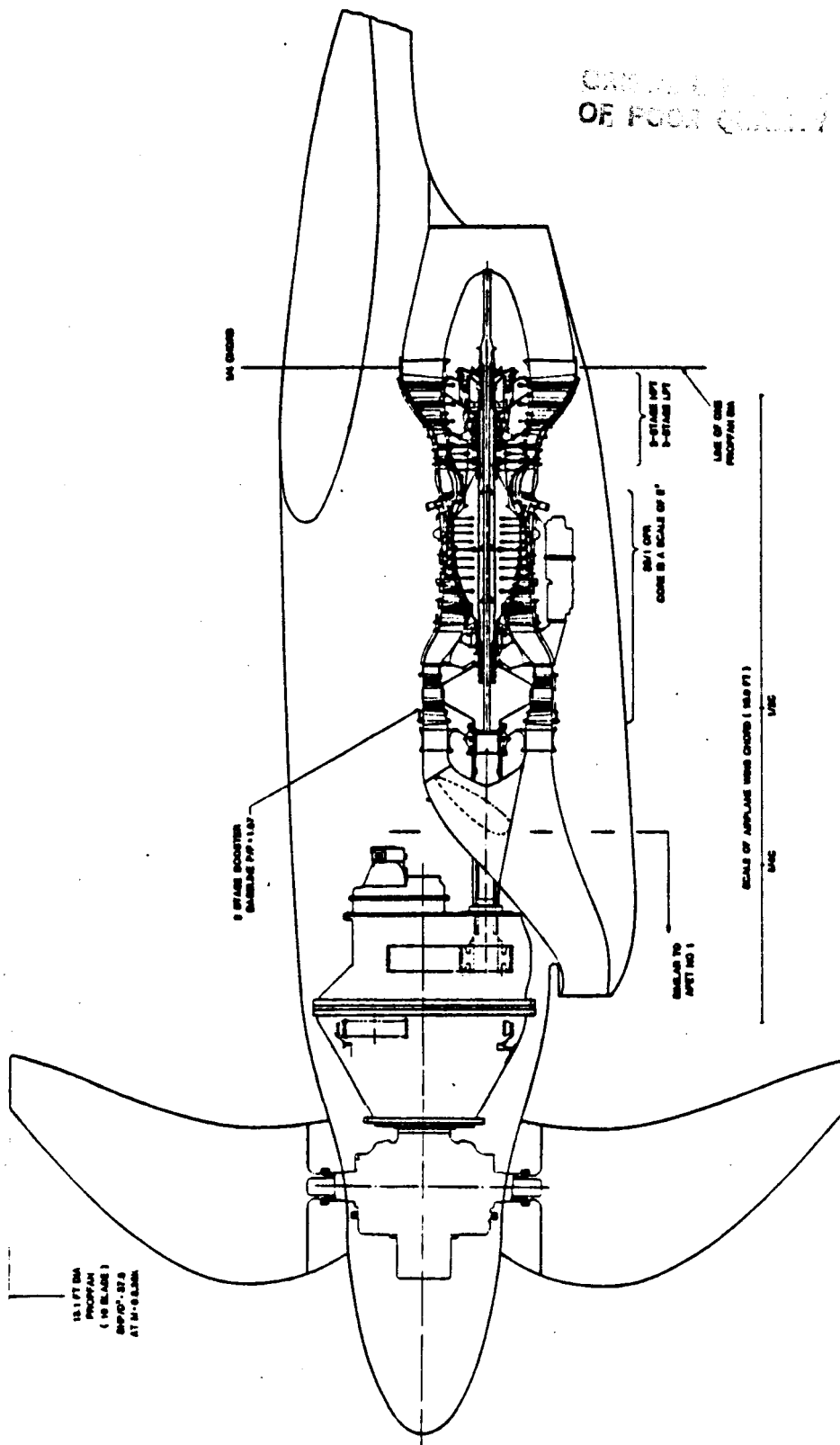


Figure 4.4-3. APET Engine No 2B Boosted Turboprop
 (All Axial Compression System)
 2 Shaft Engine.

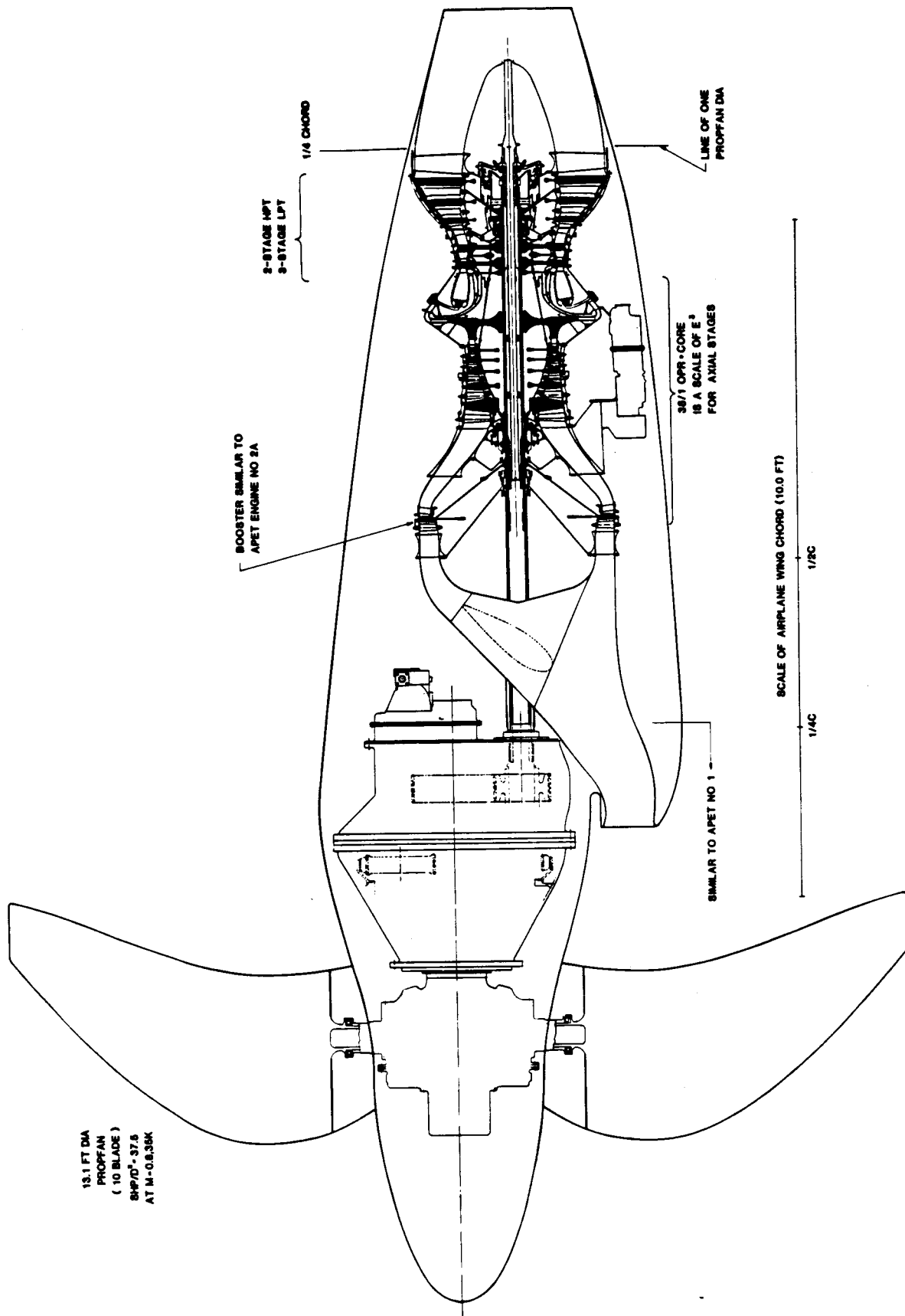


Figure 4.4-4. APET Engine No 3A-Boosted Turboprop
 (Axi-Centrifugal Compression System)
 2 Shaft Engine.

OF HIGH QUALITY

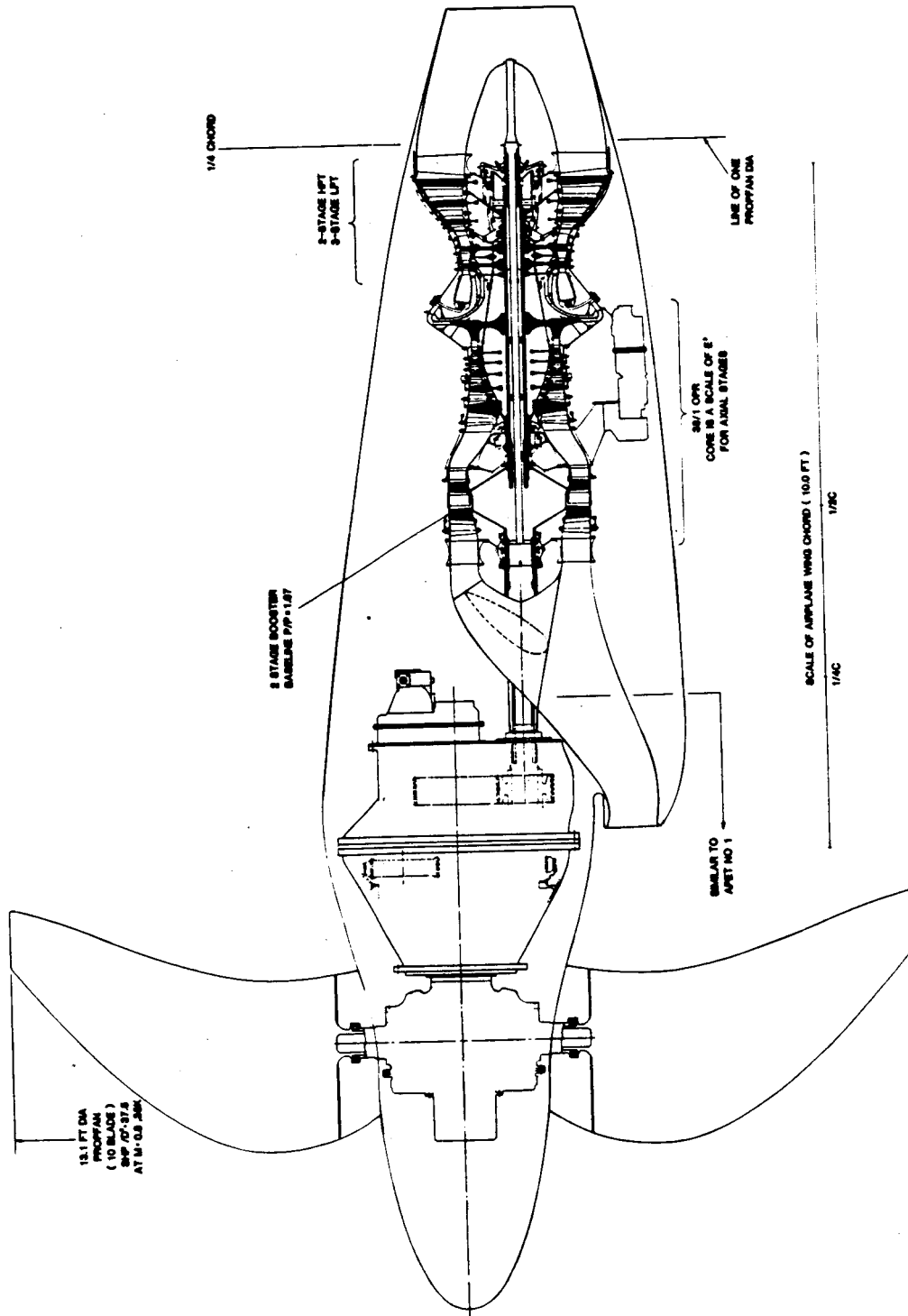


Figure 4.4-5. APET Engine 3B-Boosted Turboprop (Axi-Centrifugal Compression System) 2 Shaft Engine.

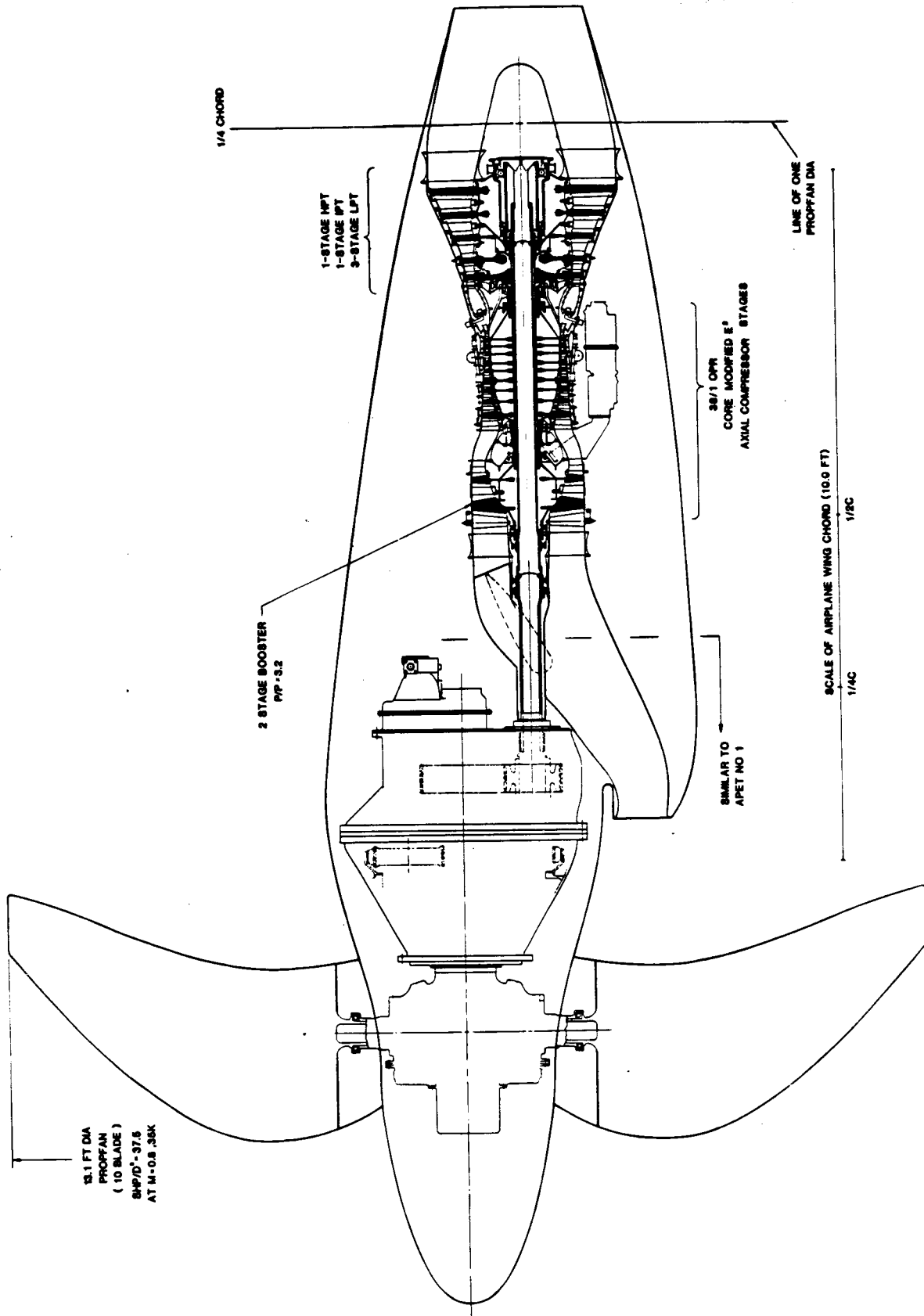


Figure 4.4-6. APET Engine No 4-Boosted Turboprop
 (All Axial Compression System)
 3 Shaft Engine.

This value of 13,000 SHP then falls halfway between the lower end of the NASA desired study level of 8,000 SHP and their desired upper end value of 18,000 SHP. This selection thus gives extra credibility to both the up and down scaling exponents used for the principal elements of the propulsion system.

Temperature lapse rates and ratings have been selected from studies that determined that only a small delta value between take-off and end of climb should be used to hold the core engine size to minimum values, and 100° F has been used in all latter parts of the APET shaft engine studies.

4.4.2 Selected Study Engines and Cycles

From the six candidate turboshaft engines, NASA selected engines 2(b) and 3(b) for further study. Both these selected engines have the low radius ratio 2-stage booster arrangement with Variable Inlet Guide Vanes (VIGV's) and are projected to achieve optimum performance when the boost pressure ratio is set at 1.75. The overall pressure ratio of the machines is then raised from the baseline 38:1 to just over 40:1 at full corrected speed. It is not certain at this time whether a 3-stage or a 4-stage LP turbine would be selected as prime; and it is recommended in the component development plan shown later in this report that a significant effort should be made to design and test high-flare low pressure turbine layouts employing orthogonally directed blade airfoils, at a power size that would lead credibly to the establishment of the required technology. The 4-stage design arrangement efficiency projections have been used throughout this study for the determination of the engine cycle performance.

Both engines are heavily dependent on the core technology already demonstrated in the NASA/GE E³ program with engine 2(b) being even more dependent than engine 3(b) in this regard. Both engines are equally dependent on the two-stage booster technology that has been previously demonstrated on the NASA/GE J101/VCE demonstrator engine programs.

Engine 3(b)'s high-pressure compressor is based on experimental work accomplished at Lynn on smaller power size turboshaft engines. The T700

turboshaft engines and the CT7 commercial turboprop engines all employ axi-centrifugal compressor arrangements - primarily to achieve ruggedness in the highest pressure stage of the compressor. In addition to these production engines, GE has developed an experimental compressor with a similar axi-centrifugal engine configuration that has demonstrated a pressure ratio of 22:1 at its design speed. (This compressor arrangement was included in the GE27 engine proposal for the MTDE* competition). The GE27 at 5000 SHP, is then just less than half-scale of the proposed APET engine 3(b), and there would be a high level of confidence in the ability to upscale the flow size to that required by the APET engine, and maintain high efficiency.

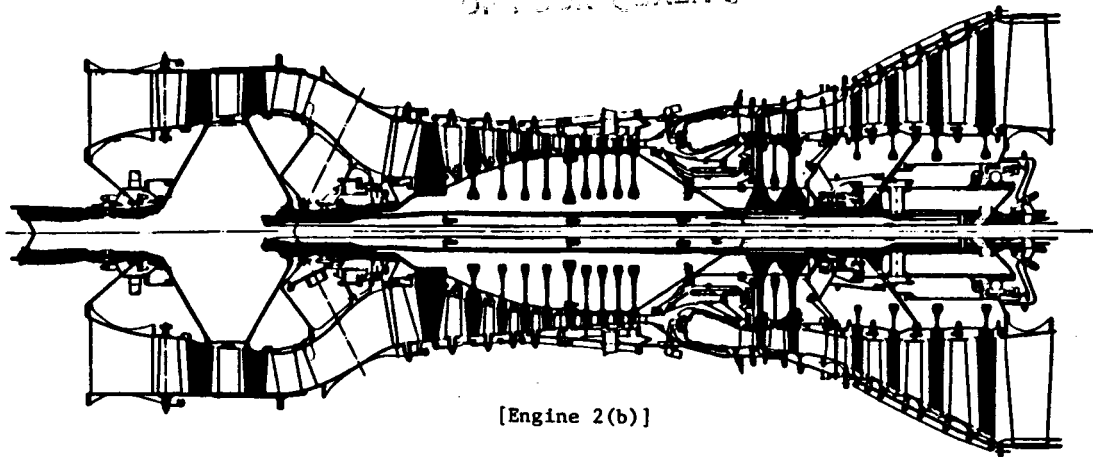
The selected engines are rated equal in the development of both HP and LP turbine efficiencies to meet the goals, and turbine technology programs would thus equally apply. Engine 3(b) has a more difficult set of design problems in the combustor stage, but high efficiency combustors have already been demonstrated at a smaller scale size.

Overall, either engine would be equally rated in their ability to produce the power levels and efficiencies being quoted in this report and other factors than those considered in this study would swing the selection from one to the other, in a final choice for an airplane development program.

These two engines are shown in Figure 4.4-7 [APET 2(b)] and Figure 4.4-8 [APET 3(b)]. The figures show engine cross sections and the principal characteristics of each are included in the figure. It may be noted that both engines shown include 4-stage low pressure power turbines - which configurations were used in the estimation of engine performance, weight and cost. Three-stage low pressure turbine arrangements were also designed and the APET (2b) engine with this turbine has been included. See Figure 4.4-9. As may be noted on this latter figure, estimation of fuel burn and DOC for this configuration is shown to be inferior to the engine shown in Figure 4.4-7 so it was dropped from further studies.

Engines 2(b) and 3(b) were then drawn attached to a "referee" offset gearbox, and enclosed within a nacelle which employs a single, offset, air inlet scoop to supply the engine inlet. The nacelle configuration shown has a radius

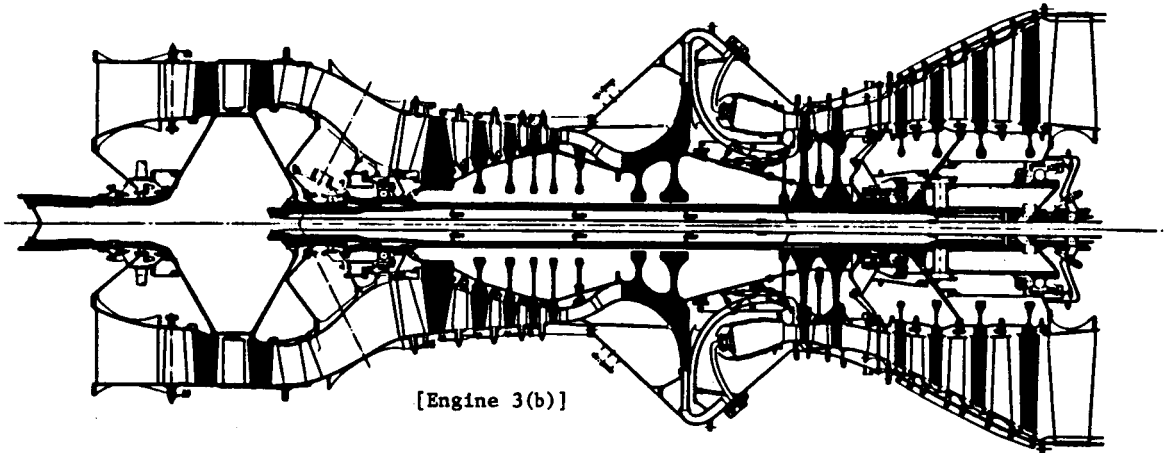
* MTDE is the Modern Technology Development Engine.



[Engine 2(b)]

<u>Booster</u>	<u>Core</u>	<u>Power Turbine</u>
$V_{Tip}/\sqrt{\theta} = 924$	Scaled E^3	$P/P = 7.6$
$r/r = .67$	$V_{Tip}/\sqrt{\theta} = 1498$	$\psi_{PAvg} = .95$
$PR = 1.75$	$PR = 23$	

Figure 4.4-7. APET Turboprop Gas Generator Axial Flow Compressor Four Stage Power Turbine.



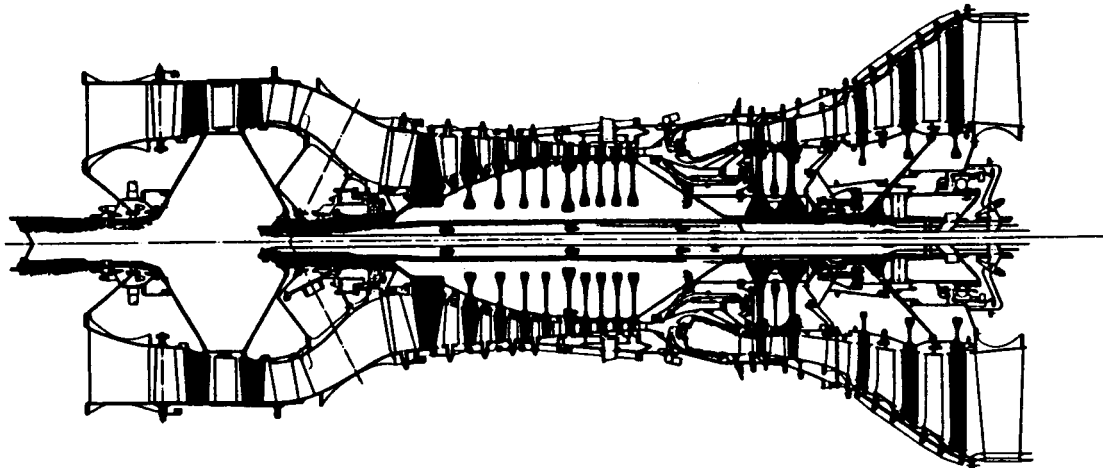
[Engine 3(b)]

<u>Booster</u>	<u>Core (PR_{OA} = 23)</u>	<u>Power Turbine</u>
$V_{Tip}/\sqrt{\theta} = 924$	Axial - $V_{Tip}/\sqrt{\theta} = 1498$	$P/P = 7.6$
$r/r = .67$	$PR = 7.12$	$\psi_{PAvg} = .95$
$PR = 1.75$	Centrifugal - $V_{Tip}/\sqrt{\theta} = 1407$	
	$PR = 3.23$	

Figure 4.4-8. APET Turboprop Gas Generator Axi-Centrifugal Compressor Four-Stage Power Turbine.

ORIGINAL FIGURE
OF TECHNICAL DRAWING

Rel to ④ Stage LPT, $\Delta\eta_{LPT} = -1.5\%$, $\Delta FB = +1.5\%$, $\Delta DOC = +0.8\%$



<u>Booster</u>	<u>Core</u>	<u>Power Turbine</u>
$V_{Tip}/\sqrt{\theta} = 924$	Scaled E^3	P/P = 7.8
r/r = .67	$V_{Tip}/\sqrt{\theta} = 1498$	$\psi_{PAvg} = 1.17$
PR = 1.75	PR = 23	

(Engine 2(b) alternate)

Figure 4.4-9. APET Turboprop Gas Generator Axial Flow Compressor Three Stage Power Turbine.

ratio (r/R) of 0.30 when comparing the axi-symmetric nacelle body to the propfan radius value. This step in the design process is illustrated in Figures 4.4-10 and 4.4-11 which show that a "basic" nacelle outline can satisfactorily enclose either selected engine. Further investigation of the nacelle designs studied are included in Section 4.7 of this report.

The preliminary design studies of the two selected engines resulted in a set of cycle assumptions and comparisons that are included in Table 4.4-2 while Table 4.4-3 is included to show the comparison in terms of the individual aerodynamic components.

These cycle assumptions and comparisons were made after some configuration studies had estimated the effect on cycle parameters when varying booster pressure ratio and cycle temperature. Figure 4.4-12 shows the summary of these studies.

Booster and core corrected flow changes are shown as a function of booster pressure ratio, on the left hand side of the figure as solid lines, while the dashed lines represent the additional change due to an increase of 100° F in T_{41} . The center portion of the figure shows the effect of the same variations in booster pressure ratio on the size of the high pressure turbine and the maximum takeoff compressor delivery temperature.

The right hand side of the figure shows again the same variable boost pressure and its effects on the minimum SFC at cruise and the shaft horsepower to the gearbox.

The results of these studies led to the selection of the cycle assumptions shown in Table 4.4-2 where it may be noted that the booster pressure ratio of 1.75 has been selected, as has a cycle temperature of 2390° F. These values may be compared with the original assumption which used a 1.67 P/P booster and a 2350° F cycle set-up temperature.

The final APET turboshaft engine sizes for the three different cruise Mach numbers considered are summarized on Figure 4.4-13 where booster and core engine corrected airflow as well as propfan diameter, shaft horsepower and thrust are shown for each cruise Mach number studied.

- 4-Stage LPT
- Referee Offset Gearbox
- Referee Nacelle (0.30 r /R)
- Single Scoop Inlet

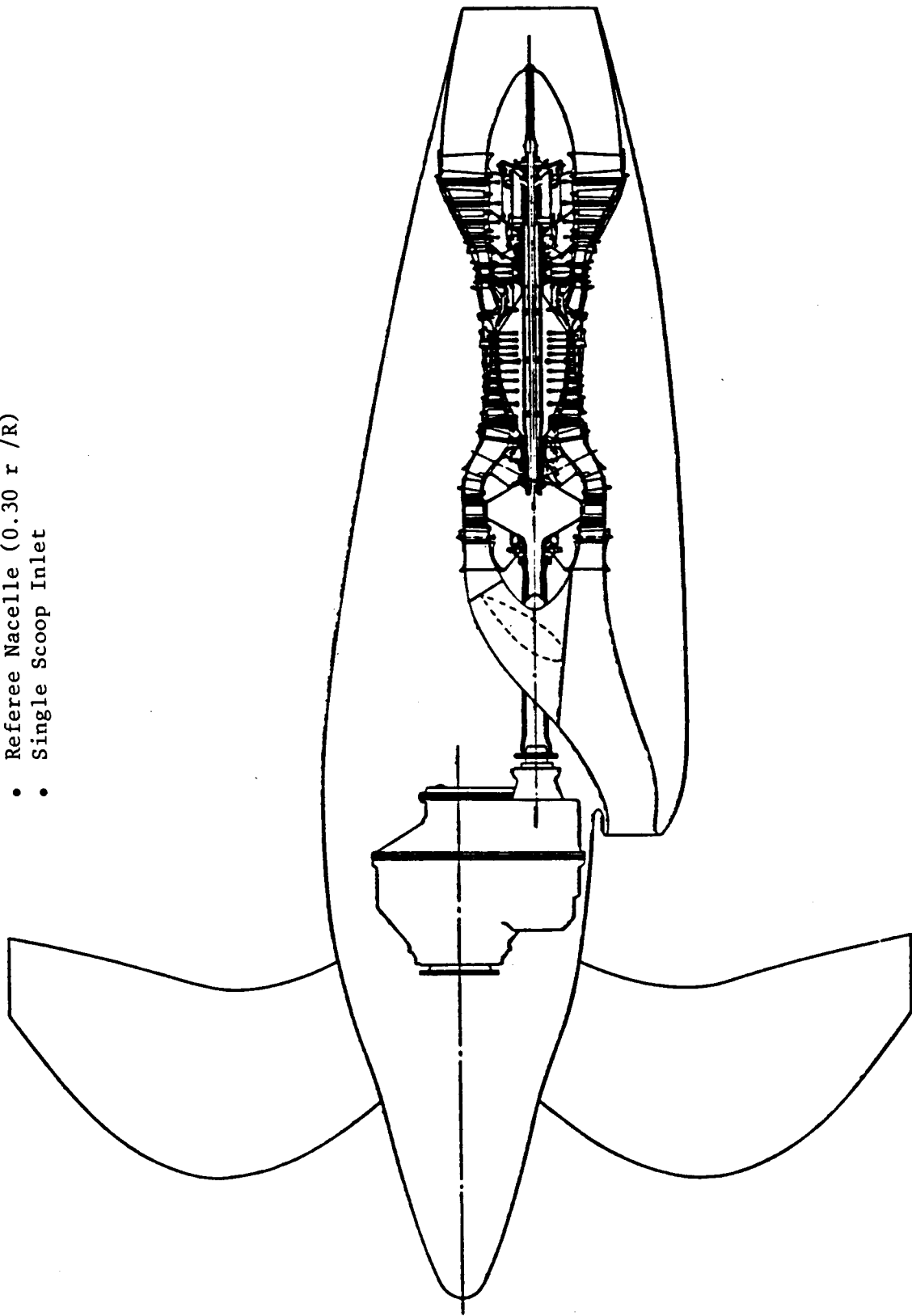


Figure 4.4-10. APET 2B "Baseline" Engine (12,500 SHP).

OF FOUR QUALITY

- 3-Stage LPT
- Referee Offset Gearbox
- Referee Nacelle (0.30 r /R)
- Single Scoop Inlet

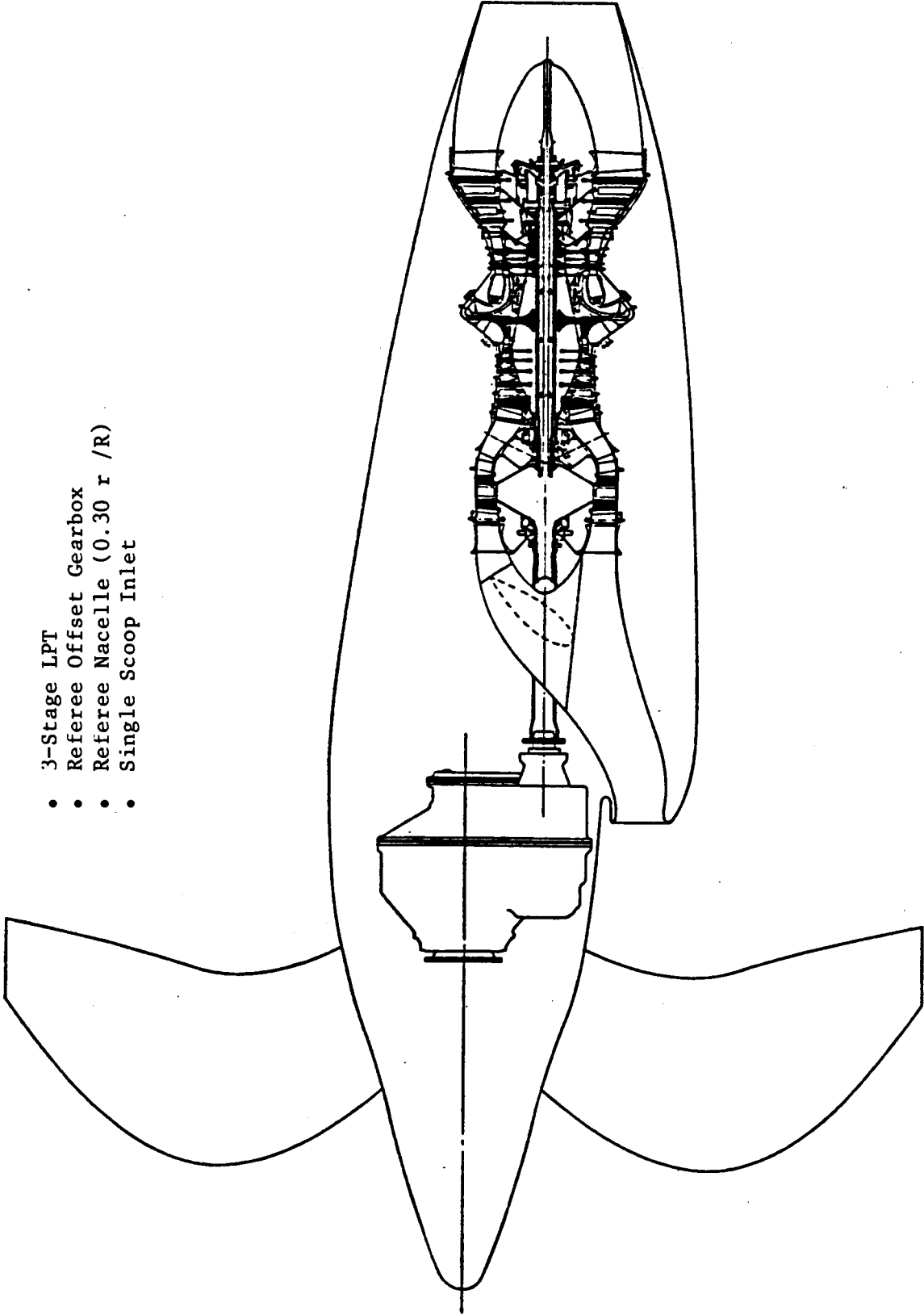


Figure 4.4-11. APET 3B "Baseline" Engine (12,500 SHP).

Table 4.4-2. APET Turboprop Configuration Studies - Cycle Assumption Comparisons.

	All Axial	Axi Centrifugal
● At M0.80/35000' + 18°		
Thrust	4000	4000
PR Overall	40.2	40.2
T41 - ° F	2390	2390
$W\sqrt{\theta}/\delta$ LP	69.9	70.3
PR _{LP}	1.75	1.75
η_{LP} Poly/Adia	0.888/0.881	0.888/0.881
ΔP Gooseneck	1.5%	1.5%
$W\sqrt{\theta}/\delta$ Core	44.2	44.5
PR Core	23.0	23.0
η_C Poly/Adia	0.898/0.848	0.897/0.846
ΔP Combustor	4.95%	6.0%
$\eta_{Combustor}$	0.995	0.995
No. HPT Stages	2	2
$W\sqrt{T}/P$ HPT	6.53	6.65
η_t (Cycle)	0.914	0.915
	---	---
$\Delta h/T$ LPT	0.101	0.100
P/P LPT	7.6	7.4
η_{LPT}	0.920	0.920
P8/PO	1.50	1.50
Total Cooling Air	17.0	17.0
Total Chargeable	9.3	9.3
η_{Prop}	0.809	0.809
SFC	Base	+0.5%
Propeller HP @ 0.8/35K + 18°	6450	6445
Propeller HP @ 0.2/SL + 27°	12500	12500

Table 4.4-3. APET Turboprop Configuration Studies - Component Aerodynamic Comparisons.

Engine Configuration	All Axial	Axi Centrifugal
A. <u>Booster/LP Spool</u>		
No. Stages	2	2
$W\sqrt{\theta}/\delta$	69.9	70.3
W_A/A_A	39.0	39.0
V Tip/ $\sqrt{\theta}$	924	924
r/r	0.67	0.67
PR	1.75	1.75
B. <u>Compressor</u>		
No. Stages	10	5+1
$W\sqrt{\theta}/\delta$	44.2	44.5/8.43
W_A/A_A	38.0	38.0/32.3
V Tip/ $\sqrt{\theta}$ Axial	1498	1498
V Tip/ $\sqrt{\theta}$ Impeller	---	1407
PR	23.0	7.12 x 3.23 = 23
Last Blade Height	0.51"	0.42"
C. <u>HP Turbine</u>		
No. Stages	2	2
$W\sqrt{T}/P$	6.53	6.65
$\Delta h/T^*$	0.086	0.086
P/P	5.14	5.16
ψ Pitch (Avg)	0.66	0.66
1st Stage Blade Height	1.12"	1.13"
D. <u>LP Turbine</u>		
No. Stages	4	4
$\Delta h/T$	0.100	0.100
P/P	7.6	7.6
ψ Pitch (Avg)	0.95	0.95
AN ²	42.5 * 10 ⁹	42.5 * 10 ⁹
*Altitude Thrust = 4000 lbs		

Cycle PR, T41 Impact on Performance Component Sizes, T3 Levels

- 4000# M_{XCL} Thrust Sized Engines
- T41 = 2350°F M_{XC} , 2450°F @ T-O
= 2450°F M_{XL} , 2550°F @ T-O

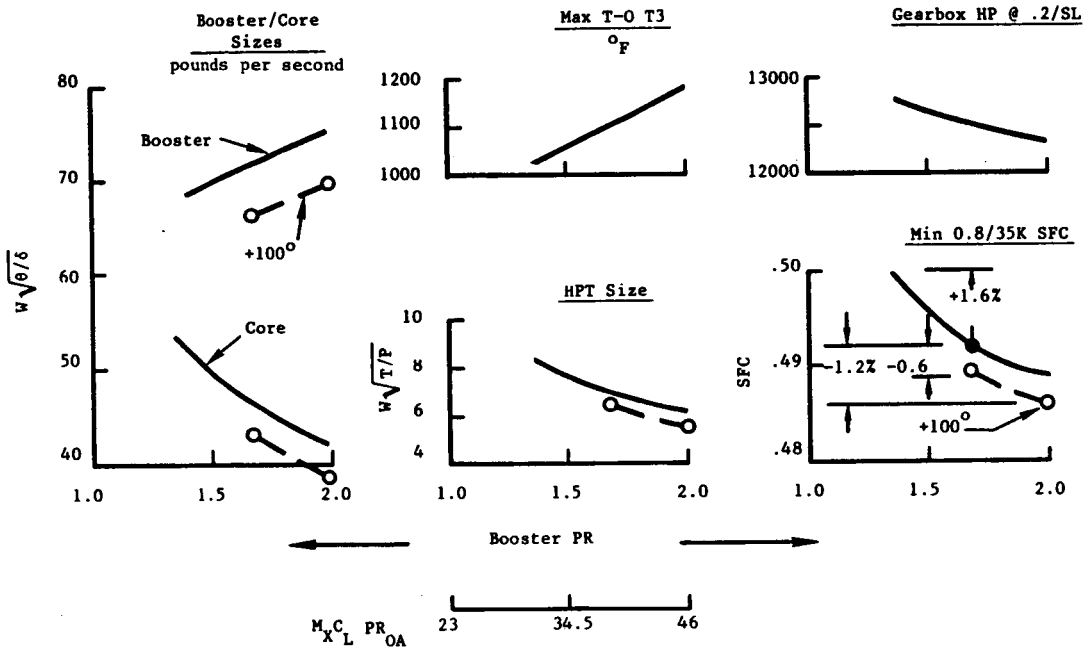


Figure 4.4-12. Turbo Prop Configuration Studies.

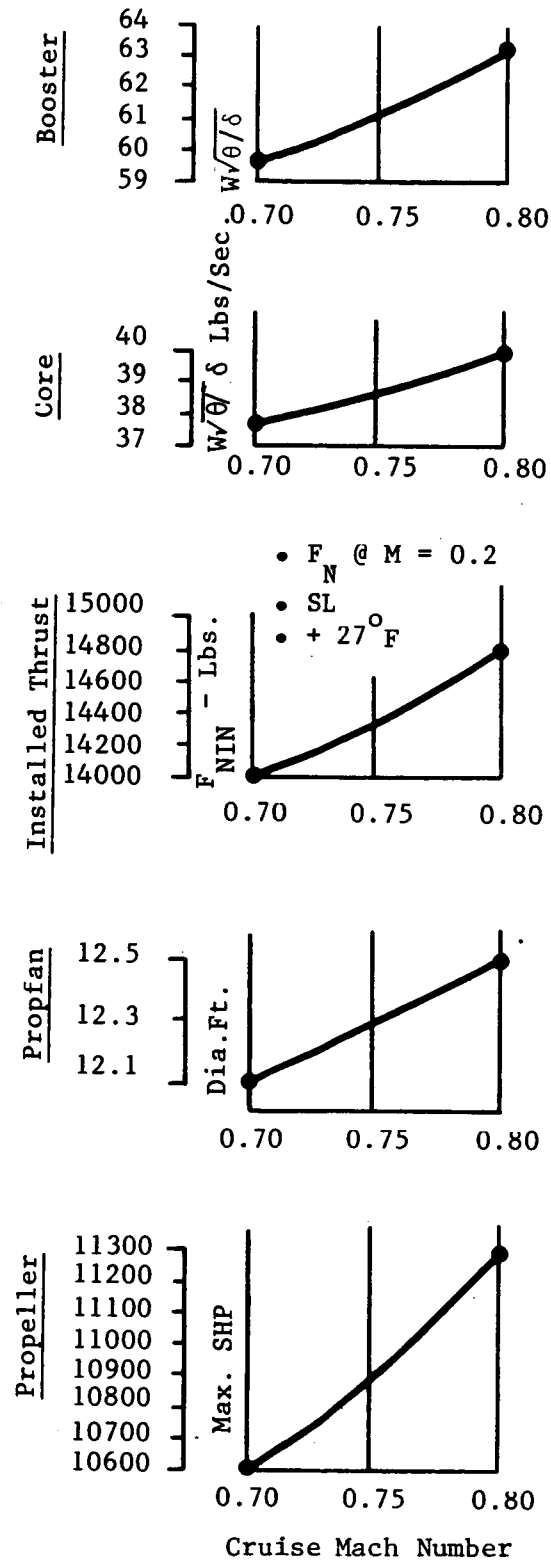


Figure 4.4-13. Final AEPT Turboshaft Engine Sizes.

4.4.3 Engine Weight and Cost

As outlined in Section 4.2.5, computer programs linked to the design program are used to generate engine weights and costs. Gearboxes and other drive components were estimated separately. This study also required that the selected engines and gearboxes together with their performance decks be formatted into scalable data packages for future airframe preliminary designs. As already indicated in Section 1, the baseline APET propulsion systems were frozen at a value of 12,500 shaft horsepower, and this is the value that was used for generating the cost and weight data baselines. The selected engines (2b and 3b) were laid out in a geometry that is usable for propulsion installation studies. Figures 4.4-14, -15 and -16 have been included to show the three baseline configurations, geometry, weights and center of gravity.

These referenced figures are also included as part of Appendix III at the end of this report, and appropriate scaling laws for dimensions and weights are provided therein. Thus it should be possible to use the APET engine computer deck, which is a "deliverable" contract item in this NASA sponsored study, and conduct airplane preliminary design studies in a large range of shaft horsepowers, using the data scaling laws. Cost data is supplied to NASA under separate cover, and is not reproduced here.

4.4.4 Cycle Selection Summary

The selected cycle characteristics for the baseline engines designated 2(b) and 3(b) are given in Figure 4.4-17. It may be noted that the temperature set-up is fixed so that the Denver hot-day takeoff rating T41 (turbine temperature) is 100° F above the hot-day, end-of-climb rating point. These ratings establish the cooling airflow required by the turbine stages and establish the final core size at a corrected airflow level of 44.2 pounds per second. Resultant engine thrust for the selected 10-bladed, 800 ft/sec tip speed, propfan is 20,000 pounds at Sea Level Static and 16,600 pounds at Mach 0.20, Sea Level, +27° F; the propeller shaft horsepower being held to the 12,500 value already established for the design of the baseline gearboxes. As indicated in the previous section, an Appendix has been provided in this report so that airframe designers may select the power level of their choice, using scaling laws, and match propulsion system to airframe requirements.

ORIGINAL DRAWING
OF POOR QUALITY

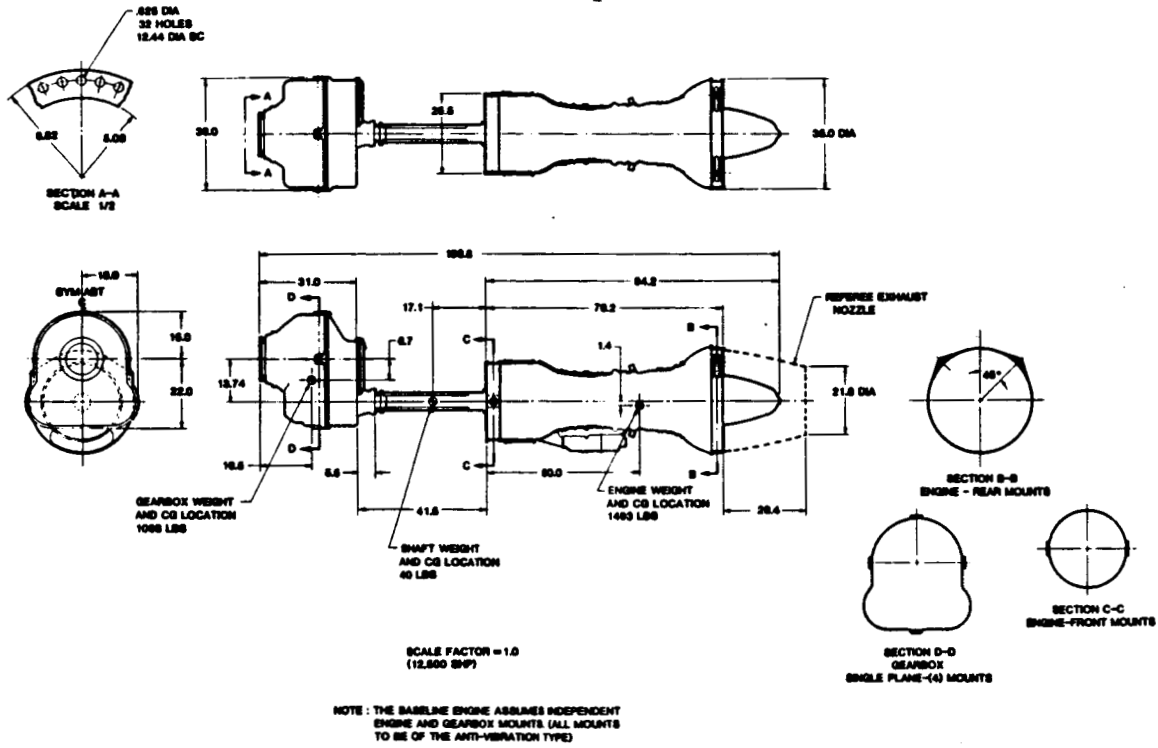


Figure 4.4-14. APET Baseline (Axi-Axi) Engine and Gearbox.

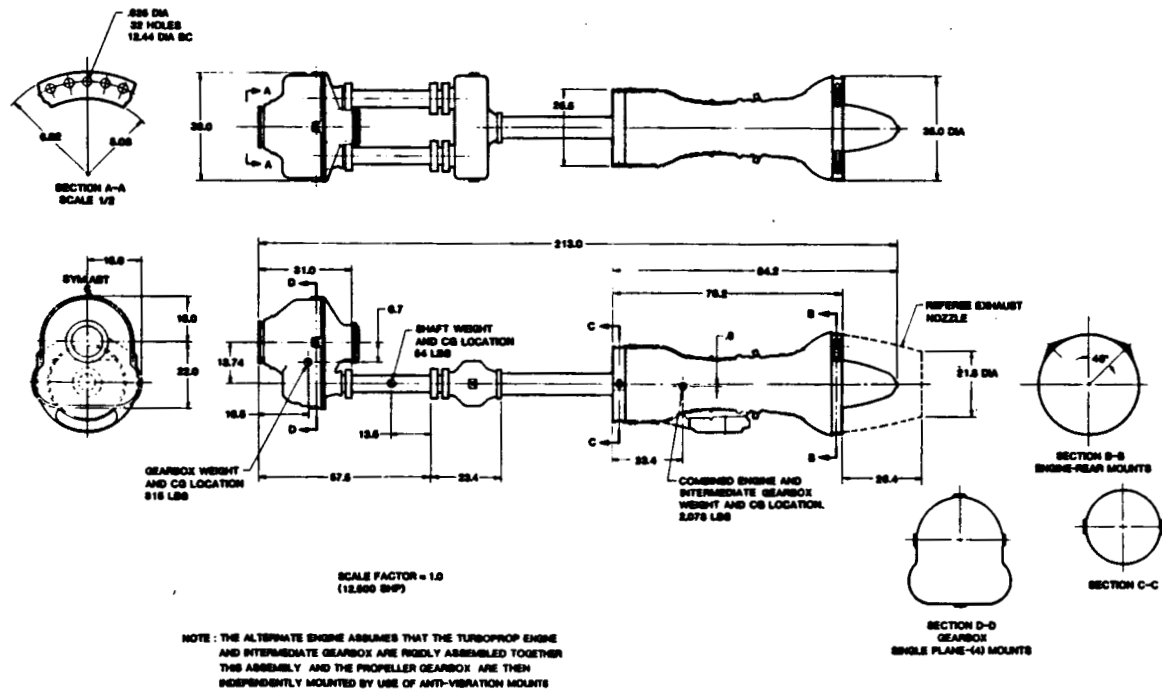


Figure 4.4-15. APET Alternate (Axi-Axi) Engine with Split Gearbox.

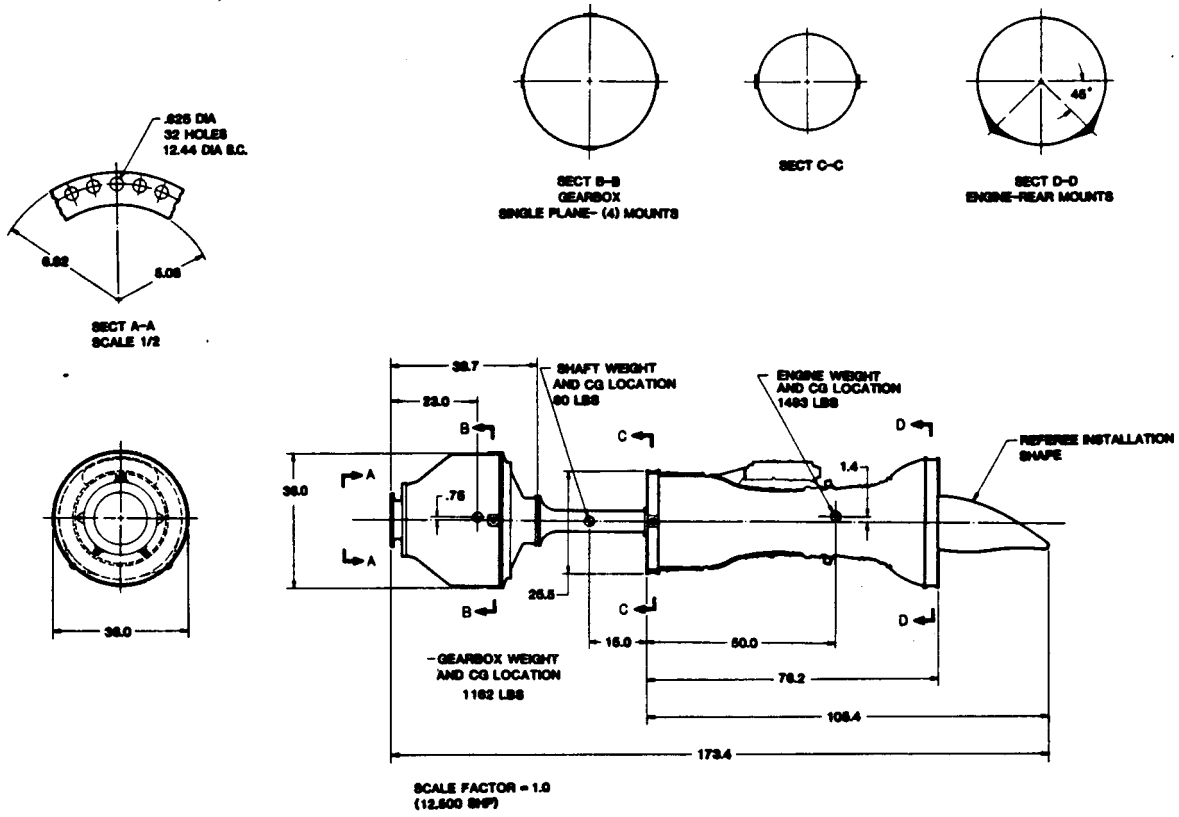


Figure 4.4-16. APET Engine (Axi-Axi) With Concentric Gearbox.

- Cycle Parameters at M0.80/35000 ft + 18°

PR Booster = 1.75
 PR Core = 23.0
 PR Overall = 40.2
 Turbine Temp., ° F = 2390/2490° F (MxC1/Denver)

- Configuration

- 2 Stage VIGV Booster
- Scaled Version of 10 Stage Ref. Turbofan Core
- 4 Stage Power Turbine that Drives VIGV
Booster and Prop

- Prop, Gearbox, Gas Generator Sizes for 4000 lb MxC1
Thrust at M0.8/35K + 18°

- Booster $W\sqrt{\theta}/\delta$ = 69.9
- Core $W\sqrt{\theta}/\delta$ = 44.2 SLS FN = 20000
- Propeller Dia. = 13.1 ft at SHP/D2 = 37.5 0.2/SL FN = 16600
- Propeller HP Max. = 12500

Figure 4.4-17. Baseline APET Boosted Turboprop Description.

4.4.5 Other Cycle Parameters

The selection of the engine parameters required prior examination of the effects of the variables for the propfan as well as the basic engine cycles. These examinations were then carried through both uninstalled and installed performance comparisons, using the appropriate installation losses in a clearly defined bookkeeping system.

Typical flight paths encompassing climb and cruise were evaluated using installation drag effects that were directly subtracted from the thrust available. These drags were further broken down into those that are chargeable to the nacelles and those that were additive, in the case of the propfan installation, to the effects due to propeller slipstream.

These studies are summarized in the following identified Figures and Tables: Figures 4.3-1 and 4.3-2 have been shown for the reference turbofan installation. Figures 4.4-10 and 4.4-11 and Table 4.4-2 have also been shown for the turboshaft engines. These four figures and table summarize the propulsion systems that were subjected to the installation and performance studies that provide the data necessary for the final cycle selection.

The propfan variables of tip speed, disk loading and net efficiency are shown in Figure 4.4-18. The flight conditions in the figure show the effects of the variables for the three cruise Mach numbers at a constant cruise altitude. Uninstalled performance of the APET turbofan versus the APET turbopropfan are shown in Figure 4.4-19, where the three identical Mach numbers have been used at the same constant cruise altitude. This figure represents the power hook of the uninstalled engines in terms of changes in Specific Fuel Consumption (SFC) and also illustrates the delta percentage between the competing propulsion systems. Although cruise SFC is of great interest, the performance of the competing systems must also be evaluated through the remainder of the flight regimes. In the Program Overview (Section 3.0) Figures 3.4-4 and 3.4-5 have been presented as being typical of the Takeoff and Climbout performance of the two competing propulsion systems. Note that these figures show fully installed comparisons which are using installation factors shown in Figure 3.5-1. These figures, with modification for the uninstalled systems, can be used as a guide to the large differences between the two competitors during climb to final cruise altitude, and it may be noted that the performance deltas and SFC's are much larger than the values being shown for the selected cruise points in Figure 4.4-19. Clearly the short-haul airplane performance is largely being dominated by the deltas during take-off and climb out, and this is highly beneficial for the propfan powered aircraft. These uninstalled comparisons are summarized in Table 4.4-4. Note that a Denver hot day takeoff has also been included in this table.

The APET studies also included evaluations of delta SFC's and delta thrusts for propfans that are designed for 700, 750 and 800 feet per second tip speeds. In each case, the propfan was power sized (at a constant $\text{SHP}/D^2 = 37.5$) to provide equal thrust at the end of climb. This is illustrated in Figure 4.4-20. This figure clearly shows that for a constant thrust objective

V Tip Impact on η Prop Net @ 35000'

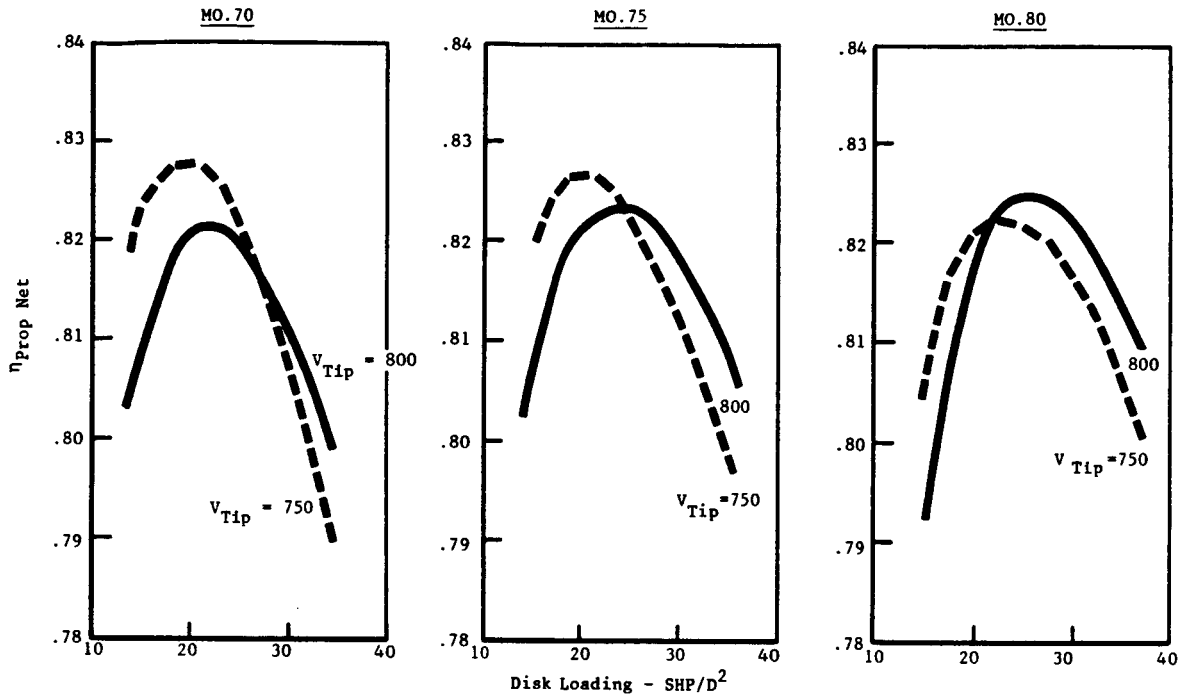


Figure 4.4-18. Prop Fan Propeller Performance - 10 Blade Configuration.

- Standard Day, No Customer Extractions
- H - S 10 Blade Prop Fan Performance
- $SHP/D^2 = 37.5$ @ MO. 8

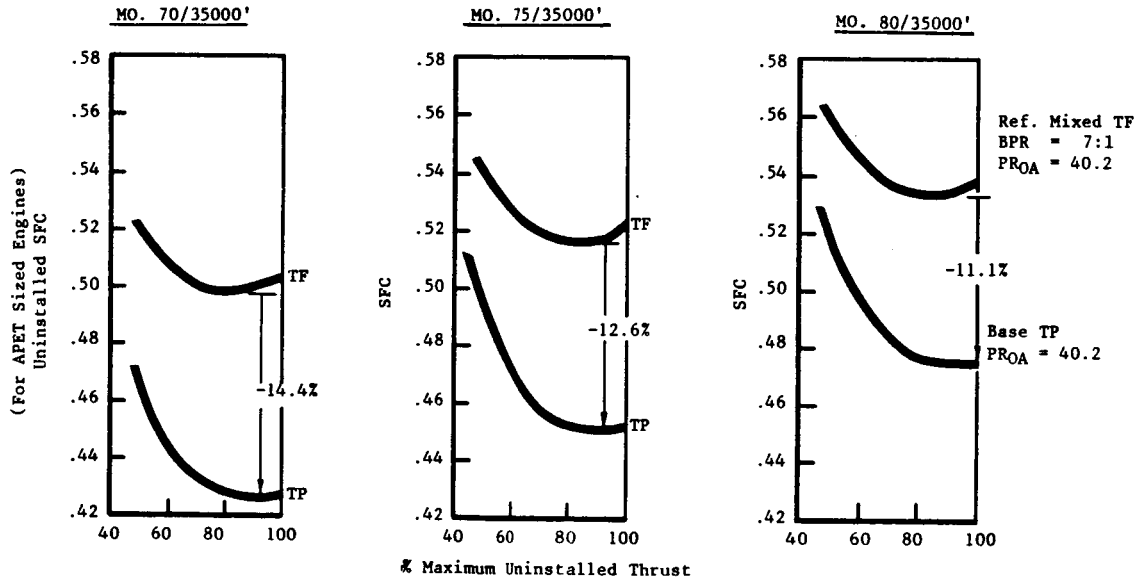


Figure 4.4-19. APET Uninstalled Performance Comparisons.

MO.80/35000' - Std Day, SHP/D² = 37.5

- Equal MO.80/35K + 18 Thrust

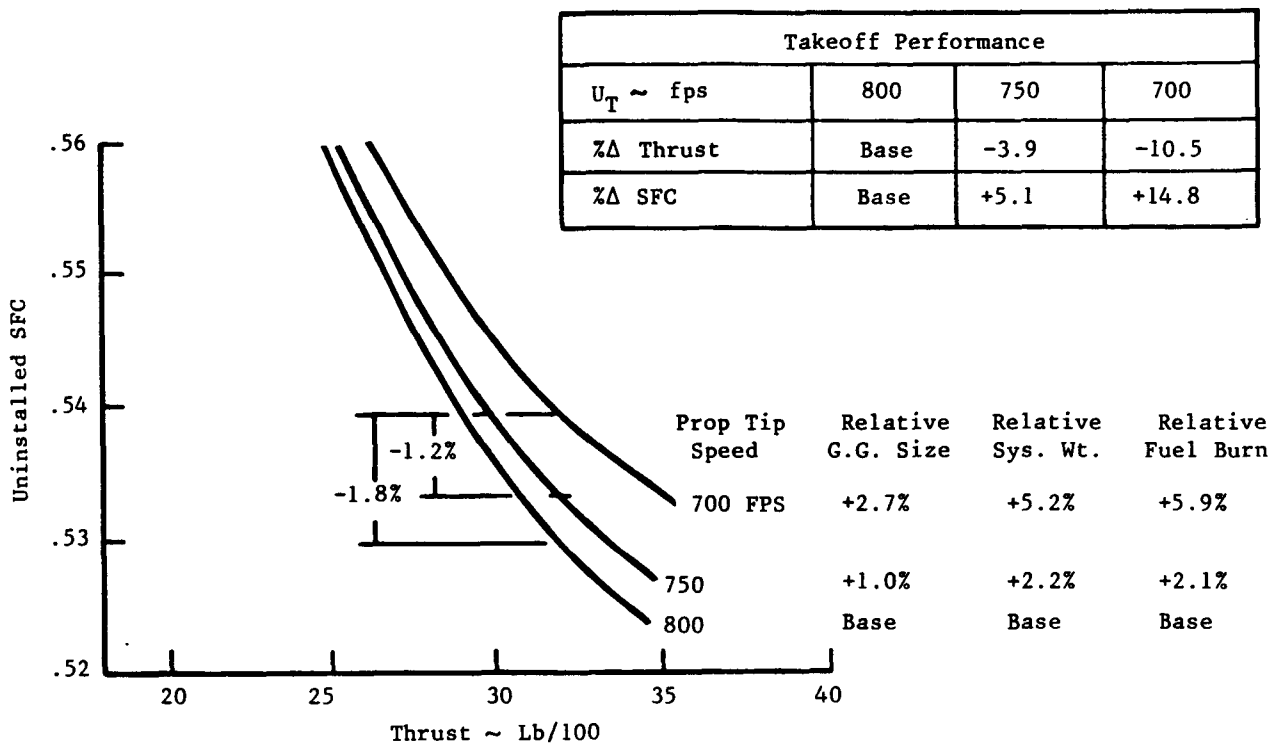


Figure 4.4-20. APET Propeller Tip Speed Study.

Table 4.4-4. APET Uninstalled Comparisons.

	Engine	
	Reference TF	Base TP
● M0.80/35K + 18° - FN - SFC	4000 Base	4000 -10.6%
● M0.2/SL + 27° - FN - SFC	Base Base	+18.1% -31.0%
*● M0.2/5330 + 52° - FN - SFC	Base Base	+13.2% -31.7%
● M0.6/20000' + 18° - FN - SFC	Base Base	+8.0% -16.4%
*Denver, Hot Day Takeoff		

there are penalties in fuel burn, engine gas generator size and system weight for tip speeds below 800 fps. The inset block on the figure also shows the relatively severe penalty that would be incurred by the use of lower tip speeds during the takeoff. In all these examples the aircraft design has been optimum for the selected cruise speed and the aircraft weights have been adjusted to reflect the design differences.

4.4.6 Propeller Selection

The propeller (or propfan) as a system concept is illustrated in Figure 4.4-21. For this study, the performance block data was derived from the Hamilton Standard Data Package No. SPO 4A80 dated October 1980. In the systems block it is assumed that a hydromechanical pitch change mechanism (PCM) would be included with the propfan and be supplied by gearbox oil at high pressure. Normally, the propeller drive gearbox requires a lubrication system that operates at low pressures (50 - 200 PSI), while the PCM is estimated to require a 3000 PSI supply pressure. Thus the gearbox is required to drive two hydraulic pumps - one for lubricating service to the gearbox while the second pump boosts the 50 PSI pressure level to the requisite high pressure for the PCM.

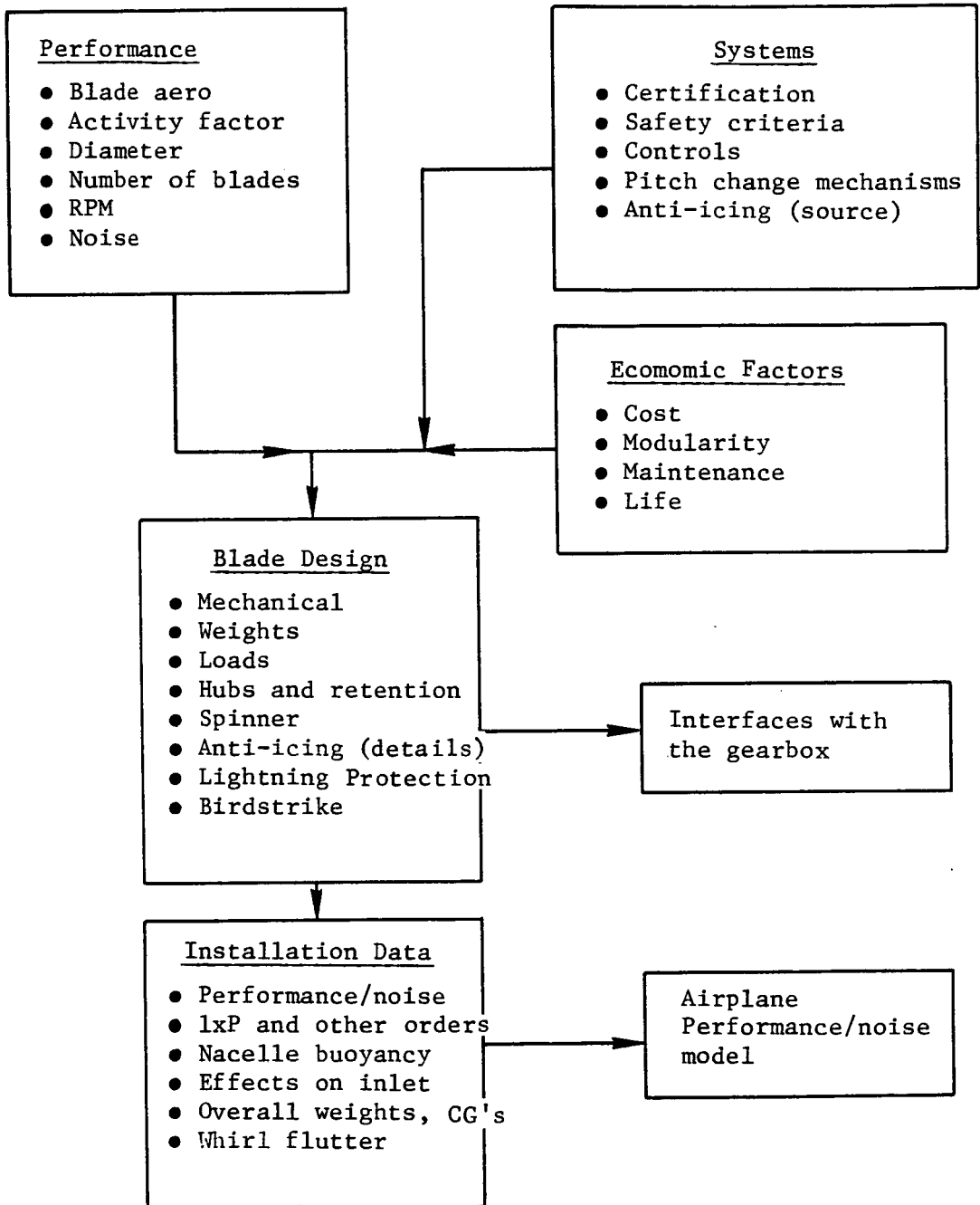


Figure 4.4-21. The Propeller System.

The Pitch Change Control Unit (PCMCU) is mounted on the gearbox and communicates with the propeller driveshaft. The PCMCU contains electrohydraulic servo valves which are responsive to control commands from the propulsion system Full Authority Digital Engine Control (FADEC). When the servo valves receive signals from the FADEC unit, they direct the high pressure oil to either the coarse or fine pitch side of the hydraulic piston assembly which is connected to the propeller blades by mechanical linkage. Oil is transferred, within the PCMCU, across the stationary to rotating barrier by a series of sliprings that seal around the driveshaft stub extension, and operate the PCM in an axial manner. Rotation of the propfan blades in the hub housing is achieved by axial-to-rotational motion via the mechanical linkage and its geometry.

Also contained within the PCM are the safety devices for ground and flight operations. A fixed flight fine pitch stop is provided that precludes selection of blade angles finer than the fine pitch setting unless a separate command has been received to remove the device that locks the pitch stop. Also, a travelling mechanical pitch stop is included that follows the commanded blade angle by 1-2 degrees when pitch is being coarsened, and leads the blade angle by the same amount when finer pitch is being commanded. This travelling pitch stop, or mechanical pitch lock as it is sometimes called, is a prime safety-of-flight mechanism in that it positively precludes inadvertent movement of the blades to hazardous drag or RPM regimes.

Safety of flight considerations demand that failure mode analyses of both the engine and the propfan are conducted. Hamilton-Standard has provided the propfan data that has been used in this study. For some flight conditions it is necessary to compute feather drag while for other failure modes it is appropriate to calculate windmilling propfan drag forces. For example, with an engine inoperative during cruise, the airplane drag model would use the feather drag values. For engine failure at V_2 , windmilling drag would be used in the drag model until safe climb-out parameters have been established and the airplane can be cleaned-up by commanding the affected propfan to the feather position.

Figure 4.4-22 shows the data used for calculating feather drag, and Figure 4.4-23 shows, versus propfan diameter, the estimated hydraulic flow rate required to feather the propfan.

Windmilling drag estimates were made by using selected values from the data shown on Figures 4.4-24 through 4.4-27 which cover the physical drag forces for two levels of Mach number and altitude (for a 13.0 ft. diameter propfan), and the estimated drags and propfan tip speeds for design Mach numbers between 0.70 and 0.80 at cruise altitude and also, on Figure 4.4-27 values for the V₂ engine failure case. Propfan power loading is also a variable parameter for the realization of both the drag forces and the windmilling RPM.

$$\text{Feather Drag} = \frac{(M_o C_K)^2 C_{DF} (\rho / \rho_o) D^2}{1476}$$

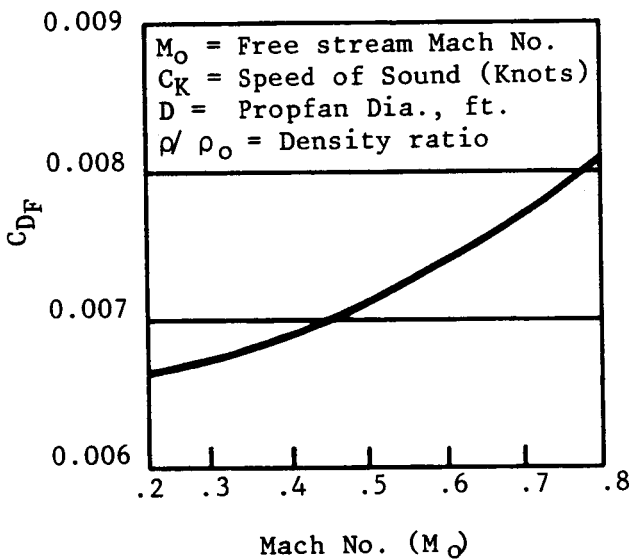


Figure 4.4-22. 10-Blade, 1986 Propfan Projections- Drag Coefficient Versus Mach Number.

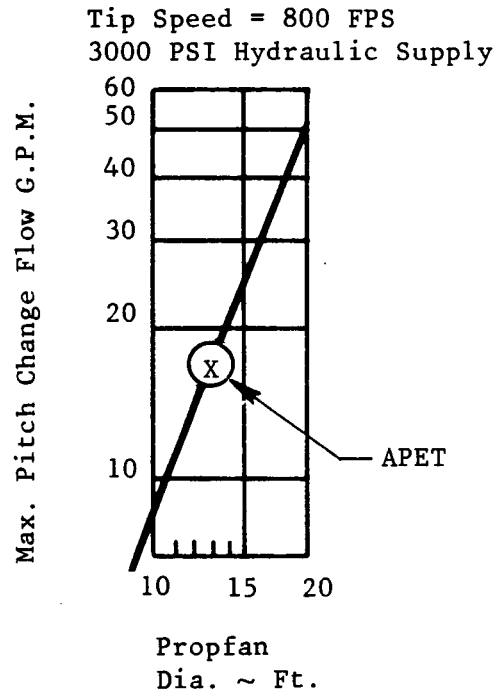


Figure 4.4-23. Single Rotation 10-Blade Propfan - Maximum Pitch Change Flow Versus Diameter.

10 Bladed - 13.0 Ft. Dia. Propfan - 1986
 At Mach = 0.20, Sea Level, ISA

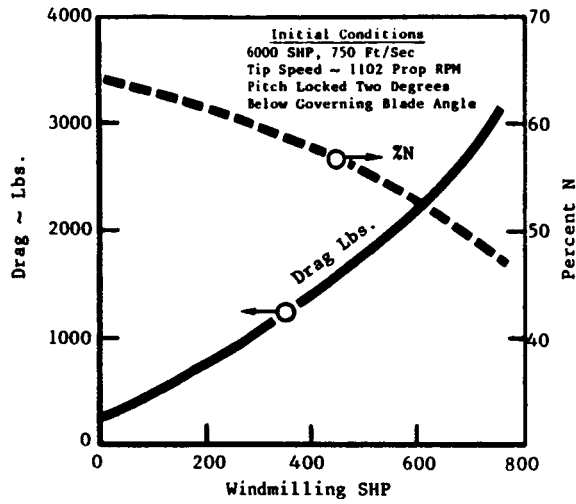


Figure 4.4-24. Drag and Propeller Speed Versus Windmilling SHP at Pitch Lock.

10 - Blade - 13.0 Ft. Dia. Propfan - 1986
 At Mach = 0.74, 35,000 Ft, ISA

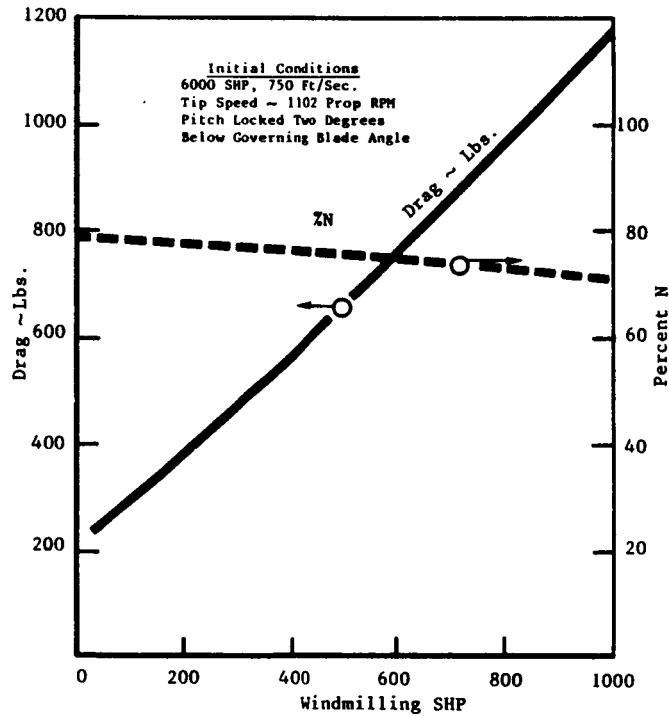


Figure 4.4-25. Drag and Propeller Speed Versus Windmilling SHP at Pitch Lock.

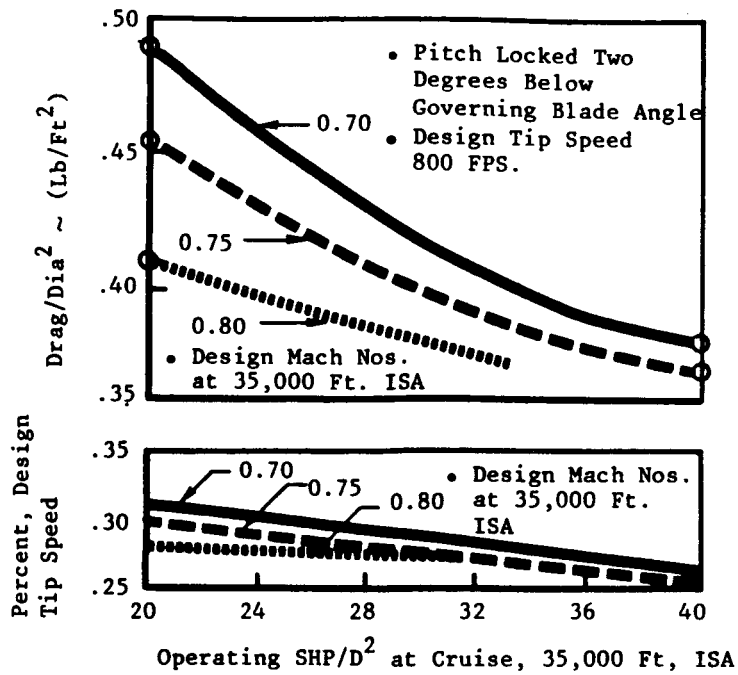


Figure 4.4-26. Windmilling Drag and Percent Tip Speed Versus Design SHP/D² and Tip Speed 10-Bladed, 1986 Propfan.

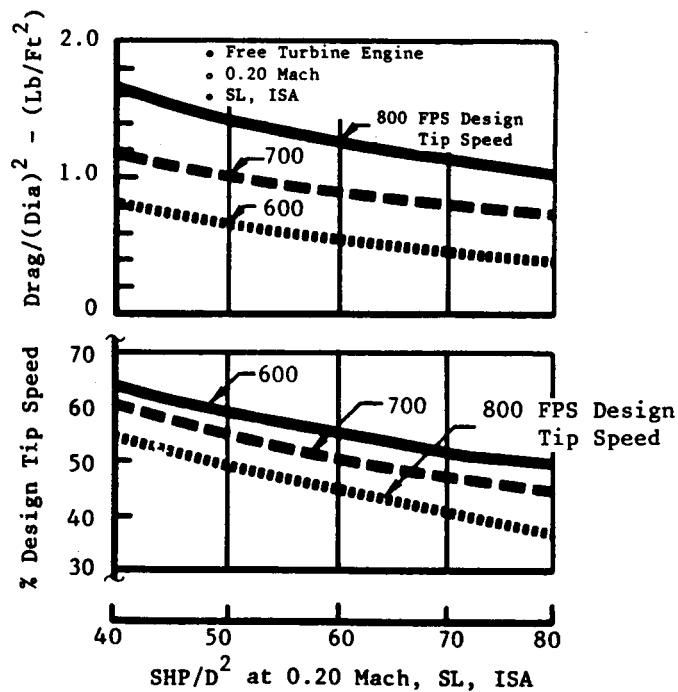


Figure 4.4-27. Windmilling Drag and Percent Tip Speed Versus Design SHP/D² and Tip Speed 10-Bladed, 1986 Propfan.

SECTION 4.5
IMPACT OF DESIGN FEATURES ON ENGINE DETERIORATING MODES

4.5 IMPACT OF DESIGN FEATURES ON ENGINE DETERIORATION MODES

The mechanical design of the APET turboshaft engines takes into account the significant deterioration in performance with time effects found in other turboshaft engines, and introduces alleviation by the selection of the design features.

The core compressor tip clearance control is due to the selection of the E³ engine compressor geometry which has a low L/D ratio that ensures a very stiff rotor spool. Rotor to shroud clearances are improved by using double-walled stators that reduce the thermal gradients at the flanges.

High pressure turbine clearance control measures will use the same system that was designed for the full-scale E³ engine. This system has already been tested successfully.

Controls over the low pressure turbine clearances are made in two ways. First, axial clearances are maintained by locating the thrust bearing at the rear of the engine. This location reduces the axial excursions due to differential thermal expansions and helps to reduce seal wear and minimize flowpath wall steps. Second, the incorporation of a bearing support through the Stage 1 low pressure turbine nozzle produces a stiffer system and improves the control of concentricity between the rotor and the stator. Also, differential bearings and their associated problems have been eliminated.

Maintenance of labyrinth seal clearance is improved by the use of seals that are significantly smaller in diameter than is current engine practice.

Overall engine maintainability is enhanced by a modular design concept that allows separation of major assemblies without disturbance of adjacent hardware. Also, the high pressure compressor is provided with horizontal split flanges to aid in compressor maintenance.

PRECEDING PAGE BLANK NOT FILMED

SECTION 4.6

GEARBOXES, LUBRICATION AND HEAT EXCHANGERS

<u>Section</u>	<u>Page</u>	
4.6.1	Data Base	163
	4.6.1.1 Gearboxes	163
	4.6.1.2 Initial Candidates	164
	4.6.1.3 Initial Screening	166
	4.6.1.4 List of Final Candidates	168
4.6.2	Preliminary Design Studies	168
	4.6.2.1 Influence of Propfan on Gearbox Design	168
4.6.3	Gearbox Design Approach	172
	4.6.3.1 Design Requirements	172
	4.6.3.2 Gear Design Approach	174
	4.6.3.3 Bearing Design Approach	174
4.6.4	Description of Detailed Preliminary Designs	175
	4.6.4.1 Design #1 - Offset Planetary	175
	4.6.4.2 Design #2 - Offset Star	177
	4.6.4.3 Design #3 - Simple Planetary	179
	4.6.4.4 Design #4 - Double Reduction Triple Branch	180
	4.6.4.5 Design #5 - Double Branch Double Reduction	184
	4.6.4.6 Design #6 - Compound Star	184
	4.6.4.7 Design #7 - Coupled Planetary	184
4.6.5	Final Selection Process	190
	4.6.5.1 Criteria Affecting Direct Operating Cost (DOC)	190
	4.6.5.2 Maintenance Cost	192
	4.6.5.3 Base Price	193
	4.6.5.4 Weight	193
	4.6.5.5 Power Loss (Efficiency)	194
4.6.6	Criteria Not Affecting DOC Directly	194
	4.6.6.1 Reliability	194
	4.6.6.2 Frontal Area	196
	4.6.6.3 Reverse Rotation	196
	4.6.6.4 Pitch Change Access	197
4.6.7	Selection	199
4.6.8	Design Description of Two Selected Designs	199
	4.6.8.1 Offset Dual Branch, Two Stage Reduction Gearbox	199
	4.6.8.2 Inline Triple Branch Compound Star Reduction Gearbox	206
4.6.9	Lubrication	211

SECTION 4.6 (Continued)

GEARBOXES, LUBRICATION AND HEAT EXCHANGERS

<u>Section</u>		<u>Page</u>
4.6.10	Heat Exchanger System Design	212
4.6.11	Cost and Weight Estimating Methodology	214
4.6.11.1	Gearbox Costs	214
4.6.11.2	Weight Determination	215

FIGURES

<u>Figure</u>		<u>Page</u>
4.6-1.	T64 SDG (Speed Decreaser Gearbox).	165
4.6-2.	APET Gearbox Study - Ratio and Configuration Effect on Weight Factor.	167
4.6-3.	APET Study Gearboxes.	169
4.6-4.	APET Gearbox Study - Effect of Scaling and Propeller Technology.	171
4.6-5.	Typical APET Mission Horsepower Versus Time.	173
4.6-6.	APET Gearbox - 12,500 SHP Offset/Planetary.	176
4.6-7.	APET Gearbox - 12,500 SHP Offset/Star.	178
4.6-8.	Modern High Horsepower Gearbox III (Simple Planetary).	182
4.6-9.	APET Gearbox - 12,500 SHP Double Reduction - Triple Branch.	183
4.6-10.	APET Dual Branch, Two Stage Reduction Gearbox - Features.	185
4.6-11.	APET Dual Branch, Two Stage Reduction Gearbox - Materials.	186
4.6-12.	APET Dual Branch, Two Stage Reduction Gearbox - Weight Breakdown.	187
4.6-13.	APET Triple Branch Compound Star Reduction Gearbox - Features.	188

SECTION 4.6 (Continued)

GEARBOXES, LUBRICATION AND HEAT EXCHANGERS

FIGURES (Concluded)

<u>Figure</u>		<u>Page</u>
4.6-14.	APET Triple Branch Compound Star Reduction Gearbox - Materials.	188
4.6-15.	APET Triple Branch Compound Star Reduction Gearbox - Weight Breakdown.	189
4.6-16.	APET Coupled Planetary Reduction Gearbox.	189
4.6-17.	APET Gearbox Economics.	191
4.6-18.	Input Stage Reversing - Schemes.	198
4.6-19.	Gearbox Facewidth vs. First Stage Ratio - Parametric Curve.	202
4.6-20.	APET Dual Branch Two Stage Reduction Gearbox.	205
4.6-21.	APET Triple Branch Compound Star Reduction Gearbox.	208
4.6-22.	APET Gear and Shaft Example.	215

TABLES

<u>Table</u>		<u>Page</u>
4.6-1.	Weight Breakdown of APET Offset Planetary Reduction Gearbox.	177
4.6-2.	Weight Breakdown of APET Offset Star Reduction Gearbox.	179
4.6-3.	Weight Breakdown of APET Simple Planetary Reduction Gearbox.	181
4.6-4.	Weight Breakdown of APET Double Reduction Triple Branch Gearbox.	181
4.6-5.	Gearbox Design Ranking.	195
4.6-6.	Gearbox Rotation.	197

SECTION 4.6 (Concluded)

GEARBOXES, LUBRICATION AND HEAT EXCHANGERS

TABLES (Concluded)

<u>Table</u>		<u>Page</u>
4.6-7.	Gearbox Candidate Rating.	200
4.6-8.	Gearbox Candidate Ranking.	200
4.6-9.	Gear Stresses for Offset Dual Branch Two Stage Gearbox.	204
4.6-10.	APET Dual Branch Two Stage Reduction Gearbox.	207
4.6-11.	Gear Stresses For Inline Triple Branch Compound Star Reduction Gearbox.	209
4.6-12.	APET Triple Branch Compound Star Reduction Gearbox.	210
4.6-13.	Calculation of APET Double Branch Gearbox Total Weight and C.G. Location.	216

4.6 GEARBOXES, LUBRICATION AND HEAT EXCHANGERS

4.6.1 Data Base

4.6.1.1 Gearboxes

General Electric has been an industry leader in providing Marine and Industrial systems powered by steam and/or gas turbine engines, and has also provided land transportation (Diesel/Electric) and is engaged in Military activity on Tank propulsion and transmission design. Many of these applications, on a worldwide basis, have used main power transmission gearboxes designed and manufactured by the various divisions of the Company. Aerospace power transmissions have included the T58 and T64 engine families of applications. Also the NASA/GE QCSEE Program designed and developed two high-horsepower, single stage reduction gearsets for driving the Variable Pitch and the Fixed Pitch engine configurations. These have most recently been joined by the commercial CT-7 turboprop engine now engaged in flight tests on the Saab/Fairchild SF 340 commuter aircraft. From these diverse activities a large data base has been built-up that includes a full range of theoretical tools for analyses, and an equally extensive library of empirical data. It was on these data that the APET gearbox design activity was based.

Initial efforts were directed to establishing the validity of the use of scaling laws in the extension of shaft powers from the known 4-5000 SHP base to the new level required (approximately 12,500 SHP). Three offset and three in-line gearboxes were preliminary designed and weighed. Complexity and reliability indices were used in a grading process to obtain comparative judgments of practicality and worth.

Before examining the details of the APET gearboxes, it is appropriate to summarize the attributes considered to be the most desirable (not necessarily in the order of importance for ranking purposes).

1. High Efficiency - Losses in the gearbox directly subtract from the shaft horsepower available and hence reduce propeller thrust.
2. Lightweight - The advanced turboprop has many hurdles to overcome and gearboxes exhibiting the weight technology level of previous turboprops would probably be unacceptable.

3. Reliability - This can run counter to (2) above but must have precedence in design selection. The advanced gearbox must be a simple layout, uncluttered with extraneous drives and have the bearings and bearing support arrangements chosen to ease the achievement of required L10 (system) life. It seems certain that very high gearbox reliability levels will have to be established and demonstrated before an airline operator would seriously consider the advanced turboprop propulsion system.
4. Initial Price - Gearboxes are expensive - in the order of two hundred and fifty to three hundred dollars per pound (and this assumes amortization of development and tooling costs over a 2000 unit production run). If R&D costs prior to development start, and facilities costs for special test rigs including water brakes are added in, the per pound cost can be increased by 20 - 30 percent. Once in service and achieving the maintainability goals being set by this APET study, overhaul and spare parts cost should be a small item.

The GE designed T64 gearbox is an excellent example of a modern in-service gearbox. Figure 4.6-1 shows a cross section of the T64 gearbox and a summary of the principal materials used.

Some physical characteristics of this gearbox are:

Ratios

Overall	13.44
Stg. 1 (offset)	2.58
Stg. 2 (planetary)	5.21

Horsepower 3400

Speeds

Input (rpm)	15,590
Output (rpm)	1,160

Weight (lbs) 340

This gearbox was reviewed in depth as it serves as an excellent point of departure for more advanced gearboxes.

4.6.1.2 Initial Candidates

It was felt that every configuration that had ever been employed in a turboprop reduction gearbox (whether or not the engine had entered production) had earned the right to a place on the list of initial candidates. In addition other configurations thought to be of possible interest were added to the list. These candidates include all those that have been described favorably in recent industry studies.

ORIGINAL PAGES
OF POOR QUALITY

TABLE OF MATERIALS

- Gears - AMS 6265 - Carburized and Ground
Shot Peened - Black Oxided
- Ring Gear Support - AMS 6415 - Shot Peened -
Black Oxided
- Bearings - 52100 and M50 - Cages Silicon
Iron Bronze or Steel
- Casings - AMS 4218 (356-T6 Al) Anodized -
Outside Surface Epoxy Coated
- Prop Shaft - AMS 6415 - Shot Peened -
Black Oxided

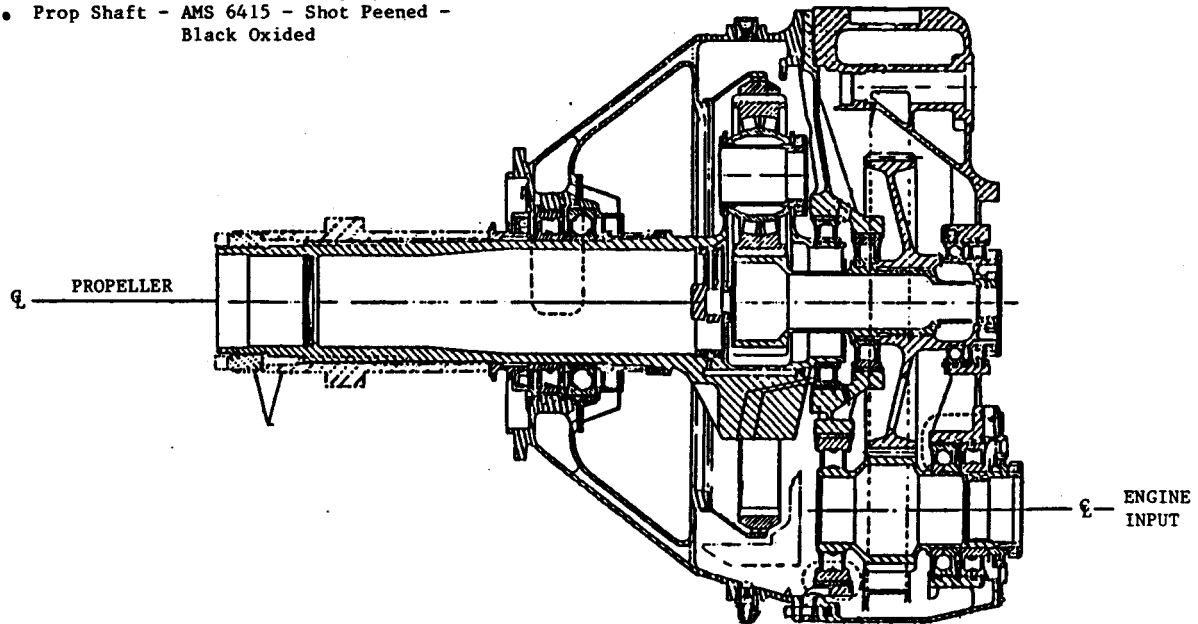


Figure 4.6-1. T64 SDG "Speed Decreaser Gearbox".

4.6.1.3 Initial Screening

The measure of merit for the initial selection of the various gear configurations was weight. The configurations were analyzed and compared using the methodology developed by R.J. Willis (Reference 40). This method permits quick comparisons to be made and readily enables the effect of parameters such as ratio and number of branches on weight to be determined. Figure 4.6-2 is an example of a plot made using this method that show the effects on weight of ratio and configuration. The experience gained using this tool during the APET study both affirmed its simplicity and usefulness and at the same time suggested the need for some possible refinement. The system keys on gear weight (or gear solid rotor volume) as opposed to total system weight.

If gearboxes of diverse configurations all had gear weights that were the same fraction of total system weight this would not be a problem, but unfortunately they do not. An example of this is the contrast between a planetary system which has relatively light gears with many heavy supporting components such as bearings, planet carrier, etc. and a single branch double reduction gearset where the gears themselves are a much larger percentage of the total weight.

The above issue is currently being addressed so that for future studies this proven method will be even more precise. Another refinement under development is to better enable the method to reflect desired technology levels. This can be done by revising both the K-value factor (surface durability constant which relates to allowable tooth Hertzian stress) as well as the application constant, k.

The judgment of experienced personnel also entered the selection process. An example of screening by judgement is the two stage planetary (double planetary) configuration. Although a possible candidate for a conventional turbo-prop where the ratio would be in the neighborhood of 15:1, two planetary units in series are just not needed for propfan ratio levels. The high parts count of such a gearbox impacts cost greatly.

As a final issue in the preliminary screening process there was a desire to see those configurations that had been used with great success on production turboprop programs survive the initial screening and be among the group

Effect on Weight Factor of Ratio & Configuration

F = face width

d = pitch dia.

$$C = \frac{2T}{K}$$

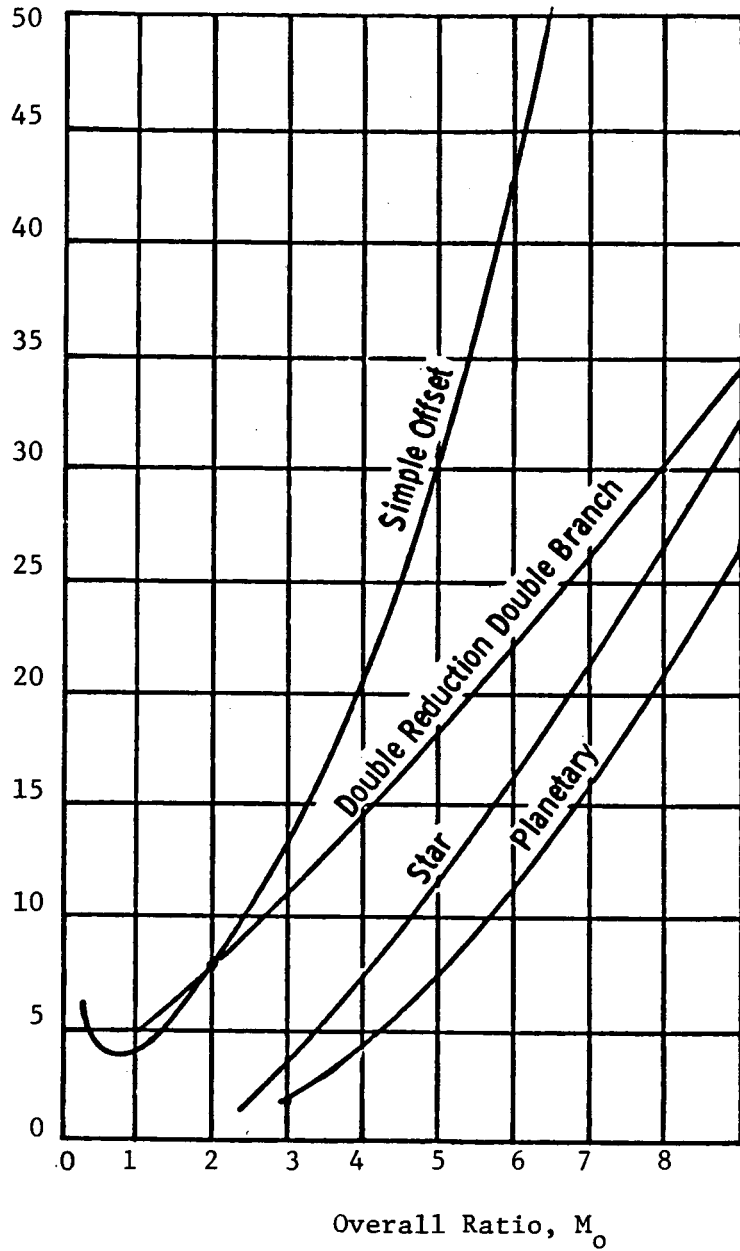
T = input torque

K = Technology constant
(surface durability)

$$\text{Weight} = \sum Fd^2 k$$

k = application constant

Weight Factor, $\Sigma \frac{Fd^2}{C}$



Total Weight Curves

Figure 4.6-2. APET Gearbox Study.

selected for detailed preliminary designs. As an example, had the offset planetary fared poorly during the initial screening we would probably have felt obligated to include it among the detailed preliminary design candidates solely because of the successful history of the T56 and T64 engines which use this configuration.

4.6.1.4 List of Final Candidates

Figure 4.6-3 shows illustrations of the seven gearbox configurations that survived the initial screening process. Preliminary designs were made of the first six and a conceptual sketch was made of the seventh. Five of the seven are epicyclic and the remaining two are double reduction layshaft designs. Also four of the designs are concentric and three are offset.

4.6.2 Preliminary Design Studies

4.6.2.1 Influence of Propfan on Gearbox Design

Virtually all turboprop propeller speed decreasing gearboxes (SDG's) have their ratios falling within a relatively narrow band regardless of the size of the engine. Some examples are:

<u>Engine</u>	<u>SDG Ratio</u>
T64	13.44
T56 (early)	12.5
T56 (late)	13.54
CT-7	15.9
Tyne	15.6

The gear ratio is a function of propeller and turbine technology and is virtually independent of scale size. The explanation is that both propellers and turbines have a well-defined tip speed and as engines are scaled to larger sizes, the ratio between propeller and turbine diameters remains constant. Thus, for unvarying tip speeds the speed ratio (and hence gear ratio) between propeller and power turbine is not a function of scale size.

A fixed ratio, as engines are scaled to larger sizes, unfortunately works to the decided disadvantage of SDG weight and size as is explained by the

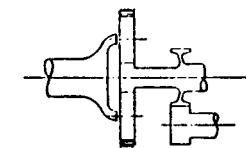
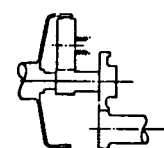
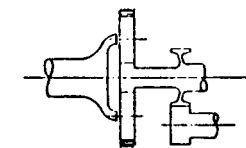
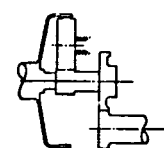
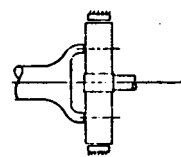
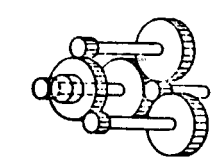
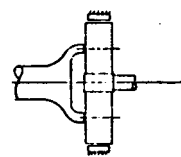
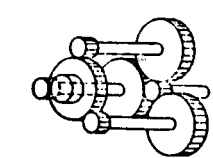
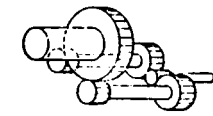
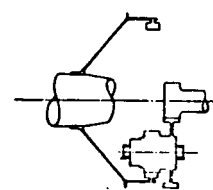
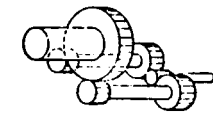
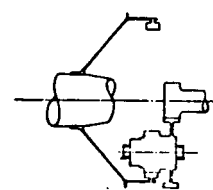
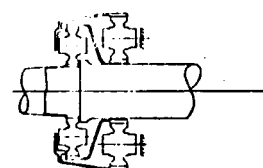
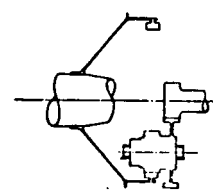
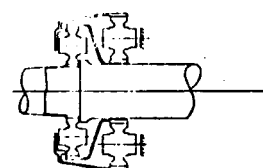
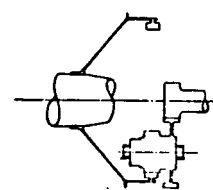
	<u>Type</u>	<u>Example</u>		
1.	Offset Planetary	T56, T64		
2.	Offset Star	-		
3.	Simple Planetary (Inline)	-		
4.	Triple Branch Double Reduction (Inline)	-		
5.	Double Branch Double Reduction (offset)	CT7; PW100		
6.	Triple Branch Compound Star (inline)	Dart		
7.	Coupled Planetary (inline)	T55		

Figure 4.6-3. APET Study Gearboxes.

upper half of Figure 4.6-4. The principal factor driving gear volume and weight in a particular gear stage is torque, and in a speed reducing gearbox output torque. In a multi-stage SDG the output stage is the largest and, therefore, the heaviest, and is the greatest contributor to the overall weight and size of the gearbox. When combining the above we are led to the inescapable conclusion that for a particular configuration of SDG the size and weight is principally driven by the output torque requirement. The upper part of the figure, reading from left to right, shows what happens to the various propeller and gearbox parameters as a hypothetical engine is scaled up tenfold (from 1300 to 13,000 horsepower). Since the SDG ratio is constant, the torque could be expected to rise as the horsepower increases, but, in fact, the rise is much faster because the propeller tip speed is constant regardless of size and, therefore, the speed varies inversely with the diameter. The conclusion to be drawn is that, for constant propeller technology (similar levels of tip speed and SHP/D^2), the principal parameter (output torque) driving gearbox size and weight scales with the 1.5 power of the horsepower level. If there were no relief in sight, turboprops that were much larger than is current practice would be disadvantaged by having SDG's that were a much larger fraction of total propulsion system size, weight, and cost.

Fortunately, propeller technology is capable of providing great relief as is again shown by reading the figure from top to bottom. The upper half of the figure represents current levels of propeller technology whereas the bottom half of the figure is constructed using propfan levels of tip speed and SHP/D^2 . The higher tip speeds permitted by the propfan design provide modest relief by propeller speed increases proportional to the tip speed increase, but the much more significant factor superimposed on this is the effect of the much larger levels of takeoff SHP/D^2 permitted by propfan technology. The much greater power loading permits a large reduction in diameter that therefore demands a greatly increased RPM to maintain the tip speed. As is shown, propfan technology permits reducing the ratio (and therefore the SDG output torque) by the factor of 2.63, for the hypothetical example.

It should be noted that the propulsion system is not the only beneficiary of propeller diameter reduction as the aircraft benefits by permitting closer spacing of wing mounted engines. This enables a reduction in wing structural

Effect of Scaling & Propeller Technology

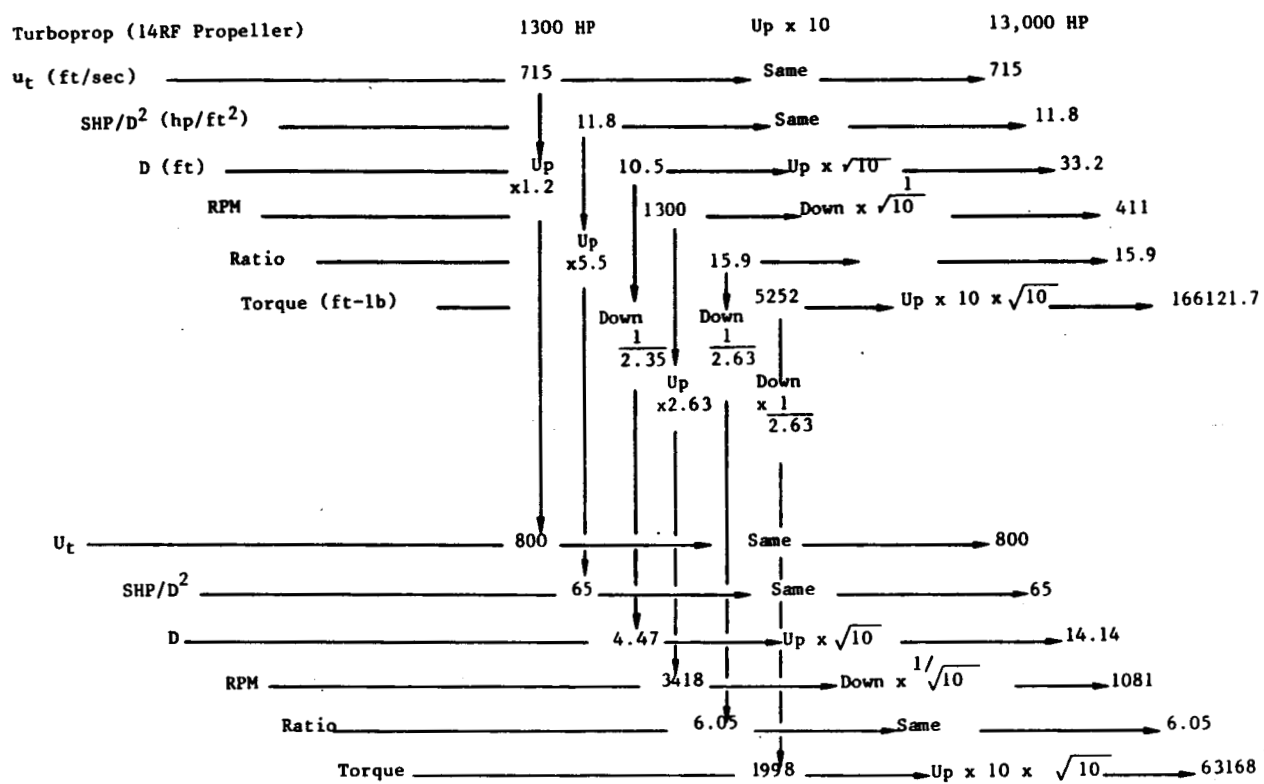


Figure 4.6-4. APET Gearbox Study.

weight and smaller tail size because of easier engine-out control. Shorter, lighter landing gear is still another benefit of smaller propellers.

4.6.3 Gearbox Design Approach

A consistent design approach has been used for all the candidate designs. This design approach draws upon General Electric's data base already described and also includes results of work currently in process. Bearing and gear design analysis computer programs currently active at General Electric have been used.

4.6.3.1 Design Requirements

The design requirements used for the preliminary design of the candidate gearboxes are as follows:

Power = 12500 HP Max (at the propeller shaft)
Bearing System = 15000 hr.
L10 Life

From a typical mission cycle shown in Figure 4.6-5 the cubic mean torque and an average operating speed was determined and used in calculating the bearing lives. The cubic mean propeller thrust load was also calculated to evaluate the life of the output shaft thrust bearing. These design loads are as follows:

Cubic mean torque = 56150 in lbs
Average input speed = 7727 rpm
Cubic mean power = 6885 HP
Cubic mean output bearing thrust load = 6390 lbs (15600 max.)

In addition to the radial loads caused by the gear reactions, the effects of the LP shaft moments were also included when sizing the output shaft bearings.

The design approach used to size the APET gearbox is principally involved with the design methods or techniques used for the gears and the bearings.

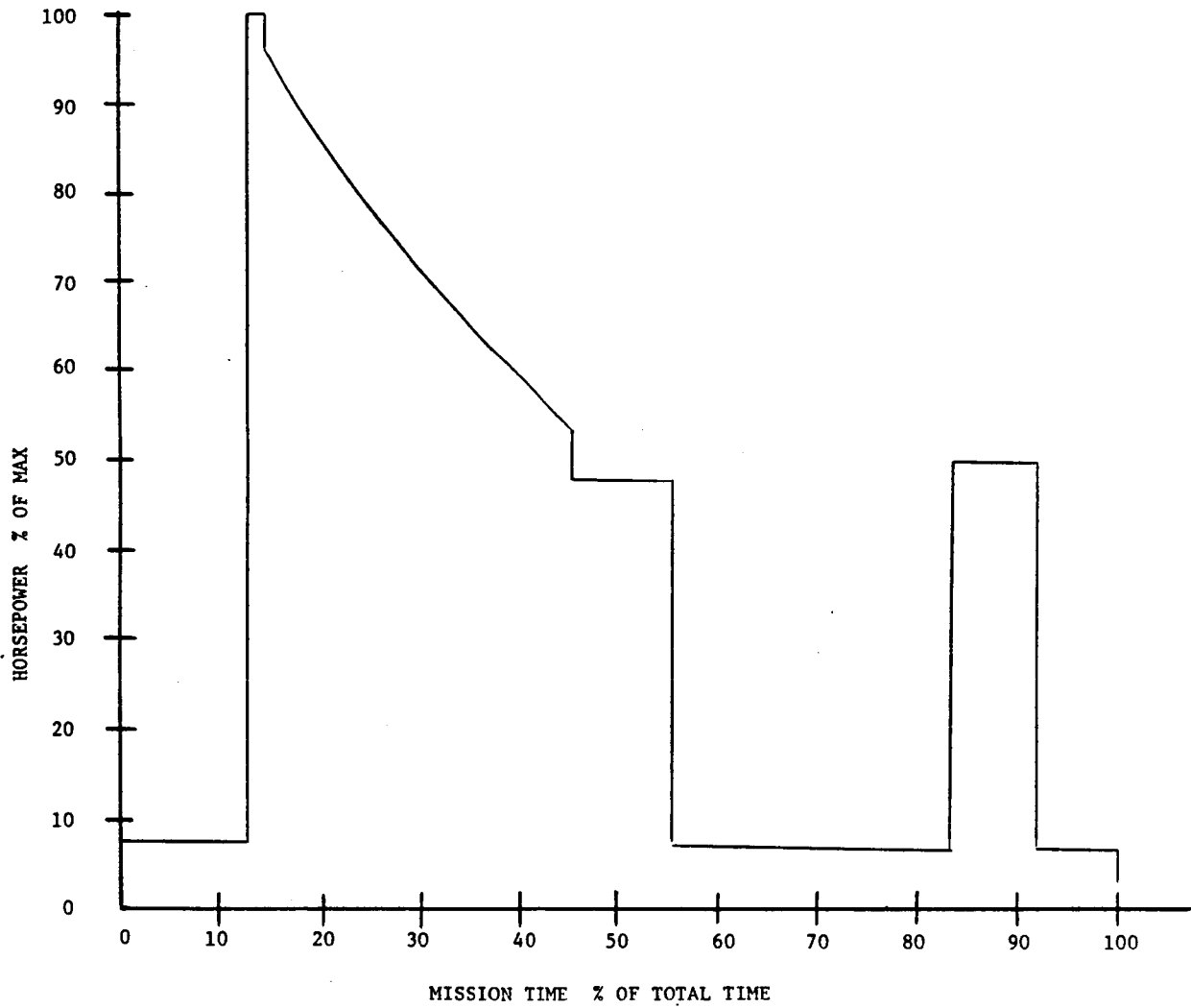


Figure 4.6-5. Typical APET Mission Horsepower Versus Time.

Preliminary designs have used the approaches outlined in the following paragraphs.

4.6.3.2 Gear Design Approach

The gear design allowables used in this study are as follows:

Compressive stress	165 ksi
Bending stress	55 ksi
Flash temperature	≥ 325 ° F

These design allowables do represent improvements over current design limits of commonly used AMS6265 (AISI 9310). Present design limits are 136 - 151 KSI for compressive stress and 44 - 50 KSI for root stress for 10^{10} stress cycles depending on the material heat treat procedure.

Some experimental data on CBS600, Vasco-X2 Modified and Cartech EX-53 have indicated improvements in load capacities over the present capability of AMS6265 although all experimental data does not substantiate the higher capability of Vasco-X2 Modified (Reference 35). Reference 36 indicates a bending stress improvement of approximately 20% for Vasco-X2; another source, Reference 37 indicates an improvement of about 24% in compressive stress capability when compared to AMS6265. Additional evaluation of CBS600 will be needed to determine its relationship to AMS6265 since Reference 38 indicates no basic difference in compressive stress capability. Unreported testing of Cartech EX-53 at NASA Lewis indicates this material shows a life improvement when compared to AMS6265 material.

All of these materials have higher tempering temperature which should move the threshold at which scoring occurs upwards from AMS6265. A flash temperature goal has been established at 325° F because of the higher temperature capability of the materials under consideration. The present limit for low risk is 275° F with MIL-L-7808 lubricant (Reference 39).

4.6.3.3 Bearing Design Approach

For this design study an L10 system life of 15000 hr. has been used. System life is calculated by the following equation:

$$L_{\text{sys}} = \left[L_1^{-\beta} + L_2^{-\beta} + \dots + L_n^{-\beta} \right]^{-1/\beta}$$

L = L10 of individual bearing using cubic mean power

β = Weibull slope constant of 1.5 which is consistent with General Electric engine experience.

Bearing lives are calculated using computer programs available at General Electric. AFBMA life calculations were used in this study. Multiplying factors of 12 for ball bearings and 6 for roller bearings were applied to AFBMA life calculations. Multiplying factors consistent with high horsepower gearboxes will have to be developed for gearbox bearings by component test; multiplying factors of 12 for ball bearings and 6 for roller bearings may be too conservative. Main shaft bearings for large bypass fan engines have demonstrated multiplying factors of 30 or more.

Bearing material is VIM-VAR M50 which is utilized extensively in the General Electric's line of engines. Some recent encouraging work on fracture tough bearing material will make this material a serious contender for high horsepower reduction gearbox bearings.

4.6.4 Description of Detailed Preliminary Designs

4.6.4.1 Design No. 1 - Offset Planetary

Gearbox (1) is similar in layout to the T64 turboprop gearbox. The design intent was to see what effects the upscale from 3-4000 SHP (T64 level) to 12,500 SHP (APET level) would have. The APET design is shown in Figure 4.6-6. This gearbox design includes all the lessons learned from T64 experience and incorporates the latest features introduced from a long history of development. It does however, have one major difference - the overall reduction gear ratio which is 13.44 for the T64 vs the 7.8:1 required by the APET propfan and engine.

Well established materials and lubrication methods are included and an adequate space has been allotted to accommodate a prop brake. A free access bore of 3-inch diameter has been reserved in extension of the prop shaft to the extreme aft face of the accessory gearbox, which is provided with a mounting pad for the benefit of through-the-shaft propeller controls.

ORIGINAL DESIGN
OF POOR QUALITY

RATIOS:

OVERALL 7.844
OFFSET 1.512
PLANETARY 5.189

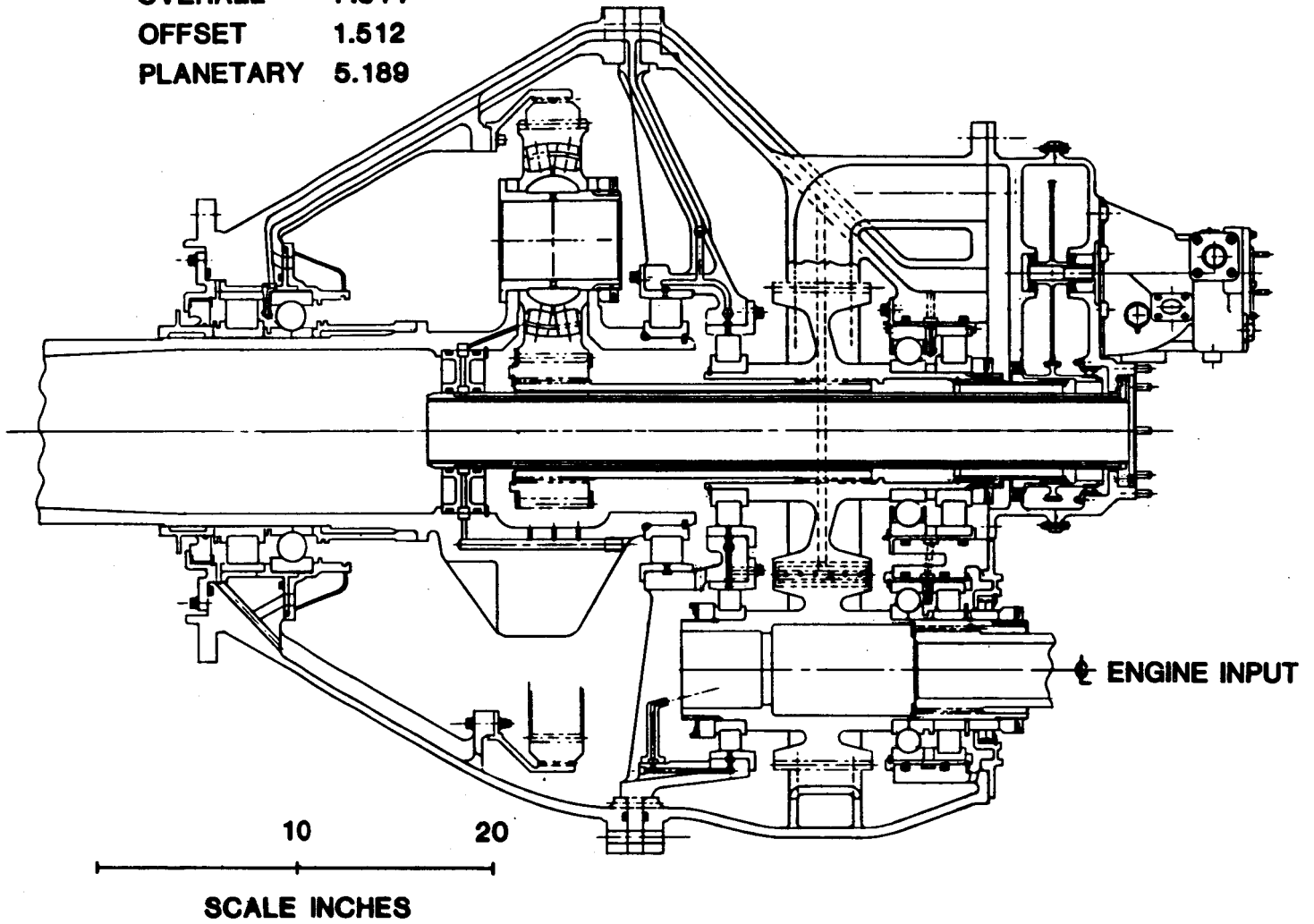


Figure 4.6-6. APET Gearbox 12500 Shp Offset/Planetary.

The principal characteristics of this design are:

Prop shaft rpm: 1104 rpm
Input rpm: 8660 rpm
Ratio (overall): 7.844:1
Input (offset ratio) 1.5116:1
Planetary Reduction 5.1892:1

A weight breakdown of this design is shown by Table 4.6-1..

Table 4.6-1. Weight Breakdown of APET Offset Planetary Reduction Gearbox.

	Weight, lb	
● Front housing	200	cast
● Aft housing + midframe	270	cast
● Accessory drive housing	60	cast
● Propeller shaft	300	forged
● Planet assemblies (4)	200	forged
● Bull gear	120	forged
● Input pinion	75	forged
● Sun gear	25	forged
● Ring gear	70	forged
● Ring gear support	30	forged
● Propshaft thrust bearings	36	
● Scavenge and lube pump	50	
	1436	

4.6.4.2 Design No. 2 - Offset Star

Gearbox (2) was designed to evaluate a star versus a planet system, i.e. it can be directly compared with gearbox (1). This gearbox, shown in Figure 4.6-7, also has space allocated for a prop brake and has a free access bore of 3 inches to the extreme aft face of the accessory gearbox. A mounting pad is provided for a through-the-shaft propeller control.

RATIO:

OVERALL 7.807
OFFSET 1.561
STAR 5.00

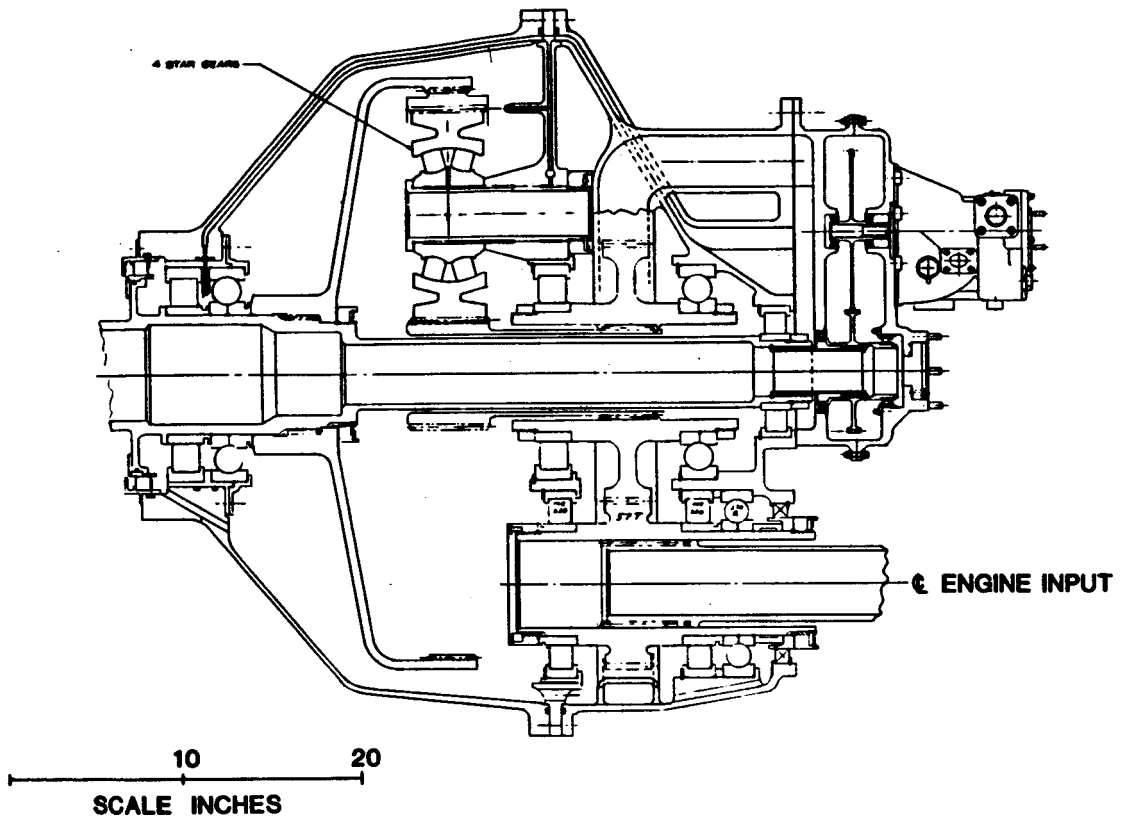


Figure 4.6-7. APET Gearbox 12500 Shp Offset/Star.

The principal characteristics of this design are:

Prop shaft rmp: 1104
Gearbox Input rpm: 8619
Ratio (Overall): 7.807:1
(1st) Ratio (Input-Off Set): 1.5614
(2nd) Ratio (Star): 5.00

A weight breakdown of this design is shown by Table 4.6-2.

Table 4.6-2. Weight Breakdown of APET Offset Star Reduction Gearbox.

	Weight, lb	
• Front housing	200	cast
• Aft housing + midframe	270	cast
• Accessory drive housing	60	cast
• Propeller shaft	100	forged
• Internal gear	210	forged
• Star assemblies (14)	280	forged
• Bull gear	125	forged
• Input pinion	80	forged
• Sun gear	20	forged
• Propshaft thrust bearing	36	forged
• Scavenge and lube pump	50	
	1431	

4.6.4.3 Design No. 3 - Simple Planetary

The ratio requirement for a propfan gearbox is within the capability of a single planetary stage. The third configuration selected for a preliminary design is a single stage in-line simple planetary. This design is shown in Figure 4.6-8. A through-the-shaft access for propeller control purposes is not possible in this configuration due to the absence of a parallel shaft. A unique feature of this design is that the gears are double helical.

The principal characteristics of this design are:

Prop shaft rpm: 1104

Input rpm: 8587

Ratio (Overall, One-step, Planetary) = 7.7778:1

A weight breakdown of this design is given by Table 4.6-3.

Usually planetary configurations are among the lightest in weight, and because there is no input offset stage this design might have been expected to be the lightest of all. Such was not the case as it is essentially at the weight of the first two designs discussed. The principal reason for this is that the ratio required, though still within the practical capability of a single stage simple planetary, is outside the range where the planetary performs to best advantage from a weight standpoint.

Note that the weight of this configuration includes an internal propeller brake. The brake is shown in Figure 4.6-8. As mentioned earlier, the gearboxes shown in the earlier Figures are designed such that they can accommodate a similar type of brake.

4.6.4.4 Design No. 4 - Double Reduction Triple Branch

The fourth candidate configuration selected for a preliminary design is the double reduction triple branch gearbox shown in Figure 4.6-9. A detailed weight breakdown of this design is shown by Table 4.6-4. Unlike the other double reduction gearbox in this study (double reduction, double branch; Figure 4.6-10), this one is reverted rather than offset, having its input and output shafts on the same centerline. As is the case with the simple planetary, through-the-shaft access for a propeller control mounted on the rear of the gearbox is not possible. The screening method referred to in Section 4.6.1.3 indicates a weight saving as the number of branches is increased. This particular design, however, did not capitalize on this theoretical advantage as it is the heaviest gearbox in the study and was the first one rejected solely because of its weight.

Table 4.6-3. Weight Breakdown of APET Simple Planetary Reduction Gearbox.

	Weight, lb
• Front housing	200
• Aft housing	270
• Accessory drive housing	60
• Propeller shaft	250
• Planet assemblies (3)	300
• Ring gear	120
• Ring gear support	120
• Sun gear	25
• Input shaft	25
• Propeller shaft thrust bearing	36
• Scavenge and lube pump	50
• Propeller brake	70
	1526

Table 4.6-4. Weight Breakdown of APET Double Reduction Triple Branch Gearbox.

	Weight, lb
• Front housing	236
• Aft housing + midframe	440
• Accessory drive housing	60
• Propeller shaft	525
• 3 Forward pinions	157
• 3 Quill shafts	49
• 3 Aft gears	306
• Input pinion	36
• Propeller thrust bearing	36
• Scavenge and lube pump	50
	1895

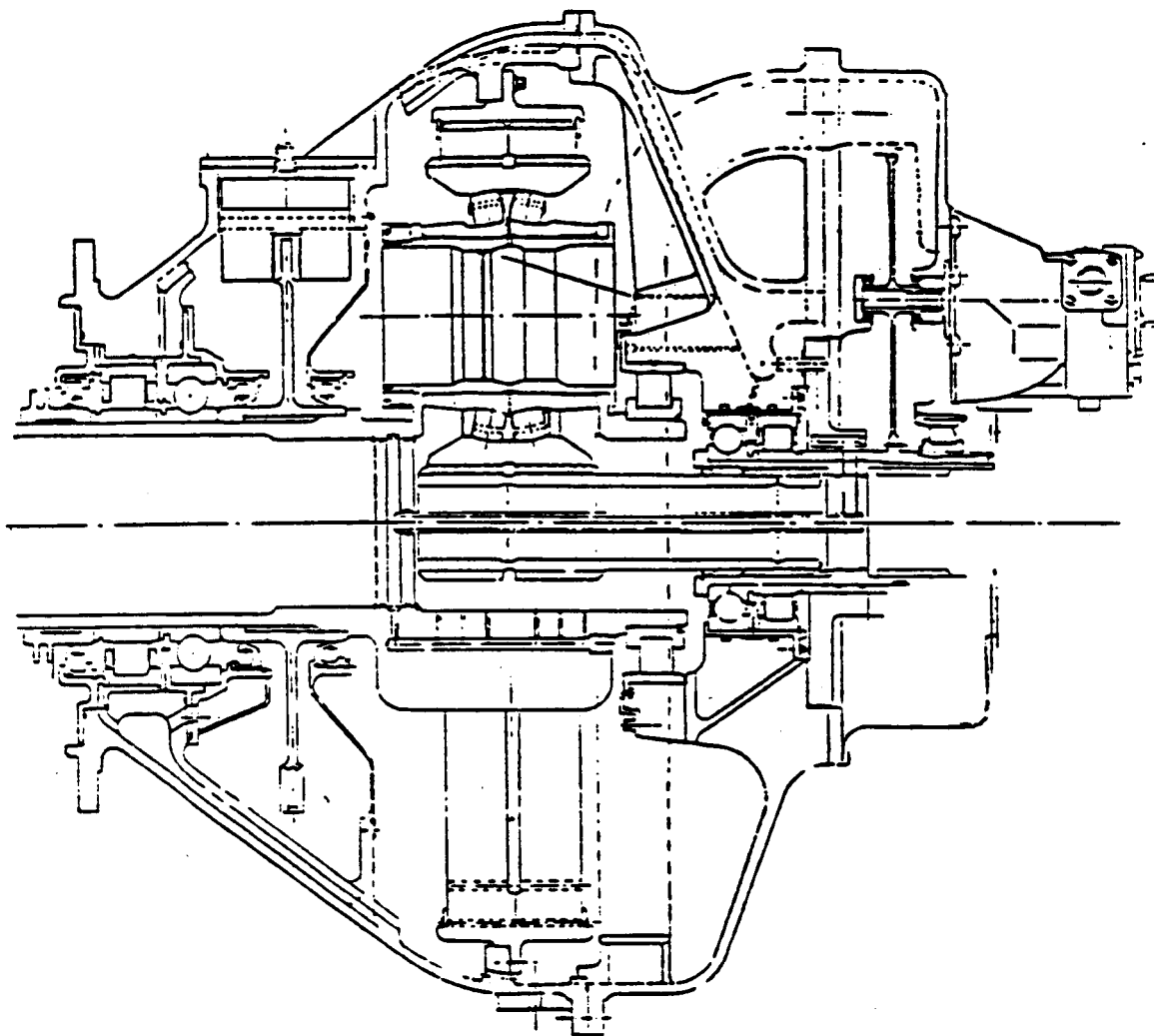


Figure 4.6-8. Modern High Horsepower Gearbox III (Simple Planetary).

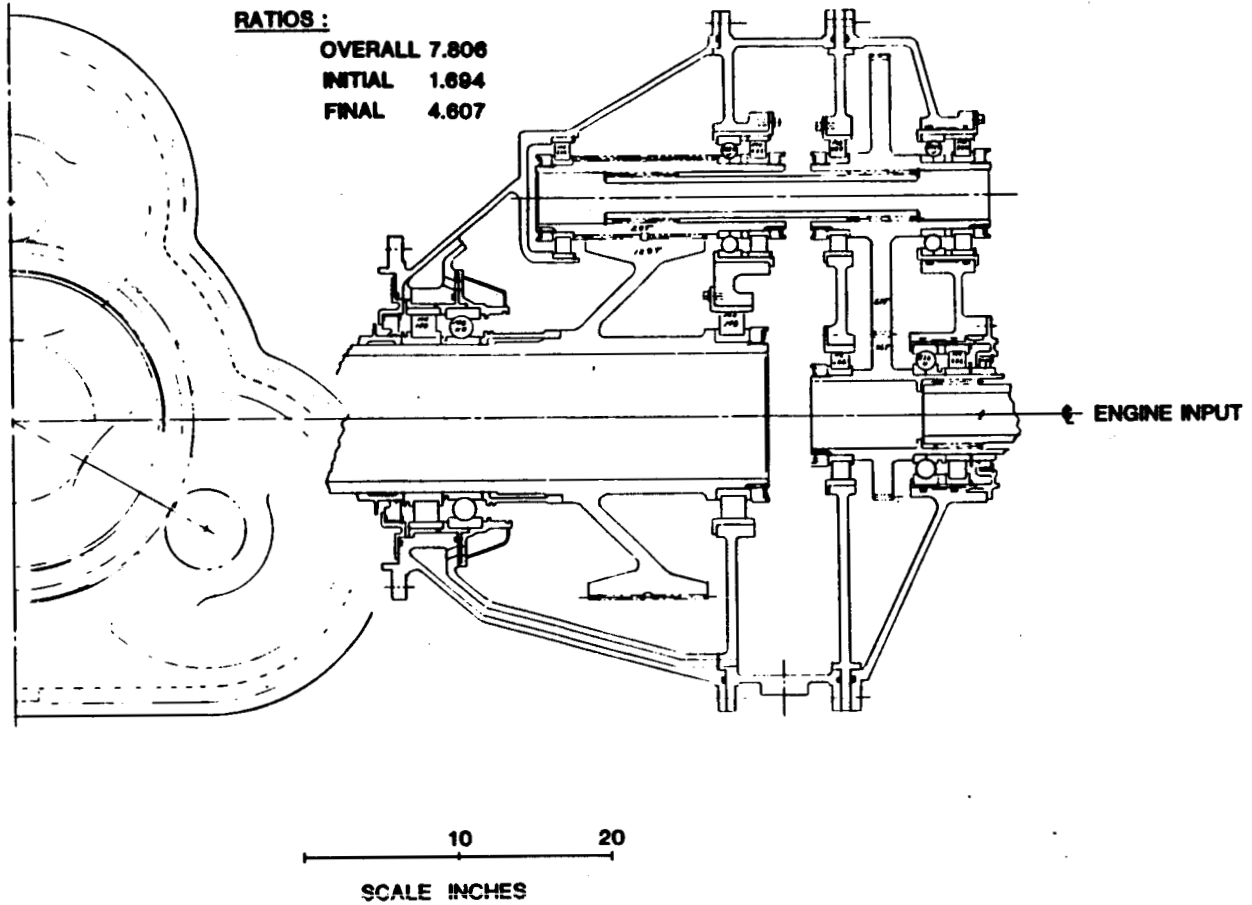


Figure 4.6-9. AEPT Gearbox 12500 Shp Double Reduction Triple Branch.

4.6.4.5 Design No. 5 - APET Dual Branch, Two-Stage Reduction Gearbox

The fifth selected candidate gearbox is a APET dual branch, two-stage reduction gearbox design. The principal features of which are shown by Figure 4.6-10. This configuration has received favorable comment in recent industry literature and is also the configuration used by both the CT-7 and PW-100 turboprops. The materials are shown by Figure 4.6-11 and the weight summary is given by Figure 4.6-12.

This configuration was subjected to a rigorous weight determination process using the GE computerized graphics system. See Section 4.6.11 for an example of the weight calculation process.

This design was subjected as well to a detailed preliminary cost estimating procedure. The details of this process are also to be found in Section 4.6.11.

4.6.4.6 Design No. 6 - Compound Star

The sixth gearbox configuration that was selected for a preliminary design is a triple branch compound star layout. The principal features of this gearbox are shown in Figure 4.6-13. Figures 4.6-14 and 4.6-15 respectively show the materials of the principal components and the weight summary. This gearbox, like the single stage simple planetary, and the double reduction triple branch are inline configurations, whereas the remainder are all offset. This design, like the other inline configurations, does not permit through-the-shaft access to the propeller from a rear mounted control.

Configurations 5 and 6 were subjected to a rigorous weight determination process using the GE computerized graphics system. See Section 4.6.11 for an example of the weight calculation process.

4.6.4.7 Design No. 7 - Coupled Planetary

A conceptual design as opposed to a preliminary design was made of a 7th candidate configuration. This configuration (see Figure 4.6-16) is a coupled planetary or a dual-path planetary as it is sometimes known. The conceptual design was used to compare with the configuration of Figure 4.6-10 (double

ORIGINAL DESIGN
OF POOR QUALITY

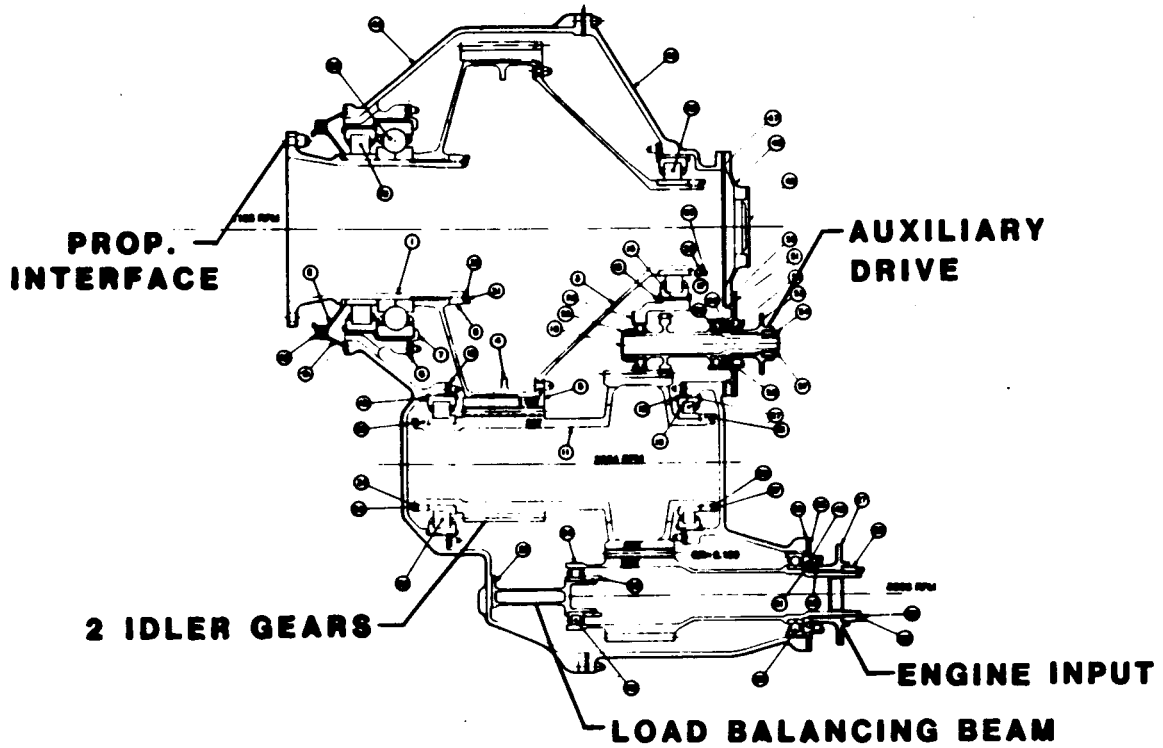


Figure 4.6-10. APET Dual Branch, Two-Stage Reduction Gearbox.

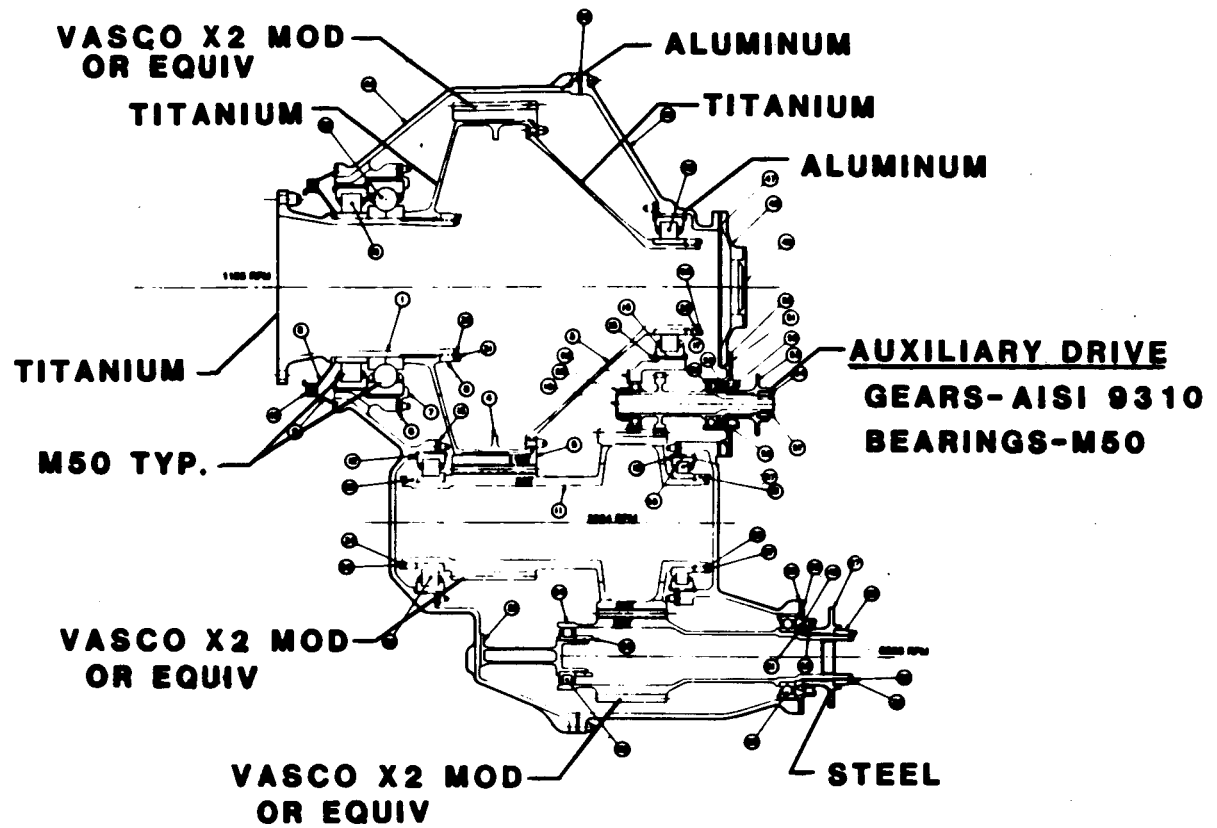


Figure 4.6-11. APET Dual Branch Two-Stage Reduction Gearbox.

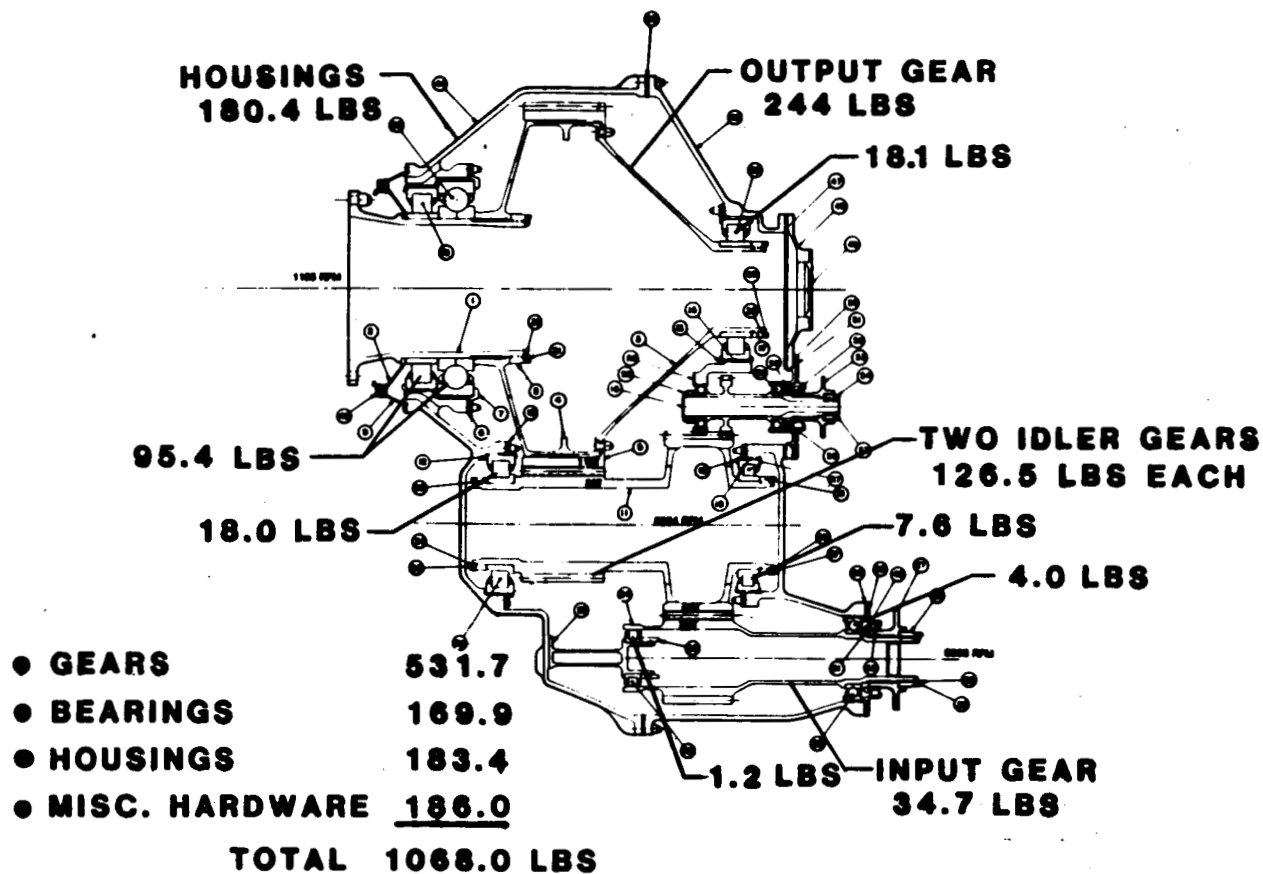


Figure 4.6-12. APET Dual Branch Two-Stage Reduction Gearbox.

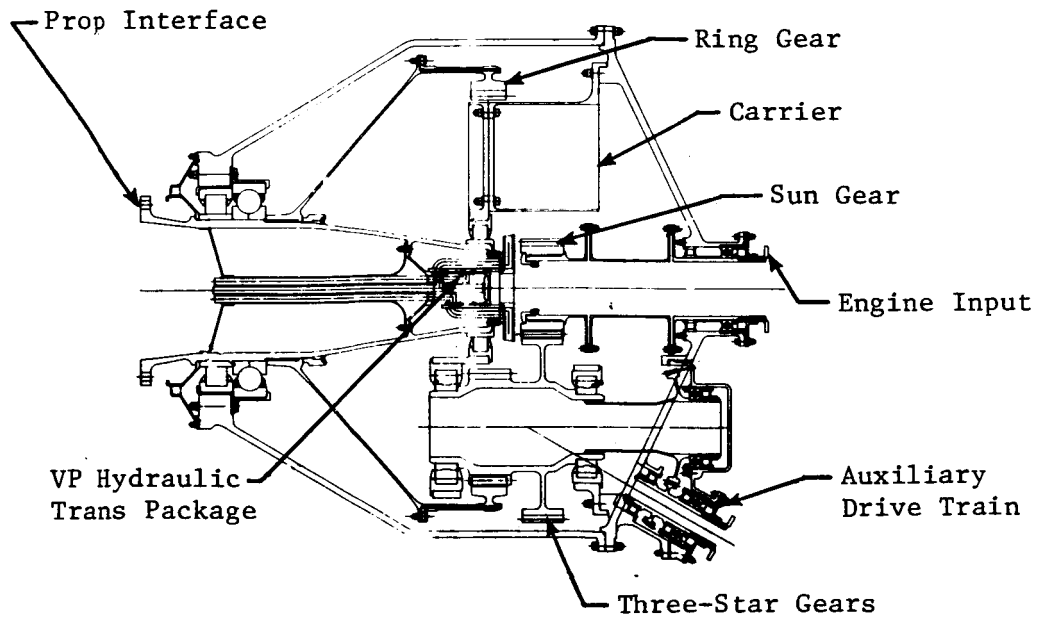


Figure 4.6-13. APET Triple Branch Compound Star Reduction Gearbox.

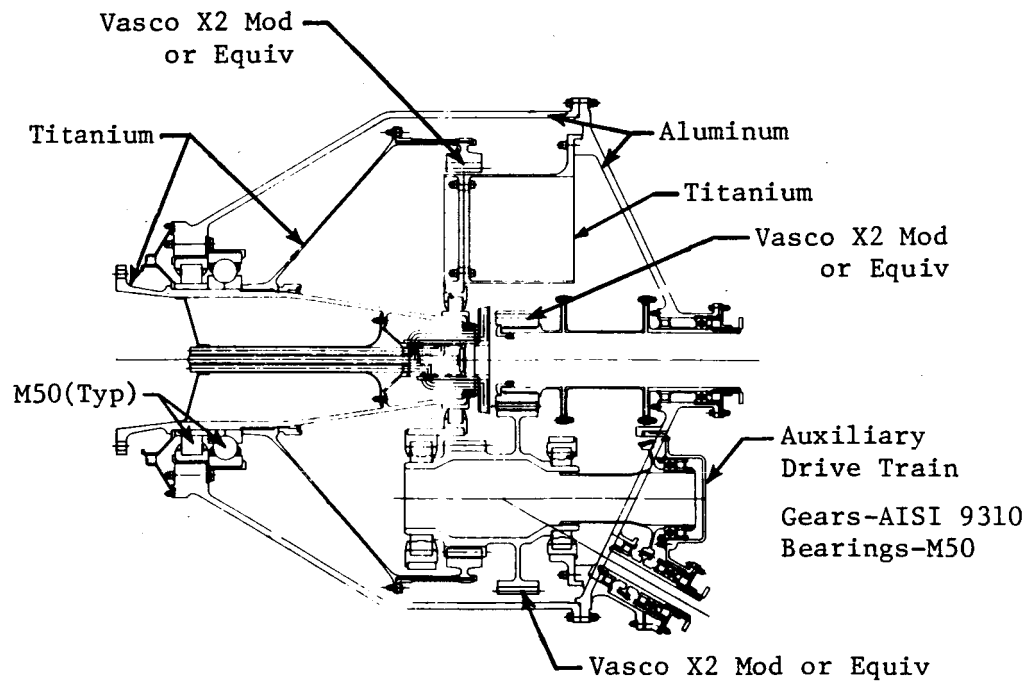


Figure 4.6-14. APET Triple Branch Compound Star Reduction Gearbox.

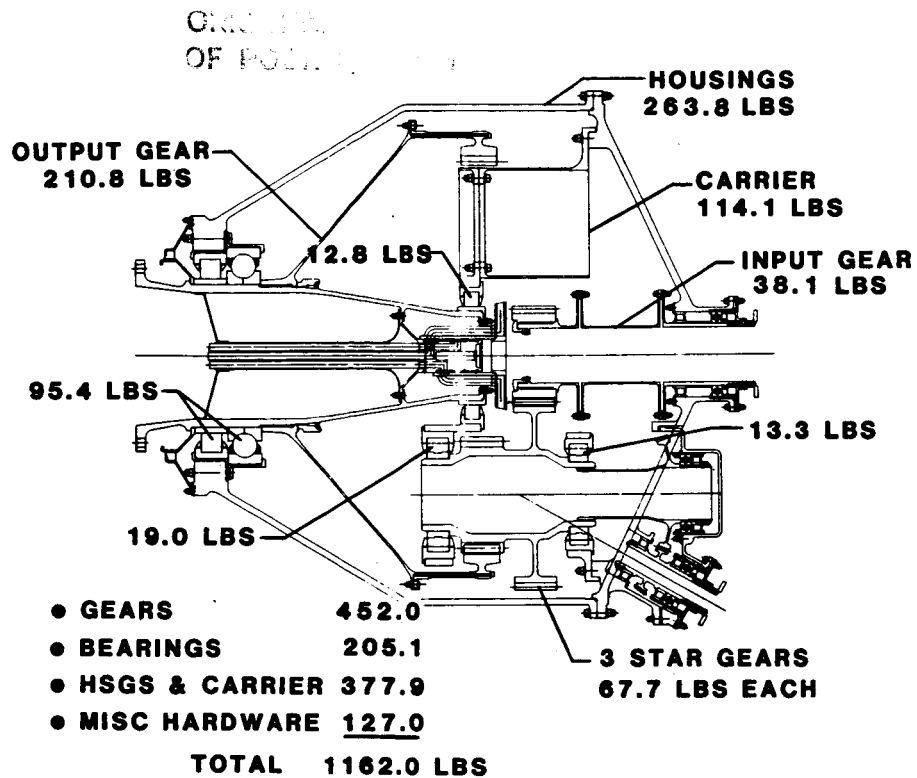


Figure 4.6-15. APET Triple Branch Compound Star Reduction Gearbox.

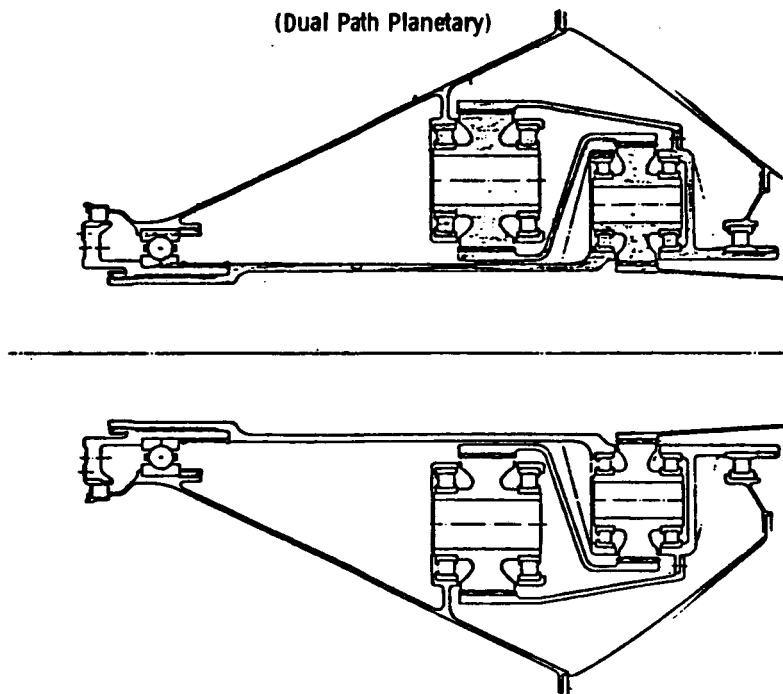


Figure 4.6-16. APET Coupled Planetary Reduction Gearbox.

reduction, double branch) for the purpose of determining the relative cost between the two designs. The high parts count weighed heavily against this design, making it among the most expensive.

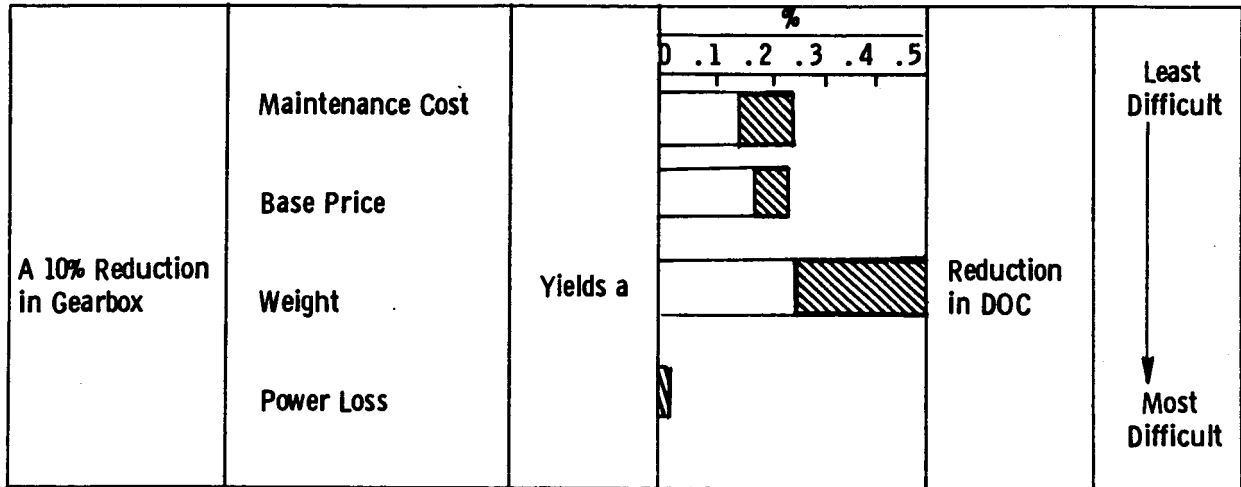
4.6.5 Final Selection Process

4.6.5.1 Criteria Affecting Direct Operating Cost (DOC)

The DOC cost model developed as part of this study for the defined APET mission was exercised for the purpose of identifying the sensitivity of the gearbox parameters known to affect DOC directly. In addition, these same parameters were ranked by experienced gearbox design personnel from the standpoint of degree of difficulty in achieving a measure of improvement above current levels. The results of both exercises are shown by Figure 4.6-17. This figure shows that weight is the significant gearbox parameter insofar as effect on DOC with maintenance cost and base price virtually tied for a lesser but still significant effect. Power loss has but a small effect on DOC as shown by the chart. When looking at the absolute levels of the effect upon DOC of the various gearbox parameters, it might seem that the gearbox drives DOC very lightly, but it must be remembered that the gearbox is but a component of the propulsion system, not unlike a compressor or power turbine. The levels of sensitivities of these other components are of the same magnitude as the SDG, and although the contribution of each is small, the cumulative effect is large indeed. The other significant item in Figure 4.6-17 is the last column which ranks the four variables as to the difficulty of achieving a 10% improvement.

When both features of Figure 4.6.4-17 are considered together they suggest where the emphasis should be placed in SDG development. For example, the small impact of power loss coupled with the difficulty in achieving a significant improvement suggest that this should not be a priority issue. Of course, this should not be interpreted as an endorsement of inefficient gearboxes, but rather that this analysis suggests that if invested in the reduction of maintenance costs, for instance, a unit of development effort has the probability of producing a much greater positive effect on DOC. Following is a discussion of how the design can influence each variable.

**Impact on Aircraft DOC
of a Change in Gearbox Variables**



- The values for each parameter are expected to lie within the shaded boxes.
- The uncertainty of each value is directly attributed to the overall uncertainty of the total DOC.

Figure 4.6-17. APET Gearbox Economics.

4.6.5.2 Maintenance Cost

This is a heavy driver of DOC and it is the area that will probably be responsible for the most significant design practice departures from past gearboxes. Three approaches are suggested which will produce the most significant reductions in maintenance costs.

1. Modularity

A modular design of the gearbox itself is a significant departure from past practice in SDG's and will permit greatly reduced maintenance costs. Only those functions directly related to the primary job of speed reducing (bearings, gears, seals) should be permitted to occupy space within the relatively inaccessible gearbox housing interior. Items such as scavenge pumps, propeller brakes, hydraulic slip rings, etc. should be accessories external to the gearbox itself. In addition the installation of the entire propulsion system should permit component replacement with minimum disturbance of adjacent items. Modular construction will do little for the overall system reliability but it will greatly improve the reliability of the SDG itself as failures of the accessory modules will not be charged against the SDG because SDG removal and teardown will not be required to repair faults in these other areas. Modular construction can have an undesirable effect on weight, as the lightest weight designs tend to be associated with integrated construction. Overall system reliability may also suffer slightly as, for example, modular construction may increase the number of fluid connections that are subject to leak.

2. Condition Monitoring

Effective vital function and diagnostic instrumentation that is part of the original design will be effective in keeping maintenance costs down. When combined with modular construction, diagnostic instrumentation in conjunction with an appropriate information processing capability will afford the ability to fault isolate to an individual line replaceable unit (LRU). The goal should be early realization of on-condition maintenance. This will demand some minimum complement of vital function instrumentation.

3. Basic Design Considerations

The factors here that will most affect maintenance cost are:

- a. Design for long system life. This will simultaneously enhance reliability but will come at the cost of weight and base price.
- b. Design for assemblability. This will both show to advantage in base price as well as in overhaul cost.
- c. Low parts count. Maintenance costs are a function of the number of piece parts that must be stocked, inspected, refurbished, and assembled.

4.6.5.3 Base Price

Modularity will greatly reduce the base price of the SDG itself, although, like weight, overall system price may be favored by integrated designs. Making these detailed trades is considered beyond the scope of the present study. The features of the basic design that most influence base price are simplicity and low parts count. Specific attention to design for producibility and design for easy assembly are the factors other than the selection of an inherently low cost configuration that will be most effective in controlling base price. Lastly, development costs will be reflected into the base price. The more complicated configurations, particularly the planetary units, are the ones most likely to have the highest development costs.

4.6.5.4 Weight

This is the most vexing variable both because it is the largest driver of DOC and also because it is difficult to make significant gains over past levels. In addition, the bulk of the previously mentioned desirable attributes of a modern gearbox (modular construction, design for long system life, added instrumentation, and cost reductions in design) tend to affect weight undesirably. The most effective approaches to a lightweight SDG are:

1. Selection of a configuration that is inherently lightweight. An example is that increasing the number of branches reduces weight.
2. Employment of weight saving design features and construction. An example of this is the built-up output gear assembly in the double branch double reduction configuration.

3. The greatest opportunity for gain, and the most challenging technology, is to increase successfully the K-value factor of the design. This will permit more torque to be carried through a given mesh. The APET study activities pointed to the following most promising avenues:
 - a. Improved materials
 - b. Advanced lubricants
 - c. Revised tooth form.

4.6.5.5 Power Loss (Efficiency)

The payoff in making a breakthrough in this area will not be great. What is recommended is proceeding with sound engineering practices and using fully the technology already in hand. Reducing the speed dependent losses in a given configuration is a major concern. Areas deserving attention are:

1. Proper jetting and application of lubricant to introduce only the minimum flow necessary and thus reduce churning losses.
2. Good practice in effective scavenging is essential to remove the lubricant as soon as its job is done to minimize the energy it will absorb from rotating elements.
3. Proper use of windage screens, baffles and internal clearances will reduce the windage losses to low levels.
4. A novel approach not currently used is to reduce or modulate the lubricant flow as a function of torque such that the flow is never in excess of what is required.

The configuration selected can affect the losses. Each mesh represents a loss, so single stage units have the edge over double reduction designs. The number of branches, however, should have a negligible effect on efficiency.

4.6.6 Criteria with Lesser Effect on DOC

4.6.6.1 Reliability

As stated in Section 4.6.1.1 it is a virtual certainty that to be a commercially acceptable product, a future SDG will have to possess a very high level of reliability much in excess of what has been exhibited by past designs. All of the candidate gearbox configurations have the capability of evolving

into highly reliable designs therefore it is not the issue as to which candidates possess the most inherent reliability but instead how difficult is it to achieve a given level of reliability with each design. An example to illustrate the foregoing is bearing system L10 life. The expression for system life is

$$L_{\text{sys}} = \left[L_1^{-\beta} + L_2^{-\beta} + \dots + L_n^{-\beta} \right]^{-1/\beta}$$

where $L_{1,n}$ represents the L 10 lives of the individual bearings. It can be readily seen from this equation that designs having a large number of bearings must have greatly elevated life for each individual bearing to maintain system life. Designing individual bearings to these high L 10 values impacts weight and cost greatly. The foregoing strongly suggests that the configurations with low parts count will have a significant advantage.

The seven candidate designs are ranked in Table 4.6-5 from the standpoint of difficulty in design of achieving a common base reliability goal.

Table 4.6-5. Gearbox Design Ranking.

Configuration	Ranking (higher number is more desirable)
1. Offset planetary	2
2. Offset star	3
3. Simple planetary	3
4. Triple branch	3
5. Double branch	4
6. Compound star	3
7. Coupled planetary	1

Another approach to increased reliability is the proper use of vital function and diagnostic instrumentation and supporting devices in the SDG and

its systems. This approach is considered beyond the scope of the present study, however.

4.6.6.2 Frontal Area

The various preliminary design gearboxes differed in frontal area which has been a measure of merit in some past installations. In the case of the APET study, however, all the candidate designs described in Section 4.6.4 could be contained within the 0.3 radius ratio propfan nacelle designs described in Section 4.7. As a result, frontal area was not used as a criteria in choosing among the designs. As a matter of interest, the coupled planetary is probably the smallest, and the portions of the housing adjacent to the two layshafts in the double branch double reduction gearbox described in Section 4.6.4.5 leave the least clearance to the nacelle outer skin.

4.6.6.3 Reverse Rotation

Opposite rotation on opposite engine locations of a twin engined aircraft with wing mounted tractor engines (the configuration of the APET study airplane) is viewed as a possible requirement from the standpoint of reduced cabin noise or the desire for aerodynamic symmetry. Opposite rotation could be achieved either by left and right hand gas generators or by reverse rotation within the gearboxes. Insofar as accommodating reverse rotation requirements within the gearbox it would be noted that some of the candidate gearboxes have output shaft rotation in the same direction as the input shaft whereas the remainder have opposite rotation.

Table 4.6-6 summarizes gearbox rotation.

One solution to the problem would be to select entirely different configurations for opposite engines, for example an offset star for the left hand engine location and an offset planetary for the right hand location. The obvious disadvantage of this solution is that it requires the development, manufacture, and support of two different designs with great impact on first cost and maintenance cost.

None of the inline or concentric designs in Table 4.6-5 (No's 3, 4, 6, and 7) have the capability for absorbing a practical modification to provide

Table 4.6-6. Gearbox Rotation.

Configuration	Input vs. Output Rotation
1. Offset Planetary	opposite
2. Offset star	same
3. Simple Planetary	same
4. Triple Branch	same
5. Double Branch	same
6. Compound Star	opposite
7. Coupled Planetary	same

reverse rotation. The offset designs, on the other hand, could be fitted with appropriate idler gears in the first or input stage (where the torque levels are lowest) to reverse the rotation. The split gearbox configuration already shown in Figure 4.4-15 is also capable of reverse rotation modification. Figure 4.6-18 shows the reversing idlers in the various input stages. Gearbox weight just resulting from the added parts would increase approximately 100 pounds as a result of incorporating idlers. There would be an additional weight increase, as in order to hold the line on system L 10 life the increased number of parts would require that existing parts be redesigned with increased individual lives. Gearbox efficiency would be impacted by approximately 1/2% which would actually be a 50% increase in power loss resulting from the addition of reversing idlers. The lubrication and heat exchanger systems would also receive an unfavorable weight impact.

4.6.6.4 Pitch Change Access

All the offset designs among the candidates (1. Offset planetary, 2. Offset star, and 5. Double branch double reduction) have provisions for through-the-shaft access to the propeller pitch change mechanism from a propeller control mounted on the rear of the gearbox. Unfortunately, such access is not possible in any of the remaining designs, which are all concentric or in-line

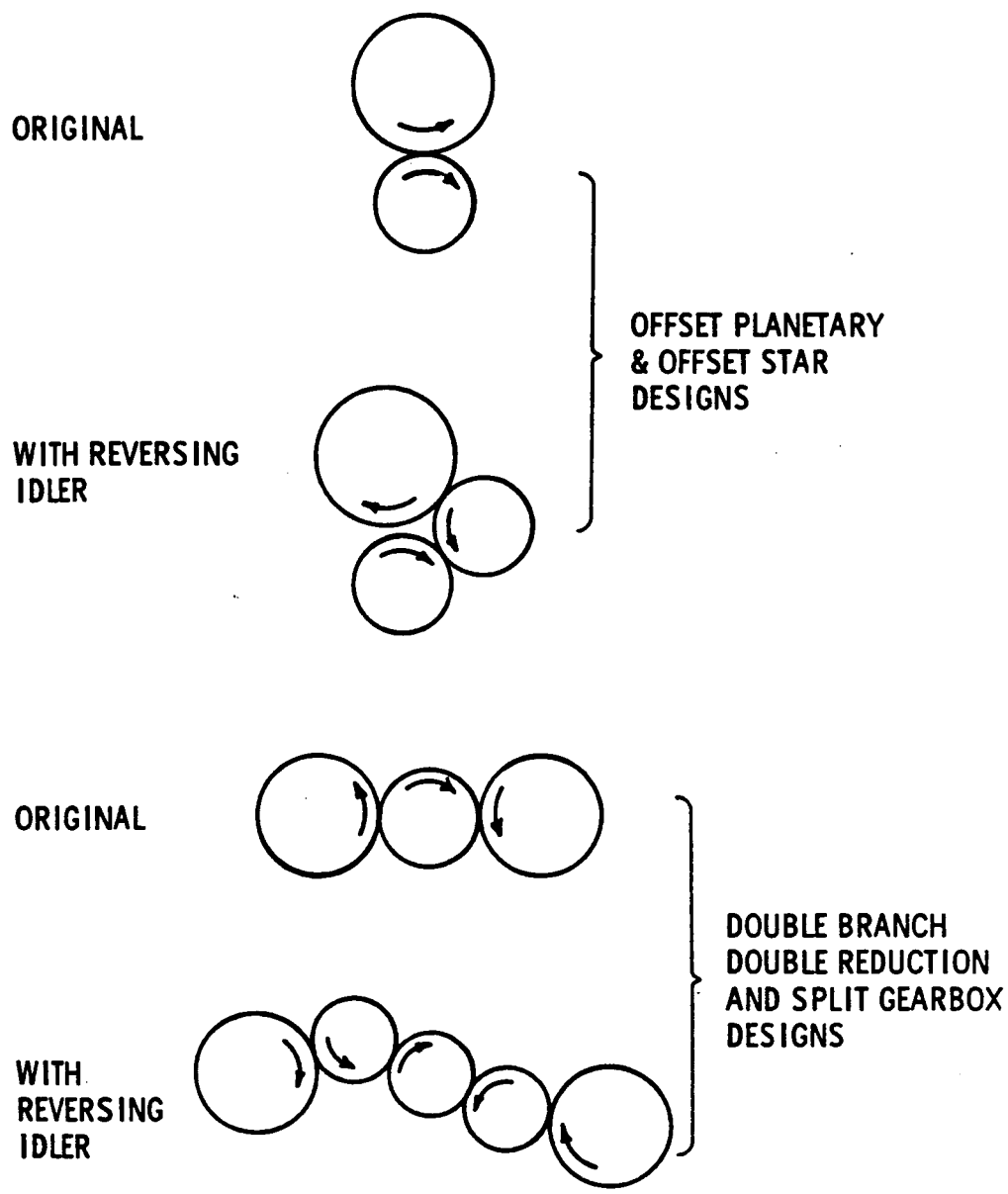


Figure 4.6-18. Input Stage Reversing Schemes.

designs. Although it is recognized that this lack of access could have serious propeller system implications, the concentric designs were not derated because of this. A potential solution to this concern might be the development of a modern technology all-electric propeller pitch change system.

4.6.7 Selection

The original field of seven configurations which survived the preliminary screening process was further reduced to two final designs that are recommended for future study and development. The final selection was based on the DOC effect of the properties of the various candidates. The candidate gearboxes were ranked for each merit category. The ranking number was then multiplied by an adjusted weighting factor to obtain a measure of merit value that is representative of DOC impact. The weighting factors used are consistent with the sensitivities shown in Figure 4.6-17. The scores for the various merit categories were then totaled to obtain an overall rating value for each gearbox configurations. The higher values represent more favorable DOC impact. The tabulations are shown by Table 4.6-7. The selected configurations are #5, the double branch double reduction, and No. 6 the compound star.

Although not used in this selection, the criteria discussed in Section 4.6.6 are also of great interest. The rankings previously developed in this Section are summarized in Table 4.6-8. The candidate with the highest score (No. 5) also rated highest in this table.

4.6.8 Design Description of Two Selected Designs

From the matrix of seven gearbox configurations screened two have been selected as prime candidates for further development. These two are an offset dual branch, two stage reduction gearbox and an inline triple branch compound star reduction gearbox.

4.6.8.1 Offset Dual Branch, Two Stage Reduction Gearbox

The offset gearbox already shown in Figure 4.6-10 contains the following features:

Table 4.6-7. Gearbox Candidate Rating.

Type		Merit Category (Merit Values)			Overall Rating Value	
		Weight	Maint. Cost	Base Price		Power Loss
1. Offset Planetary		11.7	4.6	4	.8	21.1
2. Offset Star		11.7	6.8	6	.8	25.3
3. Simple Planetary (Inline)		11.7	6.8	6	2.3	26.8
4. Triple Branch Double Reduction (Inline)		5.9	6.8	6	.8	19.5
5. Double Branch Double Reduction (offset)		17.6	9.1	10	.8	37.5
6. Triple Branch Compound Star (inline)		17.6	6.9	8	2.3	34.8
7. Coupled Planetary (inline)		17.6	2.3	2	1.5	23.4

Table 4.6-8. Gearbox Candidate Rating.

Type		Can accept modification for reverse rotation	Through-the shaft PCM access	Design for Reliability
1. Offset Planetary		Yes	Yes	2
2. Offset Star		Yes	Yes	3
3. Simple Planetary (Inline)		No	No	3
4. Triple Branch Double Reduction (Inline)		No	No	3
5. Double Branch Double Reduction (offset)		Yes	Yes	4
6. Triple Branch Compound Star (inline)		No	No	3
7. Coupled Planetary (inline)		No	No	1

- Inherently high reliability due to minimum number of parts.
- Propeller shaft bearing span consistent with long bearing life.
- Built up output shaft featuring sectional properties that enhance shaft stiffness.
- High speed auxiliary drive for accessories drive.
- Housing that incorporates internal lube tank (similar in concept to General Electric CT7).
- Straight through prop fan pitch change mechanism control accessibility.

As shown in the figure, engine power drives a 30T input pinion gear which then drives two double idler gears. It is important in a multi-branch gearbox to provide for equal load sharing between the branches. This has been accomplished in similar designs (CT7) by allowing the input gear to move along the line of action until equal load sharing has been achieved. There are several ways of accomplishing this, one of them being by using a double balancing beam which is the selection for the APET gearbox.

The idler gears are a one-piece configuration with the large gear having 63 teeth and the smaller gear having 28 teeth. The 28 tooth gears drive the large 96 tooth output gear.

A high speed auxiliary drive is provided by meshing a power takeoff gear with one of the 63 tooth idlers. This inherently provides a high speed drive with the minimum number of gears.

It is proposed to use the gearbox housing cavity as a lubricant reservoir with a lube pump driven from the reduction gear train. The internal cavity of the housing will be shrouded to minimize windage losses due to oil churning.

The gearbox has an overall gear ratio of 7.191:1. The gear arrangement has two stages of reduction and the ratio split for the lightest weight was determined from Figure 4.6-19. This figure plots the total disk volume (S face width \times dia²) of the gearbox versus the first stage gear ratio. For minimum weight the first stage ratio is 2.1:1 which has been used in this study. The second stage ratio is 3.428:1.

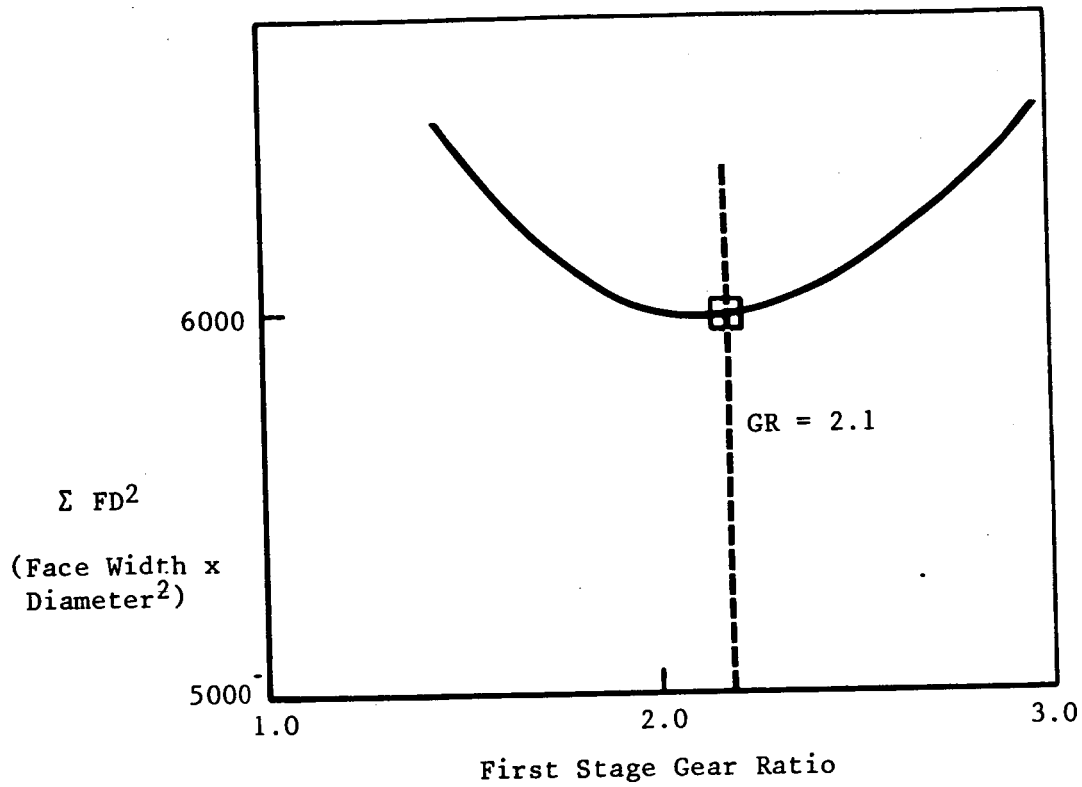


Figure 4.6-19. Gearbox Facewidth vs. First Stage Ratio - Parametric Curve.

For this study a standard involute gear tooth system has been utilized with a zero helix angle. This will result in the lowest bearing loads and the output and input bearings will not have to react thrust loads due to helix angle. Some of the other gearboxes studies did use helical gears and as future refinements are introduced the final design consideration of tooth geometry must consider at least the following:

- High profile contact ratio gearing which could increase the Hertzian stress capability of the gear set by approximately 30%. This type of gearing has been used very successfully on the NASA QCSEE engine but is very sensitive to load sharing between teeth since the bending stress capability of individual teeth is less than standard teeth (see Reference 43).
- Helical gearing with a face overlap ratio over two to reduce both the bending and Hertzian stress in the gear teeth. Loads in the double idler would be balanced by properly selecting the helix angle of each stage. The bearing loads would be higher but overall there may be advantages. This is expected to reduce gear noise significantly as well.

Preliminary stress analysis has been performed on the gears utilizing American Gear Manufacturing Association Standards (AGMA) 210.02, 220.2 and 217.01. A computer program developed at General Electric, which includes AGMA analysis design equations, was used in the analysis. The gear stresses shown in Table 4.6-10 have not been modified by any factors given in the AGMA standards (overall deration factor = 1.0).

As can be seen in Table 4.6-9, the compressive stress will be the criteria that will size the final design.

Computer techniques were used to determine the bearing loads and load direction for each gear. Figure 4.6-20 shows the graphic output from this computer program for the 63/30 tooth idler gear. The bearing configuration and life summary is given in Table 4.6-10. A system life of 15000 hours has been calculated for the nine bearings in the system. Individual bearing lives were calculated utilizing Anti Friction Bearing Manufacturers Association (AFBMA) methods by computer techniques long established at General Electric. The lowest individual bearing life is 27200 hours using overall life multiplying factors of 6 and 12 for rollers and ball bearings, respectively.

Table 4.6-9. Gear Stresses for Offset Dual Branch Two Stage Gearbox.

	Stage 1	Stage 2
No. Teeth		
- Pinion	30	28
- Gear	63	96
Diametral Pitch (P)	5.00	3.738
Pressure Angle (degree)	22.5	22.5
Face Width (F)	4.80	5.85
K Factor	811	784
Compressive Stress (KSI)	161	161
Unit Load (UL)	16500	17000
Bending Stress (KSI)	39.3	40.5
Flash Temp. Index (°F)	325	313

The K factor and Unit Load (UL) are defined as follows:

$$K = \frac{WT}{FD} \times \frac{MG \pm 1}{MG}$$

$$UL = \frac{WT}{F} \times P$$

WT = Tangential Driving Load

MG = Gear Ratio (>1) (use - for internal gear mesh)

D = No. Teeth/P = Pitch dia. of smaller gear

ORIGINAL PAGE 15
OF POOR QUALITY

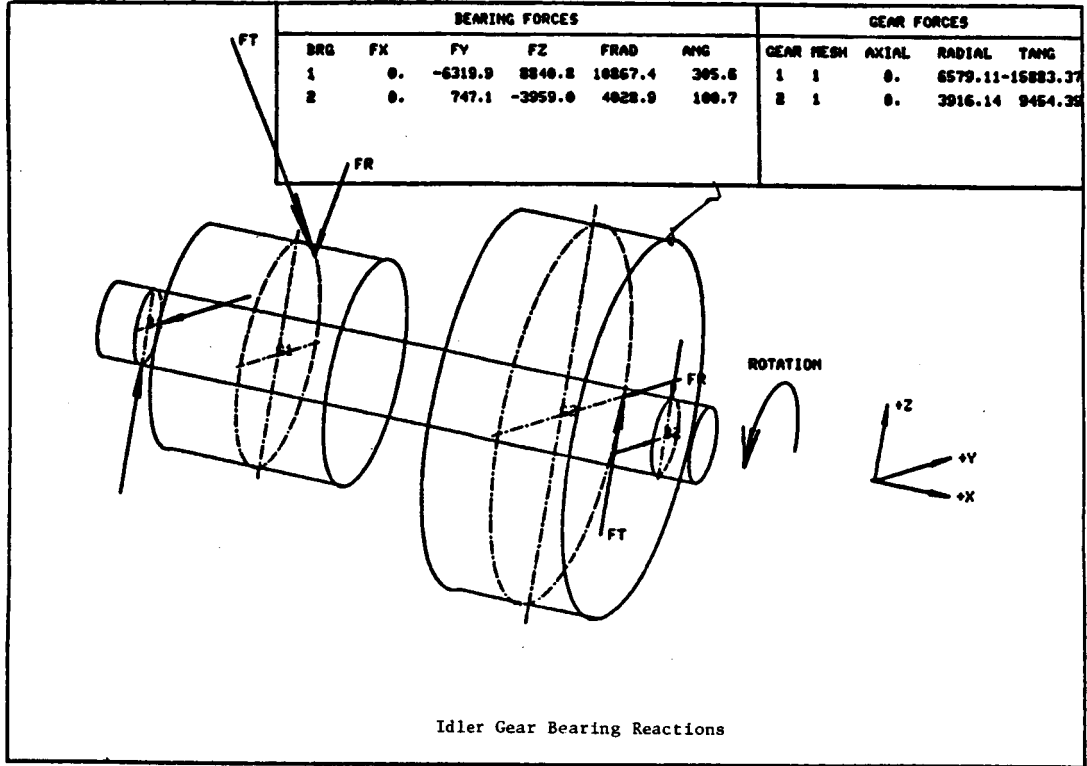


Figure 4.6-20. APET Dual Branch Two-Stage Reduction Gearbox.

Using the gears and bearings designs shown in Tables 4.6-9 and 4.6-10 and the materials shown in Figure 4.6-11 the gearbox was calculated to weigh 1068 lbs.

4.6.8.2 Inline Triple Branch Compound Star Reduction Gearbox

The inline gearbox configuration shown in Figure 4.6-21 contains the following features:

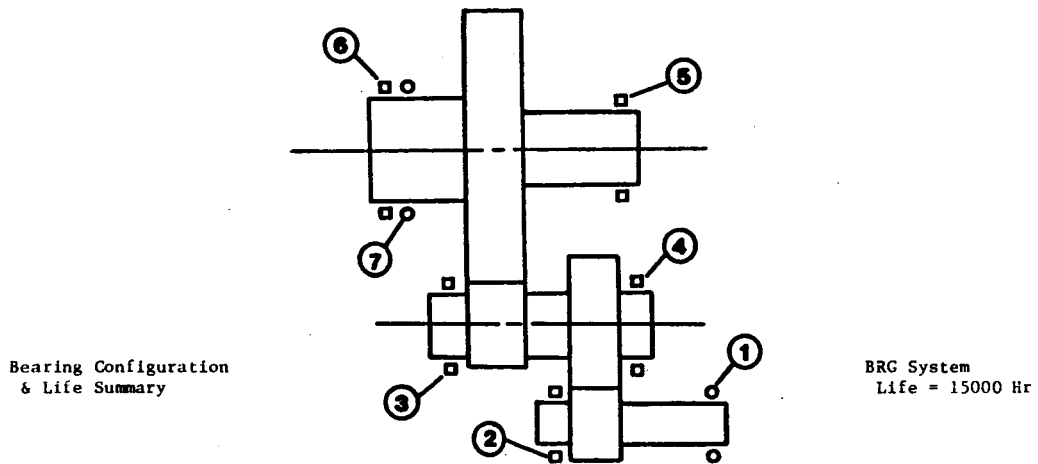
- Simple compact kinematic arrangement.
- Propeller shaft bearing span consistent with long bearing life. Span is increased by mounting aft bearing in the star gear cavities.
- Floating ring and sun gear for gear tooth load sharing.
- Triple branch for inherent gear tooth load sharing.
- High speed auxiliary drive for accessories drive.
- Access to hydraulic pitch change system transfer bearing through stationary gear carrier.

As shown in the figure, engine power drives a 33T input pinion gear which drives three double idler gears. These three equally spaced idler gears drive a large 87T internal gear. The internal gear is splined to the propeller output shaft. The propeller output shaft aft roller bearing has been mounted in the idler gear carrier to maximize the bearing span distance. A stiff two piece carrier is used to allow assembly of the internal gear past the forward bearings of the three idler gears. Load sharing is accomplished by "floating" the internal gear utilizing three planets, and allowing the input gear to center between the three idler gears by the use of flexible couplings.

A one piece design is shown for the 33/66 idler gear. Whether machined as one piece, or providing for an in-process inertia or EB weld between the two gears will have to be evaluated as the design progresses.

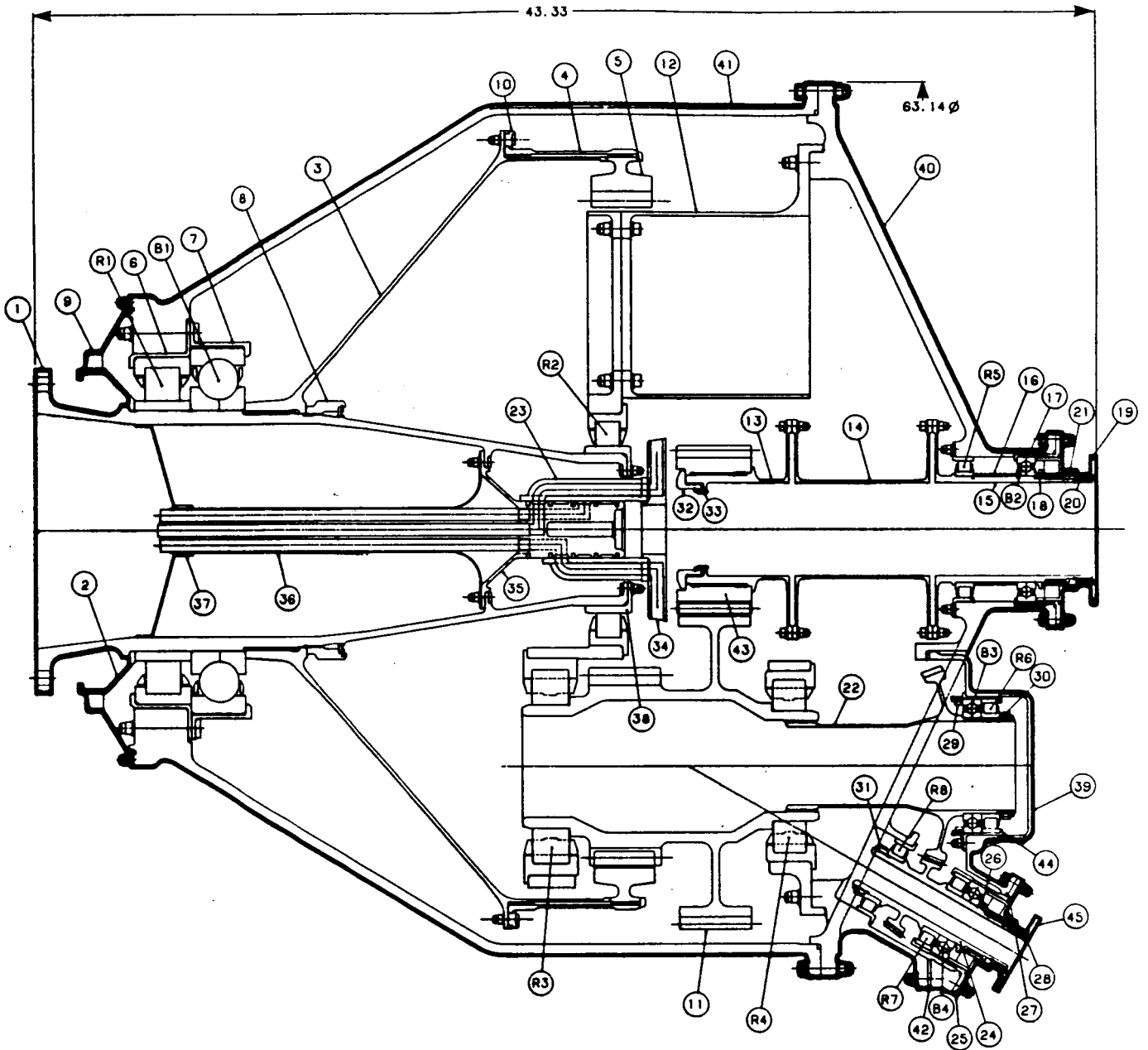
An important consideration for the assembly of a "star" gear arrangement is the proper selection of teeth numbers; this will have to be optimized along with stress and scoring considerations.

Table 4.6-10. APET Dual Branch Two-Stage Reduction Gearbox.



Pos.	Mean Dia. (Inches)	Element Size (Inches)	Number Elements	Dynamic Capacity (Lbs)	Load (Lbs)	Speed (Rpm)	B10 Life (Hours)
1	-	-	-	-	-	-	200000
2	-	-	-	-	-	-	200000
3	7.96	1.38x1.38	14	107480	10900	3677	56000
4	7.84	.79x.79	24	52780	4030	3677	144000
5	7.96	1.18x1.18	16	85990	12730	1073	47600
6	12.10	1.50x1.50	20	154000	20170	1073	27200
7	12.44	1.68 Dia.	18	55300	6390	1073	120800

ORIGINAL DRAWING
OF POOR QUALITY



12500 HP

Figure 4.6-21. APET Triple Branch Compound Star Reduction Gearbox.

The design shown in the figure also provides a high speed accessory drive at an angle of 30° from the horizontal. The offset angle will be selected based on the location of the accessory gearbox in the nacelle.

This gearbox has an overall gear ratio of 7.25:1 with the first stage ratio being 2.00:1 and the second stage being 3.625:1.

In this gearbox, as in the offset gearbox, a standard involute gear tooth system with zero helix angle has been designed. Consideration will have to be given to utilizing high contact ratio gearing or helical gearing, in any further development effort.

Preliminary stress analysis has been completed on the gears using AGMA standards for calculation. The gear stresses are shown in Table 4.6-11 with an overall deration factor of 1.0.

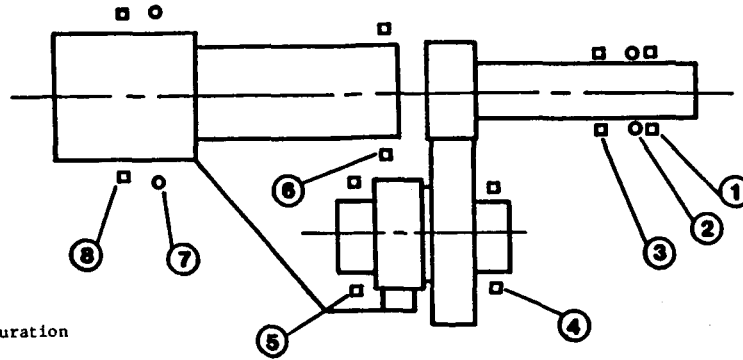
Table 4.6-11. Gear Stresses for Inline Triple Branch Compound Star Reduction Gearbox.

No. Teeth	Stage 1	Stage 2
- Pinion	33	24
- Gear	66	87
Diametral Pitch (P)	5.077	3.230
Pressure Angle (degrees)	22.5	22.5
Face Width (F)	2.90	2.90
K Factor	774	572
Compressive Stress (KSI)	156	145
Unit Load (UL)	17040	18965
Bending Stress (KSI)	38.7	43.1
Flash Temperature (°F)	324	302

For this design the compressive stress will be the sizing criteria.

Shown in Table 4.6-12 are the bearing configurations and the life summary. For this gearbox arrangement the system life calculated to be 17500 hours. The lowest individual life is 52000 hours. Since the system life is

Table 4.6-12. APET Triple Branch Compound Star Reduction Gearbox.



Bearing Configuration
& Life Summary

Brg. System
Life = 17500 Hr

Pos.	Mean Dia. (Inches)	Element Size (Inches)	Number Elements	Dynamic Capacity (Lbs)	Load (Lbs)	Speed (Rpm)	B10 Life (Hours)
1	-	-	-	-	-	7727	>200000
2	-	-	-	-	-	7727	>200000
3	-	-	-	-	-	7727	>200000
4	5.81	1.30x1.30	12	78570	7080	3864	78260
5	6.50	1.46x1.46	12	97600	9020	3864	71950
6	7.87	.83x.83	26	58090	8550	1066	52000
7	12.44	1.68 Dia.	18	55300	6390	1066	121600
8	12.00	1.34x1.34	22	13340	8550	1066	673700

a function of the individual bearing lives and the number of bearings the individual bearing lives have to be higher in the inline design when compared to the offset design because three additional bearings are required.

Using the gears and bearing designs shown in Table 4.6-11 and 4.6-12 and the materials shown in Figure 4.6-14 the gearbox was calculated to weigh 1162 lbs.

4.6.9 Lubrication

Current U.S. turboprop engines generally use the same type of oil in the power transmission (gearbox) as is used in the gas-turbine, in a shared lubrication system which, in some cases, is also used in the propeller pitch change mechanism. The oil specifications used are for low-viscosity MIL-L-7808 or MIL-L-23699, which oils are more directly tailored to the high temperature requirements of engine main shaft bearings. Thus the engine, not the gearbox, is favored in the selection made.

Ideally, gear systems would be better lubricated by a higher viscosity oil - which could also have boundary additives to increase the maximum load capacity of the gear sets and thus a non-shared lubrication system has obvious merits. This study has therefore concentrated on a non-shared system with an attempt being made to answer the following question:

"Can Synthetic oils be selected, or formulated, to accept much higher gear mesh loads than MIL-L-7808 (or MIL-L-23699) at bulk oil temperatures approaching 300° F?"

The TELSGE computer program (Reference No. 44), has been used, together with other analytical techniques, to provide a strong data base for future efforts. Comparisons have been made with an empirical data base from T64 sun and planet gear sets when lubricated with MIL-L-7808 oil operating through a range of elevated temperatures. Having established a good T64 gearbox correlation with Elastohydrodynamic Theory (EHD) for existing, known, viscosity versus temperature behavior for surface finish of gears in the range of current manufacturing capability, various input parameters were modified according to the characteristics of some newer, synthetic, oils. The effects of

increasing hypothetical viscosity of existing oils has also been studied and compared with results obtained from running the programs with the quoted capabilities of some experimental lubricants. Some conclusions are listed below:

1. Good agreement exists among the following: Actual T64 testing up to the point of gear set surface distress with high temperature lubricants; the TELSGE analytical process; the method of Wellauer and Holloway (Reference 41)
2. The minimum specific EHD film thickness has been established for the T64 sun and planet gears.
3. An Emgard EP 75W-90 ("Frigid Go") lubricant appears to have a good balance of physical properties, cost and near-term availability for high-performance gear transmissions.
4. Other good candidates may be available from formulations of high-viscosity synthetic esters, paraffinic hydrocarbons, and perfluorinated polyethers.

These conclusions are tentative and experimental programs should be instituted perhaps using an advanced design of disc type test machine, to evaluate load carrying capacity with additive effects.

4.6.10 Heat Exchanger System Design

The air-to-oil heat exchanger studied for the APET application is a Hughes-Treitler design with a 319 sq. in. airflow cross section. For the nacelle-mounted installation the heat exchanger has been located in the lower portion of the engine nacelle near the engine inlet in an area which would otherwise be unoccupied. The design selected for the external nacelle shape accommodates the inlet and the exhaust nozzle and tailors the system external lines as closely as possible to basic nacelle contours to minimize additional drag while incorporating the requirements of the inlet flowpath and heat exchanger volume.

The heat exchanger shape chosen for this nacelle location is an annular segment with its center on the engine centerline. The radial depth limit of the heat exchanger was determined by consideration of the inlet contour and a

two inch clearance envelope between the heat exchanger and engine envelope. This results in an annular depth of 15.3 inches. Combined with the 319 sq. in. cross-sectional area, this would correspond to a segment arc of 54.4°. However, the arc limit of the annular segment is set by a desire not to extend the heat exchanger beyond the engine inlet circumferentially. This arc was computed to be approximately 90°. An evaluation of the two limits, arc length vs. radial depth, indicates the arc length is favorable because it allows the shortest overall pod length for a smooth blend from external pod contour to engine nacelle contour. The radial depth of the annular segment was thus determined to be 10.21 inches for the selected 90° arc segment.

The heat exchanger exhaust duct contour is designed for the M.8/35K ft. cruise condition. The airflow, temperature and pressure of the heat exchanger at this condition were used to determine nozzle exit area of 16.98 in.². The extremely low duct Mach numbers, less than 0.1, make internal duct losses largely insensitive to duct contour; and for this reason, a duct having a smooth transition from the heat exchanger to the nozzle exit was considered sufficient. Due to the relatively large radial spacing between the heat exchanger and the external contour, i.e., 4.6 inches, and the desire to keep weight down, the internal duct lower surface contour has been designed to rapidly approach the external contour. In this way, the aft portion of the duct/pod could be fabricated from a single sheet of material. The shape contour change has, as already mentioned, little effect on the internal duct losses due to low duct Mach numbers. The flow, temperature and pressure of the heat exchanger system at the takeoff condition were used to determine the maximum required nozzle exit area of 72.62 in.²; and a hinge position on the duct/pod wall for nozzle area variation has been selected to minimize angular rotation of the nozzle and keep the exhaust flow at takeoff (open area) axially aligned.

Heat exchanger system loss calculation procedures are detailed in Appendix I. Also included in this Appendix are diagrams and figures for the selected heat exchangers.

4.6.11 Cost and Weight Estimating Methodology

4.6.11.1 Gearbox Costs

The APET double branch, double reduction offset gearbox design was manufacturing cost-evaluated by General Electric's Advanced Value Process Engineering personnel. Each individual part was subjected to a "make or buy" scrutiny, and in the case of decisions to "make" a manufacturing process plan was set up and run on the computer. In the case of "buy" decisions, vendors costs for similar items were used. All the estimates were made in 1982 dollars. Variables used included:

- Labor Rate
- Direct and indirect overhead costs
- Year Dollars
- Manufacturing lot size
- Percent variance
- Percent rework
- Percent scrap

Certain assumptions were made regarding the selected materials in the parts, especially with regard to wall thickness of the gearbox castings, coring of oil delivery and scavenge passages, forgability, castability and machineability. These assumptions were cross-checked against specifications for similar production parts for production costs.

A manufacturing price, based on the 250th unit (manufactured as an element of a production batch of 20) was estimated to be 183K dollars. This price does not include amortization of R&D including development testing, facilities costs, design costs, etc. However, the price as defined above is considered to be surprisingly reasonable for an advanced production gearbox, and certainly does not appear to be a negative factor in the development of the high horsepower turboprop system. The true selling price of the gearbox, with all the development and test costs properly allocated would be expected to add between 70 and 80 percent to the quoted manufacturing price for a production run of 1000 gearboxes.

4.6.11.2 Weight Determination

The gearboxes described in Sections 4.6.4.5 (double branch, double reduction) and 4.6.4.6 (triple branch, compound star) were both subjected to a very rigorous weight determining process. Every major component was entered into the GE Interactive Graphics System (IGS). A computer program would then perform a volume calculation of the part and then calculate the weight using the appropriate material density. Where appropriate, centers of gravity and moments of inertia were also calculated. The results of the individual parts calculations were tabulated by hand to produce the overall gearbox weight and center of gravity location. Figure 4.6-22 is a copy of the IGS plot of item 11 gearshaft (one of the two layshafts) in the double reduction double branch gearbox described in Section 4.6.4.5. The lower half of the Figure is a copy of a portion of the computer printout showing the calculated weight of this part. Table 4.6-13 is a worksheet which tabulates all the weights and center of gravity locations. The worksheet page chosen for inclusion has the data for the item 11 gearshaft tabulated in addition to those of many other parts.

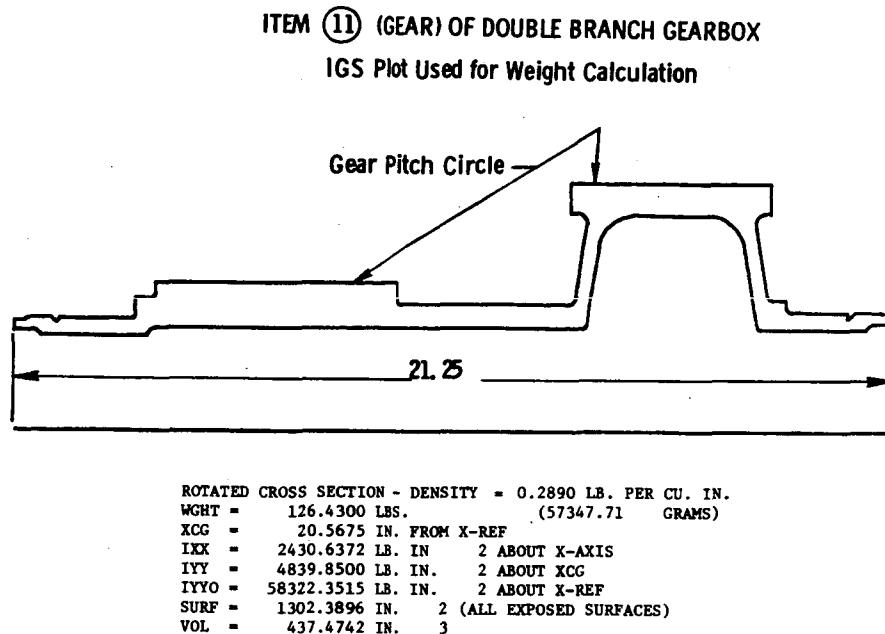


Figure 4.6-22. APET Gear And Shaft Example.

Table 4.6-13. Calculation of APET Double Branch Gearbox Total Weight and C.G. Location.

302.1 RFW DB0230 Weight Gearbox									
Identification	Nomenclature	Material	Weight	XCG	Weight XCG	YCG	Weight YC6	ZCG	Weight ZCG
1*	Shaft, Upper/Forward	Titanium	32.095	5.092	163.428	0.00	0.00	0.00	0.00
2*	Seal, Ret.	Steel	5.485	3.017	16.548	0.00	0.00	0.00	0.00
3*	Shaft Extension	Titanium	24.705	21.441	529.700	0.00	0.00	0.00	0.00
4*	Shaft	Titanium	42.070	13.231	556.628	0.00	0.00	0.00	0.00
5*	Gear	Steel	145.134	15.228	2210.100	0.00	0.00	0.00	0.00
6	Seat, Bearing	Steel	14.435	6.398	92.355	0.00	0.00	0.00	0.00
7	Retainer, Bearing	Steel	7.028	8.768	61.622	0.00	0.00	0.00	0.00
8*	Nut, Shaft	Steel	4.654	11.923	55.490	0.00	0.00	0.00	0.00
9	Seal, Sta.	Steel	4.398	3.102	13.643	0.00	0.00	0.00	0.00
10*	Gear	Steel	5.270	29.165	153.700	- 6.699	-35.304	-4.535	-23.899
11a*	Gear	Steel	126.430	20.568	2600.412	-13.738	-1736.895	-9.30	-1175.799
11b*	Gear	Steel	126.430	20.568	2600.412	-13.738	-1736.895	+9.30	+1175.799
12a	Seat, Bearing	Steel	3.035	10.579	32.107	-13.738	-41.695	-9.30	-28.226
12b	Seat, Bearing	Steel	3.035	10.579	32.107	-13.738	-41.695	+9.30	+28.226
13a	Retainer, Bearing	Steel	1.940	11.359	22.036	-13.738	-26.652	-9.30	-18.042
13b	Retainer, Bearing	Steel	1.940	11.359	22.036	-13.738	-26.652	+9.30	+18.042
14*	Gear	Steel	2.647	31.375	83.050	0.00	0.00	0.00	0.00
15	Seat, Bearing	Steel	4.839	27.182	131.534	0.00	0.00	0.00	0.00
16	Retainer, Bearing	Steel	2.021	26.270	53.092	0.00	0.00	0.00	0.00
17*	Nut, Shaft	Steel	2.250	28.920	65.070	0.00	0.00	0.00	0.00
18a	Seat, Bearing	Steel	3.382	28.342	95.853	-13.738	-46.462	-9.30	-31.453
18b	Seat, Bearing	Steel	3.382	28.342	95.853	-13.738	-46.462	+9.30	+31.453
19a	Retainer, Bearing	Steel	2.444	27.713	67.731	-13.738	-33.576	-9.30	-22.729
19b	Retainer, Bearing	Steel	2.444	27.713	67.731	-13.738	-33.576	+9.30	+22.729
20a*	Nut, Shaft	Steel	2.105	9.271	19.515	-13.738	-28.918	-9.30	-19.577
20b*	Nut, Shaft	Steel	2.105	9.271	19.515	-13.738	-28.918	+9.30	+19.577
			575.703		9861.268		-3863.700		-23.899

*Rotating Part

SECTION 4.7

NACELLES AND NACELLE TECHNOLOGY

<u>Section</u>		<u>Page</u>
4.7.1	Turboprop Introduction and Historical Survey	221
4.7.2	Geometric Selection Criteria	223
	4.7.2.1 Axial Locations	225
	4.7.2.2 Spanwise Locations	230
4.7.3	Nacelle Descriptions	230
	4.7.3.1 Under-The-Wing Layouts	230
	4.7.3.2 Over-The-Wing Layouts	237
	4.7.3.3 Moment - Index Analyses	241
4.7.4	Inlet Aero Studies (Single Scoop and Double Scoop)	241
	4.7.4.1 Cross Sectional Shape of Single Scoop Inlet	243
	4.7.4.2 Duct Design Analysis	243
	4.7.4.3 Internal Lip Shape	245
	4.7.4.4 Prop-Fan/Inlet Spacing	248
	4.7.4.5 Forebody Shape	248
	4.7.4.6 Boundary Layer Diverter	249
	4.7.4.7 Throat Area	251
	4.7.4.8 Drive Shaft Fairing	251
4.7.5	Bifurcated Scoop Inlet	251
	4.7.5.1 Cross-Sectional Shape	251
	4.7.5.2 Duct Design	252
	4.7.5.3 Internal Lip Shape	252
	4.7.5.4 Prop-Fan/Inlet Spacing	252
	4.7.5.5 Forebody Shape	252
	4.7.5.6 Boundary Layer Diverter	254
	4.7.5.7 Throat Area	254
4.7.6	Summary of Selected Inlet Design Parameters	254
4.7.7	Exhaust System Aero Design	254
	4.7.7.1 Nozzle Selection Criteria	254
	4.7.7.2 Nozzle Design	256
	4.7.7.3 Nozzle Installation Factors	259
4.7.8	Nacelle Installation Aerodynamics	259
	4.7.8.1 Nacelle Requirements and Constraints	259
	4.7.8.2 Isolated Nacelle Design	262
	4.7.8.3 Installed Nacelle	265
4.7.9	Nacelle Drag Calculation	267

SECTION 4.7 (Continued)

NACELLES AND NACELLE TECHNOLOGY

<u>Section</u>		<u>Page</u>
4.7.10	Mounting and Vibration Isolation	269
4.7.11	Maintainability and Accessibility	270
4.7.12	Systems and Controls	272
4.7.13	Fire Safety	272
4.7.14	Performance Comparisons - Turbofan Versus Turboprop	276

FIGURES

<u>Figure</u>		<u>Page</u>
4.7-1.	Lockheed Electra Installation (Lower Offset Gearbox).	222
4.7-2.	Typical Nacelle for 6000 ESHP R-R "Tyne".	222
4.7-3.	Model Configuration Used in a Wind Tunnel Program.	224
4.7-4.	APET Baseline Nacelle Principle Features and Assemblies.	227
4.7-5.	APET Nacelle Axial Spacing Criteria.	229
4.7-6.	APET Alternate Nacelle - Split Gearbox, Principal Features and Assemblies.	233
4.7-7.	APET Study Nacelles.	236
4.7-8.	Hamilton-Standard Propfan and Nacelle Recommended Relationships.	236
4.7-9.	APET Over-the-Wing Nacelle with Concentric Gearbox.	239
4.7-10.	APET Powerplant Moment Index Definition.	242
4.7-11.	APET Nacelles Powerplant Moment Index.	242
4.7-12.	Schematic Design Approach for APET Inlets/Nacelles.	244
4.7-13.	APET Single Scoop Inlet-Front View.	244

SECTION 4.7 (Continued)

NACELLES AND NACELLE TECHNOLOGY

FIGURES (Continued)

<u>Figure</u>		<u>Page</u>
4.7-14.	APET Flow Separation Analysis.	246
4.7-15.	APET Inlet Duct Recovery Schedule - Single Scoop.	246
4.7-16.	APET Swirl Model.	247
4.7-17.	APET Single Scoop Inlet - Lip and Cowl Contours.	250
4.7-18.	APET Single Scoop Inlet - Diverted Height Study.	250
4.7-19.	APET Bifurcated Scoop Inlet.	253
4.7-20.	APET Inlet Duct Recovery Schedule - Bifurcated Scoop.	253
4.7-21.	Exhaust Nozzle Internal Flowpath - Initial Design.	257
4.7-22.	Exhaust Nozzle Exit Coefficients - Initial Design.	257
4.7-23.	Exhaust Nozzle External Flow Suppression.	258
4.7-24.	Exhaust Nozzle Internal Flowpath - Final Integrated Design.	260
4.7-25.	Exhaust Nozzle Exit Coefficients - Final Integrated Design.	260
4.7-26.	Nacelle Blending Approaches.	261
4.7-27.	Initial Conditions For Nacelle Blending.	261
4.7-28.	Engine Nacelle Envelope Limits.	263
4.7-29.	Nozzle Afterbody Initial Design.	263
4.7-30.	APET Diverter Contour.	264
4.7-31.	APET Nacelle Structural Requirements.	266
4.7-32.	APET Afterbody Closure.	266
4.7-33.	Anti-vibration Mount Concept for APET Turboprop Gearbox.	271

SECTION 4.7 (Concluded)
NACELLES AND NACELLE TECHNOLOGY

FIGURES (Concluded)

<u>Figure</u>	<u>Page</u>
4.7-34. APET Baseline Nacelle-Principal Features Axi-Axi Engine, Offset Gearbox - Underwing Layout.	273
4.7-35. APET Study Alternate Nacelle-Principal Features Axi-Axi Engine with Split Gearbox and Offset Propeller.	274
4.7-36. APET Alternate Nacelle - Principal Feature - Axi-Axi Engine with Concetric Gearbox.	275
4.7-37. APET Installation Loss Bookkeeping.	277
4.7-38. APET Propeller Gearbox Related Drag Accounting - Prop Wash Drag.	278
4.7-39. APET Propeller Gearbox Related Drag Accounting - Gearbox Heat Exchanger.	278
4.7-40. APET Heat Exchanger Core.	279
4.7-41. APET Turbofan and Turboprop Installation Loss Bookkeeping.	279
4.7-42. APET Turbofan and Turboprop Installation Loss Comparisons - Typical Climb Path Drags.	280
4.7-43. APET Turbofan and Turboprop Installation Loss Comparisons - Cruise Drags.	280

TABLES

<u>Table</u>	<u>Page</u>
4.7-1. Comparative Summary of Selected Inlet Design Parameters.	255

4.7 NACELLES AND NACELLE TECHNOLOGY

4.7.1 Turboprop Introduction and Historical Survey

It is appropriate to review previous installations of turboprop engines (particularly the high horsepower systems) for guidance in selecting nacelle technology level and design methodology for the higher speed prop-fan installations. The two (Western World) high volume production turboprop engines in the "over 4000 shp" class have been the DDA T56 family and the R-R "Tyne" family, with the latter engine producing over 6000 shp in certain models.

The T56 is noted primarily for its use on all the variants of the Lockheed C130 (Hercules) aircraft, the Lockheed P3 (ORION) ASW Navy aircraft, the Lockheed "Electra" commercial aircraft, and, in lesser numbers, on the Grumman E2C (Hawkeye), Early Warning Aircraft, the Grumman C2 (Greyhound, COD) aircraft, and a number of conversions of the Convair 340 and 440 series aircraft to commuter role.

The Tyne has been used in the Vickers "Vanguard" commercial aircraft, the CL44 Military and Commercial Cargo aircraft, the Short "Belfast" Military transport aircraft, the Breguet "Atlantique" ASW aircraft, and the Franco-German "Transall" Military Transport. Installations have also been made on export versions of the Fiat G222 Military Transport.

The T56 in general has used three- and four-bladed propeller configurations in the 13- to 14-foot-diameter range, and with activity factors in the 160 to 185 band. The Tyne has used 14-foot diameter four-bladed propellers on the Vanguard, 16-foot diameter four-bladed propellers on the CL44, the Belfast and the Atlantique, and 18-foot diameter four-bladed propellers on the Transall. Activity factors have been generally lower than the T56 propellers and lie in the 125 to 145 range.

Figure 4.7-1 shows a sketch of the T56 installation in the Electra airplane (inboard location is shown). The Electra included wing and nacelle structural changes introduced as a result of the failures which occurred due to propeller/nacelle/wing whirl flutter instability discovered in service on the early models. Noteworthy in this installation are the offset gearbox arrangement with structural interconnection to the forward frame of the

engine. The center drive housing is one element in the engine-to-gearbox structural entity, and large side-mounted Vee braces are used to react the vertical and torque loads from the propeller gearbox back to the nacelle structure. Propeller induced side loads are reacted by a smaller Vee brace in plan view that interconnects the propeller gearbox with the nacelle structure. Dual redundant mounts also attach to the top of the propeller gearbox and these react combination loads to the shell structure surrounding and including the engine air inlet. The engine rear casing is also provided with steady mounts to react vertical and side loads in a redundant mounting system.

A typical Tyne installation is shown in Figure 4.7-2. It may be noted that the installation is almost "dominated" by the tubular mount structure to the nacelle. In addition to the main mounts which are reacting loads at Plane A in the figure, a redundant reaction load path for loads in any direction (except along or parallel to the thrust axis) is provided at Plane B on the figure. This rear mount at Plane B comprises an ingenious system of hard points built around the engine turbine frame contracting a flexible ring structure that surrounds the engine rear casing. The entire system is sealed by graphite high-temperature machined ring segments fitted within a spring-loaded containment compartment.

Also noteworthy of the Tyne installation is the fact that the engine essentially supplied no bleed for aircraft accessory services. Instead, a special gearbox has been added to the low-pressure engine spool to provide shaft horsepower transmitted remotely, through a drive shaft with self-aligning joints, to an aircraft-mounted accessory gearbox. This latter gearbox typically provides pads for all the required aircraft services.

The combining of systems onto a separate gearbox from the engine itself, was a precursor to the modular design approach now favored for the new turbo-propfan accessory systems.

4.7.2 Geometric Selection Criteria

For the turboprop high cruise speed installations, nacelle design work has been performed for NASA by a number of airframe companies starting with

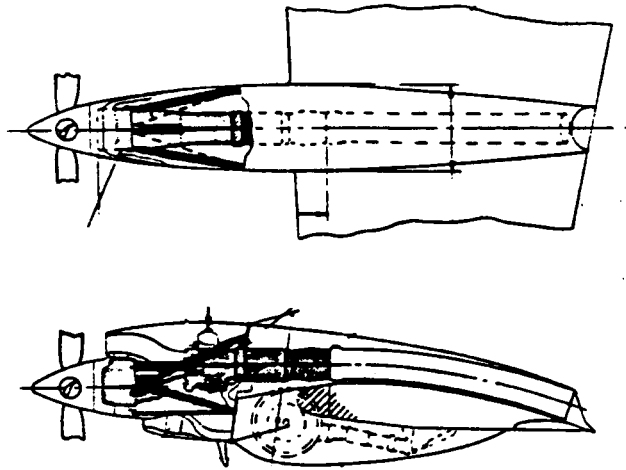


Figure 4.7.1. Lockheed Electra Installation (Lower Offset Gearbox).

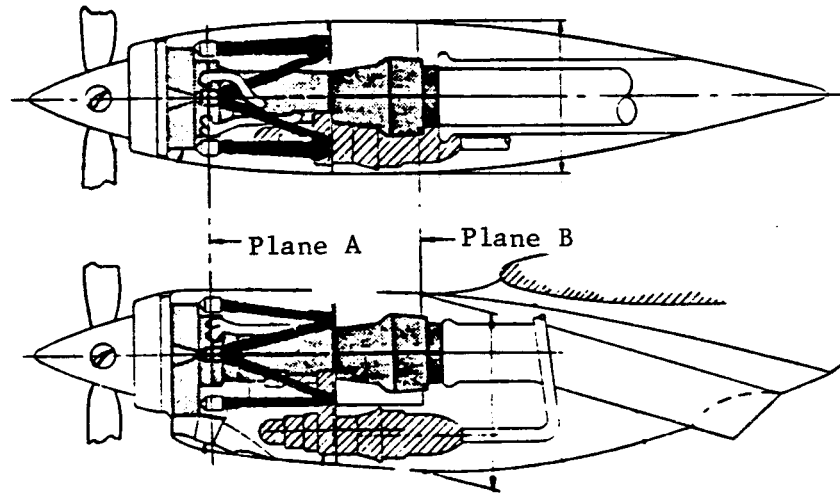


Figure 4.7-2. Typical Nacelle for 6000 ESHP R-R "Tyne".

ORIGINAL PAGE IS
OF POOR QUALITY

SPECIAL CORRELATIONS
(RIGHT/LEFT SYMMETRY)

ANGLE DEG (in)	R (in)	H (in)
0.0	1.000	0.0
0.5	1.000	0.000
1.0	1.000	0.000
1.5	1.000	0.000
2.0	1.000	0.000
2.5	1.000	0.000
3.0	1.000	0.000
3.5	1.000	0.000
4.0	1.000	0.000
4.5	1.000	0.000
5.0	1.000	0.000
5.5	1.000	0.000
6.0	1.000	0.000
6.5	1.000	0.000
7.0	1.000	0.000
7.5	1.000	0.000
8.0	1.000	0.000
8.5	1.000	0.000
9.0	1.000	0.000
9.5	1.000	0.000
10.0	1.000	0.000
10.5	1.000	0.000
11.0	1.000	0.000
11.5	1.000	0.000
12.0	1.000	0.000
12.5	1.000	0.000
13.0	1.000	0.000
13.5	1.000	0.000
14.0	1.000	0.000
14.5	1.000	0.000
15.0	1.000	0.000
15.5	1.000	0.000
16.0	1.000	0.000
16.5	1.000	0.000
17.0	1.000	0.000
17.5	1.000	0.000
18.0	1.000	0.000
18.5	1.000	0.000
19.0	1.000	0.000
19.5	1.000	0.000
20.0	1.000	0.000
20.5	1.000	0.000
21.0	1.000	0.000
21.5	1.000	0.000
22.0	1.000	0.000
22.5	1.000	0.000
23.0	1.000	0.000
23.5	1.000	0.000
24.0	1.000	0.000
24.5	1.000	0.000
25.0	1.000	0.000
25.5	1.000	0.000
26.0	1.000	0.000
26.5	1.000	0.000
27.0	1.000	0.000
27.5	1.000	0.000
28.0	1.000	0.000
28.5	1.000	0.000
29.0	1.000	0.000
29.5	1.000	0.000
30.0	1.000	0.000

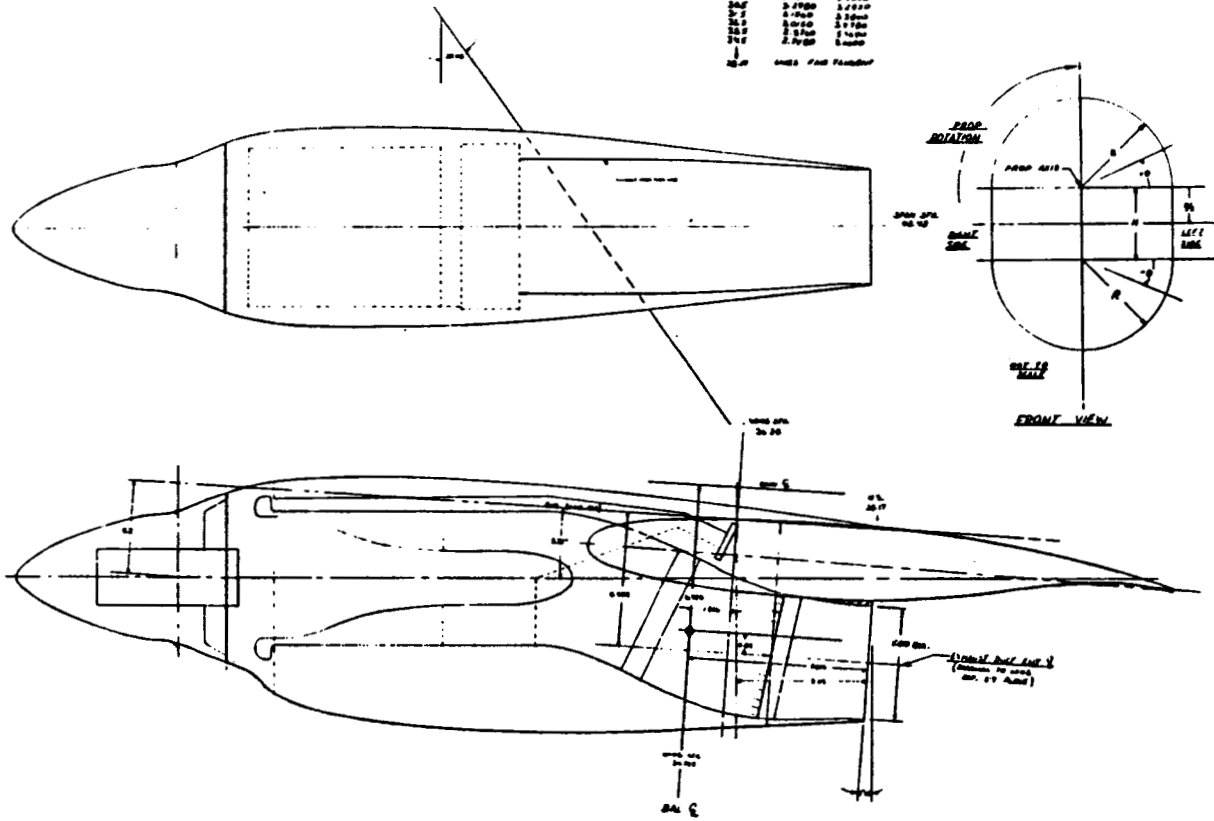


Figure 4.7-3. Model Configuration Used in A Wind Tunnel Program.

the RECAT studies in the middle 1970's. More recent designs have been developed by Douglas as part of the DC-9 reengining study contract, and by Lockheed (Georgia) on the Langley Contract for "Turboprop Cargo Aircraft Systems Study." NASA Ames, working with Douglas, has been performing wind-tunnel studies of a powered prop-fan model on a representative supercritical wing section. Figure 4.7-3 shows the model configuration being used in the wind-tunnel program. This configuration of nacelle shape and location was considered to be a strong contender for the high cruise speed/supercritical wing combination, and drag test data together with profile pressure data is now becoming available from Ames as a result of the tests. Consequently for the APET Study the first nacelle configuration that was proposed is very similar to the model configuration. This is shown in Figure 4.7-4.

Before embarking on a description of this nacelle it is considered appropriate to review the geometric data that has been used to select nacelle locations on the wing.

4.7.2.1 Axial Locations

Early studies used a Hamilton-Standard recommendation for the axial location of the plane of the propfan (pitch change axis). This recommended that the location, relative to the wing chord, should observe as a minimum a dimension of at least one propfan diameter from the reference plane to the quarter chord station of the wing along the plan view centerline of the nacelle.

Locating the propfan in this manner appears to satisfy most concerns on moderately swept wings but places the inboard propfan tip fairly close to more sharply swept wings (as is typical for the Mach Cruise 0.80 airplane). It was therefore decided for this study to invoke an additional constraint that had been used in some earlier propfan powered airplane designs. This additional constraint restricts the clearance between the inboard propfan tip and the chord of the local wing at that butt line location. A combination of these two constraints has therefore been used for the study airplanes. This axial relationship is depicted in Figure 4.7-5 for the wing geometry of the MCR = 0.80 Airplane.

ORIGINAL PAGE IS
OF POOR QUALITY

ORIGINAL PAGE IS
OF POOR QUALITY

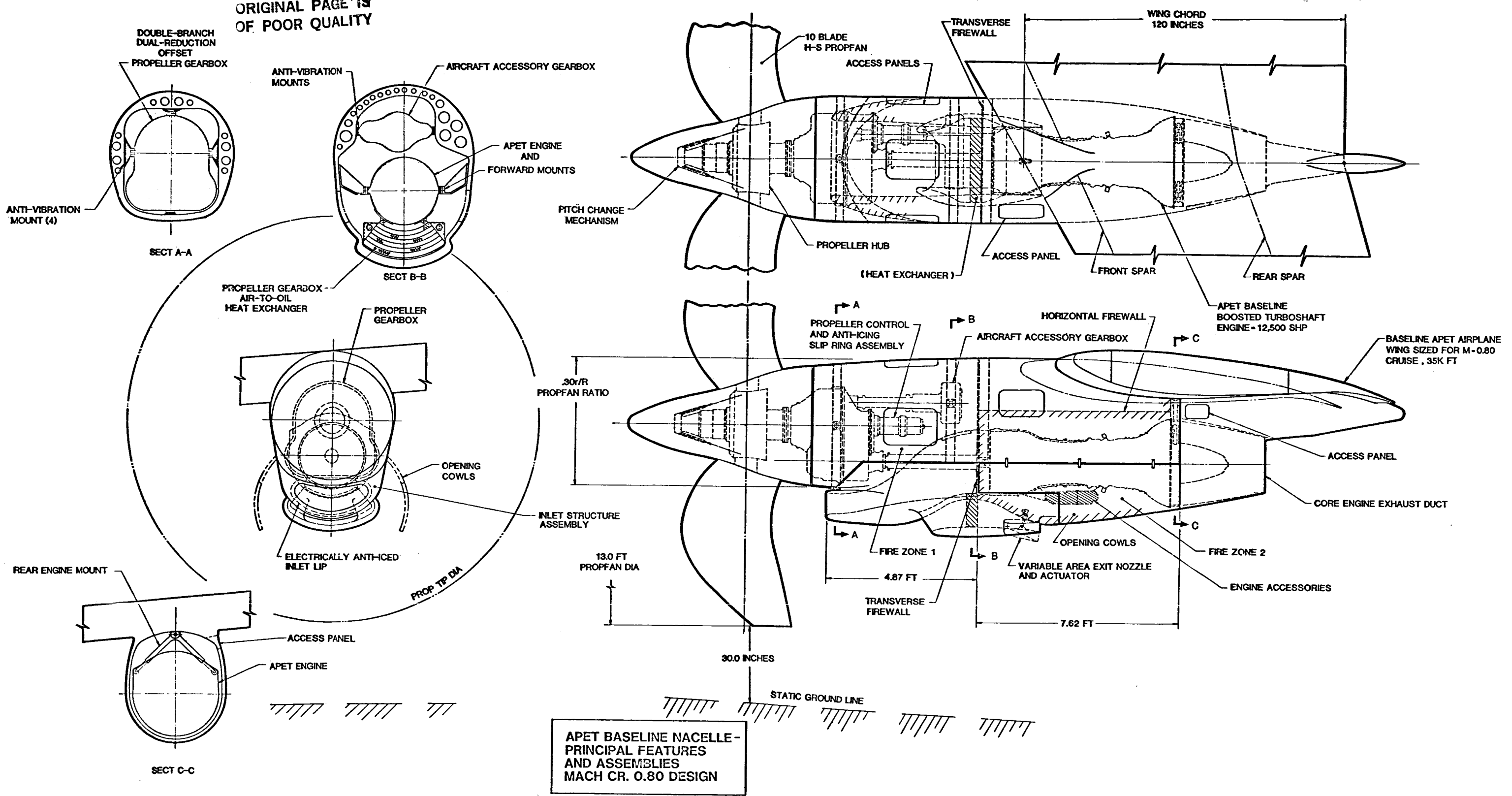


Figure 4.7-4. APET Baseline Nacelle-Principal Features and Assemblies.

FOLDCUT FRAME

2 FOLDCUT FRAME

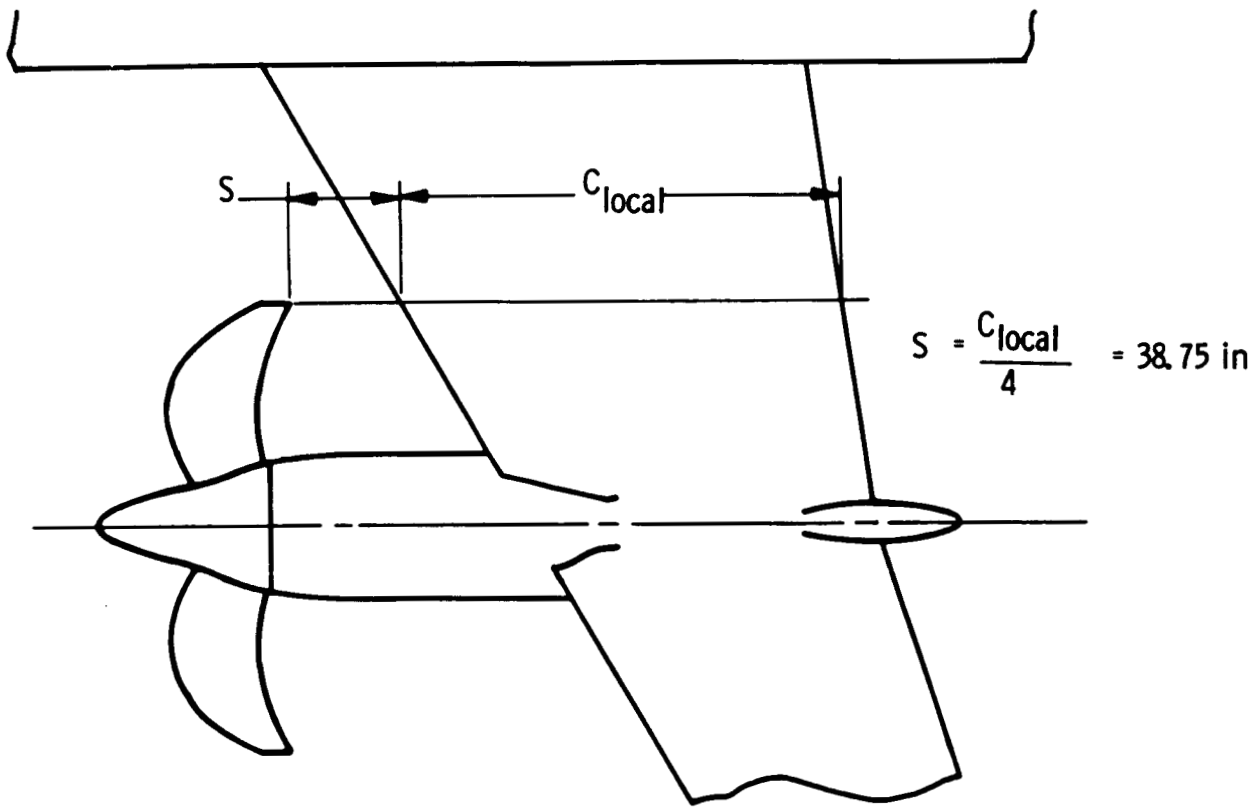


Figure 4.7-5. APET Nacelle Axial Spacing Criteria.

ENCLOSING EDGE OF THIS DOCUMENT

PAGE 276 INTENTIONALLY BLANK

4.7.2.2 Spanwise Locations

Nacelle lateral position was not established using rigorous ground rules. For the long duct mixed flow turbofan engines an average of spanwise location by airframe contractors when they conducted E³ powered airplane studies for NASA, was used. Axial spacing was held to a value with the common exhaust nozzle being set at one quarter chord and reasonable values for the channel height between the top of the nacelle and the underside of the wing. The lateral spacing value used was 0.30 of the semi-span. This location gave values of 131 sq. ft. and 133 sq. ft. for the vertical tail areas of the turbofan MCR 0.80 and MCR 0.70 airplanes respectively.

Lateral spacing of the turbopropfan nacelles was dictated by considerations of propfan tip spacing distance from the fuselage skin, engine out effects on the vertical tail size (the thrust moments are larger for the propfan than the turbofan), and propulsion weight effects for wing bending relief.

For the first consideration, advice was sought from the results of previous studies and conversations with airframe design companies. In the early days of propfan acoustic investigations a lateral spacing of 0.80 propfan diameter for fuselage/tip clearance was suggested. Later airframe studies have indicated that the overall trade for additional acoustic material in the fuselage can support a value of 0.50 of propfan diameter, and this is the value used for the APET turbopropfan powered airplanes, irrespective of cruise Mach number. This value provides a centerline of fuselage to centerline of propulsion thrust of 19.0 feet for the turbopropfan (this may be compared with 16-2/3 feet for the turbofan). The effect of engine out on vertical tail sizing dictated an increase for the turboprop airplanes of approximately 16 percent over the values used for the turbofan airplanes.

4.7.3 Nacelle Descriptions

4.7.3.1 Under-The-Wing Layouts

As can be seen in the views shown on Figure 4.7-4 an offset gearbox arrangement is used where the propeller thrust centerline is above the core engine centerline. It can also be seen that the physical separation distance

of the core engine behind the propeller gearbox is larger than seen on the current turboprops using offset gearboxes.

The reason for this is simply the fall-out of requirements that now exist for the inlet design parameters of an installation designed for cruise at Mach 0.8 as compared with the earlier, slower cruise speed aircraft which typically operated in the Mach 0.5 to 0.6 band.

This large separation distance also helps the installation in other ways. Clearly, there is widespread industry agreement that, if possible, the airframe system accessories that are required to be mechanically powered should not be driven on pads provided by the propeller gearbox. The high torque propeller gearbox is a challenging enough task on its own, to meet reliable life and unscheduled removal rate guarantees, without being penalized by a number of additional gearsets, bearings, lube oil supply and scavenge systems, overhang moments of the accessories, etc. Therefore, a remote location, shaft driven accessory gearbox dedicated solely to the support of aircraft services, provides one acceptable design solution. Such a system is shown on the referenced figure. Also, the nacelle internal volume is large enough to house the propeller control unit (on the back of the propeller gearbox and coaxial with the propeller centerline) as well as the system oil tank, heat exchanger, ducts, and controls. Engine dedicated accessories shown are mounted on the underside of the turboshaft gas generator and would be easily maintained or removed through a lower, hinged, access door.

This installation sketch also indicates the structural concept for engine and propeller gearbox interconnection and for mounting to the airframe structure. As has been noted already, turboprop installations tend to be dominated by structural requirements, and this nacelle installation, as shown, is no exception. The structural concept employs a stressed skin nacelle enclosure that could be integrated directly with the wing structure. The forward section of the nacelle is a barrel which becomes cut-away for the wing penetration and for the cowl doors below the turboshaft engine centerline.

Another possibility is shown in Figure 4.7-6 where the propfan gearbox has been split into two pieces. The engine drives forward to a first stage reduction gearset that provides twin driveshafts, that are parallel to each

ORIGINAL PAGE IS
OF POOR QUALITY

ORIGINAL PAGE IS
OF POOR QUALITY

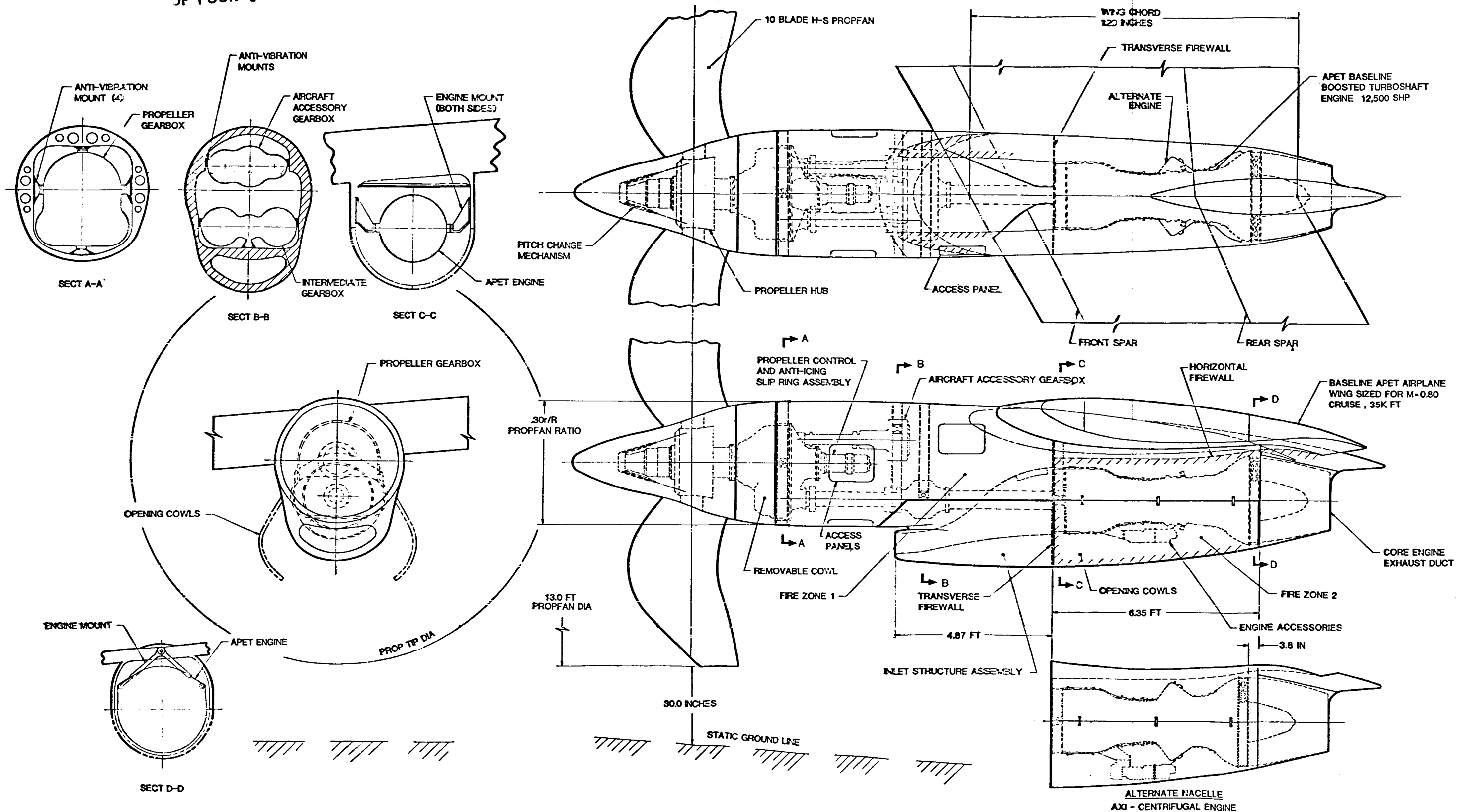


Figure 4.7-6. APET Nacelle-Split Gearbox Principal Features and Assemblies.

FOLDCUT FRAME

PRECEDING PAGE BLANK NOT FILMED 233

FOLDCUT FRAME

other, which then connect to dual inputs in the propeller gearbox. It would be appropriate at this point in the discussion of nacelle geometry to open up the subject to embrace all possible concepts.

Figure 4.7-7 shows a family of nacelle installations - some of which are above wing layouts and some are below wing layouts. In all the sketches on the figure there are constants.

All wing chords are identical (but the wings are not necessarily at the same height above the ground). All the propfans are identical in diameter and the shaft engines and gearboxes are to an equal scale for transmitting 12,500 SHP at a propfan RPM of 1155 (800 ft/sec tip speed). Also, the tip clearance of the propfans above the ground is also a constant 30 inches in each case. An additional constant is that all the nacelles apply an identical r/R value of 0.30 to their maximum radius relative to the propfan radius.

Early in the study it was found that for the advanced gearboxes and engines, values of r/R higher than 0.30 would unduly penalize nacelle weight and performance. Figure 4.7-8 shows the recommended value versus propfan disc loading contained in an earlier NASA study. Inquiries provided that the propeller thrust loss (from ideal values) would be about one half percent for cruise at $M = 0.8$ reducing linearly to zero at a cruise value of 0.75 by using 0.30 r/R (or d/D as shown in the figure) rather than the 0.35 recommended. This thrust loss was considered to be an acceptable trade factor, in that the MCR 0.80 airplane spends very little proportion of its flight time at MCR on the 300 N.Mi ranking mission.

Also referring again to Figure 4.7-7 the sketches identified as Number 1 and Number 2 depict nacelles incorporating the "split gearbox" concept. One of the concerns being addressed by this concept is the local moment effect around the wing-box structure occasioned by a forward suspended nacelle configuration. Another concern is the desire among some airframe designers to keep the "line-of-sight" of the HP and LP turbines away from the plane of fuel contained within the wing integral tanks. The split-gearbox arrangement does provide alleviation of these two concerns at the expense of some installation weight and some increase of nacelle drag due to additional wetted area.

RECORDING PAGE BLANK NOT FILMED

PAGE 234 INTENTIONALLY BLANK

ORIGINAL DRAWING
OF POOR QUALITY

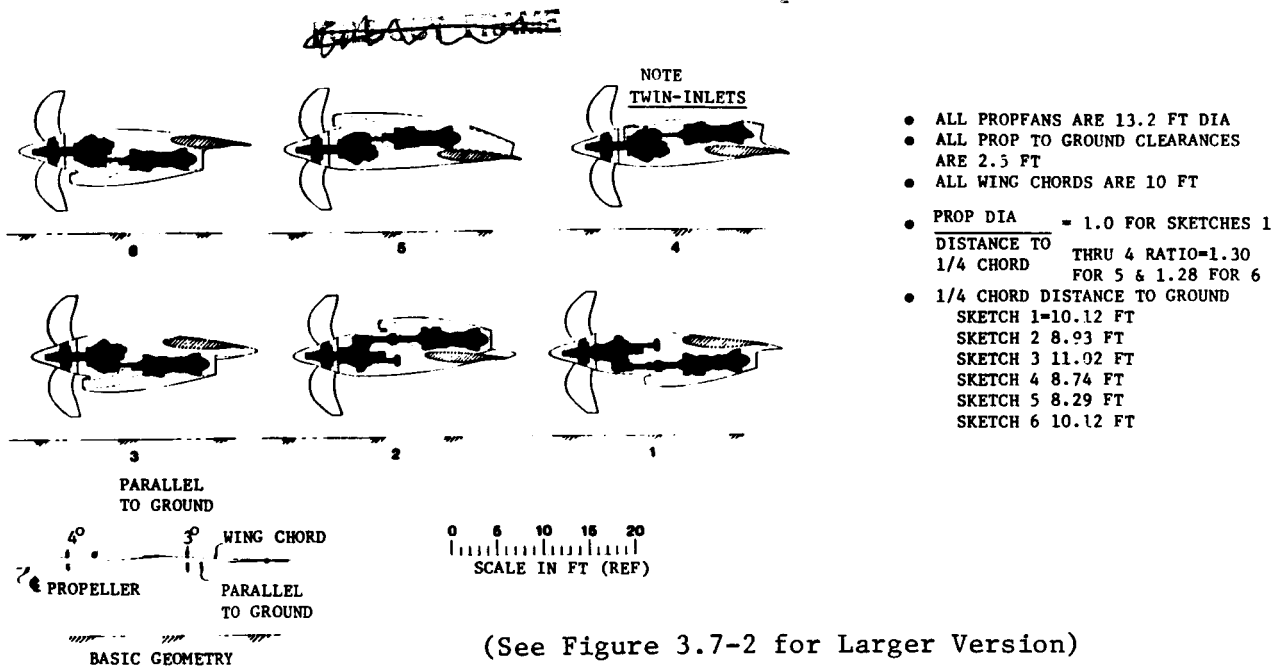


Figure 4.7-7. APET Study Nacelles.

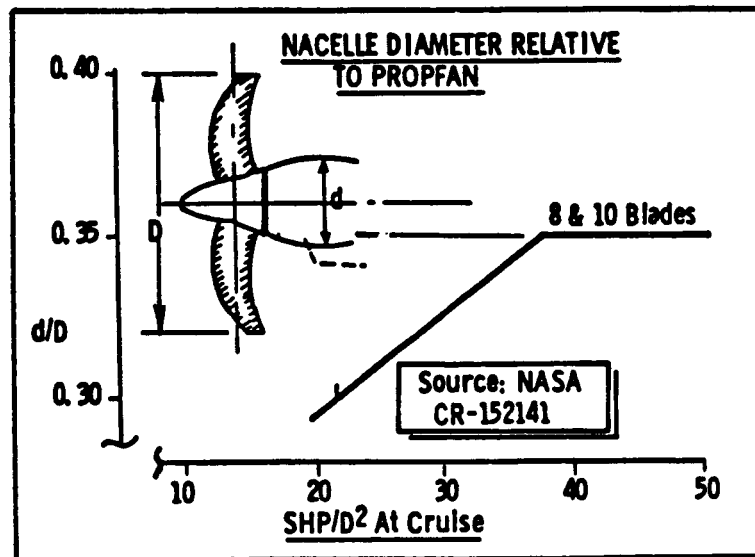


Figure 4.7-8. Hamilton Standard Propfan and Nacelle Recommended Relationships.

The two under-the-wing installations designed use offset drive systems to the propfan, i.e., the prop centerline of thrust, in each case, is above the rotational centerline of the turboshaft engines, and inlet air is supplied via a single scoop located on the underside of the nacelle. Discussions with NASA and with airframe designers indicated that an in-line gearbox and engine arrangement located in an above-the-wing layout should also be studied, and any problem areas relative to the under-the-wing arrangement should be identified.

4.7.3.2 Over-The-Wing Layouts

An in-line gearbox was designed (this was previously shown on Figure 4.6-13) and has been integrated with APET Engine Number 2(b). The full installation configuration is shown on Figure 4.7-9. Noteworthy features that are different in this installation compared with the under-the-wing variety are:

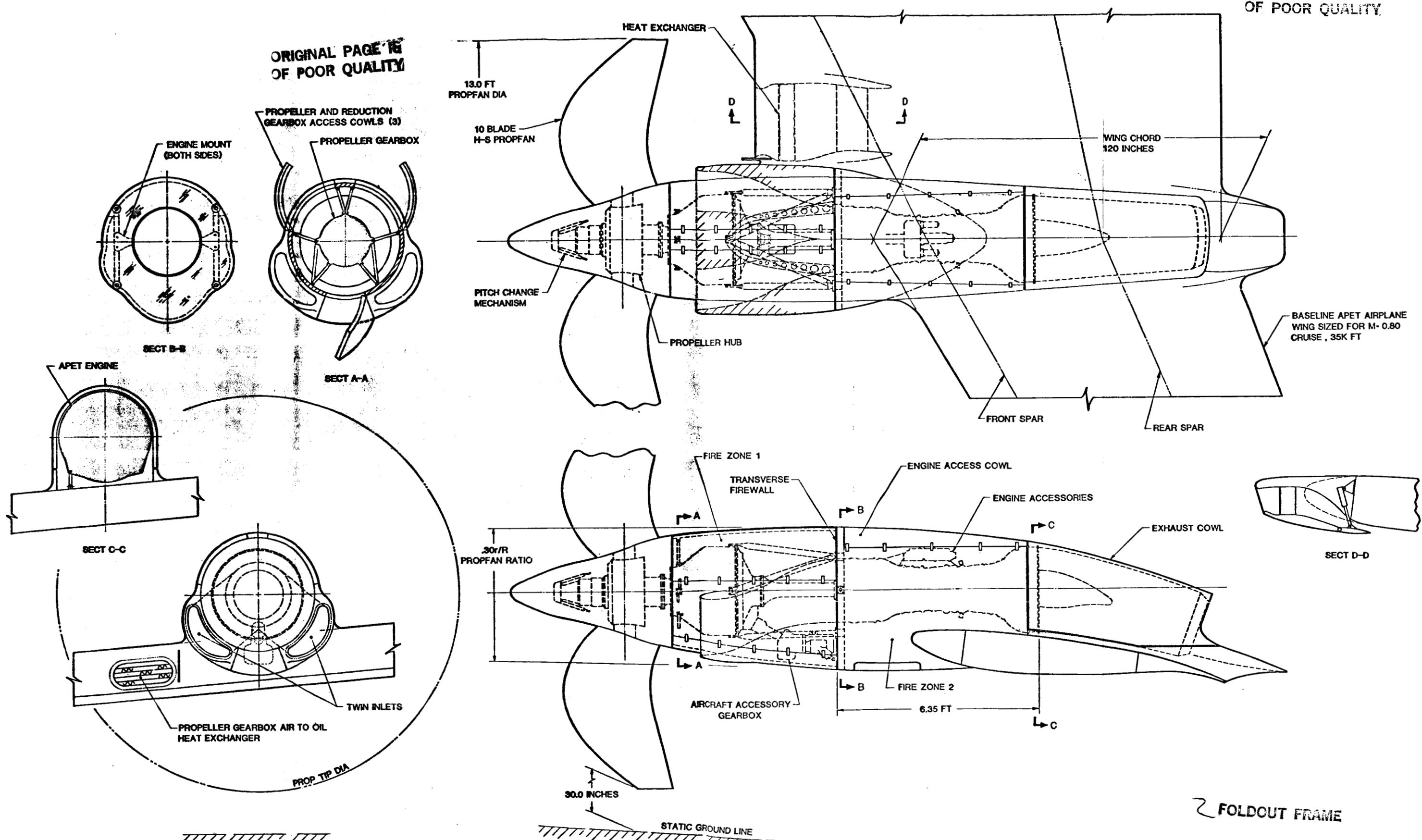
- Bifurcated inlet for engine air supply
- Gearbox supported by a tubular truss structure
- Gearbox heat exchanger located in an extension of the inboard wing leading edge.
- Aircraft accessories driven from the propeller gearbox via an angled drive
- Principal axial length of the nacelle is based on a substantially circular cross-section.

Also it may be seen that the current Hamilton-Standard propfan hydraulic pitch change mechanism has been retained.

This design layout automatically provides an improved propfan-to-ground clearance geometry, i.e., the wing is less high above the ground and therefore the landing gear length can be reduced. Structurally and aerodynamically it should be at least as good as the best under-the-wing layout and the twin-inlet arrangement should pose only minor design problems.

ORIGINAL PAGE IS OF POOR QUALITY

ORIGINAL PAGE IS OF POOR QUALITY



FOLDOUT FRAME

FOLDOUT FRAME

Figure 4.7-9. APET Over the Wing Nacelle with Concentric Gearbox Mach Cruise 0.8 Design.

The major problem in the layout is the less desirable means of transfer of hydraulic power from the propfan controller to the hydraulic pitch change mechanism. A change from a hydraulic to an all-electric propeller control might be very desirable for this installation.

4.7.3.3 Moment-Index Analyses

The relationships of the available wing-box area to the suspended weight of both the turbofan and turboprop propulsion systems was examined in this study. Some early concern was expressed, as a result of the geometry ground rules for both axial and lateral spacing of the propulsion systems, that excessive moments might be resulting from these geometries.

It was certainly a fact that the wing selected with an AR of eleven provided only a chord length of approximately 120 inches, at the lateral centerline of the turboprop system, and using spar locations of 15 and 65 percent of local chord for the front and rear spars respectively, the wing box chord length available was about 60 inches. Using thickness/chord ratios of a typical supercritical airfoil section enabled the calculation of the area bounded by the wing spars and the upper and lower wing surfaces. If the center of gravity location of the propulsion system is now identified and geometrically related to the centroid of the wing-box area, it is possible to define what might be called a Powerplant Moment Index. This index is illustrated in Figure 4.7-10 and has been used in the data shown in Figure 4.7-11, to compare the APET systems with some examples of "real" turboprop and turbofan aircraft. The conclusion that may be drawn is that the APET designs do not apply excessive moments to the wing, and that the "split gearbox" configuration would provide a substantial moment relief which might be used to advantage in reducing overall wing weight.

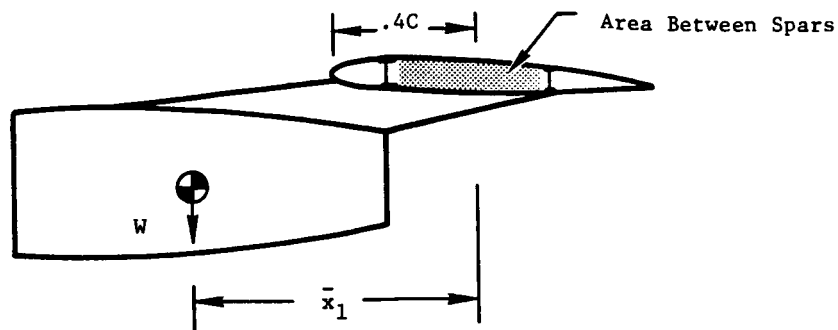
4.7.4 Inlet Aero Studies (Single Scoop and Double Scoop)

The work described in this section was based on: related experience accumulated during the General Electric Company's design and development of several commercial turbofan nacelle installations and participation in other joint programs with airframers and government agencies; available literature

PRECEDING PAGE BLANK NOT FILMED

PAGE 240 INTENTIONALLY BLANK

PAGE



$$\text{Moment Index} = \left[\frac{(W) \times (\bar{x})}{(\text{Area Between Spars})} \right]$$

W = Suspended Weight of the Propulsion System, pounds

\bar{x}_1 = Distance of the Propulsion System Center of Gravity from the 40% Wing Chord Station

C = Wing Chord at Propulsion System Centerline

Figure 4.7-10. APET Powerplant Moment Index Definition.

Powerplant Type	Aircraft Type	Approx. Moment Index (in-lb/in ²)
Turboprop	Electra (outboard)	286
	Belfast (outboard)	372
	SAAB-Fairchild SF-340	123
	DC-9 with propfan	772
	APET — Baseline	610
	APET — Split Gearbox	346
Turbofan	747	497
	DC10-30	537
	757	683
	A310	666
	737-300	590
	KC-135 (CFM56)	515
	APET — Turbofan	415

Figure 4.7-11. APET Nacelles Powerplant Moment Index.

pertaining to propeller and propfan installations; discussions with Lockheed-Georgia (GELAC) designers; access to some details of the design work for the NASA-Lewis Propeller Test Rig (PTR); and selective use of in-house analytical techniques.

The work scope is outlined in Figure 4.7-12, which was prepared at the outset to illustrate the various tasks and interactions involved as well as the broad approaches initially planned for their completion. The following discussion describes what was actually done, relative to the flow chart format of the figure. As indicated, two types of inlet systems were designed; a single scoop, with an offset gearbox; a bifurcated scoop having an in-line gearbox and over-the-wing engine arrangement. Those two designs are now described sequentially.

4.7.4.1 Cross Sectional Shape of Single Scoop Inlet

Figure 4.7-13 illustrates the end view of the throat, highlight and maximum radial envelope planes. It also reflects the design of the internal lip, forebody, boundary layer diverter, and throat area discussed below. Noteworthy features embodied in the design include:

- Inlet circumferential extent is within the maximum diameter of the propfan body enclosing the gearbox, in order to facilitate integration of the engine inlet/nacelle into that body without increasing its lateral envelope.
- Boundary layer diversion around the engine inlet is facilitated by arranging the inner cowl flowpath so that the diverter channel height increases in the lateral direction from its value at the vertical centerline.
- The side "corner" radius is based on a GELAC design. That region is important, since its leading edge must tolerate incident propfan swirl without flow separation thus reducing distortion and engine operability problems.

4.7.4.2 Duct Design Analysis

Because of its importance to the remainder of the installation, this component's bend proportions and length were established by a combination of computer flow analysis and empirical estimates of pressure loss.

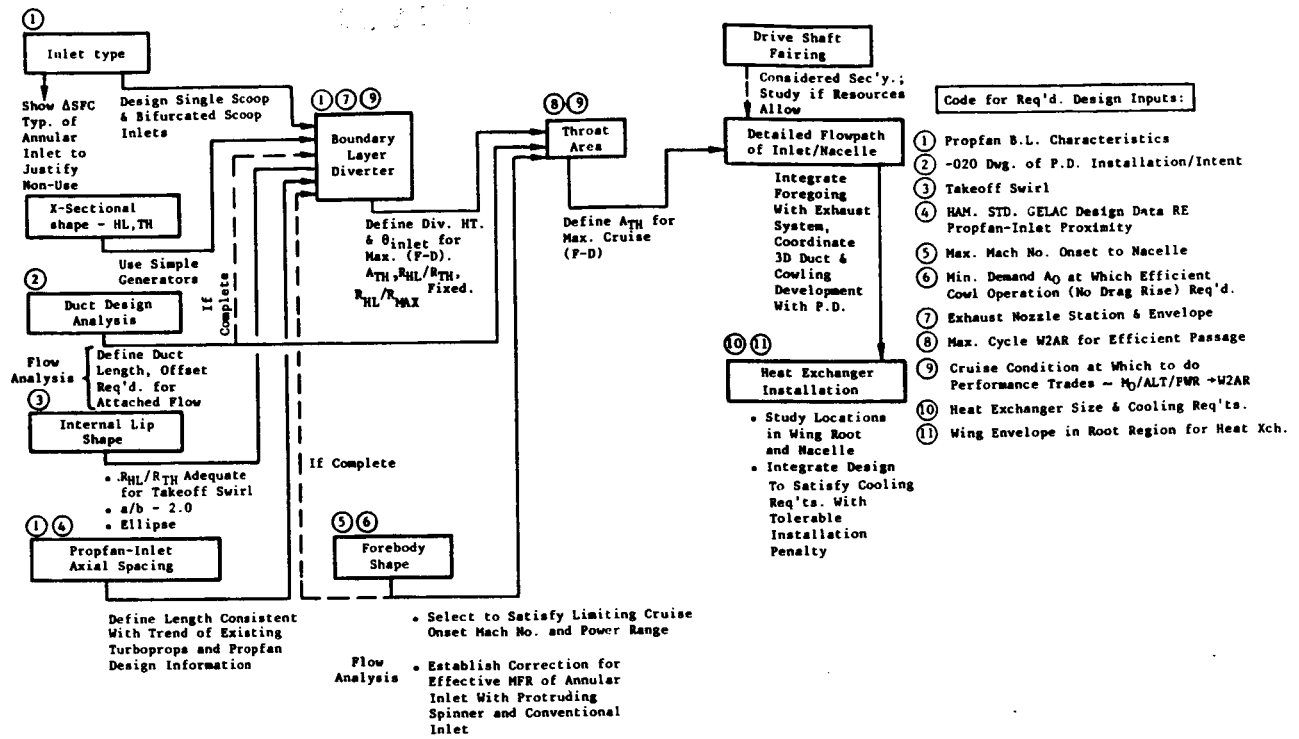


Figure 4.7-12. Schematic Design Approach for APET Inlets/Nacelles.

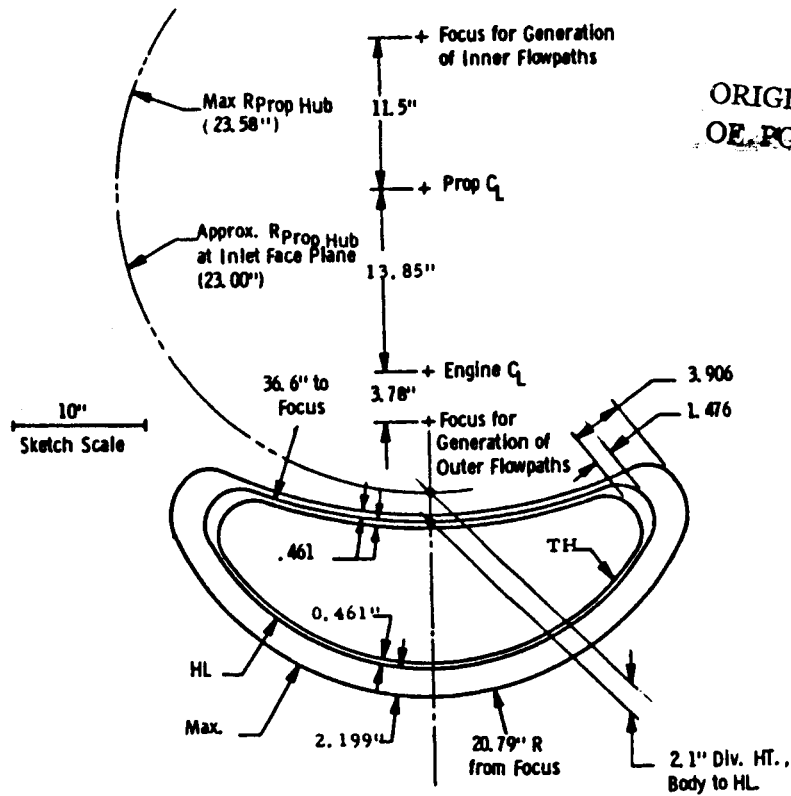


Figure 4.7-13. APET Single Scoop Inlet-Front View.

Initially, the Streamtube Curvature (STC) computer code (Reference 12) was used to establish meridional flowpaths producing attached flow in a duct whose vertical offset and length were prescribed by a preliminary engine installation layout. An important indicator emerged from the flow separation parameter, F_{sep} , commonly used by General Electric. The F_{sep} results are shown in Figure 4.7-14 for a corrected flow rate corresponding to about 83% of maximum power at $M = 0.80/35K$. The significance of this plot, per the inset scale, is that, for such an inlet offset and length, attached flow throughout the duct is only predicted for a relatively constant duct flow area. Based on that result, a constant area duct was selected, to provide some flow stability margin.

Subsequently, a new, shorter gearbox was designed. Also, empirical pressure loss estimates based on the analysis and data of Reference 27 were made that indicated higher pressure recovery could be attained with a longer duct allowing larger bend radii. Consequently, the duct was lengthened 10 inches from the initial value on which the flow analysis was based. Recovery estimates for the final duct design are shown in Figure 4.7-15 for the range of diverter height considered. The 2.1 inch height was ultimately chosen, per the discussion of Section 4.7.4.6.

4.7.4.3 Internal Lip Shape

The internal lip design was tailored around the inlet periphery, to place maximum thickness at the sides, which must tolerate the incident swirl from the prop-fan, and relatively little thickness on the inner and outer flowpaths, on which no significant flow incidence is presumed to act. APET engine cycle data were used to construct the Figure 4.7-16 plot of hub region swirl vs. discharge Mach number, to establish design requirements akin to those employed for turbofan installations. Empirical information was used to select the required side lip proportions, assuming that swirl and pitch-type incidence are numerically equivalent, since no evidence regarding that relationship is in hand. With that assumption, as shown in Figure 4.7-16, it is projected that the selected side lip design will tolerate 25° flow incidence at a 0.31 onset Mach

$W\sqrt{\theta}/\delta = 64.26 \text{ lb/sec} \sim 82.7\% \text{ Power @ } .80/35K$

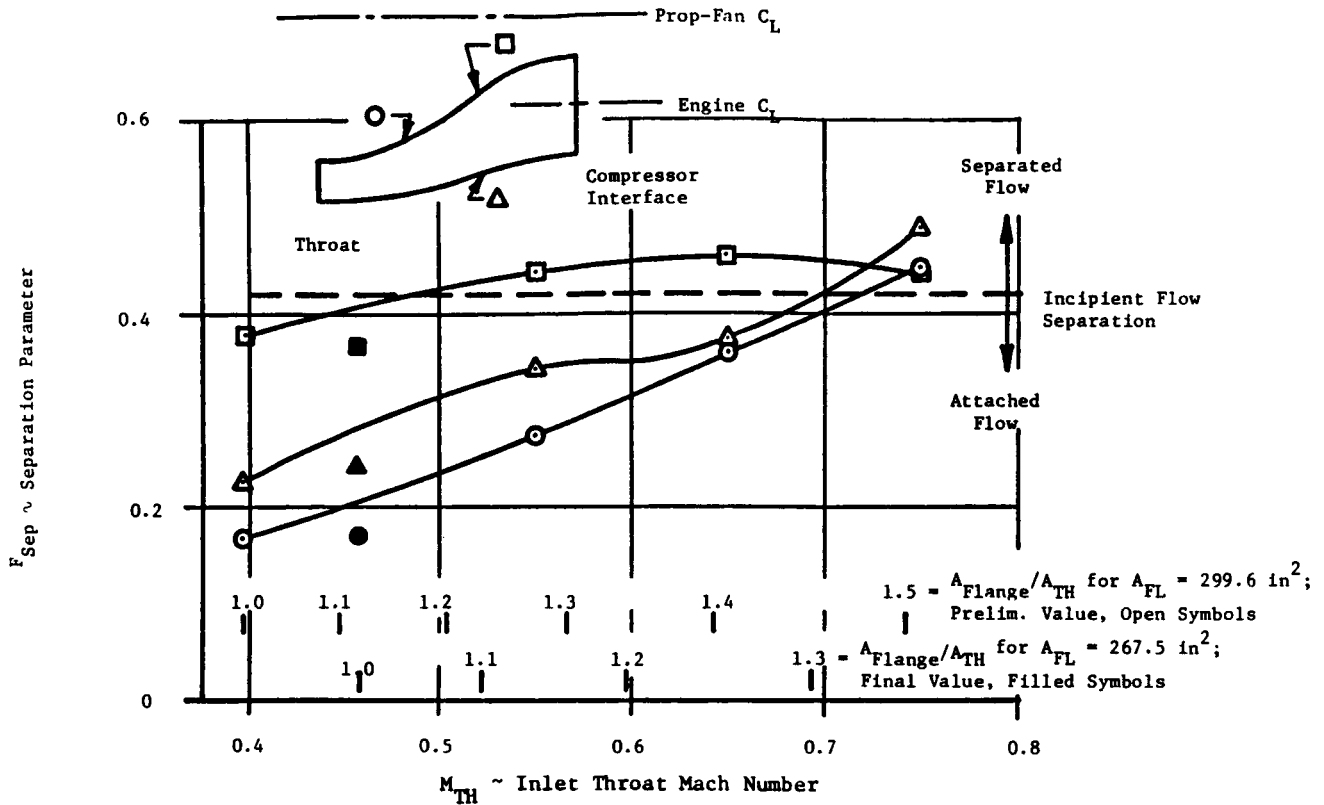


Figure 4.7-14. APET Flow Separation Analysis.

Based on:

- Final Gearbox Design. $A_{TH} = 267.5 \text{ in}^2$
- Duct Offset Dictated by Foregoing & Indicated Diverter Ht.

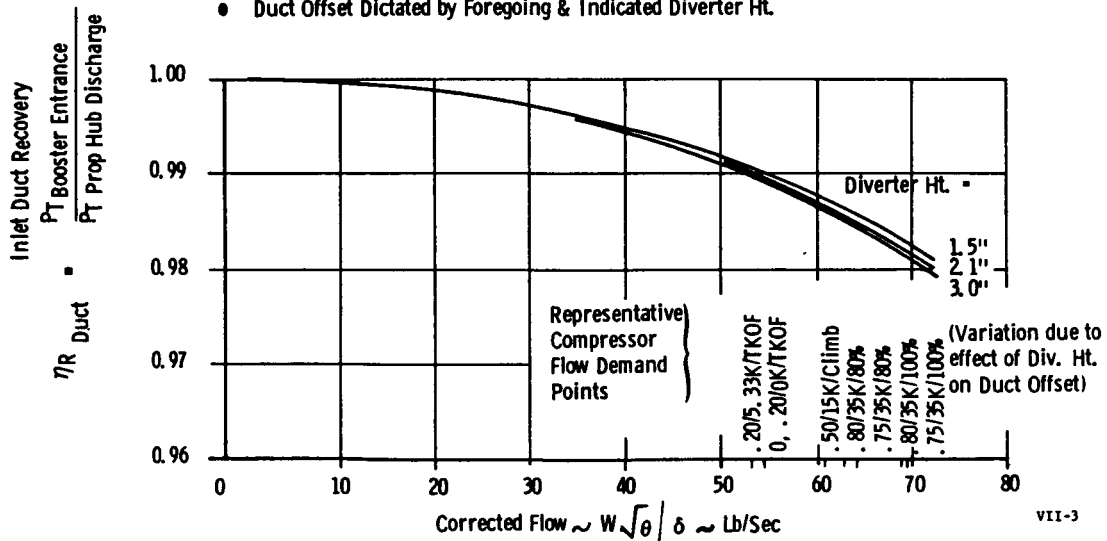


Figure 4.7-15. APET Inlet Duct Recovery Schedule (Single Scoop).

Prop-Fan Hub Region ($r/R=0.4$)

Estimated Flow Incidence
 Capability of Elliptical
 Internal Lip Designed
 Having $R_{HL}/R_{TH} = 1.16$,
 $a/b=2.0$

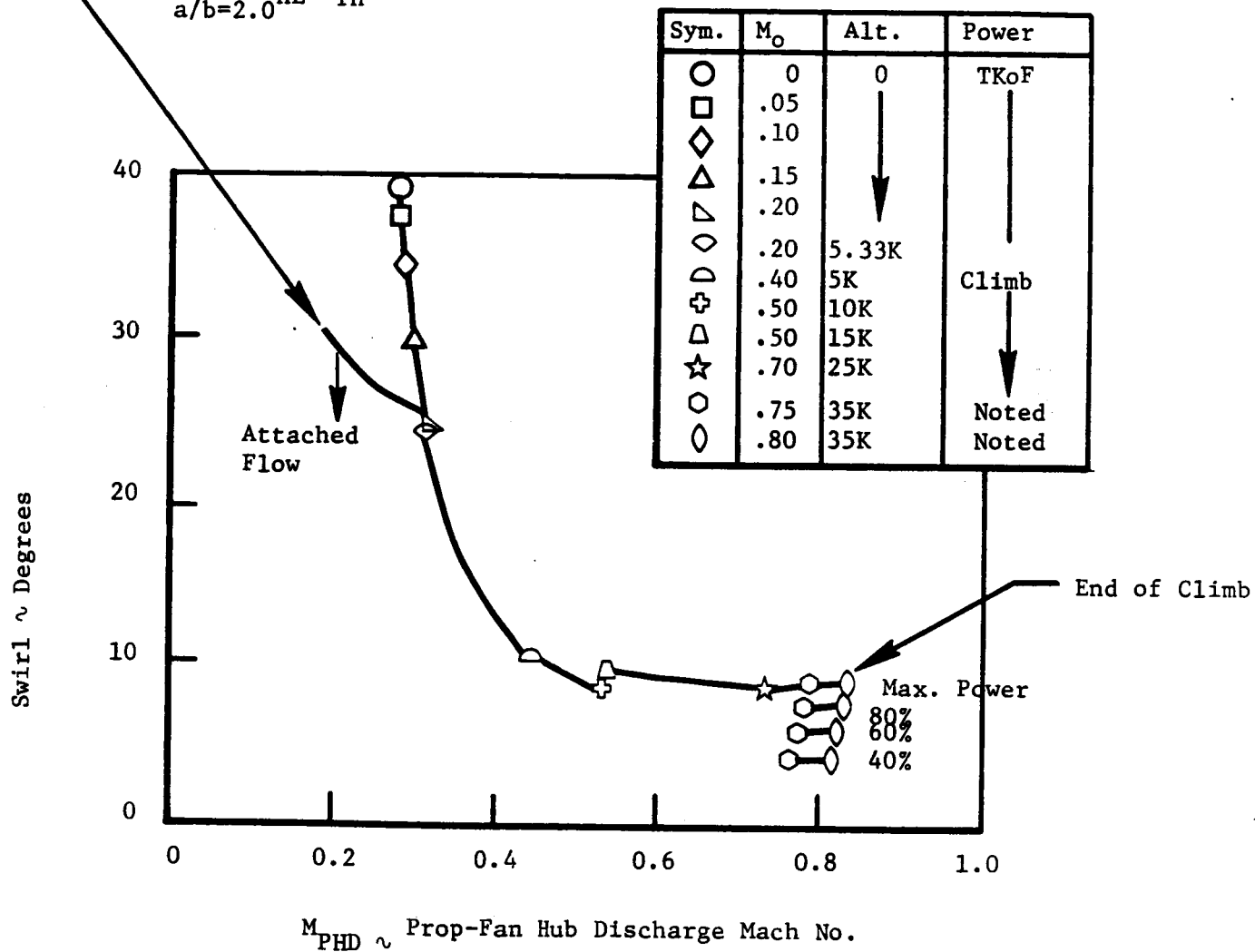


Figure 4.7-16. APET Swirl Model.

number, which satisfies the APET takeoff requirements for $M_0 \geq 0.20$. Satisfaction of the higher swirl levels occurring during the $M_0 < 0.20$ portion of the takeoff roll depends on one or more of the following factors:

- The cycle data employed for swirl requirements represent only a nominal prop-fan pitch schedule; it may be possible to reschedule pitch during the takeoff roll to reduce swirl.
- A given amount of swirl may be less taxing than the same numerical value of conventional pitch-type incidence, in terms of its potential to cause flow separation from a similar lip design. Then the inlet lip capability would be greater than the projection of the figure.
- The prop-fan flow acceleration contracts the captured streamtube, relative to a turbofan installation of the same inlet area and flight Mach number. For the APET design, which produces relatively low operating mass-flow ratio, $A_0/A_{HL} = 1.01$ to 1.14 during the takeoff roll, this effect should significantly ease the problem, by reducing the flow turning requirement around the inlet lip.
- The long inlet duct may significantly alleviate any flow distortion caused by lip separation before it reaches the compressor.

On balance, the lip design was selected in the belief that engine operability during the takeoff roll is not a barrier problem that necessitates the drag and weight penalty that would result from a thicker inlet lip.

4.7.4.4 Prop-Fan/Inlet Spacing

This parameter was determined directly by the gearbox and inlet duct designs. The resulting placement is farther from the prop-fan trailing edge than either the GELAC inlet design or the Hamilton-Standard forward boundary layer rake position in the test summarized in Reference 28. This was considered acceptable and of minimal performance significance, since no appreciable additional boundary layer growth is expected over the incremental length, due to the local flow acceleration anticipated in that region, per the above reference.

4.7.4.5 Forebody Shape

The forebody design requirements consist of the need to operate without drag rise at flight Mach numbers up to 0.80 and power settings down to 80% of maximum. The design was tailored around the periphery. Conventional cowl

design data were used to provide shapes adequate to avoid either spillage or wave drag on the side and outer flowpaths exposed to the high velocity discharge flow from the prop-fan. A relatively thin cowl was placed on the inner flowpath forming part of the diverter region, under the premise that the relatively low velocity in that region does not require much projected area for drag rise avoidance. The internal lip and forebody flowpaths selected for the inner, outer, and side regions are shown in Figure 4.7-17.

4.7.4.6 Boundary Layer Diverter

An estimate was made of the net "thrust-minus-drag" effect attributable to various diverter heights, in order to select that design feature. The following performance effects were evaluated:

- Variation of duct pressure recovery with change in the duct vertical offset, via the pressure loss methodology discussed in Section 4.7.4.2.
- Variation in average total pressure of the flow captured from various spanwise regions of the prop-fan discharge. This was evaluated by integrating a model of the prop-fan's discharge total pressure profile that was synthesized in turn from data of Reference 28 and APET cycle data.
- Drag on the incremental portion of the nacelle area attributable to the diverter's presence.

The friction drag component was calculated conventionally while the pressure drag calculation was parametricized, since no applicable pressure drag data for such an arrangement are known to exist.

The overall result of those calculations is shown in Figure 4.7-18 in terms of the relative diverter net thrust-minus-drag effect vs. diverter height. The datum for the thrust-minus-drag ordinate was chosen to represent the indicated nominal values contained in the APET cycle deck. The results shown in this figure do not indicate an optimum diverter height, due to the uncertainty in pressure drag, which is potentially the dominant effect. After some consideration, a 2.1 inch diverter height was selected, which represents about 70% of the main deficit in discharge pressure and lies between the optima indicated by pressure drag coefficients of 0+ and 0.25. That selection was based on the judgment that the relatively gradual streamwise blend of the diverter channel into the basic cowl surface of this design should facilitate

ORIGINAL DESIGN OF POOR QUALITY

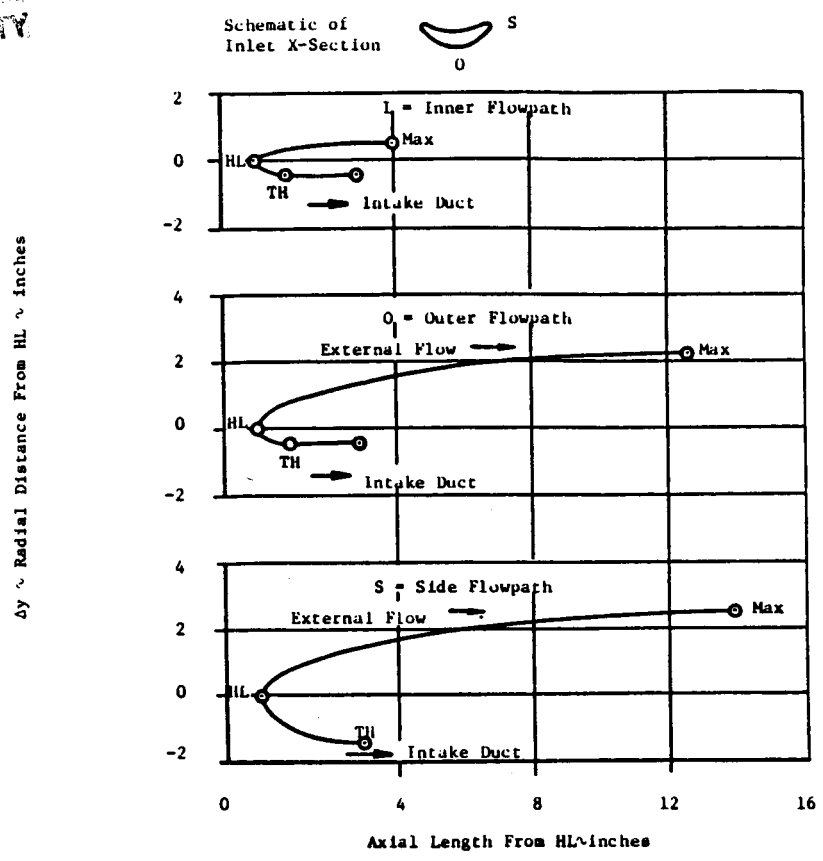


Figure 4.7-17. APET Single Scoop Inlet Lip and Cowl Contours.

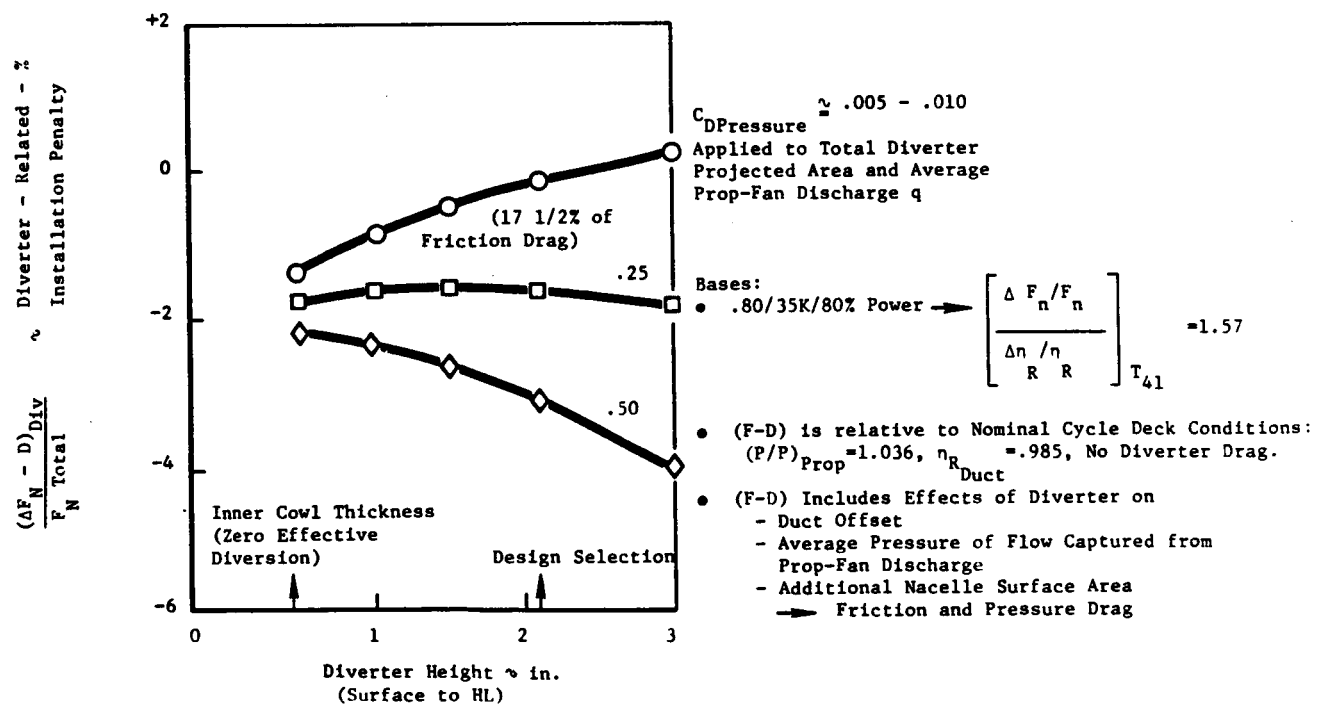


Figure 4.7-18. APET Single Scoop Inlet Diverter Height Study.

realization of pressure drag approaching the value of a well-designed turbofan nacelle. In terms of the Figure 4.7-18 portrayal, the "best-guess" pressure drag coefficient is between 0+ and 0.25 and nearer 0+.

An additional design feature related to the diverter is the provision there for an air intake to ventilate the entire nacelle cavity. That concept was studied for feasibility, including estimating the total pressure loss of several combinations of intake area and diffuser arrangement. Results showed that the area needed to provide the required six air changes per minute is easily available in the diverter as designed but that some means, such as an exit flap or ejector, of lowering the cavity exhaust pressure below ambient are needed for flight Mach numbers below about 0.4 to assure positive flow through the system.

4.7.4.7 Throat Area

Per the discussion of the duct design in 4.7.4.2, a constant area duct was selected to provide attached flow in the duct and thereby preclude engine operability problems.

4.7.4.8 Drive Shaft Fairing

No separate study of the drive shaft fairing was made. Per the experimental investigation summarized in Reference 29, a recovery improvement of 0.15 to 0.25% would be anticipated from the inclusion of a fairing designed to provide a smooth longitudinal area distribution, as opposed to a simple abrupt cylinder-cone arrangement approaching the compressor.

4.7.5 Bifurcated Scoop Inlet

A less extensive study effort was applied to the bifurcated scoop inlet design than to the single scoop inlet. Accordingly, the bifurcated inlet's definition is discussed in the same format, but less extensively, with maximum attention to those items differing from the single scoop design.

4.7.5.1 Cross-Sectional Shape

In general, a similar approach to that of the single scoop inlet was followed, with two exceptions. The centerline of each inlet face, in the front

view, was located 30° below the horizontal centerline, to avoid the large boattail angles found to occur on the top nacelle with a top/bottom inlet arrangement. Also after some iteration, the prop-fan centerline was selected as the generator of the outer flowpaths, rather than a nearer point as on the single scoop inlet. This was done to make the inlet circumferential extent more like the GELAC designs and also to reduce the cowl's radial extent. The resulting design's end view is shown in Figure 4.7-19.

4.7.5.2 Duct Design

The duct bend proportions, length, and placement were established by (1) applying the bend radius-to-duct height ratios of the APET single scoop design and (2) locating the throat plane about as far forward as possible without placing the inner duct flowpath closer than 0.5 inch to the limiting corner of the gearbox. The resulting duct length produces chordal angles intermediate between those of the APET single scoop (largest) and GELAC PTR twin (smallest) inlets.

Total pressure loss estimates were made, using empirical methods for both friction and turning components. The overall duct recovery results are shown in Figure 4.7-20. The bifurcated inlet has less turning loss and more friction loss than the single inlet, netting to slightly less overall loss.

4.7.5.3 Internal Lip Shape

This was handled akin to the single duct procedure, with an obvious allowance for the smaller absolute size of each of the bifurcated ducts.

4.7.5.4 Prop-Fan/Inlet Spacing

This feature was again determined by the duct design, i.e. the need to avoid duct-gearbox interference and the desire for minimum possible prop-engine proximity. The resulting proximity value is about 12% larger for the bifurcated than the single inlet.

4.7.5.5 Forebody Shape

The same approach as for the internal lip, 4.7.5.3, was followed.

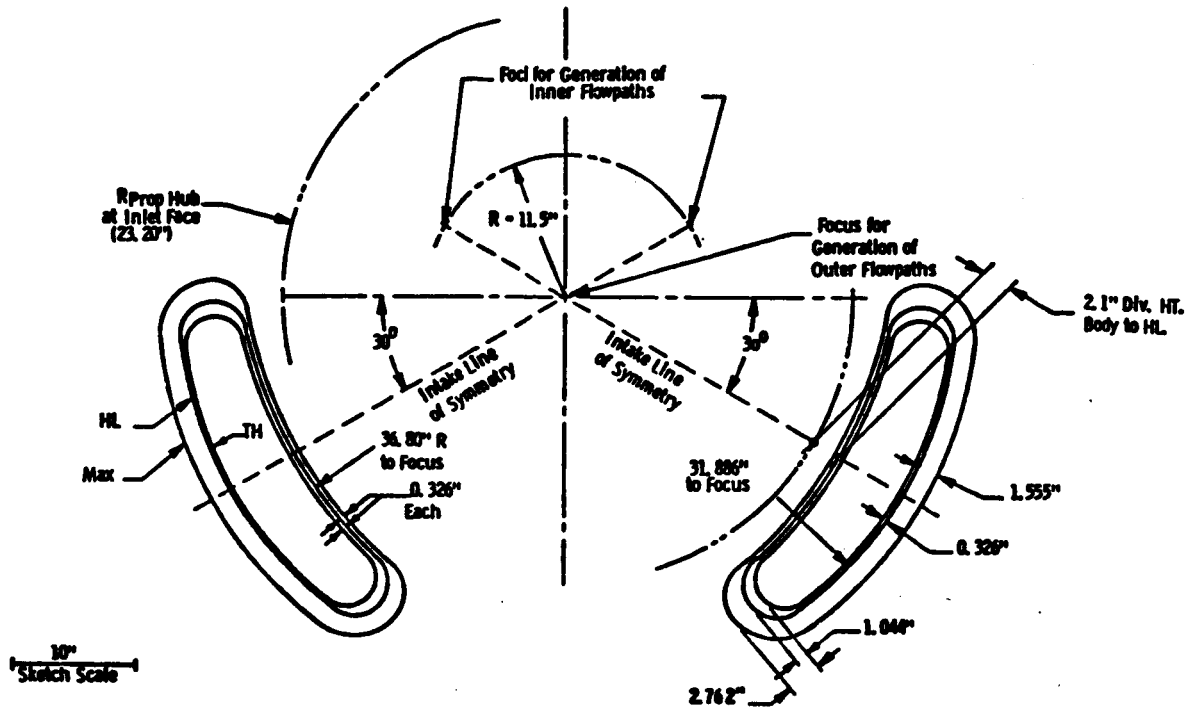


Figure 4.7-19. APET Bifurcated Scoop Inlet.

- Bases:
- In-Line Gearbox Design
 - Total $A_{TH} = 267.5 \text{ in}^2$
 - Div. Ht. $_{TH} = 2.1''$

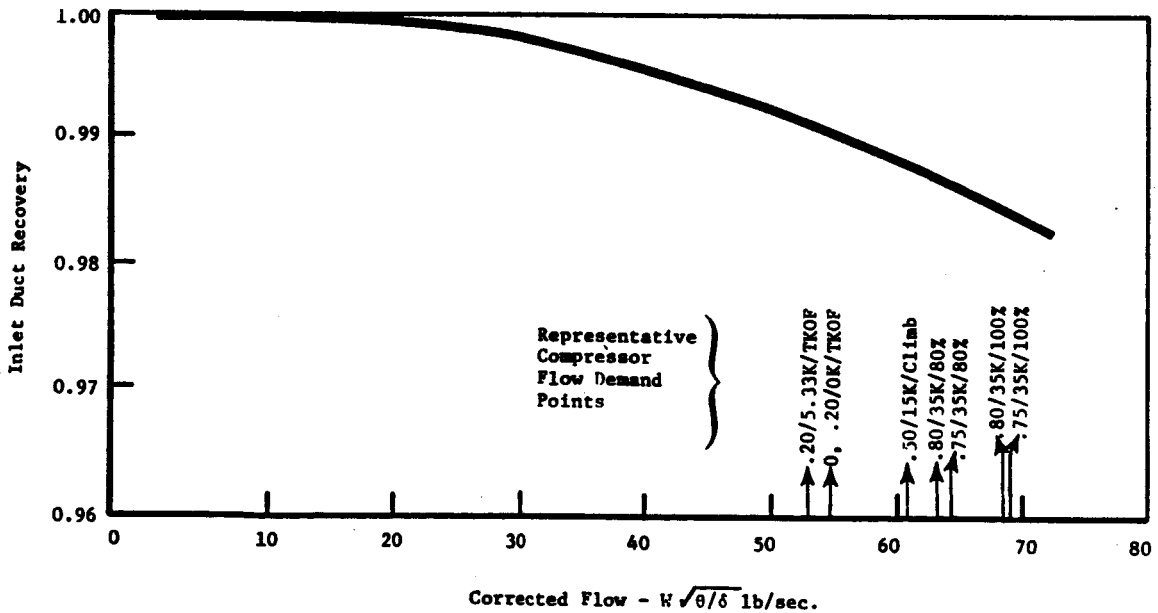


Figure 4.7-20. APET Inlet Duct Recovery Schedule Bifurcated Scoop.

4.7.5.6 Boundary Layer Diverter

The same 2.1 inch height as for the single scoop inlet was used, as no separate assessment of this feature on the bifurcated inlet was made.

4.7.5.7 Throat Area

The same total throat area as the single inlet was selected. That choice was prompted by results of the single inlet duct design analysis described in 4.7.4.2.

4.7.6 Summary of Selected Inlet Design Parameters

For perspective, Table 4.7-1 provides a tabulation of several design parameters for each of the APET inlets, with comparative GELAC values where available. Two general comments regarding this summary are appropriate. The APET configurations represent "level one" nacelle designs based on advanced engine and gearbox concepts. Also, the inlet designs are intended to be aggressive, rather than conservative, particularly in terms of duct length and lip/cowl projected area, to the extent feasible without obvious compromises in performance and/or operability. The premise behind that approach is that high-performance systems will only be identified by initially proposing aggressive designs for subsequent development and improvement, as required.

4.7.7 Exhaust System Aero Design

4.7.7.1 Nozzle Selection Criteria

The exhaust system for turboprop engines operates at low nozzle pressure ratios (1.5 or below) and, therefore, does not have to deal with supersonic flow. The general configuration can thus be a simple conic nozzle or alternatively have an external plug/centerbody. Initial studies showed little difference in performance for either approach. Thus, for the APET design, it was decided to select the conic nozzle approach which is the more simple of the two. For a more detailed design scope (i.e., full scale development program) this selection of conic vs. external plug may be directed by wind tunnel test

Table 4.7-1. Comparative Summary of Selected Inlet Design Parameters.

	Single Scoop		Bifurcated Scoop	
	GE APET	GELAC Test, PTR	GE APET	GELAC, PTR
$L_{Duct}/D_{Compressor}$	2.28	2.77	1.58	~2.5
$Y_{Duct} \ C_L / L_{Duct}$	0.303	0.226	~0.49*	~0.34
A_{HL}/A_{TH}	1.10, 1.346 Side	1.15, 1.20 Side	1.10, 1.346 Side	1.15, 1.20 Side
a/b	2.0	≤2.0	2.0	≤2.0
$L_{Prop} \ TE/D_{Prop}$ →HL	0.097	0.045	0.109	N/A
R_{HL}/R_{Max}	0.955, 0.815	N/A	0.955, 0.815	N/A
Diverter H/δ	~0.7	≤1.0	~0.7	≤1.0
A_{CF}/A_{TH}	1.00	1.00, 1.25	1.00	N/A

*Lateral Offset from Mid-point of Throat to 1/2 Compressor Tip Radius

results considering nacelle/nozzle afterbody drag and external flow suppression effects on nozzle flow coefficients. The following paragraphs describe the analyses which produced the APET exhaust nozzle and performance.

4.7.7.2 Nozzle Design

Initially, the exhaust nozzle was designed on an isolated nacelle basis. It was decided to keep the nozzle as short as possible to lower the friction losses (both internal and external) as well as weight, but at the same time maintain reasonable external boattail angles that reduce external pressure drag. Nozzle afterbody angles of 15° are considered to be about the maximum which can be employed on isolated axisymmetric nacelles without incurring excess afterbody drag. Therefore, the 15° angle was selected for the initial design. The selection of the 15° angle, combined with the required cycle nozzle flow area and a minimum radial clearance between the external nacelle and the turbine rear frame aft flange, established the exit plane of the nozzle. The internal centerbody and flowpath were defined consistent with the turbine frame rear flange dimensions to keep low values for the internal duct pressure loss. The resulting flowpath is shown in Figure 4.7-21. The internal pressure loss calculated for this flowpath from the turbine frame to the nozzle exit was 0.32 percent ΔP_T at M.8/35K. The nozzle velocity coefficient was estimated from empirical data and is nearly constant at 0.9985. Likewise, the exit flow coefficient was determined from conic nozzle data for a 15 degree half angle. The resulting nozzle coefficient curves are shown in Figure 4.7-22. The flow coefficient in this figure is derived from data with no external flow. Wind tunnel tests of nacelles installed on wings have shown that external flow can suppress (lower) the flow coefficient of an exhaust nozzle due to a change in the static pressure near the nozzle exit plane. This effect, which can be substantial, is most pronounced for unchoked nozzle conditions and is configuration dependent. Estimates of this suppression effect have been made from previous wind tunnel test experience and are shown in Figure 4.7-23. These curves were included in the APET cycle deck and were used for the cycle iteration to arrive at the physical area which defined the nozzle exit diameter in Figure 4.7-21. In a detailed development program, these curves would have

ORIGINAL PAGE IS
OF POOR QUALITY

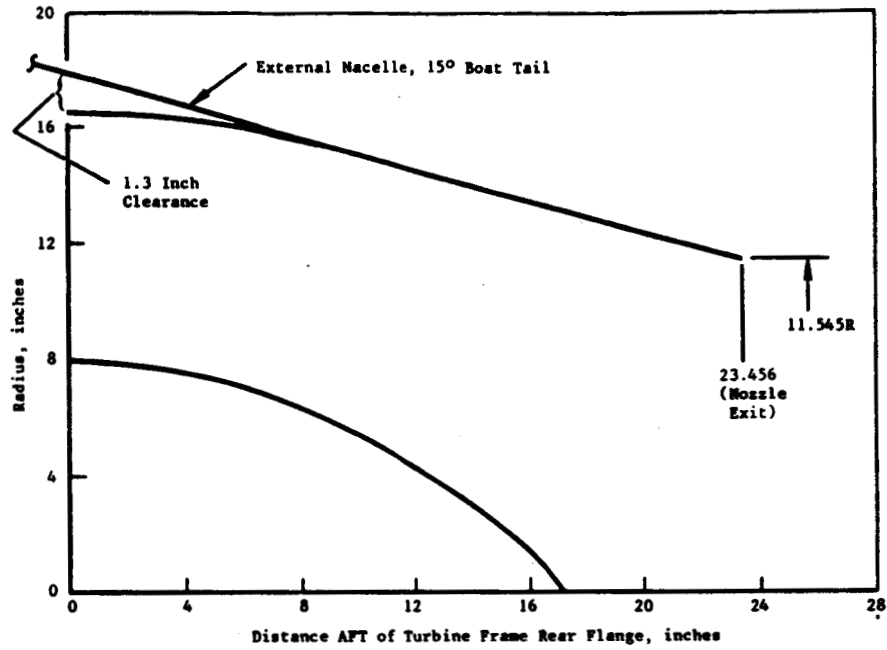


Figure 4.7-21. Exhaust Nozzle Internal Flowpath - Initial Design.

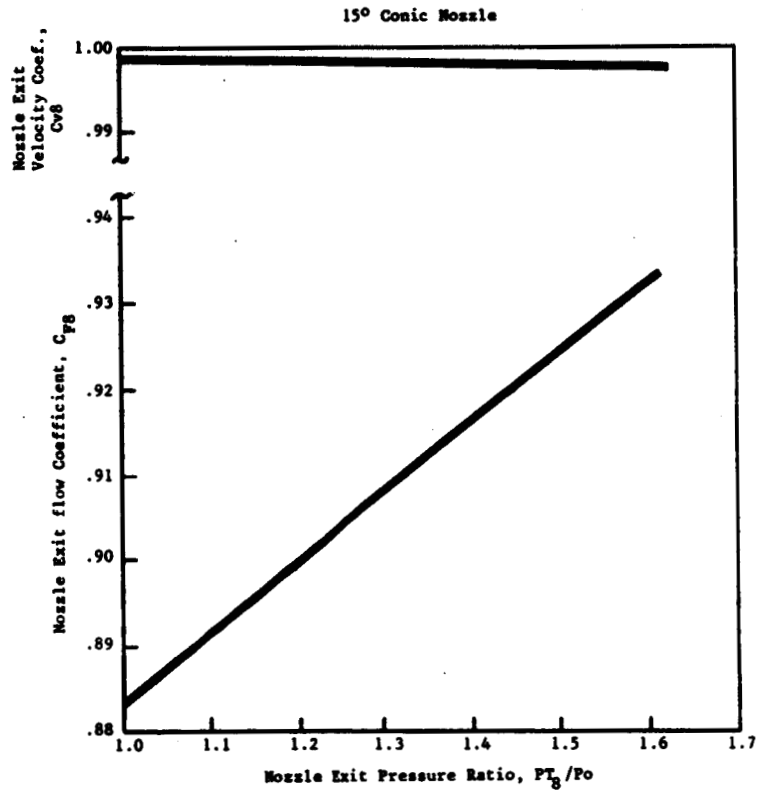


Figure 4.7-22. Exhaust Nozzle Exit Coefficients, Initial Design.

M = Prop. Discharge Mach Number
(At Ambient Pressure)

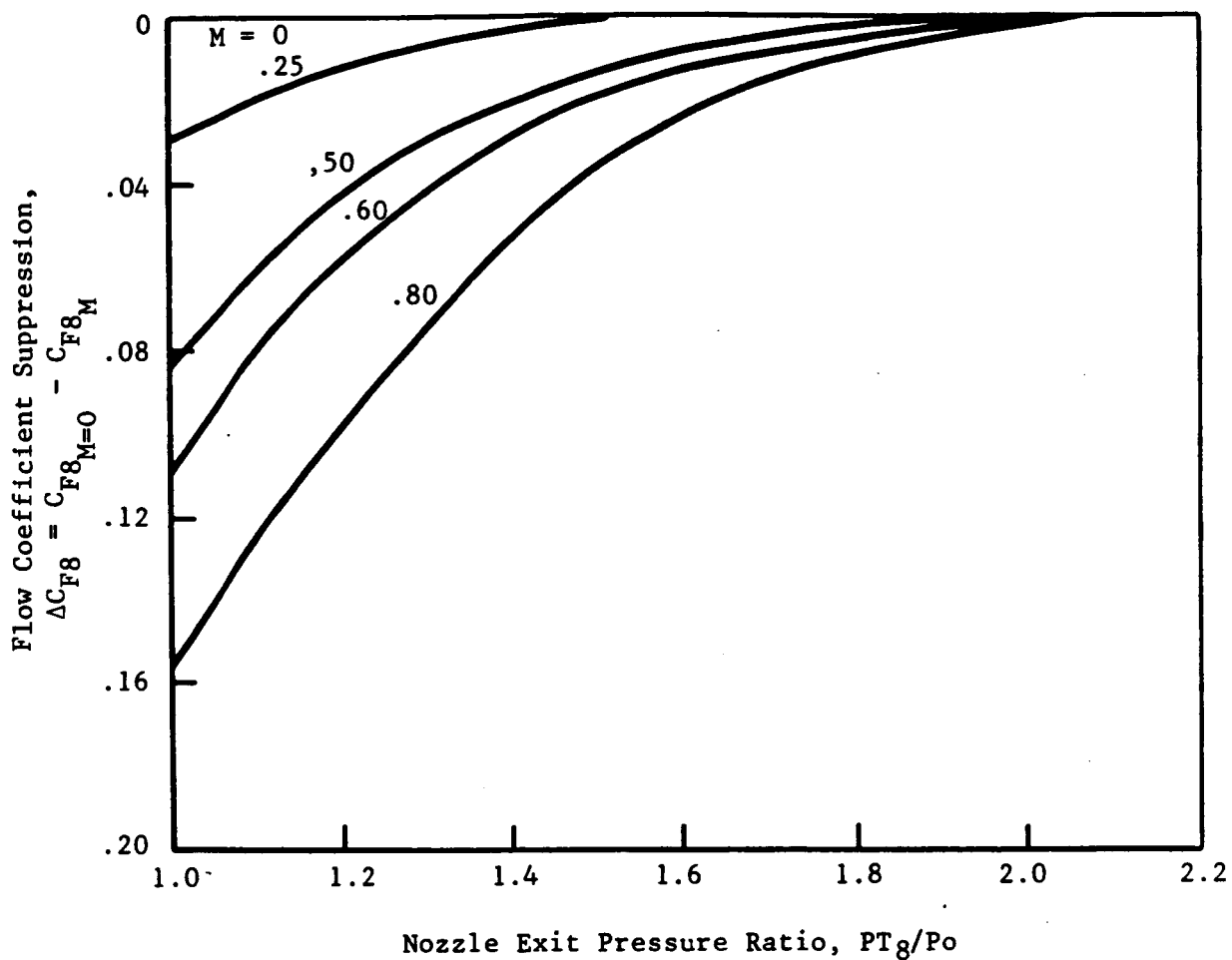


Figure 4.7-23. Estimating Exhaust Nozzle External Flow Suppression.

to be defined from wind tunnel tests of the specific nacelle and aircraft installation.

4.7.7.3 Nozzle Installation Factors

The flowpath defined in Figure 4.7-21 was used as a starting point to define the nacelle geometry on an isolated basis as discussed in the next section. Subsequent studies (also discussed in Section 4.7.7) to install the nacelle on the wing revealed that the exhaust nozzle afterbody defined on an isolated nacelle basis could result in a poor installation and high drag. The final exhaust nozzle configuration identified from the installation study had to be extended approximately 15 inches using a 10° boattail angle to make the total installation and nacelle closeout acceptable. The final nozzle design is shown in Figure 4.7-24, and the corresponding exit coefficients are shown in Figure 4.7-25; only the flow coefficient changes due to the half angle reduction are shown. The calculated pressure loss at cruise increased to 0.37% due to the added surface area.

4.7.8 Nacelle Installation Aerodynamics

The nacelle design was defined to minimize drag and weight consistent with required installation constraints. A baseline under-the-wing nacelle was first identified on an isolated basis. The installed nacelle was subsequently defined considering the total nacelle/installation drag and constraints.

4.7.8.1 Nacelle Requirements and Constraints

For discussion purposes, it is convenient to consider the nacelle as a blended combination of two nacelles: the engine nacelle and prop nacelle as shown in Figure 4.7-26. An engine nacelle was first defined on an isolated basis from the following two initial conditions. First, the nozzle afterbody was the initial design (15° afterbody) discussed in Section 4.7.7. And, second, it was decided to make the maximum diameter of the engine nacelle equal to the maximum diameter of the prop nacelle at a forward point near the location of the prop nacelle maximum diameter. Figure 4.7-27 shows these two starting points. The dashed line portion of the isolated nacelle contour in the figure was then defined by determining the minimum drag configuration,

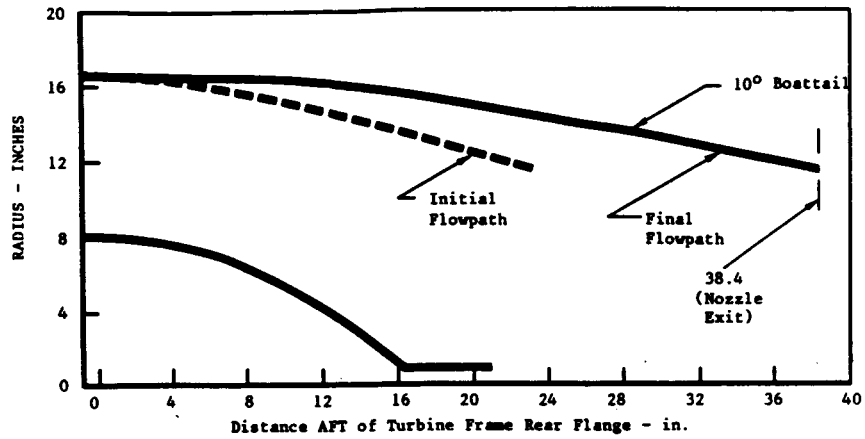


Figure 4.7-24. Exhaust Nozzle Internal Flowpath, Final Integrated Design.

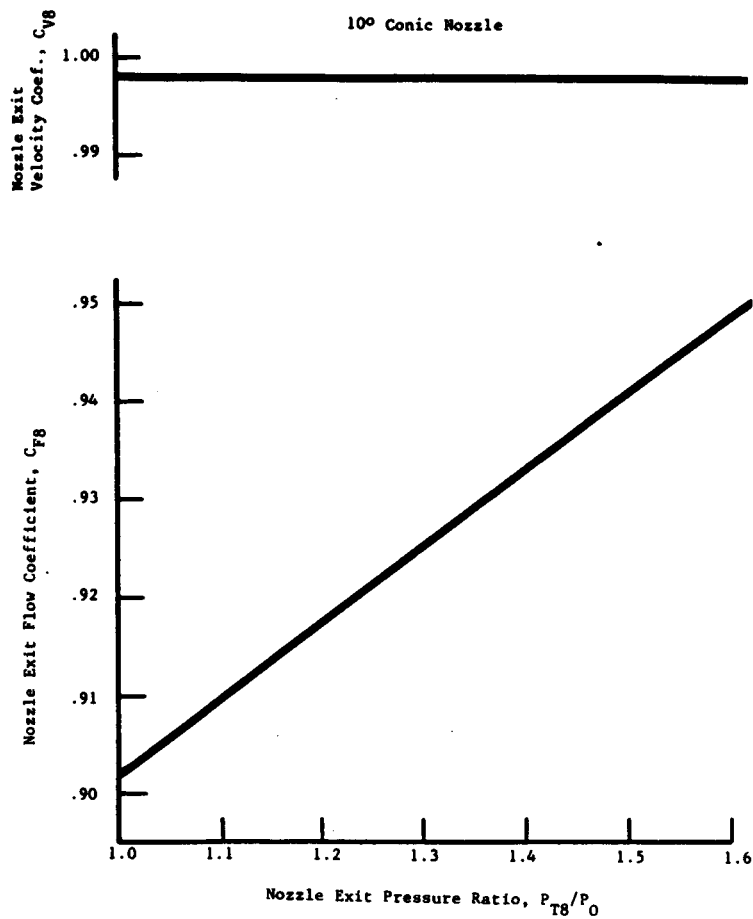


Figure 4.7-25. Exhaust Nozzle Exit Coefficient, Final Integrated Design.

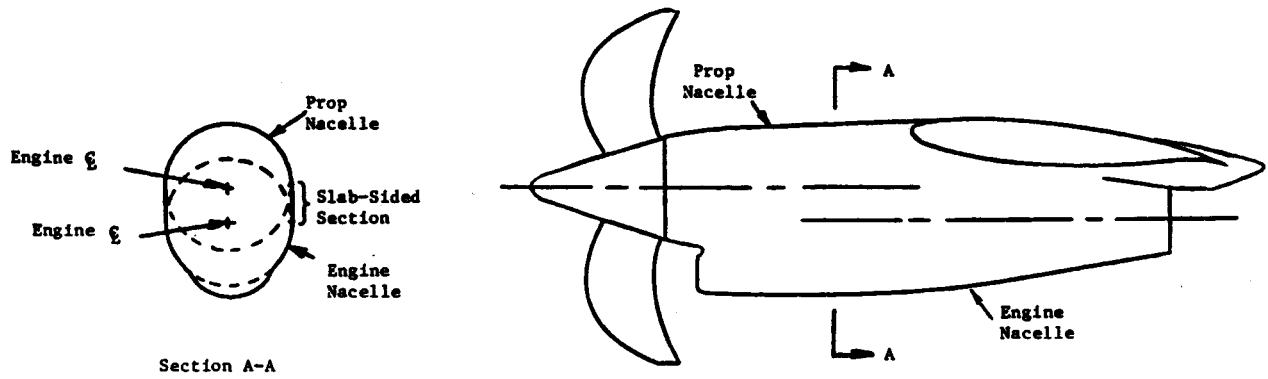


Figure 4.7-26. Nacelle Blending Approaches.

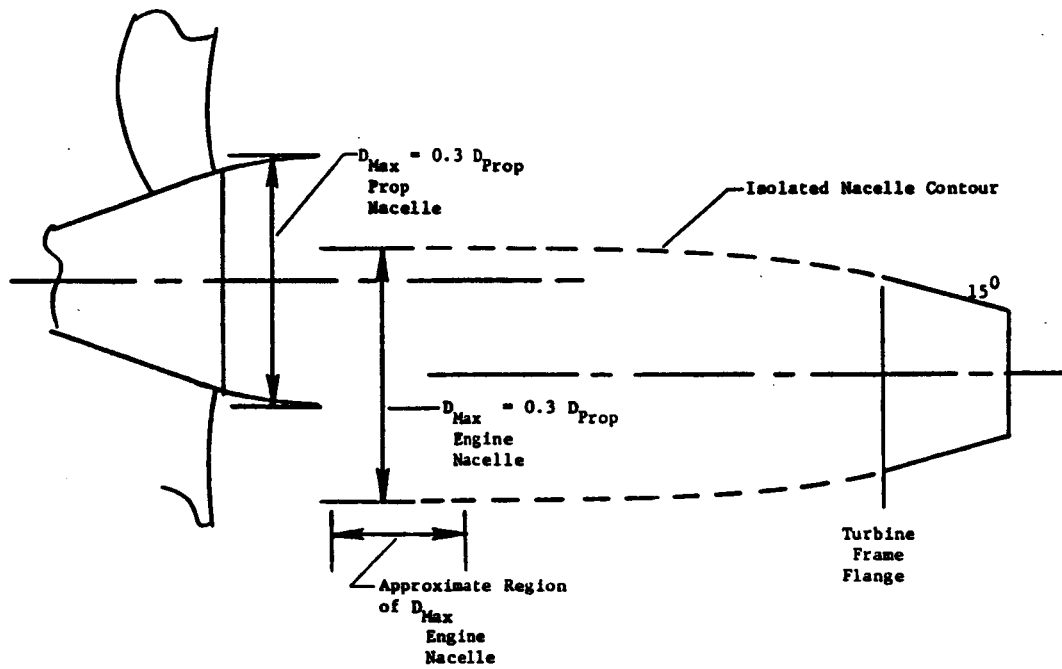


Figure 4.7-27. Initial Conditions For Nacelle Blending.

trading skin-friction drag for pressure drag. Skin friction drag can be reduced by employing a small afterbody radius of curvature which reduces the average diameter of the nacelle and the surface area. However, the smaller radius of curvature will tend to increase afterbody pressure drag. A trade study was conducted to determine the optimum combination for minimum drag. The nozzle afterbody and nacelle diameter limited the range of variation as shown in Figure 4.7-28. The study showed an almost insignificant difference in drag between the two limits; 0.03% F_n at cruise with the maximum envelope case having lower drag. Because the two drags were so very close, it was decided to "shade" the nacelle toward the minimum envelope side to keep the weight down. An $R_c/D_{max} = 3.0$ was selected and blended to D_{max} with a 1° forebody. This initial design, isolated nacelle (engine) flowpath is shown in Figure 4.7-29.

4.7.8.2 Isolated Nacelle Design

The inlet flowpath analysis discussed in Section 4.7.3 established the relative axial spacing of the isolated nacelle components. This included the prop-to-inlet spacing and inlet-to-engine face spacing. The bottom centerline of the inlet is also the bottom centerline of the nacelle.

The next step in the nacelle definition was the blending of the prop nacelle with the engine nacelle. Structural requirements dictated that the prop nacelle diameter be maintained constant at $D_{max} = 0.3/D_{prop}$ aft of the max diameter point. This results in a "barrel-type" structure along the top of the nacelle. The blending of the two nacelles was a simple slab-sided connection as shown by the schematic in Figure 4.7-30. With this portion of inlet analysis selected the diverter height, and a planform view of the diverter was used to define the diverter blendout starting from an initial half angle of 30° . The diverter was completely blended out at about the axial midpoint of the engine nacelle. The diverter planform view and several station cuts are also shown in the above figure.

1. Max Envelope; Cylindrical Forebody with $R_c/D_{Max} = 3.8$ (Largest Value)
2. Min Envelope; Smallest $R_c/D_{Max} = 2.5$

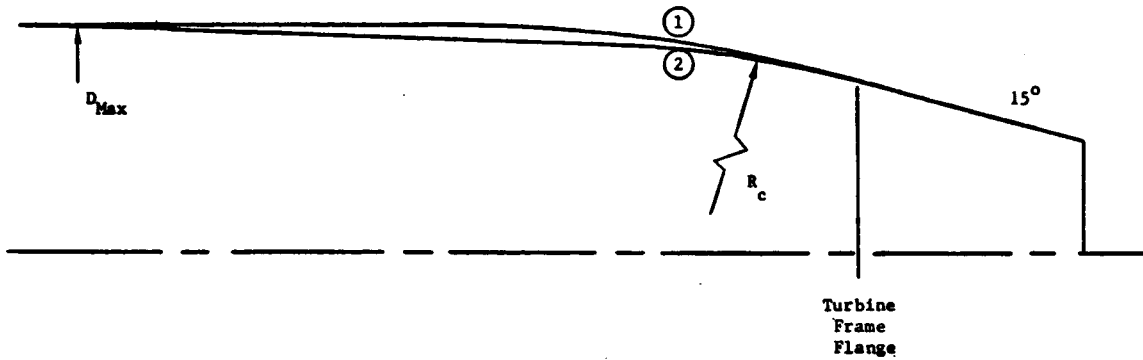


Figure 4.7-28. Engine Nacelle Envelope Limits.

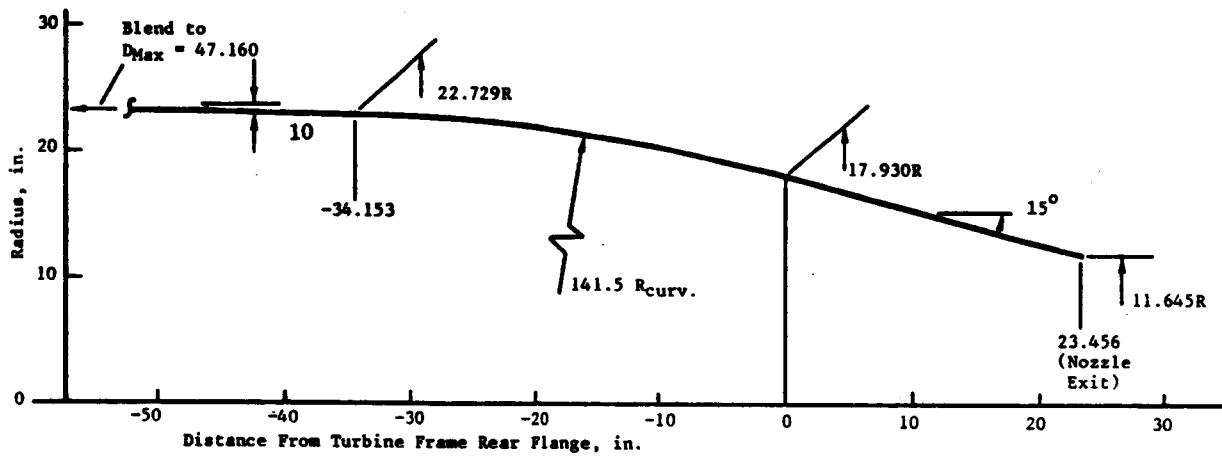


Figure 4.7-29. Nozzle Afterbody Initial Design.

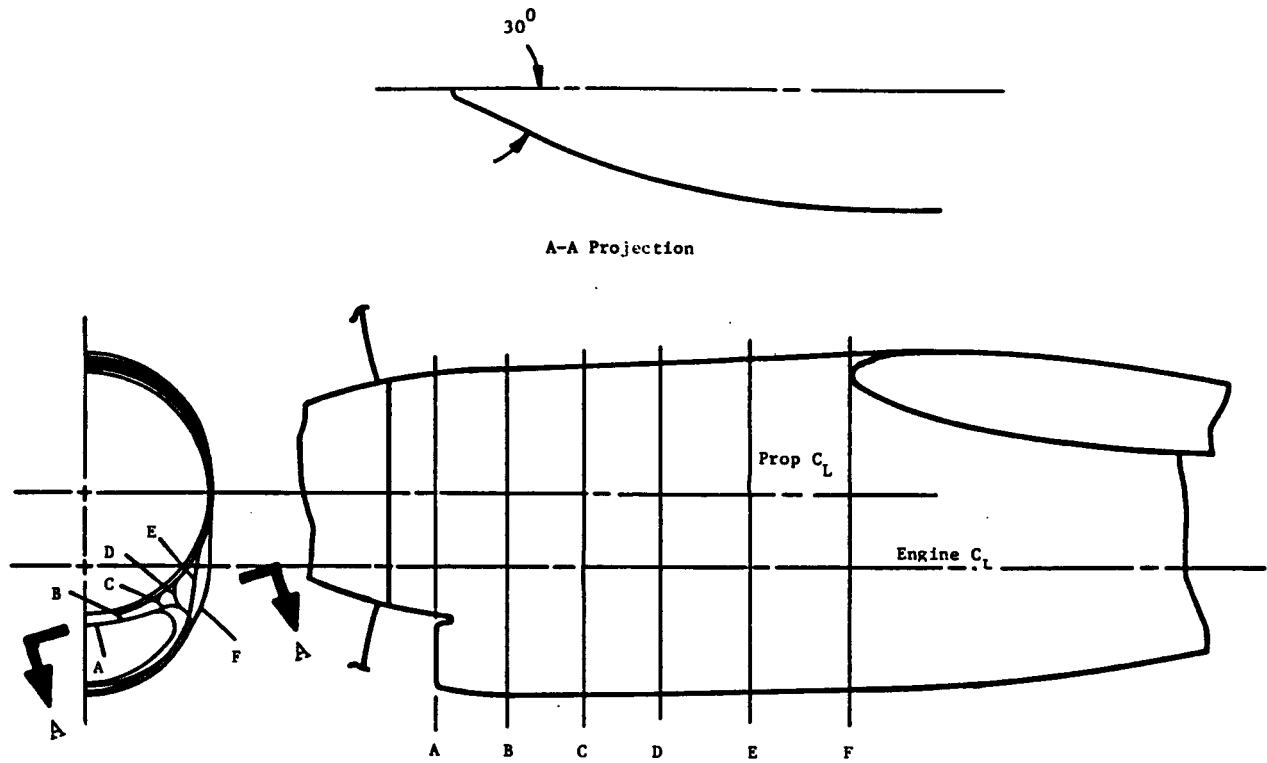


Figure 4.7-30. APET Diverter Contour.

4.7.8.3 Installed Nacelle

Most of the overall nacelle was now defined on an isolated basis. Nacelle placement was next established from two parameters. Axial placement relative to the wing was determined by maintaining a minimum clearance between the prop and wing leading edge on the inboard side. This clearance amounted to one-fourth of the local wing chord as shown in Figure 4.7-5. Vertical spacing was set by the requirement to maintain a four inch spacing between the wing lower surface and the engine nacelle contour at the turbine rear frame. This spacing was required to provide room for the required structural member to connect the engine and wing. This requirement is shown on Figure 4.7-31.

The last task was to "blend out" the nacelle at the wing-nacelle interface in the region of the nozzle/nacelle afterbody. Attempts to do this with the nacelle as defined resulted in closure rates which were considered too large in view of the fact that three bodies (wing, nacelle, and pylon) and were all closing out simultaneously. For typical, high-bypass turbofan installations, the structural pylon is relatively narrow and is easily faired over. In the case of the turbo-prop installation, the requirement for the constant nacelle diameter "barrel-structure" results in a very wide "pylon" (same width as the engine nacelle) at the wing leading edge. In order to close this pylon out and not have a pylon nearly equal in width to the nozzle at the nozzle exit plane, the pylon closure becomes excessive. Figure 4.7-32 pictorially displays the closeout problem of the three bodies; each body "turns away" from the other creating a significant diffusing channel along the afterbody. It appeared that a lengthening of the nozzle afterbody was required to reduce the severity of the closeout. A nozzle extension of about 15 inches relative to the initial design, 15° afterbody was the end result of this effort. This reduced the nozzle afterbody angle to 10° and the pylon closure half angle was comparable at 11°. With this closure rate, the pylon fairing extends past the wing trailing edge by about 17 inches and requires a small fairing to go forward a short distance over the upper surface of the wing.

It was not appropriate for this APET study to attempt a sophisticated, three-dimensional computational evaluation of the nacelle geometry to analyze and design the flowpath. Little technology currently exists to assess drag

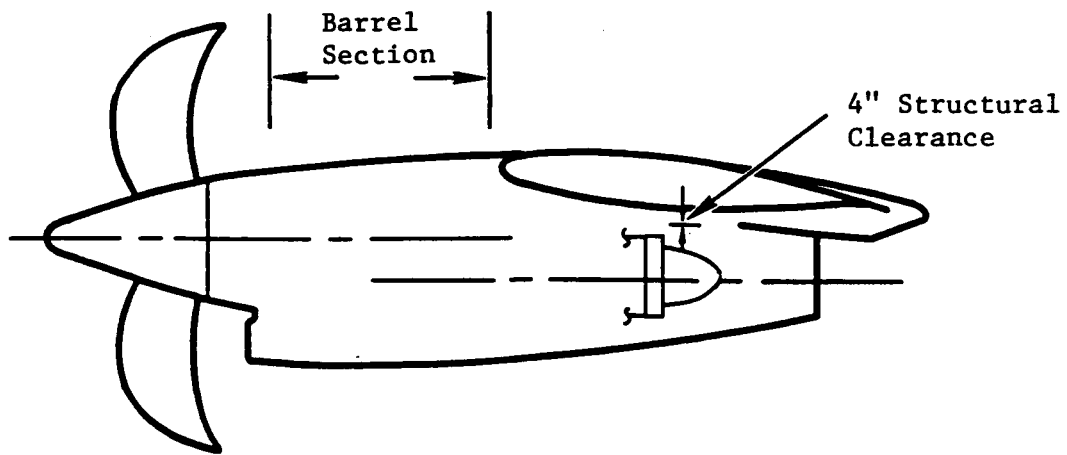


Figure 4.7-31. APET Nacelle Structural Requirements.

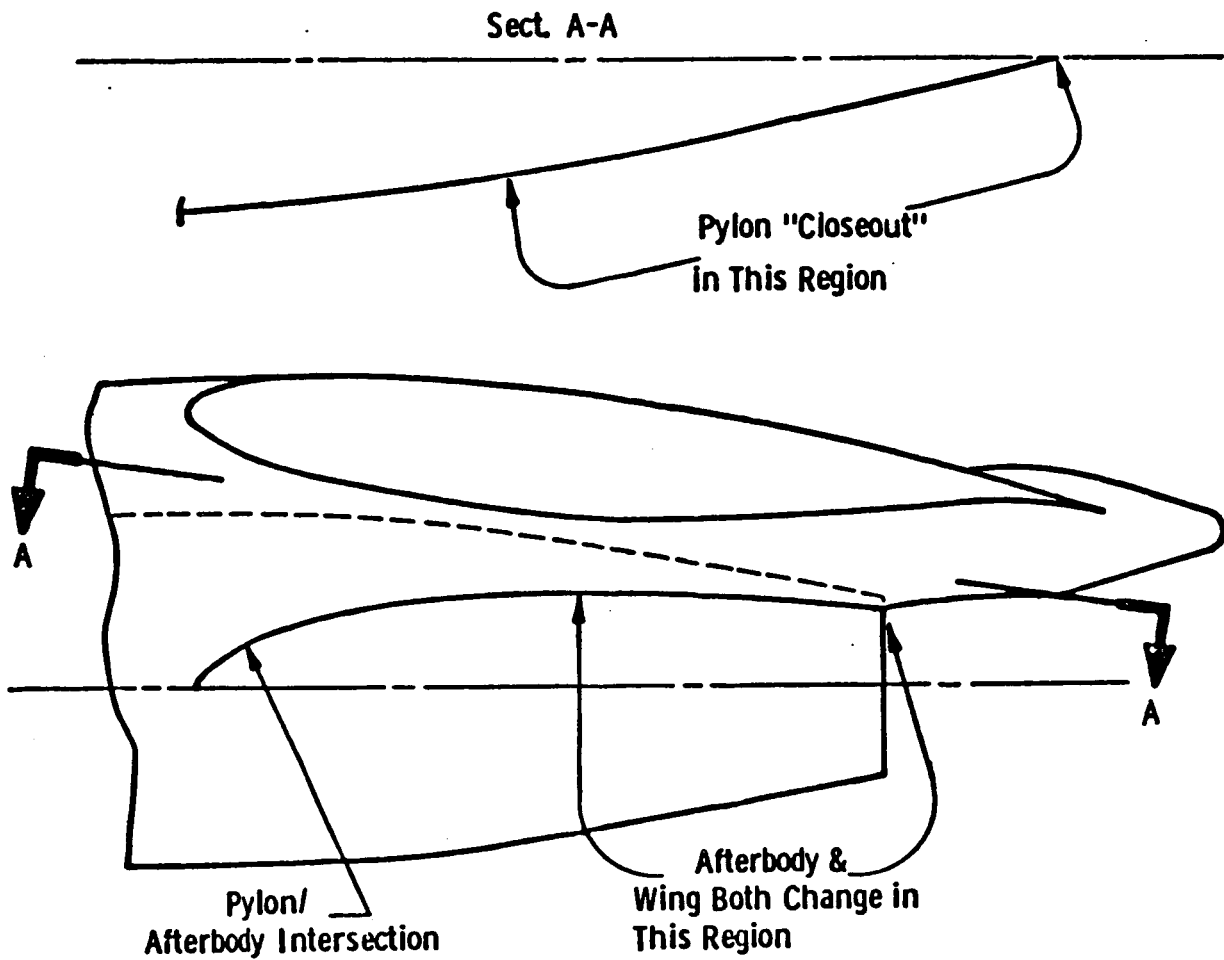


Figure 4.7-32. APET Afterbody Closure.

increments associated with turboprop installations. Thus, the nacelle configuration, with the exception of the inlet, was determined by the forementioned qualitative approach using general guidelines. Successful nacelle aerodynamic integration is a particular area of concern, and, in a detailed, development program, computational analyses and wind tunnel tests would be conducted to identify an optimum system. This need to develop turboprop nacelle installation technology is addressed in the Development Plan, Section 12. Also, the scope of the APET study was not sufficient to make an equivalent evaluation of an over-the-wing nacelle as has been shown in the sketches numbered 2, 4, and 5 of Figure 4.7-7.

4.7.9 Nacelle Drag Calculation

The nacelle external drag includes both friction and pressure drag on the entire nacelle aft of the prop spinner trailing edge and directly up to the wing surface. Conventional techniques currently employed in high bypass turbofan nacelle analysis were used to calculate the nacelle friction drag. This technique treats the nacelle as a flat plate and calculates the average, incompressible flat plate skin friction coefficient assuming a turbulent boundary layer. The Frankl-Voishel compressibility correction is applied to account for Mach number effects. The specific equations for this calculation are as follows:

$$D_{\text{fric}} = C_{\text{fi}} \frac{C_{\text{fc}}}{C_{\text{fi}}} q_o A_{\text{surf}} K_r$$

where:

$$C_{\text{fi}} = 0.455 (\log_{10} Rn)^{-2.58} \quad \text{Avg, flat plate, turbulent friction coefficient}$$

$$\frac{C_{\text{fc}}}{C_{\text{fi}}} = \left[1 + \left(\frac{\gamma-1}{2} \right) M_o^2 \right]^{-0.467} \quad \text{Compressibility correction}$$

$$q_o = \frac{\gamma}{2} P_o M_o^2$$

$$R_n = 144 P_o M_o \left(\frac{\gamma g}{RT_o} \right)^{1/2} \frac{C}{\mu_o}$$

$$u_o = 2.27 g \left(\frac{T_o^{1.5}}{T_o + 198.6} \right) 10^{-8}$$

and:

M_o = Reference freestream Mach number = average prop discharge Mach number

P_o = Ambient pressure, psia

T_o = Ambient temperature, ° R

γ = Ratio of specific heats = 1.4 for air

g = Gravitational constant = 32.174 ft/sec²

R = Gas constant = 53.35 ft-lb/lb ° R

C = Characteristic nacelle length, ft.

A_{surf} = Nacelle surface area, sq. inches

K_R = Roughness factor

Results of this technique have been compared against detailed boundary layer analyses and have been shown to be in very good agreement with the detailed analysis approach.

For axisymmetric or semi-elliptical nacelles, the determination of surface area for the friction drag calculation is straightforward. For nacelles such as the turboprop nacelle, the wide variation in nacelle shape is handled by plotting nacelle perimeter versus station and integrating the curve. Since the APET nacelle surface area is so highly "front-loaded", use of a characteristic length based directly on nacelle length to calculate the average friction coefficient will result in a drag which will be lower than the true value. This is because significantly more surface area is located near the front of the nacelle where the local Reynolds numbers are lower and the local skin friction coefficient is higher. To account for the surface area distribution unique to this nacelle design, calculation of the nacelle drag at cruise was

performed in three sections treating each section independently and adding up the total drag. Then, several nacelle lengths were used to calculate the overall nacelle drag, and a characteristic length was subsequently determined which gave the same drag as the "integrated" drag. The resulting characteristic length was 134 inches compared to a physical nacelle length of 223 inches. Use of the physical length would have calculated the friction drag low by ~9 lb at M.8/35K. This information was included in the engine cycle deck to allow external nacelle friction drag calculation at any flight condition and power setting.

Analytical and experimental studies have shown that for conventional separate flow turbofan nacelles, the nacelle pressure drag is typically 15 to 20 percent of the friction drag. This drag ratio range is about 10 to 15 percent for long duct nacelles. From the standpoint of nacelle fineness ratio, the turboprop nacelle is more like a long duct nacelle, and it would be expected to have similar drag relationships. However, the turboprop nacelle, as defined and analyzed herein, includes all surfaces and fairings exclusive of the wing. Thus, it is not the clean, relatively axisymmetric, design of conventional long duct nacelles. It is expected that the pressure drag may be closer to the 15 to 20 percent range of the separate flow nacelles. For this reason, it was assumed that the pressure drag would be 17.5 percent of the friction drag. As with the basic nacelle/installation design, this drag level would require substantiation/verification in a wind tunnel test.

4.7.10 Mounting and Vibration Isolation

The figures referenced and shown in Section 4.7.2 that depict the nacelle concepts designed for this study included only cursory considerations of engine and gearbox mounting and dynamic suspension. The engine alone - approximately 1500 lb in weight and with an 8000 RPM output driveshaft - presents no significant problem unless it becomes part of the system of dynamics which include the gearbox and the propfan. As is well understood, the T56, T64 and CT-7 type turboprop offset-drive installations directly couple the engine and gearbox in a mechanical manner which combines the two major elements into a single entity from the point of view of propulsion system mounting and dynamic suspension.

It is by no means clear that the up-scale from the current 4-5000 SHP systems to the 12,500 SHP of the APET engine is best addressed by designs that are similar to these historical examples, and the APET nacelles shown assume that the engine and gearbox are separately mounted from the dynamic viewpoint. This change is somewhat radical and would have to be justified in further study efforts because it introduces the problem that the engine driveshaft must use couplings which have degrees of flexibility at both the engine and gearbox drive interfaces.

Follow-on APET studies already planned will address this problem area and hopefully provide some design ideas and guidance for the future, high horsepower, turboprop installations. For the current APET studies, the baseline offset gearbox has been examined in conjunction with the Lord Manufacturing Co. of Erie, Pa. Figure 4.7-33 shows one approach to the dynamic suspension of the gearbox and propfan that has resulted from a preliminary design discussion.

All gearbox torque loads are reacted by the links shown that terminate in Points A and B. Loads at these two points, due to torque reaction only, are transmitted directly to the nacelle structure. Anti-vibration mounting material can be included in a sandwich which forms part of the pedestal type support brackets that enclose the large, laterally disposed, torque tube. Additional elastomer may also be introduced at the end fittings that join the offset levers to the torque tube.

Thus, the additional mount points identified as C, D, E and F play no part in reacting torque and may be optimized for the isolation of thrust, vertical and side loads, or combinations thereof. This system also has excellent redundancy for safety aspects that would be considered in any final design - such as whirl/flutter phenomena and analyses.

4.7.11 Maintainability and Accessibility

The nacelle designed for the baseline engine with offset gearbox has already been illustrated (see Figure 4.7-4). The concept for maintainability/accessibility is discussed below:

The engine and gearbox are located and mounted within the nacelle as separate entities and are coupled to each other by a drive shaft that uses

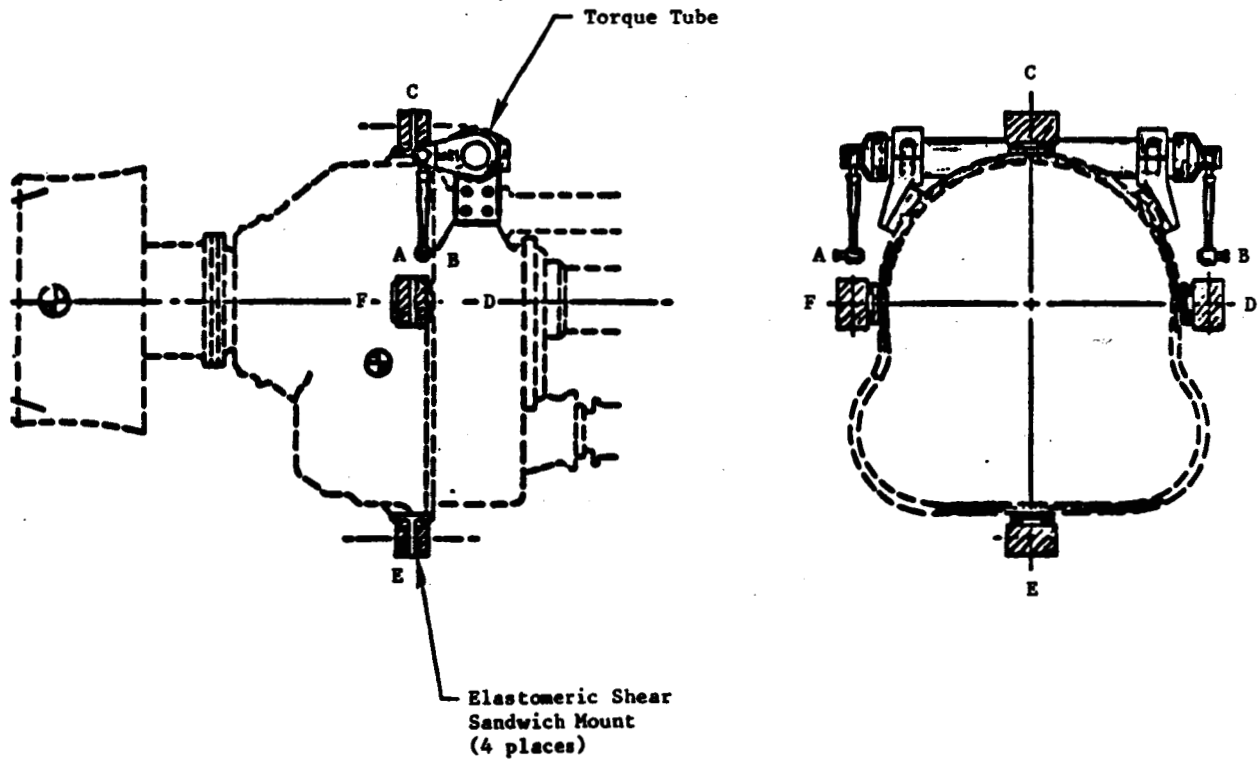


Figure 4.7-33. Anti-Vibration Mount Concept for APET Turboprop Gearbox.

flexible couplings at each end. Both these couplings use flange joints that permit removal of the driveshaft proper without requiring any axial displacement of the engine or the gearbox. Access to these joints is via the large lower cowling doors and via the special access doors in each side of the nacelle opposite the rear face of the propfan gearbox.

In this manner, the engine and gearbox installation or removal can be effected without disturbance to each other. The engine is three-point supported by the nacelle mountings provided and is installed/removed by pure vertical motion. The gearbox is four-point supported by the nacelle mountings provided and is installed/removed by pure axial motion. The PCM and the propfan controls are modular and may be installed or removed without disturbing other components or assemblies.

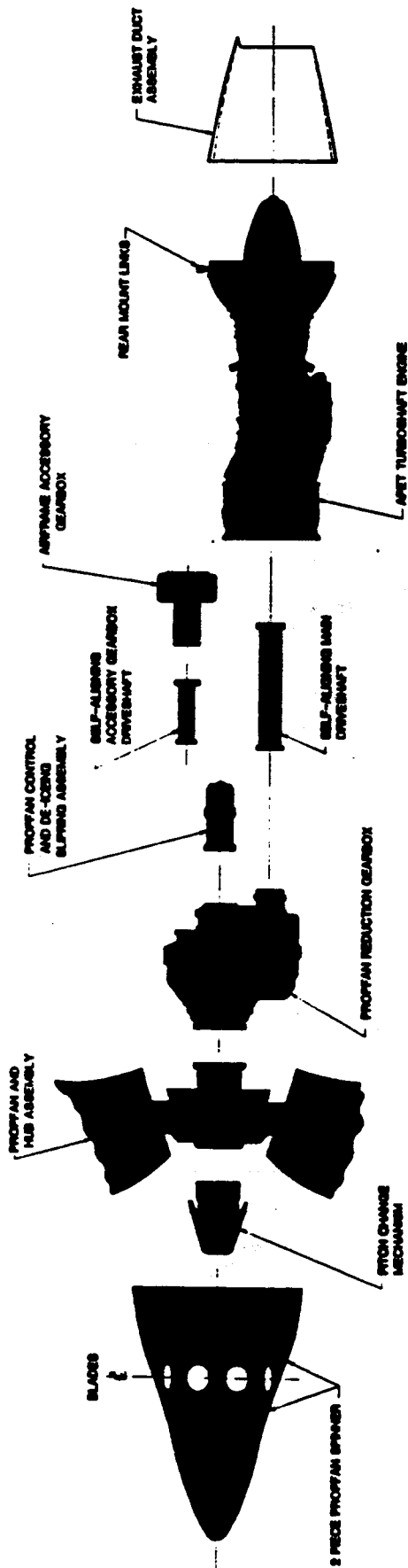
The engine inlet is shown as part of a removable assembly, as is the engine exhaust duct. Both these assemblies would be removed from the nacelle prior to engine removal and would be reinstalled after the engine has been locked to the nacelle mounts. Access provisions have been located so that installation or removal is in a straight forward manner. "Exploded" views of the three nacelles designed for the APET studies are included as Figures 4.7-34, -35, and -36. These sketches are believed to be self-explanatory in showing the principal features that have been designed to assure adequate maintainability.

4.7.12 Systems and Controls

The development of the design concepts shown into a detail consideration of the engine installation might possibly be of value if further APET studies are warranted. This is particularly true of the FADEC system and the heat exchanger installation. The FADEC system is recommended in the Development Plan in Section 4.12 as a key technology item and is the subject of its own development and cost plan. All the other systems are deemed to be straightforward and within current design and hardware experience.

4.7.13 Fire Safety

Isolation of zones within the nacelles has been indicated on the nacelle studies made. The high-speed turboprop installation does not appear to have



ORIGINAL PAGE IS
OF POOR QUALITY

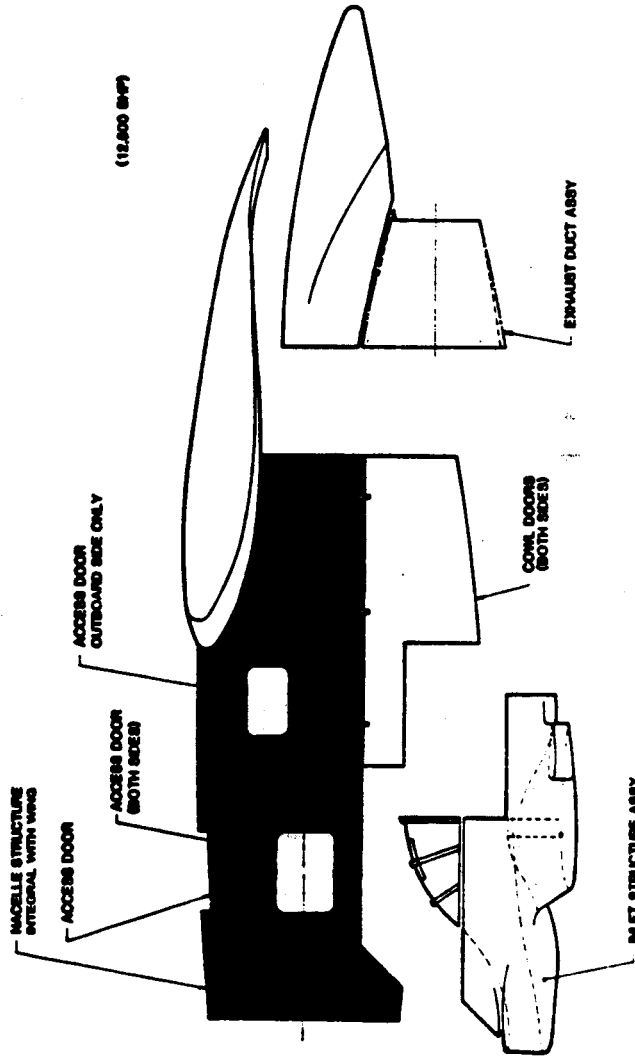


Figure 4.7-34. APET Baseline Nacelle-Principal Features
Axi-Axi Engine, Offset Gearbox
Underwing Layout.

ORIGINAL PAGE IS
OF POOR QUALITY

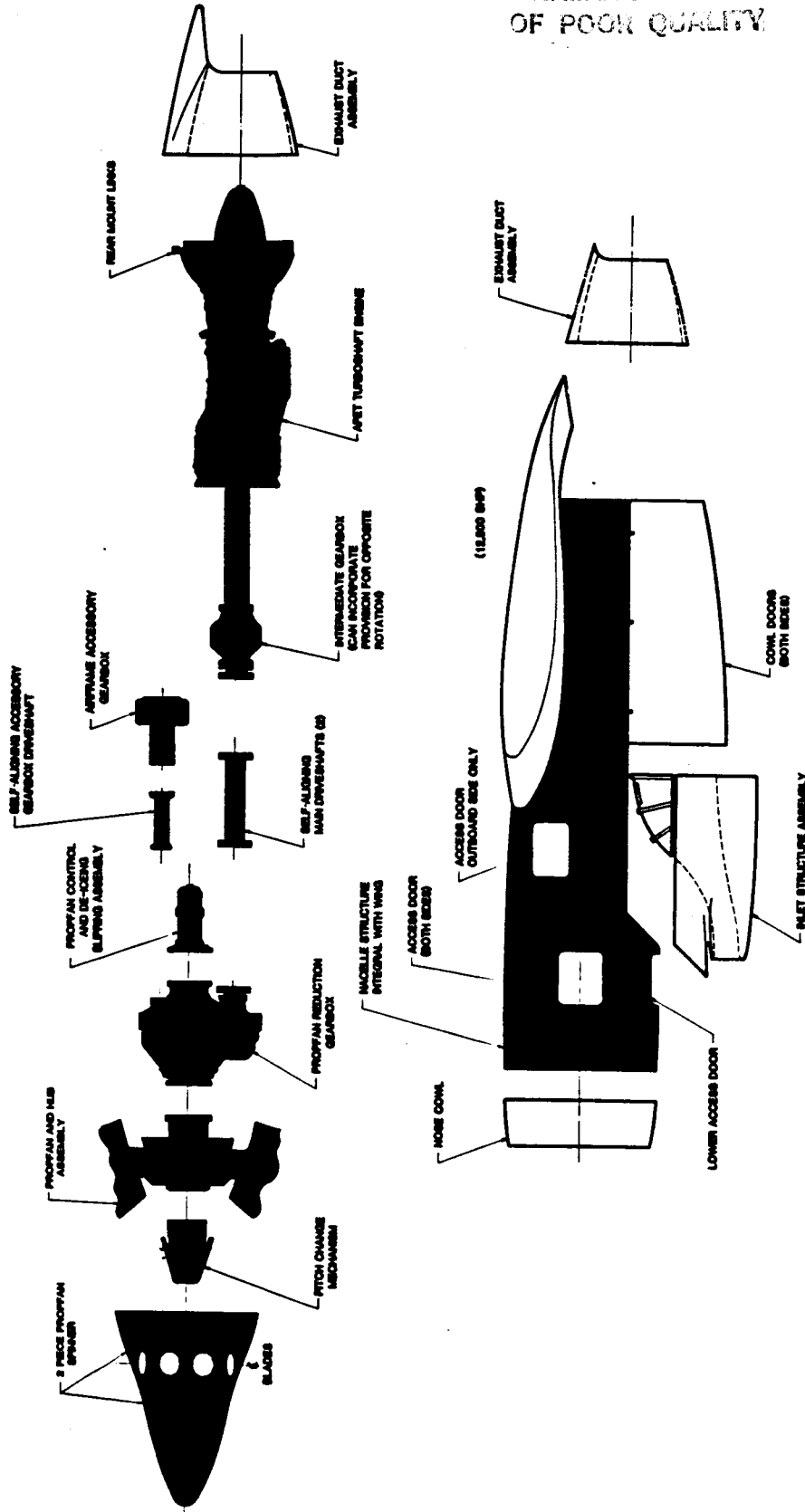


Figure 4.7-35. APET Study Alternate Nacelle Principal Features. Axi-Axi Engine with Split Gearbox and Offset Propeller.

ORIGINAL PAGE IS
OF POOR QUALITY

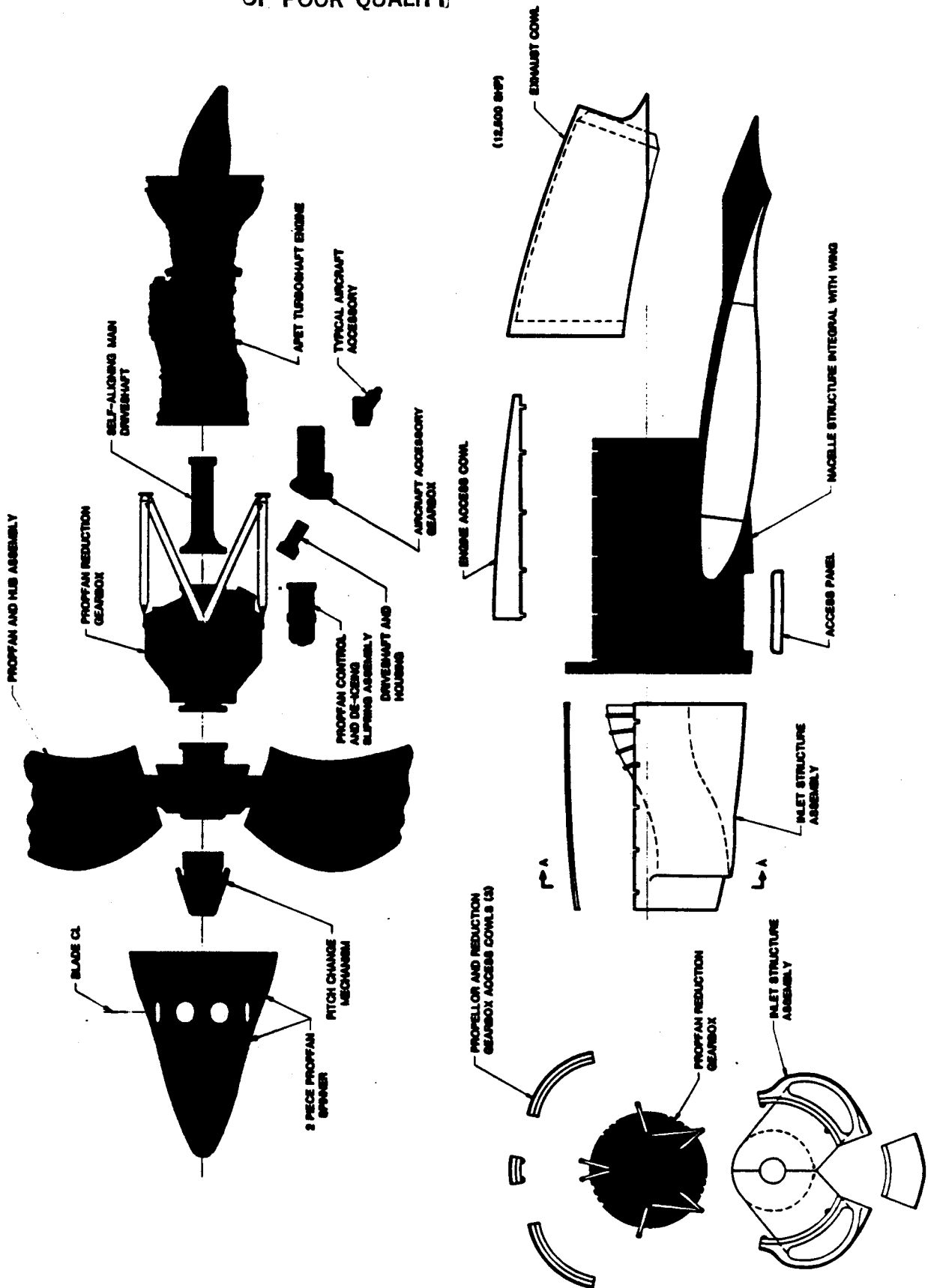


Figure 4.7-36. APET Alternate Nacelle Principal Features. Axi-Axi Engine with Concentric Gearbox.

SECT A-A

any unusual requirements for fire safety except with regard to the care taken to protect the engine and propeller control means from degradation or destruction by internal nacelle fires. Obviously, these areas will require careful attention in any final design effort. Fire extinguishing and nacelle ventilation will be more demanding than the low-speed turboprop because of the low-drag nature of the nacelle aerodynamic design and the desire to keep external flow excrescences to a minimum.

4.7.14 Performance Comparisons - Turbofan Versus Turboprop

4.7.14.1 Installation Models

Simplified installation models for both the turbofan and turboprop aircraft were used in this study. Simplification was achieved by eliminating drag items that are difficult to assess or that are controversial. Restricting the installation models to "basic" drags yields a clear picture of the fundamental differences between the two propulsive systems although admittedly, some of the omitted drags may have significant consequences. However to make arbitrary estimates at this point in time would cloud the picture to the point that more harm than good may result.

Items included in the installed performance drag bookkeeping are:

- Nacelle Scrubbing
- Nacelle Pressure Drag
- Δ Wing Scrubbing Due to Δ Mach No.
- Gearbox Heat Exchanger
- Boundary Layer Diverter and Nacelle Purge System

Items acknowledged but omitted are:

- Swirl Angle of Attack Induced Δ Lift, Δ Drag
- Swirl Recovery
- Compressibility Effects
- Nacelle/Wing/Propwash Interaction

The applicability of the various included drag items to the two propulsive systems is shown in Figure 4.7-37.

	Turbofan	Turboprop
Nacelle Friction Drag	X	X
Nacelle Pressure Drag	X	X
Ram Recovery	X	1
Spillage	X	+
Prop/Gearbox Losses	-	X
Boundary Layer Diverter and Purge System	-	X

1	}	<ul style="list-style-type: none"> • Constant 1-1/2% Inlet ΔP Subtracted From Prop Hub ΔP Rise • Prop Hub ΔP and ΔT Rise Included in Cycle Bookkeeping + Included in Nacelle Drag
---	---	---

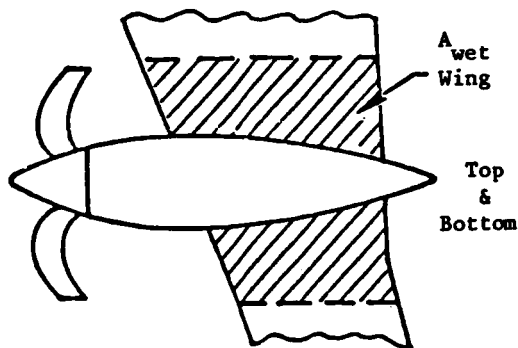
Figure 4.7-37. APET Installation Loss Bookkeeping.

Design details for the nacelle and inlet along with a description of drag calculation have already been shown in this Section. A brief description of the bookkeeping system and a summary of results are presented here.

The wing and nacelle scrubbing model is shown in Figure 4.7-38. The wing area, less the nacelle footprint, scrubbed by the prop wash is charged with drag resulting from the change in Mach number through the prop (ΔM). The nacelle itself is charged with drag resulting from the full prop discharge Mach number ($M_0 + \Delta M$). The nacelle pressure drag is considered to be 15-20% of the nacelle friction drag.

The heat exchanger loss, Figure 4.7-39. can be put into two categories; ducting and external losses and heat exchanger core loss. The ducting and external loss estimation procedure are fairly straight forward. The heat exchanger core is more complex; it operates as a pressure loss generator and provides heat addition to the flow. The pressure loss and temperature rise across the core are important to determining the heat exchanger internal drag.

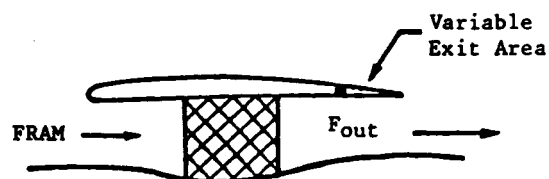
• Prop Wash Drag



1. Nacelle Friction Drag From Δ Mach Across Prop (~+.04 Mach @ MO. 80)
2. Wing Friction from Prop Δ M

Figure 4.7-38. APET Propeller Gearbox Related Drag Accounting - Prop Wash Drag.

• Gearbox Heat Exchanger



- Core Loss Levels Supplied by Hughes-Treitler Mfg. Corporation.
- GE Estimates of Inlet, Exhaust and External Losses
- Baseline Design is Nacelle Mounted
- Alternate Design is Mounted in Wing Glove

$$\text{Drag} = F_{\text{Out}} - F_{\text{Ram}} - F_{\text{External}}$$

Figure 4.7-39. APET Propeller Gearbox Related Drag Accounting - Gearbox Heat Exchanger.

General Electric contacted a heat exchanger manufacturer, Hughes-Treitler Manufacturing Corporation, who provided a preliminary heat exchanger design based on the APET turboprop specification. The critical heat exchanger data supplied by Hughes-Treitler is given in Figure 4.7-40. A boundary layer diverter and purge system loss is associated with a turboprop and not with a turbofan. The boundary layer diverter loss was analyzed but the purge system loss was estimated.

A typical loss breakdown for an end of climb flight condition is shown in Figure 4.7-41. Climb path loss levels are shown in Figure 4.7-42. The impact of cruise speed and part power on installation loss level is shown in Figure 4.7-43.

Data Supplied by Hughes-Treitler Mfg. Corporation

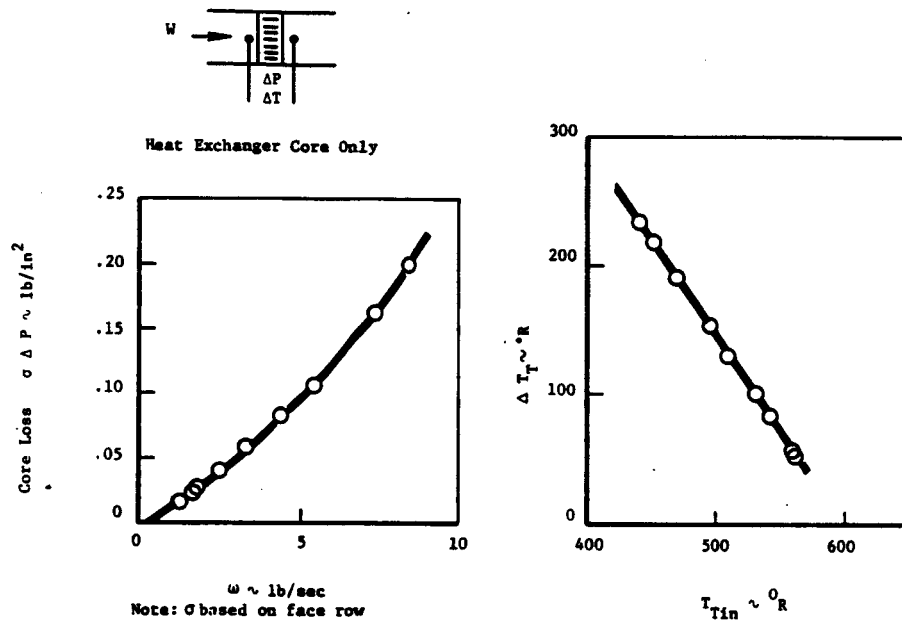


Figure 4.7-40. APET Heat Exchanger Core.

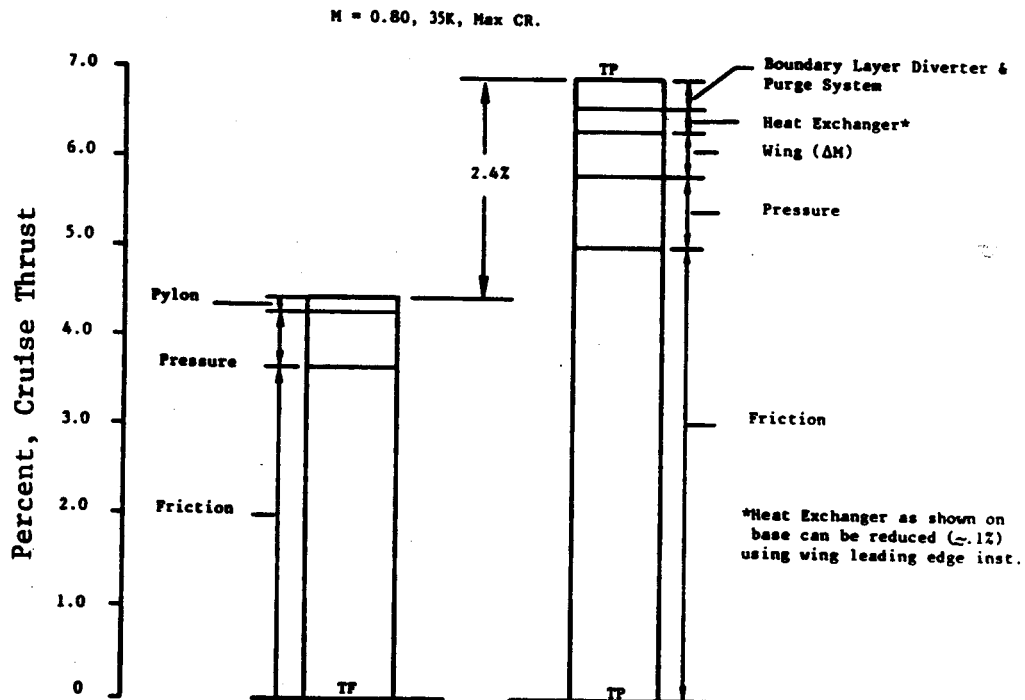


Figure 4.7-41. APET Turbofan & Turboprop Installation Loss Bookkeeping.

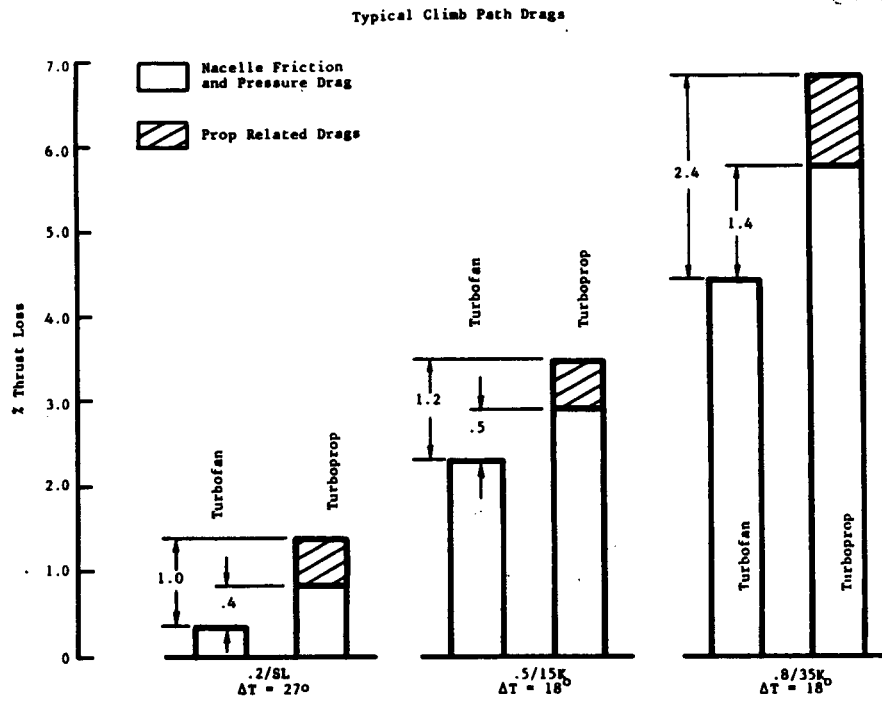


Figure 4.7-42. APET Turbofan and Turboprop Installation Loss Comparisons.

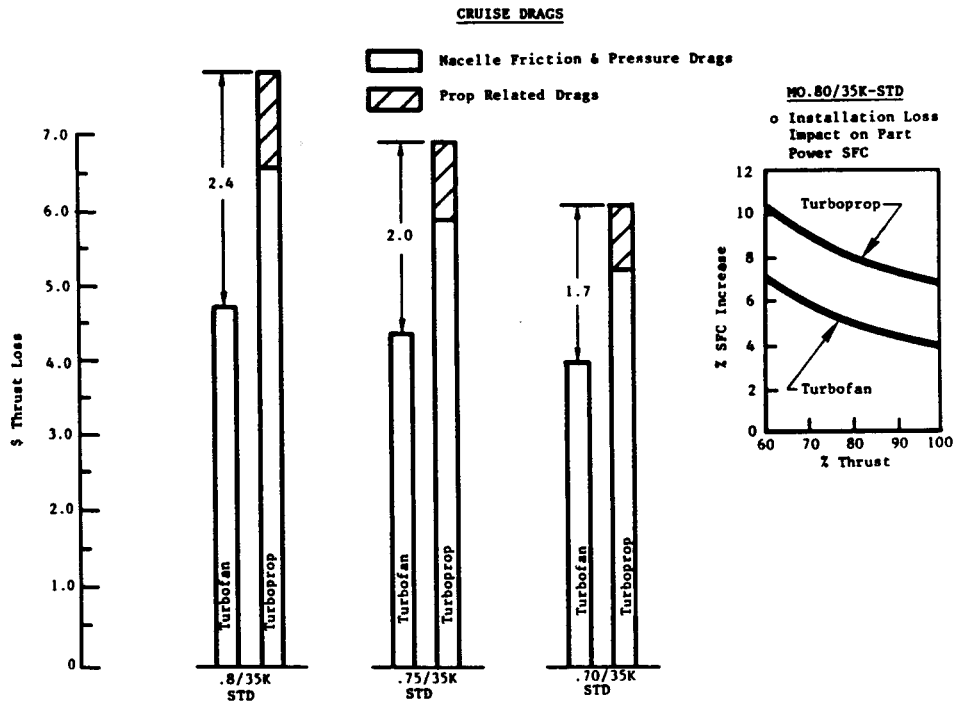


Figure 4.7-43. APET Turbofan and Turboprop Installation Loss Comparisons.

SECTION 4.8
MISSION ANALYSES

<u>Section</u>		<u>Page</u>
4.8.1	Scope	283
4.8.2	Measures of Merit	284
4.8.3	Fuel Price Forecast	284
4.8.4	DOC Method	285
4.8.5	Fuel Burn Analysis Results - Ranking Missions	286
4.8.6	Fuel Burn Analysis Results - Alternate Studies	288
4.8.7	Mission Analysis - Sensitivities	291
4.8.8	Mission Analysis - DOC Results	293

FIGURES

<u>Figure</u>		<u>Page</u>
4.8-1.	APET Optimized Airplanes - 100% Load Factor.	287
4.8-2.	APET Optimized Airplanes - 65% Load Factor.	287
4.8-3.	APET Installed Performance Comparisons - Baseline TF vs. Baseline TP.	289
4.8-4.	APET Installed Performance Comparisons - Baseline TF vs. Baseline TP - Climb SFC's.	290
4.8-5.	APET Mission Fuel Usage.	290
4.8-6.	APET Results Fuel Burn vs. Technology vs. MCR vs. Range, 65% L.F.	292
4.8-7.	APET Economic Results - Baseline Cases.	297
4.8-8.	APET DOC Comparisons - Propfan vs. Turbofan.	298

SECTION 4.8
MISSION ANALYSES

TABLES

<u>Table</u>		<u>Page</u>
4.8-1.	APET Turbofan/Turboprop Mission Assessment.	289
4.8-2.	Technology Study - Turbofan Civil Transport Study - 150 PAX.	292
4.8-3.	APET Mission Sensitivities.	293
4.8-4.	APET DOC Results - APET Baseline Cases Propulsion Prices Equal.	294
4.8-5.	APET Baseline Turboprop Mach 0.8 Design Price of Fuel \$1.50.	295
4.8-6.	APET Baseline Turbofan Mach 0.8 Design Price of Fuel \$1.50.	296
4.8-7.	APET Baseline Turbofan Mach 0.8 Design Supplemental Breakdown.	297

4.8 MISSION ANALYSES

4.8.1 Scope

As indicated earlier in Section 4.2.4, mission analyses covered both turbofan and turboprop powered airplanes at the three cruise design Mach numbers of 0.70, 0.75 and 0.80. Each airplane (six in all) was a point design for its selected cruise Mach number. The analyses were performed on a computer using a General Electric mission analysis program which (for this study) was limited to estimates of fuel burn and flight time expended in the following flight modes:

- Takeoff (fuel allowance only)
- Constant altitude acceleration
- Constant Mach number climb
- Constant altitude and Mach number cruise
- Constant Mach number climb to optimum Breguet cruise altitude.
- Constant altitude and Mach number cruise after discontinuous change in altitude and Mach number
- Breguet cruise
- Decelerated descent along a specified path
- Constant Mach number descent
- Maneuver mode (used for reserves).

The nondimensional aircraft drag characteristics (drag polar) and weight were inputted to the program. A matrix of engine performance data (net thrust as a function of altitude and Mach number) was run on the cycle deck and placed in a file. This file was then read by the mission program.

The mission program "flew" a "rubber" airplane. That is, aircraft weight, engine weight and engine thrust were adjusted (scaled) to match the mission requirements. The output of the mission program (aircraft weight, fuel burn) reflect the complex interaction of engine thrust - SFC characteristics and aircraft design. Wing loading and thrust loading were systematically varied.

The computer program was also capable of determining the effects of small changes and, hence, could be used to obtain sensitivity factors.

Airplane weight estimating procedures have already been discussed in Section 4.2.5 and will not be repeated here. However, it should be noted that the sensitivity studies included the effects of both propulsion and aircraft structure weight assumptions, and these are later reported in the Section devoted to "Sensitivities".

Operating costs, as described in Section 4.1.3, used the ATA method, with Boeing modifications, updated to the 1981 economy. Aircraft and propulsion prices used in-house methodology, while fuel price was subject to prior agreement with NASA and was set at $\$1.50 \pm 0.050$ per gallon.

Acoustic and emission analyses of selected mission sized airplanes were also made and are reported later in this section.

4.8.2 Measures of Merit

Three measures of merit were considered; fuel burn, available seat miles per gallon (ASM/GAL) and direct operating cost (DOC). Fuel burn is the most direct measure of efficiency; it depends solely on the technical accuracy of the aircraft performance, aircraft weight and engine performance. ASM/GAL is as direct a measure as fuel burn but has some of the advantages of a nondimensional parameter in that it can be used for direct comparison of advanced technology and current technology aircraft/engine systems. The DOC measure of merit is the most all encompassing index, and the one most important to operators. The DOC, however, is the most difficult of the three measures to assess accurately. The very element that makes the DOC valuable, incorporation of economic factors, also increases the uncertainty of its value.

4.8.3 Fuel Price Forecast

The Statement of Work (SOW) for this study called for the Contractor to estimate the future expected price of fuel and then conduct Direct Operating Cost (DOC) analyses with these values of fuel price. In the past prior to 1973, the price of aviation fuel was both low and predictable.

Currently, the pricing of fuel is in a state of flux; and predictions of future fuel price vary considerably from one source to another. The future cost of the fuel relative to costs of other goods and services is an important parameter in comparing the economics of different airframe/engine systems as fuel cost is the dominant items amongst the nine that collectively make up the DOC of an airplane. Of these nine DOC elements, two are independent of inflationary pressures, i.e., utilization and block distance. Six of the remaining items (airframe and engine purchase price, spares, depreciation, insurance, maintenance and crew costs) were all subject to similar economic forces and inflationary pressures. Fuel prices, however, because fuel is a depletable resource item, is subject to different economic pressures and also is sensitive to political conditions.

4.8.4 DOC Method

As part of the economic assessment of the aircraft, unit airplane fly-away prices have been estimated by dividing the airplane into two basic categories - (1) Airframe, including avionics, and (2) Propulsion. Estimating relationships were devised to allow for the variation of airframe price with variations in airplane size. These relationships were primarily based on the data contained in the following two reports:

- NASA CR-151970 "Parametric Study of Transport Systems.....Weight" -- Report by "Science Applications, Inc.," Published in April 1977. (Reference 33)
- Society of Allied Weight Engineers Paper 1416 "Price-Weight Relationships of General Aviation, Helicopters, Transport Aircraft and Engines" dated May 1981, by Joseph L. Anderson. (Reference 25)

In addition to the above, General Electric used Hamilton-Standard data for estimating propfan and controls price and maintenance costs and used in-house programs for estimating engine, gearbox, and nacelle structure and system costs to achieve total propulsion system costs:

Three DOC methods have been evaluated in detail. They are:

- EURAC method (Reference 31).
- ATA method as modified by Boeing and updated to 1981 (Reference 32).
- NASA method (Reference 30).

Currently, the pricing of fuel is in a state of flux; and predictions of future fuel price vary considerably from one source to another. The future cost of the fuel relative to costs of other goods and services is an important parameter in comparing the economics of different airframe/engine systems as fuel cost is the dominant items amongst the nine that collectively make up the DOC of an airplane. Of these nine DOC elements, two are independent of inflationary pressures, i.e., utilization and block distance. Six of the remaining items (airframe and engine purchase price, spares, depreciation, insurance, maintenance and crew costs) were all subject to similar economic forces and inflationary pressures. Fuel prices, however, because fuel is a depletable resource item, is subject to different economic pressures and also is sensitive to political conditions.

4.8.4 DOC Method

As part of the economic assessment of the aircraft, unit airplane fly-away prices have been estimated by dividing the airplane into two basic categories - (1) Airframe, including avionics, and (2) Propulsion. Estimating relationships were devised to allow for the variation of airframe price with variations in airplane size. These relationships were primarily based on the data contained in the following two reports:

- NASA CR-151970 "Parametric Study of Transport Systems....Weight" -- Report by "Science Applications, Inc.," Published in April 1977. (Reference 33)
- Society of Allied Weight Engineers Paper 1416 "Price-Weight Relationships of General Aviation, Helicopters, Transport Aircraft and Engines" dated May 1981, by Joseph L. Anderson. (Reference 25)

In addition to the above, General Electric used Hamilton-Standard data for estimating propfan and controls price and maintenance costs and used in-house programs for estimating engine, gearbox, and nacelle structure and system costs to achieve total propulsion system costs:

Three DOC methods have been evaluated in detail. They are:

- EURAC method (Reference 31).
- ATA method as modified by Boeing and updated to 1981 (Reference 32).
- NASA method (Reference 30).

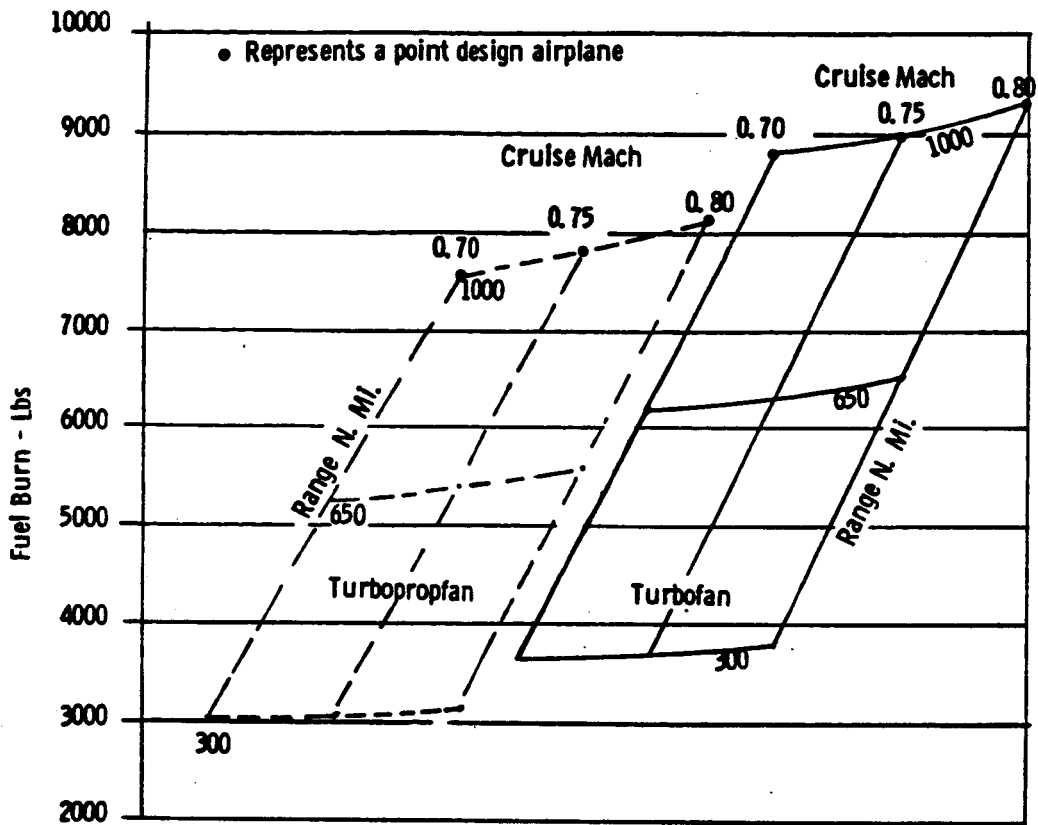


Figure 4.8-1. APET Optimized Airplanes 100% Load Factor.

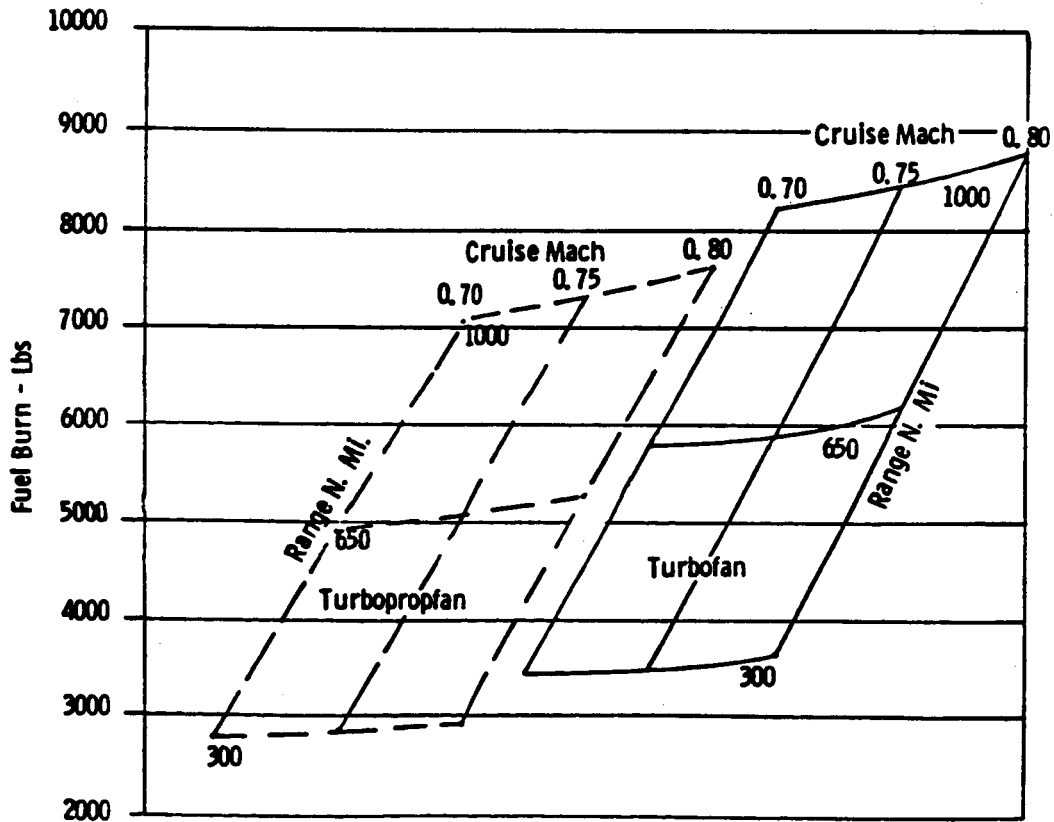


Figure 4.8-2. APET Optimized Airplanes 65% Load Factor.

In terms of the installed performance turbofan versus turboprop mission assessment results are listed in Table 4.8-1. At the "ranking" mission range of 300 N. Mi. the curve of fuel burn versus Mach number is very flat, as the fuel burn value changes only a small amount for the variation between Mach 0.70 and Mach 0.80. (170 pounds difference at 300 N. Mi. for the turbofan, and 130 pounds for the turboprop). These values of about one pound of fuel per passenger over the "ranking" mission are really insignificant and indicate quite clearly that the selected cruise speed for some future high speed turbofan (or turboprop) short-haul airplane will be driven by other factors than just the fuel burn values calculated here. Nevertheless, the difference in fuel burn between the turbofan and turboprop, irrespective of the selected cruise Mach number, is around 18 percent. This value may seem lower than those reported in other propulsion studies, but is believed to be quite accurate for the APET airplanes analyzed. Part of the reason may be that the APET turboprop airplane is charged (at cruise speed) with 2.4 percent more installation loss than the turbofan. Other differences may lie in the very high performance of the advanced design, E³ type, turbofan engine installed in a mixed flow nacelle. The similarity of all the airplanes studied and the weights that have been used, practically preclude anything but propulsive efficiency providing the delta fuel burns. The installed SFC of the three different Mach number airplane designs is shown in Figure 4.8-3, which directly compares the turbofan versus turboprop at their correct cruise thrust size values for the point design airplanes on a standard day. The bucket SFC's are shown for each Mach number and these percent values are less than the percent values calculated for the mission fuel burn. The reason for this is the large advantage of the turboprop during the climbout to cruise altitude. This comparison is shown on Figure 4.8-4 (for a non-standard day) while Figure 4.8-5 compares (for two Mach numbers) the mission fuel usage of turbofan versus turboprop at 1000 N. Mi. and 300 N. Mi. From here it can be seen that the climb fuel dominates the bar chart for the shorter range flights.

4.8.6 Fuel Burn Analyses Results - Alternate Studies

During the course of the APET studies, some questions were raised by NASA and the USAF Propulsion Laboratory relative to an evaluation of some alternate configurations and design parameters. The objective of these inquiries was

Table 4.8-1. APET Turbofan/Turboprop Mission Assessment.

- 1000 NM Design Range
- 300 NM Ranking Mission

	0.80/35000		0.75/35000		0.70/35000	
	Reference TF	Base TP	Reference TF	Base TP	Reference TF	Base TP
TOGW	111970	110990	109310	108850	108040	107310
OEW	64390	65490	62480	64080	61690	63100
W $\bar{0}$ /6 Fan or Booster	721	63.3	679	61.1	657	59.6
W $\bar{0}$ /6 Core	56.1	40.0	52.8	38.7	51.1	37.7
Fan Diameter	4.9'	---	4.8'	---	4.7'	---
Prop Diameter	---	12.5'	---	12.3'	---	12.1'
FNIN @ 0.2/SL / 27°	13940	14870	13120	14370	12690	14000
Fuel Burned						
Design Mission	9270 lb	-12.7%	8950 lb	-13.2%	8775 lb	-14.3%
Ranking Mission	3780 lb	-18.3%	3460 lb	-17.4%	3410 lb	-18.0%

(η_{Ram} , Customer HPX, Macelle Drags, Prop Wash, Heat Exchanger)

- Engines Sized for 150 PAX APET A/C, Mo. 80/35000' Cruise
- VTip Prop = 800 FPS, SHP/D² = 37.5 @ 0.8/35K

Mixed Flow TF

BPR = 7.1
PRQA = 40.2
Fan Dia = 4.9'

Boosted TP

PRQA = 40.2
Dia Prop = 12.5'

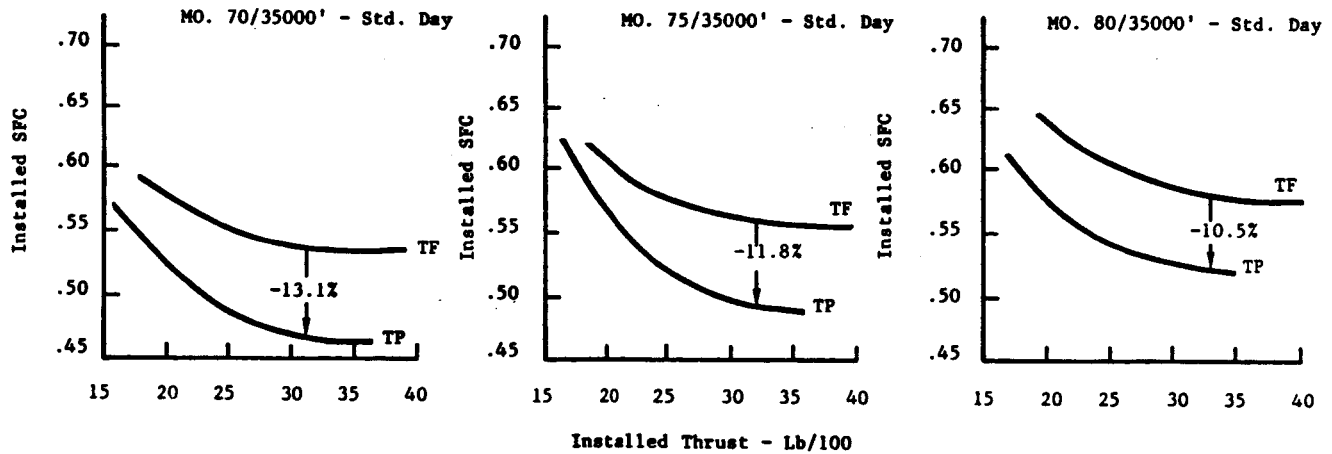


Figure 4.8-3. APET Installed Performance Comparisons Baseline TF Versus Baseline TP.

(η_{Ram} , Customer HPX, Nacelle Drags, Prop Wash, Heat Exchanger)

(Equal End of Climb Thrust)
Mixed Flow TF

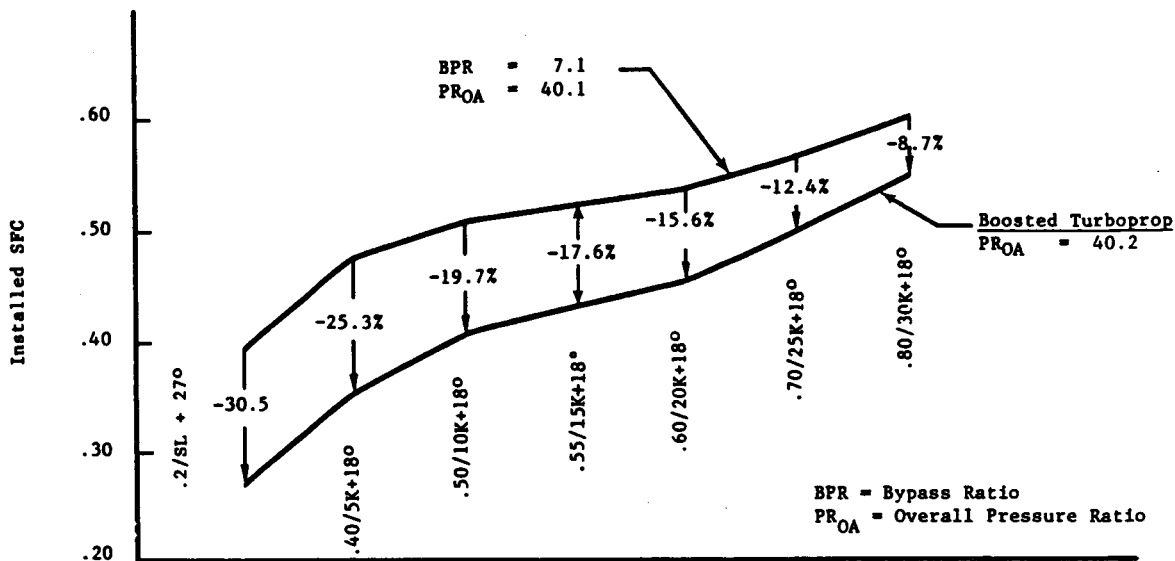


Figure 4.8-4. APET Installed Performance Comparisons
Baseline TF vs. Baseline TP Climb SFC's.

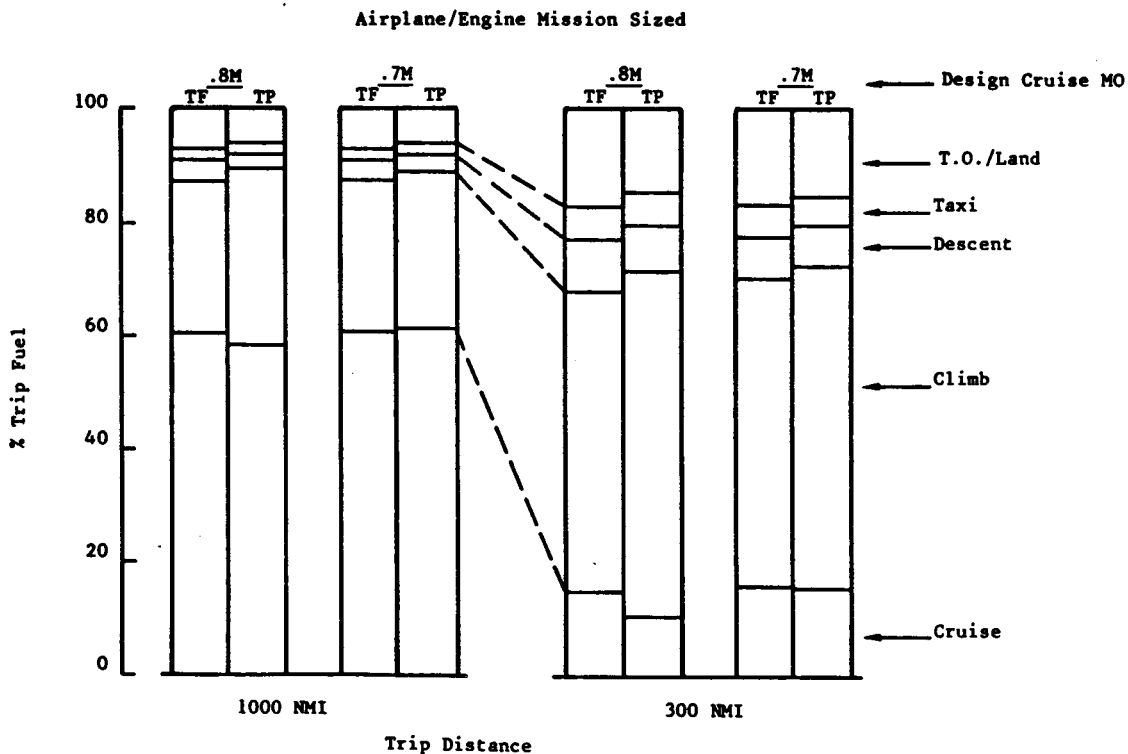


Figure 4.8-5. APET Mission Fuel Usage.

to quantify the value, or level, of improved performance that is attributable to each of the assumptions made for the definitive APET airplane and its selected turboprop propulsion system.

Consequently, efforts were made to modify the mission analysis computer program with revisions to the input assumptions. The NASA contract required that the APET turboprop performance be evaluated in the Mach Cruise Range of 0.70 to 0.80, at cruise altitudes that are typical for the current generation of turbofan powered airplanes. Therefore, changes were made towards defining what the differences might be between an airplane designed for service circa 1972 versus one designed for service in 1992. These differences are summarized below:

- The maximum payload range point would be fixed at 2000 N. Mi. (versus the APET limit of 1000 N. Mi.).
- The weight of the airplane would use 1972 level of technology (versus the APET 1992 level).
- The turbofan propulsion system weight and specific fuel consumption would be related to CF6-50 technology (versus the APET E³ + technology).
- The wing would be non-supercritical in airfoil section and would be designed for an aspect ratio of 9 (nine) (versus the APET supercritical assumption with an aspect ratio of 11).
- Finally, the quantitative value of the E³ fan as a propulsor would be changed (APET uses the H-S prop fan). These levels, or steps, were evaluated one at a time, but not necessarily in the order presented above.

Table 4.8-2 shows in terms of both reduction of Takeoff Gross Weight (TOGW) and fuel burn the benefits which accrue due to the performance improvements postulated for the turbofan powered APET airplane. These results are also depicted on Figure 4.8-6 which graphically portrays the data of Figure 4.8-2 with the steps enumerated above, and which also includes the benefits due to the propfan.

4.8.7 Mission Analyses - Sensitivities

The conventional parameters of SFC for various mission segments, weights and drags were varied to determine the resultant airplane sensitivity at

ORIGINAL DESIGN
OF POOR QUALITY

Table 4.8-2. Technology Study - Turbofan Civil Transport Study - 150 PAX.

• Effects of Varying Technology Assumptions

Code	Engine Technology	Airframe Aero	Airframe Weight	Design Range	TOGW	Percent Reduction in TOGW	Fuel Burn 1000 NMI, 65% LF	Percent Reduction in Fuel Burn	Fuel Burn 300 NMI, 65% LF	Percent Reduction in Fuel Burn
	CF6	AR = 9	1972	2000	155606*		12949*		5335*	
	"APET"	AR = 9	1972	2000	143583	>7.7	10613	>18.0	4361	>18.2
	"APET"	AR = 11	1972	2000	140860	>1.8	10131	>3.7	4222	> 2.6
	"APET"	AR = 11	1995	2000	125823	>9.6	9212	>7.1	3818	> 7.6
	"APET"	AR = 11	1995	1000	112000	>8.9	8749	>3.6	3759	> 3.4

*Baseline Values for Percentage Calculations

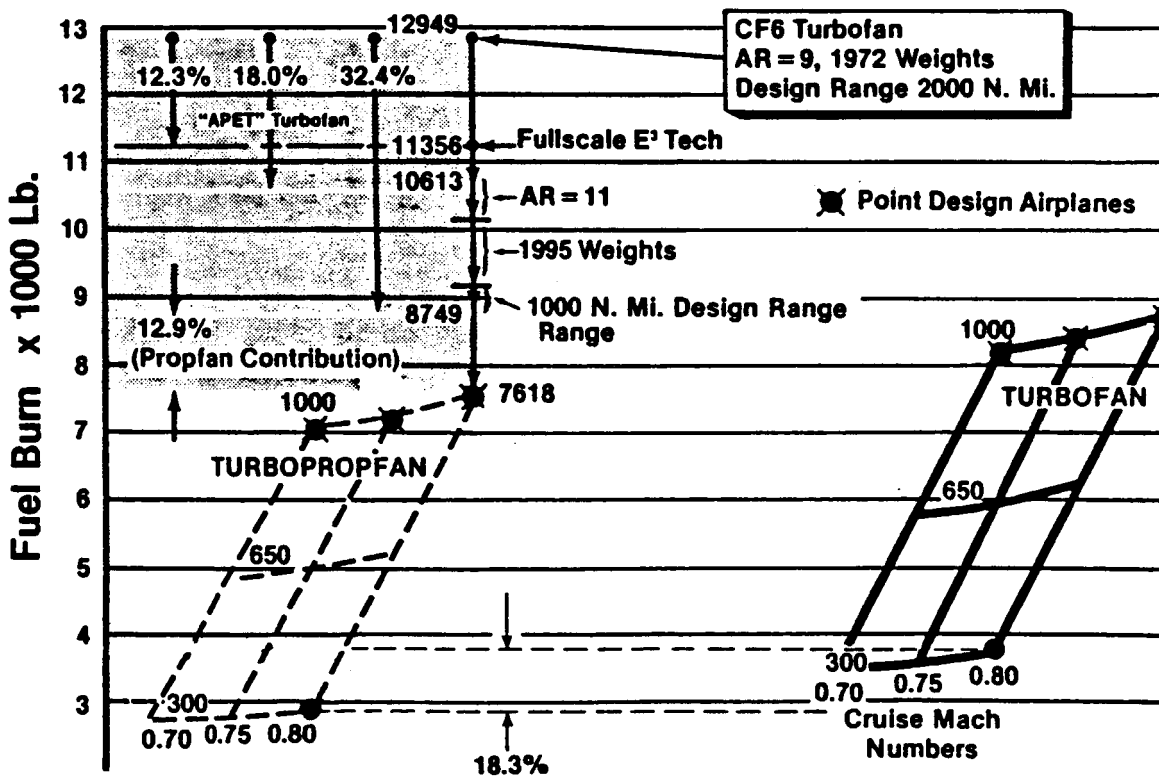


Figure 4.8-6. APET Results Fuel Burn Versus Technology Versus MCR Versus Range, 65% L.F.

both the 1000 N. Mi. design range, and the 300 N. Mi. "ranking" range. These results are shown (for the Mach 0.80 turboprop) in Table 4.8-3.

Overall SFC is clearly the most sensitive parameter, followed by aircraft structural weight and drag (C_{D0}). These sensitivity results are generally in accord with values shown on other contractor studies in the literature and are therefore believed to reasonably represent the APET airplanes.

Table 4.8-3. APET Mission Sensitivities.

0.8M - Design Turboprop

Parameter		% Δ Fuel Burned	
		Design Range	300 NMI
SFC Cruise	+1%	+0.66	+0.18
	-1%	-0.65	-0.18
SFC Climb	+1%	+0.33	+0.64
	-1%	-0.33	-0.64
SFC Descent	+1%	+0.03	+0.08
	-1%	-0.03	-0.08
SFC Overall	+1%	+1.14	+1.03
	-1%	-1.12	-1.01
Propulsion Weight	+1%	+0.10	+0.11
	-1%	-0.09	-0.11
A/C Drag (C_{D0})	+1%	+0.60	+0.53
	-1%	-0.58	-0.51
A/C Structure Weight	+1%	+0.62	+0.69
	-1%	-0.60	-0.67

4.8.8 Mission Analyses - DOC Results

Table 3.1-1 given in the "Program Overview" Section has already listed the DOC parameters that were selected for APET analyses. Using these data as input to the computer programs, DOC values were obtained at the ranking mission for all six APET airplanes, with three different values for fuel price. These results are shown on Table 4.8-4.

Table 4.8-4. APET DOC Results - APET Baseline Cases Propulsion Prices Equal.

DOC in \$'s/Passenger/Statute Mile

Propulsion Type	Turboprop			Turbofan			
	Design Mach No.	0.7	0.75	0.8	0.7	0.75	0.8
DOC (Fuel @ \$1.00/Gal)		0.0311	0.0314	0.0320	0.0334	0.0336	0.0344
DOC (Fuel @ \$1.50/Gal)		0.0352	0.0355	0.0362	0.0383	0.0386	0.0395
DOC (Fuel @ \$2.00/Gal)		0.0392	0.0396	0.0404	0.0432	0.0435	0.0447

The DOC's in this table are as calculated using the ATA method, modified by Boeing and are in 1981 dollars. Table 4.8-5 gives a sample of the computer printout.

A supplemental breakdown, directly applicable to the flight case analyzed and reported in Table 4.8-6, is given in Table 4.8-7.

A plot of the DOC results for the point design airplanes flying at their design Mach number at the Figure of Merit range of 300 nmi is shown in Figure 4.8-7. Additional data on this figure shows the effect of the point design Mach 0.80 turbofan and turboprop airplanes flying at the reduced cruise speed of Mach 0.70. Also, the effect of reducing cruise altitude from 35 thousand feet to 30 thousand feet is also noted.

Figure 4.8-8 depicts the rate of change in DOC as variable fuel cost assumptions and variable engine price assumptions are made for turbofan and turboprop airplanes. At the relative total price of turbofan versus turboprop airplane equal to unity, and with the price of fuel pegged at 1.50 dollars per gallon, the turboprop airplane has a favorable relative DOC of just over eight percent.

Table 4.8-5. APET Baseline Turboprop Mach 0.8 Design
Price of Fuel \$1.50.

Aircraft Data

Aircraft:	APET	Engine:	GE-APET
T/O Gross Wgt. lbs :	110986.	Number of Seats:	150
Airframe Weight lbs :	51930.	No. of Crew Members:	2
Propfan Dia. feet :	12.5		

Operating Data: Domestic Flight

Stage Length St. Mi. :	345.0	Block Fuel lbs :	2922.0
Block Time hrs :	1.134	Shaft Horsepower:	11389.0
Ground Maneuver Time Hr :	0.24	Assumed Number Trips/Year:	2960

Financial Data

A/F Price \$:	12467000.	Price of Fuel \$/Gal :	1.500
Propulsion Sys. \$EA :	3628094.	Labor Rate \$/M-hr :	14.19
Fly-Away Price \$:	19723188.	Maint. Burden % :	200.0
		Fuel Price Base Yr.:	81

	<u>A/F</u>	<u>Core</u>	<u>Propfan</u>	<u>GE</u>	<u>Nacelle</u>
Spare Ratio:	0.06	0.30	0.30	0.30	0.06
Depreciation Period Yrs:	15.0	15.0	15.0	15.0	15.0
Residual Value % :	10.0	10.0	10.0	10.0	10.0

Calculated Data

Contributing Factors

Utilization, Block Hrs/Yr	3356.6
Total Investment, \$	22429998.

	<u>\$/Block Hour</u>	<u>\$/St. Mi.</u>
Depreciation	400.91	1.3178
Insurance	29.36	0.0965
Crew, Cockpit Only	356.33	1.1712
Fuel	573.45	1.8849
Airframe Labor, Burden Incl.	134.61	0.4400
Airframe Material	29.09	0.0956
Engine Labor, Burden Incl.	51.15	0.1681
Engine Material	75.83	0.2492

Cost to Fly = \$959.14/Block Hour

Direct Operating Cost

<u>\$/Block Hours</u>	<u>\$/ST. Mi.</u>	<u>\$/ASM</u>	<u>\$/Flight Hr</u>
1650.73	5.43	0.0362	2097.79

Table 4.8-6. APET Baseline Turbofan Mach 0.8 Design
Price of Fuel \$1.50.

Aircraft Data (APET-Fan Engine)

T/O Gross Wgt. lbs :	111970.	Number of Seats:	150
Airframe Weight lbs :	50974.	No. of Crew Members:	2

Operating Data: Domestic Flight

Stage Length St. Mi. :	345.0	Block Fuel lbs :	3578.0
Block Time hrs :	1.136	Thrust lbs :	17429.0
Ground Maneuver Time Hr :	0.24	Assumed Number Trips/Year:	2960

Financial Data

A/F Price \$:	12540000.	Price of Fuel \$/Gal :	1.500
Propulsion Sys. \$EA :	3628094.	Labor Rate \$/M-hr :	14.19
Fly-Away Price \$:	19796188.	Maint. Burden % :	200.0
		Fuel Price Base Yr.:	81

	<u>A/F</u>	<u>Core</u>	<u>Reverser</u>	<u>Nacelle</u>
Spare Ratio:	0.06	0.30	0.30	0.06
Depreciation Period Yrs:	15.0	15.0	15.0	15.0
Residual Value % :	10.0	10.0	10.0	10.0

Calculated Data

Contributing Factors

Utilization, Block Hrs/Yr	3362.6
Total Investment, \$	22477040.

	<u>\$/Block Hour</u>	<u>\$/St. Mi.</u>
Depreciation	401.05	1.3206
Insurance	29.41	0.0968
Crew, Cockpit Only	367.49	1.2101
Fuel	700.96	2.3081
Airframe Labor, Burden Incl.	132.84	0.4300
Airframe Material	28.53	0.0939
Engine Labor, Burden Incl.	50.55	0.1665
Engine Material	90.51	0.2480

Cost to Fly = \$1097.86/Block Hour

Direct Operating Cost			
<u>\$/Block Hours</u>	<u>\$/ST. Mi.</u>	<u>\$/ASM</u>	<u>\$/Flight Hr</u>
1801.34	5.93	0.0395	2288.09

Table 4.8-7. APET Baseline Turbofan Mach 0.8 Design Supplemental Breakdown.

	Investments (Incl. Spares)	Depreciation \$/B. Hr.	Insurance \$/B. Hr.	Labor \$/B. Hr.	Material \$/B. Hr.
Airframe:	13292400.	237.18	18.64	132.84	28.53
Core Engine(s):	7567121.	135.02	8.65	50.555	88.443
Reverser(s):	520400.	9.28	0.59	0.	1.822
Nacelle(s):	<u>1097119.</u>	<u>19.57</u>	<u>1.53</u>	<u>0.</u>	<u>0.246</u>
Totals:	22477040.	401.05	29.41	183.390	119.038

Note: Burden included in labor

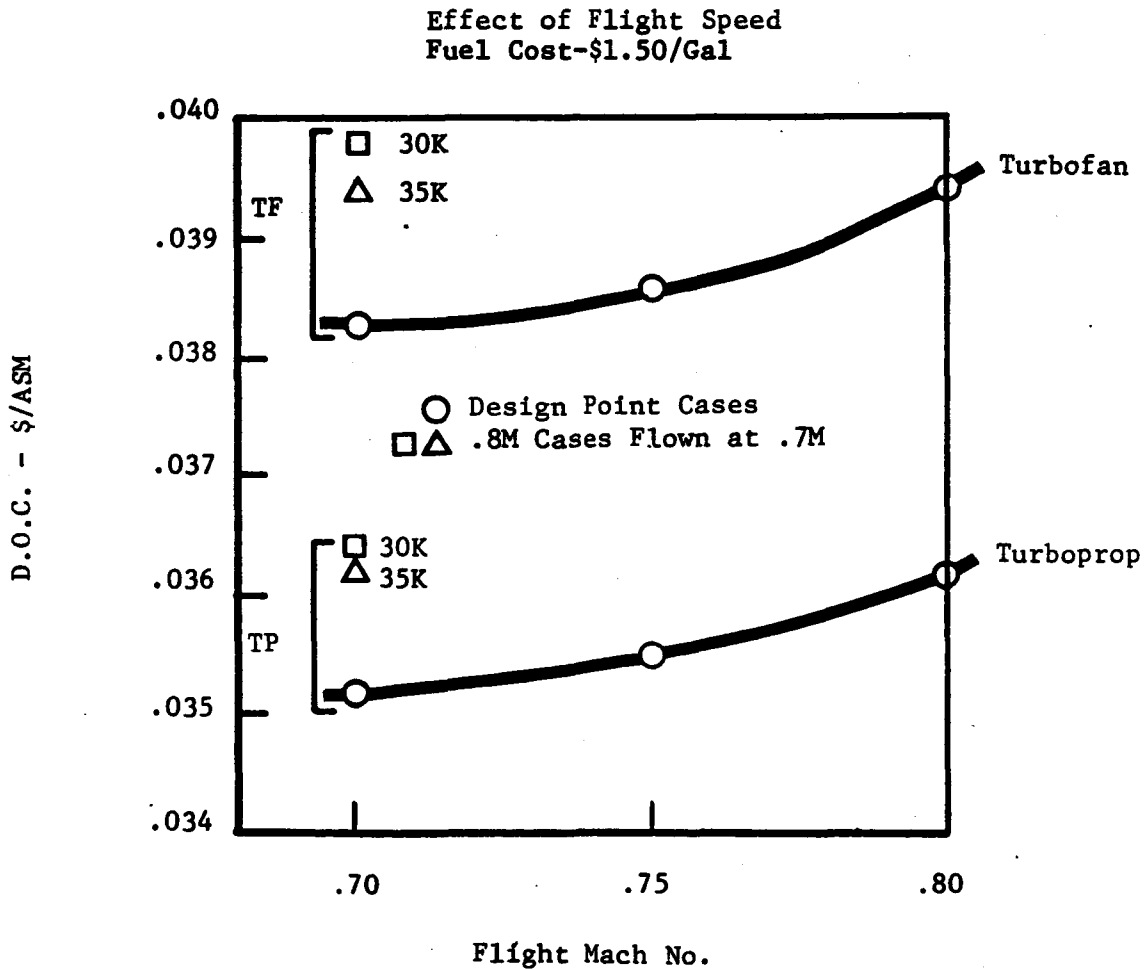


Figure 4.8-7. APET Economic Results - Baseline Cases.

Effect of Uncertainty in Propfan Propulsion Prices
 .8M Design - 300 NMI Leg

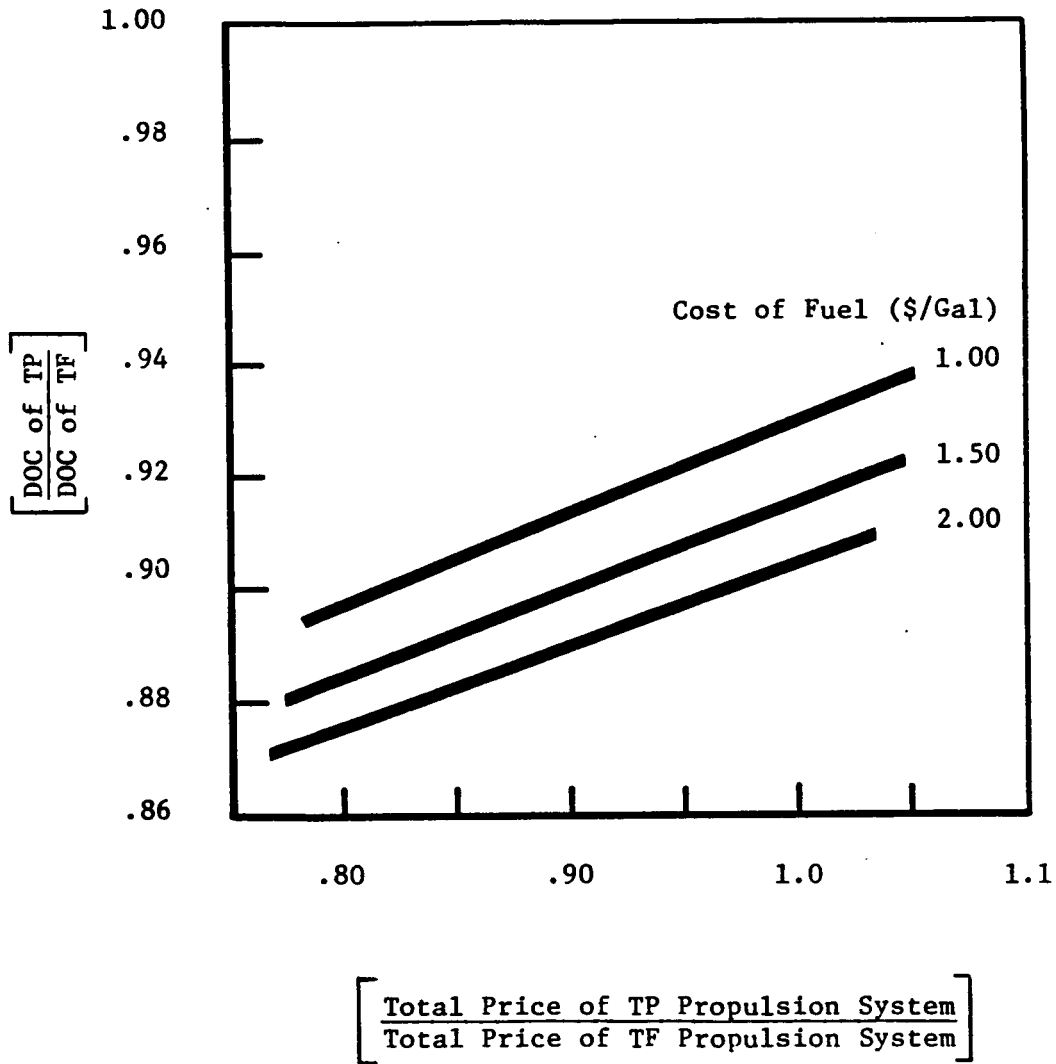


Figure 4.8-8. APET DOC Comparisons
 Propfan Vs. Turbofan.

SECTION 4.9

ACOUSTICS

Section	Page
4.9.1 Methodology and Assumptions	301
4.9.1.1 Aircraft Flight Conditions	301
4.9.1.2 Propeller Noise	301
4.9.1.3 Compressor/Fan Noise	301
4.9.1.4 Turbine Noise	301
4.9.1.5 Combustor Noise	302
4.9.1.6 Airframe Noise	302
4.9.1.7 Jet Noise	302
4.9.2 Noise Predictions and Adjustments	303
4.9.2.1 Mach Cruise = 0.80, Turbofan	303
4.9.2.2 Mach Cruise = 0.80, Turboprop	304
4.9.2.3 Mach Cruise = 0.70, Turboprop	304
4.9.3 Conclusions and Recommendations	304

TABLES

4.9-1 APET Aircraft Noise Levels.	303
-----------------------------------	-----

4.9 ACOUSTICS

4.9.1 Methodology and Assumptions

4.9.1.1 Aircraft Flight Conditions

Three different airplane designs were acoustically evaluated in this study. All the airplanes are twin-engined and have under-wing-nacelle layouts. They are:

1. Mach cruise = 0.80, turbofan powered
2. Mach cruise = 0.80, turboprop powered
3. Mach cruise = 0.70, turboprop powered

Tables of data for the flight conditions at the acoustic measuring points are noted in Appendix II.

4.9.1.2 Propeller Noise

NASA-CR-145105 and SAE AIR 1407 (References 44 and 45) were used to develop a preliminary design methodology which computed a scaled OASPL based on the SAE procedures discussed in the NASA CR. This procedure is discussed in more detail in Appendix II.

4.9.1.3 Compressor/Fan Noise

A NASA developed method was used for the turboprops and for the fan inlet and discharge noise for the turbofan. The method is reported in NASA TM X-71763 (Reference 49). The method determines one-third octave band SPL's for broadband, discrete tone and combination-tone noise components. This is also discussed in Appendix II.

4.9.1.4 Turbine Noise

Turbine noise has been predicted using techniques discussed in AIAA 75-449 (Reference 50) which is based on rig and engine data that correlates pressure ratio, tip speed and exit areas. This prediction method is further discussed in Appendix II.

PRECEDING PAGE BLANK NOT FILMED

PAGE ³⁰⁰ INTENTIONALLY BLANK

4.9.1.5 Combustor Noise

The prediction methodology used for this component is developed from SAE ARP 876B, Appendix "D" (Reference 51) and it correlates predicted combustor noise with mass flow rate, inlet total pressure, total temperature rise and the total temperature extraction associated with the take-off conditions. Appendix II also expands on the methodology used.

4.9.1.6 Airframe Noise

NASA TN-D-7821 (Reference 52) is used for this prediction, The equations used, and definition of terms is included in Appendix II.

4.9.1.7 Jet Noise

These predictions are made using the procedure described in SAE ARP 876B - Appendix A (Reference 53) and is based on a correlation of fully-expanded mean jet velocity, temperature ratio, nozzle area and Strouhal number. An extensive model data base is in existence to support this prediction methodology. Appendix II contains the equations that are used and the definition of terms.

4.9.1.8 Flight Predictions and Adjustments

Air attenuation and corrections are based on the method published in SAE ARP 866 (Reference 54) and ground reflection correlation and relationships use the method shown in FAA Report RD-71-85 (Reference 55). The procedure corrects for spherical divergence air attenuation, ground reflection, Doppler shifting, dynamic effects, jet noise flight effects, and extra ground attenuation. See Appendix II for further details.

4.9.1.9 Cabin Noise

In paragraph 4.9.1.2 the references are given for the establishment of the propfan as a noise source, and nearfield values have been applied to estimates for the sound pressure level at the fuselage wall. A cabin wall transmission loss is applied and this then determined an A-weighted interior SPL. Transmission losses through the wall are estimated using the method described in

NASA CR 159200 (Reference 57). Appendix II, Table II.1-2 gives the values of the transmission loss (in dB) versus frequency.

4.9.1.10 Treatment Assumptions

The two turboprop engines in this study do not require any treatment surfaces. The turbofan requires fan inlet, fan exhaust and turbine treatment areas and the materials and technologies used are similar to those developed during the course of the NASA/GE E³ program. Details of the suppression levels assumed in terms of ΔdB versus Hz are given in Tables II.1-3A and -3B included in Appendix II.

4.9.2 Evaluation

The three study aircraft have been acoustically evaluated relative to FAR 36, 1978 Stage III limits as dictated by the FAR Part 36 regulations (Reference 58) Table 4.9-1 gives the results of these evaluations, and these results are also included in Appendix II.

Table 4.9-1. APET Aircraft Noise Levels.

Condition	0.8 Mach Turbofan TOGW = 111,970 lbs			0.8 Mach Turboprop TOGW = 110,986 lbs			0.7 Mach Turboprop TOGW = 107,309 lbs		
	FAR 36 (EPNdB)	Estimated Level (EPNdB)	Margin (EPNdB)	FAR 36 (EPNdB)	Estimated Level (EPNdB)	Margin (EPNdB)	FAR 36 (EPNdB)	Estimated Level (EPNdB)	Margin (EPNdB)
Takeoff	89.3	85.8	3.5	89.3	90.5	-1.2	89.1	90.2	-1.1
Cut Back	89.3	85.3	4.0	89.3	88.9	0.4	89.1	88.7	0.4
Sideline	95.4	91.3	4.1	95.4	95.4	1.9	95.2	93.2	2.0
Approach	99.3	94.9	4.4	99.2	97.2	2.0	99.1	96.7	2.4

4.9.2.1 Mach Cruise = 0.80, Turbofan

As can be determined from Table 4.9-1 this airplane will meet the FAR 36 limits without trades. Some observations on other factors that would help improve the system margins are included in Appendix II, and also where the component levels are given in Table II.2-2 for values at the measuring point for this aircraft and the two turboprop airplanes.

4.9.2.2 Mach Cruise = 0.80, Turboprop

This airplane will also meet the FAR 36 limits using cutback. For all conditions examined the propeller generated noise dominates and system noise thus becomes directly dependent on propeller acoustic level reductions.

4.9.2.3 Mach Cruise = 0.70, Turboprop

The remarks above for the Mach = 0.80 airplane, equally apply.

4.9.3 Conclusions and Recommendations

This study shows that for the airplanes considered, FAR 36 Stage III limits can be met, and that the NASA objective for cabin interior noise is also within reach for some fuselage acoustic treatment weight penalty. Growth of the turboprop airplanes is foreseen provided source noise (the propeller) is capable of some reduction. This may well be provided by a combination of reduced tip-speed at take-off and some improvement in the blades acoustic signatures.

SECTION 4.10

EMISSIONS

<u>Figure</u>		<u>Page</u>
4.10-1.	EPA Smoke Emission Standards - Turbojet/Turbofan Engines.	308
4.10-2.	EPA Smoke Emission Standards - Turboprop Engines.	308

TABLES

<u>Table</u>		<u>Page</u>
4.10-1.	... Certified Large Engines (Federal ...)	...
4.10-2.	... for Emissions Calculations.	...
4.10-3.	... Certified Large Engines (Federal Register March 24, 1978)	309

4.10 EMISSIONS

The exhaust streams of aircraft turbine engines usually contain very low concentrations of objectional gaseous and particulate emissions. However, aircraft turbine engines do produce exhaust emissions of concern from an air pollution standpoint. These emissions, in the category of air pollutants, consist of carbon monoxide (CO), unburned or partially oxidized hydrocarbons (HC), oxides of nitrogen (NO_x), and carbon particulates such as soot or smoke.

Emission standards have been issued by the U.S. Environmental Protection Agency (EPA) to regulate the quantities of CO, HC, NO_x, and smoke emissions that may be discharged by various different categories of commercial engines when operating within or near airports. The presently prescribed standards, as published in the Federal Register of July 17, 1973, for newly certificated large turbojet/turbofan and large turboprop engines, are presented in Table 4.10-1 and Figures 4.10-1 and 4.10-2. The standards for turbojet turbofan engines are based on the engine thrust rating and the turboprop standards are based on the engine shaft power rating. A direct comparison of emissions for these two engines can be estimated, on a total weight per cycle basis, using the appropriate EPA prescribed landing-takeoff cycle. The current prescribed cycles for emissions calculations for turbofan/turbojet and turboprop engines are presented in Table 4.10-2.

Some changes to the presently prescribed standards have been proposed by the EPA. The proposed revisions to the standards were issued by the EPA as a Notice of Proposed Rule Making (NPRM) on March 24, 1978. The revised standards, for newly certified large-size engines, are presented in Table 4.10-3. Metric (SI) units are used for these new standards.

Recently, extensive further revisions to the NPRM standards have been proposed by the EPA. The newly proposed revisions eliminate the existing CO and NO_x standards and the HC standard is relaxed. However, the NPRM smoke standards are unchanged by these proposed revisions. Based on these currently proposed revisions, projections of the emission regulations applicable to large-size turboprop engines in the post-1990 time period are as follows:

Table 4.10-1. Current Standards - Newly Certified Large Engines.

(Federal Register - July 17, 1973)

	Large Turbojet/ Turbofan Engines (>8000 lb Thrust)	All Turboprop Engines
HC	0.4*	4.9 [†]
CO	3.0*	26.8 [†]
NOx	3.0*	12.9 [†]
Smoke No.	(Fig. 4.1-4)	(Fig. 4.1-5)
*Lbs/1000 lb-Thrust Hrs/Cycle		
†Lbs/1000 HP-Hrs/Cycle		

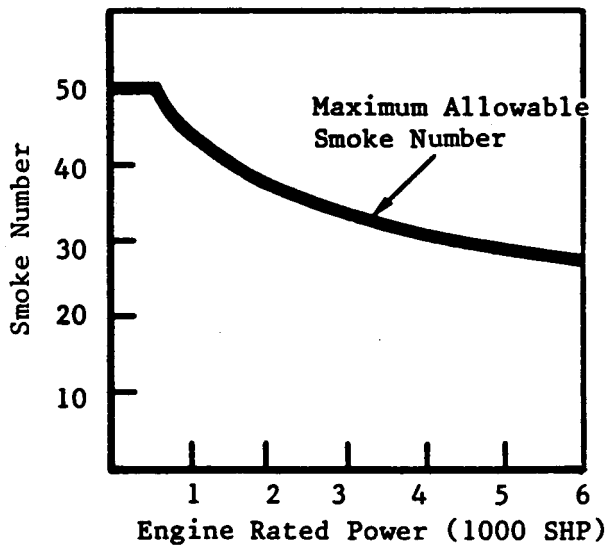


Figure 4.10-1. EPA Smoke Emission Standards-Turboprop Engines.

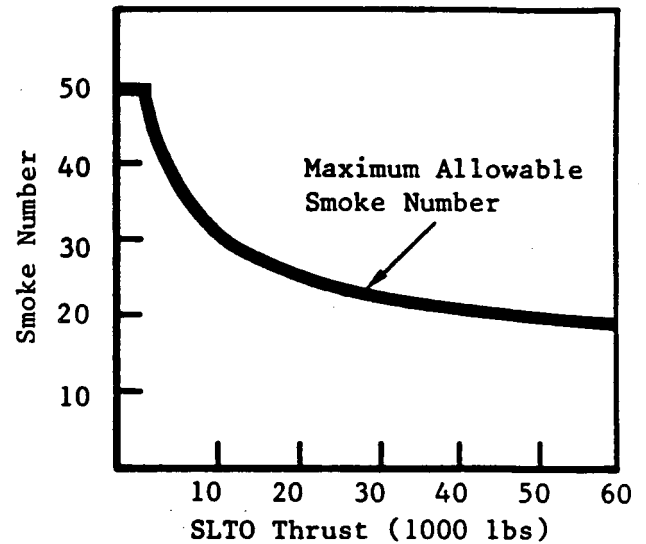


Figure 4.10-2. EPA Smoke Emission Standards-Turbojet/Turbofan Engines.

Table 4.10-2. Current EPA Prescribed Cycles for Emissions Calculations.

Time-in-Mode at Percent Rated Power

Mode	Turbojet/Turbofan Engines		Turboprop Engines	
	Time, Minutes	Power Percent	Time Minutes	Power Percent
Taxi Idle	26	*	26	*
Takeoff	0.7	100	0.5	100
Climbout	2.2	85	2.5	90
Approach	4.0	30	4.5	30

*Idle power setting determined by manufacturer

Table 4.10-3. NPRM Standard - Newly Certified Large Engines.

(Federal Register - March 24, 1978)

	Large Turbojet/ Turbofan Engines (>27 KN Thrust)	Large/Turboprop Engines (>2000 KW Power)
HC	3.3*	0.045 †
CO	25.0*	0.34 †
NO _x	33.0*	0.45 †
Smoke No.	79* (KN Thrust)-0.265	277* (KW Power)-0.280

* Grams per Cycle/KN Thrust
 † Grams per Cycle/KW Power

- No CO and NO_x standards.
- Less stringent HC standards - not likely to be more stringent than NPRM values.
- Same smoke standards as proposed in the NPRM of 1978 (as presented in Table 4.10-3).

SECTION 4.11
MILITARY RELEVANCE

ORIGINAL PAGE IS
OF POOR QUALITY

<u>Figure</u>		<u>Page</u>
4.11-1.	APET Military Relevance.	315

TABLES

4.11-1.	Military Relevance of APET Study.	313
4.11-2.	Possible Differences Between Military and Commercial Propfan Breakdown Retention Factors.	314

C-4

4.11 MILITARY RELEVANCE

As indicated in Section 1, many aspects of this APET study have relevance to potential Military aircraft programs that include Cargo Aircraft or other bulk airlifters. These aspects are highlighted in Table 4.11-1. Although no military studies have yet been conducted that use the APET engine data, it is recommended that some future work is initiated to see what advantages might accrue if the Military considered the use of high-speed turboprops for some selected missions. The "concern" items from the APET study regarding Military applications are summarized in Table 4.11-2, and Figure 4.11-1 has been introduced to indicate what the stretched version of the Lockheed C141 might look like if re-engined with APET technology propulsion systems.

Table 4.11-1. Military Relevance of the APET Study.

- Turboshaft engine computer decks can be used for both commercial and military applications.
- Nacelle/engine/wing integration problems are similar (Mach 0.70 to 0.80 range).
- Engine weight prediction methods are valid within the scalable range of approximately 8 - 18,000 SHP.
- Advanced gearbox design concepts will be identified.
- Development plan for critical technology components can be used equally for a military turboshaft engine.
- Introduction of FADEC to propeller controls.
- Acoustic (and other) "observables" are being quantified.
- Fuel conservation and low maintenance cost objectives are similarly shared by both the military and civil sectors.

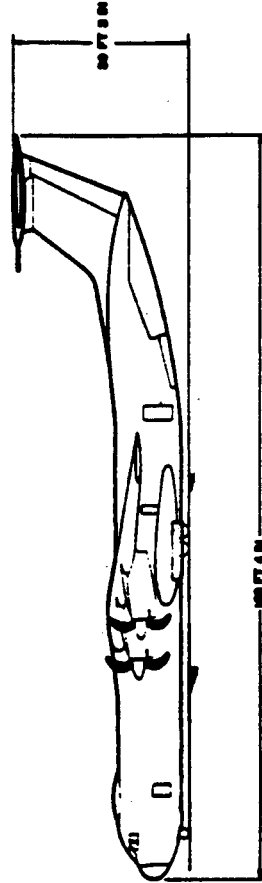
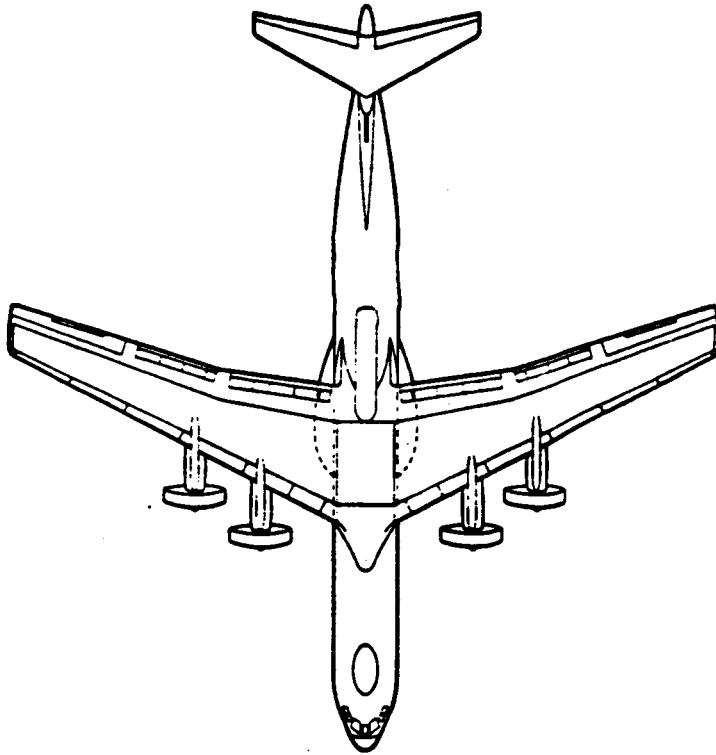
PRECEDING PAGE BLANK NOT FILMED

PAGE 3/2 INTENTIONALLY BLANK

Table 4.11-2. Possible Differences Between Military and Commercial Propfan Propulsion Selection Factors.

- Takeoff and landing performance may be more important for the military airlifter.
 - This alters engine temperature ratings and affects thrust lapse rate requirements.
- Optimum propfan selection likely to peak at lower SHP/D² loadings, lower tip speeds and possibly lower flight speeds.
 - Output torques (through the gearbox) may be higher.
- Aircraft layout may be radically different, causing substantial design changes to the propulsion system.
 - High wing most probable. Nacelle integration will be different.
 - Some unusual layouts may be explored, i.e. tail mounted engines, pushers.
- Engine duty cycles, utilization factors are different.
 - Different relative importance of fuel burn.
 - Economic considerations are aimed at reduced life cycle costs rather than the DOC or ROI formulae used in commercial programs.
- Engine power size could be drastically affected by considerations of 4 rather than 2-engined airplanes.

ORIGINAL PAGE IS
OF POOR QUALITY



- C141B Re-engineing
- Turboprops on same centerlines as existing engines

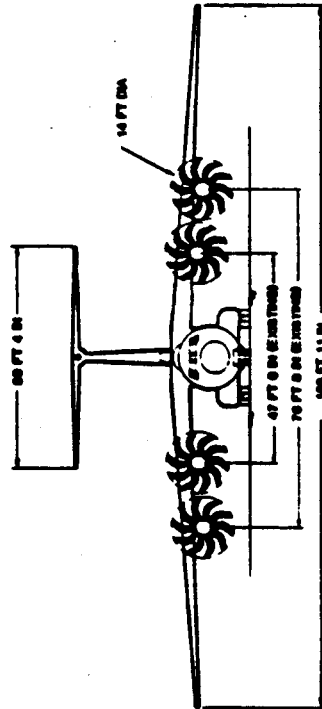


Figure 4.11-1. APET Military Relevance.

SECTION 4.12
RECOMMENDATIONS

ORIGINAL PAGE IS
OF POOR QUALITY

<u>Section</u>		<u>Page</u>
4.12.1	Introduction	319
4.12.2	Nacelle Placement	319
4.12.3	Thrust Matching	321
4.12.4	Aeromechanical Loads	321
4.12.5	System Dynamics	322
4.12.6	Structures	322
4.12.7	Nacelle Aerodynamics	322
4.12.8	Propfan Turbines	322
4.12.9	Turboprop Turbine Driven Booster Stages	322
4.12.10	Engine Controls	329
4.12.11	Propfan Gearbox	329
4.12.12	The Propfan Pitch Change Mechanism	333
4.12.13	APET Combustor	334
4.12.14	Final Recommendations	335

<u>Figures</u>		<u>Page</u>
4.12-1.	Advanced Propfan Technology-Key Technical Areas and Concerns.	320
4.12-2.	APET LPT Technology Plan.	326
4.12-3.	APET Booster Test.	328
4.12-4.	Turboprop Reduction Gearbox Program.	333
4.12-5.	Combustor Test Plan.	336

PRECEDING PAGE BLANK NOT FILMED

PAGE 310 INTENTIONALLY BLANK

TABLES

<u>Table</u>	<u>Page</u>
4.12-1. Comparison of the Full Scale E ³ and the Scaled Sized APET Configuration.	324
4.12-2. APET LPT Technology Mechanical Assessment.	325
4.12-3. APET Booster Unique Technology Features.	326
4.12-4. Low Pressure Booster.	327
4.12-5. APET Booster Test.	328
4.12-6. Turboprop Reduction Gearbox Development Program.	330
4.12-7. Program Elements.	330
4.12-8. Mechanical Design and System Analysis.	331
4.12-9. Hardware Procurement.	331
4.12-10. Bearing and Gear Component Tests.	332
4.12-11. Full Scale Back-to-Back Rig Test.	332
4.12-12. APET Combustor Development.	334
4.12-13. Combustor Test Plan.	335

4.12 RECOMMENDATIONS (INCLUDING DEVELOPMENT PLAN)

4.12.1 Introduction

The APET Study has identified numerous key technical areas and concerns. The nacelle design, its location relative to the wing and fuselage require the development of criteria before an airplane design can be explored with confidence. The power drive train which comprises the shaft engine, gearbox drive shaft and gearbox are also key technology items requiring development tests which must include the demonstration of life and reliability that is compatible with commercial operation. Control over the engine and propfan will almost certainly require a specialized FADEC using advanced signaling techniques and microprocessors. The propfan pitch change mechanism and its power source should be subjected to a separate design and development program, so that the opportunity to explore modern concepts and devices is not overlooked.

Figure 4.12-1 summarizes the above in a pictorial manner. It may be seen that the upper part of the figure is largely representative of technology items that are principally airframe design oriented, although a propulsion company would be required to make substantial inputs and for some areas (e.g., the engine inlet and exhaust) they may well be prime. In the lower half of the figure are the drive train elements and controls which together require development into a well-matched system. These key areas are the prime responsibility of the propulsion company, and have therefore been addressed in some depth in this study section.

4.12.2 Nacelle Placement

A number of assumptions have been made in this study regarding the desirable (for performance and noise) placement of the nacelles on the airplane wing. Rigorous analyses are not possible in light of the lack of a data base for these criteria. Airplane drag, weight, acoustic considerations, engine-out safety and maintainability are all factors which become impacted by the nacelle placement criteria. The performance of the propfan may also be affected, to a lesser extent, but the excitation factors through the propfan plane may present a much more significant problem.

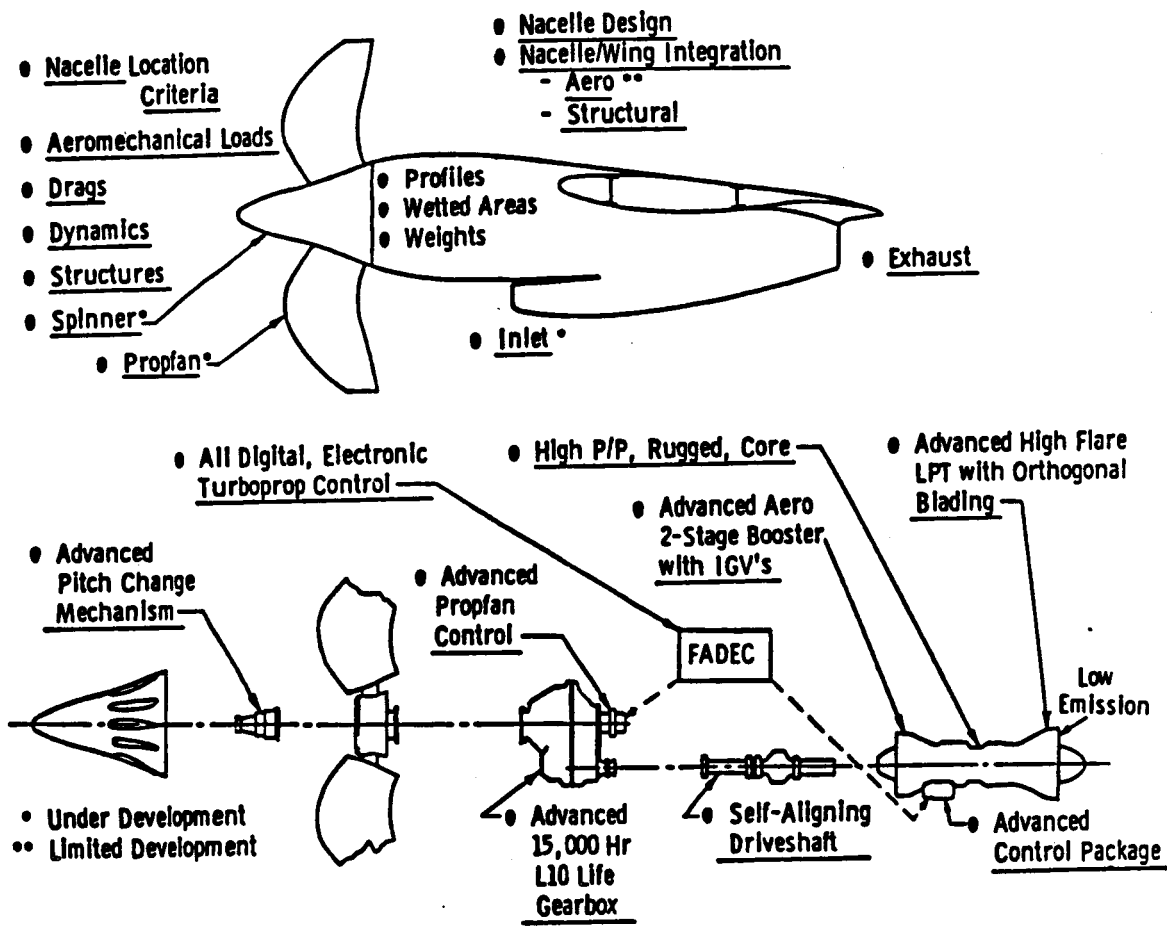


Figure 4.12-1. Advanced Propfan Engine Technology - Key Technical Areas and Concerns.

Wing weight and flutter avoidance criteria with considerations of the propfan whirl phenomenon subsequent to some assumed failure of a principal element in the nacelle structure has likewise not been addressed. The whirl mode loadpath could play a major role in the nacelle structural design concept and the selection of the methods and varieties of the dynamic suspension of both the engine and the propfan gearbox.

The aircraft aerodynamics, for both cruise and high-lift configurations, are also largely assumed due to the lack of a data base; and there are obviously some real questions to be answered regarding optimum flap and other high-lift features, particularly leading edge high-lift devices.

4.12.3 Thrust Matching

In this study the turbopropfans have been designed to produce identical thrust levels as the turbofans at 35K altitude, Mach 0.80 flight speed, using maximum climb power. With this design point matched, the propfan powered airplane has superior runway and climbout performance when compared with a high-bypass-ratio turbofan. Credit or debit for this takeoff performance has been taken in terms of the fuel burned by the competitive systems, but no other side studies have been made to judge the effects if some other match point had been selected.

For example, if the turbofan powered airplane was constrained to have equal takeoff field length capability as the turboprop, the airplane wing size would be increased as would also the installed thrust-to-weight ratio. These factors would cause additional degradation of fuel burn values.

It is therefore recommended that NASA further evaluate the selection criteria for thrust matching.

4.12.4 Aeromechanical Loads

NASA, at their Ames wind-tunnel facility and with the support of air-frame contractors, are pursuing the installation aerodynamics of the propfan and developing analytical techniques for optimum integration of the propfan flowfield with the wing. It is recommended that these efforts be expanded to include the measurement of the aeromechanical loads.

4.12.5 System Dynamics

It is strongly recommended that NASA contracts for the dynamic simulation of a turbopropfan propulsion system installed in a nacelle and coupled to a representative wing. Both fatigue data and mode loadpaths can be predicted and evaluated with good accuracy expectations. These data would be invaluable for an engine and airplane design program.

The forthcoming NASA PTA program should address this technical area, and lay the groundwork for an improved computer software package that could be used in future propfan powered airplane studies.

4.12.6 Structures

The nacelles conceived in the APET study are seen to be radically different from previous design experience. A structural design study, possibly best accomplished together with 4.12.4 and 4.12.5 above, is recommended with emphasis on advanced composite shell structures integrated with the airplane wing.

Fireproofing of composite structures is also an area of technology which needs some practical test programs, and these should be integrated with the above program.

4.12.7 Nacelle Aerodynamics

NASA should continue inlet studies to the extent of answering questions regarding pressure recovery behind the propfan, inlet stability in the swirling flowfield, and the trade-offs which relate to single offset inlets versus two (or more) offset inlets. The important criteria for lip shape and external forebody geometry must also be determined.

The exhaust system suppression effects due to the propfan flowfield should be tested in a scale model program so that the estimated nozzle performance coefficients can be verified.

The current NASA turboprop inlet programs are noted as important steps in defining the parameters for a well designed offset inlet configuration operating at high subsonic speeds. Some existing turboshaft engine should be

selected and an inlet design should then be tailored for this engine. The system should then be run in a tunnel with simulation of the pulsed dynamic flow from the root area of the propfan blade, and a full spectra of inlet distortion parameters and engine operability criteria be demonstrated.

4.12.8 Engine Low Pressure Turbines

As already indicated in this report, the achievement of high turbine efficiency using the minimum number of turbine stages is a critical item in the propulsion system's development. In order to effect a compact design, the stage pressure ratios and wall slope angles (flared surfaces) are beyond current technology testing. Component aerodynamic and mechanical test programs are therefore considered to be essential elements of any key technology development program.

The goals for these programs are as follows:

1. Develop technology to minimize aero losses associated with highly-sloped flowpath configurations
2. Incorporate recently developed OGV technology for low radius ratio APET flowpath
3. Reduce Reynolds number effects on efficiency

The expected payoffs are as listed below.

1. Improved efficiency via loading reduction for fixed number of stages, or decreased cost, length, and weight via stage number reduction at fixed efficiency level
2. Potential for 0.5 points in η_{TT} for more uniform stage-by-stage energy distribution allowed by OGV
3. Improved efficiency for altitude operation

The approach to the recommended program is as follows:

1. Execute a two part rig test program to evaluate multiple approaches to accomplishing goals, including
 - Orthogonal Blading
 - Improved Transition Duct Configurations
 - Improved Endwall Axial Gap Geometry
 - Efficient Deswirl with Low Radius Ratio OGV's

COMPARISON OF
OF POWER QUALITY

It is considered that the test program should include two blocks of testing with an appropriate time being allowed for hardware redesign between Block 1 and Block 2. The configurations proposed are noted below:

1. Block I, consisting of 3 configurations for Stages 1 and 2
2. Block II, consisting of complete LPT configuration including redesigns of Stages 1 and 2 based on Block I results

A comparison of the full scale E³ LPT and the scaled sized APET configurations is given in Table 4.12-1. The mechanical assessment being proposed is included in Table 4.12-2.

Table 4.12-1. Comparison of the Full Scale E³ and the Scaled Sized APET Configuration.

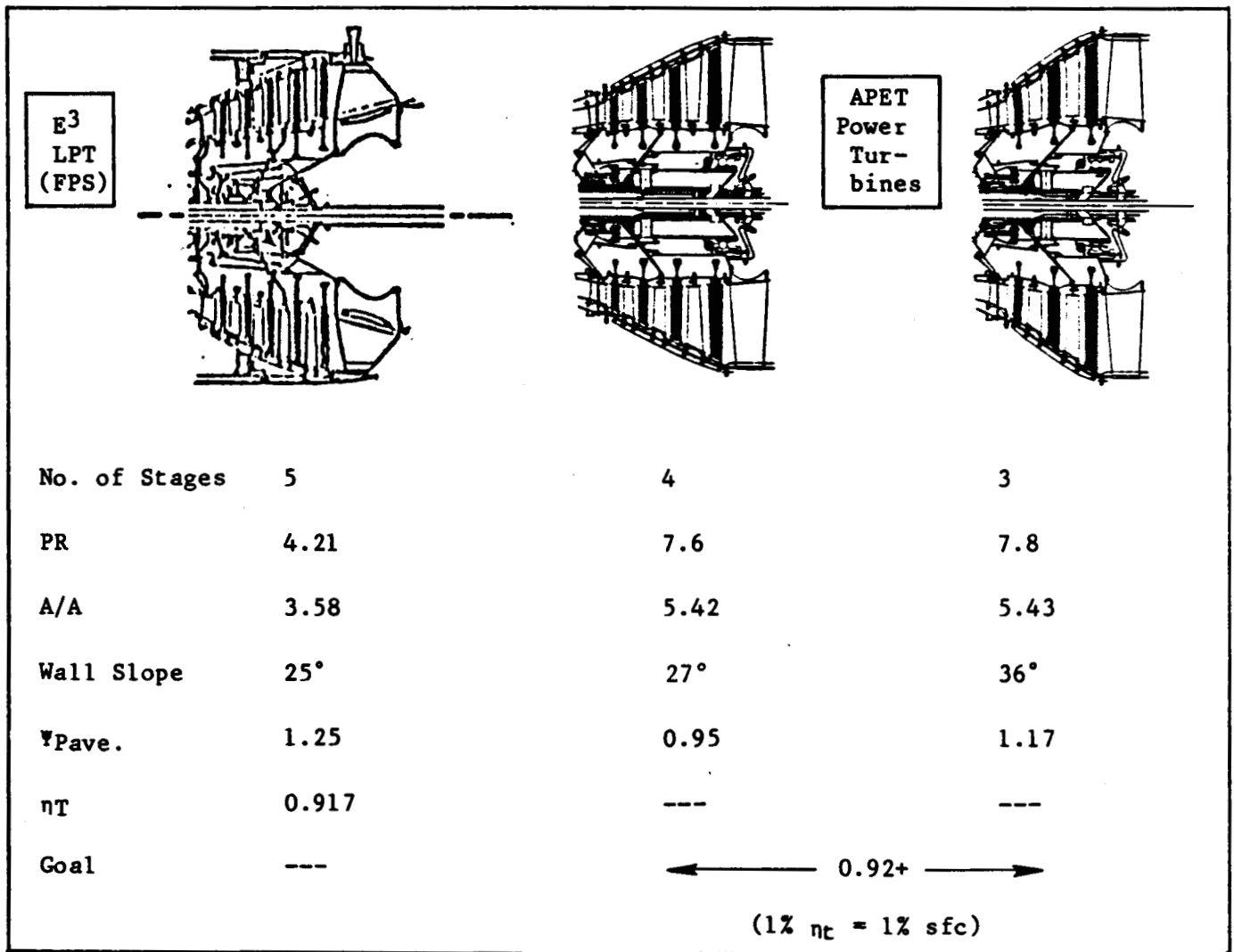


Table 4.12-2. APET LPT Technology Mechanical Assessment.

Evaluation of aerodynamic features (high AN², orthogonality) on blade stress/life and vibration, include:

- Vibrations - Geometry Effects: On Frequencies
On Vibratory Stress Distribution
- Fatigue - High Cycle Fatigue Life Effects of Geometry
- Hot Engine Environment
- Photoelastic - Identify Peak Local Stress Concerns
- Modeled Using Vibration/Fatigue Hardware
- Configurations - Four Variations
- Limited Quantity of Parts (12 of Each Variation)

The overall LPT technology plan and the key milestones are as shown in Figure 4.12-2.

4.12.9 Engine Low Pressure Turbine Driven Booster Stages

The APET engines in this report contain two-stage boosters with variable inlet guide vanes (VIGV's). The boost pressure called for in these designs is about 1.75 (total for the two stages). In order to maintain flow matching between the booster output (driven by the LP turbines) and the compressor inlet (driven by the HP turbines), some flow control variable geometry is required. This may be achieved by flow dumping via interstage bleed valves (which is wasteful) or by modulating the flow via the VIGV's. Development test programs for the booster configuration are essential to understand the system behavior and to establish a methodology for flow control scheduling. A test program to verify booster performance and control scheduling is therefore also a key component technology development recommendation.

The program identifies some unique technology features relative to current state-of-the-art boosters as exemplified by the T700 engine design. These features are identified in Table 4.12-3.

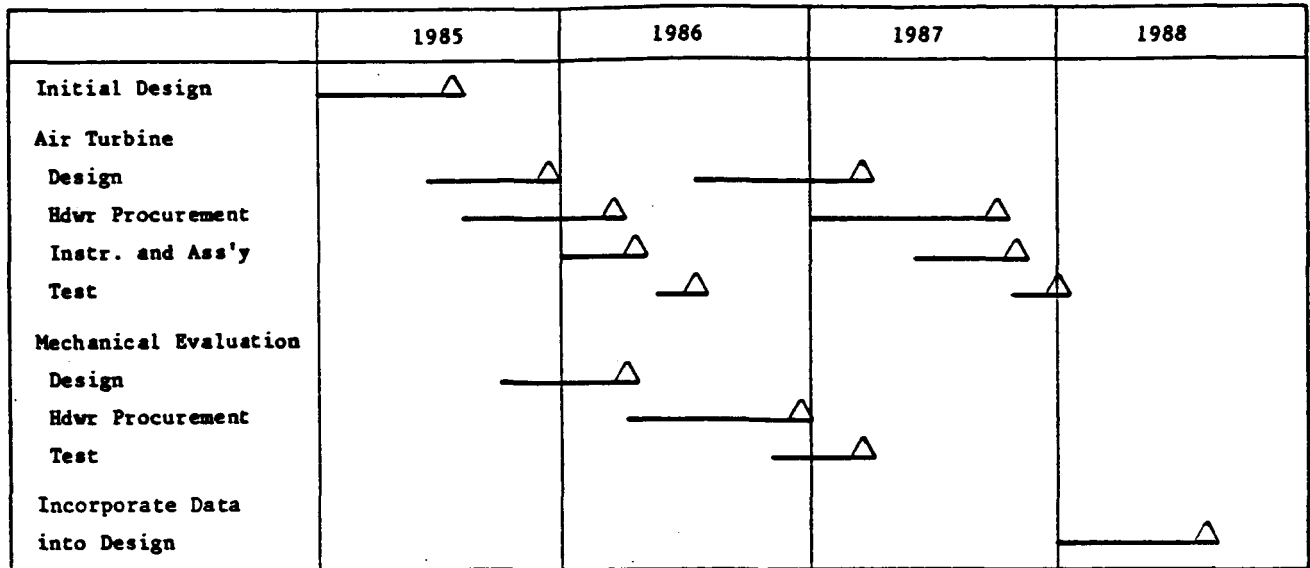


Figure 4.12-2. APET LPT Technology Plan.

Table 4.12-3. APET Booster Unique Technology Features.

1. Variable Geometry Varies Flow at Constant Speed
 - More Efficient at Part Power (Low Flow, High Speed)
 - Low Loss Variable IGV, Stator Configurations
 - Airfoil Sections With Broad Incidence Range
 - Vector Diagrams That Maintain Good Radial Balance of Loading

2. More Highly Loaded Than T700 Booster
 - Aero Design Challenge

3. High Tolerance to Heavy, Unsteady Inlet Distortions
 - High Inherent Stall Margin
 - Low Aspect Ratio Blading

Table 4.12-4 below compares the configuration of the T700 versus the APET booster and a 100 hour test program is outlined in Table 4.12-5.

Table 4.12-4. Low Pressure Boosters.

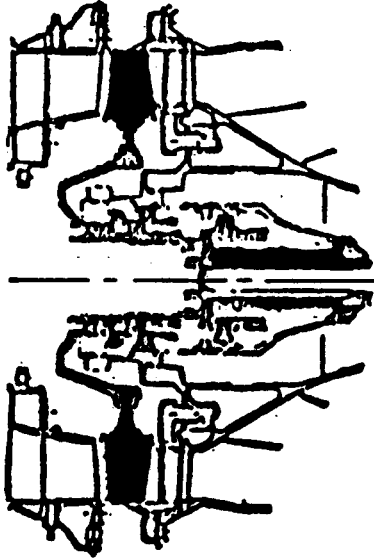
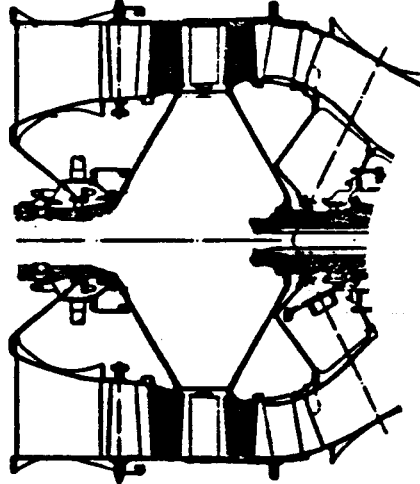
	<u>T700</u>	<u>APET</u>
		
No. of Stages	1	2
PR	1.38	1.75
$V_{Tip}/\sqrt{\theta}$	1172	969
r_h/r_c	0.737	0.67

Table 4.12-5. APET Booster Test.

100 Hours of Testing to Include:	
1. Performance Mapping	
- Operating and Stall Lines	
- Off-Design Regimes	
2. Inlet Distortion	
- Hub and Tip Radial	
- 1/Rev	
3. Radial Traversing	
- Interstage Radial Profiles	
4. Hardware	
- One Set Plus Spares	

The overall schedule for the proposed booster test program is shown on Figure 4.12-2.

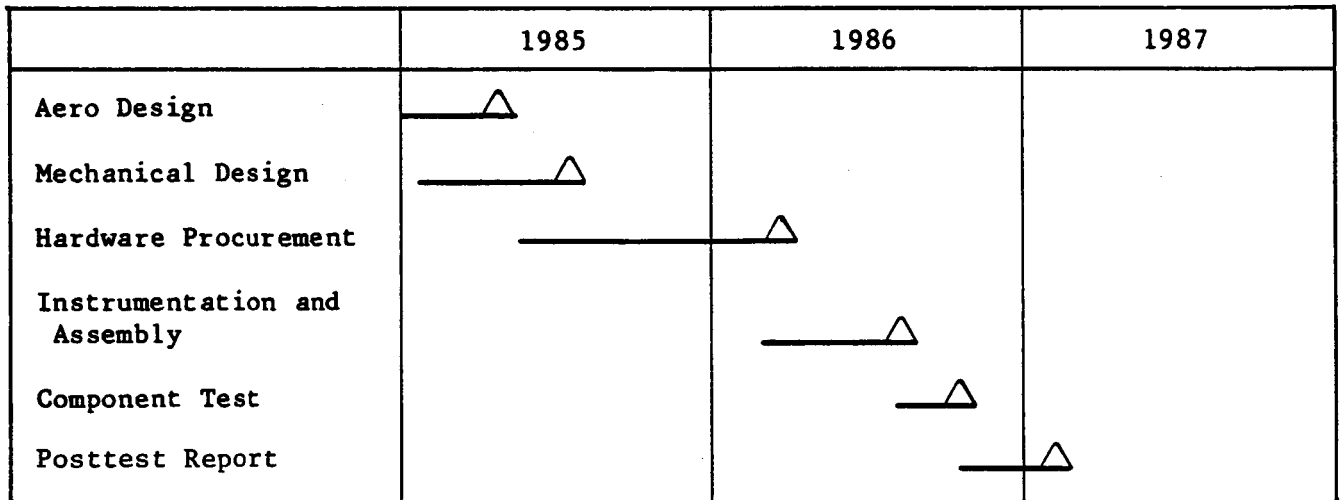


Figure 4.12-3. APET Booster Test.

4.12.10 Turboprop Controls

The turboprops in service today all use some version of hydromechanical fuel flow scheduling and hydromechanical propeller pitch change scheduling. The future turboprop is almost certainly going to be equipped with a FADEC system that simultaneously controls both the turboshaft engine power output (and all its variable geometry features) and the propeller system. Substantial design and development efforts will be required for these new control technologies, and it is recommended that NASA create a separate advanced turboprop control effort to demonstrate a FADEC system on a turboprop in an operational environment. This program should include the design and demonstration of the micro-processor based logic for the control, coupled with a digital redundant output which communicates with the engine and propeller using advanced signaling techniques. These technologies are also considered key to the success of the high cruise speed turboprop airplane.

This program is recommended to be identified in terms of cost and schedule when Task VIII of the APET program is completed. (Task VIII is currently in process of study.) This task addresses the design of an advanced pitch change mechanism (PCM) and includes the concept of control from a FADEC system. Because the modern turboprop engine and propeller control are perceived as being commanded and regulated by the same central processing system, the program will address both the engine and propeller systems.

4.12.11 The Propfan Gearbox

NASA is well aware of the critical nature of the gearbox and is pursuing, through further study tasks, detail design investigations which will cover all the aspects required to propose an advanced, lightweight gearbox with reliability indices for in excess of those being currently demonstrated in service.

These studies must be followed by a hardware development program which includes very substantial resources for hardware, rigs and testing. New levels of Hertzian stress in gear teeth coupled with improved lubrication and lubricants must be verified in an orderly manner. It is foreseen that some major cooperative industry and NASA programs may provide the best balance of effort, and the definition of these programs will be one of the prime objectives of APET Task VII due to be completed by the end of 1984.

In the meantime, that is before Task VII report is due, a program outline for a 12,500 SHP turboprop gearbox has been prepared. This program plan is discussed below. Table 4.12-6 gives the outline for the program plan.

Table 4.12-6. Turboprop Reduction Gearbox Development Program.

<p>Program Leads to:</p> <ul style="list-style-type: none">● Advanced Technology Reduction Gearbox 12,500 hp● Aimed at Late 1980's

The main elements for the proposed program are six in number. These are described in Table 4.12-7.

Table 4.12-7. Program Elements.

<ol style="list-style-type: none">1. Mechanical Design2. System Analysis<ul style="list-style-type: none">- Vibration- Lubrication3. Procure Hardware4. Outside Contractors Coordination5. Bearing and Gear Component Tests6. Full Scale Back-to-Back Rig Test
--

In the mechanical design and system analysis area there are eight sub-elements to the program. These are given in Table 4.12-8.

Table 4.12-8. Mechanical Design and System Analysis.

<p>Program Elements:</p> <ol style="list-style-type: none">1. Select Design Configuration2. Prepare Detail Drawing3. Analysis4. OV Coordination5. Engineering Coverage During Manufacture6. Component Test Coverage7. Full Scale Test Coverage8. Documentation

Hardware procurement requirements are given in Table 4.12-9, and comprise two subelements.

Table 4.12-9. Hardware Procurement.

<ol style="list-style-type: none">1. 3 Sets + Spares of Gearbox for Full Scale Back-to-Back Testing2. Component Test Bearings and Gears
--

It is possible that outside contractors will be invited to participate in certain areas of the gearbox design and hardware test effort because of their recognized technical expertise in specialist areas. These areas could include the following:

Possible Outside Contractors

Mechanical Design and Test Hardware

- Dynamic Mount System
- Input Drive Shafting
- Condition Monitoring (GE?)

Included in Table 4.12-9 there is an item which covers the component tests for bearings and gears. The plan outline for these components is given in Table 4.12-10.

Table 4.12.10. Bearing and Gear Component Tests.

<p>Bearings</p> <ol style="list-style-type: none">1. Planet/Star or Idler Bearings2. Include Gear Mesh Separating Load Effects3. Equivalent Loading4. Determine Stability at Various Cooling Rates5. Determine Heat Rejection6. Endurance Test <p>Gears</p> <ol style="list-style-type: none">1. Single Mesh Testing2. Scale of Test Gears (To be Determined)3. Determine Scoring Characteristics4. Determine Heat Rejection5. Load Endurance
--

A full scale back-to-back rig test is planned for the assembled gearbox. Table 4.12-11 highlights this test.

Table 4.12-11. Full Scale Back-to-Back Rig Test.

<ol style="list-style-type: none">1. New Facility2. Minimum Testing Requirements<ul style="list-style-type: none">● Initial Assembly and Final Teardown● 4 Inspections● Mechanical C/O and Test Plan Testing (100 to 500 hours)● Only Torque Testing, No Prop Load Testing3. Reporting

The overall timing and key milestone events are shown in Figure 4.12-4.

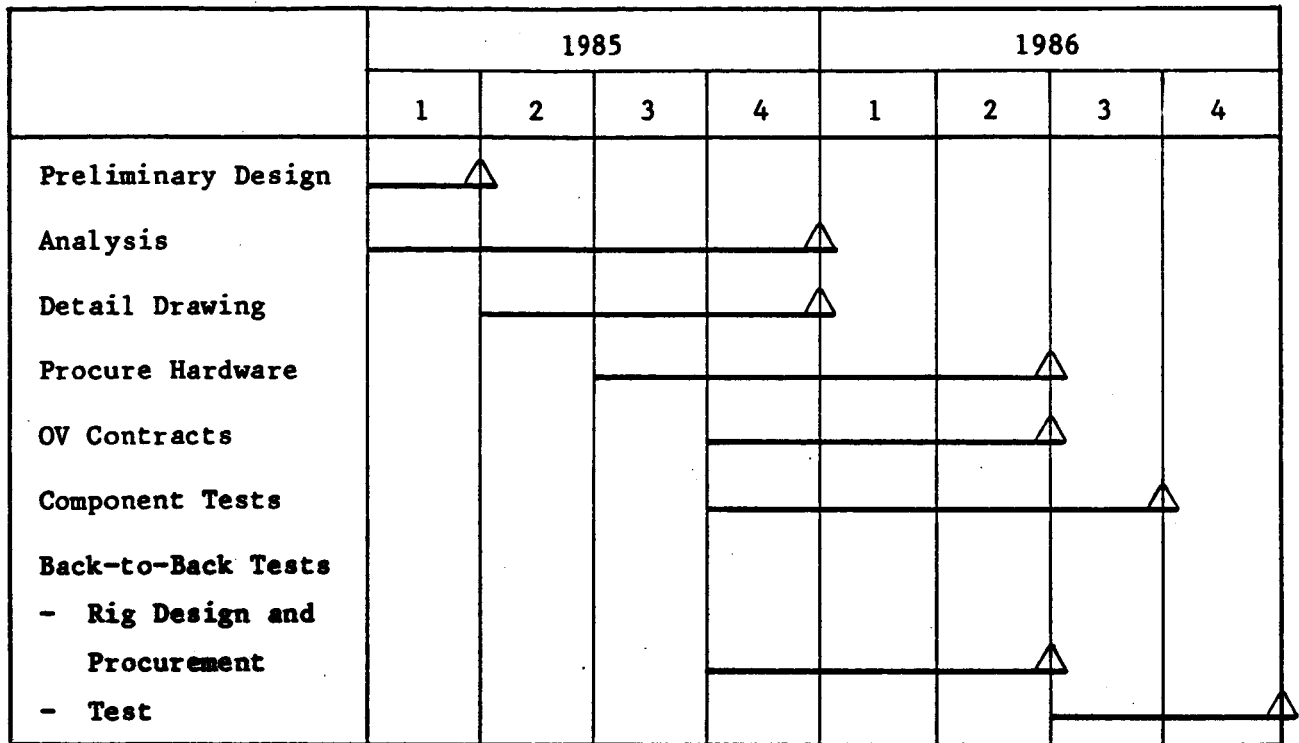


Figure 4.12-4. Turboprop Reduction Gearbox Program.

4.12.12 The Propfan Pitch Change Mechanism

General Electric has identified some novel design approaches which may offer significant improvements in terms of reliability, system stiffness, and blade position accuracy. Safety of operation is an absolute requirement which will be addressed by using levels of stress that are conservative for the materials considered, coupled with advanced redundant control concepts and advanced instrumentation which monitors vital functions as well as diagnostic functions. Like the gearbox above, the PCM will be further refined in APET Task VIII, which will produce a detailed recommendation for further efforts to include hardware appraisal and development.

4.12.13 APET Combustor

A technology plan is required to address the performance implied in the APET study engines combustors. The objective and the challenges are outlined in Table 4.12-12.

Table 4.12-12. APET Combustor Development.

Objective - Develop Full Annular Combustor Technology for Advanced Propfan Engine Applications.

Technology Challenge

1. 20% Reduction in Nondimensional Burning Length (1.75 L/H_D Versus Current Production Designs of 2.2)
 - Reduced System Weight
 - Reduce NO_x Emissions
2. 30% Reduction in Liner Cooling Relative to E³.
 - Advanced Technology Design
 - Increase Available Air for Aerothermal Mixing
3. 100% Increase in HP Nozzle Leading Edge Back Flow Margin
 - Increase HP Nozzle Cooling Efficiency
 - Reduce Sensitivity to Combustor Thermal Nonuniformity
4. ICAO Research Goals for Future Subsonic Engine Gaseous Emissions*
 - Carbon Monoxide - 42.00 grams per Kilonewton Cycle
 - Hydrocarbons - 4.35
 - Oxides of Nitrogen - 58.00
5. Low Visibility
 - Smoke* -20 SAE

*Using "ERBS" Fuels

The development plan includes a number of subelements which lead to a full scale annular test program including the diffuser. This plan is outlined in Table 4.12-13.

Table 4.12-13. Combustor Test Plan.

Development Plan	
1.	Parallel, but Interactive, Component Sector Test Programs. <ul style="list-style-type: none">● Single Cup Sector - Swirl Cup Development (Atmospheric)● Five Cup Flat Sector - Stability, Temperature Profile, Primary Zone Stoichiometry, Liner Hole Patterns (Atmospheric)● Five Cup Annular Sector - Ignition, Emissions, Ignitor Location, Subidle Performance (Sub-Atm + 7 Atm)
2.	Full Annular Test Program - Profile, Pattern Factor, Stability, Emissions, Life (Sub-Atm + 35 Atm)
3.	Full Annular Diffuser Test Program - Water Table Studies, Performance, Sensitivity, Stability

The overall plan including milestones and events is as shown in Figure 4.12-5.

4.12.14 Prioritized Recommendations

In order of priority, the recommendations are listed below:

Priority One

- (2) ● Low pressure turbine design/development
- (3) ● Booster with VIGV's design/development
- (2) ● FADEC controls design/development
- (1) ● Propfan gearbox design/development
- (3) ● Propfan PCM design/development
- (3) ● Combustor design/development

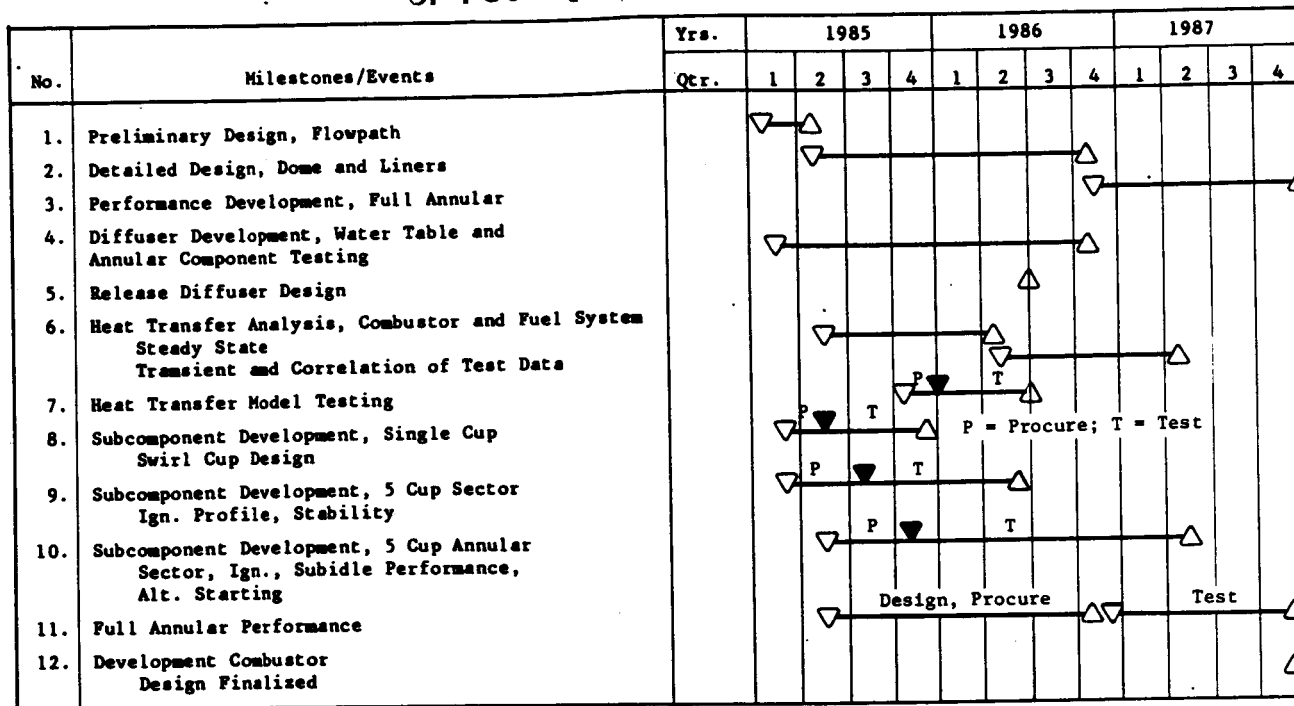


Figure 4.12-5. Combustor Test Plan.

The numbers in parentheses are the suggested order of priority based on the estimated individual program time span. It would be recommended that design engineering efforts on all five items be conducted in parallel.

Priority Two

- (1) ● Nacelle placement design studies/Wind Tunnel testing
- (2) ● Thrust matching design studies
- (3) ● Aeromechanical loads design studies
- (4) ● Nacelle structures design studies
- (1) ● Nacelle aerodynamics Wind Tunnel testing

The numbers in parentheses are the suggested order of priority based on the impact that the individual programs may have on an overall design effort. Also, it should be noted that these five subjects are mostly airframe design prime areas.

TASK VII PRELIMINARY DESIGN OF PROPFAN REDUCTION GEARBOX

<u>Section</u>		<u>Page</u>
4.13.1	Summary	339
	4.13.1.1 Objectives	339
4.13.2	Design Constraints	340
4.13.3	Trade Studies	340
4.13.4	Design Criteria	341
4.13.5	General Arrangements (Current and Advanced)	342
	4.13.5.1 Current	342
4.13.6		343
4.13.7	Preliminary Design Details	343
	4.13.7.1 Arrangement	343
	4.13.7.2 Gears	350
	4.13.7.2.1 Gear Stress Analysis	353
	4.13.7.2.2 Gear Materials	353
	4.13.7.2.3 Gear Scoring	354
	4.13.7.2.4 Load Sharing Provisions	355
	4.13.7.3 Bearing Design	355
	4.13.7.4 Lubrication System Design	356
	4.13.7.5 Heat Generation and Efficiency	361
	4.13.7.6 Reliability	362
	4.13.7.7 Gearbox Housing Design	363
	4.13.7.8 Gearbox/Propfan Interface	365
	4.13.7.9 Engine/Gearbox Interface	365
	4.13.7.10 Gearbox Physical Description	366
	4.13.7.11 Maintenance	366
	4.13.7.12 Opposite Rotation Gearboxes	368
	4.13.7.13 Gearbox Weight	368
	4.13.7.14 Costs	374

FIGURES

ORIGINAL PAGE IS
OF POOR QUALITY

<u>Figure</u>		<u>Page</u>
4.13-1.	APET 4-Branch Propfan Reduction Gearbox.	343
4.13-2.	Compressive Stress Comparison for Helical and Spur Gears.	351
4.13-3.	Bending Stress Comparison for Helical and Spur Gears.	351
4.13-4.	Bearing Load and Life Summary.	356
4.13-5.	Typical APET Mission Profile.	356
4.13-6.	Star Gear Forces and Bearing Reactions.	357
4.13-7.	Lube System Schematic.	360
4.13-8.	Modular Breakdown.	367
4.13-9.	APET Propulsion System Mounts.	369
4.13-10.	Offset and In-Line Opposite Rotation Gearboxes.	370
4.13-11.	Added Star Gear Idlers and Reversed LP Turbine Rotor of Reversed Rotation.	371
4.13-12.	Star Versus Epicyclic and Compromised Star Gear Arrangement for Opposite Rotation.	372
4.13-13	APET Gearbox Weight.	373

TABLES

<u>Table</u>		<u>Page</u>
4.13-1.	Comparison of Three to a Four-Star Kinematic Arrangement.	349
4.13-2	Gear Data, HP = 12,500, Total Gear Ratio = 7.3:1.	352
4.13-3	Calculated Gear Parameters.	353
4.13-4	Gear Design Allowables, Current Versus Advanced.	353
4.13-5	Opposite Rotation Comparison Studies.	364

4.13 TASK VII PRELIMINARY DESIGN OF PROPFAN REDUCTION GEARBOX

4.13.1 Summary

A continued design effort on a propfan reduction gearbox has been made as a follow-on to Tasks III and IV of Contract NAS3-23044. As a result of conceptual design studies, two basic designs evolved; an in-line compact design and a simple offset configuration.

These designs were ranked in Task III of the above-mentioned contract and were rated approximately equal. The Westland Helicopter Co. (working at no cost to the U.S. Government) was developing a preliminary design for a novel offset gearbox. Because of this activity, GE chose, in-house, to expand upon the design of the in-line design so two gearboxes, one of each principal type (in-line and offset), would result from Task VII. This report however is restricted to reporting on the in-line design only.

4.13.1.1 Objectives

This study included the following objectives:

- Identify the specifications judged appropriate for a 1990 IOC (Initial Operational Capability) propfan gearbox
- Provide a viable gearbox preliminary design for a 1990's propfan propulsion system. The gearbox to include advanced technology systems, features, materials.
- Identify the constraints on the gearbox design
- Identify the required technologies
- Identify areas needing technology development
- Quantify the benefits of these advanced technologies
- Provide a Development Plan which will develop these technologies for timely introduction into a "product" gearbox.
- Identify other components (gearbox related or gearbox adjacent) requiring technology advances or development.

4.13.2 Design Constraints

The propfan reduction gearbox of the 1990 time period must have maintainability and reliability levels in excess of current experience. This will require a design for Mean Time Between Unscheduled Removals (MTBUR) in excess of 20,000 hours. This then in turn will require designing for very high bearing and gear lives in order to achieve system lives of 20,000 hours. Also demanded are that individual bearings and gear meshes have lives in excess of 100,000 hours depending on the total number of bearings in the system. Thus the design constraint is to keep the kinematics simple and the number of fatigue prone components to a minimum.

Also important are interfaces of the Pitch Change Mechanism (PCM) and the gearbox. Transfer of electric or hydraulic power to the mechanism and access for servicing also constrains the gearbox design.

To achieve favorable weight factors the design should include integrating features which have in the past been separate, such as lube oil coolers and the oil reservoir. Thus the packaging of the gearing arrangement into a multifunctional housing becomes an important aspect of the selected design.

The gearbox that is being reported was preliminarily designed to meet the following criteria:

- Compatibility with the aircraft, engine, and mission developed in Tasks I through IV.
- Mean time between unscheduled removals (MTBUR) in excess of 20,000 hours
- Integrate all the gearbox support systems into the basic gearbox; i.e. no systems to be remote from the gearbox.
- Keep accessory drive systems separate from the basic gearbox.

4.13.3 Trade Studies

Configuration

Initially the configuration of all gearboxes that had ever flown (as determined from the historical survey) were considered as initial candidates

along with other configurations that were thought to have possible potential. This rather large field of candidates was narrowed to seven final candidates. As a part of Tasks II and III conceptual designs were made of these candidates prior to judging them on the following properties:

- Weight
- Cost
- Technical risk
- Development requirements
- Build where possible from an established data base
- Capability of achieving life and maintainability goals
- Installation consideration including dynamic mountings

The two leading candidates, which were virtually tied for first place, were an in-line compound star configuration and an offset double branch double reduction configuration. The details of this configuration comparison are reported in Section 4.6 of this report.

With the approval of NASA, Task VII was contracted to explore further the preliminary design of an in-line compound star configuration. Also as a separate issue General Electric Company continued with an advanced offset configuration, using novel gearing designs. This work was not performed as part of the NASA-funded contract and therefore is not reported herein.

4.13.4 Design Criteria

The design criteria established for the in-line design included the following considerations:

- A design that was established from the mission profile shown in Figure 4.6-5. This mission profile was used to establish the Cubic Mean Power for bearing system lives.
- A maximum power capability of 12,500 HP at takeoff. This was a "nominal" power selection and is applied to the propfan driveshaft.
- An overall gear ratio of $7.4:1 \pm 0.1$
- A system life in excess of 20,000 hours.
- Compatibility with an advanced PCM to be conceptually designed in Task VIII of this study. This gearbox must include the source of

hydraulic or electric power and any lubrication requirements for the total propfan system.

- Simple kinematic arrangement leading to a low parts count thus enhancing maintainability, reliability and DOC.
- Use of advanced concepts to help achieve any of the above criteria.

4.13.5 General Arrangements (Current and Advanced)

4.13.5.1 Current

The baseline gearbox design, which is used for the purpose of determining the worth of the advanced technology features, is shown earlier in this report as Figure 4.6-13. This design is an in-line compound star configuration having three branches and is the in-line having the highest rating in the trade study discussed in Task 4.6 of this report. Desirable attributes of this design are:

- Simple compact kinematic arrangement.
- Propfan shaft bearing span consistent with long bearing life. Aft bearing is mounted in the star gear carrier.
- Floating ring and sun gear for gear tooth load sharing.
- High speed drives for the Pitch Change Mechanism (PCM) and the auxiliary drive for the accessories.

4.13.5.2 Advanced

Task VII, with the approval of NASA, took the configuration shown in Figure 4.6-13 and incorporated into it advanced features. The advanced configuration, shown in Figure 4.13-1, is also an in-line star configuration, which is an evolution of the current design. The configuration choice remains the same for the same reasons.

The general arrangement of the advanced gearbox designed under this task is shown in Figure 4.13-1. For this arrangement engine power drives a 30-tooth input pinion gear which then drives four double idler gears. These four gears engage a 91-tooth internal gear for a total gear ratio of 7.3076:1. The ring gear is splined to the output shaft to provide flexibility and the output shaft bearing system consists of a ball and roller bearing mounted in the forward

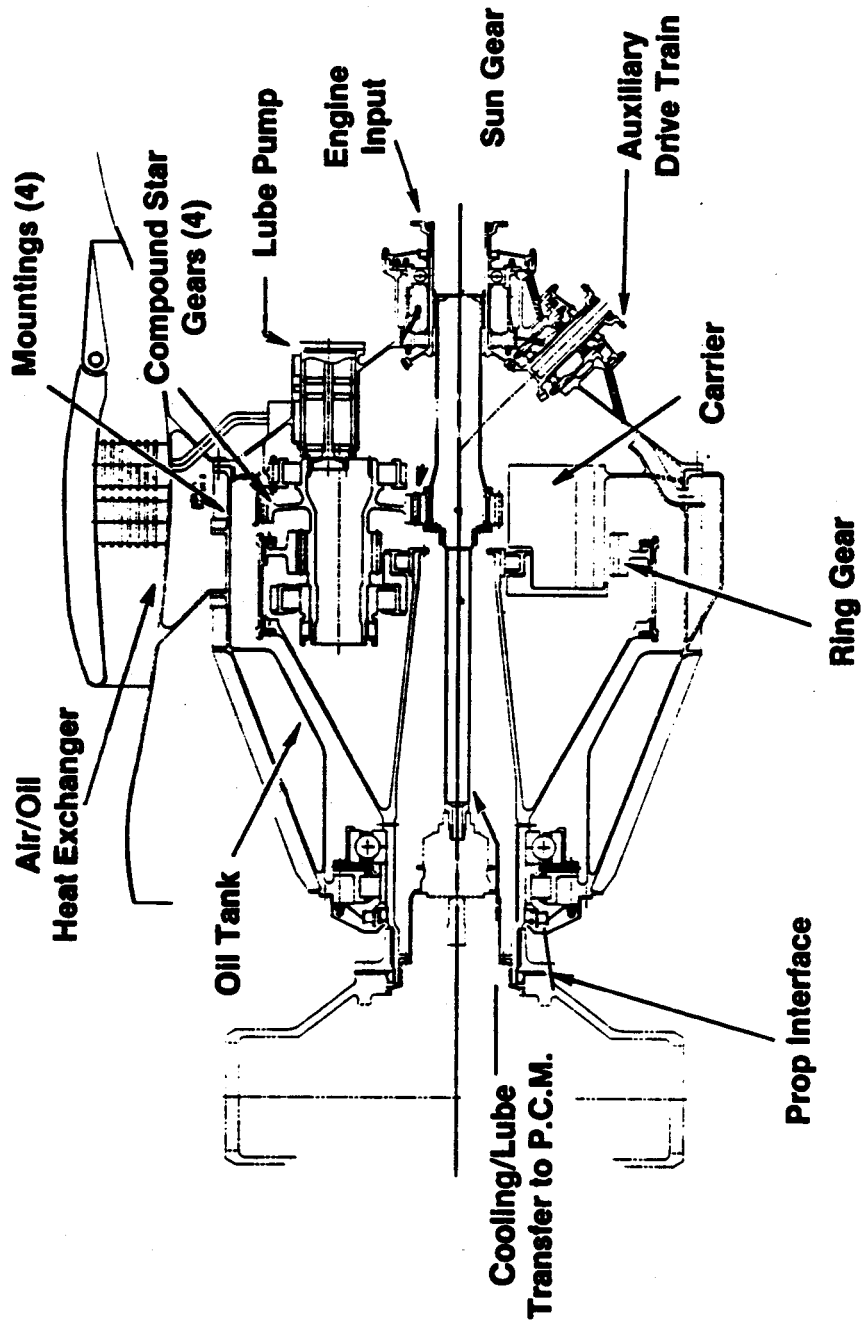


Figure 4.13-1. APET 4-Branch Compound Star Reduction Gearbox.

housing and a roller bearing mounted in the star-gear carrier. The carrier is a stiff, two piece design to allow for assembly of the internal gear past the forward support bearings of the four idlers. The 22/53 tooth star gears are of a welded design with the weld located in the web of the 53 tooth gear. The differences between the gearboxes of Figure 4.6-13 and Figure 4.13-1 are:

- Slight ratio modification which enables the use of four (instead of three branches) with a resulting improvement in weight and volume.
- Use of bulk oil temperatures approximately 100° F higher than permitted by current technology. A reduction in size of both the lube system and heat exchanger is then a direct result.
- Use of a titanium alloy rather than a light alloy housing. This change is partly necessitated by the higher operating temperature, but there are other benefits as well from this change that are discussed in Section 4.13.7.9, later in this report.
- Anticipated improvements in Multiplying Factors for bearings. These improvements will occur as experience continues to mount on the high bypass ratio fan engines.
- A modulated lube system oil flow rate for improved efficiency at cruise power settings.
- Ability to exploit more fully the properties of advanced gear materials (higher hot hardness) as a result of the elevated operating temperature.
- Incorporation of an oil tank as part of the gearbox housing. This has advantages of increased reliability as well as saving weight.
- Incorporation of a heat exchanger as part of the gearbox. This saves weight, increases reliability, as a result of fewer fluid lines and connections, and possesses installation advantages. It also ensures that new production gearboxes can be factory "system" tested, and flushed for cleanliness before being installed as part of the overall propulsion system.
- Incorporation of finer filtration to improve bearing and gear wear.

The gear configuration is a compound star layout, which means that the star pinions are stepped, each containing two gears. The star pinions also serve as convenient locations from which accessory power can be extracted. The twin lube and scavenge pumps are driven from the two lower star pinions. The sun gear meshes with the larger diameter gear on each pinion, with the ring

gear meshing with the other, or smaller, gear. This arrangement preserve the advantages of the simple star configuration (which has unstepped, or single pinions) but greatly increases the ratio capability at which the gearbox can still be very competitive in weight. The pinions are, of course much longer in this configuration and this plus the fact that the tangential forces at the input and output of the pinion do not lie in the same plane give rise to a couple that tends to skew the centerline. This tendency places additional importance on the rigidity of the star gear support such that changes in deflections as the load goes from zero, or even negative, to full load, do not unacceptably change the meshing contact pattern. In order to meet these demanding design considerations, the use of a fabricated (welded) titanium shell and support members are highly beneficial. Fabricated assemblies, when analyzed with the latest Finite Element Analytical techniques, can much more easily be designed for stiffness in the right places than can a monolithic constant shell thickness aluminum casting. The housing of this gearbox is therefore an advancement in that it is a titanium weldment rather than the more conventional light alloy casting. Additional unique features are that the gearbox incorporates a built-in oil tank and heat exchanger. Mounting provisions to absorb thrust, roll, (torque reaction), and vertical and side loads are included at four locations on the outside of the housing in the plane of its largest diameter.

Because of the unique design features of the electric pitch change which is mated with the gearbox in this study, minimum demands are placed upon the gearbox insofar as accommodating propfan pitch change system requirements. The gearbox, however, does supply energy within the propfan hub via a high speed central shaft which is coaxial with the output drive shaft. Approximately 30 horsepower maximum is transmitted, and this is used by the propeller assembly for:

- Powering the blade pitch change actuator.
- Providing power to de-ice the blades and spinner shell.
- Powering the on-board electronic control.
- Powering, when necessary, the following pitch lock to prevent a lock up situation and permitting authorized blade movement toward fine pitch.

Additionally, a low pressure (50-60 psig), low flow hydraulic slipring is provided within the SDG (Speed Decreaser Gearbox) to supply cool, filtered oil to channels within the high speed central shaft. This oil is used:

- To lubricate the alternator bearings and speed increaser device.
- To cool both the alternator and motor.
- To activate the emergency feather clutch, if necessary.

Because of the low pressure, this slipring is not a demanding design and it can be of small diameter as the flow is low. Zero leakage performance of this slipring is not a requirement as the location within the oil-wetted interior of the gearbox makes the slipring extremely leak-tolerant. Reliable delivery of the required flow is the only necessary condition.

4.13.6 Accessories

Removal of an accessory drive section from the propfan speed reducing gearbox greatly simplifies the SDG and eases the task of attaining the reliability goal. The accessory drives are envisaged as being on an aircraft mounted accessory drive system (AMADS). The AMAD system is powered by a single high speed power extraction pad on the SDG. This pad is shown on Figure 4.13-1 and is virtually identical with that also shown on the three branch SDG of Figure 4.6-13. The maximum rating of this power extraction pad is nominally:

400 horsepower (at)
20,000 RPM

These values are believed to be more than adequate for the AMADS.

This AMADS drive consists of a high speed bevel gear drive providing a 45° power takeoff (PTO). The airframe required accessories, including the propfan brake would be on this remote gearbox. The design of this gearbox was not undertaken as part of this study. The PTO bevel gears from the main reduction gearbox were designed for 400 hp which is judged to be consistent with the airframe requirements for the 1990 time period. Current gear design stress levels were used for this bevel gear mesh. Bending stresses of 27.9 ksi and compression stresses of 156.6 ksi were considered suitable for this design and are within the state of the art. Bearing lives over 20,000 hours were calculated.

As will be discussed in later sections this gear train operates at 100° F higher temperatures than current technology. The gears would use the same material as the main reduction gears and the bearings would be M50 or M50NIL.

This pad is located at the lower rear of the SDG and a typical connection to an AMADS is shown by the installation of Figure 4.7-9. The majority of the drive components are on a single removable module that contains the shaft, bearings, oil seals, spline, and gear. Only the mating gear cannot be removed without an SDG disassembly.

Mounted to the aft side of the main reduction gearbox are two lube and scavenge pumps. Two are provided for redundancy consistent with helicopter experience and these are mounted directly to the main housing to facilitate internal porting and lube transfer to eliminate any need for external lines.

An internal drive has been provided for the Pitch Change Mechanism (PCM). The PCM intended for use with this reduction gearbox is the electric system described in Task VIII. This PCM does not require a conventional speed governor or control powered by the reduction gearbox, so none is provided.

4.13.7 Main Reduction Gearbox Preliminary Design Details

The detailed discussion of the main reduction gearbox covers the following areas:

- Configuration.
- The kinematic arrangement with a four-stage design compared to a three-star configuration.
- The gear design and certain advanced concepts.
- The bearing arrangement and bearing criteria.
- Lubrication system.
- Heat generation and efficiency.
- Reliability.
- Gearbox housing design.
- Gearbox/Propfan interfaces.

- Engine/Gearbox interfaces.
- Gearbox Physical Description.
- Maintenance.
- Gearbox weights.
- Costs.

4.13.7.1 Configuration

The configuration chosen, that of a compound star gear, possesses many desirable attributes for this application which caused it to be the preferred selection. The principal advantages of the compound star are:

- Elimination of planet bearings operating in a high "G" field
- Favorable score in the trade study
- Compound configuration has the efficiency of a single stage simple star with the ratio capability of a two-stage star system
- Produces an in-line SDG, which is desired, as the alternative SDG designed was an offset configuration.
- Simpler design with projected lower development costs than an equivalent planetary system
- Configuration easily accommodates both a high speed shaft coupled to the bore of the sun gear, which powers the PCM, and an oil transfer bearing for lube and cooling flow to the PCM
- Earlier generation turboprops required an SDG with a much higher numerical ratio (see Section 4.6.2.1 for this summary). A requirement for a much higher ratio than that required by current propfan technology would make the single-stage compound star gear arrangement much less competitive.

4.13.7.2 Kinematic Arrangement

A compound star arrangement is basically simple kinematically but there are certain considerations which require attention. These include the selection of the number of stars, after which the selection of teeth numbers must be made.

The "current technology" in-line design utilized a three star arrangement. During Task VII, efforts were made to reduce the size/weight of the gearbox by adding one more star gear to produce a reduction of the overall size and weight. A study of the gear ratio of the first and second stage of gearing was made to define ratios that would allow an additional star and also provide adequate material between the stars for the carrier support structure.

Also very important is the proper selection of the individual gear teeth numbers. A computer program was used to consider the following criteria:

- Assembly with four branches
- "Hunting" tooth action
- Non factorizing with number of stages

For a four-star arrangement, a gear ratio range and gear mesh tooth numbers were studied and possible combinations meeting the above criteria were calculated. Table 4.13-1 shows the final selection made compared to the 3-star design.

Table 4.13-1. Comparison of Three to a Four Star Kinematic Arrangement.

	4 Star	3 Star
<u>Stage 1</u>		
Pinion	30	33
Gear	53	66
<u>Stage 2</u>		
Pinion	22	24
Gear	91	87

Notice that the 3-star arrangement did not meet "hunting" tooth action in Stage 1, but the same computer techniques could have been applied to this arrangement. The teeth number would have varied slightly but the basic sizing would be unaffected. The gear ratio of the first stage was reduced by 13% to allow more material between the gears in the structure.

The final gear ratio selected was 7.3076:1 which meets turbomachinery and propfan speed matching requirements.

4.13.7.3 Gears

Various gear tooth geometries were studied during the preliminary design of the reduction gearbox. The following geometries considered:

- Spur versus helical gears
- High profile contact ratio gearing

Spur versus Helical

Although helical gears do offer desirable characteristics such as higher efficiency, quiet operation, and higher load capacity (as can be seen in Figures 4.13-2 and 4.13-3), axial loads generated in the mesh must be reacted. The axial load from the output ring gear can be reacted by the ball thrust bearing, and the axial loads in the star gear can be balanced by careful selection of the helix angle in each gear, but to react the thrust load from the input sun gear, a large high speed thrust bearing must be used. From a study made, it was decided to use "zero" helix angle gearing to eliminate the need for this bearing. It would be possible to react the axial load by the engine Low Pressure (LP) turbine but this would introduce difficulties because of the connecting shafting arrangement between the gearbox and the engine. The engine LP turbine is thrust reacted at the rear of the APET turboshaft engine.

An additional problem with the thrust load produced by helical gearing when idler gears, such as the star gears in this SDG, are used is that the thrust loads at the input and output meshes of the idler are in opposite directions. This situation gives rise to a couple, which must be reacted by the idler (or star, in this case) gear bearings. Because of the critical design problem of these bearings, any design which introduces additional bearing loads was avoided.

Tooth Form

Table 4.13-2 shows a summary of the gear design data. The selection of gear tooth pitch has been such as to allow margin in the bending stress (tooth

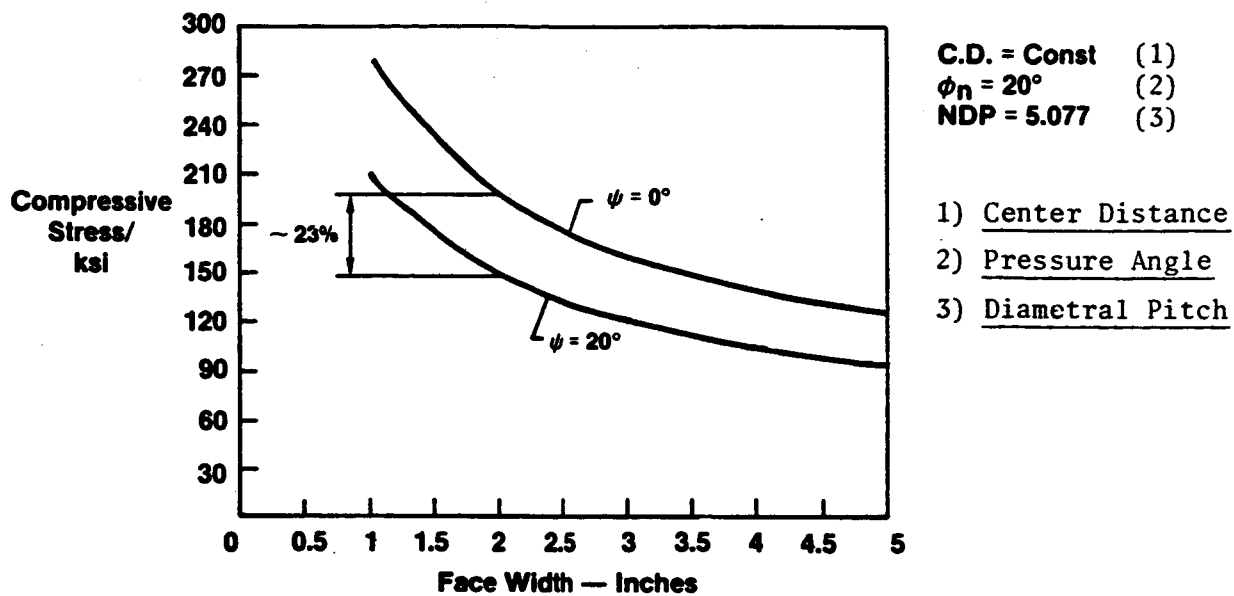


Figure 4.13-2. Compressive Stress Comparison for Helical and Spur Gears.

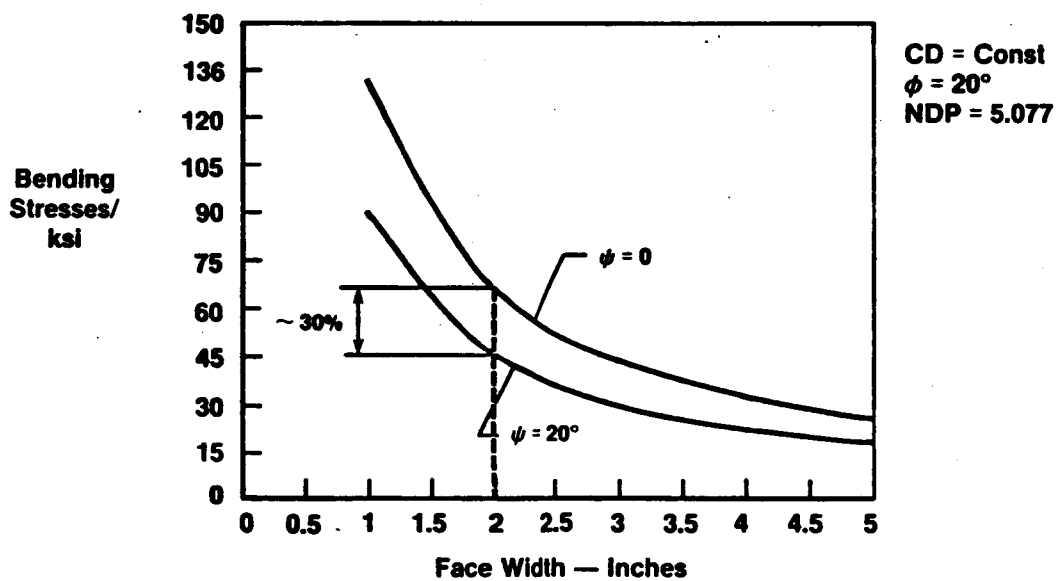


Figure 4.13-3. Bending Stress Comparison for Helical and Spur Gears.

breakage criteria); compressive stress is being used as the design limit although scoring will need further investigation to ascertain whether it may in fact be the actual limiting criteria.

Table 4.13-2. Gear Data, HP = 12,500, Total Gear Ratio = 7.3:1.

	Stage 1	Stage 2
● No. Teeth		
- Pinion	30	22
- Gear	53	91
● Diametral Pitch P	5.00	4.15
● Pressure Angle (deg)	22.5	22.5
● Face Width F (in)	2.35	3.00
* ● K Factor (lb/in ³)	860	742
● Compressive Stress (ksi)	163	162
** ● Unit Load UL (lb/in)	16510	21500
● Bending Stress (ksi)	37.2	48.4
● Temperature Rise (° F)	118	69
<p>*K = $\frac{WT}{FD} \frac{MG + 1}{M_G}$</p> <p>**UL = $\frac{WT}{F} \times P$</p> <p>WT = Tangential Driving Load</p>		

High profile contact ratio gearing could increase the Hertzian stress capability of the gear set by approximately 30%. This type of gearing has been used very successfully by GE on the NASA QCSEE engine but it is sensitive to load sharing between teeth since the bending stress capability of individual teeth is less than that of standard teeth (see Reference 43).

A study was made to ascertain the benefit (if any) of the use of high contact ratio gearing in this application. For this specific instance the benefit is not significant. The incorporation of high contact ratio gearing would also impose an efficiency penalty of approximately 0.3%; which would disadvantage

the system. Although it is recognized that high contact ratio gearing can be a worthwhile feature for some designs, in this particular SDG it was not assessed to have sufficient advantage to warrant further consideration for the detail design.

4.13.7.3.1 Gear Stress Analysis

Stress analysis was performed utilizing American Gear Manufacturing Association Standards (AGMA) 210.02, 220.2 and 217.01. A computer program developed at General Electric, which includes AGMA design equations, was used in the analysis. The calculated stresses are shown in Table 4.13-3 for the output design horsepower of 12,500.

Table 4.13-3. Calculated Gear Parameters.

	Stage 1	Stage 2
Diametrical Pitch	5.0	4.15
Pressure Angle (degrees.)	22.5	22.5
Face Width (in)	2.35	3.00
Compressive Stress (ksi)	163	122
Bending Stress (ksi)	37.2	48.4
Mesh Temperature Rise (° F)	118	69

4.13.7.3.2 Gear Materials

For a gearbox of the 1990's it is anticipated that the design allowables must be improved. Design allowables for an advanced gearbox are shown in Table 4.13-4

Table 4.13-4. Gear Design Allowables, Current Versus Advanced.

	Current (AMS 6265)	Advanced
Compressive Stress (ksi)	135-151	165
Bending Stress (ksi)	40-50	60
Scoring Flash Temp.(° F)	275 (Low Risk)	Testing Required
Max. Operations Temp.(° F)	350	450

As can be seen, these are extensions over current practice. Justification for the use of these higher values are:

- More precise determination of material allowables (both bending and compressive).
- Improved lubricant (compressive, scoring).
- Change in gear material (compressive & bending).
- Better control over bearing center distance variations by thermal management.

Some experimental data on CBS600, Vasco-X2 Modified and Cartech EX-53 have indicated improvements in load capacities over the present capability of AMS6265 although all experimental data does not substantiate the higher capability of VASCO-X2 Modified (Reference 35). Reference 36 indicates a bending stress improvement of approximately 20% for Vasco-X2; another source, Reference 37 indicates an improvement of about 25% in compressive stress capability when compared to AMS6265. Additional evaluation of CBS600 will be needed to determine its relationship to AMS6265 since Reference 38 indicates no basic difference in compressive stress capability. Unreported testing of Cartech EX-53 at NASA Lewis indicates this material shows a life improvement when compared to AMS6265 material.

Another material being developed by the General Electric Company under Air Force Contract is a modified M50 material. These modifications allow this normally through hardened material to be case hardened for improved fracture toughness. This material has been successfully tested for turbine mainshaft bearings and would certainly be a candidate for a high temperature gear material. Gear testing must be accomplished to confirm its suitability as a gear material.

All of these materials have higher tempering temperatures which should move the threshold at which scoring occurs upwards from AMS6265. The flash temperature capability would have to be determined by component testing.

4.13.7.3.3 Gear Scoring

Gear scoring, especially when operating at the elevated temperatures proposed for this design needs further investigation. Scoring thresholds are dependent not only on the gear tooth meshing geometry but also mesh sliding

velocities, and the compatibility of the lubricant and the gear material. An improvement in life is forecast if the gear tooth flank surface finish is improved from the current standard combined with an overall improvement in filtration of the lubricant. A 5 micron absolute system filtration level would be selected for the advanced gearbox, for both bearing and gear life improvement objectives.

4.13.7.3.4 Load Sharing Provisions

When calculating gear-mesh stresses, load sharing must be considered. Some designs are derated to account for this but for the proposed gearbox it will be accounted for by careful attention to detail design.

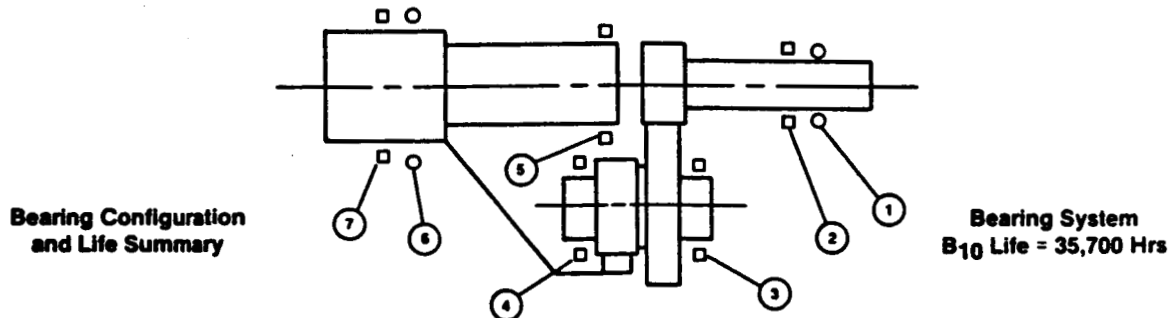
Three principal areas in this SDG bear the responsibility for assuring that the torque is appropriately shared by the four branches. They are:

- Precision and Tolerancing: Each star pinion, because of the compound design, carries two gears. These gears must be timed, one relative to the other. A second critical area is the relative accuracy of location of the centers of rotation of the star pinions.
- Mesh Centered Sun Gear: The sun pinion is not constrained radially but is instead free to be mesh centered by the four mating star pinions. The center distance of each meshing pair (with the sun gear always being one gear of the "pair") will be what is required for equal load sharing. Four pinions is the maximum number that can be used and still allow this mechanism to perform at maximum effectiveness, although this is still a viable concept with a greater number of pinions.
- Flexible Ring Gear: The ring gear is not designed to be a rigid structure, but instead is a compliant band. In addition, the ring is attached to the SDG output shaft by a flexible coupling that allows both radial misalignment as well as a deviation from perfect roundness of the ring. This coupling is shown in Figure 4.13-1. As a result, each segment of the ring that is in contact with its mating star pinion at any instant may be thought of as being "mesh located" in a fashion similar to that of the sun gear.

4.13.7.4 Bearing Design

Shown in Figure 4.13-4 is a summation of the bearing characteristics, loads and lives. The bearing Cubic Mean Loads (CML) were calculated from a typical mission profile shown in Figure 4.13-5. With a maximum power level of

12,500 hp the calculated cubic mean power is 6885 hp. The resultant system life is 35,700 hrs which is in excess of the goal for the next generation of turboprop reduction gearboxes. Figure 4.13-6 shows the output from the computer analysis of the bearing reactions of the star gear.



Pos.	Mean Dia. (Inches)	Element Size (Inches)	Number Elements	Dynamic Capacity (lbs)	CML Load (lbs)	Max Speed (rpm)	B10 Life (Hours)
1	5.500	.800	18	18,270	AX. 390 Rad. 370	8460	1,053,000
2	5/5--	.800	18	42,970	720	8460	7,130,000
3	6.600	1.250	14	88,800	6850	4790	182,000
4	6.600	1.250	14	88,800	7365	4790	143,000
5	7.870	.830	26	61,400	5650	1160	254,100
6	12.440	1.680	18	55,800	8950	1160	178,000
7	12.000	1.340	22	132,700	7630	1160	1,290,000

Figure 4.13-4. Bearing Load and Life Summary.

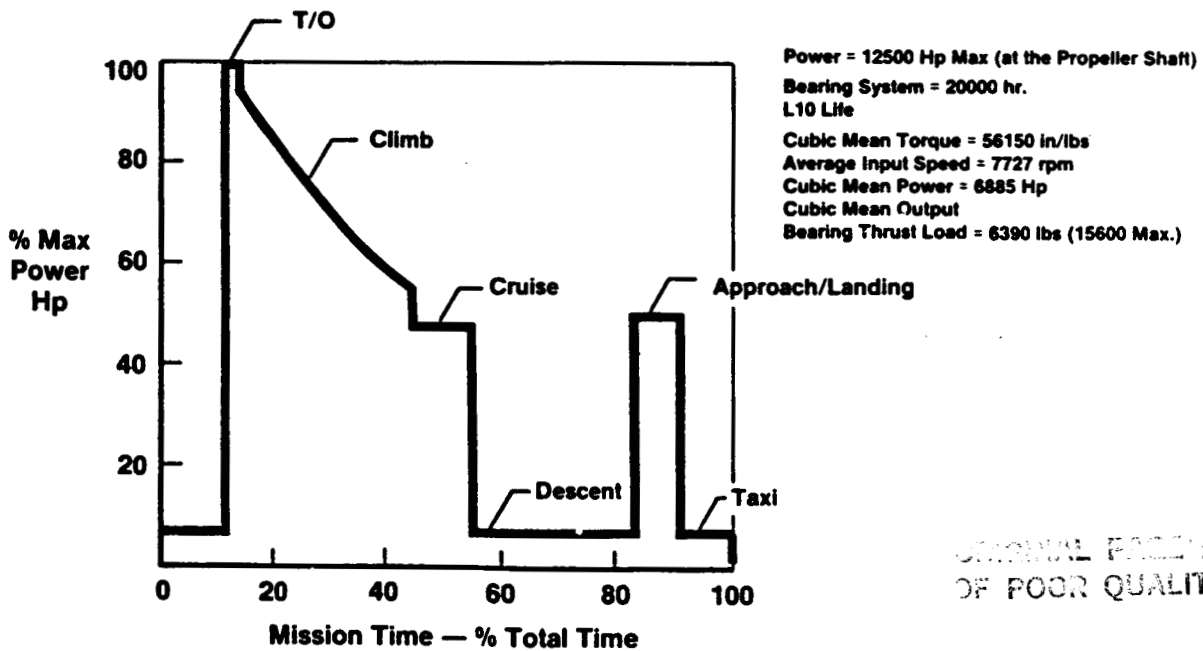


Figure 4.13-5. Typical APET Mission Profile.

ORIGINAL PAGE IS
OF POOR QUALITY

Gear Forces					Bearing Forces					
Gear	Mesh	Axial	Radial	Tang	Bearing	FX	FY	FZ	Frad	Ang
1	1	0.	3471.46	9537.75	1	0.	7155.6	1744.9	7365.3	193.7
2	1	0.	1625.67	-4466.50	2	0.	6848.7	100.9	6849.4	180.8

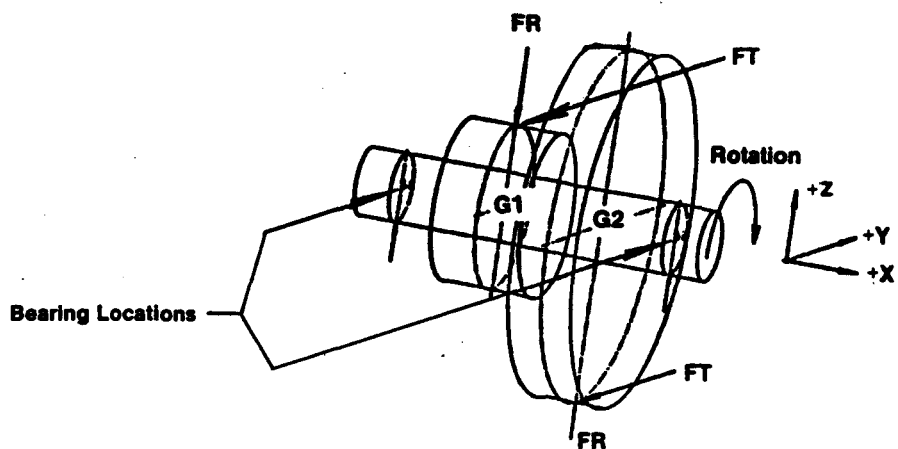


Figure 4.13-6. Star Gear Forces and Bearing Reactions.

System life is calculated using the expression

$$L_{\text{sys}} = \left[L_1^{-\beta} + L_2^{-\beta} + \dots + L_n^{-\beta} \right]^{-1/\beta}$$

L = L10 of individual bearing using cubic mean power.

β = Weibull slope constant of 1.5 which is consistent with General Electric engine experience

where L_n represents the L10 lives of individual bearings. The number of bearings can greatly affect the system life and individual bearing lives must be high to achieve the desired overall life.

Fatigue type failures are only one of the modes of distress for antifriction bearings. Other important considerations are:

- Race rotation which leads to excessive clearance between the bearing and the gearshaft causing gear misalignment and premature failure.
- Cage failure which creates a vibration and secondary damage to surrounding hardware.
- Contamination scratches leading to earlier than anticipated fatigue failures.
- Material subsurface defects that are undetermined by nondestructive inspections.

Race rotation is controlled by maintaining tight fits throughout the operating range, and the gearbox requires a detailed thermal analysis with speeds and initial shaft fitups to determine the operating fits of bearings on their respective shafts. As shown in Figure 4.13-1 each bearing inner ring is clamped with a highly torqued nut, and if the inner ring can be eliminated this should be done. The bearing outer races are all bolted in place.

Cage failure is minimized by careful attention to design details such as materials, coatings, pocket fitup and clearances to adjacent rings.

Contamination damage is greatly reduced by initially providing a clean lubrication circuit and maintaining it during operation. The inclusion of a low micron absolute filtration system, assembly clean room procedures, and elimination of external lubrication circuits all contribute to the improvement in reliability of this design.

4.13.7.5 Lubrication System Design

The lube system schematic is shown in Figure 4.13-7. Major features of the lube system are:

- A lube tank integral with the forward support housing.
- Dual supply and scavenge pumps for redundancy.
- Separate lube subsystem for the PCM to provide oil which is cooler than that supplied to the main reduction gearbox.
- Modulating flow valve to vary the main gearbox flow rate proportional to torque demand.
- Elimination of most external lines.
- Revised oil chemistry to provide high load carrying and temperature and the selection of a high temperature capability oil.
- Improved filtration.
- Clean room assembly and test.

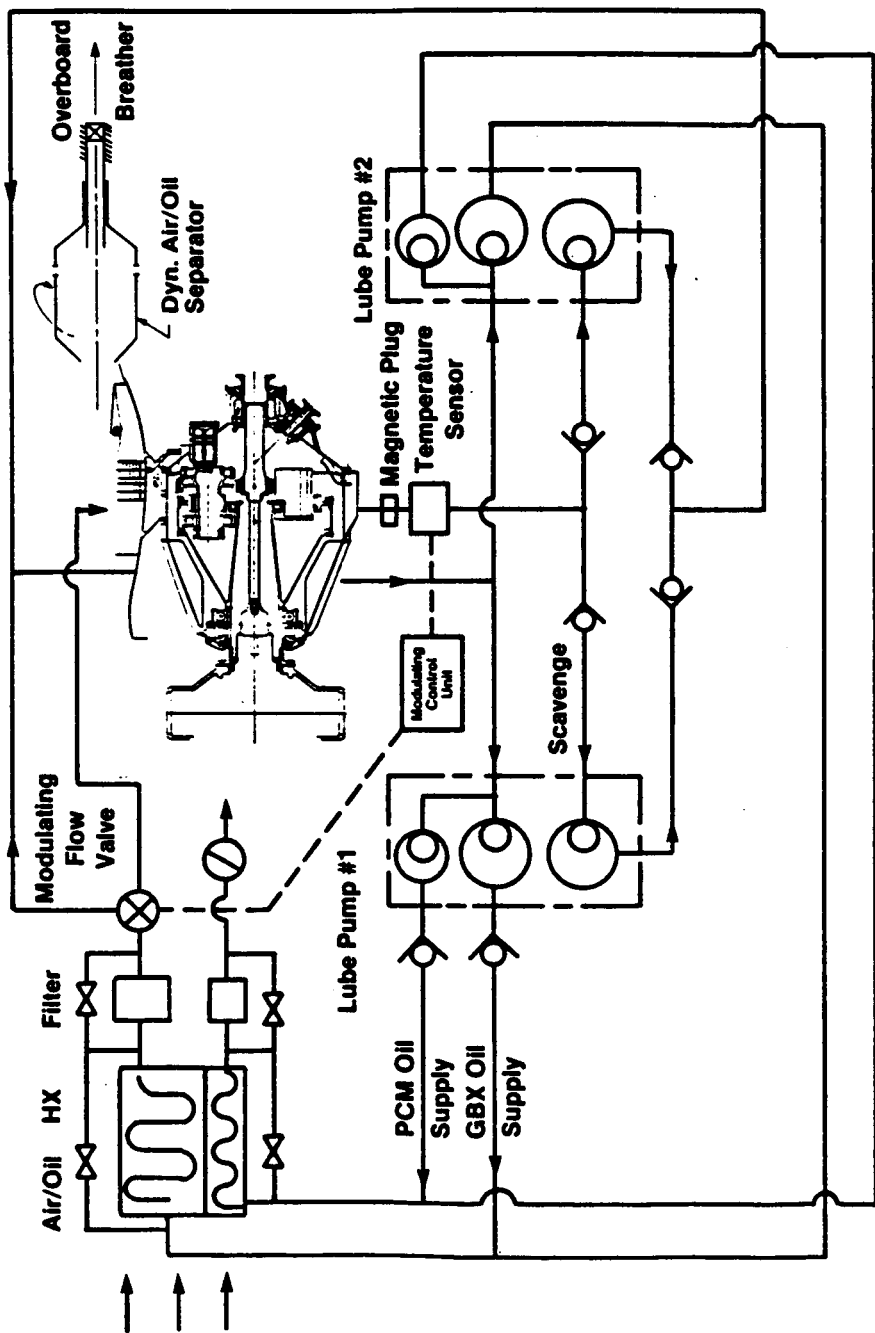
An important consideration in the development of the next generation of turboprop reduction gearboxes will be the lubricant evaluation and selection. The use of present light viscosity turbine engine oils (Mil-L-7808 or 23699) unnecessarily penalize the design objectives of a lightweight, efficient and highly reliable gearbox. The proposed gearbox lube system would be totally separate from the engine system. The lubricant requirements proposed are as follows:

- 300° F Oil supply temperatures
- 450° F Gear blank temperatures
- -20° F Cold starting temperatures *
- 165 ksi Allowable compressive stress

* Cold starting below -20° F would be facilitated by using the built-in electric heater before engine start to bring the gearbox oil temperature up to the -20° level.

Some preliminary studies indicate a Synthetic Hydrocarbon, Diester oil (for example, Emgard EP75W-90) optimized for 300° - 350° F would generate

ORIGINAL QUALITY OF PRINT GUARANTEED



- Check Valve
- ⊗ Cooling Flow
- ⊘ Bypass Valve

- Oil Tank Includes:**
- Oil Heater
 - Static Air/Oil Separator

Figure 4.13-7. Lube System Schematic.

adequate specific film thickness parameters to support the gear loads through the operating range. Extensive evaluation work in regard to both gears and bearings remains to be accomplished.

4.13.7.6 Heat Generation and Efficiency

The principal features of this reduction gearbox design that promote high efficiency are:

Single Stage Design: The choice of a compound star configuration allows the demanded ratio to be achieved by a single stage while still permitting the geometry to remain in a weight-advantaged range. The choice of a simple star design would have necessitated two stages of reduction, with essentially twice the losses, or if a single stage design were executed, it would be severely weight disadvantaged. In order to accomplish the required ratio in a single stage, the star pinions would be very large compared to the sun pinion. This would restrict the number of branches that could be incorporated, thus impacting the weight. Figure 4.6-2 in Section 4.6.1.3 shows the effect of ratio of a star system on weight factor.

Use of Spur Gears: Had high contact ratio gearing been employed, the meshing losses would increase, as the efficiency of this type is somewhat lower.

Lubrication System Features: The use of an elevated oil operating temperature (approximately 100° F higher than the current level permits a greater differential temperature (oil in to oil out). This enables the heat generated due to gearbox losses to be picked up by a smaller quantity of oil. Reduced oil flow also results in reduced churning losses, and a lightweight heat exchanger.

In addition, an oil flow modulating system is included. Only when operating at peak torque levels is maximum oil flow provided. At reduced torque levels the flow is reduced proportionately, which further aids in the reduction of churning losses. The oil flow is modulated as a function of oil differential temperature, thus the system functions with a nearly constant differential temperature even though the power transmitted (and hence the losses) varies throughout the mission.

4.13.7.7 Reliability

For economic reasons it is clear that in order to achieve commercial acceptance, a modern propfan gearbox must exhibit levels of reliability more than twice that demonstrated by previous turboprop gearboxes. The goal set for this study is a MTBUR (mean time between unscheduled removals) in excess of 20,000 hours.

The approaches taken in this study to achieve a high reliability goal are as follows:

- Bearing system life is compatible with the gearbox MTBUR goal. The bearing lives are shown by Figure 4.13-4.
- Elimination of all functions from the reduction gearbox which are not related to the primary job of driving the propfan and the PCM. The one exception is a power takeoff to drive the AMADS.
- Choice of a single-stage design with its attendant simplicity and low parts count.
- Choice of a star design instead of a planetary configuration. The problems of planet bearings operating in a high G-field are thus avoided. The problems of jetting oil to planet pinions are also circumvented, as moving jets mounted onboard the planet carrier are not necessary. In summary, the inherent simplicity, as compared to more complicated planetary configurations, of this design is seen as working to the advantage of reliability.
- Where deemed advantageous, separable bearing races are avoided.
- Use of spur rather than helical gearing. This relieves the bearing system of the task of reacting thrust loads.
- Splines are used sparingly in the design. Only the minimum number necessary are employed and care is taken to avoid placing them in areas that will not provide an optimum environment, such as areas where shaft bending is high. All splines are straddled by double pilots to preclude the possibility of bending loads impairing the spline function.
- Both the oil tank and the heat exchanger are designed integral with the gearbox. This eliminates any external fluid lines and connections, all of which are opportunities for leaks.

4.13.7.8 Gearbox Housing Design

The three branch compound star gearbox of Figure 4.6-13 was designed with a light-alloy housing. Given the fact that the density and the modulus of elasticity of typical engineering materials suitable for housings vary together, the best stiffness-to-weight ratio is obtained with the least dense material, typically magnesium alloys. This conclusion is further enhanced by the fact that frequently wall thicknesses are chosen not because of stiffness or strength considerations, but because of casting limitations, and requirements for internally cored passages.

The housing material chosen for the three branch design, however, was aluminum rather than magnesium. A slight sacrifice in stiffness-to-weight was deemed appropriate as magnesium is a very active metal and approaches to corrosion protection must be carefully considered. Another factor mitigating against the choice of magnesium is its softness, which necessitates greater use of fastener inserts and bearing liners.

A 100° F elevation of lube temperature for the four branch compound star gearbox design of Figure 4.13-1, however, essentially rules out the choice of a light alloy housing because the material strength has begun to degrade unacceptably at the projected maximum operating temperatures. A fabricated titanium housing was selected instead. Additional benefits, other than retention of strength at temperature, are:

- Inherently good corrosion protection, thus additional operations in surface treatment are eliminated.
- Low coefficient of thermal expansion, thus critical dimensions remain more stable throughout the operating temperature range.
- Experience of General Electric in the fabrication of large titanium structures.

Table 4.13-5 summarizes the various properties of all the examined candidate housing materials.

The housing of the four-star gearbox also incorporates the heat exchanger and the oil tank. As a fabricated assembly, it is clearly superior and less costly to integrate these functions compared with a cast gearbox housing necessitating external system components.

Table 4.13-5. Opposite Rotation Comparison Studies.

• Option	$\Delta W\%$	$\Delta \text{Eff. } \%$	Comments
- Offset Adapter Gearbox	13	-.76	No Longer "In-Line"
- In-Line Adapter Gearbox	25.7	-1.44	Many Gears and Bearings
- Additional Star Gear Idlers	19.3	-.80	Probably 3 Star Gear System 3 Additional Gears 6 Additional Bearings
- Reversed LP Turbine Rotor	0	0	Major Engine Changes
- Star Gear and Epicyclic Arrang.	0	0	Two Unique Gearbox Designs
- Compromised Star Gear Arrang.*	Ext. Mesh		No Additional
	13.2	+ .08	Gears and Bearings
	Int. Mesh		But Larger Than Baseline
	26.7	-.10	

*Compared to Baseline

4.13.7.9 Gearbox/Propfan Interface

The propfan, with the electric PCM of Task VIII (as shown by Figure 4.14-1) places three principal requirements upon the gearbox.

- The connection between the gearbox output shaft and the propfan hub is by a flanged, bolted joint with a curvic coupling to provide concentricity and to transmit the torque. The propeller thrust load is taken by the bolts in tension; bolt bending and shear is thus eliminated.
- A high speed shaft concentric with the SDG output shaft powers the electric PCM alternator. In the case of the advanced SDG, this shaft is splined into the bore of the sun gear, and thus rotates at engine low pressure turbine speed.
- The stationary portion of the optical slipring is supported by the nose of the SDG and must be positioned with suitable concentricity relative to the centerline of the output shaft. The redundant optical cables supplying the signals are routed over the outside of the SDG housing to make connections with the stationary half of the slipring.

4.13.7.10 Engine/Gearbox Interface

There are two physical connections between the engine and the gearbox. The gearbox input drive shaft is constructed integral with the sun gear. The rear of this shaft is splined into the engine low pressure turbine shaft which, at this station, is more properly considered the booster front shaft. A spline permitting slight misalignment is required, as the sun gear is mesh-centered and slight radial movement is permitted to effect load-sharing among the branches. This splined joint is configured such that the SDG input shaft is axially constrained relative to the booster front shaft and thus the SDG sun gear is positioned axially by the engine low pressure system thrust bearing. Gage spacers may be used, if necessary, to ensure that the sun gear assumes the correct axial position relative to the mating SDG pinions.

An outer tube with a stiff flanged connection at either end connects the gearbox housing rigidly to the engine. Discussions with the Lord Corp., indicated that a rigid gearbox/engine connection was the preferred mounting and installation arrangement. Such considerations as assuring safety from whirl flutter in the case of a failed elastomeric mount situation are made easier with this design.

Four equally-spaced pads for elastomeric mounts are provided on the exterior of the gearbox housing. These mounting points are responsible for reacting thrust, vertical and side loads, and torque. A rear engine mount is provided for reacting vertical and side loads but it does not restrain the engine against axial movement (thrust) or torque (roll about the engine centerline). This mounting arrangement is shown in Figure 4.13-8.

4.13.7.11 Gearbox Physical Description

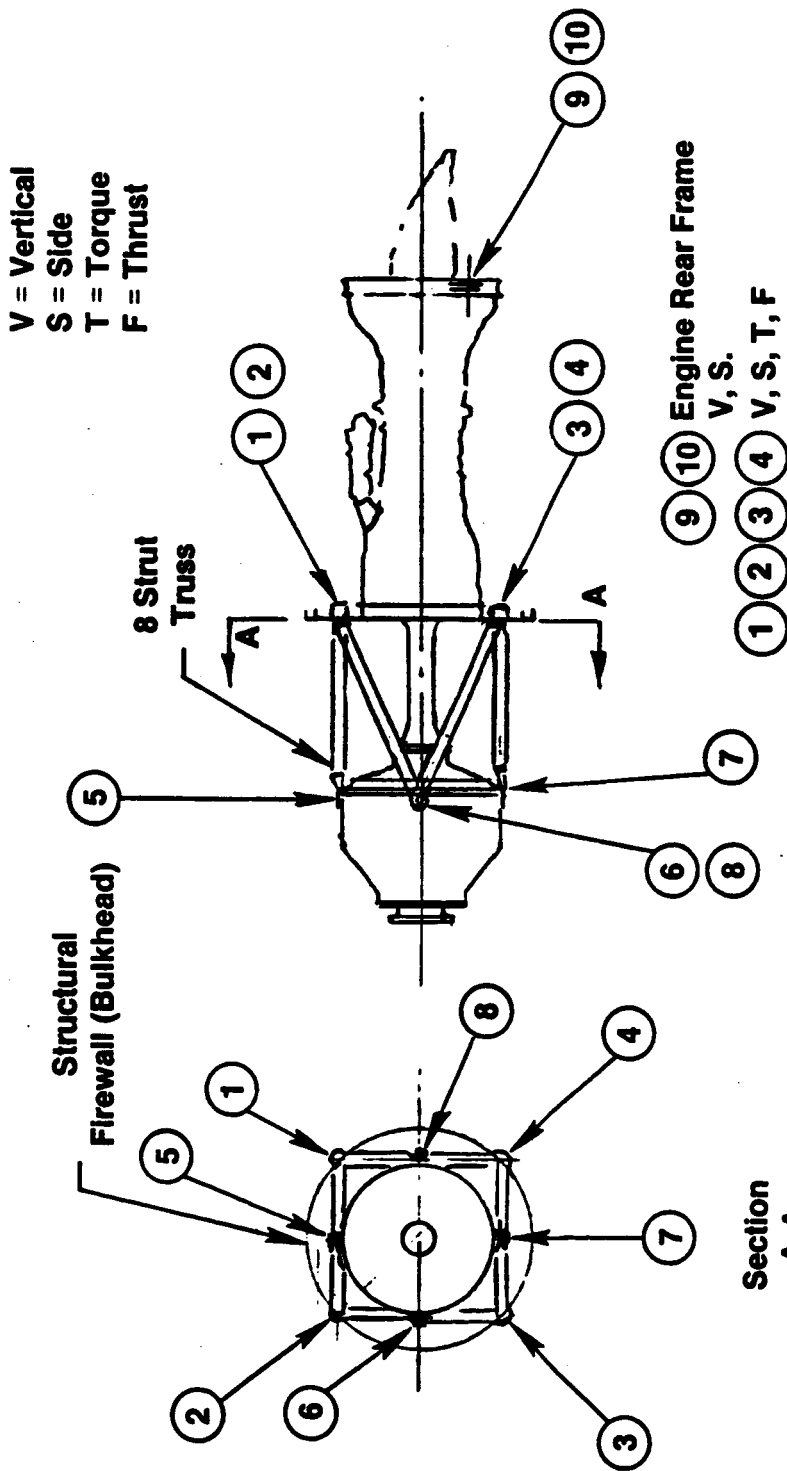
The gearbox preliminary design produced in Task VII is an in-line design (input and output shafts on the same centerline). From a gearbox designer's standpoint there is little to choose between in-line and offset configurations; the choice is largely affected by installation considerations of the aircraft application.

The ratio of this gearbox is 7.3075:1, which is a slight change in numerical ratio from the 7.25:1 of the gearbox described in Task III. This slight ratio change permits more desirable tooth action as is described in Section 4.13.7.2. The weight saving between the three branch gearbox of Task III and the four branch gearbox of Task VII is 178 pounds.

4.13.7.12 Maintenance

Many features in the gearbox of Task VII are responsible for a projected reduced maintenance burden. They are:

- Design is for a long system life. Conservative criteria is used for bearing and gear selection.
- The titanium housing is inherently corrosion resistant. Also because of the hardness of titanium, the use of inserts and bearing liners as compared to the use of a light alloy casting is greatly reduced.
- The use of an integral oil tank and a heat exchanger attached to the housing eliminates all external lines and fluid connections thus reducing the areas that traditionally require significant maintenance.
- Elimination of all functions possible that do not relate directly to the primary job of driving the propfan remove whole systems which have proven to be significant maintenance burdens in the past. An example is the replacement of an accessory drive section by a single power extraction pad for driving an AMADS.



In-Line Gearbox (Side View)

- Engine and Gearbox are Rigidly Interconnected
- Pads 1, 2, 3 and 4 are for a Redundant System of Anti-Vibration Mounts. These are to be Used for Attachment to the Nacelle Structure

Figure 4.13-8. APET Propulsion System Mounts.

- Elimination of splines, where possible, and placement of the remaining splines such that adequate lubrication is present and the probability for wear is low.
- Use of modular construction where feasible. The lube and scavenge pumps are removeable as modules without the necessity of disconnecting any external plumbing. The accessory drive pad is removeable as a module as well. The propfan PCM high speed drive shaft and hydraulic slipping can be removed from the bore of the output shaft without the necessity of disassembling the gearbox or even the need of removing it from the aircraft.
- Shaft oil seals are designed to be externally replaceable without a gearbox disassembly.
- Where possible, separable bearing inner races are eliminated and bearing races are integral with the gear shafts.

Figure 4.13-9 shows the proposed modular arrangement of the gearbox.

4.13.7.13 Opposite Rotation Gearboxes

A preliminary study was done in regard to opposite rotation gear boxes for right and left wing applications. There appear to be at least seven options to accomplish this. These are summarized in Table 4.13-5. Shown in Table 4.13-5 are weight and efficiency delta's compared to the baseline which is the four star in-line configuration. Figure 4.13-10 through 4.13-12 show schematics of these seven arrangements along with some general comments.

4.13.7.14 Gearbox Weight

The total weight and the weight of the various components of the four branch gearbox is shown by Figure 4.13-13. For the same mission, this gearbox is 178 pounds lighter than the three branch gearbox discussed in Task III. The breakdown of this weight savings is as follows:

105 lb	less total weight of gearbox system
34 lb	weight of heat exchanger included in 4-branch G/B
20 lb	weight of heat exchanger support and flowpath
<u>19 lb</u>	additional housing weight to incorporate integral oil tank (3-branch has neither integral tank or heat exchanger)
178 lb	

CRITICAL PARTS
OF POOR QUALITY

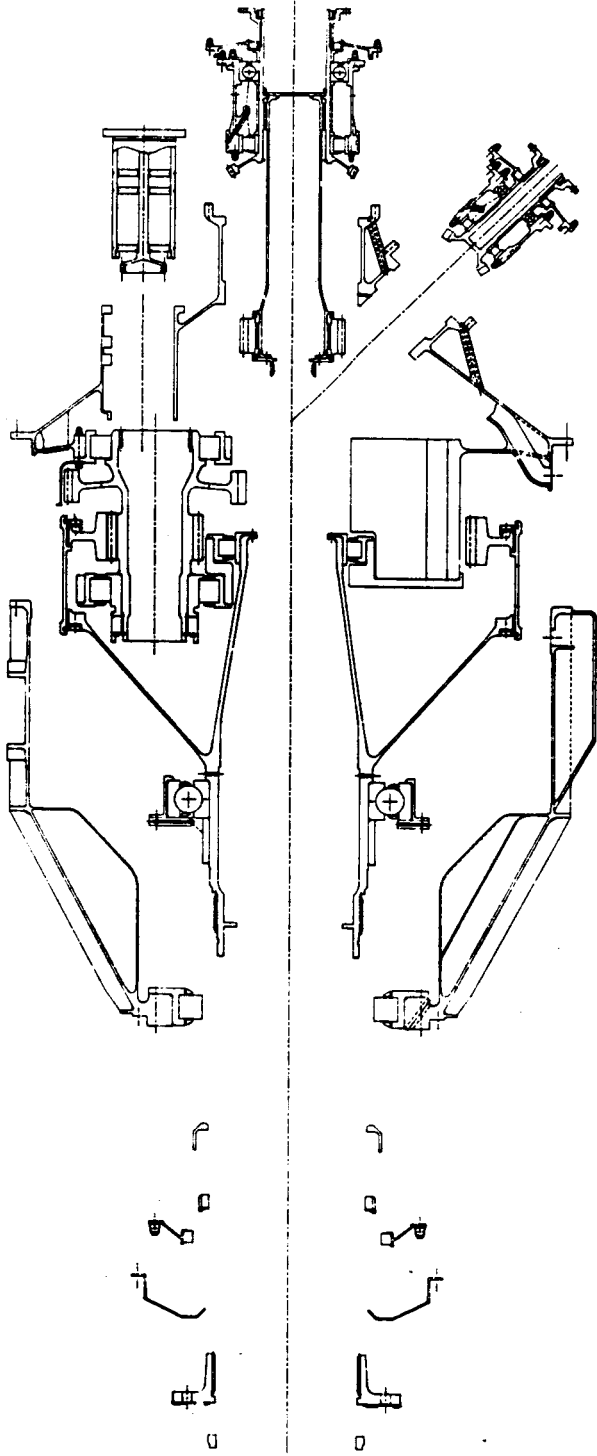
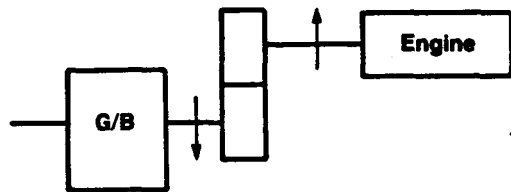
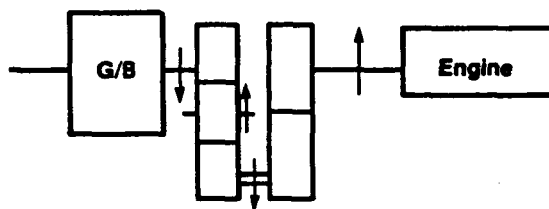


Figure 4.13-9. Modular Breakdown.



- **Offset Adapter Gearbox**
 - 2 Large Additional Gears
 - 4 Bearings
 - Housing and Structure
 - Additional Heat Generation



- **In-Line Adapter**
 - 5 Large Additional Gears
 - 8 Bearings
 - Housing and Structure
 - Additional Heat Generation

Figure 4.13-10. Offset and In-Line Opposite Rotation Gearboxes.

ORIGINAL PLAN OF
OF POOR QUALITY

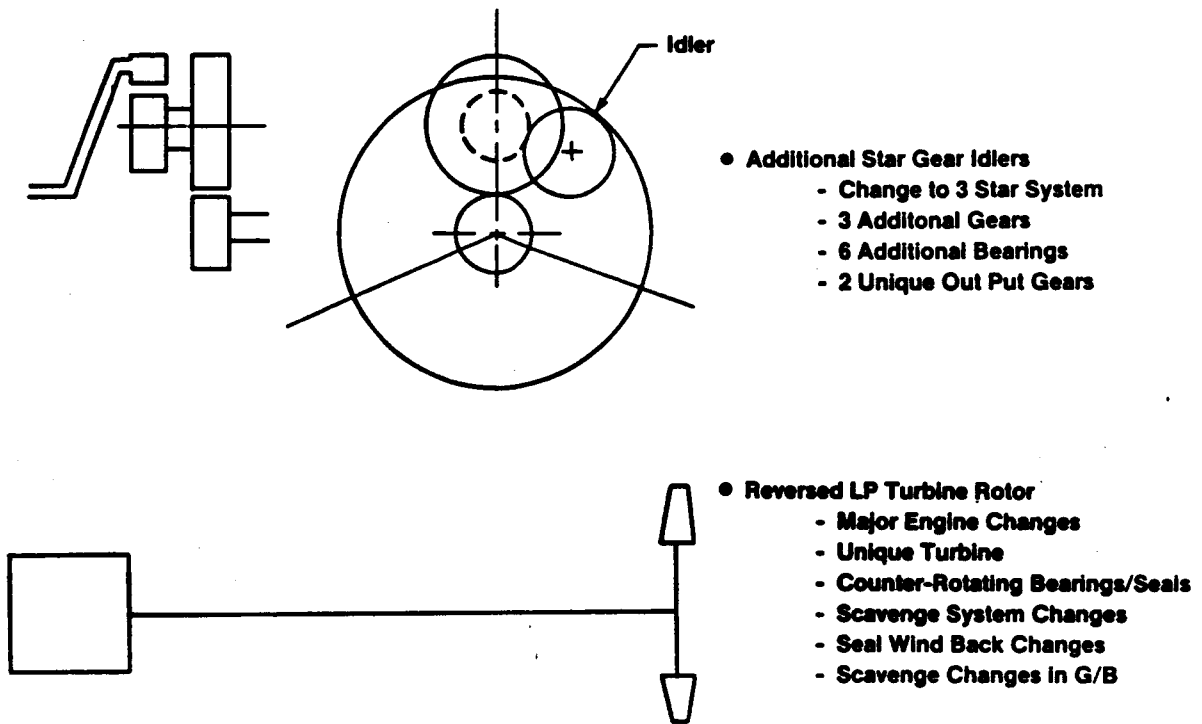


Figure 4.13-11. Added Star Gear Idlers and Reversed LP Turbine Rotor of Reversed Rotation.

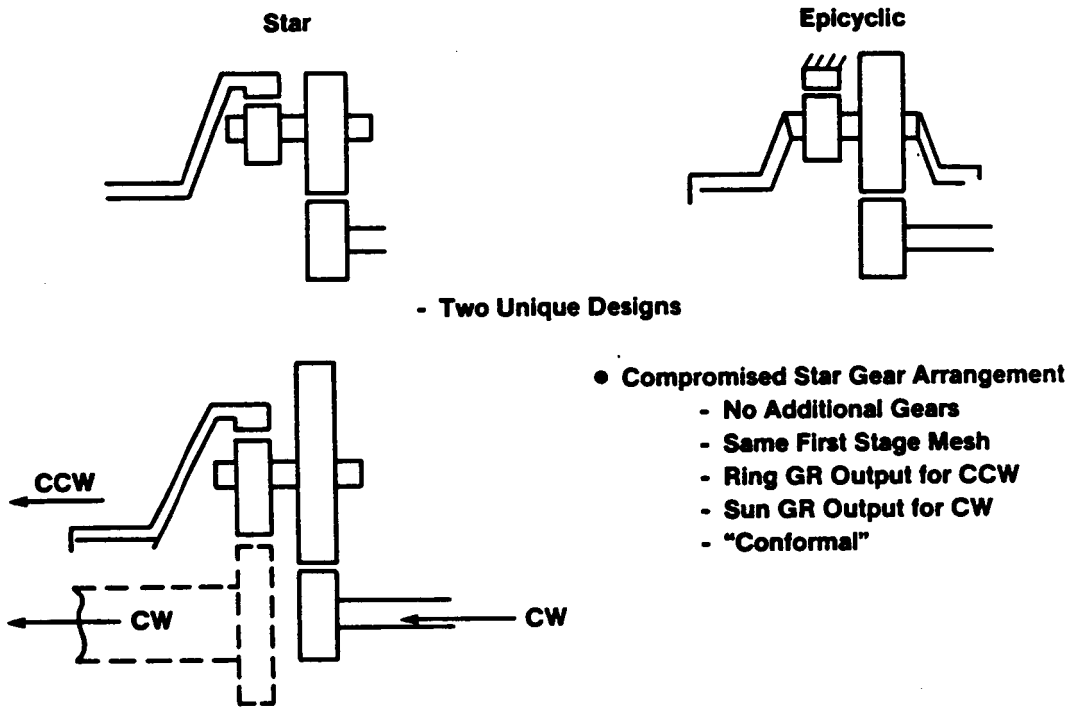


Figure 4.13-12. Star Versus Epicyclic and Compromised Star Gear Arrangement for Opposite Rotation.

ORIGINAL PAGE IS
OF POOR QUALITY

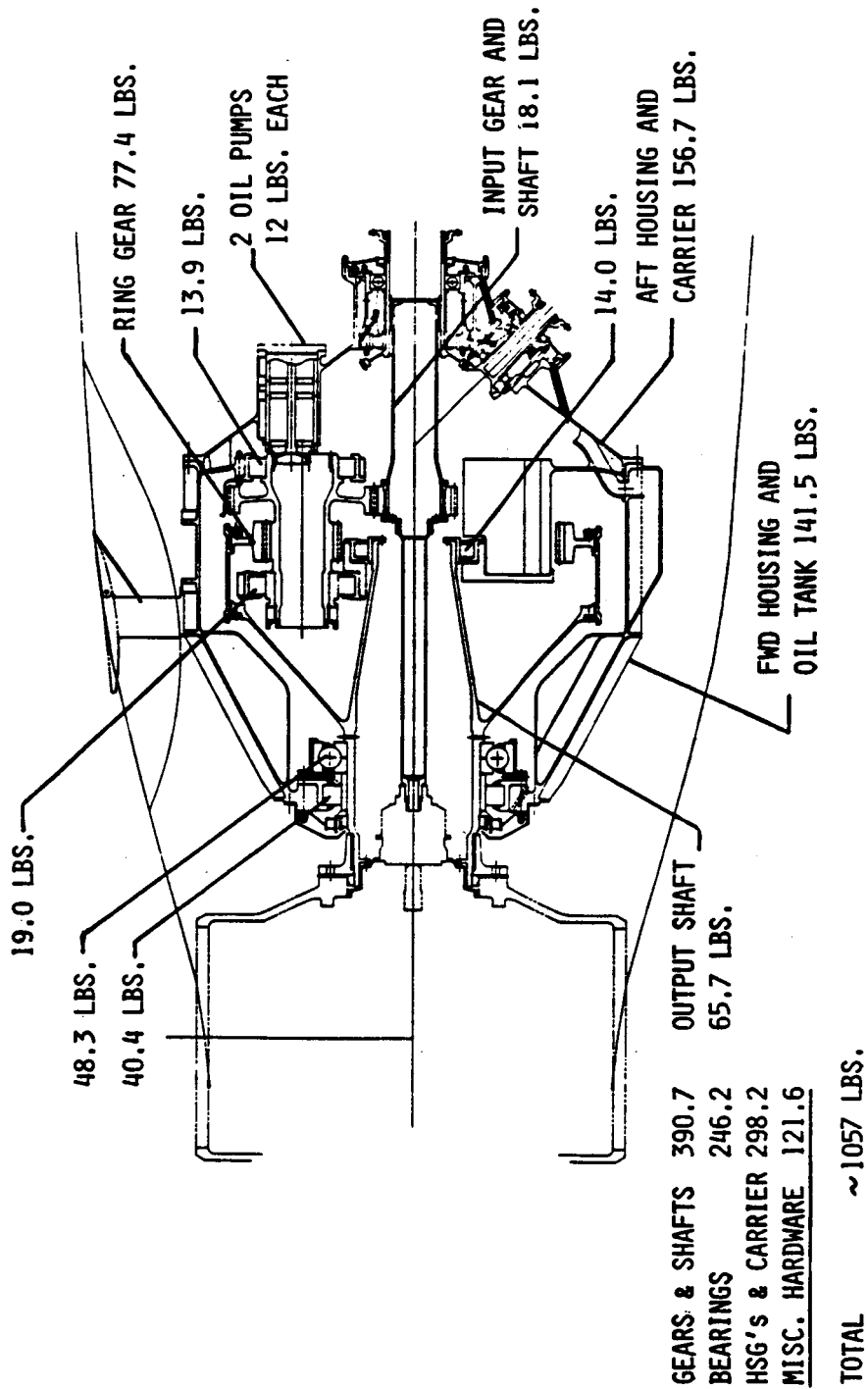


Figure 4.13-13. APET Gearbox Weight.

Weight Scaling

The weight scaling trends shown by Figure III-3 in Appendix III are valid for the four branch compound star gearbox as well as for the offset gearbox.

4.13.7.15 Costs

First costs and maintenance costs have historically been hard to establish. Many turboprop gearbox designs are intimately configured with the gas generator engine, and thus are not amenable to "break out" the isolated costs of gearboxes from the rest of the propulsion system.

In-house manufacturing estimates for the in-line, 4-branch, star configuration have been developed from a detailed cost estimate that was made in Tasks I through VI. The manufacturing shop cost of the gearbox will be in the order of \$180,000 at the 250th unit. However, with normal amortization of design and development costs, the selling price of the gearbox at the 250th unit is likely to be about \$330,000. This price will vary drastically downward if different assumptions are made on the amortization factors.

Maintenance costs for gearboxes in commercial service have historically been low when compared to the maintenance cost of the propeller driven by the gearbox. In general terms, propellers cost about four times as much to maintain as do gearboxes. For this study not much improvement was seen in gearbox first cost factors where parts count heavily favors the least numbers of gears, shafts, bearings, splines, and seals. The selection of titanium fabrication for the gearbox housing is adverse on first cost, but does allow the achievement of lower maintenance costs.

A maintenance "cost factor" of about 15% of gearbox first cost is estimated to be achievable with a gearbox designed for 20,000 hours MTBUR. On a \$330,000 gearbox price this then equates to an overhaul cost of \$49,500, or \$2.475 per flight hour. This is at least as good a value as is being achieved by gearboxes from 1/3 to 1/2 the horsepower of the APET gearbox.

SECTION 4.14

PITCH CHANGE MECHANISM CONCEPTUAL DESIGN

<u>Section</u>	<u>Page</u>
4.14.0	377
4.14.1	382
4.14.2	385
4.14.2.1	385
4.14.2.2	388
4.14.3	388
4.14.3.1	388
4.14.3.2	391
4.14.4	392
4.14.5	392
4.14.6	400
4.14.7	402
4.14.7.1	402
4.14.7.2	409
4.14.8	409
4.14.9	412
4.14.10	412
4.14.10.1	412
4.14.10.2	413
4.14.11	413
4.14.12	417

FIGURES

<u>Figure</u>	<u>Page</u>
4.14.1. Advanced Technology Pitch Control System.	383
4.14.2. Pitch Control Mechanism Based on Dual Drive Bevels.	387
4.14.3. Pitch Control Mechanism Based on Ballscrew and Nut.	389
4.14-4. Combined Speed-Increasing Train and Emergency Feather Mechanism.	390

FIGURES (Concluded)

<u>Figure</u>	<u>Page</u>
4.14-5. Pitchlock Schematic Normal Operation.	393
4.14-6. Pitchlock Schematic Lock Engaged.	393
4.14-7. Pitchlock Drive.	395
4.14-8. Cross Section of Optical Slipring.	397
4.14-9. Schematic of Slipring.	397
4.14-10. On-Axis View of Slipring.	398
4.14-11. Source Reflection Patterns.	398
4.14-12. Modulation from Source Pattern.	399
4.14-13. Slipring With 3 Source Fibers and 4 Detector Fibers.	399
4.14-14. Traction Drive Arrangement for 210:1 Ratio.	403
4.14-15. Traction Drive Arrangement for 210:1 Ratio.	404
4.14-16. Basic Interior PM Synchronous Motor.	406
4.14-17. Basic Switched Reluctance Motor.	407
4.14-18. PCM Control Schematic.	411
4.14-19. Full Power Losses.	414

TABLES

<u>Table</u>	<u>Page</u>
4.14-1. Design Parameters Used for This Study.	386
4.14-2. Performance Estimate.	401
4.14-3. Performance Estimate.	401
4.14-4. APET PCM-Motor/Generator Choices.	405
4.14-5. Recent Technological Advances Important for AC Drives.	407
4.14-6. Motor Design.	408
4.14-7. Motor Scaling.	408
4.14-8. Generator Design.	410
4.14-9. Generator Scaling.	410
4.14-10. Failure and Effects.	415
4.14-11. Failure and Effects.	416
4.14-12. Propfan Summary.	417

4.14 PITCH CHANGE MECHANISM CONCEPTUAL DESIGN

4.14.0 Design Objectives and Concepts

About three years ago General Electric identified the need for substantial improvements in the overall level of reliability that would be required for a propfan pitch change mechanism (PCM) and its controls. These were formulated into the following list of highly desirable features:

1. An autonomous power source. Do not recommend use of gearbox oil.
2. Completely separate motive power for emergency feather.
3. "Closed loop" functions within the rotating propeller assembly.
4. Redundancy of control inputs with FADEC having the highest level of authority. Complete ground check-out capability.
5. Modularity and ease of component(s) removal.
6. A traveling mechanical pitch lock. External power required only for un-lock functions.
7. Highly precise pitch selection. Hysteresis held to a minimum.
8. Self-generated anti-icing power supply
9. Self-test systems and diagnostics.
10. Ease of maintenance e.g. no external lubrication of components required.
11. Friction/wear points (e.g. seals) held to a minimum.
12. No filters, no centrifugal dirt traps.

Each feature in this list was expanded into concepts that appeared to have the necessary advantages for an "advanced" PCM. The paragraphs that follow are number keyed to the list above.

1.0 ADVANCED PITCH CHANGE MECHANISM - AUTONOMOUS POWER SOURCE

- 1.1 Electromechanical system combining a motor/generator assembly corotating with the propfan is one option.
- 1.2 Control for the above could be all-electronic using GE ECM Technology. Signalling could be fiberoptic.

ECM = ELECTRONICALLY COMMUTATED MOTOR

- 1.3 High rotational speed pneumatic motor. Mounted on the back of the propfan gearbox is one option. Also could be located on the forward face of the propeller hub and be supplied by high pressure air delivered through either a stationary or a rotating supply tube.

- 1.4 Control for the above could be an all-fluidic logic unit. Signalling could be fiberoptic. Power source would be a dedicated pressure-regulated bleed system from the turboshaft engine compressor.
- 1.5 Ground operations with engine shutdown could be regulated pressure from the aircraft APU.
- 1.6 Emergency operation could be from a high-pressure air storage bottle communicating directly with a ram actuator connected to the mechanisms that rotates the blades in the pitch sense.

2.0 ADVANCED PITCH CHANGE MECHANISM - EMERGENCY FEATHER

- 2.1 A very attractive system could be developed that used the rotational windmilling propfan energy as the motive power source.
- 2.2 Control over the above could be by a clutch/brake unit that does not operate at all during normal control functioning.
- 2.3 The concentric, high-speed, gearbox provided shaft that penetrates completely through the propfan hub may prove to be a highly desirable concept for any emergency feathering system.
- 2.4 Signalling for the above could be fiberoptic using a completely separate light source, and completely separate fiberoptic bundle, from the "normal" signal system.

3.0 ADVANCED PITCH CHANGE MECHANISM - 'CLOSED LOOP' FUNCTIONS

- 3.1 It is possible to devise a pitch change mechanism and control system that is corotating with the propfan and which controls all the normal operations of the propfan.
 - It senses its own rotational speed.
 - It has stored programs that contain all the necessary information for each significantly different phase of flight, e.g., start, taxi, take-off, climb, cruise, descent, land, "normal" feather. (Emergency feather could be separately commanded) Reverse on landing, etc.
- 3.2 FADEC control over the above could be in a simplistic manner. FADEC would select the appropriate "Closed Loop" Program function for the flight condition and then command the rotating system to be autonomous.

- 3.3 FADEC would monitor the autonomous systems performance and would step in with higher authority should programs limits be exceeded.

4.0 ADVANCED PITCH CHANGE MECHANISM - REDUNDANCY OF CONTROL

- 4.1 If fiberoptic signalling is used there may be two triple-redundant FADEC outputs with majority voting logic.
- One will be the "normal control system.
 - The other will be the "emergency" control system.
- 4.2 Loss of both sets of signals will be an automatic command to coarsen pitch and supply an appropriate cockpit warning.
- 4.3 The normal and emergency controls will be physically separated from each other by the maximum allowable geometry. The emergency system may be totally enclosed in a fireproof sleeve.
- 4.4 There may also be a third signal which is a simple confirmation. In closed-loop form, that both systems are alive and well, i.e., controls functions are at nominal settings, power supply is O.K., etc.

5.0 ADVANCED PITCH CHANGE MECHANISM - MODULARITY

- 5.1 Insofar as practical, all mechanisms and controls will be stacked on each other, with quick attach/detach modules.
- 5.2 The diagnostic circuit features being monitored by FADEC will resolve faults to the module level.
- 5.3 It will never be necessary to uncouple the propfan from the gearbox for control or PCM malfunction.
- 5.4 Traction drives, if used, will be sealed units that are located where normal maintenance will not disturb their mechanical connections.

6.0 ADVANCED PITCH CHANGE MECHANISM - MECHANICAL PITCH LOCK

- 6.1 A mechanical pitch lock will be provided that leads propeller pitch when finer pitch is commanded and lags propeller pitch when coarser pitch is commanded.
- 6.2 The pitch lock will be set in the range of commanded pitch minus one to two degrees.

- 6.3 External power is only required to unlock the mechanism. Conversely, no power is required for the lock to be operative.
- 6.4 Spring power will not be used in critical functions.
- 6.5 The locking unit, as an assembly, will be an easily removed module.
- 6.6 The normal pitch change function will be routed through the lock. Any pitch lock malfunction will automatically restrict the propfan to obey coarser pitch commands only.

7.0 ADVANCED PITCH CHANGE MECHANISM - PRECISE PITCH SELECTION

- 7.1 It is believed that the inherent "stiffness" of traction drive speed reducers may lead to excellent use in precise pitch selection systems, when powered by equally precise rotary power units.
- 7.2 An alternative using linear ball-screw actuators has been identified. The nut and rod end balls would be preloaded against each other to obtain zero backlash.
- 7.3 Again, traction drives may be an attractive solution for the high reduction ratios required to convert the rotation speed of the power source into precise axial positioning.
- 7.4 For all systems, the accuracy of the final engagement of the mechanisms to the individual propfan blades is a critical design selection. No favorite method has yet been identified.

8.0 ADVANCED PITCH CHANGE MECHANISM - ANTI-ICING POWER SUPPLY

- 8.1 Although not considered to be a "critical" item there are many and obvious advantages for the propfan/spinner anti-icing (or de-icing) system to be an autonomous subsystem of each rotating propfan assembly.
- 8.2 For an electromechanical PCM the power source could be variable frequency A.C. derived from the PCM generator. In this case, the generator would be sized to provide the requisite power output to supply PCM and anti-icing functions simultaneously.
- 8.3 A cursory examination of the practicality of carrying a continuously rechargeable electric battery subsystem has been made. This idea may be worthy of a separate investigation, particularly if the battery could also provide the power source for "emergency" feathering.
- 8.4 The elimination of powered sliprings and brushes is a primary objective, and has obvious merits.

9.0 ADVANCED PITCH CHANGE MECHANISM - SELF TEST AND DIAGNOSTICS

- 9.1 Dependent on the selection of the PCM power source, there are a number of desirable self-test and diagnostic functions.
- 9.2 Each designated module must monitor its own health and report to the FADEC diagnostic center.
- 9.3 Noncritical fault data will be memorized and read out after flight, on a maintenance diagnostic test device. Critical faults will be analyzed by FADEC and appropriate safety control measures will be initiated.
- 9.4 The system will be completely self-checking, on the ground, when supplied with an external power source. FADEC will be responsible for recognizing any anomalies and will report (via CRT messages) to the cockpit propulsion display system.

10. ADVANCED PITCH CHANGE MECHANISM - EASE OF MAINTENANCE

- 10.1 Modular design is the objective.
- 10.2 Components that require lubrication will be sealed, enclosed units.
 - Propfan blade bearings.
 - Traction drive fluid, ball-screw actuator lubricant.
 - Electric or pneumatic motor bearings.
- 10.3 Consideration will be given to air bearings where practical.
- 10.4 Links, link bearings or items that wear through fretting, will only be used where the primary load is in tension.
- 10.5 Maintenance errors elimination is a key objective.

11. ADVANCED PITCH CHANGE MECHANISMS - FRICTION, WEAR POINTS

- 11.1 No piston rings, no seals thus no wear.
- 11.2 All motion will be via antifriction bearings that are designed for 35,000 hours of system operation.

- 11.3 Stability of joints will be maintained by accurately machined faces and lands. All splines will have positive lands that relieve spline teeth of bending loads.
- 11.4 Axial fit-up of components will account for thermal environment. Matched axial and radial expansion/contraction of internal mechanisms to their casings will be a design objective.

12. ADVANCED PITCH MECHANISMS - FILTERS, DIRT TRAPS

- 12.1 The design and manufacturing philosophy will use the latest techniques in the use of assembly clean rooms.
- 12.2 Because hydraulic systems will not be used, all oil filters are eliminated.
- 12.3 Cross contamination of the gearbox and the PCM cannot occur. There will be no interfaces that can contaminate each other.
- 12.4 The use of sealed units and the elimination of hydraulic fluids will eliminate dirt traps in rotating "G" fields.

4.14.1 Description of System

Figure 4.14-1 is a cross section of the final configuration that evolved from this study. The propeller hub is connected to the gearbox output shaft by means of a bolted joint incorporating a curvic coupling. A high speed driveshaft, coupled at the rear to the gas generator low pressure turbine (in the case of an installation with a concentric gearbox) extends forward along the centerline of the gearbox output shaft. It is this shaft that transmits the energy required for pitch change and anti-icing to the propeller. In addition to the foregoing, the gearbox must support the stationary portion of the optical slipring required to transmit signals to and from the propeller assembly.

The demands, or constraints, that a propeller of this design places upon the system of which it is a part may be summarized as follows:

- A flanged, hollow drive shaft is required to support and drive the propeller.
- A hydraulic slipring is required for lubrication of the motor/generator unit and emergency feather oil supplies.

ORIGINAL FACTS
OF POOR QUALITY.

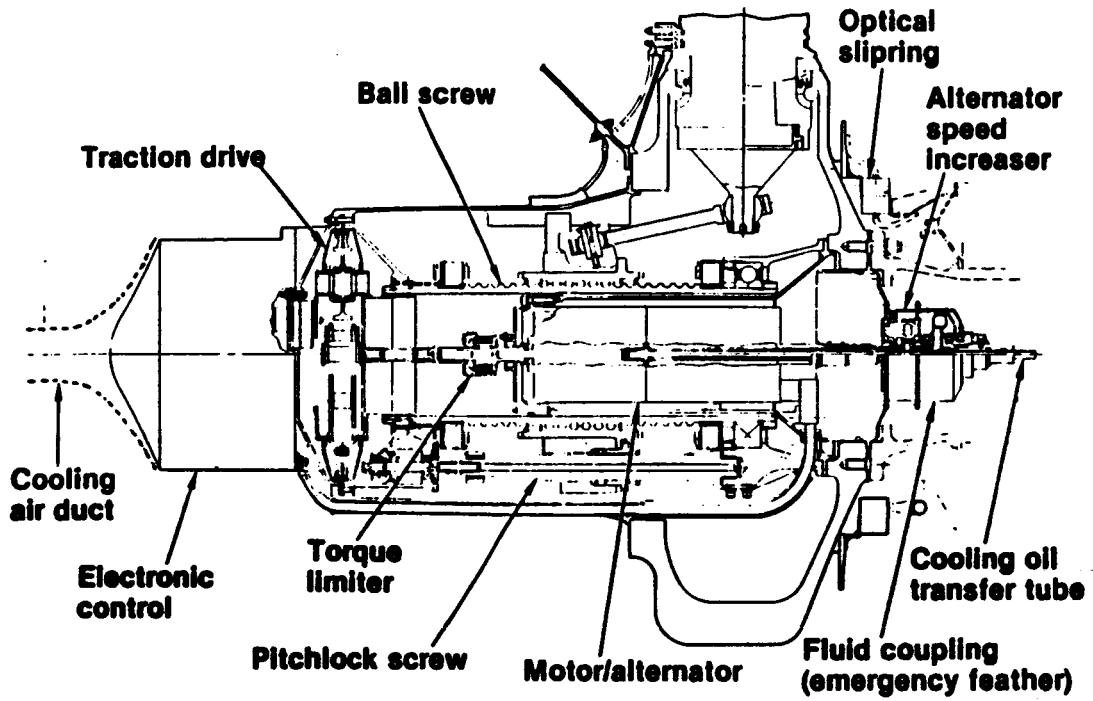


Figure 4.14-1. Advanced Technology Pitch Control System.

- A high speed drive shaft is required to provide the energy to the propeller pitch change mechanism.
- A support for the stationary portion of the optical slipring is also required and a control system that provides the necessary optical signals to the slipring and which will also accept return signals from the propeller assembly.

A speed increaser, when used, steps up the speed of the high speed drive shaft to the speed required by an optimized alternator. The speed increaser drives the alternator, which is the next most forward component, by means of a hollow shaft. A power cable exits from the rear of the alternator and transfers the generated power to the electronic module which is located at the extreme front of the propeller assembly. When appropriate, electric power is returned along this same cable route to the rear of the alternator where it is carried to the motor via internal conductors. The motor is located immediately forward of the alternator, and when servicing is required, they are removed together as an electrical machinery module.

The solid electric motor drive shaft extends rearward through the hollow alternator shaft and couples with the driven half of the emergency feathering clutch. The motor shaft also extends forward and drives the sun roller of a traction drive reduction unit through a torque limiting clutch. During normal operation control logic prevents the end-of-travel stops from being impacted at high speed, but the possibility of mis-rigging the system during an overhaul does exist, and in this situation the stops could be impacted with sufficient energy to damage portions of the system were it not for the protection afforded by the torque limiting clutch.

The traction drive provided is a hybrid unit, meaning that a portion of the total reduction is performed via contact between smooth rolling elements, but at the output stage, where the torque is high, it utilizes rollers carrying outboard pinions which drive an output gear. A rotary transducer monitors rotation of this stage and supplies a signal to the electronic control. This signal is a function of blade pitch angle, and is used both for display in the cockpit and for control refinement.

The output of the traction drive rotates a ball screw assembly. The ball nut, which is translated axially by screw rotation, carries the forward ends of links which are connected to crank arms mounted to the inboard ends of the propeller blade trunnions. By this arrangement, rotation of the ball screw causes blade rotation about the pitch changing axis. Elastomeric torsional stops are located at both ends of the ballscrew. The ball nut carries forward and aft facing tangs which engage the full feather and full reverse stops at the end of travel and prevent further rotation of the ballscrew in that direction. The crank arms are positioned on the blade trunnions such that during forward flight the blade centrifugal twisting moment loads the links in tension rather than compression and thus they are not subjected to buckling.

4.14.2 Preliminary Designs

The design parameters used in this study are listed in Table 4.14-1. These parameters were obtained from Hamilton-Standard who acted as a subcontractor for this task. The loads and forces being presented were appropriate for a "baseline" propfan with an 800 ft/sec tip speed.

4.14.2.1 Dual Bevel Gear Blade Design

The first design consisted of a blade drive scheme using pinions attached to each blade root which were driven by a pair of opposing large bevel gears which rotated about the propeller hub centerline. Figure 4.14-2 is a cross section of this design. As can be seen from the figure, this configuration had the motor located at the extreme forward end of the PCM with the electronic control unit placed in a surrounding annulus. The motor drives rearwards into the sun roller of the traction drive. In this device the traction drive has a ratio of 101:1. The output of the traction drive in turn powers a star gear reduction gearset. This star gear reduction stage drives the input of a planetary differential reduction unit which in turn drives the opposing dual bevel gears in opposite directions. The planetary differential stage is built into an annulus surrounding the alternator.

Historically many successful propellers have been built where a bevel gear has driven pinions attached to the blade trunnions. The problem in this

Table 4.14-1. Design Parameters Used For This Study.

Pitch Control Slew Rates

<u>Condition</u>	<u>Blade Pitch Rate (Deg/Sec)</u>
Normal Control	0-3
Synchro-Phasing	0-3
Feather	15
Reverse	15
Ground Operation (Engine Inoperative)	0-3

Pitch Control Blade Angles

<u>Condition</u>	<u>Degrees (3/4 Blade Span)</u>
Feather	+85°
Flight Idle (0.3 Mn)	+39°
Max Reverse	-7°
Min Prop Torque (Static Conditions)	0°
Emergencies	Approx 1° Below that when Condition Occurred

Pitch Control Torque

Max Total Blade Twisting Moment at 100% RPM =
489,000 in-lbs

Total Blade Twisting Moment on Pitch Lock at 100% RPM =
461,000 in-lbs

Basic design Requirements

Max SHP at Prop	12,500
Prop RPM	1160
Overall Speed Ratio	7.4:1 (+ 0.1)
1-P Shaft Moment	
At 0.2 Mn Climb	172,000 in-lb
At 0.74 Mn Cruise	68,400 in-lb
Shear Load (Up)	
At 0.2 Mn Climb	2620 lb
At 0.74 Mn Cruise	2230 lb
Shaft Gyro Moment	
At 0.1 Rad/Sec	35,300 in-lb
Prop Thrust	
Static Take-Off	19,500 lb
0.2 Mn Climb	16,000 lb
0.74 Mn Cruise	3,800 lb
Ambient Temperature	-40° F

ORIGINAL FACILE
OF POOR QUALITY

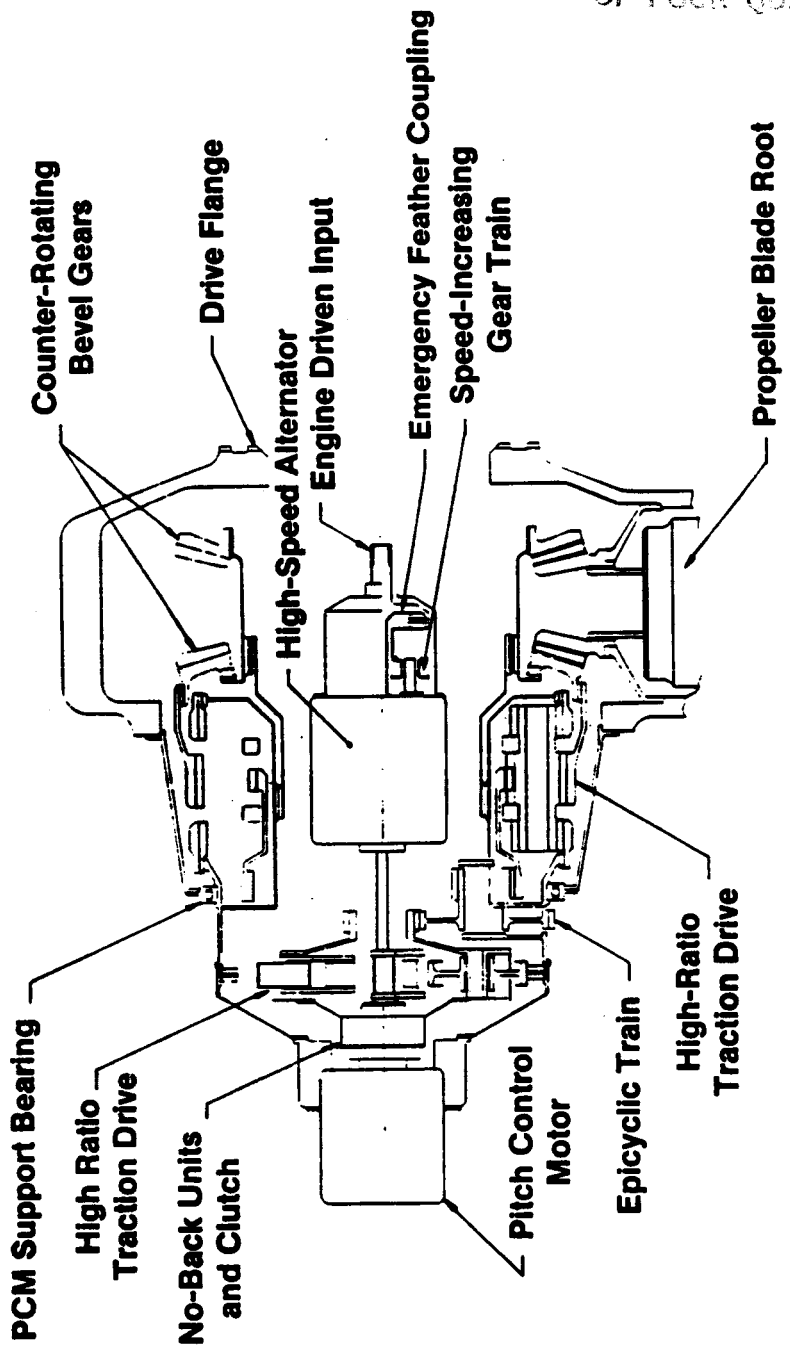


Figure 4.14-2. Pitch Control Mechanism Based on Dual Drive Bevels.

instance is that when ten blades (and ten pinions) are used, the pinion diameter must of necessity be significantly smaller in diameter than the bevel gears. This condition produces a ratio in the final blade drive that is in the wrong, or speed-increasing direction. This requires that additional reduction be designed into the stages preceding the final stage. This additional reduction produces extremely high torque to the input of the speed increasing stage, which results in robust, heavy, components.

4.14.2.2 Ballscrew Blade Drive

In a successful effort to evade the weight shortcoming of the previously described design, a PCM having blades rotated by links about their pitch trunnions was designed. These links have their forward ends translated by a ballscrew/ballnut device which is concentric with the propeller centerline. Figure 4.14-3 is a cross section of this design. At this stage of development the PCM still retained the forward motor location and a no-back type of pitch lock.

Further development of this concept resulted in the final design. The significant differences between the scheme of Figure 4.14-3 and the final configuration are the combining of the motor and alternator into a single module placed at the center of the PCM and the addition of a following pitch lock mechanism.

4.14.3 Speed Increaser and Emergency Feather Module

Although serving separate functions, the speed increaser and emergency feathering clutch have been combined into one module which is located just to the rear of the alternator. Figure 4.14-4 is a cross section of this module.

4.14.3.1 Speed Increaser

The speed increaser raises the low pressure turbine speed (rpm) of the gas generator to the rpm required by an optimized alternator. Some installations may have this function incorporated as part of the main speed decreasing gearbox which drives the propeller. The installation shown here is typical

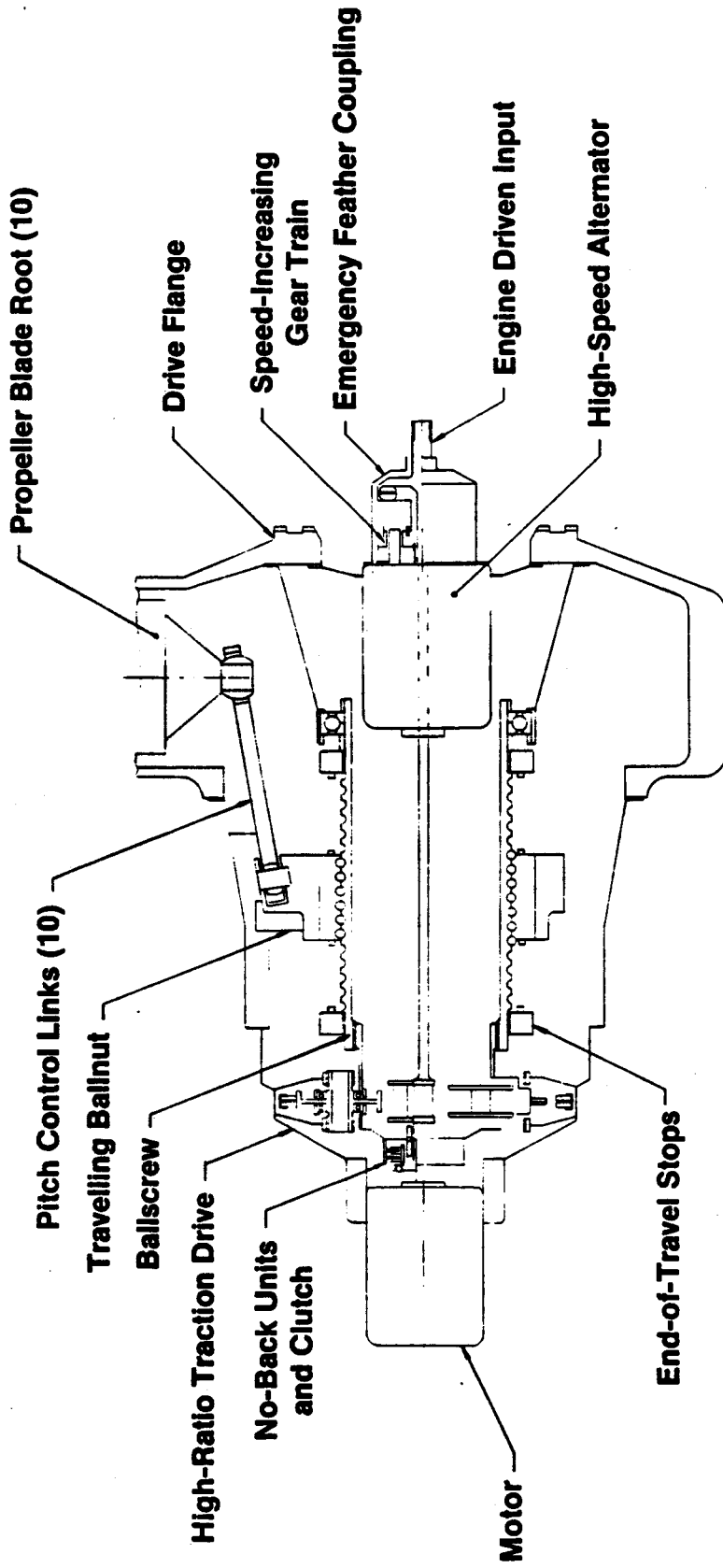


Figure 4.14-3. Pitch Control Mechanism Based on Ballscrew and Nut.

ORIGINAL PAGE IS
OF POOR QUALITY

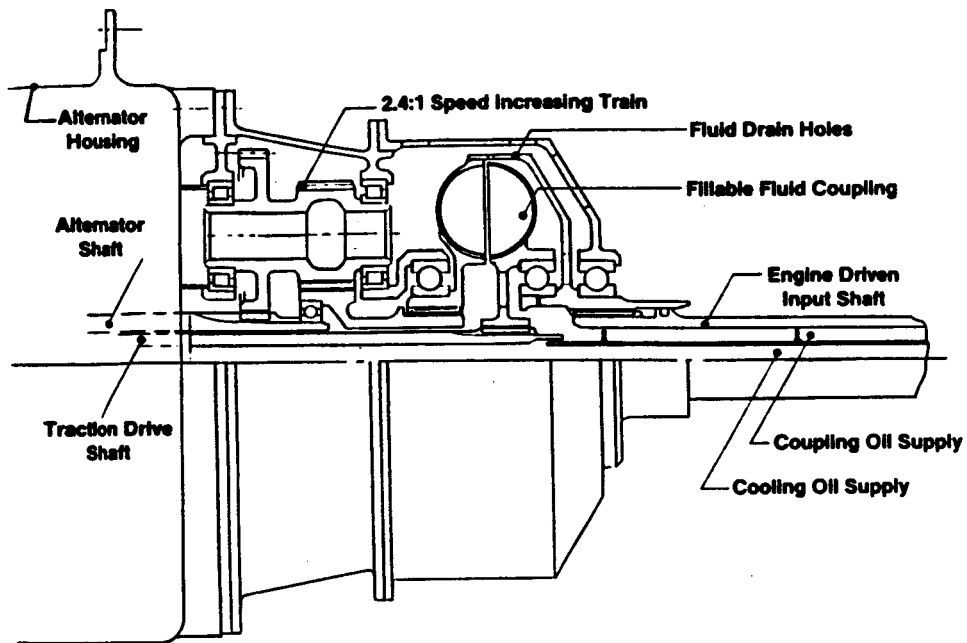


Figure 4.14-4. Combined Speed-Increasing Train and
Emergency Feather Mechanism.

of installations having concentric main gearboxes mechanism. The speed increaser is a three branch double reduction reverted arrangement. Lubrication to the speed increaser as well as lubrication to the alternator bearings is supplied by means of a channel in the high speed drive shaft.

As is the case with all the other major components of the pitch change mechanism, the speed increaser may be removed as a module along with the emergency feathering mechanism.

4.14.3.2 Emergency Feathering Mechanism

An entirely separate, all-mechanical mechanism is provided to feather the propeller in an emergency in the event that a prior failure has occurred in the normal pitch control system, which includes normal feathering capability. This separate, backup system consists of a fluid coupling that serves as a dump-and-fill clutch which, when engaged, couples the high speed drive shaft directly with the traction drive sun roller. The alternator shaft is hollow and an extension shaft of the motor extends rearward through the alternator and couples to the driven half of the fluid coupling.

This coupling is filled, when commanded, by means of a second fluid channel which is independent of the other channel in the high speed drive shaft used to supply cooling and lube flow to the PCM. The directions of rotation within the system are chosen such that when the propeller is windmilling (or engine driven) in the normal direction of rotation, coupling of the high speed shaft directly to the motor will drive the ballscrew via the traction drive in the direction to cause movement to a coarser pitch. As long as the propeller continues to windmill, the high speed drive shaft will be driven by the propeller via the main speed decreasing gearbox and alternator speed increaser. By virtue of this, if the feathering clutch continues to be engaged, the blades will continuously coarsen their pitch until the system comes to rest with the blades fully feathered. Should flight conditions cause reverse windmilling of the propeller, as long as the clutch is engaged all rotation within the system will be reversed and the blades will appropriately change pitch setting such that the system will again come to rest fully feathered.

A means of supplying oil to the emergency feathering channel within the high speed shaft that is independent of normal operation, and can be activated from the cockpit, is a requirement. This can be achieved by an electric motor/pump unit which is integrated with the propfan gearbox, and which draws on a "reserved" section of the oil tank for its oil supply. In this manner it is entirely analogous to the emergency feather provision of a hydraulic propeller.

4.14.4 Pitch Lock Mechanism

The two initial schemes shown by Figure 4.14-2 and Figure 4.14-3 utilized no-back devices for the purposes of pitch locking. Although used successfully in the QCSEE variable pitch turbofan, a similar application here posed four major problems. They are:

1. By its very nature, the no-back device possesses some lost motion which is not desirable in a precision positioning device.
2. During continuous synchrophasing operation the device would be frequently locking and unlocking and therefore would absorb and dissipate significant energy.
3. To assure complete safety all components downstream of the device would be required to be prime reliable.
4. The very high centrifugal twisting moments (CTM's) of the propfan blades demand a very strong mechanism in the pitchlock.

In order to circumvent the above difficulties a different pitchlocking scheme was decided upon. It is shown by two isometric sketches, Figure 4.14-5 depicting normal operation, and Figure 4.14-6 depicting a lockup situation. In Figure 4.14-5 all the arrows indicating direction of movement show motion in the coarsening pitch direction. Movement in this direction, even if inappropriate, does not compromise flight safety as it cannot lead either to a propeller overspeed or to a high drag condition. Therefore, travel in this direction is never inhibited by the mechanism. When coarser pitch is commanded, the ball screw rotates in the direction of the arrow. The lugs come into contact, and the large gear is rotated by the ballscrew. This large gear

ORIGINAL PAGE IS
OF POOR QUALITY

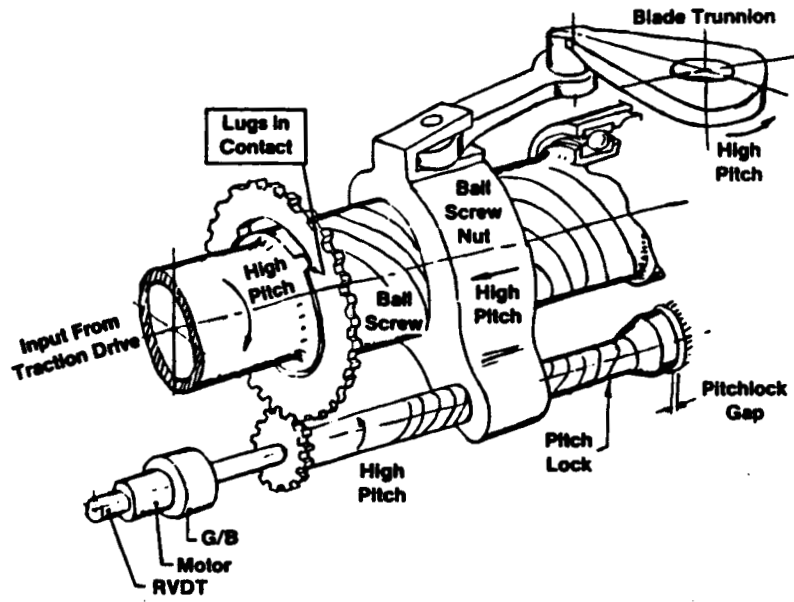


Figure 4.14-5. Pitchlock Schematic Normal Operation.

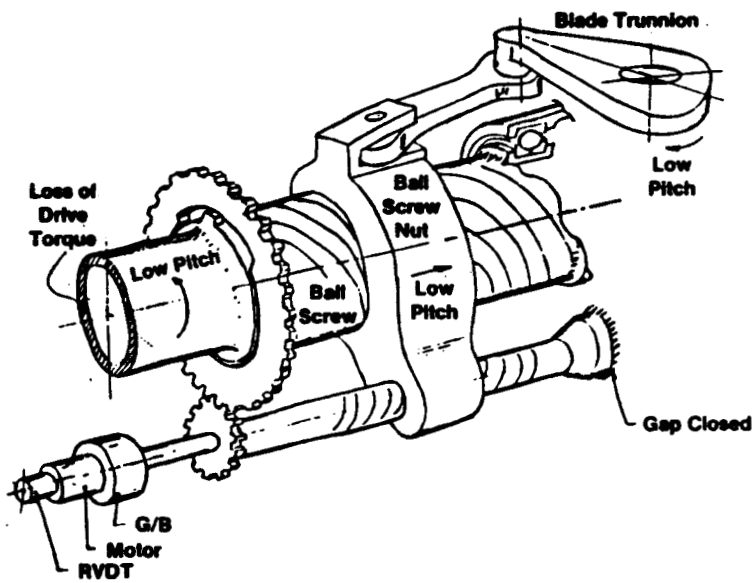


Figure 4.14-6. Pitchlock Schematic Lock Engaged.

drives the smaller gear which in turn rotates one of the two locking screws (the second screw is omitted from the sketch). Because of the proper relation between gear ratio and thread lead, the pitch lock screw advances to the right through the ear attached to the ball nut at exactly the same rate that the ball nut itself moves to the left. Thus, the screw is stationary with respect to the propeller hub and the pitchlock gap is maintained unchanged.

In an authorized move toward fine pitch, all the directions of motion shown on Figure 4.14-5 are reversed. The description of operation is as before with one significant exception. In the move toward coarse pitch the pitchlock screw was driven by the gears as a result of lug contact. Movement toward fine pitch requires the lock screw to be driven instead by its motor in order to maintain lug contact and avoid pitch lock engagement (gap closure).

Refer to Figure 4.14-6 for a sketch depicting an unauthorized move toward fine pitch which will result in a system lockup. Being an unauthorized move, the motor will not cooperate in the move and drive the pitchlock screw. Without the contribution of the motor the lugs on the ballscrew and large gear will come out of contact which results in rotation of the ballscrew without any corresponding movement of the gear. Since neither the gear or the motor is driving the lockscrew, it will remain stationary. As a result, when the ballscrew nut moves to the right, it will carry the nonrotating lockscrew along with it. After very little movement, corresponding to less than a degree of blade pitch angle change, the locking gap will close, preventing further movement of the system by precluding further movement to the right of the ballscrew nut. Figure 4.14-7 is a section through the propeller hub in the plane of the large gear showing the relationship of the parts as they are intended to be.

4.14.5 Optical Slipring

The position of the optical slipring relative to other components of the pitch control system is shown by Figure 4.14-1. The ring is located in the plane of the propeller drive flange. In the upper portion of Figure 4.14-1 one set of the triply-redundant optical fiber bundles can be seen leading from the gearbox exterior surface to the stationary inner part of the ring and from

ORIGINAL DRAWING
OF POOR QUALITY

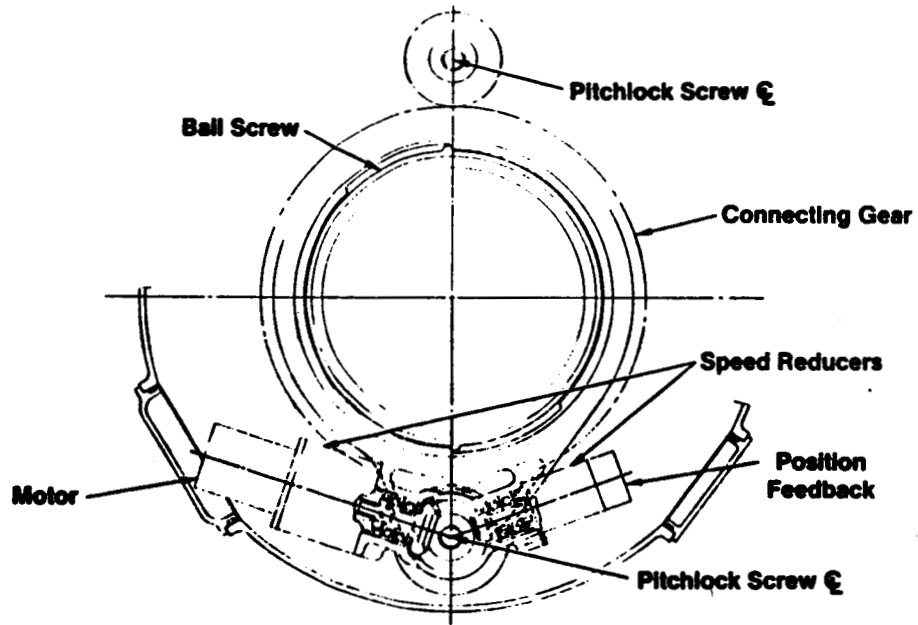


Figure 4.14-7. Pitchlock Drive.

the rotating outer portion of the ring to the propeller hub. In the lower part of the same figure the tube can be seen that supplies warm, filtered purge air from the engine to the slipring. This air prevents condensation within the ring and protects the interior reflective surfaces from contamination by the environment in the area of the slipring.

Figure 4.14-8 shows a cross section of the slipring. The labyrinth seals which contain the purge air are clearly visible as are the cylindrical reflective surfaces and the counterbores for the fiber bundles and lenses. The operation of the ring is best understood by referring to Figure 4.14-9 which schematically shows how the reflective patterns cross the rotating boundary. The light signal is injected at an angle through a hole in one cylindrical reflective surface and it is repeatedly reflected until it exits through a similarly angled hole in the opposite reflective surface. Figure 4.14-10 schematically represents a slipring cross section showing the three pairs of transmitter and receiver ports on the inner (stationary) ring and the four pairs of ports on the outer (rotating) ring. By an examination of the figure it can be seen that for any relative angular position of outer ring to inner ring there are always three channels in communication. This situation prevails both for transmission radially outward (sending signals to the propeller) and transmission radially inward (receiving signals from the propeller).

There is a modulation loss in the slipring which is a function of the reflection pattern. This pattern is in turn a function of the geometry of the slipring and the aperture of the light source. Figure 4.14-11 shows three examples of reflection patterns. The ratio x/d (spot spacing to spot diameter) is referred to as the lateral offset ratio. Figure 4.14-12 is a curve of modulation loss versus lateral offset ratio.

A further loss exists in the ring that is a function of the number of reflections required before the signal passes through the ring. This is a function of the circumferential length between the launching, or source port and the exit, or receiver port. This length depends on the angular position of the rotating portion of the slipring. Figure 4.14-13 is a plot showing the loss versus angle for all three active channels for a slipring of assumed dimensions.

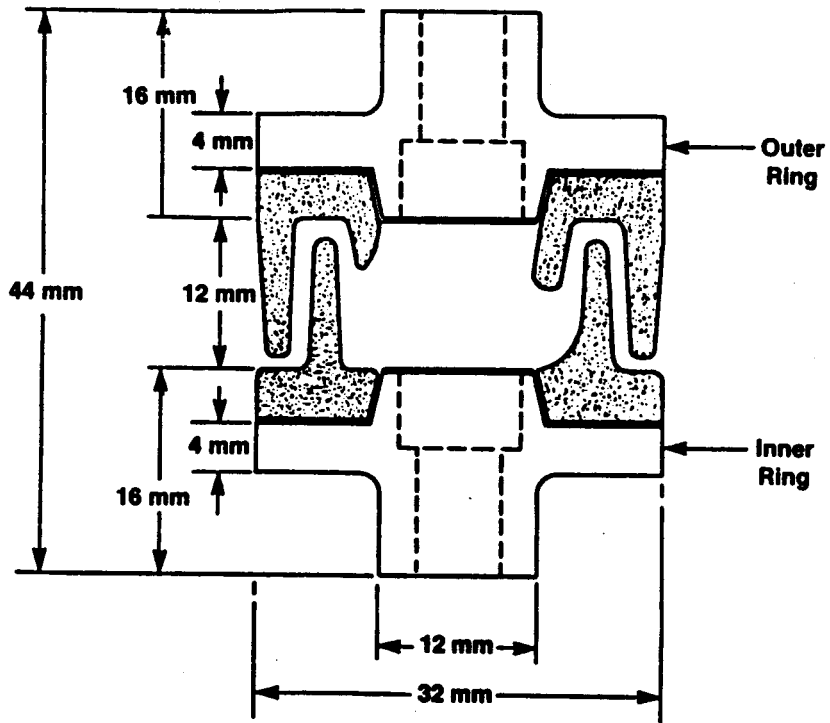


Figure 4.14-8. Cross Section of Optical Slipring.

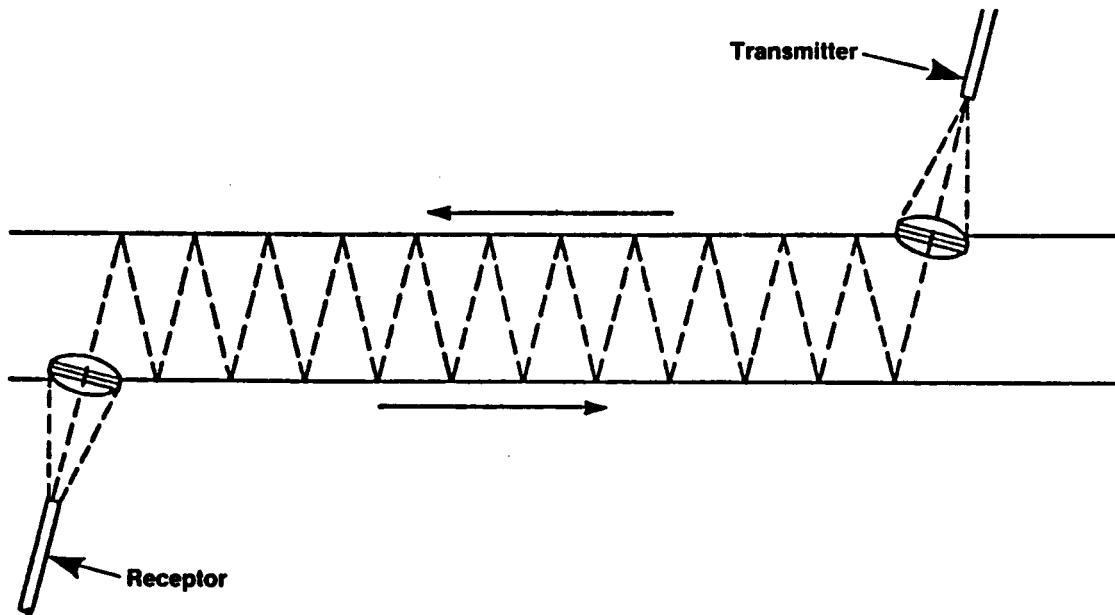


Figure 4.14-9. Schematic of Slipring.

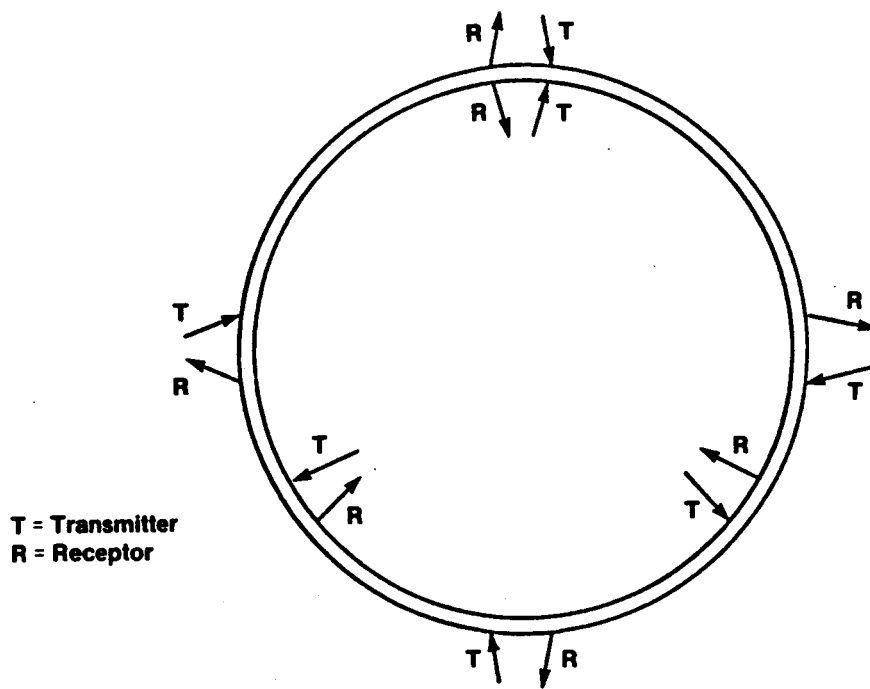


Figure 4.14-10. On-Axis View of Slipring.

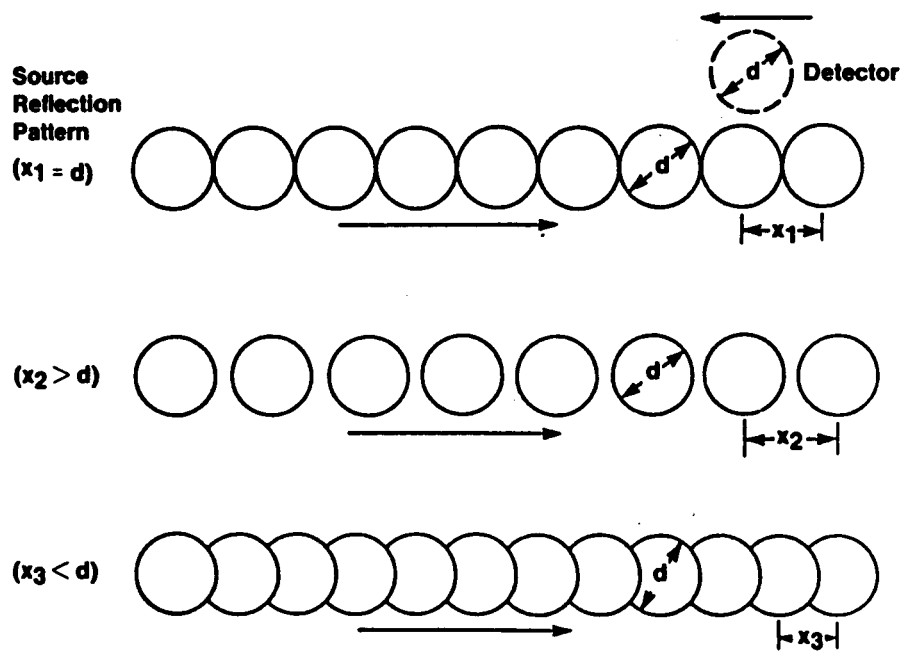


Figure 4.14-11. Source Reflection Patterns.

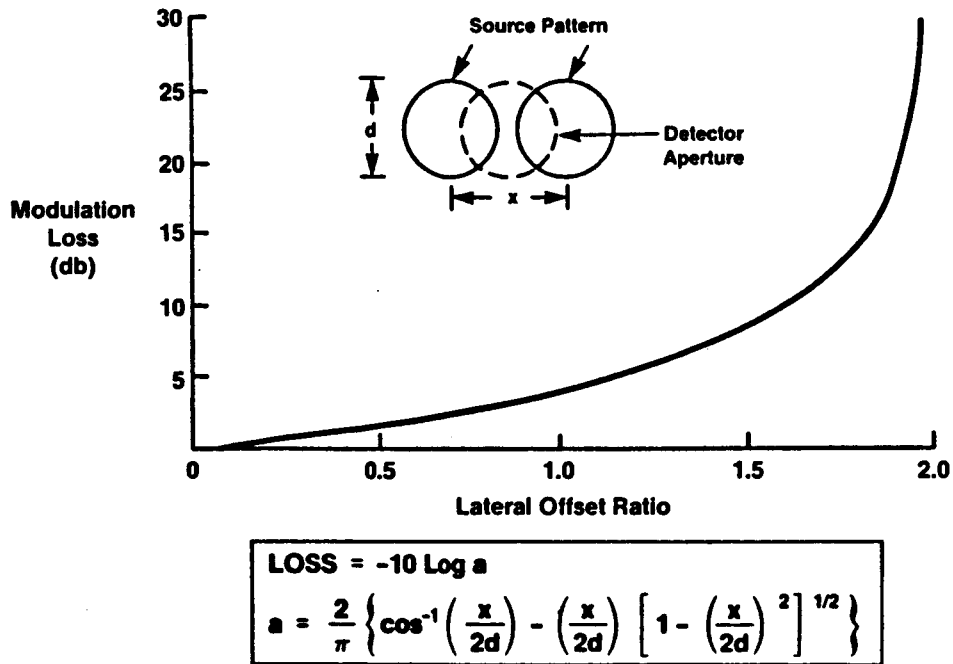


Figure 4.14-12. Modulation from Source Pattern.

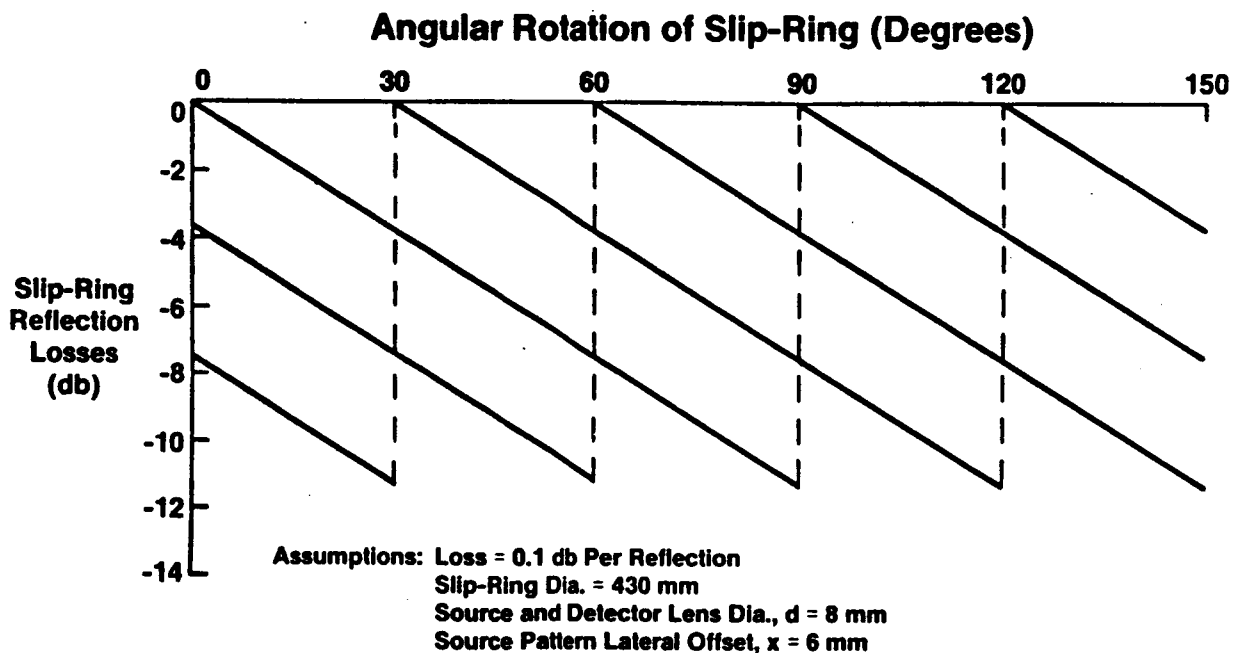


Figure 4.14-13. Slipring with 3 Source Fibers and 4 Detector Fibers.

Some deterioration of the slipping with time may be expected principally due to deposits on the reflective surfaces and lenses. Several features have been incorporated to successfully cope with this trend. Condition monitoring can be used to track the rate of deterioration. A signal of known strength is launched into the fiberoptic bundle and the perceived strength of this signal as seen by the electronic control is reported back as health information. A comparison is made and the data is stored for trending purposes. A projection can be made as to when corrective action should be taken.

As mentioned previously, the ring is pressurized with warm, filtered engine bleed air. This prevents condensation and infiltration of air which may be laden with contaminants.

The ring is also equipped with washout ports that permit the ring to be flushed with an agent to enable it to be cleaned without disassembly or removals. Lastly, the ring is constructed of three segments, which permit easy ring removal and replacement without disturbing the propeller.

Performance estimates of the optical slipping are given by Tables 4.14-2 and 4.14-3.

4.14.6 Traction Drive Module

The reduction unit chosen for the pitch change mechanism is a traction drive device which has multiple rows of smooth rollers in contact which transfer the power to adjacent rollers utilizing friction, or elasto-hydrodynamic traction as it is more properly termed. The benefits of the traction drive that especially suit it to this application are:

- High reduction ratio in a single unit
 - 101:1 ratio for the dual bevel PCM design
 - 210:1 ratio for the ballscrew PCM design
- Axially compact
- High efficiency for the ratio--94%
- Ability to run with marginal grease lubrication
- Very high torsional stiffness

Table 4.14-2. Performance Estimate.

	Expected	Worse Case
● System Losses		
- Source-to-Fiber	-2.94 db	-3.5 db
- Connectors (2)	-2.0 db	-3.0 db
- Optical Fiber Link (2)	-0.02db	-0.03db
- Lens (2)	-2.4 db	-3.0 db
- Photodiode Coupling	-0.1 db	-0.2 db
- Optical Slip Ring	-10 db	-15 db
- Misalignment in Slip Ring	-3 db	-5 db
- Total System Loss	-20.46 db	-29.73 db
● Source Output (P_{in})	2.4 MW	2.0 MW
● Detector Responsivity (R)	0.5 A/W	0.45 A/W
● Detector Dark Current (I_d)	1 nA	20 nA

Table 4.14-3. Performance Estimate.

$$\text{System Loss} = 10 \text{ Log } (P_{in}/P_{out}) \quad (1)$$

$$\text{Signal Current} = I_s = P_{out}R \quad (2)$$

$$\text{Signal-to-Noise} = \text{SNR} = 10 \text{ Log } (I_s/I_n) \quad (3)$$

	Expected	Worst Case
System Loss	20.46 db	29.73 db
P_{in}	2.4 MN	2.0 MN
R	0.5 A/W	0.45 A/W
I_d	1 nA	1 nA
P_{out} (From 1)	21.6 μ W	2.1 μ W
I_s (From 2)	10.8 μ A	0.95 μ A
SNR (From 3)	40.3 db	16.8 db

- Zero backlash
- High ratio of output torque to weight
- Low torque ripple
- Clean room, sealed, assembly

The creep, which represents about a 2% speed loss at full torque, associated with traction drives is not a problem in this application and it does not degrade the system performance in any way. The 210:1 ratio drive is termed a hybrid traction drive as it combines gears with rollers as it has geared pinions driving an output gear in the final stage. Figure 4.14-14 shows an end view of the hybrid unit and Figure 4.14-15 shows a cross section. This unit is constructed as a module, and as such it can be removed virtually intact from the PCM assembly.

4.14.7 Electrical Machinery

4.14.7.1 Motor Design

Table 4.14-4 shows the choices, and characteristics of each choice, considered for types of motors and generators. The one selected for this study was the permanent magnet synchronous design because its advantages make it particularly well suited to this application and because the technology is well developed. Figure 4.14-16 shows a cross section of this type of machine.

Another very attractive motor type is the switched reluctance motor, a cross section of which is shown by Figure 4.14-17. Table 4.14-5 shows some of the recent advances that make AC drives more competitive with other systems.

Table 4.14-6 lists some of the factors affecting motor design. Table 4.14-7 lists the variables of motor scaling and gives the characteristics of the motor selected for the PCM application. Note that at the time the mechanical drive for the PCM was designed the optimum motor was thought to be a 20,000 rpm design and so the gear ratios were selected accordingly. Further efforts at optimizing the motor design produced the 40,000 rpm machine, which is smaller, lighter, and less costly. Although a new drive design was not made, a study indicated that the system would be more attractive with the

ORIGINAL PAGE IS
OF POOR QUALITY

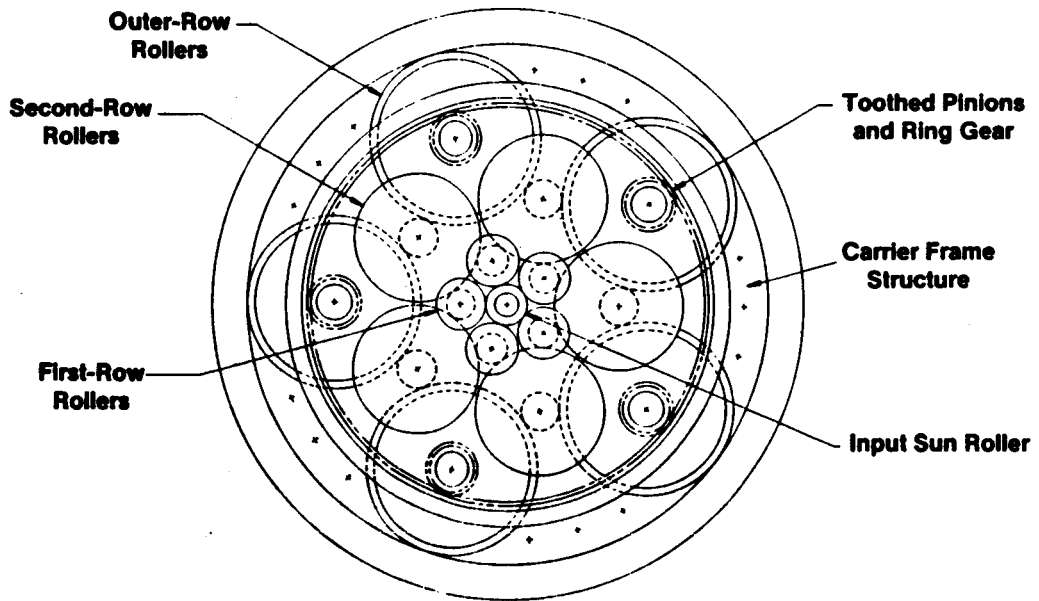


Figure 4.14-14. Traction Drive Arrangement for 210:1 Ratio.

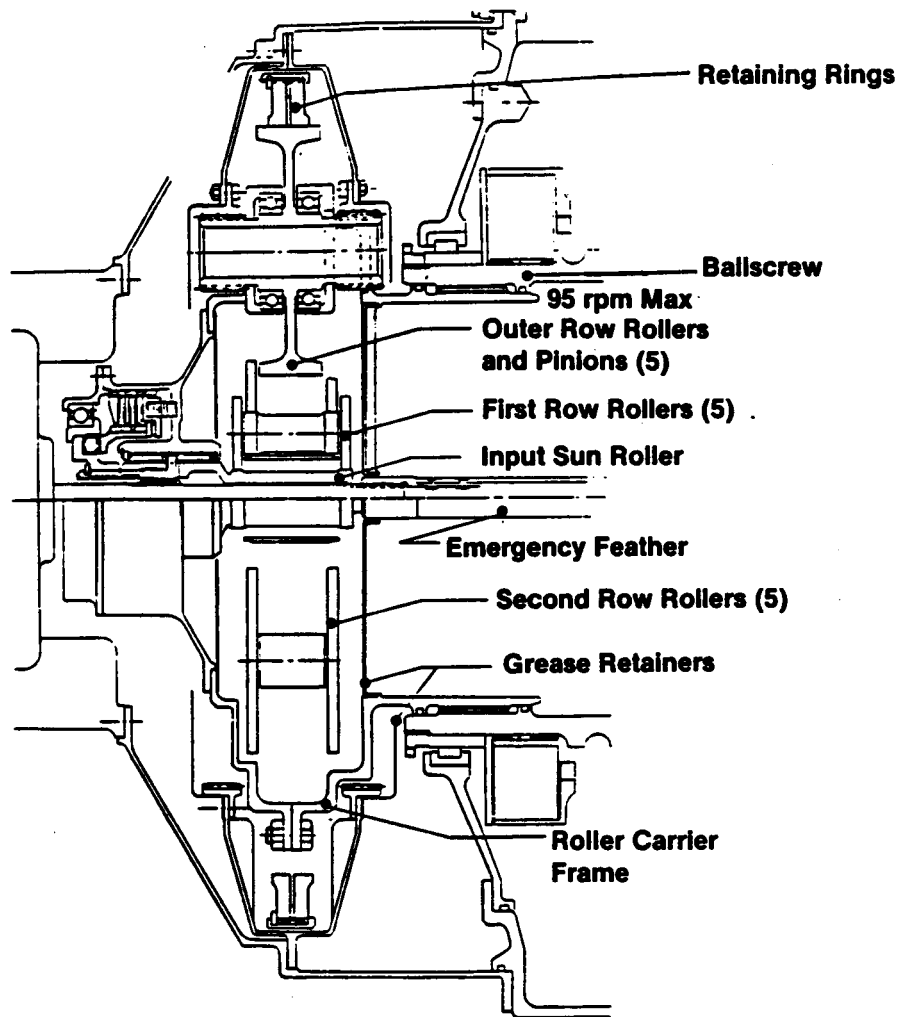


Figure 4.14-15. Traction Drive Arrangement for 210:1 Ratio.

Table 4.14-4. APET PCM-Motor/Generator Choices.

(Only Brushless Machines Considered)

Motor

- **Induction**
 - Standard Technology
 - Complex Control
- **PM Synchronous**
 - High Efficiency
 - Simplified Control
 - Wide Speed Range
 - High Power Factor
- **Switched Reluctance**
 - Low Cost
 - No Magnets or Rotor Conductors
 - Reliability
 - Cooling
 - Insulation
 - Wide Speed Range
 - No Temperature Effects
 - Fewest Power Semiconductors (3 Instead of 6)
 - Well Suited for DC Power Supply

Generator

- **PM**
 - Short-Circuit Protection With Co-Sm
 - High Power Density
- **Induction Alternator — Not Recommended**

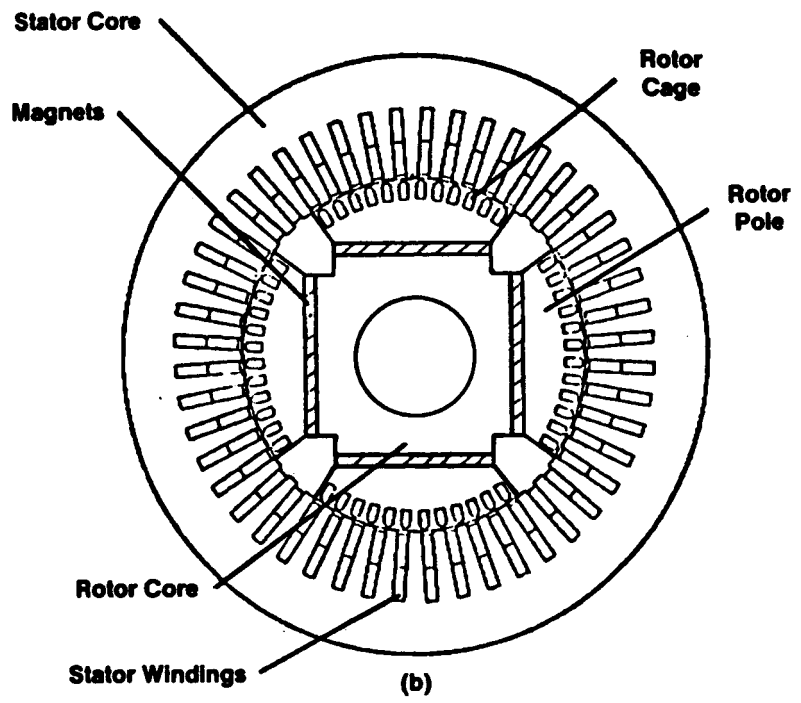


Figure 4.14-16. Basic Interior PM Synchronous Motor.

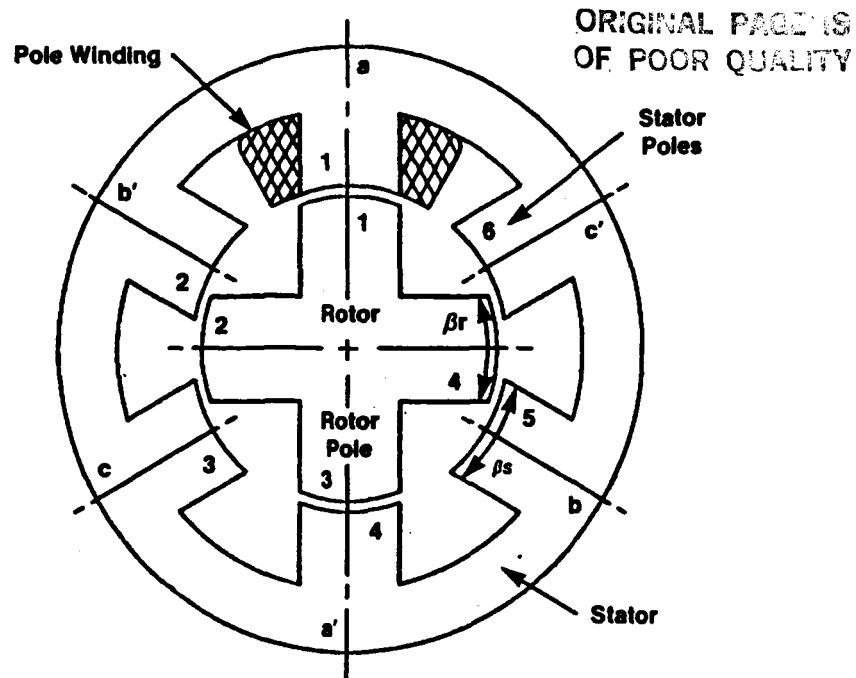


Figure 4.14-17. Basic Switched Reluctance Motor.

Table 4.14-5. Recent Technological Advances Important for AC Drives.

Advance	Reason for Its Importance
1. Invention of Insulated Gate Transistors	Reduction in Parts Count and Overall Simplification of Gate or Base Drive Circuits for High Power Semiconductor devices
2. Increased Availability of Gate Turn-Off Thyristor	Reduction in Parts Count and Overall Simplification of Inverter Circuits; Elimination of Auxiliary Circuits for Forced Commutation.
3. Discovery of Neodymium Iron Permanent Magnet Material	May Lead to the Feasibility of High Power Surface-Magnet Motors Having Low Inverter kVA Requirement; Also to Low-Cost, High-Performance Interior-Magnet PM Motors.
4. Development of Switched Reluctance Motor	Completely New Motor/Converter System With Potential for High Efficiency, Small Inverter Size and Low Cost. SR System and its Derivatives Have a Wide Range of Potential Applications.
5. VLSI and Advanced Microcontrollers	Permit Sophisticated Control Systems to be Implemented at Low Unit Cost; Possibly Enabling a Wider Use of Advanced Control Concepts Including Adaptive Algorithms. Also to Permit the Development of Improved Feedback and Sensing of Motor Parameters.
6. Availability of Higher-Power Bipolar Transistors and MOSFET's	Increases the Range of Applicability of Pulse-Width Modulation Techniques for Induction Motor Drives; Facilitates the Rapid Development of Technology for PM and SR Drive Systems.

Table 4.14-6. Motor Design.

- **Maximum Motor Speed (rpm) is Determined by:**
 - **Maximum Switching Frequency (Less Than 300 Hz)**
 - **Iron Losses (Start to Reduce Flux Density Around 3000 Hz)**
 - **Maximum Bearing Speed (DN) (Good Bearing Fundamentals)**
 - **Rotor Stresses (140,000 psi Maximum)**
 - **Rotor Dynamics (System Response Concerns)**
- **Permanent Magnet Motor (Evaluated In Most Detail)**
- **Motor Rating Can Be Influenced by Inverter Selection**
 - **Force Commutated Inverter Allows Motor Operation at Its Lowest Possible Rating**
 - **Also Requires Less Magnetic Material Than a Load Commutated Inverter**
 - **Both 4-Pole and 2-Pole Designs Can Meet Design Criteria.**
 - **Operating The Motor at Constant Power Over a Wide Speed Range (Mandates a Force Commutated Inverter)**
- **Switched Reluctance Motor (Merits Further Evaluation)**
 - **Half The Number of Power Semiconductor Devices**
 - **No Magnets or Rotor Winding**
 - **Simple Torque Control**

Table 4.14-7. Motor Scaling.

- **Variables Are: Speed (rpm)—Range From 20,000 to 60,000 rpm (60,000 rpm was dropped—Inconsistent With Stress Limits for the Diameters That are Practical)**
 - **Number of Poles — Range From 6 Poles to 2 Poles Was Evaluated**
- **Motor Selected Is a 6-Pole Design @ 40,000 rpm**
 - **Rated Power** 24 KVA
 - **Stator Diameter** 4.36 Inches
 - **Stack Length** 1.84 Inches
 - **Frame Diameter** 4.76 Inches
 - **Motor Length** 4.58 Inches
 - **El. Mag. Weight** 8.70 lbs.
 - **Motor Weight** 10.50 lbs.



higher speed motor as the drive could accommodate the additional ratio without much penalty. All the figures of the PCM show the envelope of the larger electrical machinery.

4.14.7.2 Generator Design

The selected generator was scaled from an existing machine. Table 4.14-8 gives the characteristics of this larger, parent machine. Table 4.14-9 shows the scaling factors and gives the characteristics of the generator selected for the advanced PCM. Again the speed increaser was designed when a 20,000 rpm generator was thought to be optimum but further work indicated the 30,000 rpm machine was to be preferred. This higher speed machine would produce a more desirable PCM as the speed increaser can also accommodate the higher ratio with little penalty.

4.14.8 Controls

Figure 4.14-18 shows a control schematic for the all-electric PCM. The schematic as drawn is designed to be illustrative rather than depict actual intended hardware, as, for example, the schematic shows a DC link whereas the power conversion would more likely be handled by a cycloconverter type of device.

As can be seen from the figure, there is two-way communication across the optical slipring. The blade angle resolver produces blade angle information which is transmitted back to the stationary propulsion system FADEC for ultimate cockpit display. Health data for condition monitoring and trending is also transmitted in this same direction. All other information is transmitted to the rotating assembly for normal or emergency operation of the propeller or for checkout.

One very important benefit of this type of PCM is its capability of continued near-normal operation in the event of a propeller control failure or of communication failure. The in-hub speed sensor is continually looking rearwards across the rotating boundary at the stationary portion of the system and is therefore capable of supplying a signal proportional to propeller speed



Table 4.14-8. Generator Design.

- **A Base Machine For Scaling Was Selected From An Existing PM-Generator For a 60 kVA VSCF System**
 - **Characteristics**
 - **System Rating of 60 kVA in the Generator Speed Range of 15-30,000 rpm**
 - **Electro Magnetic Dimensions for Generator**
 - **Rotor OD** 5.0 Inches
 - **Stator OD** 6.05 Inches
 - **Stack Length** 4.75 Inches
 - **Electrical Rating of Generator (9 Phase)**
 - **59A @ 155V and 0.76 PF (Continuous)**
 - **110A @ 145V and 0.72 PF (For 5 Seconds)**
 - **The Continuous Generator Rating Amounts to 82.3 kVA**
- VSCF = Variable Speed, Constant Frequency
OD = Outside Diameter
PF = Power Factor

Table 4.14-9. Generator Scaling.

- **Considerations:**
 - rpm (Range From 15 to 30,000)
 - Rotor Dimensions — Stack Length, Shrink Ring
 - ① - Number of Poles — 8 to 6
 - ② - Frequency — 750 Hz to 1500 Hz
 - Weight of Electromagnetics
 - Total Weight
- ① **Pole Number is Selected by Pole Pitch for Manufacturing Reasons**
- ② **Resulting Frequencies Also Influence Rectifier/Inverter Design**
- **The 30,000 rpm Machine is shorter at the same diameter**
- **The Bearing System Has Been Built and Demonstrated**
- **The Selected Generator (Force Commutated Inverter)
Rating 25 kVA @ 0.922 PF, 30,000 rpm, 1500 Hz**
- **Dimensions**
 - **Frame Diameter** 4.76 Inches (Same as Motor)
 - **Frame Length** 5.09 Inches
 - **Total Weight** 13.1 lbs.

ORIGINAL PAGE 15
OF POOR QUALITY

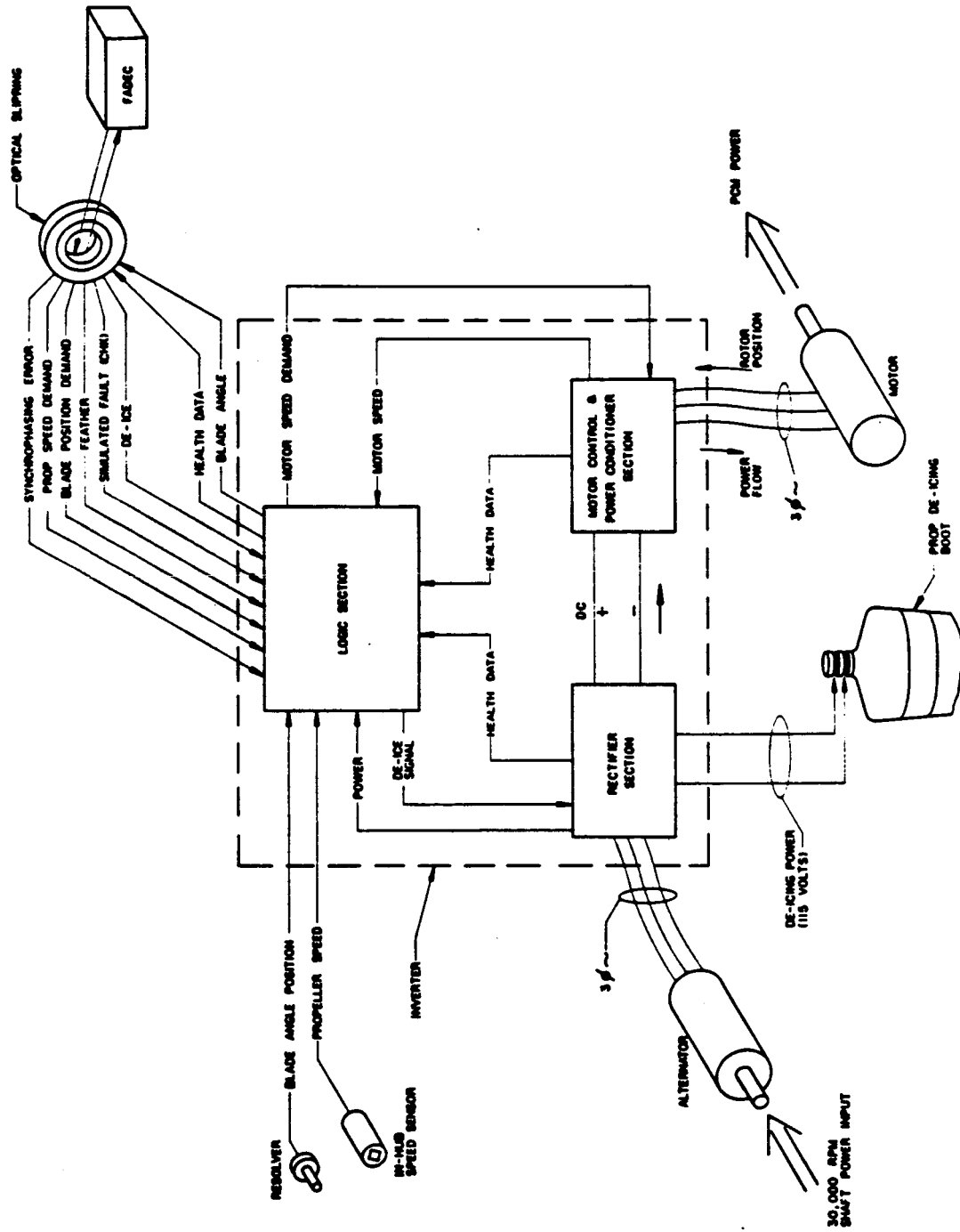


Figure 4.14-18. PCM Control Schematic.

to the rotating logic unit. In the event of a stationary control or communication failure, the cessation of proper signals to the rotating logic unit would be sufficient to cause the system to revert to a backup or default mode of operation. In this backup mode the signal from the in-hub sensor would be compared to that of a preprogrammed desired constant propeller speed and the speed or error would be used to adjust blade pitch to cancel the error. Synchronizing might be lost but, if so, it could be re-established by assigning the engine operating in the backup mode as the master and permitting the engine with normal operation to assume the slave role.

4.14.9 Lubrication and Cooling

The electronic control module, located at the extreme forward end of the propeller assembly, is air cooled. An inlet is provided in the tip of the spinner to capture ram air. This air is ducted to the control module and provides the necessary cooling. Air egress passages are provided in the large diameter portion of the spinner shell. Because of the exit holes being located at a large radius and the entrance being on the centerline, the rotation of the propeller aids in pumping cooling airflow.

The alternator rotates continuously at high speed and therefore its bearings are provided with pressurized oil which is supplied through a channel in the high speed drive shaft. This same oil is used to lubricate the speed increaser and bearings in the emergency feathering mechanism. In addition this oil is used for cooling both the motor and alternator. Suitable channels are supplied for cooling purposes in both the motor and alternator structures. No separate system is provided for the scavenging of this lubricating and cooling flow as the used oil is spilled into the bore of the gearbox output shaft and, ultimately, this oil joins the main gearbox lubricant, and is scavenged by the gearbox system.

4.14.10 Efficiency and Heat Rejection

4.14.10.1 Mechanical Efficiency

The traction drive as used in the final design (210:1 ratio) has an estimated efficiency of 94%. The efficiency of the entire drive system downstream

of the motor, including the traction drive and the ballscrew and links, is over 90%.

4.14.10.2 Electrical Efficiency

Figure 4.14-19 shows the full power efficiency, losses, and how the losses vary with current and voltage of the motor, alternator, and inverter. In summary, at full load 33.1 hp enter the alternator and 26.4 hp is produced by the motor.

It should be noted that the motor in this installation has a very unusual duty cycle for an electric machine. During synchrophasing operation, which represents the majority of the mission time, the motor is essentially operating stalled at near full torque as it is moving only a few revolutions, or fractions of a revolution, as necessary to achieve synchrophasing. This does not represent a problem for a properly designed machine as the losses at this condition are less than the full power losses. What is demanded is a motor cooling scheme that is independent of motor speed, as is provided here with oil cooling for both the motor and alternator.

The propeller having the master role in synchrophasing would have much less activity than the slave propeller as the master system has only the job of modulating blade pitch to run constant speed, a much less demanding task than matching blade phase with the master.

4.14.11 Failure Modes and Effects

A very important attribute of this advanced PCM is its ability to produce useable, controllable thrust in the event of a single serious failure, or even in the event of combinations of failures. Most competing systems would require that the affected propulsion system be shut down and the propeller feathered in the event of similar failures. Tables 4.14-10 and 4.14-11 lists possible failures and their effects on operation.

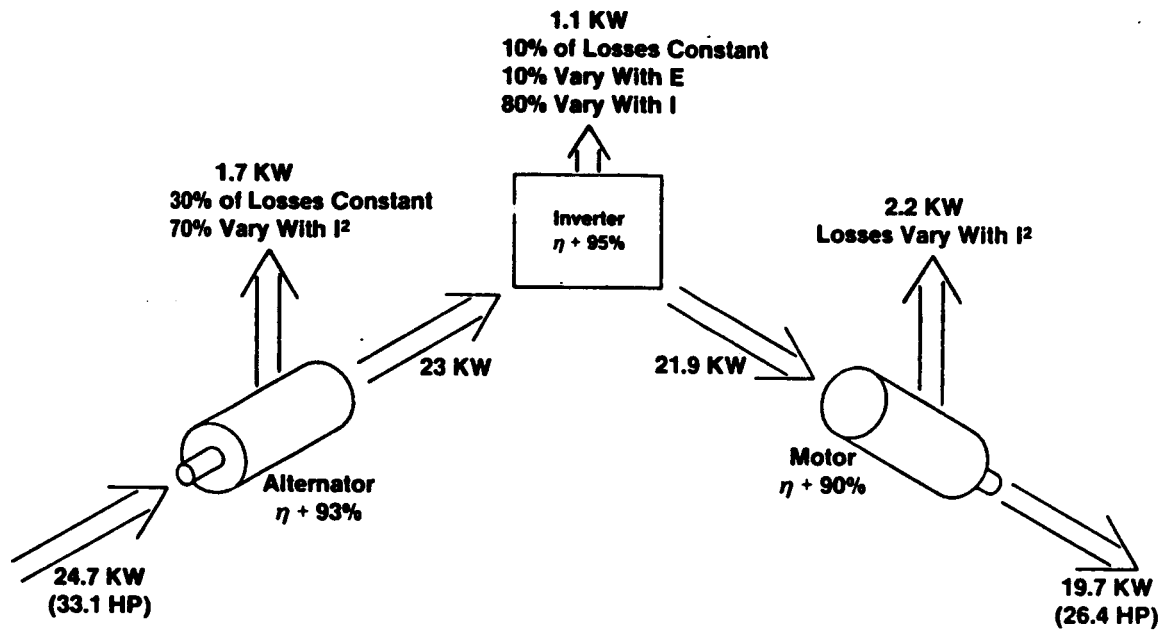


Figure 4.14-19. Full Power Losses.

Table 4.14-10. Failure and Effects.

If a Failure Occurs In The	Then	and	But
<ul style="list-style-type: none"> Optical Fibers 	Redundant Fiber Bundles Are Available to Transmit All Signals	The Mission Can Continue Normally.	
<ul style="list-style-type: none"> Silp Ring or FADEC 	The System Reverts to Internal Speed Loop Control.	The Mission Can Continue Safely. Emergency Feather Is Still Available. Constant Speed Operation and Thrust Modulation is Normal.	Synchronphasing, Reverse, and Reduced Speed Selection Not Possible.
<ul style="list-style-type: none"> Motor, Alternator, or Inverter 	The Blades Settle Back 1° Onto the Pitch Lock.	Useable Thrust Can Still Be Produced. Overspeed Protection (Wf Cutback) and Emergency Feather Capability Still Exist.	Constant Speed Operation, Synchronphasing, and Thrust \geq than that just Prior to Failure Not Possible.
<ul style="list-style-type: none"> Non-Prime Reliable Drive Components (Driveshaft, Traction Drive) 	Same as Above.	Same as Above Except No Capability of Emergency Feather	Same as Above.

Table 4.14-11. Failure and Effects.

If a Failure Occurs In The	Then	and	But
<ul style="list-style-type: none"> Pitch Lock Motor, or Control 	Pitch Settings < 1° of That at Instant of Failure Not Available.	Operation at or Above Power Setting at Instant of Failure is Normal.	No Negative Thrust is Available. Thrust Response From Low Power Reduced.
<ul style="list-style-type: none"> Cooling Circuits 	Blades Must Be Allowed to Settle onto Pitch Lock.	All Functions Retained Except Duty Cycle Greatly Restricted.	No Synchronphasing; Constant Speeding Probably Affected.
<ul style="list-style-type: none"> Lubrication Circuit 	Alternator Bearings Will Fail and Rotor Will Seize.	Driveshaft Will Fail in Shear Section.	Subsequent Operation Will Be the Same as With a Drive Failure.
<ul style="list-style-type: none"> Emergency Feather System 	All Normal Operation is Unaffected.	Feathering Can Be Accomplished in an Emergency Using the Normal Systems.	There Will Be No Backup Feathering Capability

4.14.12 Reliability, Cost, and Weight

Table 4.14-12 compares the advanced electric PCM with a current hydraulic system. The first generation advanced electric system is very competitive in all areas except acquisition cost. The situation here may soon change to the advantage of the electric system as the enabling technology in motors, controls, power switching devices, and optics is progressing at a very rapid rate and significant reductions in cost of components utilizing these technologies may be expected.

Table 4.14-12. Propfan Summary.

	Pitch Control Technology	
	Current	Advanced
● Reliability		
- MTBUR, Propfan Assembly (Chargeable) — Hours	18,400	18,800
- Mean Time Between All Maintenance Actions (All Causes) — Hours	2,700	3,580
● Maintenance Cost	Base	-11%
● Acquisition Cost	Base	+10%
● Weight	Base	-5%

Base is Defined as the Offset Gearbox System Presented in the GE APET Contract

SECTION 4.15

RECOMMENDATIONS FOR TASK VII AND VIII

<u>Section</u>		<u>Page</u>
4.15.1	Advanced Propfan Gearbox	421
4.15.2	Pitch Change Mechanism	422

FIGURES

<u>Figure</u>		<u>Page</u>
4.15-1.	Overall Timing and Key Milestones.	425
4.15-2.	Development Plans and Recommendations - PCM.	427
4.15-3.	Turboprop Pitch Change Mechanism Fiberoptic Technology Program.	428
4.15-4.	FADEC Technology Program.	429
4.15-5.	Turboprop Pitch Change Mechanism Electric Motor/Generator Technology Program.	430
4.15-6.	Traction Drive Module Program.	432
4.15-7.	Turboprop Pitch Control Technology Program.	433
4.15-8.	Turboprop Pitch Control Technology Program.	434
4.15-9.	Turboprop Pitch Control Technology Program.	435

TABLES

<u>Table</u>		<u>Page</u>
4.15-1.	Program Elements.	423
4.15-2.	Mechanical Design and System Analyses.	423
4.15-3.	Hardware Requirements.	424
4.15-4.	Outside Vendor Participation.	424
4.15-5.	Bearing and Gear Component Tests.	424
4.15-6.	Full-Scale Back-to-Back Rib Test.	425

4.15 RECOMMENDATIONS FOR TASK VII AND VIII

Some preliminary recommendations for the gearbox development effort have already been included in 4.12.11 and now need amplification. The Pitch Change Mechanism (PCM) of Task VIII has not yet been covered and is therefore fully described in this section.

4.15.1 Advanced Propfan Gearbox

Subsequent to the recommendations in 4.12.11, the design effort to take the gearbox from a "conceptual" current technology standard to a "preliminary" design standard for the early 1990's time period has resulted in some notable changes although the basic concept of an "in-line" star configuration has not been superseded.

Noteworthy changes include:

- A four star layout versus a three star has been selected.
- A fabricated titanium housing rather than one cast in aluminum alloy is now proposed.
- The integration of all gearbox "services" into the basic design layout has been accomplished.
- More attention to modularity has been paid.
- A thermally controlled lubrication supply, whereby oil flow is metered as a function of torque applied is the selected system concept.
- More detailed efforts in system integration with both the propfan, its pitch change mechanism, and the design of the enclosing nacelle.

A number of the component elements already given in 4.12.11 need not be repeated for this amplified program definition, and these elements still apply to the gearbox designed in Task VII.

The emergence of through and case-hardened M50 NIL material for toughness in antifriction bearing applications would indicate that some additional materials should be investigated for the power gearsets. First by Ryder type gear

PRECEDING PAGE BLANK NOT FILMED

tests and second in some existing power gear setup. It is definitely recommended that the M50 NIL material be critically evaluated for possible use in aerospace gearing.

Improvements that are being constantly made in both Finite Element and Dynamic Modeling suggest that some significant efforts, using these modern tools, should be made to theoretically compare with the empirical results from test rigs. The effects of friction and wear must also be countered using the best data available from the tribological experts - particularly where elevated gear blank temperatures, modulated lubrication flow, a more advanced lubricant chemistry with additives, are all to be explored in both component and full-scale test programs.

Also considered important, but not a part of the recommendations for the in-line gearbox, is the development of a technology data base for conformal gears. This type of gearing is strongly recommended for a high-stage-ratio, single gearset, for a 12,500 SHP gearbox with offset geometry. If airplane layouts of single row propfans are better served with propulsion systems using offset gear arrangements, then the technology inherent in conformal gearing could play a dominant part in the overall picture.

The program elements for the in-line gearbox development are included as Table 4.15-1. These are further broken down in Table 4.15-2 which defines the tasks for mechanical design and system analysis.

Table 4.15-3 describes the hardware required for the test programs and Table 4.15-4 indicates the technical areas which would most probably require some outside vendor support.

Tables 4.15-5 and 4.15-6 indicate the component and full-scale tests required, while Figure 4.15-1 gives the program overall schedule.

4.15.2 Pitch Change Mechanism

A 3-year technology program has been laid out which would accomplish NASA's primary objective of establishing a solid foundation for an advanced

Table 4.15-1. Program Elements.

- Mechanical Design
- System Analyses
 - Stress/Deflections
 - Vibration
 - Lubrication
 - Finite Element Modeling
- Procure hardware
- Outside Contractors Coordination
- Bearing and Gear Component Tests
- Full-Scale Back-to-Back Rig Test

Table 4.15-2. Mechanical Design and System Analyses.

Program Elements

- Select Design Configuration
- Prepare Detail Drawings
- Analysis - Stress, Finite Element
- Outside Vendor Coordination
- Engineering Coverage During Manufacture
- Component Test Coverage
- Full-Scale Test Coverage
- Documentation

Table 4.15-3. Hardware Requirements.

- 3 Complete Gearbox Assemblies Plus Spares - Gears, Shafts Bearings.
- Bearings and Gears for Component Tests (3 or 4 Gearsets with Modified Profiles).

Table 4.15-4. Outside Vendor Participagion.

- Mounts Design and Analysis
- Mounts Hardware
- Input Driveshaft, Couplings, Torque Tube
- Condition Monitoring Instrumentation
- Test Rig Instrumentation

Table 4.15-5. Bearing and Gear Component Tests.

- Bearings*
 - Planet/Star or Idler Bearings
 - Include Gear Mesh Separating Load Effects
 - Equivalent Loading
 - Determine Stability at Various Cooling Rates
 - Determine Heat Rejection Versus Load
 - Endurance Test
- Gears*
 - Single Mesh Testing
 - Scale Size of Test Gears (To Be Determined)
 - Determine Scoring Characteristics (Materials)
 - Determine Heat Rejection Versus Load
 - Load Endurance

*Assumes a Single Lubricant Has Been Selected.

Table 4.15-6. Full-Scale Back-to-Back Rig Test.

- New 4 Square Rig Facility
- Minimum Testing Required
 - Four Test Sequences
 - Inspections at Initial Assembly/Teardown
 - Intermediate Inspections as Required by the Test Plan
 - Initial Checkout
 - "Test Plan" testing (4-500 Hours)
 - Torque Testing Only
 - Measured Delections
- Addition of Prop Load Testing is a Program Option

	First Year				Second Year			
	1	2	3	4	1	2	3	4
Preliminary Design	▲							
Analysis				▲				
Detail Drawing				▲				
Procure Hardware							▲	
Outside Vendor Contracts							▲	
Component Tests								▲
Back-to-Back Tests								
Rig Design and Procurement							▲	
Test Plan Testing								▲

Figure 4.15-1. Overall Timing and Key Milestones.

electromechanical PCM controlled by a fiberoptic, digitally encoded, data link. The program includes 2 years of design and manufacturing effort on the intrinsic components and modules with a further 1-year effort to complete both static and dynamic tests. It is emphasized that the program is strictly geared to the generation of a technology base in that no propfan blade activities are warranted or included in the plan although, of necessity, a prototype of a flight-type propfan hub would be required.

There are a number of module units which can be developed independent of each other and subjected to appropriate component tests prior to being assembled into a complete hub mechanism. Also, in parallel with this activity there can be ongoing efforts to design and manufacture the hardware and slave drives that will be needed during the 3rd year's tasks. i.e., complete system checkout.

Figure 4.15-2 is an overview of the PCM development recommendations. Basically, what is foreseen, are requirements in three main areas:

- Mechanisms
- Electrical (and electro-optical)
- Specialized test rigs.

Figure 4.15-3 shows a 3-phase program for the required fiberoptic technology. Note that Phase 1 concentrates on the problems that must be solved in the successful execution of the design and development of the low noise, optical slipring. Phase 2 contributes a laboratory prototype for bench testing and Phase 3 contributes a "developed" laboratory prototype which can be used in the ensuing full-scale rig program.

Figure 4.15-4 describes the efforts needed to add an optical data link for an engine FADEC unit. Note that the converted FADEC is both a transmitter and receiver of optical data. These efforts culminate with a "brassboard" test of an existing FADEC suitably modified for the optical role. This unit would also play a part in the ensuing full-scale rig program.

Figure 4.15-5 represents the key item development for the electrical machinery. Both the motor and the alternator are to be designed and manufactured together with a compatible control system. Like the previous technology

- **Mechanisms**
 - **Clutch and Speed Increaser, Input Shaft, Module**
 - **Traction Drive, 210 to 1 Stage Ratio, Module**
 - **Duplicate Ball Nut* and Ball Screw, Recirculating Type, Module**
 - **Torque Limiter, Pitch Locks, Modules**
 - **Pitch Links, Individually Balanced and Replaceable**
- **Electrical**
 - **Motor and Generator, Oil Cooled, 30-40,000 rpm, Modules**
 - **Servomotor for Pitch Locks, Module**
 - **Alternator, Power Conditioning, Module ****
 - **FADEC Signal Generating, Electronic Optic, Module**
 - **Optical Slipring, With Purge System, Module**
 - **Ground Operating, Power Supply, Module**
- **All the Above to be Rig Tested, Individually, and as an Assembly With Fullscale Loading**
 - **Redundant 2 Track Design**
 - ** **Includes Optic to Electronic Converter. Is Air Cooled**

Figure 4.15-2. Development Plans and Recommendations - PCM.

3 Phases

- **Phase 1**
 - **Mirror Surfaces, Select Materials, Evaluate by Test**
 - **Select Components for Data Link, Evaluate by Test**
 - **Select Data Transmission Protocols, Including Redundancy**
 - **Verify Signal-to-Noise Ratio**
 - **Verify Operation in Adverse Conditions (Contamination)**
- **Phase 2**
 - **Design, Manufacture, Test a Laboratory Prototype System Including an Optical Slip Ring**
- **Phase 3**
 - **Design, Manufacture, Test a Developed Laboratory Prototype**

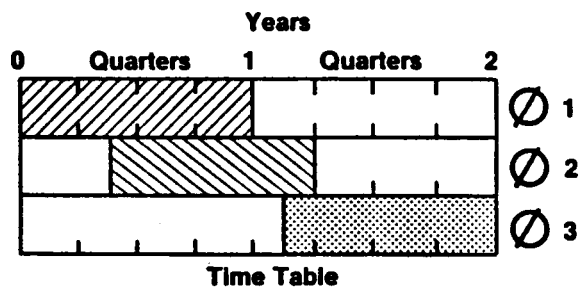


Figure 4.15-3. Turboprop Pitch Change Mechanism Fiberoptic Technology Program.

Program Objectives

- 1) ● Define a FADEC That Controls Both the Shaft Engine and the Propeller With Fiberoptic Data Links
- 2) ● Define the Converters — Electronic to Fiberoptic and Vice Versa (FADEC Both Transmits and Receives Fiberoptic Data)
- 3) ● Determine Communication Logic — Pulse Width Modulation Versus Frequency Modulation
- 4) ● Test a Brassboard System Based on Modifying an Existing FADEC Unit

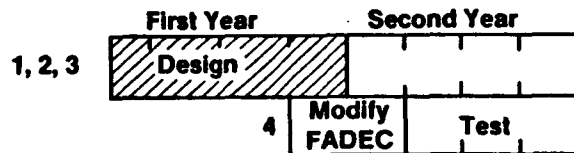


Figure 4.15-4. FADEC Technology Program.

- 1) • Select Motor Type and Generator Type (Trade Studies)
- 2) • Select and P.D. Control Circuits (Trade Studies)
- 3) • Design Electric Machinery and Control Module
- 4) • Assemble Breadboard Control and Test (Inc. Heat Rejection)
- 5) • Manufacture Machinery and Brassboard Control
- 6) • Test Machinery and Control
- 7) • Participate in Fullscale PCM Testing, Modify as Required

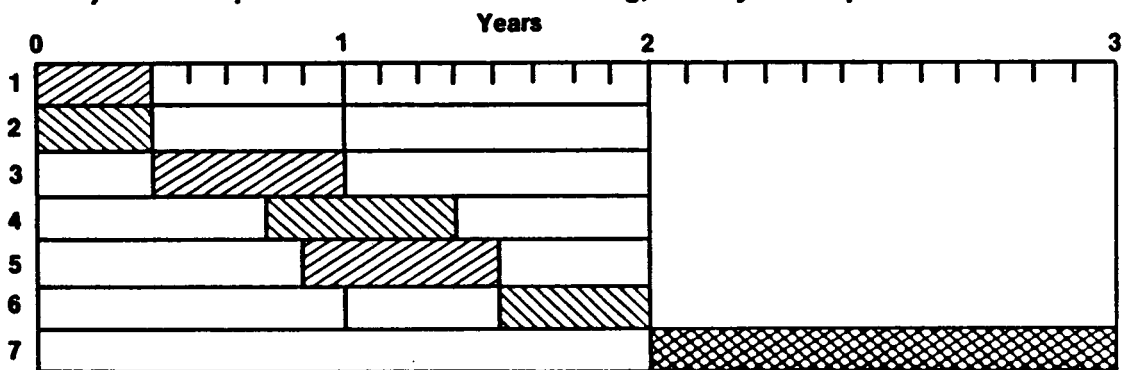


Figure 4.15-5. Turboprop Pitch Change Mechanism Electric Motor/Generator Technology Program.

items, the electrical machinery is first tested as a modular set of components before being committed to the test program on the full-scale rig.

Figure 4.15-6 delineates all the necessary steps that must be taken to design, manufacture, and component test a traction drive with a 210:1 reduction ratio. Similarly to the other modules it also finds its way eventually to the full-scale rig test program.

Figure 4.15-7 outlines the necessary hardware that must be designed, manufactured, and supplied by Hamilton-Standard in support of the full-scale test rig. Naturally, these major components must be integrated in form and function with the remainder of the modules which are also highlighted in this figure.

Figure 4.15-8 addresses the design and manufacture of a specialized test stand which will be required to provide the drive and loading in the full-scale rig. Figure 4.15-9 summarizes the total effort required from full-scale rig testing which is estimated to require about a 1-year effort.

Costs for implementation of the total PCM program have been provided to NASA under separate cover.

Milestones	Year 1	Year 2	Year 3	Year 4
	J F M A M J J A S O N D	J F M A M J J A S O N D	J F M A M J J A S O N D	J F M A M J J A S O N D
<ul style="list-style-type: none"> • Module Units - Hub and Blade Assembly - BallScrew/Nut Assembly - Motor/Ail Assembly - Electronic Controls - Traction Drive Assembly - Blade Roots and Links - Fiber Optic Slipring - Pitchlock Mechaniam - Pitchlock Motor and Controls • Speed Increase and Feather Unit - Shafting and Structures - Lube and Cooling System 	<p>Hamilton Standard</p> <p>Hamilton Standard</p> <hr/> <hr/> <p>Hamilton Standard</p> <hr/> <hr/>	<hr/> <hr/> <hr/>		

Figure 4.15-7. Turboprop Pitch Control Technology Program.

Milestones	Year 1	Year 2	Year 3	Year 4
	J F M A M J J A S O N D	J F M A M J J A S O N D	J F M A M J J A S O N D	J F M A M J J A S O N D
<ul style="list-style-type: none"> • Test Cell - Test Stand Construction - Loading and Absorb. Motors - Instrumentation - External Lube System - Blade Loading Actuators - Hub Rotation Drive 				

Figure 4.15-8. Turboprop Pitch Control Technology Program.

SECTION 5.0
CONCLUSIONS

ORIGINAL PAGE IS
OF POOR QUALITY

PRECEDING PAGE BLANK NOT FILMED

437

PAGE 436 INTENTIONALLY BLANK

5.0 CONCLUSIONS

The General Electric findings from the APET study are positive; the fuel burns of the APET airplanes have been quantified between 300 and 1000 N.Mi ranges with payload factors of 100% and 65%. Great care was taken throughout the study to ensure that consistent airplane and engine technology was used when making comparisons between turbofan and turboprop powered airplanes for the 1990's. The various steps, or levels, of enabling technology have been identified to project current technology gas turbine-powered airplanes into the next decade. Both the fuel burn results and the DOC results show sufficient improvement to warrant continued efforts on the high-speed turboprop. NASA has been supplied with the necessary propulsion system technology program plans required to demonstrate the component improvements that are needed.

The propulsion configurations and performance results of this study have not yet been critically reviewed by the airframe and the airline industry. General Electric recommends that NASA contracts with these industries to confirm these results. GE believes that the APET Contract effort should be continued with the objective of providing another, and more detailed, study of some of the critical technology components. These components, which have been identified within this study's recommendations section, require commitment of major financial and developmental resources to accomplish the objective performance.

The computer generated engine performance decks and the scaling laws for propulsion weights and dimensions need exercising in airframe study programs. These computer decks are fully described in Appendix III.

Aircraft/engine integration is a major problem for any new propulsion system and the high-speed turbopropfan falls directly into this category. Substantial Government resources and programs are considered necessary for the eventual successful development of the airplane and matching propulsion system. Apart from the basic aerodynamic development, required through wind tunnel test programs to ensure a low-drag installation at cruise speeds, other aero programs are required. Areas requiring more work are low speed

handling, high lift configurations, engine out and other asymmetric flight conditions, basic stability and control derivatives, thrust-matching studies, nacelle placement studies, and more detailed investigations into acoustic and vibration environments.

Finally, General Electric would welcome the opportunity to continue the APET investigations. For propulsion prime areas we would propose solo efforts. For all subjects that require airframe/engine integration it is recommended that the airframe companies should have the prime contracts and that propulsion companies should be subcontracted. In both areas, Government funding support with continued development efforts also occurring in parallel is recommended to make the full scale propfan a success.

The advantages of counterrotating propfan systems must also be systematically examined for both tractor and pusher configurations. New technologies in gearboxes, pitch change mechanisms, exhaust system designs and controls techniques, should be pursued and integrated into practical nacelles and airplane configurations. Both military and commercial applications should be considered. The APET study is supplying NASA and the airframe industry with a solid technical base, and future efforts are confidently expected to define the advanced propulsion systems required by a new subsonic generation of airplanes.

REFERENCES

1. Task Force Report, "Aircraft fuel Conservation Technology," NASA Office of Aeronautics and Space Technology, September 10, 1975.
2. NASA CR-137926 Final Report and NASA CR-137927 Summary Report, "Study of the Cost/Benefit Tradeoffs for Reducing the Energy Consumption of the Commercial Air Transportation System," Lockheed-California Company, NASA Ames Contract NAS2-8612, August 1976.
3. NASA CR-137923 Final Report Volume I: Technical Analysis, NASA CR-137924 Final Report Volume II: Market and Economic Analyses, and NASA CR-137925 Summary Report, "Cost/Benefit Tradeoffs for Reducing The Energy Consumption of the Commercial Air Transportation System," Douglas Aircraft Co., NASA Ames Contract NASA 2-8618, June 1976.
4. Boeing Commercial Airplane Company - Energy Consumption Characteristics of Transports Using the Prop-Fan Concepts, NASA CA 137937, October 1976.
5. Rohrbach, C. - A Report on the Aerodynamic Design and Wind Tunnel Test of a Prop-Fan Model, AIAA Paper No. 76-667, July 1976.
6. Mikkelson, D.C., D.J. Blaha, Mitchell, G.A. and Wikete, J.E. - Design and Performance of Energy Efficient Propeller for Mach 0.8 Cruise, NASA TMX-73612, April 1977.
7. ICAS Proceedings, 1978, Edited by J. Singer and R. Staufenbiel, 11th Congress of the International Council of the Aeronautical Science (ICAS), Volume I, "Fuel Conservative Aircraft Engine Technology," D.L. Nored, NASA Lewis, September, 1978.
8. NASA CR-152186, "An Analysis of Prop-Fan/Airframe Aerodynamic Integration," Boeing Commercial Airplane Co., NASA Ames contract NAS2-9104, October 1978.
9. R.E. Neitzel, R. Hirschcron, and R.P. Johnston, "Study of Unconventional Aircraft Engines Designed for Low Energy Consumption." (R76AEG597), General Electric Co.; NASA Contract NAS3-19519.) NASA CR-135136, 1976.
10. "Study of Turboprop Systems Reliability and Maintenance Costs." (EDR 9132, Detroit Diesel Allison; NASA Contract NAS3-20057.) NASA CR-135192, 1978.
11. Little, B.H., Jr., "Propulsion System Installation Design for High-Speed Prop-Fans," AIAA-81-1649, AIAA Aircraft Systems and Technology Conference, Dayton, Ohio, August 11-13, 1981.
12. Keith, J.S., Ferguson, D.R., Merkle, C.L., Heck, P.H., and Lahti, D.J., "Analytical Method for Predicting the Pressure Distribution About a Nacelle at Transonic Speeds," NASA CR-2217, July 1973.

13. Welge, H. Robert, "Prop-Fan Integration at Cruise Speeds," AGARD Paper 33 presented to AGARD Symposium on Aerodynamics of Power Plant Installation, Toulouse, France, May 11-14, 1981.
14. Dugan, J.F., Miller, B.A., Graber, E.J., and Sagerser, D.A., "The NASA High-Speed Turboprop," NASA TM 81561, October 1980.
15. NASA TM-78962, "Fuel Conservative Aircraft Engine Technology," D.L. Nored, NASA Lewis, September 1978.
16. NASA TM-79124, "Wind Tunnel Performance of Four Energy Efficient Propellers Designed for Mach 0.8 Cruise," R.J. Jeracki, D.C. Mikkelson, and B.J. Blaha, NASA Lewis, April 1979.
17. Canadian Aeronautics and Space Journal, Vol. 24, Number 4, "Prospects for Energy Conserving STOL Transports Using Prop-Fans," B. Eggleston, deHavilland Aircraft of Canada, Limited, August 1978.
18. A Study to Define the Research and Technology Requirements for Advanced Turbo/Propfan Transport Aircraft. I.M. Goldsmith. Douglas Aircraft Company NASA CR-166138 dated February 1981.
19. Turboprop Cargo Aircraft Systems Study. Phase 1 Lockheed, Georgia. NASA CR-159355.
20. Hamilton Standard, "Ten-Blade Propfan Parametric Data Package" HSD Report No. 07A82, May, 1982.
21. Hamilton Standard, Ten Blade Prop-Fan Data Package HSD Report No. SPO4A80, October 1980.
22. This Reference is a Duplicate of Reference 13.
23. General Electric Report No. R82AEB262 dated April, 1982.
24. American Airlines Report "A New Method for Estimating Current and Future Transport Aircraft Operating Economics," 1978 (NASA CR 145190).
25. Society of Allied Weight Engineers Paper 1416 "Price - Weight Relationships of General Aviation, Helicopters, Transport Aircraft and Engines" dated May 1981, by Joseph L. Anderson.
26. Hoerner, S.F.; "Fluid Dynamic Drag," Published by Author, 1965.
27. GE Heat Transfer and Fluid Flow Data Book, Research and Development Center, Schenectady, New York, 1970.

28. Black, D.M., Menthe, R.W., and Wainauski, H.S., "Aerodynamic Design and Performance Testing of an Advanced 30° Swept, Eight Bladed Propeller at Mach Numbers from 0.2 to 0.85", NASA CR-3047, 1978.
29. Little, B.H. Jr. and Trimboli, W.S.. "An Experimental Investigation of S-Duct Diffusers for High-Speed Prop-Fans", AIAA-82-1123, June 21-33, 1982.
30. Maddalon, Molloy, and Neubauer, "Computer Programs for Estimating Civil Aircraft Economics, "NASA TM 80196, January 1980.
31. Association of European Airlines G(T) Ext. 2419/R1 "Future Aircraft Definition Group - Common DOC Method for Short/Medium Range Aircraft," 4 March 1980.
32. Boeing Presentation 6-1445-S-327 "Boeing 1979 Operating Cost Methods."
33. NASA CR-151970 "Parametric Study of Transport Systems Weight" -- Report by "Science Applications, Inc.," Published in April 1977).

GEARBOX AND LUBRICATION

34. AGM 411.02, Design Procedure for Aircraft Engine and Power Takeoff Spur and Helical Gears, American Gear Manufacturing Association, 1974.
35. Townsend, Dennis, P.; Zaretsky, Erwin, V.; Comparison of Modified VASCO X-2 and AISI 9310 Gear Steels, NASA Technical Paper 1731, 1980.
36. Lemanski, A.J., Rose, H.J., Evaluation of Advanced Gear Material for Gearboxes and Transmissions. Boeing Vertol Report for Department of Navy, D210-10345-1, 1971.
37. Mack, J.C., HLH Drive System. US Army Aviation Research and Development Command, USAAMRDL-TR-77-38, 1977.
38. Townsend, Dennis, P., Parker, Richard, J., and Zaretsky, Erwin, V.: Evaluation of CBS600 Carburized Steel as a Gear Material. NASA Technical Paper 1390, 1979.
39. AGMA 217.01, Gear Scoring Design Guide for Aerospace Spur and Helical Power Gears, American Gear Manufacturing Association, 1965.
40. Willis, R.J. Lightest Weight Gears, Product Engineering 1-21-63.
41. Wellauer, E.J. and Holloway, G.A., "Application of EHD Oil Film Theory to Industrial Gear Drives", Trans. ASME, J. Eng. Ind., 98B (2) 626-634 (May 1976).

42. NASA CR-3241 "Thermal Elastohydrodynamic Lubrication of Spur Gears," K.L. Wang and H.S. Chen, Feb. 1980.
43. Townsend, Dennis P.; Baber, Berl B.; Nagy, Andrew; Evaluation of High-Contact - Ratio Spur Gears with Profile Modification, NASA Technical Paper 1984, 1979.

ACOUSTIC REFERENCES

44. SAE AIR 1407, "Prediction Procedure for Near-Field and Far-Field Propeller Noise", May 1977.
45. Magliozzi, B. NASA-CR-145105, "The Influence of Forward Flight on Propeller Noise," February 1977.
46. Marte, J.E. and Kurtz, D.W. "A Review of Aerodynamic Noise from Propellers, Rotors, and Lift Fans, NASA JPL TR32-1462, January 1, 1970.
47. Metzger, F. "Preliminary Analysis of Prop-Fan Flight Test Data", Presentation at NASA Advanced Turboprop Acoustic Review, November 3, 1982.
48. Farassat, F. and Succi, G.P. "A Review of Propeller Discrete Frequency Noise Prediction Technology with Emphasis on Two Current Methods for Time Domain Calculations", 1980 Journal of Sound and Vibration 71, 399-419.
49. Heidman, M.F. NASA TM X-71763 "Interim Prediction Method for Fan and Compressor Source Noise", June 1975.
50. Kazin, S.B. and Matta, R.K. AIAA Paper 75-449 "Turbine Noise Generation, Reduction and Predictions", March 1975.
51. SAE ARP 876B, Appendix D "Prediction of Noise from Conventional Combustors Installed in Gas Turbine Engines", February 1980.
52. Hardin, J.C. et al., NASA TN-D-7821 "Prediction of Airframe Noise," February 1975.
53. SAE ARP876B-Appendix A, "Prediction of Single Stream Jet Mixing Noise from Shock Free Circular Noise," November 1978.
54. SAE ARP866, "Standard Values of Atmospheric Absorption as a Function of Temperature and Humidity for Use in Evaluating Aircraft Flyover Noise", August 1964.
55. Benzakein, M. FAA report RD-71-85 Section IID "Fan Compressor Noise Research," March 1972.
56. SAE AIR 923, "Method for Calculating the Attenuation of Aircraft Ground to Ground Noise Propagation During Takeoff and Landing," August 1966.

57. Rennison, D.C. et al., NASA CR 159200 "Interior Noise Control Prediction Study of High-Speed Propeller-Driven Aircraft," September 1979.
58. FAR PART36 "Noise Standards: Aircraft Type and Airworthiness Certification", 1978.

ORIGINAL PAGE IS
OF POOR QUALITY

APPENDICES

<u>Number</u>		<u>Page</u>
I	HEAT EXCHANGERS	449
II	ACOUSTICS	467
III	ENGINE WEIGHT AND DIMENSION CALCULATION MODEL	485

PRECEDING PAGE BLANK NOT FILMED

PAGE 446 INTENTIONALLY BLANK

447

APPENDIX I

I.1 INTRODUCTION

Heat exchanger system losses include inlet spillage drag, inlet recovery, heat exchanger total pressure loss, exhaust duct total pressure loss, nozzle exit velocity coefficient, external pod drag, and incremental external drag due to nozzle deflection. The heat exchanger core total pressure loss was supplied by the Hughes-Treitler Manufacturing Corporation and has been used exclusively.

I.2 BASIC DRAG AND LOSS ELEMENTS

Exhaust duct total pressure loss has been calculated using duct conditions at the heat exchanger exit and the duct geometry in a pressure loss computer program. Total pressure losses varied from 0.126% $\Delta PT/PT$ at takeoff conditions to 1.111% $\Delta PT/PT$ at cruise conditions. An appropriate model was defined for the engine cycle deck.

The heat exchanger basic external drag includes three items: pod pressure drag, pod sidewall friction drag and corner losses. (The pod bottom external friction drag is assumed equal to that part of the engine nacelle covered by the pod and therefore is included in the engine nacelle external drag.) A value of 20% of the total friction drag was used to approximate the pod pressure drag. Sidewall areas amounted to 11% of the total pod wetted area and, therefore, 11% of the total friction drag; and corner losses were assumed to be equal to 5% of the total friction drag. Therefore, the external pod drag was assumed equivalent to 36% of the external pod friction drag. The external friction drag was computed using the propeller hub discharge flow conditions and the incompressible friction coefficient, $C_{f_i} = 0.455/(\log_{10} Re)^{2.58}$, and the ratio of compressible to incompressible friction coefficients,

$$C_{f_{comp}} / C_{f_{incomp}} = \left(1 + \frac{\gamma-1}{2} M_1^2 \right)^{-0.467}.$$

The results of the calculations gave an external drag coefficient, C_D , of 0.012 based on a frontal area of 294 in.². This C_D appears consistent with the C_D values of similar bodies contained in Reference 26 (Hoerner) when the total friction drag is included. Based on this C_D and reference area, the expression for the basic pod drag was $D = 2.4696 P_o M^2$.

I.3 VARIABLE GEOMETRY EXHAUST NOZZLE

At flight conditions other than cruise, the nozzle area must be increased to meet the requirements of the heat exchanger with the maximum area being required at takeoff conditions. The exit area is increased by rotating the duct outer wall out into the external flow thereby increasing the drag. The opened nozzle will appear as a ramp but at a larger angle, approximately 19° instead of 5.25°, with respect to the local flow field. Adjusting for this difference in angles by assuming a linear relation between C_D and the ramp angle gives a C_D of 0.064. Both the C_D value and the additional frontal area due to nozzle deflection were assumed to vary with nozzle exit area by the ratio of $(A_{\text{exit}} - A_{\text{exit min}})/A_{\text{exit max}} - A_{\text{exit min}}$. This gave the following expression for the drag due to nozzle deflection

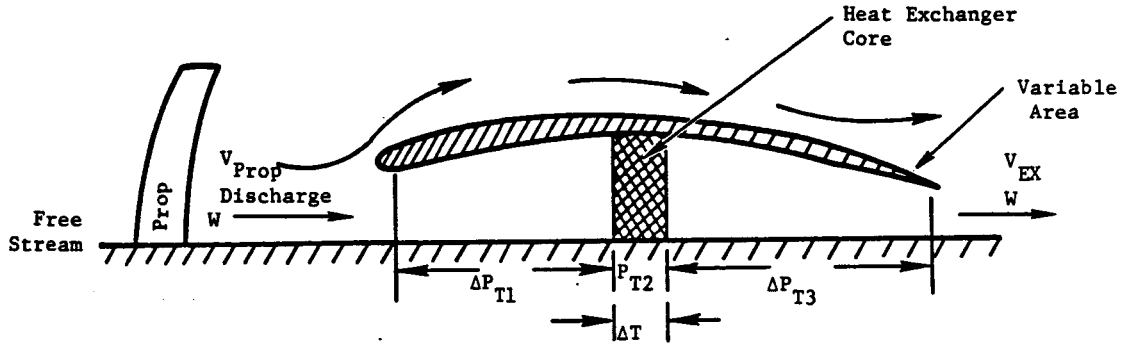
$$D = 2.4927 P_o M^2 \left(\frac{A_{\text{exit}} - A_{\text{exit min}}}{A_{\text{exit max}} - A_{\text{exit min}}} \right)^2$$

The nozzle exit velocity coefficient, C_v , was estimated using empirical data which accounts for nozzle perimeter effects for high aspect ratio, 2-D nozzles. At the cruise condition, the nozzle hydraulic diameter ratio is approximately 0.2. For this condition and an assumed C_v value of 0.99 for a standard round nozzle, the C_v of the heat exchanger nozzle was calculated to be 0.98. For this application, little change in C_v should be expected with nozzle deflection to the takeoff position. This value of C_v was assumed constant over the range of operating conditions (nozzle pressure ratios of 1.04 to 1.57 and geometry variations of the heat exchanger exhaust system). The nozzle exit flow coefficient, C_f , was to be a constant value of 0.98 over the operating range.

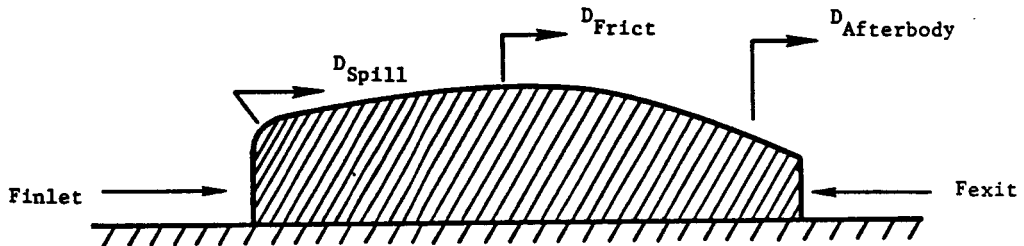
I.4 APET HEAT EXCHANGER LOSS MODEL

ORIGINAL PAGES
OF POOR QUALITY

Station Diagram



Force Diagram



$$\text{Net Force (Drag)} = (F_{Inlet} + D_{Spill} + D_{Friction} + D_{Afterbody}) - F_{Exit}$$

I.4.1 External Elements

- D_{Spill} ~ Spillage Drag; Inlet Design, Airflow Requirements
- $D_{Friction}$ ~ Friction due to Additional Wetted Area
- $D_{Afterbody}$ ~ Afterbody Drag due to Variable Area Nozzle

I.4.2 Internal Elements

- F_{inlet} ~ Prop Discharge Velocity and Airflow Required for Cooling
- F_{Exit} ~ ΔP_{T1} , Inlet Diffuser Pressure Loss
 ΔP_{T2} , Heat Exchanger Core Pressure Loss
 ΔT , Temperature Rise Across Heat Exchanger
 ΔP_{T3} , Exhaust System Pressure Loss, Friction and Turning

I.5 INTERNAL LOSS CALCULATION PROCEDURE

The heat exchanger core is at the heart of the internal loss calculation. It is essential to know the pressure loss and heat transfer characteristics of the heat exchanger core in order to assess the heat exchanger system performance. Therefore, in order to establish a credible design GE submitted the APET heat exchanger requirements to Hughes-Treitler Manufacturing Corporation, an aircraft heat exchanger manufacturer and Hughes-Treitler provided the preliminary design of the APET heat exchanger used in nacelle design and analyses.

GE has the in-house capability to design and analyze the ducting to and from the heat exchanger core. The APET heat exchanger ducting was designed by GE to meet specific APET requirements. The Hughes-Treitler heat exchanger core data was generalized (to account for small changes in the APET engine that occurred from the time the specification was issued) and used in conjunction with the GE duct analysis.

The resulting generalized heat exchanger core data are shown in Figure I-1. Note that the σ ($= \rho/\rho_0$) in Table I-1 is based on a core face density rather than the average density through the core as stated in the Hughes-Treitler report. This change was made to simplify calculation procedure.

For a generalized assessment of the heat exchanger system internal drag, the system can be viewed as a "black box". The "black box" has an entering momentum (Ram drag = $\omega/g V$); an internal loss (pressure drop); heat addition

¹APET horsepower, gearbox efficiency, flight condition relationships are given in Figure I-5 and Table I-1.

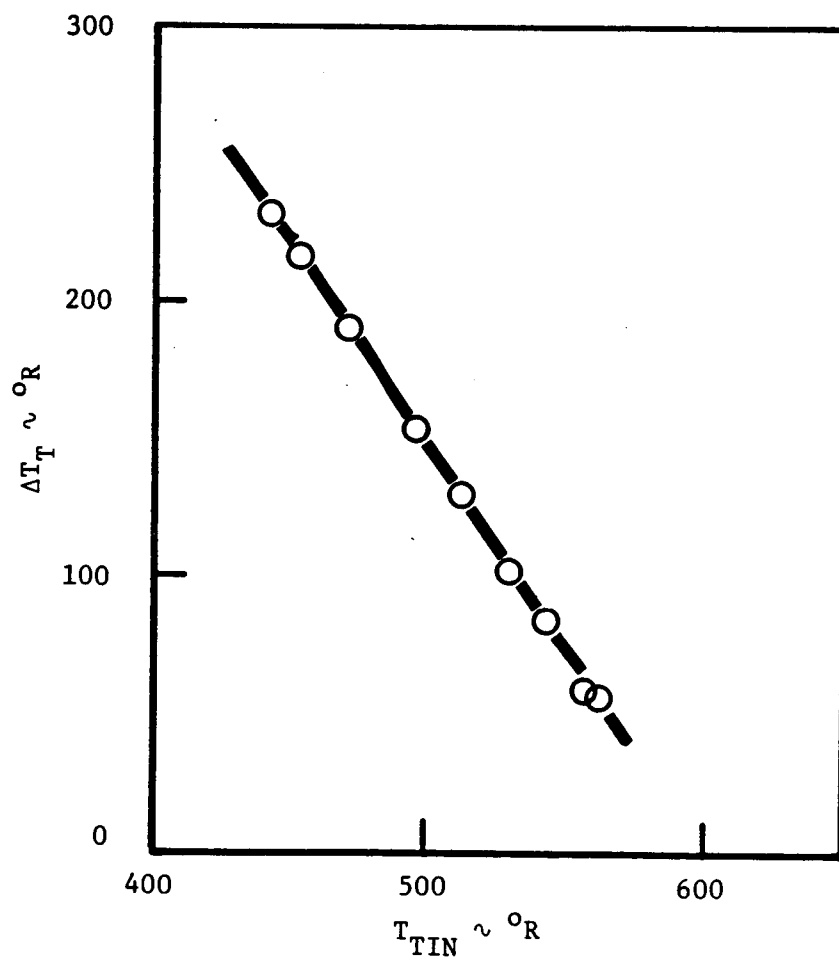
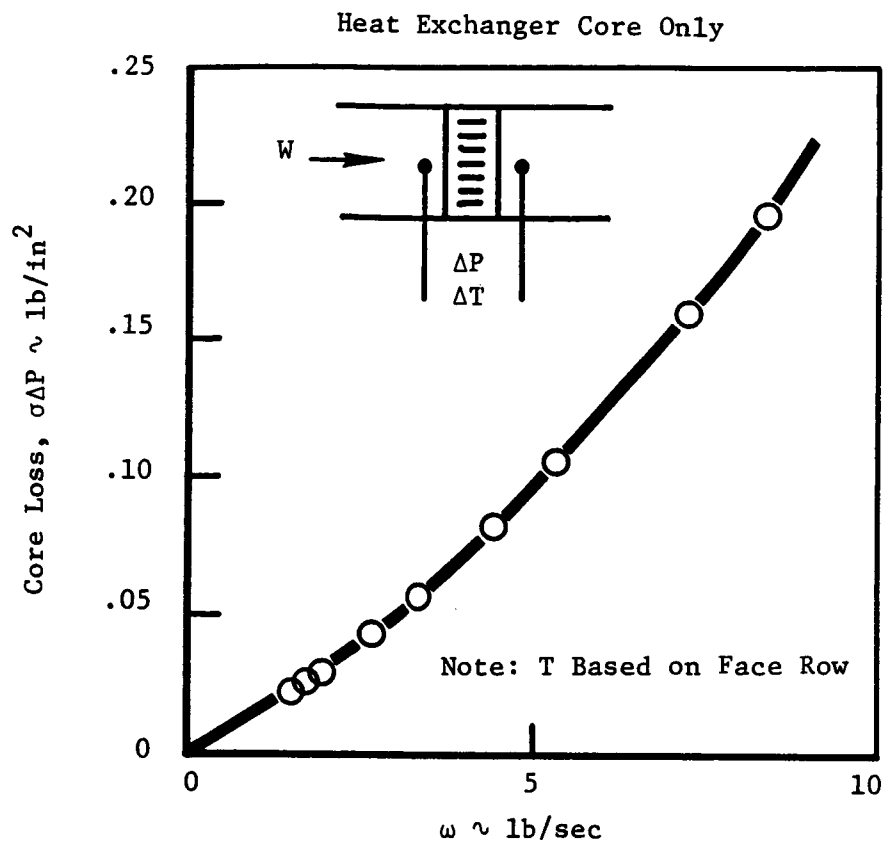


Figure I-1. Hughes-Treitler Heat Exchanger Characteristics.

Table I-1. Typical APET Turboprop Flight Path.

Case	M/h (ft)	Engine, shp	Propeller, shp	Gearbox, η
SLS	0/0	12378	12249	0.9901
SL/TO	0.20/0	12510	12385	0.9900
DEN/TO	0.20/5330	9850	9743	0.9891
Climb	0.40/5K	10986	10874	0.9898
Climb	0.50/10K	104449	10339	0.9894
Climb	0.60/20K	8966	8863	0.9885
Climb	0.80/30K	7676	7579	0.9874
EOC	0.80/35K	6550.5	6457	0.9857
CR. 100%	0.80/35K	6550.5	6457	0.9857
CR. 90%	0.80/35K	5895	5804	0.9845
CR. 80%	0.80/35K	5240	5151	0.9830
CR. 70%	0.80/35K	4585	4498	0.9810

SLS = Sea Level Static
 SL/TO = Sea Level Takeoff
 DEN/TO = Denver Takeoff
 EOC = End of Climb
 CR = Cruise

and a resulting exit momentum. The difference between entering and exit momentum is the net force (thrust or drag). The heat addition is set by the gearbox horsepower and efficiency.¹ The heat exchanger core ΔT (Figure I-1) determines the airflow requirements:

$$C_p (T_{to} - T_{tin}) = Q = W C_p \Delta T$$

(Note: The fundamental pressure loss resulting from heat addition is ignored in this analysis. The Mach numbers and temperature ratios at which the heat addition occurs are so low that this pressure loss is negligible). Knowing the heat exchanger core ΔT , a "heat exchanger internal drag map" can be generated as shown in Figure I-2. An example of how this map is generated is given below.

End of Climb, $M_o = 0.8$, $h = 35,000$ ft., + 18° Day, $F_{net} = 3999$ lb.

<u>Amb</u>	<u>Heat Exchanger Inlet</u>
T = 411.85	M = 0.8406
P = 3.458	Pt = 5.495
$M_o = 0.8$	Tt = 471.7

Engine Shaft Output 6543.92

Gearbox Efficiency, $\eta = 0.986$

Power Rejected 91.604 HP

APET
DESIGN

Heat Rejection = 91.604 HP $42.42 \frac{\text{BTU/MIN}}{\text{HP}} \frac{1}{60} \text{ SEC/MIN}$

= 64.764 BTU/SEC

Heat Exchanger ΔT , Figure 1, 187°

Airflow Required = $\frac{64.764}{0.24(187)} = 1.443$ lb/sec

NOTE: Airflow is set using a variable exit area. Inlet momentum is equal to $(W/g) \times V$.

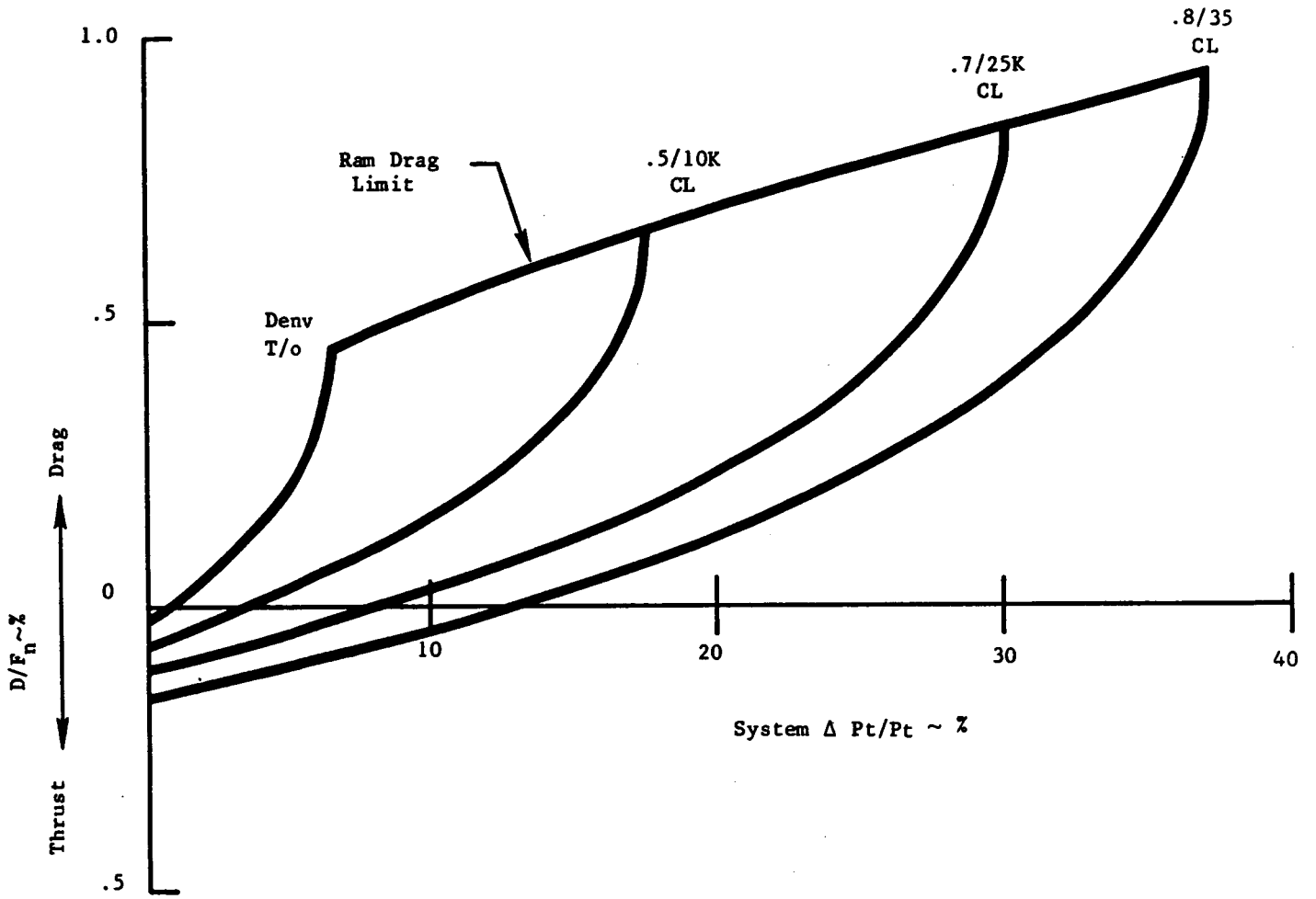


Figure I-2. Heat Exchanger Internal Drag.

$$\frac{F}{\omega \sqrt{T_T}} = \sqrt{\frac{2 \gamma R}{g(\gamma-1)} \left[1 - \left(\frac{1}{P_T/P_{amb}} \right)^{\frac{\gamma-1}{\gamma}} \right]}$$

Conventionally, the former expression is used for inlet momentum calculation and the latter used for exit momentum (thrust). The thrust function ($F/W \sqrt{T}$) may be more informative in that it directly relates force, flow, temperature and pressure.

Inlet Momentum (F_{RAM})

$$F_{RAM} = \frac{1.443}{32.174} 49.01 \sqrt{411.850} (0.8406)$$

$$F_{RAM} = 37.5$$

or

$$\frac{F}{W \sqrt{T_t}} = 3.4069 \sqrt{1 - \left[\frac{1}{(P_t/P_o)} \right]^{0.285714}} \quad \gamma = 1.4$$

$$\frac{F}{W \sqrt{T_t}} = 3.4069 \sqrt{1 - \left[\frac{1}{\left(\frac{5.495}{3.458} \right)} \right]^{0.285714}} = 1.1994$$

$$F = (1.1944) 1.443 \sqrt{471.7}$$

$$F_{RAM} = 37.5$$

To generate the heat exchanger internal drag map ΔP_t is varied from $\Delta P = 0$ to the ΔP_T that gives $P_T \text{ exit} = P_{\text{Amb}}$. $\Delta P_T = 0$ is the ideal situation, pure heat addition, zero Pressure Loss

$\Delta P_t = 2.037 \text{ lb/in.}^2$ ($P_t \text{ exit} = P_{\text{amb}}$) Worst possible case, flow disappears, or turns 90° from thrust/drag direction

For $\Delta P = 0$ The exit momentum exceeds the inlet momentum due to the temperature

$$F \text{ exit} = (1.1994) 1.443 \sqrt{633}$$

$$F \text{ exit} = 43.53$$

$$\text{Net force (drag positive)} = F_{\text{Inlet}} - F_{\text{Exit}} = 37.5 - 43.53$$

$$\text{Net force} = -6.92 \text{ lb}, \frac{-6.03}{3999} = -0.15\% \text{ (Thrust) Eng. Net Thrust}$$

For $\Delta P = (P_t \text{ exit} = P_{\text{amb}})$ There is no exit momentum

$$\text{Net force} = 37.5 - 0 = 37.5/3999 = + 0.94\% \text{ (Drag) Eng. Net Thrust}$$

Using the parameter, $\Delta P_t/P_t$ and a nozzle coefficient of 0.98, the 0.8/35 Climb curve on Figure I-3 can be generated.

$\Delta P_t/P_t$ %	$P_t \text{ exit}$	$\frac{P_{t \text{ exit}}}{P_{\text{amb}}}$	$\frac{F}{W\sqrt{t}}$	F exit	$F_{\text{in}} - F_{\text{ex}}$	$\frac{F_{\text{in}} - F_{\text{ex}}}{F_{\text{n}}} \%$
0	5.495	1.589	1.199	43.53	- 6.03	- 0.151
10	4.945	1.430	1.062	38.55	- 1.05	- 0.26
20	4.396	1.271	0.877	31.83	+ 5.67	+ 0.143
30	3.847	1.112	0.590	21.40	+16.10	+ 0.403
37.07	3.458	1.0	0	0	+37.5	+ 0.938

These points, along with curves for Denver T/O, 0.5/10K Climb, 0.7/25K are shown in Figure I-3.

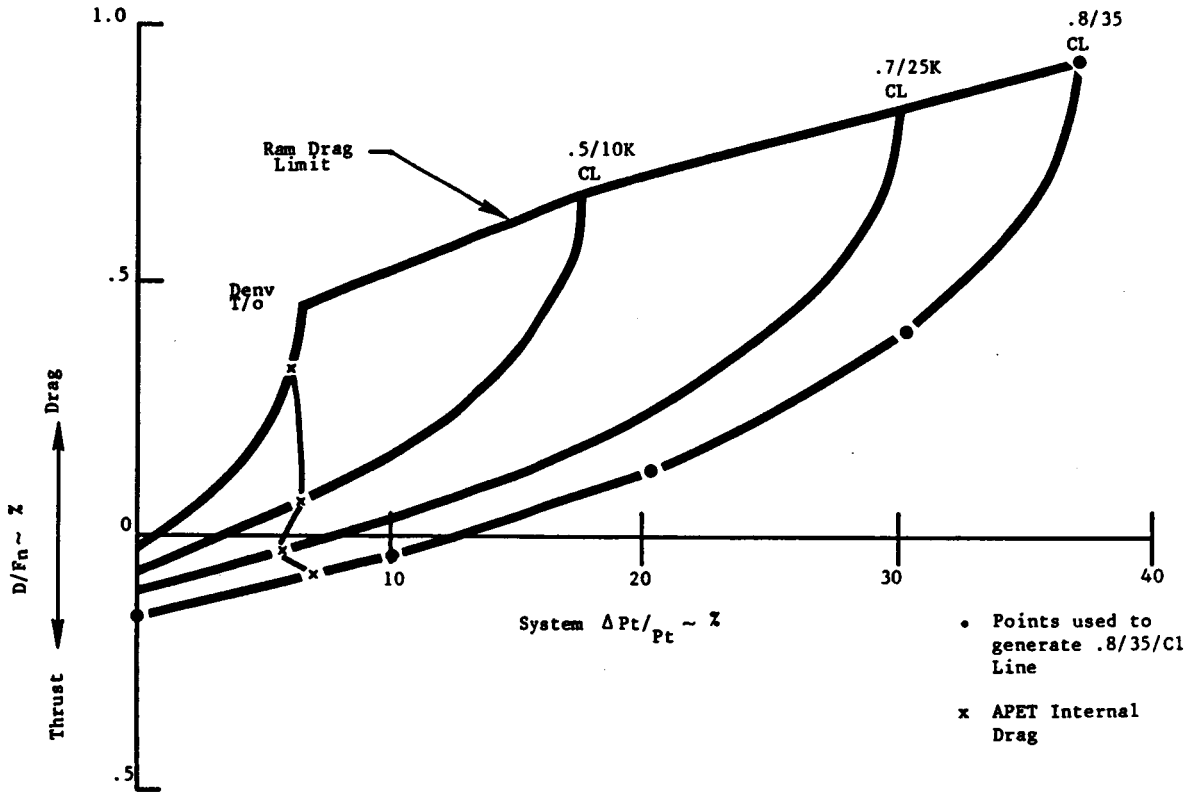


Figure I-3. Heat Exchanger Internal Drag.

Estimates for the actual internal ducting (0.8/35K/End of Climb) are given below:

Item	Pt/Pt %	Source
Inlet and Diffuser	5.0	GE
Heat Exchange Core	0.93	Hughes-Trietler
Exhaust Duct and Nozzle	1.16	GE
	<u>7.09</u>	Total

Typical total System Losses:

Ft Condition	System Internal $\Delta Pt/Pt$ %	System Internal Drag % Fn
DEN T/O	6.01	0.32
0.5/10K Climb	6.20	0.08
0.7/25K Climb	5.60	-0.02
0.8/35K End of Climb	7.10	-0.08

These points are shown in Figure I-3.

External Loss Calculation

External losses are a strong function of the location and geometry of the heat exchanger. Calculation procedures for external losses are straight forward. This section will coordinate the external and internal drags.

For a well designed system, spillage drag can be eliminated within the normal heat exchanger operating range. Some wave drag may be present at the high Mach operating conditions but this is considered negligible.

Pod drag and afterbody drag are calculated as follows:

Pod Drag (D_{Frict})

$$D_{pod} = \frac{\gamma}{2} P_o M^2 C_D A_{ref}$$

where

P_o = ambient pressure

M = hub average Mach number

C_D = 0.012

A_{ref} = 294 in.² (frontal area)

Afterbody Drag ($D_{Afterbody}$)

$$D_{noz} = 3.077 P_o M^2 \frac{A_3 - A_{3min}}{A_{3max} A_{3min}}^2$$

where

P_o = ambient pressure

M = hub average Mach number

A_3 = nozzle exit area for nozzle position

A_{3min} = minimum nozzle area

A_{3max} = maximum nozzle area

External drag levels are calculated for the same cases used as examples for external loss calculation.

Case	P_o lb/in. ²	M	Fn ~lb	Pod Drag		Afterbody Drag	
				lb	% Fn	lb	% Fn
Denv T/O	12.00	0.3117	13222	2.88	0.22	3.59	0.027
0.5/10K/CL	10.11	0.537	8795	7.20	0.082	2.12	0.24
0.7/25K/CL	5.45	0.737	5484	7.32	0.133	0.196	0.004
0.8/35K/CL	3.46	0.841	3999	6.04	0.151	0.039	0

Summary of System Performance

Summary of System Performance

Case	Pod Drag	% Fn		Total Drag
		Afterbody Drag	Internal Drag	
Denv T/O	0.022	0.027	0.32	0.369
0.5/10K/CL	0.082	0.024	0.08	0.186
0.7/25K/CL	0.133	0.004	-0.02	0.117
0.8/35K/CL	0.151	0	-0.08	0.071

For compressor purposes, the total system drag can be plotted on the internal drag map as shown in Figure I-4. The total heat exchanger drag is about 0.2% or less throughout most of the flight profile.

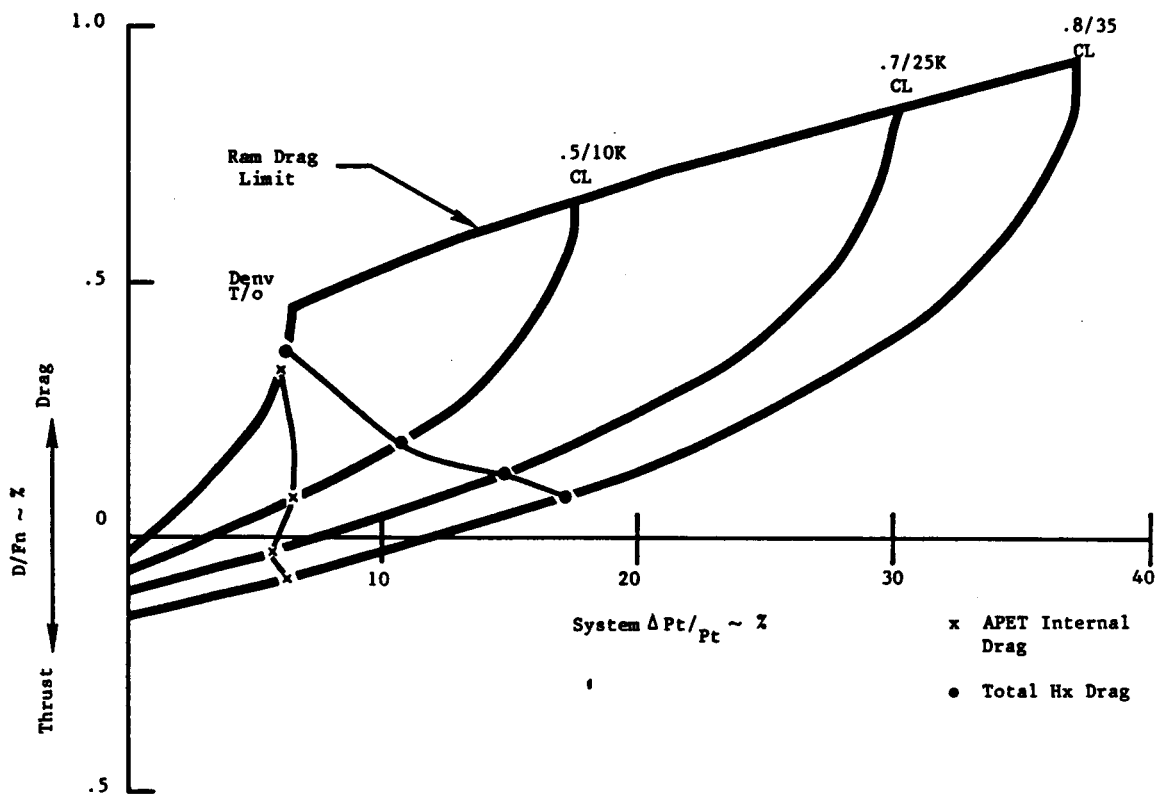


Figure I-4. Heat Exchanger Internal Drag.

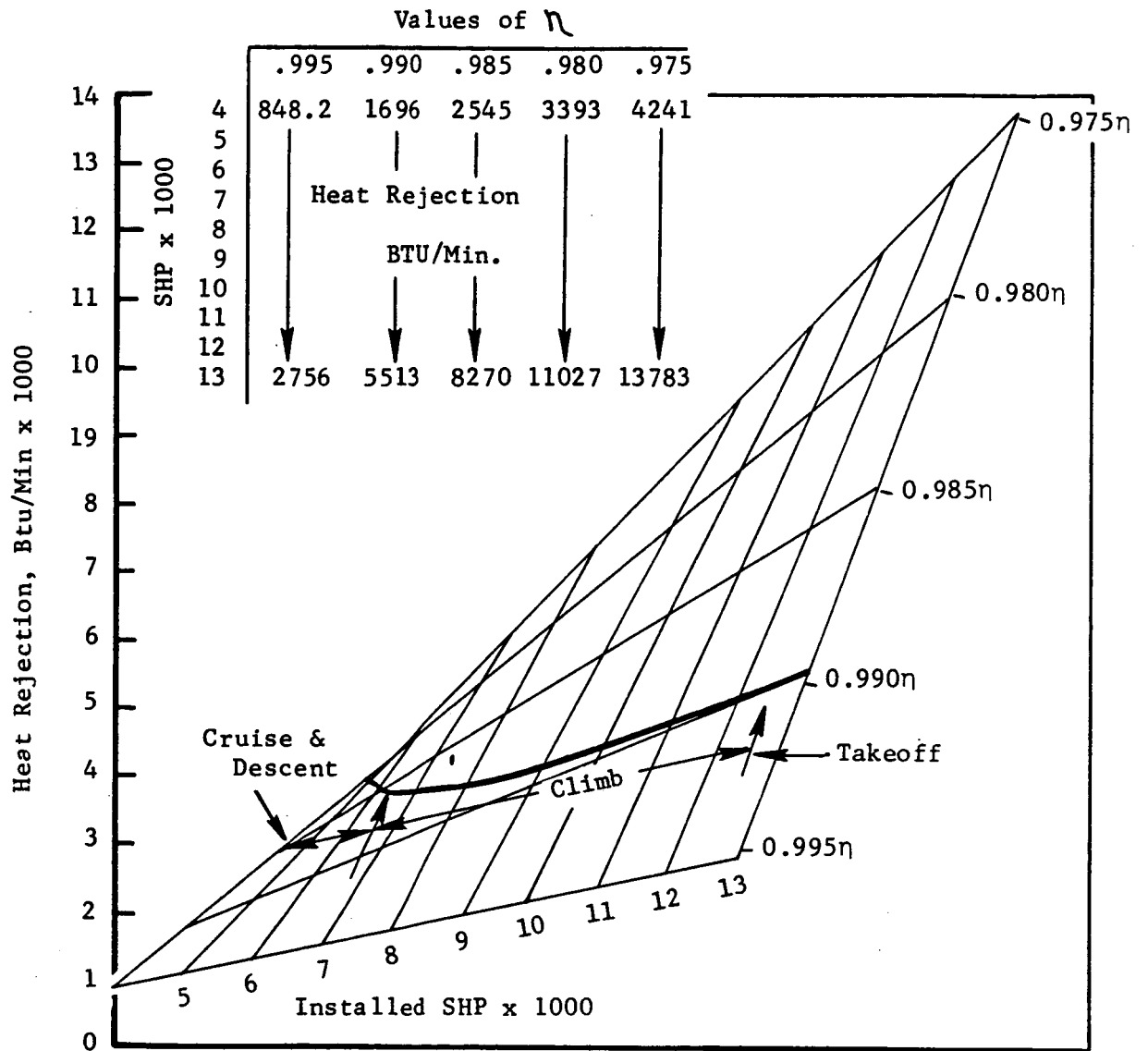


Figure I-5. APET Horsepower/Gearbox Efficiency.

APPENDIX II.

ORIGINAL PAGE IS
OF POOR QUALITY

ACOUSTICS

<u>Section</u>	<u>Page</u>
II.1 METHODOLOGY AND ASSUMPTIONS	467
II.1.1 Aircraft Flight Conditions	467
II.1.2 Propeller Noise	468
II.1.3 Compressor/Fan Noise	470
II.1.4 Turbine Noise	472
II.1.5 Combustor Noise	473
II.1.6 Airframe Noise	473
II.1.7 Jet Noise	474
II.1.8 Flight Projections and Adjustments	475
II.1.9 Cabin Noise	476
II.1.10 Treatment Assumptions	477
II.2 EVALUATION	477
II.2.1 Reference Turbofan Engine	477
II.2.2 0.8 Mach Turboprop Engine	480
II.2.3 0.7 Mach Turboprop Engine	480
II.3 CONCLUSIONS	480

PRECEDING PAGE BLANK NOT FILMED

PAGE 404 INTENTIONALLY BLANK

465

FIGURES

<u>Figure</u>		<u>Page</u>
II.2-1	APET Baseline Turbofan Engine.	479
II.2-2	APET Engine No. 28 Boosted Turboprop.	481

TABLES

<u>Table</u>		
II.1-1A	Reference Turbofan Flight Conditions - TOGW = 111970 lb.	467
II.1-1B	0.8 Mach Cruise Turboprop Flight Conditions - TOGW = 111714 lb.	467
II.1-1C	0.7 Mach Cruise Turboprop Flight Conditions - TOGW = 107309 lb.	468
II.1-2	Cabin Wall Transmission Losses.	476
II.1-3A	APET Reference Turbofan Treatment Suppressions.	478
II.1-3B	APET Reference Turbofan Treatment Suppressions Approach.	478
II.2-1	Reference Turbofan Component Levels.	479
II.2-2	0.8 Mach Turboprop Component Levels.	481
II.2-3	0.7 Mach Turboprop Component Levels.	482

ACOUSTICS

II.1 METHODOLOGY AND ASSUMPTIONS

II.1.1 Aircraft Flight Conditions

Three uniquely powered aircraft were acoustically evaluated in this study:

1. Reference turbofan powered
2. 0.8 Mach cruise turboprop powered
3. 0.7 Mach cruise turboprop powered

Tables II.1-1A to II.1-1C list the flight conditions at which these aircraft were studied. All aircraft had two wing mounted engines.

Table II.1-1A. Reference Turbofan Flight Conditions TOGW = 111970 lbs.

Cond.	Thrust Fn/δ (lbs.)	Fan rpm N1/√θ	Alt. (ft.)	Sideline (ft.)	Ground Speed (ft/sec)	A/P Climb Ang. (Deg)	Nacelle Pitch Ang. (Deg)
TO	13448	4859	2700	0	226	9.3	19.3
CB	10718	4448	2405	0	226	6.0	16
SL	13948	4859	900	1476	226	9.3	19.3
AP	3479	2928	394	0	218	-3	7

Table II.1-1B. 0.8 Mach Cruise Turboprop Flight Conditions TOGW = 111714 lbs.

Cond.	Thrust Fn/δ (lbs.)	Fan rpm N1/√θ	Alt. (ft.)	Sideline (ft.)	Ground Speed (ft/sec)	A/P Climb Ang. (Deg)	Nacelle Pitch Ang. (Deg)
TO	14887	1216	2466	0	226	8.5	18.5
CB	11563	1216	2170	0	226	6.3	16.3
SL	14887	1216	900	1476	226	8.5	18.5
AP	3931	1216	394	0	218	-3	7.0

Table II.1-1C. 0.7 Mach Cruise Turboprop Flight Conditions TOGW = 107309 lbs.

Cond.	Thrust Fn/δ (lbs.)	Fan rpm N1/√θ	Alt. (ft.)	Sideline (ft.)	Ground Speed (ft/sec)	A/P Climb Ang. (Deg)	Nacelle Pitch Ang. (Deg)
TO	14016	1253	2466	0	226	8.5	18.5
CB	10887	1253	2170	0	226	6.3	16.3
SL	14016	1253	900	1476	226	8.5	18.5
AP	3701	1253	394	0	218	-3	7.0

II.1.2 Propeller Noise

Fan field propeller generated noise was predicted using a preliminary design procedure methodology based on Reference 44 and DeHaviland Twin Otter data presented in Reference 45. This methodology computes a scaled OASPL based on the SAE procedures discussed in Reference 1:

$$\begin{aligned} \text{OASPL} = & (37.5 * M_t) + 15.8 \log (\text{SHP}) - 20 \log (\text{NB}) - 20 \log (\text{DI}) \\ & - 20 \log (\text{DIS}/500) + 43 + \text{DI} \end{aligned} \quad (1)$$

where: OASPL = Overall Sound Pressure Level for one propeller in far field

M_t = Tip Mach No.

SHP = Shaft Horse Power

NB = Number of Blades

D_t = Tip Diameter

DIS = Measurement Distance

DI = SAE Directivity Index

From this OASPL, the total spectrum is determined using a correlation of the harmonic fall-off rates vs. Helical Mach number developed from the DeHavilland data, Reference 45.

Broadband noise is then computed based on an empirical relationship discussed in Reference 46:

$$\text{SPL}_{\text{Peak}} = 10 \log \frac{(6.1 \times 10^{-27}) A_b (V_{0.7})^6}{10^{-16}} + 20 \log \frac{C_L}{0.4} - 20 \log \frac{\text{DIS}}{300} \quad (2)$$

$$f_{\text{Peak}} = \text{St} \frac{(V_{0.7})}{h} \quad (3)$$

Where: SPL_{Peak} = Peak Sound Pressure Level

A_b = Blade Area

$V_{0.7}$ = Velocity at .7 radius

C_L = Lift Coefficient

DIS = Evaluation Distance

f_{Peak} = Peak Amplitude Frequency

St = Strouhal Number

h = Projected Blade Thickness

After the peak frequency and amplitude are determined the other spectral levels are defined by a prescribed spectrum and the directivity is assumed to be uniform on a constant radius arc.

Calculations performed using this procedure yield lower levels than the standard SAE procedure, Reference 44. This reduction can be attributed to the "clean-up" that is achieved by the DeHavilland propeller in flight.

Projections of comparative measurements of advanced blade design impact no noise levels made on NASA's Jetstar (Reference 47) suggest that, at the tip relative Mach number region of interest, very little, if any, benefit of advanced blade technology can be claimed (the helical Mach numbers are low $M_h = 0.75$).

Near field propeller generated noise was predicted based on the SAE methodologies of Reference 44, as follows:

$$\text{OASPL} = 15.2 \log (\text{SHP}) - 40 \log (\text{DI}) + 20 \log (4/\text{NB}) + 10 \text{ N} \log (\text{Y}/\text{D}_t/.03) + 135.7$$

Where: OASPL = Nearfield Overall Sound Pressure Level for one propeller
 SHP = Shaft Horse Power
 DI = Tip Diameter, ft.
 NB = No. of Blades
 N = $2.6 \times \text{M}_t - 3.52$
 Y = Propeller Tip Clearance to Fuselage

Discrete tone harmonic fall-off rates are prescribed by a fall-off rate correlation developed from the data of Reference 45 and 48. These tonal levels were summed into one third octaves, and then A-weighted sound level (dBA).

II.1.3 Compressor/Fan Noise

Compressor noise for the turboprop cases and fan inlet/discharge noise for the turbofan case were predicted using the methodology discussed in Reference 49. This method, which was developed by NASA in partial support of NASA ANOPP, determines one-third octave band sound pressure levels of broadband, discrete tone and combination-tone noise components.

Broadband levels are correlated based on the following expression:

$$L = 20 \log \frac{\Delta T}{\Delta T_0} + 10 \log \frac{\dot{M}}{\dot{M}_0} + F1_B (\text{M}_{tr}, \text{M}_{trd}) + F2_B (\text{RSS}) + F3_B (\theta) + F4_B \frac{f}{f_b}$$

Where: L_B = Broadband Sound Pressure Level
 ΔT = Total temperature rise across fan or compressor
 ΔT_0 = Reference value of ΔT (1R)
 \dot{M} = mass flow rate passing through fan or compressor
 \dot{M}_0 = reference value of M (1 lbm/sec)

$F1_B (M_{tr}, M_{tro})$ = Broadband Correction Function based on rotor tip relative Mach number and design rotor tip relative Mach number.

$FZ_B (RSS)$ = Broadband rotor-stator spacing correlation function

$F3_5 (\theta)$ = Broadband Directivity Correlation function

$F4_B (f, f_b)$ = Broadband spectra distribution correlation function

Discrete tone noise levels are correlated based on the following expression:

$$L_t = 20 \log \frac{\Delta T}{\Delta T_0} + 10 \log \frac{\dot{M}}{\dot{M}_0} + F1_t (M_{tr}, M_{trd}) + F2_t (RSS) \\ + F3_t (\theta) + F4_t \frac{f}{f_b}$$

Where: L_t = Discrete tone sound pressure level

$F1_t (M_{tr}, M_{trd})$ = Tonal rotor tip relative Mach number correlation function

$F2_t (RSS)$ = Tonal rotor - stator spacing correlation function

$F3_t (\theta)$ = Tonal Directivity correlation function

$F4_t (f/f_b)$ = Harmonic tone level correlation function

Combination tone noise, as calculated for first stage fans, are correlated by:

$$L_c = 20 \log \frac{\Delta T}{\Delta T_0} + 10 \log \frac{\dot{M}}{\dot{M}_0} + F1_c (M_{tr}) + F2_c (\theta) + F3_c \frac{f}{f_b}$$

Where: L_c = Combination tone sound pressure level

$F1_c (M_{tr})$ = Combination tone rotor tip relative Mach number correlation function

$F2_c (\theta)$ = Combination tone directivley correlation function

$F3_c (f/f_b)$ = Combination tone spectrum correlation function

C = Inlet guide vane correlation factor

$F1$, $F2$, $F3$ and $F4$ are correlation functions which were curve fit from plots in Reference 49.

Comparisons of estimated levels using these procedures to commercial engine measured data show the methodology to be in good agreement with the measured data.

II.1.4 Turbine Noise

Turbine noise is predicted using the techniques discussed in Reference 50. This methodology was based on rig and engine data correlations to pressure ratio, tip speed, and exit area. The peak OASPL, which is the composite of broadband and tone noise, is determined by:

$$\text{PEAK OASPL} = 40 \log_{10} (\Delta T/T_{\text{Turbine}}) - 20 \log_{10} U_t + 10 \log_{10} A + 164.$$

Where: PEAK OASPL = combined broadband and discrete frequency OASPL at 120° and 200 ft.

$$(\Delta T/T) = 1 - (1/Pr) \left(\frac{\gamma - 1}{\gamma} \right)$$

Pr = turbine total-to-static pressure ratio

$$= P_{t0}/P_{s2}$$

U = dominant stage tip speed₂, ft/sec.

A' = core nozzle exit area, ft

Y = ratio of specific heats 1.4

Tone noise is determine by:

$$\text{PEAK SPL} = 21 \log_{10} (\Delta T/T) - 20 \log_{10} (U_t) + 10 \log_{10} A + 161.5$$

Where: PEAK SPL = tone SPL at 120° and 200 ft. sideline, without air attenuation and EGA

The dominant stage was assumed to be the next to last stage for the two configurations and the reference engine.

Broadband noise was determined by logarithmically subtracting tone levels from the overall levels, and distributing the resultant levels over a prescribed spectra.

II.1.5 Combustor Noise

The combustor generated noise prediction methodology was based on Reference 51. This methodology correlates combustor noise with combustor mass flow rate, inlet total pressure, total temperature rise, and takeoff condition total temperature extraction. The OAPWL is calculated by:

$$\text{OAPWL} = 10 \log_{10} (M_3 a_0 / \pi_{\text{ref}}) + 10 \log \left(\frac{T_4 - T_3}{T_3} \right)^2$$

$$\left(\frac{P_s}{P_o} \right)^2 \left(\frac{T_4 - T_5}{T_o} \right)^{-4} - 60.5$$

OAPWL = Overall Power Level

- Where:
- M_3 = combustor mass flow rate, kg/s
 - P_3 = combustor inlet total pressure, Pa
 - $(T_4 - T_3)$ = combustor total temperature rise, ° k
 - $(T_4 - T_5)_{\text{ref}}$ = Mn. takeoff reference total temperature extraction by the turbines, ° k
 - π_{ref} = reference power, 1 pW
 - T_o = 288.15° k
 - P_o = 1.01325 x 105 Pa
 - a_o = 340.294 M/S

This OAPWL distributed over angle and over frequency using a far field directivity index and spectrum shape factors.

II.1.6 Airframe Noise

Noise, as generated by the aerodynamic forces on the airframe was predicted using relationships from Reference 52.

$$\text{OASPL}(r, \theta) = 10 \log \left[\frac{M^{3.47} \left(\frac{W}{\rho_0 a_0^2} b_2 \right)^{0.62} \cos^2 \gamma}{\left(\frac{r}{b} \right)^{1.59} (AR)^{2.39} (1 - M_r)^4} \right] + 154.9$$

Where: OASPL (r,θ) = Overall Sound Pressure Level at radius r and angle θ
re 2×10^{-5} N/M²

M = Aircraft Mach Number

W = $C_L (1/2 \rho_0 v^2) S$

C_L = Lift Coefficient

ρ_0 = Ambient density, kg/M³

a_0 = Ambient speed of sound, M/Sec

b = Aircraft Span, M

v = Aircraft Speed, M/Sec

S = Aircraft Wing Area, M²

γ = Angle between the normal to the aircrafts wings and the observer, degrees

r = Observer distance, M

AR = Aspect Ratio

M_r = Instantaneous Mach number in observer direction

The OASPL as calculated above is distributed over a prescribed spectrum shape.

II.1.7 Jet Noise

The single stream jet mixing noise from the shock free circular exhaust nozzle was predicted using the procedure defined in Reference 53. It is based on a correlation of fully expanded mean jet velocity, temperature ratio, nozzle area, and Strouhal Number, with an extensive scale model database. This procedure calculates the component OASPL from:

$$\text{OASPL} = S + 10 \log_{10} \left(\frac{P_d}{P_o} \right)^\omega + 10 \log_{12} \left(\frac{A_j}{r^2} \right) + 20 \log \left(\frac{P_o}{P_{\text{ISA}}} \right)$$

- Where: OASPL = Overall Sound Pressure Level at angle θ ; dB
- S = Normalized Overall Sound Pressure Level at Angle θ ; dB
- P_j = Fully expanded jet density, Kg/M³
- P_o = Atmosphere density, Kg/M³
- ω = Variable density index
- A_j = Cross sectional area of jet exhaust nozzle, M²
- r = Radial distance from nozzle to observer, M
- P_o = Ambient pressure, Pa
- PISA = Ambient pressure under ISA conditions, Pa
- θ_j = Angle relative to intake axis, degrees

The OASPL is distributed over a prescribed spectra, and modified to reflect the forward speed effects when projected to flight.

II.1.8 Flight Projection and Adjustments

The procedure by which the data was projected to flight includes correlations for such things as spherical divergence, air attenuation, ground reflections, doppler shifting, dynamic effects, jet noise flight effects, and extra ground attenuation.

Spherical divergence was calculated assuming a point source and applying a "20 log" ratio of distances correction.

Air attenuation corrections were determined based on ARP 866 (Reference 54).

The ground reflection correction relationships are based on FAA report RD-71-85 (Reference 55).

The Dynamic amplitude effect correction is based on the following:

$$\text{Dynamic Effect} = 40 \log \left[\frac{1}{1 - (\text{Mac} \cos \theta)} \right]$$

Where: M_{ac} = Aircraft Mach Number
 θ = Listener angle

Jet noise flight effects are discussed in Reference 53. Extra ground attenuation effects are determined from Reference 56.

II.1.9 Cabin Noise

Cabin noise levels were assessed at take off condition (highest propeller source noise condition) for the two turboprop aircraft. The only source that was considered for the cabin noise was near field propeller noise (Reference Section II.1.2). After the near field propeller source levels were estimated at the cabin wall, a cabin wall transmission loss was applied to the one-third octave levels and a cabin environment A-weighted sound pressure level was determined. The cabin wall transmission loss values were estimated from Reference 57 and are given in Table II.1-2.

Table II.1-2. Cabin Wall Transmission Losses.

Frequency	Transmission Loss (dB)
50	10
63	13
80	16
100	21
125	29
160	33
200	40
250	47
315	51
400	56

II.1.10 Treatment Assumptions

The two turboprop engines studied did not need any duct acoustic treatments. The reference turbofan engine studied did require fan inlet, fan exhaust, and turbine treatments. The treatments for this engine are assumed to be similar to those used in the NASA/GE Energy Efficient Engine.

As the L/D factors of the reference engine (Inlet L/D \approx .67, Fan Exhaust L/H \approx 4.33) are better than the Energy Efficient Engine (Fan Inlet L/D \approx .52, Fan Exhaust L/H \approx 3.36) a conservative estimation was used by substituting the Energy Efficient Engine suppression estimates directly (reference Tables II.1-3A and II.1-3B). The actual suppressions used are comprised of the product of the suppression levels and the appropriate suppression directivity ratios.

II.2 EVALUATION

All aircraft were acoustically evaluated in relation to FAR36 1978 Stage III limits (Reference 58). In addition, the two turboprop aircraft were evaluated in relation to a cabin noise goal of 85 dBA.

Table II.2 list the estimated levels of all three aircraft, the corresponding FAR36 limits, and the limit margins at each of the flight conditions. The accuracy of those estimates are obviously limited by the preliminary status of the design cycle, the prediction assumptions, and the flight mission objectives.

II.2.1 Reference Turbofan

The Reference turbofan engined aircraft (Figure II.2-1) will meet FAR36 limits using cutback.

The sources that are controlling the system noise levels at takeoff and cut back are fan inlet and fan exhaust, (Reference Table II.2-1). Future design considerations which would help improve FAR36 margin are:

Table II.1-3A. APET Reference Turbofan Treatment Suppressions ~ Takeoff, Sideline, and Cut Back.

	Suppression Level (Δ dB)															
Freq. (Hz)	<315	400	500	630	800	1K	1.25K	1.6K	2K	2.5K	3.5K	4K	5K	6.3K	8K	10K
Fan Exhaust	5.2	5.2	5.2	5.2	5.2	7.0	4.5	7.5	8.0	8.5	8.5	11.0	12.0	14.0	15.0	15.0
Fan Inlet	0	1.2	5.2	6.0	4.9	7.0	6.1	6.5	8.0	7.0	5.1	4.5	4.3	5.1	5.4	4.6
Turbine	0	0	0	0	0	0.1	0.3	0.6	1.2	1.3	2.5	3.0	3.1	2.9	2.5	3.2

Suppression Directivity Ratio

	Angle re Inlet								
	10°	20°	23°	40°	50°	60°	70°	80°	90°
Fan Inlet	0.4	0.4	0.2	0.5	0.5	1.0	1.6	2.4	2.2

	Angle re Inlet							
	80°	90°	100°	110°	120°	130°	140°	150°
Fan Exhaust	1.1	1.1	1.4	1.3	1.0	1.3	0.9	0.8
Turbine	1.6	1.16	1.59	1.48	1.14	0.89	0.63	0.41

Table II.1-3B. APET Reference Turbofan Treatment Suppressions ~ Approach.

	Suppression Level (Δ dB)														
Freq. (Hz)	<400	500	630	800	1K	1.25K	1.6K	2K	2.5K	3.15K	4K	5K	6.3K	8K	10K
Fan Exhaust	7.1	7.1	7.3	7.2	9.6	10.9	10.7	11.7	14.5	14.0	13.3	15.0	15.1	15.0	12.8
Fan Inlet	1.8	3.1	4.1	5.3	5.6	7.5	7.7	5.8	6.5	6.2	7.2	7.2	7.3	6.5	4.4
Turbine	0	0	0	0	0.1	0.3	0.6	1.2	1.3	2.5	3.0	3.1	2.9	2.5	3.2

Suppression Directivity Ratio

	Angle re Inlet								
	10°	20°	23°	40°	50°	60°	70°	80°	90°
Fan Inlet	0.3	0.2	0.5	0.9	1.1	1.5	1.9	1.8	1.4

	Angle re Inlet								
	70°	80°	90°	100°	110°	120°	130°	140°	150°
Fan Exhaust	1.0	1.0	1.0	1.2	1.2	1.2	1.0	1.1	1.0
Turbine	1.48	1.59	1.16	1.59	1.48	1.14	0.89	0.63	0.41

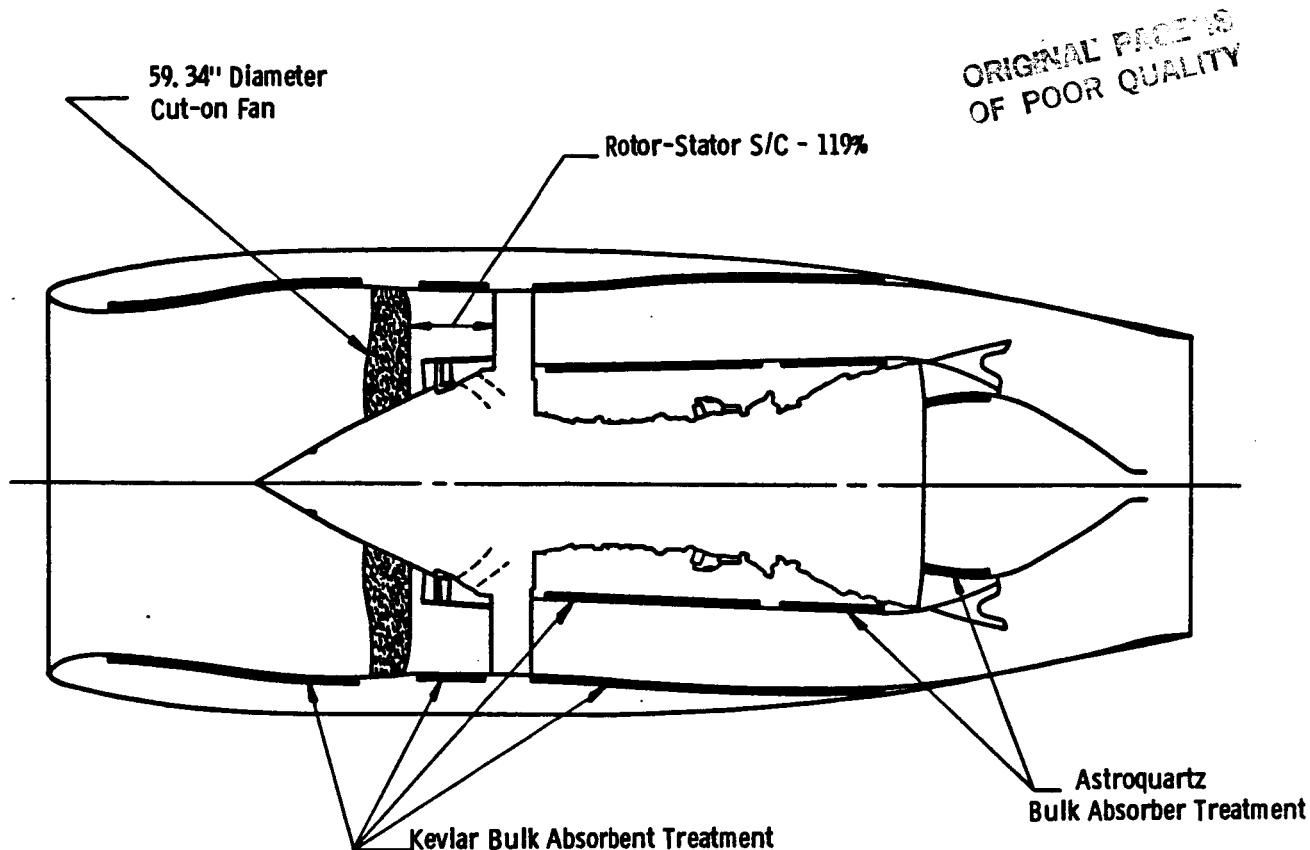


Figure II.2-1. APET Baseline Turbofan Engine.

Table II.2-1. Reference Turbofan Component Levels.

Noise Source	Measuring Point			
	Full Power (EPNdB)	Cutback (EPNdB)	Sideline (EPNdB)	Approach (EPNdB)
Airframe	---	---	---	87.6
Jet	80.5	77.9	84.2	72.5
Core	69.6	67.4	73.2	69.6
Fan Exhaust	75.0	75.7	80.7	80.9
Fan Inlet	80.6	80.9	87.3	93.0
Turbine	71.0	72.6	77.4	88.1
Engine Alone	---	---	---	94.2
System	85.8	85.3	91.8	94.9

- Reduction in fan operating speed at take off
- Improved inlet liner treatment
- Increased rotor-stator spacing

II.2.2 0.8 Mach Turboprop

The 0.8 cruise Mach turboprop engine (Figure II.2-2) aircraft will meet FAR36 limits using cutback.

Propeller generated noise controls the total system noise at all flight conditions (Reference Table II.2-2). Any advanced propeller blade design acoustic benefit which can be claimed could be directly applied to the overall system noise due to the dominance of propeller noise in the system noise.

The maximum A-weighted cabin noise for this aircraft at takeoff is 85.8 dBA. Therefore, anticipated levels during normal operation are expected to be within program goals.

II.2.3 0.7 Mach Turboprop

The 0.7 cruise Mach turboprop engine (also Figure II.2-2) aircraft will meet FAR36 limits using cut back. As in the 0.8 Mach cruise propeller generated noise controls the total system noise at all flight conditions (Reference Table II.2-3). Therefore, any advanced propeller blade acoustic benefit is directly realizable as a system noise benefit.

Maximum A-weighted cabin noise at takeoff for this aircraft is estimated to 85.8 dBA which is at the program goals.

II.3 Conclusions and Recommendations

All three aircraft evaluated in this study are expected to meet FAR36 Stage III limits for far field noise, and program goals for near field noise.

Growth of the turboprop aircraft may be permitted if advanced blade technology can provide any benefit at the low tip relative Mach number at which the propeller is operating.

There is not any significant acoustic benefit or penalty that the propeller engines in this study have over the turbofan engines.

ORIGINAL PAGES AS
OF POOR QUALITY

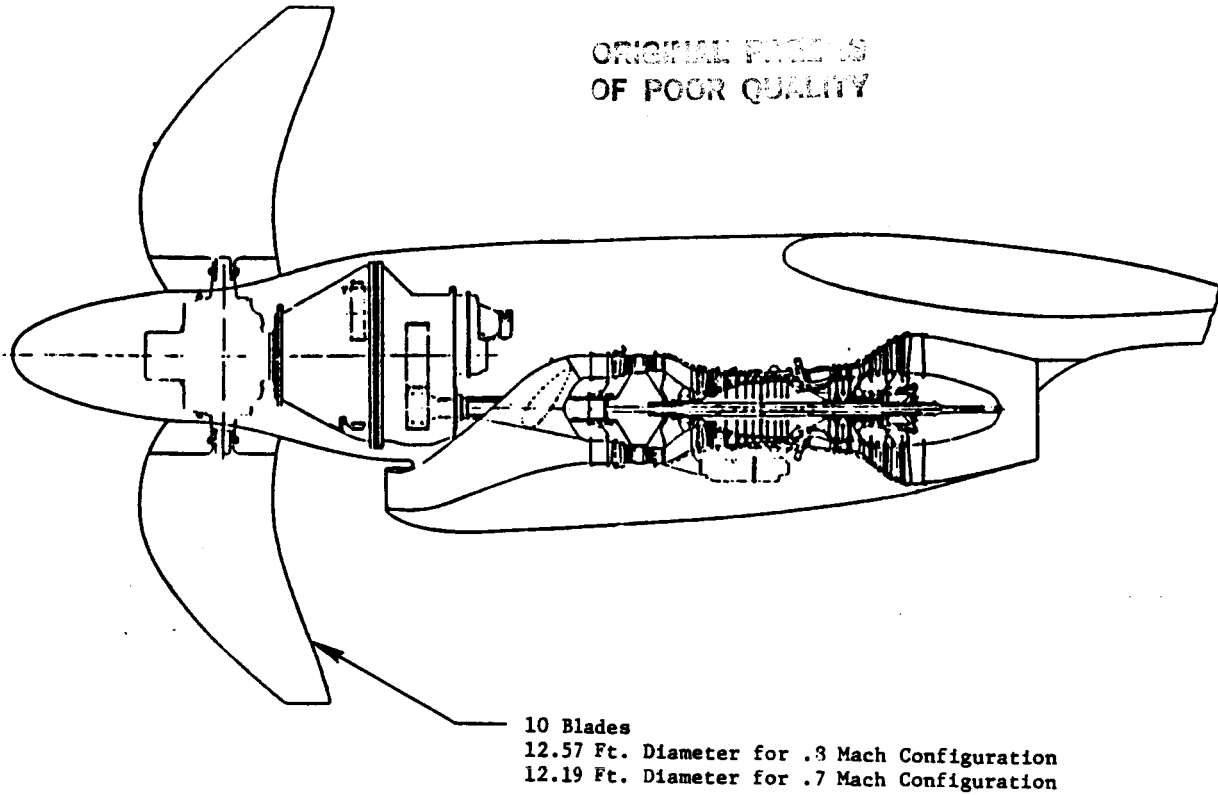


Figure II.2-2. APET Engine No. 2B Boosted Turboprop.

Table II.2-2. 0.8 Mach Turboprop Component Levels.

Noise Source	Measuring Point			
	Full Power (EPNdB)	Cutback (EPNdB)	Sideline (EPNdB)	Approach (EPNdB)
Airframe	---	---	---	87.6
Jet	67.5	61.4	70.6	57.1
Core	75.1	72.8	77.9	76.0
Compressor	63.6	59.4	72.0	88.4
Propeller	89.3	87.6	91.9	90.5
Turbine	73.4	73.9	78.8	89.5
Engine Alone	---	---	---	97.2
System	90.5	88.9	93.5	97.2

Table II.2-3. 0.7 Mach Turboprop Component Levels.

Noise Source	Measuring Point			
	Full Power (EPNdB)	Cutback (EPNdB)	Sideline (EPNdB)	Approach (EPNdB)
Airframe	--	--	--	86/7
Jet	67.3	64.9	70.4	56.9
Core	74.8	72.5	77.6	75.7
Compressor	62.8	58.3	71.1	87.5
Propeller	89.1	87.4	91.7	90.4
Turbine	72.8	73.3	78.2	88.9
Engine Alone	--	--	--	96.7
System	90.2	88.7	93.2	96.7

APPENDIX III

ENGINE WEIGHT AND DIMENSION

CALCULATION MODEL

<u>Section</u>		<u>Page</u>
III.0	INTRODUCTION	487
III.1	PREFACE	487
III.2	PROCEDURE	488
III.3	WEIGHTS (Split and Concentric Gearbox)	488
III.4	RESULTS	493
III.5	DIMENSIONS	493

FIGURES

<u>Figure</u>		
III-1	APET Gas Generator Weight Trends.	489
III-2	APET Propeller Weight Trends.	489
III-3	APET Gearbox Weight Trends - Offset Gearbox.	490
III-4	APET Nacelle Weight Trends.	490
III-5	APET Weight Trend.	491
III-6	APET Propeller Loading Trends.	491
III-7	APET Baseline (Axi-Axi) Engine and Gearbox.	495
III-8	APET Alternate (Axi-Axi) Engine with Split Gearbox.	496
III-9	APET Engine (Axi-Axi) with Concentric Gearbox.	497
III-10	APET Turboprop Configuration.	498
III-11	APET 2B "Baseline" Engine (12,500 SHP).	498

TABLES

<u>Table</u>		
III-1	Gearbox Type Effects.	492
III-2	Engine Weight and Dimensions.	494
III-3	APET Engine System Weights.	494

NAS3-23044

ORIGINAL PAGE IS
OF POOR QUALITY

March 1983

APET
ENGINE WEIGHT & DIMENSION
CALCULATION MODEL

PRECEDING PAGE BLANK NOT FILMED

GENERAL  ELECTRIC

AIRCRAFT ENGINE BUSINESS GROUP
ADVANCED TECHNOLOGY PROGRAMS DEPARTMENT
CINCINNATI, OHIO 45215

485

PAGE 484 INTENTIONALLY BLANK

III.0 INTRODUCTION

The APET customer deck includes a provision for scaling for reference engine. Thus, the user can calculate engine system performance for a range of engine sizes. To complement the scaling capability, this weight and dimensional model will provide weights and dimensions over a range of engine sizes.

The model is divided into five components:

- Gas Generator
- Propeller
- Gearbox
- Nacelle
- Installation

With this breakdown, the user can supply components with different characteristics and determine weights and dimensions for the new engine system.

III.1 PREFACE

This provides a method for determining the weights and dimensions for scaled APET engines' systems. The system includes the gas generator, gearbox, propeller, nacelle, and installation. The engine scaling capability (SWSIZE) is included in the APET customer deck for the range of gearbox horsepower (PWS) from 7800 to 20800. With the GE gearbox efficiency characteristic and customer oftakes, the resulting propeller shaft horse power (PWI) is ~7500 to ~20000. Weights and dimensional information can be calculated for the following:

- Gas generator configurations
 - All axial
 - Axi centrifugal
- Propeller Design Range H-S Prop Fan ~M0.80 Capability

- MO.70 to MO.80
- Tip Speed from 700 to 800 fps (UT1)
- SHP/D² from 30 to 37.5 (PWODS)
- Gearbox Types ~ GE Supplied
 - Offset
 - Split
 - Concentric

III.2 PROCEDURE

Weights (System with Offset Gearbox)

Determine the scale APET engine system's weights as follows:

- Select the desired airflow scale ~SWSIZE = desired value
~ (0.60 <SWSIZE<1.60)
- Choose cruise flight condition ~ ALT = 35K, Mach No. = 0.70 to 0.80
- Choose the propeller design
 - Propeller Sizing switch ~SWPROP
 - Tip Speed ~ZUT1
 - Propeller Loading ~ZPWODS
- Operate scaled engine at MO.20/SL+27, SITFK = 1, PC = 50 to find gearbox design horsepower (PWSD)

With this information, use Figures III-1 through III-6 to calculate the weight for the scaled APET engine system.

III.3 WEIGHTS (Split and Concentric Gearbox)

The procedure is the same except Reference Weights (WT) REF for the desired gearbox type are found in Table III-1.

The weights of the desired gears are then calculated using the characteristics of Figure III-3.

$$(WT)_{\text{Gears}} = (WT)_{\text{Ref}} \times \frac{WT @ PWSD \quad MO.20/SL + 27}{WT @ PWSD = 13000, SHP/D^2 = \text{Specified}}$$

$$(WT)_{\text{Nacelle Structure}} = (WT)_{\text{Ref}} \times \frac{WT @ PWSD \quad MO.20/SL + 27}{WT @ PWSD = 13000, SHP/D^2 = \text{Specified}}$$

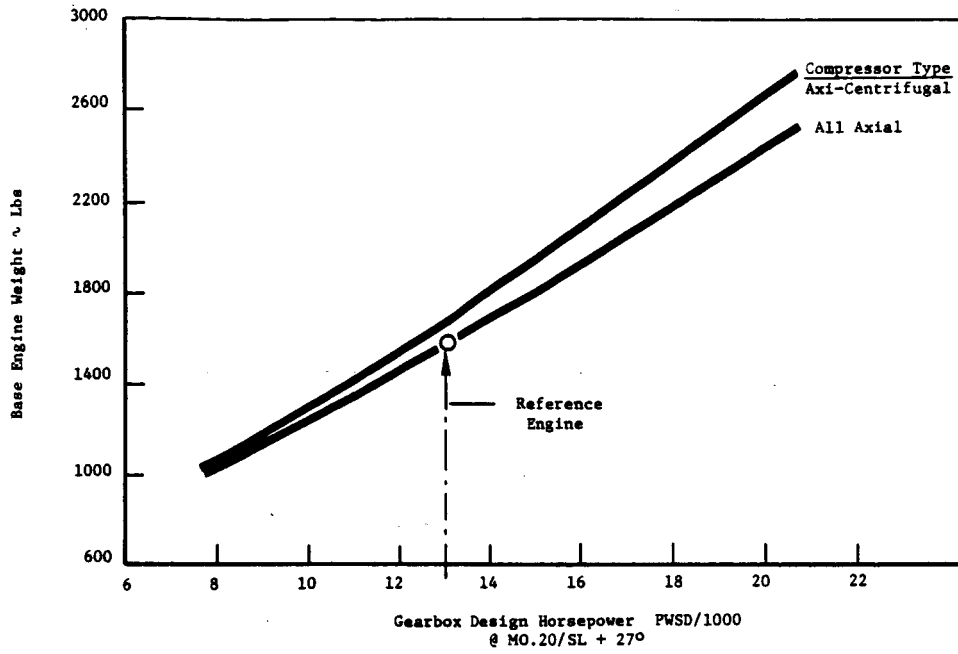


Figure III-1. APET Gas Generator Weight Trends.

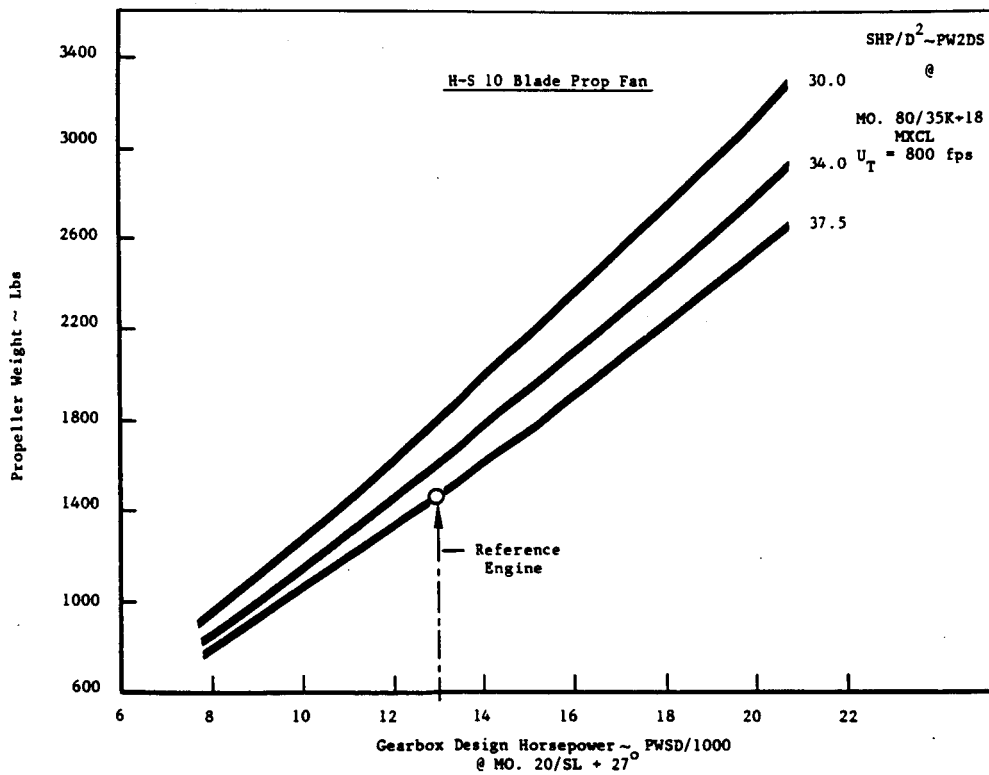


Figure III-2. APET Propeller Weight Trends.

ORIGINAL PART OF POOR QUALITY

Offset Gearbox

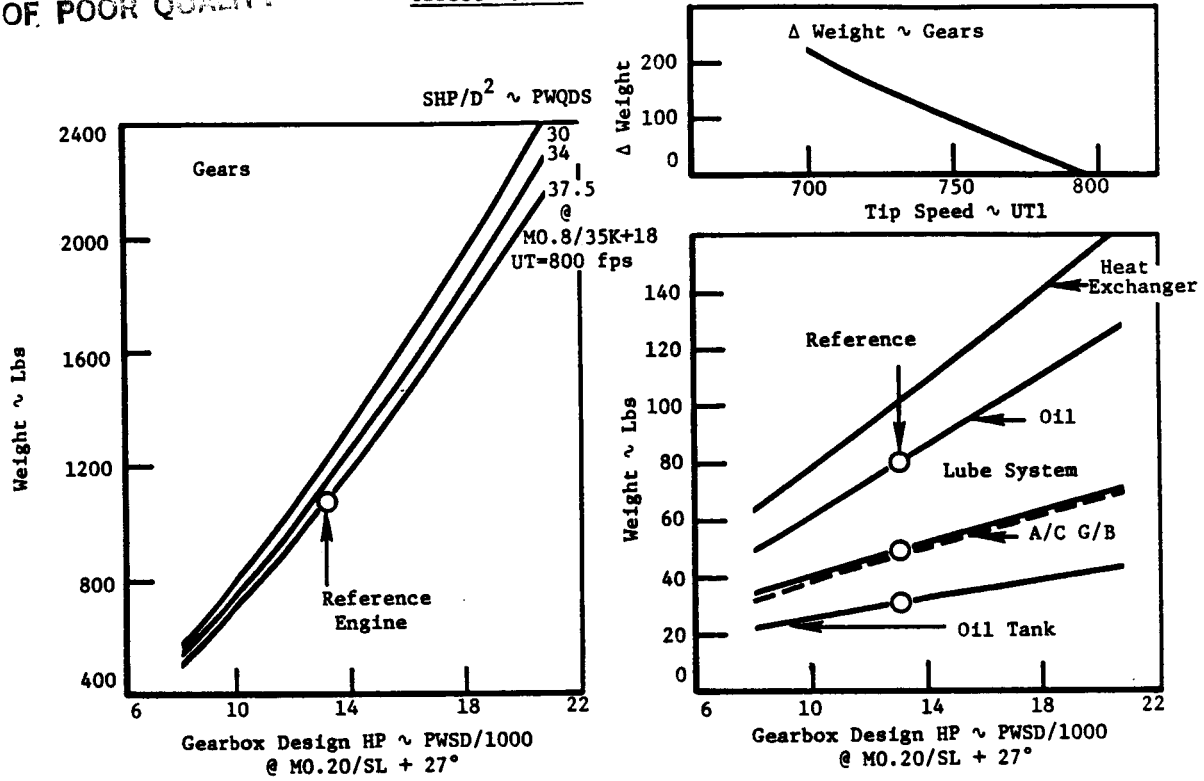


Figure III-3. APET Gearbox Weight Trends.

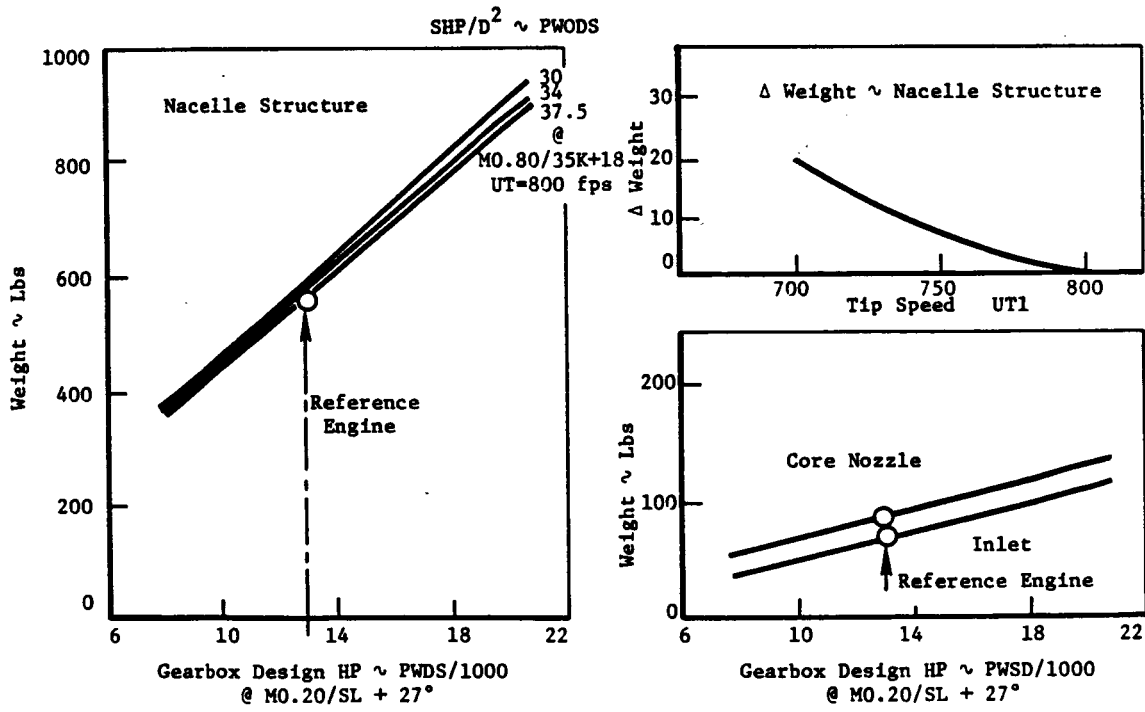


Figure III-4. APET Nacelle Weight Trends.

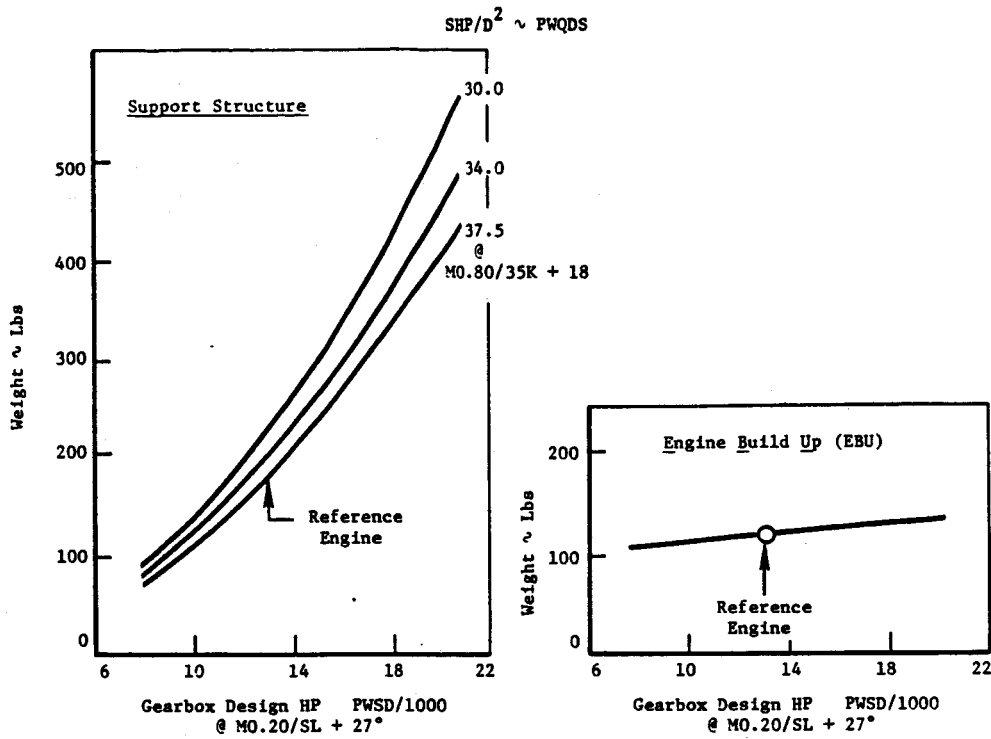


Figure III-5. APET Weight Trend.

Altitude = 35000 Ft., DTAMB = 18°

Engine Control ~ Rated Temperature (SITFK = 1)

PWX1 = GE Reference Value

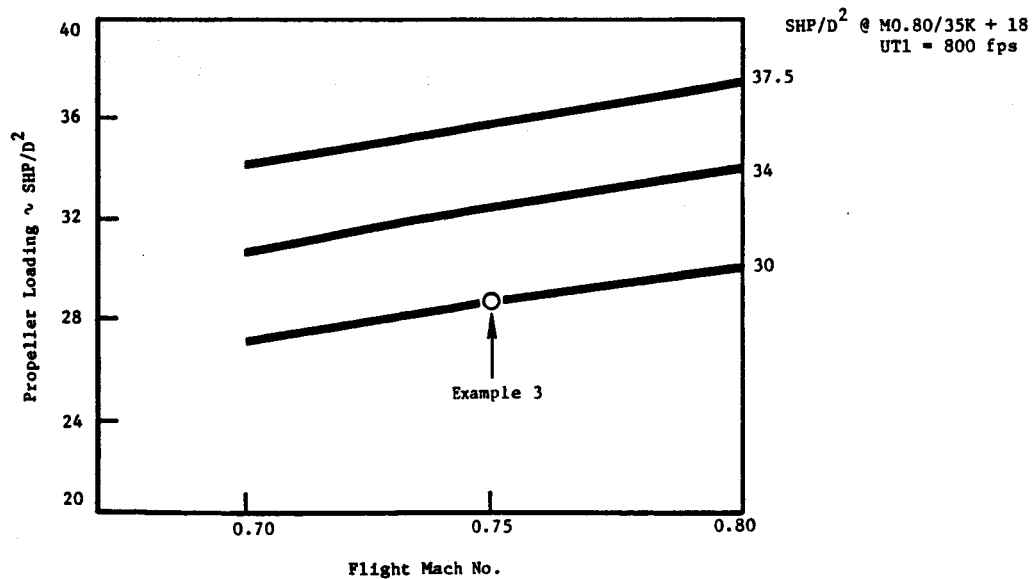


Figure III-6. APET Propeller Loading Trends (Constant Rated Temperature).

Table III-1. Gearbox Type Effects.

PWSD = 13000 @ M0.20/SL + 27°

Gearbox Type

SHP/D2 @ M0.80/35K + 18	Gears Weights		Concentric
	Offset	Split	
37.5	1068	1500	1162
34.0	1123	1577	1222
30	1184	1663	1288
<u>Nacelle Weights</u>			
37.5	567	660	594
34	578	673	606
30	594	691	622

III.4 RESULTS

The results of 3 scaling situations are contained in Tables III-2 and III-3. The reference engine is also included for comparison. Table III-2 contains the input selections to the customer deck and Table III-3 the breakdown of the contributing weights. The examples illustrates these situations.

Engine System	Reference	Example 1	Example 2	Example 3
SWSIZE	0	0.80		
Gas Generator	All Axial			Axi-Centrifugal
Gearbox Type	Offset			Concentric
Propeller	H S 10 Blade Propfan			
SHP/D2 @ M0.80/35K	37.5	37.5	34	30
Tip Speed	800	800	750	700

The listing of the APET customer deck input is included at the back of this section.

III.5 DIMENSIONS

Engine dimensions can be calculated by using Figures III-7 through III-9 along with these scaling relationships.

- Gas Generator

$$\text{Dia} = (\text{Dia})_{\text{Ref}} * (\text{SWSIZE})^{K_1}$$

$$K_1 =$$

$$\text{Length} = (\text{Length})_{\text{Ref}} * (\text{SWSIXE})^{K_2}$$

$$K_2 =$$

- Gearbox

$$\text{Dimension} = (\text{Dimension})_{\text{Ref}} * \frac{\text{PWS D}}{13000} \text{ M0.20/SL} + 27^{K_3}$$

$$K_3 = 0.50$$

ORIGINAL DESIGN
OF POOR QUALITY

Table III-2. Engine Weights and Dimensions.

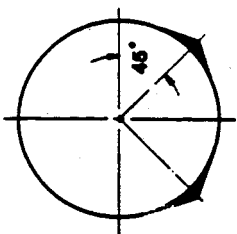
Inputs/Outputs

	Reference Engine		Example 1		Example 2		Example 3	
	Case 1	Case 2	Case 1	Case 2	Case 1	Case 2	Case 1	Case 2
Input								
Mach No.	0.80	0.20	0.80	0.20	0.80	0.20	0.75	0.20
Alt	35000	0	35000	0	35000	0	35000	0
DTAMB	18	27	18	27	18	27	18	27
RC	40	50	40	50	40	50	40	50
SITFK	1	1	1	1	1	1	1	1
PWX1	287	327	229.6	261.6	229.6	261.6	229.6	261.6
SWSIZE	0	0	0.80	0.80	0.80	0.80	0.80	0.80
Propeller	H.S. 10 Blade Propfan							
SWPROP	0	0	0	0	1	2	1	2
ZFWODS	-	-	-	-	34.0	-	28.7*	2
ZUT1	-	-	-	-	750	-	700	-
Configuration								
Gearbox	Offset		Offset		Offset		Concentric	
Gas Generator	All Axial		All Axial		All Axial		Axi Centrifugal	
Output								
PWQDS**	37.5	-	37.5	-	34.0	-	30	-
PWSD	-	-13000	-	10450	-	10450	10440	-
UT1	800	-	800	800	750	-	700	-
GR	7.45	-	7.45	7.45	8.35	-	9.52	-

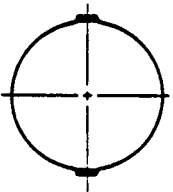
*Selected from Figure 6
 **Values to use for Figures 1 through 5

Table III-3. APET Engine System Weights.

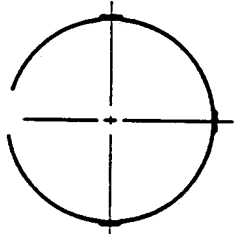
	Reference Engine		Example 1	Example 2	Example 3
	Figure	Weights			
Gas Generator	1	1568 (All Axial)	1280	1280	1345
Propeller	2	1479	1130	1230	1340
Gearbox System	3				
Gear		1068	770	810	920
Heat Exchanger & Ducts		102	81	81	81
Lube System		50	42	42	42
Oil Tank		31	27	27	27
Oil		79	64	64	64
Aircraft Gearbox		50	41	41	41
Weight (Tip Speed)		0	0	100	220
Total		1380	1025	1165	1395
Nacelle System	4				
Nacelle Structure		567	475	485	512
Inlet		70	55	55	55
Core Nozzle		88	75	75	75
Weight (Tip Speed)		0	0	7	20
Total		725	605	622	662
Installation	5				
Support Structure		184	125	137	155
Engine Build Up		122	115	115	115
Total		306	240	252	270
Total = 1 + 2 + 3 + 4 + 5		1548#	4280#	4549#	5012#



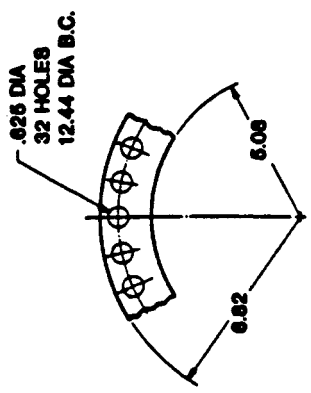
SECT D-D
ENGINE-REAR MOUNTS



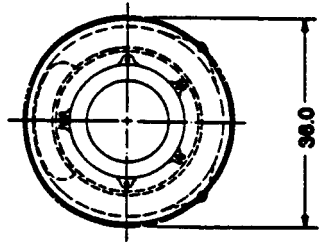
SECT C-C



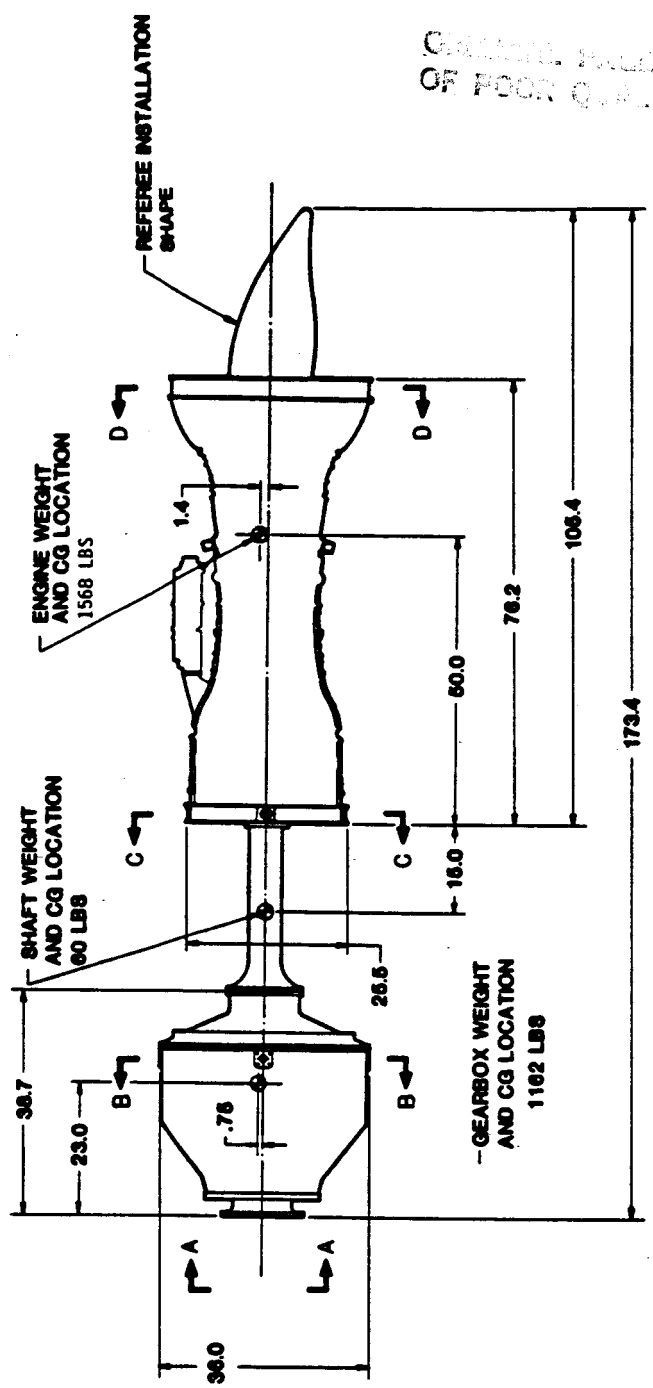
SECT B-B
GEARBOX
SINGLE PLANE-(4) MOUNTS



SECT A-A
SCALE 1/2



SCALE FACTOR = 1.0



GEARBOX WEIGHT
97 POUNDS QUALITY

Figure III-9. APET Engine (Axi-Axi) with Concentric Gearbox.

ORIGINAL PAGE IS
OF POOR QUALITY

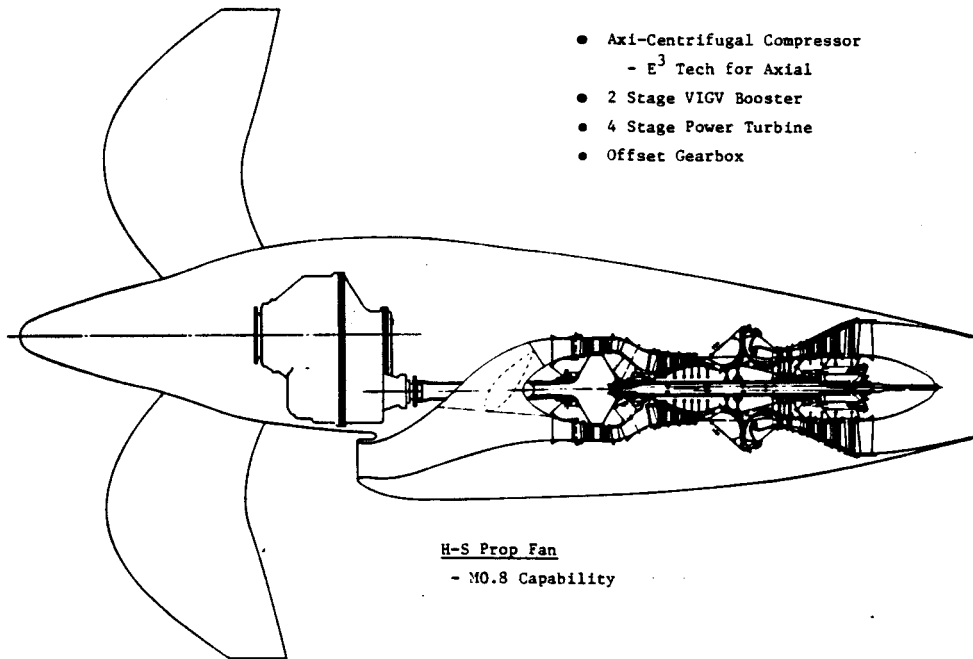


Figure III-10. APET Turboprop Configuration.

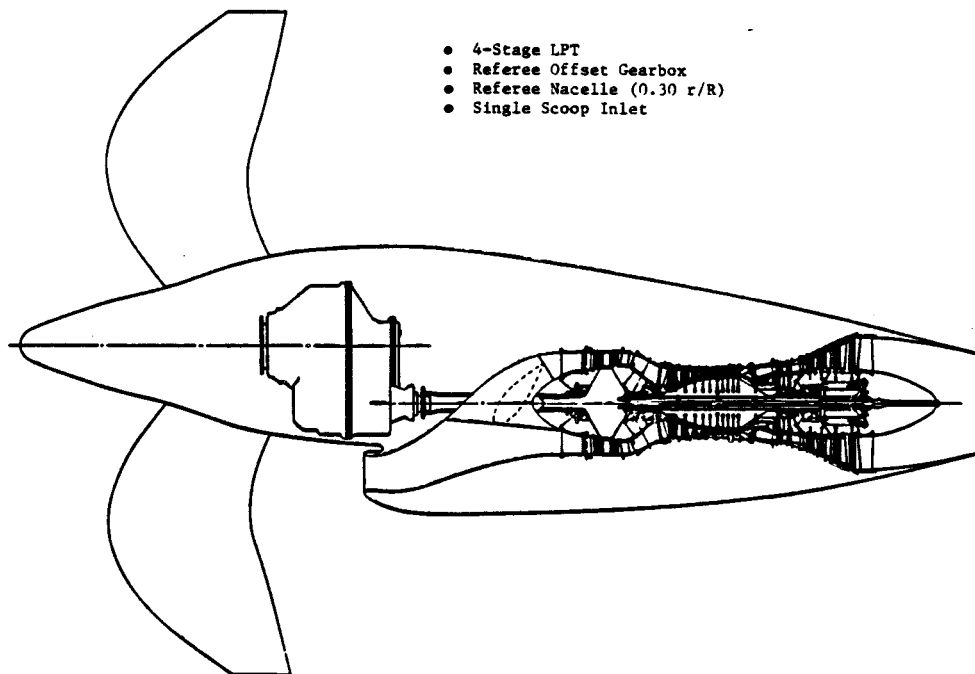
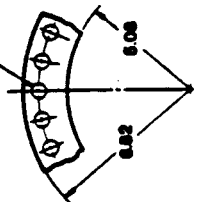
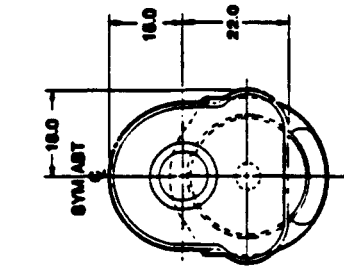
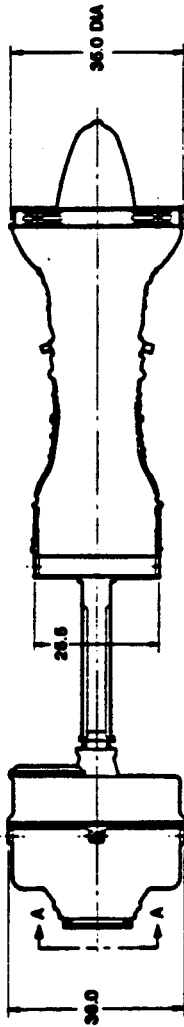


Figure III-11. APET 2B Baseline Engine (12500 SHP).

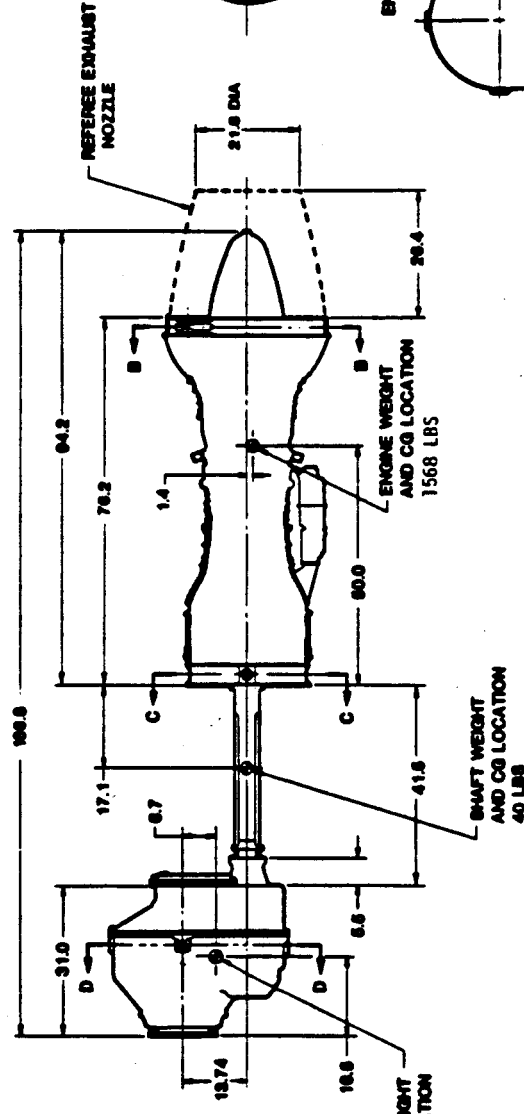
.625 DIA
32 HOLES
12.44 DIA BC



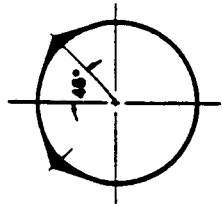
SECTION A-A
SCALE 1/2



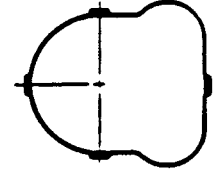
GEARBOX WEIGHT
AND CG LOCATION
1090 LBS



ORIGINAL PAGE IS
OF POOR QUALITY



SECTION B-B
ENGINE - REAR MOUNTS



SECTION C-C
ENGINE-FRONT MOUNTS

NOTE: THE BASELINE ENGINE ASSUMES INDEPENDENT
ENGINE AND GEARBOX MOUNTS. (ALL MOUNTS
TO BE OF THE ANTI-VIBRATION TYPE)

SECTION D-D
GEARBOX
SINGLE PLANE-(X) MOUNTS

Scale Factor = 1.0

Figure III-7. APET Baseline (Axi-Axi) Engine and Gearbox.

ORIGINAL DRAWING
OF POOR QUALITY

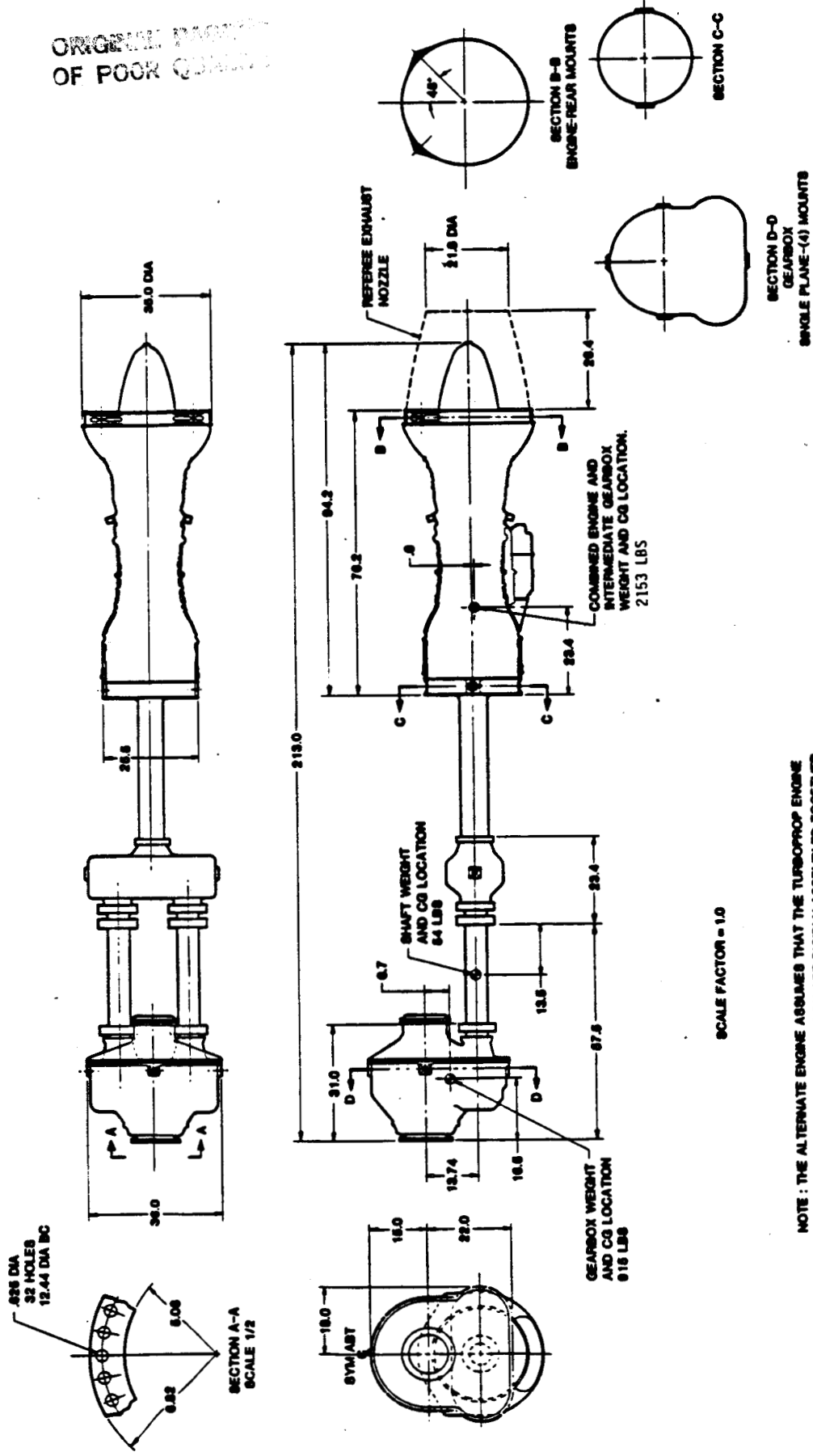


Figure III-8. APET Alternate (Axi-Axi) Engine with Split Gearbox.

Input Listing

PROBING
OF POOR QUALITY

```
$INPUT  
CASE=1;ZALT=35000;ZXM=0.80;ZDTAMB=18;  
SITFK=1;ZRC=40;ZPCNSD=100;SWPW1=1;SWPQ1Z=0;  
ZPW4=0;ZPC=0;ZP1=0;SIM=1;ZT1=0;SWPROP=0;  
ZWB3=0;ZWB3Q=0;ZPWS=0;ZDI1=0;  
ZEGB=0;ZGR=0;ZP1PQ=0;ZPQ1Z=0;  
ZPWQDS=0;ZPW1=0;ZT1PQ=0;ZUT1=0;  
ZVIAS=0;ZVTAS=0;ZWB27Q=0;ZWB27=0;SWSIZE=0;  
SWPQ1Z=0;ZPQ1Z=0;  
$  
$INPUT ZALT=0;ZXM=.2;ZDTAMB=27;  
ZRC=50;  
$
```

Reference
Engine

```
$INPUT  
SWSIZE=0.80;SWPW1=0;ZPW1=229.6;  
ZALT=35000;ZXM=0.80;ZRC=40;ZDTAMB=18;  
$  
$INPUT  
ZALT=0;ZXM=0.20;ZDTAMB=27;ZRC=40;  
ZPW1=261.6;  
$
```

Example
①

```
$INPUT  
ZALT=35000;ZXM=0.80;ZDTAMB=18;ZRC=40;  
SWPROP=1;ZPWQDS=34;ZUT1=750;  
ZPW1=229.6;  
$  
$INPUT  
ZALT=0;ZXM=0.20;ZRC=50;ZDTAMB=27;  
ZPW1=261.6;  
SWPROP=2;  
$
```

Example
②

```
$INPUT  
ZALT=35000;ZXM=0.75;ZRC=40;ZDTAMB=18;  
SWPROP=1;ZPWQDS=28.7;ZUT1=700;  
ZPW1=229.6;  
$  
$INPUT  
ZALT=0;ZXM=0.20;ZRC=50;ZDTAMB=27;ZPW1=261.6;  
SWPROP=2;  
$
```

Example
③

SYMBOLS AND ABBREVIATIONS

M - Mach Number
TOGW - Takeoff Gross Weight
OEI - One Engine Inoperative
SHP - Shaft Horsepower
KEAS - Equivalent Airspeed in Knots
ASM - Available Seat Miles
PAX - Number of Passengers
HP - High Pressure
LP - Low Pressure
SFC - Specific Fuel Consumption
MXCL - Maximum Climb
T/O - Takeoff
PR - Pressure Ratio
K - One Thousand
TF - Turbofan
TP - Turboprop
SL - Sea Level
FN - Net Thrust
DOC - Direct Operating Cost
LF - Load Factor
N.Mi - Nautical Mile
or
NMI
EPNdB - Effective Perceived Noise Level in Decibels
kN - Kilo Newton
kW - Kilowatt
OWE - Operational Weight Empty
ZFW - Zero Fuel Weight
OPR - Overall Pressure Ratio
VIGV - Variable Inlet Guide Vanes
MTDE - Modern Technology Development Engine
T41 - Turbine Gas Temperature
PCM - Pitch Change Mechanism

SYMBOLS AND ABBREVIATIONS (Concluded)

PCMCU - Pitch Change Mechanism Control Unit

PSI - Pounds per Square Inch

KSI - Thousand Pounds per Square Inch

SDG - Speed Decreasing Gearbox

STC - Streamtube Curvature

C_L - Centerline

FADEC - Full Authority Digital Engine Control

DISTRIBUTION LIST

NASA Lewis Research Center
21000 Brookpark Road
Cleveland, OH 44135

No. of Copies

Attn:	Report Control Office, MS 60-1	1
	Library, MS 60-3	2
	L. J. Bober, MS 86-7	1
	L. C. Franciscus MS 6-12	1
	E. J. Graber, MS 86-7	1
	J. F. Groeneweg, MS 86-7	1
	G. A. Kraft, MS 86-7	25
	E. T. Meleason, MS 86-7	1
	J. E. Rohde, MS 86-7	1
	D. A. Sagerser, MS 86-7	1
	G. K. Sievers, MS 86-7	1
	W. C. Strack, MS 6-12	1
	J. A. Ziemianski, MS 86-7	1

NASA Scientific and Technical Information Facility
P. O. Box 8757
Baltimore Washington International Airport, MD 21240

Attn:	Accessioning Department	20
-------	-------------------------	----

NASA Headquarters
Washington, DC 20546

Attn:	RJ/W. S. Aiken, Jr.	1
	RP/J. R. Facey	1

NASA Ames Research Center
Moffett Field, CA 94035

Attn:	D. P. Bencze, MS 227-6	1
	R. C. Smith, MS 227-6	1

NASA Dryden Flight Research Center
P. O. Box 273
Edwards, CA 93523

Attn:	R. S. Baron, MS D-FP	1
-------	----------------------	---

NASA Langley Research Center
Hampton, VA 23665

Attn: C. Driver, MS 249A 1
R. W. Koenig, MS 249 1
Research Information Center, MS 151A 1

Air Force Aero Propulsion Lab
Wright Patterson AFB, OH 45433

Attn: H. F. Jones AFWAL/POSL 3

Naval Air Systems Command
Jefferson Plaza #1
Arlington, VA 20360

Attn: G. Derderian, AIR 310-E 3
J. Klapper, AIR 532C-1 1

Naval Air Propulsion Center
P. O. Box 7176
Trenton, NJ 08628

Attn: P. J. Mangione, M.S. PE-32 2

Allison Gas Turbine Operations
General Motors Corporation
P.O. Box 894
Indianapolis, IN 46206-0894

Attn: R. D. Anderson, MS T-18 1
A. S. Novick, MS T-18 6
D. A. Wagner, MS T-18 1

Beech Aircraft Corporation
Wichita, KS 67201

Attn: R.W. Awker 2

Boeing Commercial Airplane Company
P.O. Box 3707
Seattle, WA 98124

Attn: G. P. Evelyn, MS 72-27 3

Boeing Military Airplane Company
P. O. Box 7730
Wichita, KS 67277-7730

Attn: D. Axelson, MS K77-24 2
C. T. Havey, MS 75-76 2

Cessna Aircraft Company
P. O. Box 154
Wichita, KS 67201

Attn: Dave Ellis, Dept. 178 2

Douglas Aircraft Co.
3855 Lakewood Blvd.
Long Beach, CA 90801

Attn: R. F. Chapier, MS 3641 1
S. S. Harutunian, MS 3641 1
E. S. Johnson, MS 3641 1
F. C. Newton, MS 3584 1

The Garret Corporation
One First National Plaza
Suite 1900
Dayton, OH 45402

Attn: A. E. Hause 1

General Electric Company
Aircraft Engine Business Group
1000 Western Avenue
Lynn, MA 01905

Attn: R. J. Willis, Jr., M.S. WL 345 2

Grumman Aerospace Corporation
Bethpage, NY 11714

Attn: N. F. Dannenhoffer, M.S. C32-05 1
C. Lehman, M.S. C42-05 1
J. Karanik, M.S. C32-05 1

Hamilton Standard Div., UTC
Windsor Locks, CT 06096

Attn:	J. A. Baum, M.S. 1-2-11	1
	S. H. Cohen, M.S. 1-2-11	1
	B. S. Gatzen, M.S. 1-2-11	2
	M. G. Mayo, M.S. 1A-3-2	2

Hartzell Propeller Products
P. O. Box 1458
1800 Covington Avenue
Piqua, OH 45356

Attn:	A. R. Disbrow	1
-------	---------------	---

Lockheed-California Company
P. O. Box 551
Burbank, CA 91503

Attn:	A. R. Yackle, Bldg. 90-1, Dept. 69-05	2
-------	---------------------------------------	---

Lockheed-Georgia Company
86 South Cobb Drive
Marietta, GA 30063

Attn:	W. E. Arndt, M.S. D/72-17, Zone 418	4
	D. M. Winkeljohn, M.S. D/72-79, Zone 419	1

Pratt & Whitney Aircraft
United Technologies Corporation
Commercial Products Division
400 Main Street
East Hartford, CT 06108

Attn:	J. Godston, M.S. 118-26	1
	A. McKibben, M.S. 163-12	1
	C. Reynolds, M.S. 118-26	6
	N. Sandt, M.S. 118-27	1

Pratt & Whitney Aircraft
United Technologies Corporation
Military Products Division
P. O. Box 2691
West Palm Beach, FL 33402

Attn:	L. Coons, M.S. 711-69	1
	W. King, M.S. 702-05	1
	H. D. Snyder, M.S. 711-67	1
	S. Spoleer, M.S. 702-50	1
	H. D. Stetson, M.S. 713-09	1

Sikorsky Aircraft
Transmission Engineering
North Main Street
Stratford, CN 06601

Attn: R. Stone, M.S. S-318A 3

Williams International
2280 West Maple Road
P. O. Box 200
Walled Lake, MI 48088

Attn: Edward Lays, M.S. 4-9 1

Air Canada
Dorval Base H4Y-1CZ
Quebec, Canada

Attn: Goeff Haigh - Zip 14 1
B. H. Jones - Zip 66 1

Air Transport Association
1709 New York Avenue, NW
Washington, DC 20006

Attn: D. J. Collier 1

Delta Air Lines Inc.
Hartsfield Atlanta International Airport
Atlanta, GA 30320

Attn: J.T. Davis, Engineering Department 2

Federal Express
P. O. Box 727-4021
Memphis, TN 38194

Attn: B. M. Dotson, M.S. 4021 1

Ozark Air Lines Inc.
P. O. Box 10007
Lambert St. Louis Airport
St. Louis, MO 63145

Attn: Phil Rogers - Engineering Dept. 1

Trans World Airlines Inc.
605 Third Avenue
New York, NY 10016

Attn: Engineering Dept. 2

United Air Lines
P. O. Box 66100
Chicago, IL 60666

Attn: Engineering Dept. 2

United Air Lines
San Francisco International Airport
San Francisco, CA 94128

Attn: Engineering Dept. 2